

Copyright
by
Nam Ho Kim
2013

The Dissertation Committee for Nam Ho Kim
Certifies that this is the approved version of the following dissertation:

**Mechanistic Investigations of SpnF- and SpnL-Catalyzed Cyclizations
in the Biosynthesis of Spinosyn A**

Committee:

Hung-wen Liu, Supervisor

David W. Hoffman

Seongmin Lee

Christian P. Whitman

Guangbin Dong

**Mechanistic Investigations of SpnF- and SpnL-Catalyzed Cyclizations
in the Biosynthesis of Spinosyn A**

by

Nam Ho Kim, B.S.; M.S.; M.Ed.

Dissertation

Presented to the Faculty of the Graduate School of

The University of Texas at Austin

in Partial Fulfillment

of the Requirements

for the Degree of

Doctor of Philosophy

The University of Texas at Austin

December 2013

Dedication

To my parents and parents-in-law for their incessant support and love

and

To my beloved wife, Insuk, and my lovely kids, Sumin and Suhyun, for completing me

Acknowledgements

It has been a great pleasure working in the Liu lab for the last several years. It was an experience that will remain precious throughout my life. Particularly, learning numerous strategies and mechanisms involved in studying the biosynthesis of natural products has been a constant thrill. Herein, I want to recognize and thank the people who have helped me through this invaluable experience and aided in the completion of my dissertation:

Mechanistic Investigations of SpnF- and SpnL-Catalyzed Cyclizations in the Biosynthesis of Spinosyn A

I would first like to acknowledge my advisor, Dr. Hung-wen (Ben) Liu, for agreeing to serve as my advisor as well as for his patience and feedback both during the Ph.D. courses I took with him, and during the completion of my dissertation. He has always been a nice teacher of science and a great mentor in my life. Additionally, I would like to thank Dr. Christian P. Whitman, David W. Hoffman, Seongmin Lee, and Guanbin Dong for generously agreeing to serve on my dissertation committee. I truly appreciate all of their time and assistance as I completed my researches.

Very special thanks is due my friends and colleagues in the Liu group. When I was a freshman in the Ph.D. program at the University of Texas in Austin, Dr. Hak Joong Kim and Sei-hyun Choi guided me to the Liu lab and helped me settle down in Austin. With enthusiasm and a deep knowledge of biochemistry, Dr. Kim established the foundation of the spinosyn project, and Dr. Choi worked with me to elucidate the mechanism of the SpnL-catalyzed cyclization. This dissertation would not have been possible without their support and assistance. I would like to sincerely thank Dr. Yung-

nan Liu for her kindness and friendship. Whenever I felt I was having difficulties with my family, she enthusiastically gave me advice and helped keep me from falling into despair. I also want to thank Dr. Mark Ruszczky for his willingness to help me with the spinosyn project. Whenever I needed advice on different scientific approaches for the mechanistic investigation of the SpnF and SpnL reactions, he readily spent his time and energy to assist me, giving me a lot of useful comments. In addition, I would like to thank my spinosyn project team members, Byung-sun Jeon, Geng-min Lin, Shao-an Wang, and Eta Isiorho-Mansoorabodi for their tireless efforts. As collaborators, we have shared the aspirations of this project and have worked to continuously move it forward. I want to thank Byung-sun especially for helping me understand many aspects of spinosyn project through thorough discussion.

I would like to thank Hak Joong Kim and Yeonjin Ko as good Korean friends. When I had some trouble with life in the lab, Hak Joong and Yeonjin helped me a great deal. Hak Joong was an especially great colleague and always a good friend in the Liu lab. We constantly discussed matters both in and out of the lab. I sincerely hope that he will accomplish great academic achievements in future.

Life in the Liu lab has not merely been about research, but also about interacting with nice people and having fun. For sharing in the great experience of working in this lab, I would like to thank Dr. Steven Mansoorabodi, Yasushi Ogasawara, Hui Huang, Jordi Calveras, Reid McCarty, Chi-hau Chen, Jessica White-Phillip, Christopher Thibodeaux, Eita Sasaki, and Wei-chen Chang. Steve is a person who will readily share his keen perspectives and fresh ideas with other lab members, and has helped me both to select the theme for my qualifying exam and to develop my idea into concrete hypothesis. Yasushi, Eita, and Reid have given me an abundance of advice and taught me a great deal about enzymatic mechanisms. Hui, Jordi, Wei-chen, and Chi-hau have been great

advisors during organic synthesis projects. Jess and Chris have been great colleagues and have assisted me in the areas of biochemistry and molecular biology.

I am especially thankful to Mel Cheng-Hao Liu, Grace He Sun, Chia-I Lin, Ke-Yi Lin, Meilan Wu, and Anthony Romo. When I had no idea about what to do in the lab, they helped me to adapt quickly. I was happy to meet Mel and Grace because they answered my many questions with patience, no matter the subject. Chia-I and Meilan gave me a lot of advice that helped me balance my research and Ph.D. course work during my first year in the Liu Lab. Ke-Yi was a great colleague for helping me expand my biochemical knowledge, especially while I was working through my Ph.D. courses. Anthony has helped me to become familiar with American life and has corrected my English many times. In addition, I want to thank Jake LeVieux, Jung-Kuei Chen, Aoshou Jhong, and Richiro Ushimaru. I wish they will have as great a time in the Liu lab as I did. I would like to thank Jon Gengler, who took the time to correct my English in my dissertation. His efforts helped ensure my dissertation's timely completion.

I would like to additionally express my gratitude to many colleagues in SK Chemicals Co. Ltd. for supporting me for last four years. I would like to thank Dr. Bongyong Lee and Dr. Key An Um for giving me this opportunity to get a doctoral degree from the University of Texas at Austin. Dr. Bongyong Lee guided me through my development of my R&D within SK Chemicals Co. Ltd. Dr. Key An Um the best boss I have had the pleasure of working for, and has helped me to expand my fantastic professional life. Additionally, I would like to thank Dr. Jae-Sun Kim for sharing many great moments in my professional life. He is an exceedingly cheerful person with a zest for life. Thanks are also due Dr. Ju Young Lee, Dr. Je Ho Ryu, Seon Mi Kim, Shin Ae Kim, Min Hee Lee, Hoe Chul Jung, and all of my colleagues at SK Chemicals Co. Ltd. Also, I would like to recognize some of my old colleagues, Dr. Nam Kyu Lee, Dr. Suk

Ho Lee, Dr. Jun Won Lee, and Jin Young Choi for guiding me during my professional development.

I would like to express my appreciation for my family, who has been of the utmost importance to me. I owe a great deal to my children. I am truly grateful to Sumin and Suhyun, who have adapted so well and grown so much in the time they have spent in Austin. I am sincerely thankful to my parents, Kyu Hwa Kim and Jum Don Lee as well as my parents-in-law, Won Chun Kim and Jun Hee Park. They have constantly encouraged and supported me. I would especially like to thank my mother for her endless efforts to support me and my children in Austin. I also appreciate the encouragement Kyoung-Ho Kim and Ju-Young Kim have given me. Finally, I have to express my appreciation for my wife, In Suk Kim, living in the heaven. My love for In Suk has not changed since the day I meet her. In Suk was a great friend who shared her life with me, a kind wife who loved me in totality, and a wise mother who touched Sumin and Suhyun with her love. Words cannot express my appreciation of In Suk's passion and the love she gave myself and my children. I would like to end this acknowledgement with love to In Suk.

Abstract

Mechanistic Investigations of SpnF- and SpnL-Catalyzed Cyclizations in the Biosynthesis of Spinosyn A

Nam Ho Kim, Ph.D.

The University of Texas at Austin, 2013

Supervisor: Hung-wen Liu

Spinosyn A is a particularly interesting natural product due to its structural complexity and potent insecticidal activity. The biosynthetic pathway of spinosyn A is interesting as it has two unusual features, the SpnF-catalyzed [4+2] cycloaddition and the SpnL-catalyzed cyclization to produce the perhydro-as-indacene core. The work described in this dissertation focuses on elucidating the mechanisms of the SpnF- and SpnL-catalyzed reactions.

SpnF has attracted significant interest as a possible Diels-Alderase. To explain how SpnF catalyzes the formation of cyclohexene ring, three plausible mechanisms have been proposed, the Diels-Alder reaction mechanism, the ionic rearrangement mechanism, and the biradical rearrangement mechanism. Kinetic isotope effect studies were performed using four deuterium-labeled mechanistic probes, specially the C4-D, C7-D, C11-D, and C12-D analogs. Currently, the ionic rearrangement mechanism can be excluded, based on the results using the C4-D and C7-D analogs. In addition, how SpnF accelerates the reaction was studied to assess the contribution of an entropic

preorganization compared to enthalpic transition state stabilization. To measure the relative rate enhancements due to structural perturbations, three mechanistic probes were synthesized, the linear analog, the C13-14 Unc analog, and the C2-3 Unc analog. Unfortunately, the linear analog and C13-14 Unc analog didn't show any turnover activity under either non-enzymatic or enzymatic conditions. Thus, no conclusion could be drawn from incubation with these substrate analogs.

Mechanistic studies of SpnL-catalyzed cyclization were devoted to differentiating between the Rauhut-Currier type mechanism and the Michael addition mechanism. Biochemical studies using the C13-F analog as a mechanism-based inhibitor showed the formation of a covalent adduct with SpnL, which is consistent with the Rauhut-Currier type mechanism. Additional experimental data obtained from isotope trace experiments and kinetic isotope effect studies using C12-D analog supports the Rauhut-Currier type mechanism. Biochemical studies concerning the role of SAM in SpnF and SpnL showed that SAM is required for the activity of SpnL, and were inconclusive for SpnF. SpnL mutant studies showed that Cys60 and Glu96 may be important for the catalysis of SpnL. Chemoenzymatic total synthesis of spinosyn A was completed by chemical etherification of 17-pseudoaglycone and D-forosamine.

Table of Contents

List of Figures	xiv
Chapter 1. Investigation of the Biosynthesis of the Polycyclic System	1
1.1. Background	1
1.2. Mechanistic Investigations of SpnF-Catalyzed [4+2] Cycloaddition	7
1.3. Mechanistic Investigations of SpnL-Catalyzed Cyclization	18
1.4. Deuterium-Labeled Substrate Analogs for Mechanistic Studies of Natural Product Biosynthesis	27
1.5. Fluorinated Substrate Analogs for Mechanistic Studies of Natural Product Biosynthesis	34
1.6. Dissertation Statement	39
Chapter 2. Mechanistic Investigation of SpnF-Catalyzed [4+2] Cycloaddition in the Biosynthesis of Spinosyn A	41
2.1. Introduction	41
2.2. Experimental Procedures	50
2.2.1. Materials and Equipment	50
2.2.2. Preparation of Enzymes	51
2.2.3. Synthesis of the SpnM Natural Substrate	51
2.2.4. Synthesis of the [C4- ² H] SpnM Substrate Analog	88
2.2.5. Synthesis of the [C7- ² H] SpnM Substrate Analog	92
2.2.6. Synthesis of the [C11- ² H] SpnM Substrate Analog	99
2.2.7. Synthesis of the [C12- ² H] SpnM Substrate Analog	111
2.2.8. Synthesis of the Linear SpnF Substrate Analog	117
2.2.9. Synthesis of the C13-14 Unc SpnF Substrate Analog	137
2.2.10. Synthesis of the C2-3 Unc SpnF Substrate Analog	147
2.2.11. <i>In vitro</i> activity assay of SpnM and SpnF	150
2.2.12. <i>In vitro</i> activity assay of SpnF-Catalyzed Cycloaddition by Competitive Reaction Using SpnM Natural Substrate and Deuterium-Labeled SpnM Substrate Analog	151

2.2.13. <i>In vitro</i> activity assay of SpnF-Catalyzed Cycloaddition Reaction Using the Linear, C13-14 Unc, and C2-3 Unc SpnF Substrate Analog.....	153
2.3. Results and Discussion	156
2.3.1. Synthesis of the SpnM Natural Substrate & Deuterium-Labeled SpnM Substrate Analogs.....	156
2.3.2. Synthesis of the Linear, C13-14 Unc, and C2-3 Unc SpnF Substrate Analogs	161
2.3.3. <i>In vitro</i> activity assay of SpnM and SpnF.....	164
2.3.4. <i>In vitro</i> Activity Assay of SpnF-Catalyzed [4+2] Cycloaddition by Competitive Reaction using SpnM Natural Substrate and Deuterium-Labeled SpnM Substrate Analog.....	165
2.3.5. <i>In vitro</i> Activity Assay of SpnF-Catalyzed [4+2] Cycloaddition using the Linear, C13-14 Unc, and C2-3 Unc SpnF Substrate Analogs	174
2.4. Conclusion	182
Chapter 3. Mechanistic Investigation of SpnL-Catalyzed Cyclization in the Biosynthesis of Spinosyn A.....	185
3.1. Introduction.....	185
3.2. Experimental Procedures	190
3.2.1. Materials and Equipment	190
3.2.2. Preparation of Enzymes	191
3.2.3. Synthesis of the SpnL Natural Substrate	192
3.2.4. Synthesis of the [C12- ² H] SpnL Substrate Analog.....	194
3.2.5. Synthesis of the [C13- ² H] SpnL Substrate Analog.....	195
3.2.6. Synthesis of the C13-F SpnL Substrate Analogue.....	209
3.2.7. <i>In vitro</i> activity assay of SpnL.....	216
3.2.8. Isotope Trace Experiment for the SpnL Reaction.....	217
3.2.9. Kinetic Isotope Effect Studies of the SpnL Reaction Using SpnL Natural Substrate and Deuterium-Labeled SpnL Substrate Analogs	217
3.2.10. Biochemical Studies of the SpnL-Catalyzed Cyclization Using C13-F Substrate Analog.....	219

3.2.11. Studies on the SAM-dependence of SpnF and SpnL reactions.....	222
3.2.12. SpnL mutant study using SpnL D57N, E96Q, and E96L.....	225
3.2.13. Chemoenzymatic total synthesis of spinosyn A	226
3.3. Results and Discussion	227
3.3.1. Synthesis of the SpnL Natural Substrate, and Deuterium-Labeled SpnL Substrate Analogs.....	227
3.3.2. Synthesis of the C13-F SpnL Substrate Analog	230
3.3.3. <i>In vitro</i> activity assay of SpnL.....	231
3.3.4. Isotope Trace Experiment for the SpnL Reaction.....	232
3.3.5. Kinetic Isotope Effect Studies of the SpnL Reaction Using SpnL Natural Substrate and Deuterium-Labeled SpnL Substrate Analogs	235
3.3.6. Biochemical Studies of the SpnL-Catalyzed Cyclization using the C13-F SpnL Substrate Analog	239
3.3.7. Studies on the SAM-dependence of SpnF and SpnL reactions.....	274
3.3.8. SpnL mutant study using SpnL D57N, E96Q, and E96L.....	286
3.3.9. Chemoenzymatic total synthesis of spinosyn A	291
3.4. Conclusion	294
Appendix.....	297
A.1. Spectral Data for Chapter 2.....	297
A.2. Spectral Data for Chapter 3.....	329
Bibliography	335
Vita	357

List of Figures

Figure 1-1: Representatives of polyketide natural products containing fused cyclic rings with a cyclohexene moiety	1
Figure 1-2: Chemical structures of the spinosyn family.....	3
Figure 1-3: Biosynthetic gene cluster of spinosyn family	4
Figure 1-4: Established biosynthetic pathway of spinosyn A (1).....	6
Figure 1-5: Proposed mechanisms for SpnF-catalyzed [4+2] cycloaddition in the biosynthesis of spinosyn A	7
Figure 1-6: Plausible mechanisms for SpnL-catalyzed cyclization in the biosynthesis of spinosyn A	7
Figure 1-7: Candidates for putative Diels-Alderase reactions involved in the biosynthesis of natural products containing a cyclohexene moiety....	9
Figure 1-8: Proposed mechanisms for macrophomate synthase in the biosynthesis of macrophomic acid.....	11
Figure 1-9: Mechanism of the formation of the monoterpene limonene from geranyl diphosphate (GPP)	12
Figure 1-10: Mechanism of the biosynthesis of the sesquiterpene epi-aristolochene from farnesyl diphosphate (FPP)	12
Figure 1-11: Detailed ionic rearrangement mechanism for SpnF-catalyzed [4+2] cycloaddition in the biosynthesis of spinosyn A.....	14
Figure 1-12: Synthetic scheme for the construction of hexahydrobenzofuran fragment of avermectins	16
Figure 1-13: Retrosynthetic analysis of guttiferone G and chemical structure of hyperforin.....	17

Figure 1-14: Mechanisms proposed for DNA photolyase (top) and (6-4) photolyase (bottom)	17
Figure 1-15: Detailed biradical cyclization mechanism for SpnF-catalyzed [4+2] cycloaddition in the biosynthesis of spinosyn A.....	18
Figure 1-16: Rauhut-Currier reaction reported in 1963 by the Rauhut-Currier group	19
Figure 1-17: General intramolecular Rauhut-Currier reaction	20
Figure 1-18: Synthesis of a fused tetraquinane ring system as an intermediate for the synthesis of waihoensene	21
Figure 1-19: Utilization of Rauhut-Currier reaction for the synthesis of (±)-ricciocarpin A.....	21
Figure 1-20: Synthesis of (+)-harziphilone using Rauhut-Currier reaction.....	22
Figure 1-21: Intramolecular Rauhut-Currier cycloisomerization for the preparation of <i>as</i> -indacene ring in FR182877	22
Figure 1-22: Diastereoselective synthesis of perhydro- <i>as</i> -indacene core in (-)-spinosyn A	23
Figure 1-23: Proposed mechanism of the reaction catalyzed by thymidylate synthase.....	23
Figure 1-24: General mechanism of Michael addition	25
Figure 1-25: Asymmetric synthesis of (S)-warfarin using Michael addition	26
Figure 1-26: Preparation of synthetic intermediate for (-)-tetracycline and (-)-oxytetracycline.....	26
Figure 1-27: Preparation of synthetic intermediate for (-)-kainic acid.....	26
Figure 1-28: Preparation of synthetic precursor of (+)-atisirene using intramolecular double Michael reaction	27

Figure 1-29: Preparation of synthetic precursor of atisine using intramolecular double Michael reaction.....	27
Figure 1-30: Mechanistic probes for SpnF-catalyzed cycloaddition	28
Figure 1-31: Mechanistic probes for SpnL-catalyzed cyclization	28
Figure 1-32: A Morse potential for a C-H bond showing that the activation energy for homolysis of a C-D bond is larger than for a C-H bond	30
Figure 1-33: Vibrational modes for C-H bonds on sp^3 and sp^2 hybridized carbons	31
Figure 1-34: Reaction of tryptophan 2-monooxygenase (TMO).....	32
Figure 1-35: Proposed mechanisms for TMO	32
Figure 1-36: Proposed mechanisms of D-amino acid oxidase.....	33
Figure 1-37: Mechanistic probes for SpnL-catalyzed cyclization	35
Figure 1-38: Reaction catalyzed by thymidylate synthase	36
Figure 1-39: Inactivation of thymidylate synthase by 5-fluoro-2'-deoxyuridylate... ..	36
Figure 1-40: Proposed mechanism of thymidylate synthase	37
Figure 1-41: Reaction catalyzed by CDP-D-glucose 4,6-dehydratase (E_{od}).....	37
Figure 1-42: Proposed mechanism of E_{od} inactivation by difluoroglucose derivate	38
Figure 1-43: Proposed mechanism for SpnL reaction with C13-F analog through the Rauhut-Currier type mechanisms and Michael addition mechanism	39
Figure 2-1: Established biosynthetic pathway of spinosyn A.....	42
Figure 2-2: Proposed mechanisms for SpnF-catalyzed [4+2] cycloaddition in the biosynthesis of spinosyn A	42

Figure 2-3: Diels-Alder reaction between diene and dienophile via the stereospecific <i>endo</i> -mode <i>syn</i> -addition.....	44
Figure 2-4: Mechanistic probes for SpnF-catalyzed cycloaddition.....	45
Figure 2-5: The expected secondary kinetic isotope effect for the proposed mechanisms of SpnF-catalyzed [4+2] cycloaddition.....	47
Figure 2-6: Analogs for studying the intrinsic property of SpnF.....	47
Figure 2-7: Proposed mechanisms for SpnF reaction.....	156
Figure 2-8: Retrosynthetic analysis for the synthesis of SpnM natural substrate and its deuterium-labeled derivatives.....	158
Figure 2-9: Two synthetic pathways for the preparation of SpnM natural substrate (51).....	159
Figure 2-10: HPLC trace of SpnJ-catalyzed oxidation of its natural substrate (50) into product (51).....	161
Figure 2-11: Retrosynthetic analysis for the synthesis of Linear SpnF substrate analog.....	162
Figure 2-12: Retrosynthetic analysis for the synthesis of C13-14 Unc SpnF substrate analog.....	163
Figure 2-13: Retrosynthetic analysis for the synthesis of C2-3 Unc SpnF substrate analog.....	164
Figure 2-14: HPLC trace of SpnM and SpnF reactions.....	165
Figure 2-15: Representative MS results from the competition reaction of SpnM natural substrate and C7-D SpnM substrate analog.....	168
Figure 2-16: Plots of enrichment (<i>R_x</i>) versus reaction progress for C4-D and C7-D kinetic isotope effect in the non-enzymatic reaction.....	169

Figure 2-17: Alternative mechanism describing a [6+4] cycloaddition followed by a [3+3] sigmatropic rearrangement, suggested by Ken Houk.....	170
Figure 2-18: Plots of enrichment (R _x) versus fraction of reaction (f) for C4-D and C7-D kinetic isotope effect in the enzymatic reaction.....	171
Figure 2-19: The most likely mechanism for the SpnF-catalyzed cycloaddition based on the current estimation of kinetic isotope effects at the C-4 and C-7 positions	173
Figure 2-20: The ionic rearrangement mechanism via the unusual zwitterion intermediates	173
Figure 2-21: Current estimations for non-enzymatic and enzymatic kinetic isotope effects for the [4+2] cycloaddition.....	174
Figure 2-22: Expected $RRE_{NS,Analog}$ for [4+2] cycloaddition	176
Figure 2-23: HPLC trace of Linear SpnF substrate analog.	176
Figure 2-24: HPLC trace of C13-14 Unc SpnF substrate analog	177
Figure 2-25: General procedure for the [4+2] cycloaddition.....	177
Figure 2-26: The change of HOMO and LUMO by the adjacent conjugation in the [4+2] cycloaddition.....	179
Figure 2-27: Inhibition assay of SpnF with the Linear analog and C13-14 Unc analog.....	181
Figure 2-28: Inhibition assay of SpnF with the Linear analog and C13-14 Unc analog.....	181
Figure 3-1: Established biosynthetic pathway of spinosyn A.....	185
Figure 3-2: Plausible mechanisms for SpnL-catalyzed cyclization in the biosynthesis of spinosyn A	186
Figure 3-3: Mechanistic probes for SpnL-catalyzed cyclization	188

Figure 3-4: The expected kinetic isotope effect for C12-D and C13-D analogs during SpnL reaction.....	188
Figure 3-5: Proposed mechanism for SpnL reaction with C13-F analog through the Rauhut-Currier type mechanisms and Michael addition mechanism	189
Figure 3-6: Hybridal changes of carbons at C-12 and C-13 positions, and the summary of the expected kinetic isotope effects during the SpnL reaction.....	228
Figure 3-7: HPLC trace of SpnM natural substrate (9) into SpnG product (2 , SpnL natural substrate)	229
Figure 3-8: HPLC trace of the SpnG reaction for a mixture of C13-F and natural substrate	231
Figure 3-9: HPLC trace of SpnL reaction for the SpnL natural substrate	232
Figure 3-10: Deuterium(s) incorporation during the SpnL reaction, depending on the mechanisms	233
Figure 3-11: MS (ESI, positive) results for the isotope trace experiment	234
Figure 3-12: Determination of kinetic parameters for the SpnL natural substrate and C12-D substrate analog	238
Figure 3-13: Kinetic parameters for the SpnL natural substrate and C12-D substrate analog, and the kinetic isotope effect determined under the direct comparison conditions	238
Figure 3-14: Plot of enrichment ratio (Rx) versus reaction progress for C12-D kinetic isotope effect of the SpnL	238
Figure 3-15: HPLC trace of SpnL-catalyzed cyclization using C13-F analog	240

Figure 3-16: HPLC trace of SpnL-catalyzed cyclization using SpnL and C13-F analog	241
Figure 3-17: HPLC trace of the SpnL reaction for the preincubation experiment	243
Figure 3-18: HPLC trace of SpnL reaction for the test of L-glutathione depletion by C13-F analog.....	244
Figure 3-19: Inhibition assay of SpnL with C13-F analog	249
Figure 3-20: Inhibition assay results for various concentrations of the C13-F analog.....	249
Figure 3-21: Plot for $1/k_{obs}$ versus $1/[I]$	250
Figure 3-22: ESI-MS data of SpnL incubated with SpnL natural substrate	252
Figure 3-23: ESI-MS spectroscopic data of SpnL.....	252
Figure 3-24: ESI-MS data of SpnL incubated with C13-F analog	252
Figure 3-25: Plausible covalent-modification of SpnL (or glucuronylated SpnL) by the C13-F analog.....	253
Figure 3-26: Expected MS of fragments of SpnL treated with trypsin after incubation with the C13-F analog.....	255
Figure 3-27: MS for SpnL, which was treated with 2 equivalent of C13-F analog and trypsin.....	256
Figure 3-28: MS for SpnL, which was treated with 0.5 equivalent of C13-F analog and trypsin.....	257
Figure 3-29: MS for SpnL C71A mutant.....	259
Figure 3-30: Fragment ion table in average mass for Fragment 4 in SpnL	260

Figure 3-31: Re-fragmentation of unmodified fragment 4 from the trypsin-digested SpnL C71A mutant after preincubation with the C13-F analog.....	261
Figure 3-32: ESI MS/MS for SpnL C71A mutant, trypsin-digested after incubation with C13-F analog.....	264
Figure 3-33: Two possible scenarios if Cys60 and Cys71 are located in close proximity.....	265
Figure 3-34: Expected non-enzymatic covalent adduct formation of L-glutathione with SpnL natural substrate and C13-F analog.....	266
Figure 3-35: <i>In vitro</i> activity assay of SpnL and three mutants.....	267
Figure 3-36: Comparison of reactivity of three α,β -unsaturated ketones toward nucleophilic addition in Rauhut-Currier reaction	267
Figure 3-37: The third possible scenario if Cys60 and Cys71 are located opposite to the other and in close proximity	268
Figure 3-38: HPLC trace for the single turnover experiments	270
Figure 3-39: MS of isolated compound from single turnover experiment	271
Figure 3-40: Proposed mechanism of H ₂ O incorporation into C13-F containing SpnL product.....	272
Figure 3-41: Mechanistic probes for SpnL reaction: ¹³ C13-F analog	273
Figure 3-42: Sequence comparison of SpnL and SpnF with known SAM-dependent methyltransferases	275
Figure 3-43: HPLC traces of SAM in SpnF	276
Figure 3-44: HPLC traces of SAM in SpnL	276
Figure 3-45: HPLC traces of apo-SpnF	277
Figure 3-46: HPLC traces of apo-SpnL.....	277

Figure 3-47: HPLC traces for <i>in vitro</i> activity assay of apo-SpnF with external SAM.....	278
Figure 3-48: HPLC trace of <i>in vitro</i> activity assay of apo-SpnL in the presence of (A) SAM, (B) SAH, and (C) 5'-deoxyadenosine and/or methionine	279
Figure 3-49: HPLC trace of SAM for (a) SAM standard, (b) as-isolated SpnL, (c) apo-SpnL, and (d) reconstituted SpnL	280
Figure 3-50: HPLC trace of SpnL reaction with the reconstituted SpnL	280
Figure 3-51: Three proposed structural roles of SAM in SpnL reaction	282
Figure 3-52: CD spectrum of as-isolated SpnL and apo-SpnL.....	283
Figure 3-53: CD spectrum change during the reconstitution process.....	283
Figure 3-54: New proposed role of SAM in the SpnL reaction.....	285
Figure 3-55: HPLC trace of the <i>in vitro</i> activity assay for SpnL and its mutants	289
Figure 3-56: Retrosynthetic analysis of spinosyn A by the Roush group	292
Figure 3-57: Retrosynthetic analysis of spinosyn A analog by the Tietze group	292
Figure 3-58: HPLC trace of enzymatic transformations using SpnJ, SpnM, SpnF, SpnG, SpnL, SpnI, SpnK, and SpnH to produce 17-pseudoaglycone of spinosyn A	293
Figure 3-59: HPLC trace of SpnL/I/K/H reaction versus SpnI/K/H/L reaction ..	294
Figure 3-60: Etherification of D-forosamine to 17-pseudoaglycone of spinosyn A for the chemoenzymatic total synthesis	294

Chapter 1. Investigation of the Biosynthesis of the Polycyclic System in

Spinosyn A

1.1. BACKGROUND

Fused polycyclic systems are found in a number of natural products biosynthesized by polyketide synthases. Their formation has attracted a great deal of attention in terms of the biosynthetic pathways and the mechanism (**Figure 1-1**).^{1, 2, 3} Spinosyn A, which contains a tetracyclic aglycone and two appended sugars, is a particularly interesting natural product due to its structural complexity.⁴

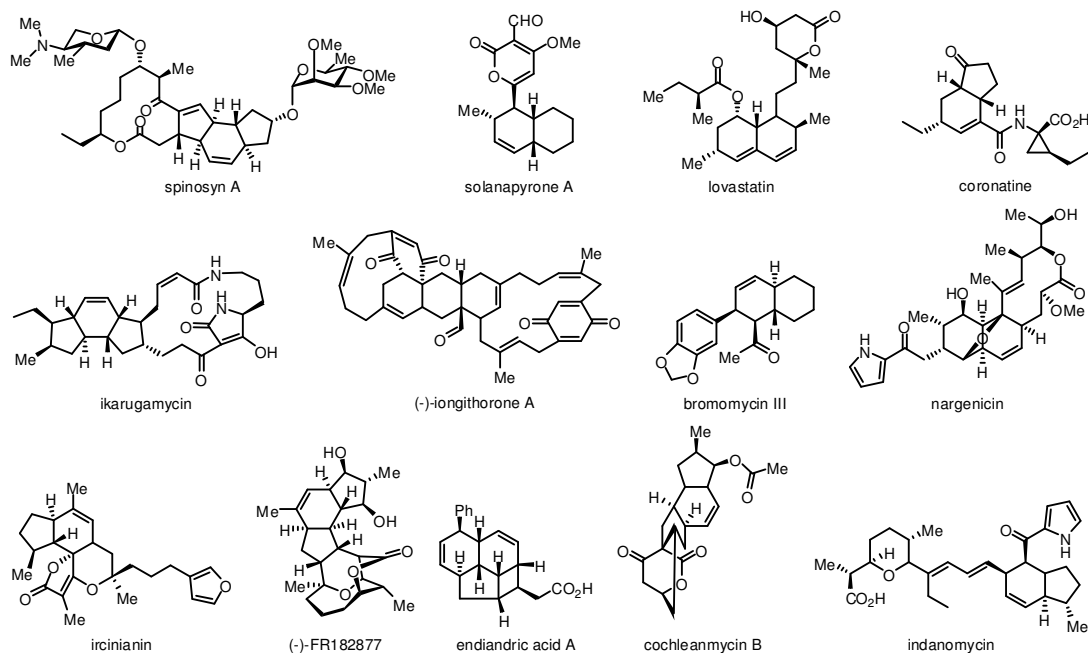


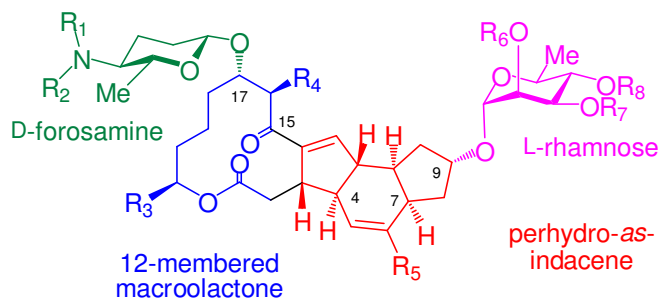
Figure 1-1. Representatives of polyketide natural products containing fused cyclic rings with a cyclohexene moiety.

The spinosyns are a family of polyketide natural products that are known for their extraordinary insecticidal activity (**Figure 1-2**).^{5, 6, 7} Spinosyns are produced by the soil

bacterium *Saccaropolyspora spinosa*. Extraction of the compounds from fermentation broths generally yields a mixture of spinosyn A (**1**, ~85%) and spinosyn D (**2**, ~15%). According to Dow AgroScience, Spinosad[®] (a mixture of spinosyn A and spinosyn D) has several attractive features when compared to most synthetic insect pest control products.^{8,9} First, it is produced through fermentation of a naturally occurring organism. Second, it has high activity even at low concentrations. Third, regardless of whether the pest ingests or simply comes into contact with the compound it is an extremely potent insecticide. Fourth, it has a lower impact on certain beneficial predatory insects. Lastly, among known insecticides, the mechanism of Spinosyn A is unique. Specifically, spinosyn A disrupts neuronal activity and excites motor neurons, causing involuntary muscle contractions. This eventually leads to paralysis and death. It has been demonstrated that spinosyn A interacts with both γ -aminobutyric acid (GABA) receptors and nicotinic acetylcholine receptors, implicating their involvement as part of the mechanism.^{10, 11} More recently, knockout studies in *Drosophila melanosaster* has established the *Da6* subunit of the nicotinic acetylcholine receptor as a target site of the spinosyn family.^{12, 13, 14}

Spinosyn A is composed of a 22-membered tetracyclic core and two sugar moieties at the C-9 (tri-*O*-methyl-L-rhamnose) and C-17 (D-forosamine) positions. The fused perhydro-*as*-indacene core, which contains the cyclohexene and cyclopentene moieties, contributes to the overall structural complexity. The possible involvement of putative “Diels-Alderase” and “Rauhut-Currier type cyclase” in the biosynthesis of this perhydro-*as*-indacene has been suggested. Because of its unusual structure and the potent

biological activity, study of biosynthesis and mechanism of enzymes in the pathway has been a hot topic.



No.	Name	R ₁	R ₂	R ₃	R ₄	R ₅	R ₆	R ₇	R ₈	LC ₅₀ (mg/L)
1	Spinosyn A	Me	Me	Et	Me	H	Me	Me	Me	0.3
2	Spinosyn B	H	Me	Et	Me	H	Me	Me	Me	0.4
3	Spinosyn C	H	H	Et	Me	H	Me	Me	Me	0.8
4	Spinosyn D	Me	Me	Et	Me	Me	Me	Me	Me	0.8
5	Spinosyn E	Me	Me	Me	Me	H	Me	Me	Me	4.6
6	Spinosyn F	Me	Me	Et	H	H	Me	H	Me	4.5
7	Spinosyn H	Me	Me	Et	Me	H	H	Me	Me	5.7
8	Spinosyn J	Me	Me	Et	Me	H	Me	H	Me	>80
9	Spinosyn K	Me	Me	Et	Me	H	Me	Me	H	3.5
10	Spinosyn L	Me	Me	Et	Me	Me	Me	Me	Me	26
11	Spinosyn M	H	Me	Et	Me	H	Me	H	Me	22.6
12	Spinosyn N	H	Me	Et	Me	Me	Me	H	Me	40
13	Spinosyn O	Me	Me	Et	Me	Me	Me	Me	H	1.4
14	Spinosyn O	Me	Me	Et	Me	H	Me	H	H	>64
15	Spinosyn Q	Me	Me	Et	Me	Me	H	Me	Me	0.5
16	Spinosyn R	H	Me	Et	Me	H	H	Me	Me	14.5
17	Spinosyn S	Me	Me	Me	Me	H	H	Me	Me	53
18	Spinosyn T	Me	Me	Et	Me	H	H	H	Me	>64
19	Spinosyn U	Me	Me	Et	Me	H	H	Me	H	22
20	Spinosyn V	Me	Me	Et	Me	Me	H	Me	H	17
21	Spinosyn W	Me	Me	Et	Me	Me	Me	H	H	>64
22	Spinosyn Y	Me	Me	Me	Me	H	Me	Me	H	20

Figure 1-2. Chemical structures of the spinosyn family. The LC₅₀ values represent the biological activity of the corresponding spinosyn against tobacco budworm, *Heliothis virescens*.

The spinosyn biosynthetic gene cluster was cloned and characterized by Waldron and co-workers in 2001 (**Figure 1-3**).¹⁵ It is approximately 74 kbp long and contains 19

open reading frames (ORFs). Combination of computational and experimental techniques including BLAST analysis, gene deletion studies, intermediate feeding and trace tracking studies, have allowed for a tentative assignment of the function of each ORF.^{15, 16, 17, 18} About half of the annotated gene cluster is comprised of five large ORFs which code for multimodular type I polyketide synthases (PKSs). Upstream of these PKS genes is involved in forosamine biosynthesis, rhamnose methylation, glycosyl transfer, and intramolecular C-C bond formation. Careful analysis of the gene cluster has led to a hypothesis that the three intramolecular C-C bond formations between C13-C14, C4-C12, and C7-C11, are probably formed from the macrolactone immediately after its release from the polyketide synthase, SpnE, but prior to the glycosyl transfers. Waldron and co-workers suggested that the gene products of SpnF, SpnJ, SpnL, and SpnM might be involved in the “cross-bridging” reactions to produce the perhydro-*as*-indacene core.^{15, 19}

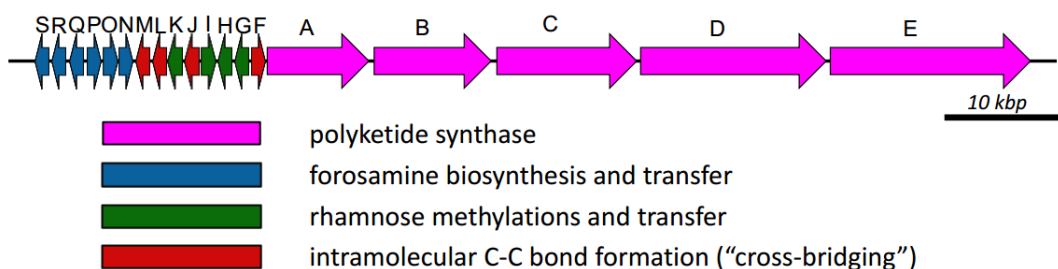


Figure 1-3. Biosynthetic gene cluster of spinosyn family.

Recently, the “cross-bridging” biosynthetic pathway of spinosyn A has been established by Liu group, as shown in **Figure 1-4**.^{20, 21, 22} The first step of post-PKS modification is the oxidation of the 15'-hydroxyl group to the corresponding ketone by SpnJ, a flavin-dependent dehydrogenase.²⁰ This result is in agreement with the proposal made by Leadlay and co-workers, implying that the “cross-bridging” process is a post-

PKS modification, initiated by the oxidation at C-15 position, and followed by a cascade of cationic cyclization.²³ However, SpnJ turned out to be a monofunctional oxidase, and didn't promote the following cyclization to generate the spinosyn carbocyclic array via an oxidative modification of a polyolefin intermediate.²⁴ Interestingly, generation of the ketone moiety at C-15 may lower the pK_a of the neighboring C-14 position, at which point deprotonation may be facilitated by SpnM, the putative hydratase in the second step, leading to the highly activated ketone-conjugated polyolefin intermediate. These two steps catalyzed by SpnJ and SpnM are particularly important to understand the intramolecular C-C bond formations leading to the perhydro-*as*-indacene core, because all of the elements involved in the formation of perhydro-*as*-indacene are established in the resulting polyolefin intermediate. In the third step, SpnF catalyzes two C-C bond formations between C-7 and C-11 and between C-4 and C-12, accelerating the rate of the [4+2] cycloaddition 500 times faster than the non-enzymatic reaction.²¹ SpnF is interesting due to its unique monofunctional facilitation of the [4+2] cycloaddition in the formation of the cyclohexene moiety in the spinosyn A aglycone.

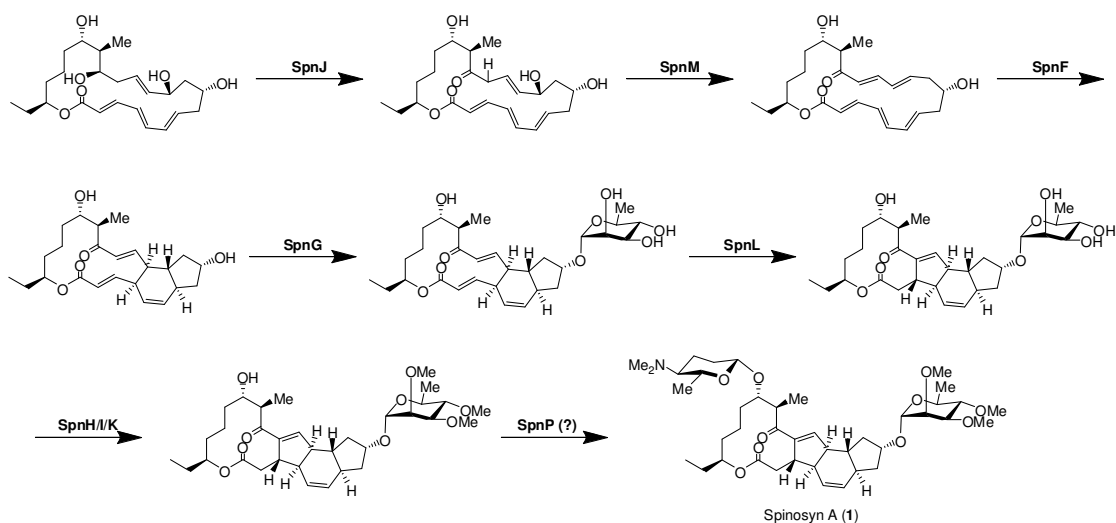


Figure 1-4. Established biosynthetic pathway of spinosyn A (**1**).

Initially, SpnL was expected to catalyze the second cyclization to complete the formation of perhydro-*as*-indacene core before glycosylation of L-rhamnose or D-forosamine. However, tricyclic intermediate turned out not to be a substrate for SpnL, but a substrate for SpnG, a rhamnosyltransferase, producing the 9'-rhamnosyl tricyclic intermediate, which is then converted to tetracyclic perhydro-*as*-indacene intermediate by SpnL. Thus, this reaction sequence consists of two steps: the glycosylation of L-rhamnose at the C-9 position catalyzed by SpnG when fed a tricyclic intermediate, and the conversion of the tricyclic to a tetracyclic core catalyzed by SpnL to give the 9'-L-rhamnosylated tetracyclic intermediate. SpnL-catalyzed cyclization is thought to be facilitated by a C-15 ketone moiety produced by SpnJ, although the reaction mechanism is uncertain. The last step for the biosynthesis of spinosyn A may be the second glycosylation of D-forosamine, catalyzed by SpnP, a glycosyltransferase. Due to difficulties in the preparation of TDP-D-forosamine, the last step of the biosynthesis of spinosyn A remains to be confirmed.

The mechanisms of the formation of the perhydro-*as*-indacene core in the biosynthesis of spinosyn A are not straightforward, although the reaction sequence of the “cross-bridging” biosynthetic pathway has been established. The specific mechanism of the first cycloaddition catalyzed by SpnF has not been conclusively determined, although there are three plausible mechanisms: Diels-Alder reaction mechanism,^{24, 25, 26, 27} ionic rearrangement mechanism, and biradical cyclization mechanism (**Figure 1-5**).

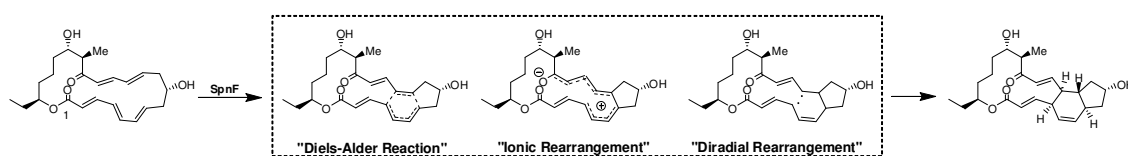


Figure 1-5. Proposed mechanisms for SpnF-catalyzed [4+2] cycloaddition in the biosynthesis of spinosyn A.

The second cyclization catalyzed by SpnL is also very interesting from a mechanistic point of view. Two suggested mechanisms are Rauhut-Currier type mechanism^{29, 30} and Michael addition mechanism^{31, 32} (**Figure 1-6**).

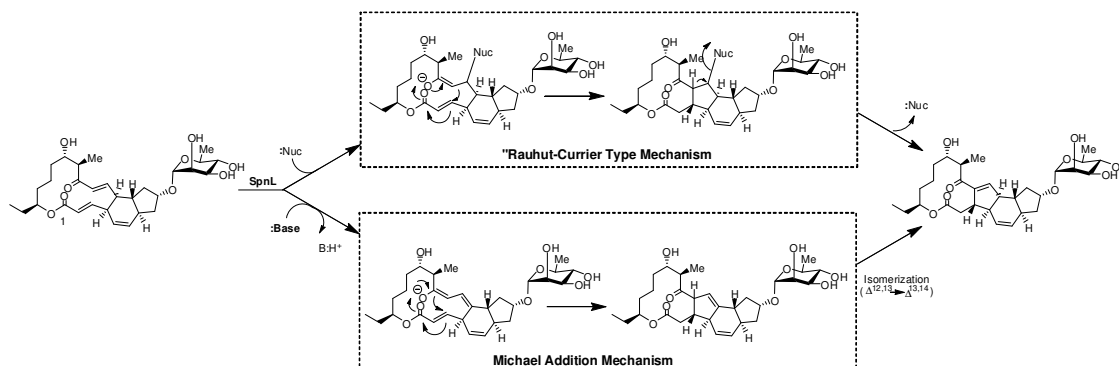


Figure 1-6. Plausible mechanisms for SpnL-catalyzed cyclization in the biosynthesis of spinosyn A.

1.2. MECHANISTIC INVESTIGATIONS OF SpnF-CATALYZED [4+2] CYCLOADDITION

In the following chapter three possible mechanisms of SpnF-catalyzed [4+2] cycloaddition, which results in the formation of a cyclohexene moiety, will be discussed.

The first possible mechanism of SpnF-catalyzed cycloaddition is the Diels-Alder reaction mechanism. The Diels-Alder reaction, named after the two Nobel Prize-winning (1950) chemists, Otto Paul Hermann Diels and Kurt Alder, who first recognized and developed this reaction.^{25, 26, 27} In a typical Diels-Alder reaction, a cyclohexene system is formed through a [4+2] cycloaddition reaction between a conjugated electron-rich 1,3-diene component and a substituted electron-deficient alkene (dienophile) via a concerted, pericyclic, and aromatic transition state.^{33, 34, 35} The Diels-Alder reaction is generally considered as one of the most useful reactions in organic chemistry because it readily produces a cyclohexene moiety in a [4+2] cycloaddition process. In fact, it has been applied to the synthesis of many natural products, which contains six membered carbocyclic ring in their structure (**Figure 1-1**).^{36, 37, 38, 39, 40} Several putative Diels-Alderase reactions have been reported to catalyze [4+2] cycloaddition reaction, but many of them appear to be involved in more than one chemical processes. For example, the biosynthetic pathways for solanapyrone^{41, 42, 43} and lovastatin^{44, 45} have been investigated in an attempt to discover naturally occurring Diels-Alderase reactions, since their 1,2-dehydrodecalin moiety has been suspected to be formed through an enzyme-catalyzed intramolecular Diels-Alder reaction (**Figure 1-7A** and **Figure 1-7B**).

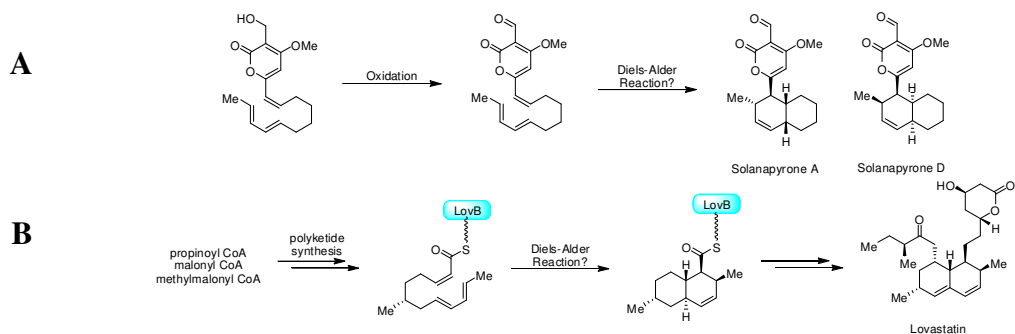


Figure 1-7. Candidates for putative Diels-Alderase reactions involved in the biosynthesis of natural products containing a cyclohexene moiety. A) Proposed functions of solanapyrone synthase and the change in the stereo-outcome of the products in the presence of partially purified enzyme, B) Proposed functions of LovB on its substrate, a cyclohexene-containing intermediate in the biosynthesis of lovastatin.

The Oikawa group was the first to show solanapyrone synthase capability to catalyze the 1,2-dehydrodecalin formation.^{41, 42, 43} The Vederas and Hutchison groups were later demonstrated the activity of LovB as a cyclase.^{44, 45} Solanapyrone synthase from the pathogenic fungus *Alternaria solani* involved in the biosynthesis of solanapyrone, and lovastatin nonaketide synthase (LovB), from *Aspergillus terreus* involved in the biosynthesis of lovastatin. Through their work, these two enzymes were shown to influence the stereochemical outcome of the corresponding [4+2] cycloaddition reactions, when the respective linear polyketide chain intermediates were used as substrates for the formation of 1,2-dehydrodecalin moiety. It was reported that Solanapyrone synthase is a multifunctional enzyme, which catalyzes both the oxidation of the linear polyketide intermediate to produce the aldehyde precursor and the subsequent Diels-Alder reaction to produce the 1,2-dehydrodecalin core of solanapyrone (**Figure 1-7 (A)**). Lovastatin nonaketide synthase (LovB) is a megasynthase responsible for the assembly of the nonaketide, which is then converted to the decalin core in the

same active site of LovB (**Figure 1-7 (B)**). Although the stereochemistries of the 1,2-dehydrodecalin products are different in the presence and in the absence of enzyme in both cases, the detailed mechanisms of these two enzymes, especially whether they affect the rate of the cyclization reaction are still obscure.

In addition to these putative Diels-Alderases, macrophomate synthase (MPS) is another enzyme known to catalyze a [4+2] cycloaddition between 2-pyrone and oxaloacetate to form macrophomic acid in the fungus *Macrophoma commelinae* (**Figure 1-8**).^{46, 47} The crystal structure of macrophomate synthase⁴⁸ and the results of many biochemical experiments showed that binding of 2-pyrone and pyruvate in the active site likely results in an electro-cyclic transition state.^{49, 50} Two plausible mechanisms are possible, a concerted Diels-Alder reaction or a stepwise Michael-aldol reaction.⁵¹ The bicyclic intermediate (**Figure 1-8**, the compound in the dotted box) proposed for the Diels-Alder reaction could be stabilized by a divalent metal ion (probably Mg^{2+}), which was used to facilitate the formation of an enolate intermediate in the final step. In the Michael-aldol reaction, a nucleophilic attack by the enolate would generate a C-C bond and the negative charge could be stabilized by the 2-pyrone core. Subsequently, the enolate of the 2-pyrone core could attack the newly formed carbonyl group to generate the bicyclic intermediate. Oikawa and co-workers insisted that the high stereospecificity observed in an aberrant cyclization product catalyzed by macrophomate synthase is consistent with a concerted mechanism, although the normal reaction product is achiral.⁴⁸ However, Jorgensen and co-workers computationally demonstrated that a stepwise mechanism is energetically more favorable for macrophomate synthase, as compared to

the pericyclic Diels-Alder reaction.⁵¹ Their conclusion was based on calculation using mixed quantum and molecular mechanics (QM/MM) methods, combined with Monte Carlo simulations and free-energy perturbation (FEP) calculations. Additionally, the Hilvert group demonstrated experimentally that macrophomate synthase operates as a promiscuous aldolase consistent with the second half reaction of the stepwise Michael-aldol reaction.⁵² Thus, combined results suggested that macrophomate synthase may not be a Diels-Alderase. Because none of the early examples can be considered as true Diels-Alderase, the mechanistic study of SpnF-catalyzed [4+2] cycloaddition reported herein represents our attempts to discover the existence of a natural Diels-Alderase.

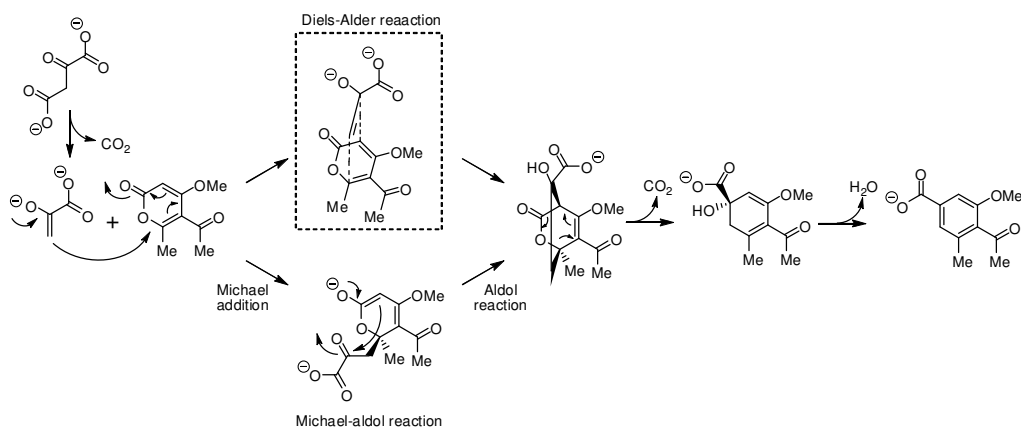


Figure 1-8. Proposed mechanisms for macrophomate synthase in the biosynthesis of macrophomic acid.

The second proposed mechanism for SpnF-catalyzed cycloaddition may occur through a series of ionic rearrangements, a process akin to those involved in terpenoid biosynthesis. Monoterpene limonene is biosynthetically produced from a cationic cyclization of geranyl diphosphate (GPP) (**Figure 1-9**).⁵³ Loss of diphosphate ion from geranyl diphosphate (GPP) results in an allylic cation, which undergoes a 1,3-cationic rearrangement and rephosphorylation to give linalyl diphosphate (LPP). A second loss of

diphosphate ion from linalyl diphosphate (LPP) initiates the cationic cyclization through a 1,5-cationic rearrangement to give a cyclohexene moiety. Finally, deprotonation completes the biosynthesis of limonene. Sesquiterpene biosynthesis also arises by cationic cyclizations of farnesyl diphosphate (FPP) through a series of cationic rearrangement (**Figure 1-10**). For example, the biosynthesis of epi-aristolochene⁵⁴ is initiated by the loss of diphosphate ion from farnesyl diphosphate (FPP), followed by 1,3-cationic rearrangement, cyclization, and deprotonation to produce a neutral triene intermediate. Further cyclization is initiated by reprotonation at C-6, followed by a 1,2-hydride migration, a 1,2-methyl shift, and then the deprotonation at C-8 to give a cyclohexene moiety and complete the biosynthesis of epi-aristolochene.

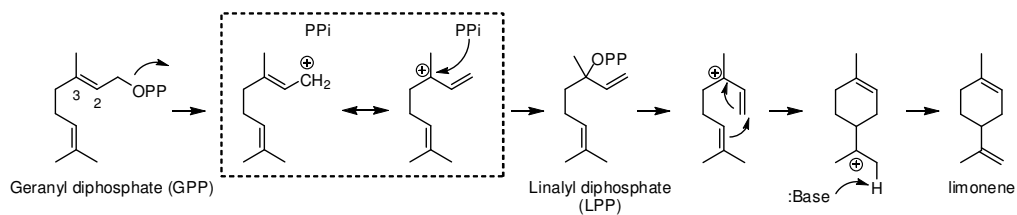


Figure 1-9. Mechanism of the formation of the monoterpene limonene from geranyl diphosphate (GPP).

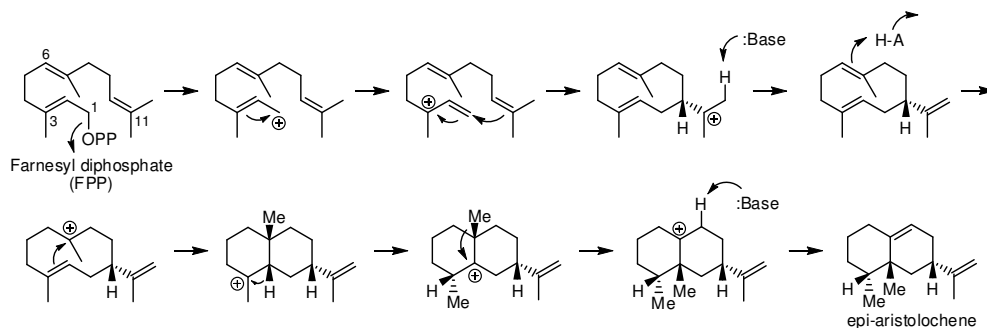


Figure 1-10. Mechanism of the biosynthesis of the sesquiterpene epi-aristolochene from farnesyl diphosphate (FPP).

The proposed ionic rearrangement mechanism for SpnF-catalyzed cycloaddition follows a similar process. Initially, an intermediate containing an anionic oxygen at C-15

and a carbocation at C-11 arises through the ionic rearrangement of the dienone component to give a highly activated dienophile moiety, where the negative charge at C-15 can be stabilized by hydrogen bonding with an amino acid residue or a metal ion in the active site of SpnF (**Figure 1-11**, upper intermediate in the dotted box). Then, diene makes the first C-C bond between C-7 and C-11 leaving a positive charge at the C-4 position (**Figure 1-11**, bottom intermediate in the dotted box). Finally, the negative charge on oxygen at the C-15 position returns to C-12, and immediately makes a C-C bond between C-4 and C-12 to finish the [4+2] cycloaddition producing a cyclohexene moiety. Alternatively, ionic rearrangement may produce the intermediate possessing anionic oxygen at the C-15 position and positive charge at the C-4 position, which can then be to make the first C-C bond between C-7 and C-11 positions (**Figure 1-11**, bottom intermediate in the dotted box). Then, the anion at C-15 can return to the carbocation at C-4 to make the second C-C bond between C-4 and C-12. Although two possible intermediates are presented, this mechanism can be referred to as the ionic rearrangement mechanism, since the overall reaction is initiated by the formation of a carbocation by ionic rearrangement. No matter the specific process is used for the SpnF-catalyzed [4+2] cycloaddition, the ionic rearrangement mechanism is obviously a series of cascade stepwise process.

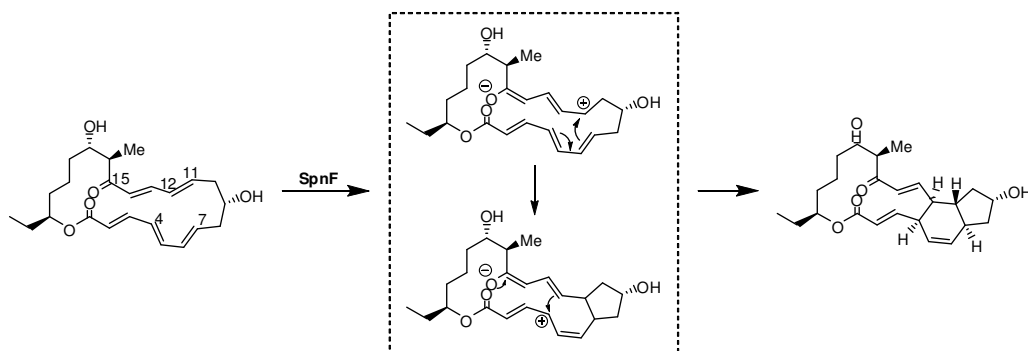


Figure 1-11. Detailed ionic rearrangement mechanism for SpnF-catalyzed [4+2] cycloaddition in the biosynthesis of spinosyn A.

Radical cyclizations are chemical transformations that yields cyclic products via radical intermediates, and are one of the most powerful and versatile methods for the construction of mono- and polycyclic systems.^{55, 56, 57, 58, 59} These reactions are widely used in the field of organic synthesis due to their high functional group tolerance, mild reaction conditions, and high levels of regio- and stereochemical product specificity. Radical cyclization reactions usually proceed in three basic steps; selective radical generation, radical cyclization, and conversion of the cyclized radical intermediate to product.⁶⁰ First, the generation of an initial carbon radical is facilitated by using one of a number of suitable precursors, such as halides, thio- and selenoethers, alcohols, aldehydes, and even hydrocarbons. The use of metal hydrides (tin, silicon, and mercury hydrides) is common in radical cyclization reactions, even though there is the possibility of reducing the initially formed radical by the metal hydride. Second, the radical cyclization step is the attack of a double or triple bond by the initially formed radical to make a carbon-carbon bond. Usually this is the intramolecular addition of the initially generated radical to a double or triple bond comprising of a carbon-carbon bond, a

carbon-oxygen bond or a carbon-nitrogen bond. Sometimes polycycles and macrocycles can be formed using radical cyclization. To generate a polycyclic system, rings can be pre-formed and a single ring closed with radical cyclization, or multiple rings can be produced in a tandem process. Macrocyclizations have the unique property of exhibiting *endo* selectivity. Finally, the resulting cyclized radical is converted to the desired product through one of several quenching methods, such as trapping with a radical scavenger, a fragmentation reaction, or an electron-transfer reaction, depending on the radical cyclization employed. It is important that the radical cyclization step must be faster than the trapping of the initially generated radical otherwise the cyclization will stop with an incomplete transformation. The most common products are five- and six-membered rings, and the formation of smaller or larger rings is rarely observed. However, various side reactions make the radical cyclization method problematic, and cyclization is especially slow for small and large rings, excepting macrocyclization. Compared to the aforementioned cationic cyclization through ionic rearrangement, the advantage of radical cyclizations include: reactions are not complicated by Wagner-Meerwein rearrangement (carbocation 1,2-rearrangement),^{61, 62} do not require strongly acidic conditions, and can be kinetically controlled. In addition, radical cyclizations are much faster than analogous anionic cyclizations, and can avoid β -elimination side reactions.

The biosynthesis of natural products through radical cyclization is rare despite many organic syntheses using radical cyclization to prepare natural products have been developed. The avermectins, a complex of chemically related agents isolated from *Streptomyces avermitilis*, show promise as an extraordinarily potent anthelmintic, were

investigated to determine if their hexahydrobenzofuran fragment is biosynthesized by radical cyclization (**Figure 12**).^{63, 64, 65, 66} Synthetically, the acyclic precursor was treated with tri-*n*-butyltin hydride and azobisisobutyronitrile (AIBN) to initiate the desired tandem intramolecular cyclization followed by the incorporation of tri-*n*-butyltin radicals by intermolecular addition to give the allylstannane intermediate, which was then oxidized with peracid to yield the desired polycyclic core system.

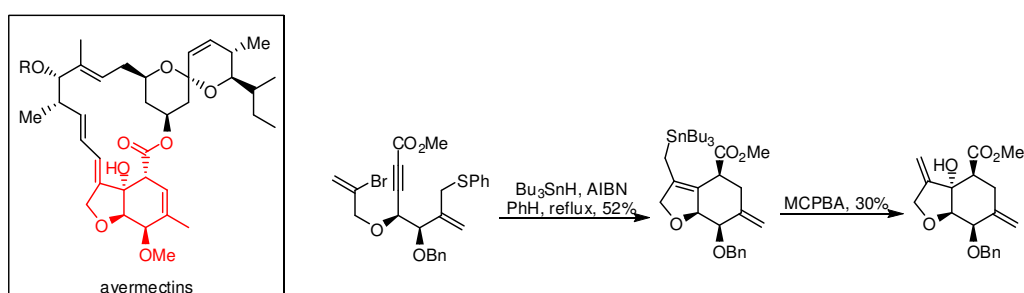


Figure 1-12. Synthetic scheme for the construction of hexahydrobenzofuran fragment of avermectins.

The Njardarson group demonstrated the utilization of radical cyclization to produce the symmetrically substituted bicyclic natural products, guttiferone and hyperforin, commonly used as a natural remedy of St. John's wort and a promising potential anticancer agent (**Figure 1-13**).⁶⁷ Retrosynthetic analysis of guttiferone G relies on the late stage desymmetrization of intermediate. This intermediate is rapidly accessed via tandem 5-*exo* radical cyclizations enabled by oxidative dearomatization of strategically functionalized *para*-hydroquinone. It has been reported that this dearomatization proceeds uneventfully to produce a ketal from the phenol intermediate, which is cyclized to form the desired symmetrical bridged bicyclic product as the only product when $(\text{TMS})_3\text{SiH}$ and Et_3B are used as the solvent with a yield of 73%.

In the “cross-bridging” reaction catalyzed by SpnF, radical cyclization is expected to proceed in a stepwise manner via two plausible biradical intermediates to make the first carbon-carbon bond between the C-4 to C-7 diene and the C-11 to C-12 alkene (**Figure 1-15**). Then, the newly generated biradical intermediate undergoes the second carbon-carbon bond formation to complete the [4+2] cycloaddition and produce the cyclohexene moiety. A biradical intermediate possessing radicals at C-4 and C-12 is believed to be thermodynamically more stable due to the delocalization of electron through resonance stabilization. By comparison, the biradical intermediate having unpaired electrons at the C-7 and C-11 may be a kinetic intermediate due to the partial stabilization of one component.

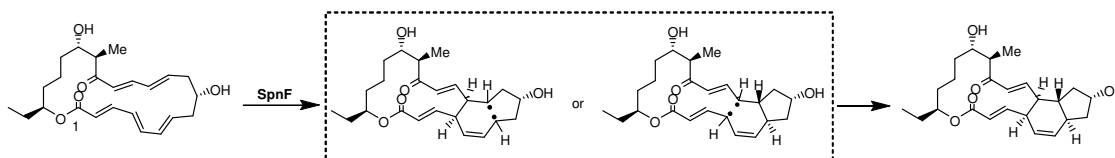


Figure 1-15. Detailed biradical cyclization mechanism for SpnF-catalyzed [4+2] cycloaddition in the biosynthesis of spinosyn A.

1.3. MECHANISTIC INVESTIGATIONS OF SpnL-CATALYZED CYCLIZATION

SpnL catalyzes the formation of cyclopentene ring between two conjugated alkenes. This begs the question, what is the mechanism SpnL uses to initiate this reaction.

At a glance, SpnL-catalyzed cyclization is similar to a well-known organic reaction, the Rauhut-Currier reaction^{29, 30} (also called the vinylogous Morita-Baylis-Hillman reaction), which describes the dimerization or isomerization of activated alkenes adjacent to electron-withdrawing functional groups such as ketones, esters, and nitriles

(specifically, enones) in the presence of an organophosphine of the type R_3P . This reaction was reported in 1963 by the Rauhut and Currier group (**Figure 1-16**).

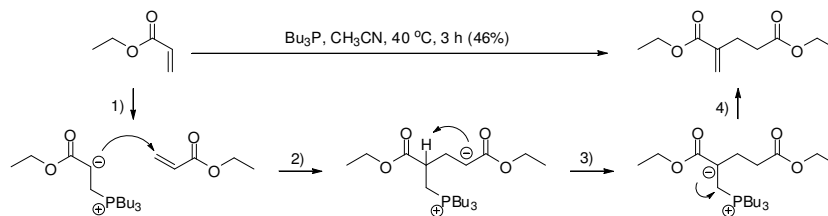


Figure 1-16. Rauhut-Currier reaction reported in 1963 by the Rauhut-Currier group.

A large number of scientific inquiries involve the Morita-Baylis-Hillman reaction,^{72, 73, 74} reflecting its potential to greatly affect organic synthesis, whereas the Rauhut-Currier reaction^{29, 30} has not received as much attention due to the low reactivity of its substrates and difficulty in controlling the selectivity of the cross-coupling reaction. Interestingly, the Morita-Baylis-Hillman (MBH) and Rauhut-Currier (RC) reactions merge the concepts of conjugate addition and latent enolate generation. Unlike the MBH reaction, which utilizes the coupling of an activated alkene (latent enolate) with an aldehyde, the definition of a Rauhut-Currier reaction has been recently extended to more general reactions, including any coupling of one active alkene (latent enolate) to a second alkenyl Michael acceptor to produce a new C-C bond between the α -position of one activated alkene and the β -position of a second alkene with a help of nucleophilic catalyst. The mechanism of the Rauhut-Currier reaction has been well studied. The Baizer and Anderson group have shown that the α -position of one alkene is first activated by a nucleophilic attack by an organophosphine to give a ylide, and that newly formed alkyl anion attacks the β -position of the second alkene to make a C-C bond. Furthermore, they demonstrated that the newly formed alkyl anion on the second alkene abstracts the

proton on the junction position to make the more stable ylide. The phosphorus ylide is then released to product a dimer molecule (**Figure 1-17**). An interesting aspect of the Rauhut-Currier reaction is that the first alkene retains its original alkene moiety and the second alkene loses its original alkene moiety. A general intramolecular Rauhut-Currier reaction is depicted in **Figure 1-8**, which may be utilized by SpnL-catalyzed cyclization in the biosynthesis of spinosyn A.

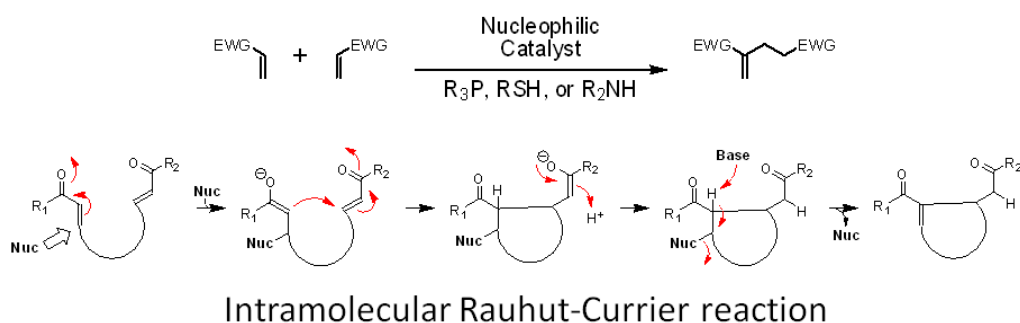


Figure 1-17. General intramolecular Rauhut-Currier reaction.

In nature, a number of natural products seem to possess a skeleton similar to the product of the Rauhut-Currier reaction. However, to my knowledge, no enzyme capable of catalyzing “Rauhut-Currier” reaction has been reported. The Moore and Erguden group have reported an interesting and unique application of the intramolecular Rauhut-Currier reaction in the synthesis of a fused tetraquinane ring system en route to the synthesis of the natural product waihoensene (**Figure 1-18**).⁷⁵ In their synthesis, the cycloisomerization of tricyclic bis(enone) catalyzed by thiophenol and sodium thiophenolate produced angularly fused tetraquinane with an excellent yield of 93%. The reaction mechanism begins with the nucleophilic conjugate addition of the thiolate to the target. This is followed by a transannular Michael reaction, resulting in a tetracyclic

intermediate. An intramolecular E2 trans-diaxial elimination reaction then proceeds to produce the desired product and regenerate the thiophenolate.

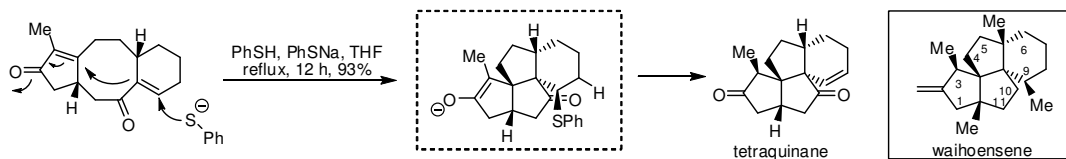


Figure 1-18. Synthesis of a fused tetraquinane ring system as an intermediate for the synthesis of waihoensene.

Krische and Agapiou demonstrated the use of highly reactive and chemoselective thioenates in the Rauhut-Currier reaction for the synthesis of the furanosequiterpene lactone (\pm)-ricciocarpin A (**Figure 1-19**).⁷⁶ Interestingly, compared to the less active analogous enolate-enone, the thienolate-enone substrate showed superior reactivity and exquisite chemoselectivity in providing the desired cyclized product with an 81% yield.

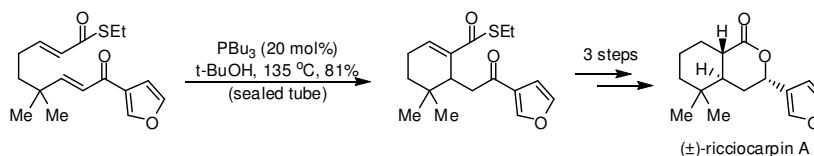


Figure 1-19. Utilization of Rauhut-Currier reaction for the synthesis of (\pm)-ricciocarpin A.

Sorensen and co-workers successfully completed the synthesis of (+)-harziphilone with the use of a tertiary amine-catalyzed Rauhut-Currier reaction (**Figure 1-20**).⁷⁷ The mechanism they proposed begins with the enone component being activated with a mild catalyst, DABCO (10 mol%) to give an DABCO-decorated enolate, which attacks the β -position of conjugated alkyne through an intramolecular Michael addition to yield a chemoselectively monocyclized zwitterion intermediate. The (+)-harziphilone is finally produced through either a direct intramolecular substitution or a β -elimination followed by 6π -electrocyclization.

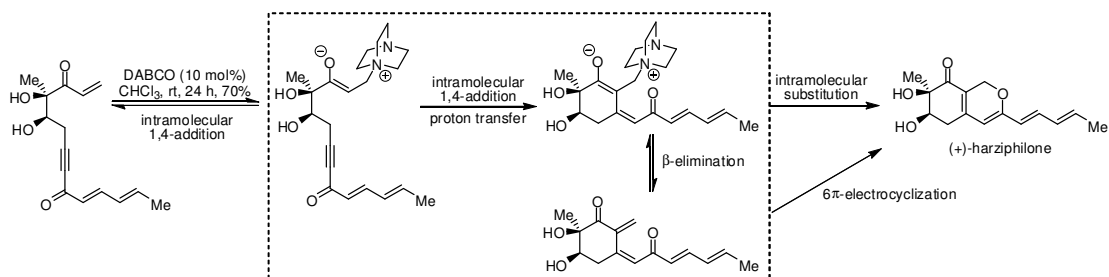


Figure 1-20. Synthesis of (+)-harziphilone using Rauhut-Currier reaction.

Roush and co-workers demonstrated the use of an intramolecular Rauhut-Currier cycloisomerization to generate the *as*-indacene core of the antimetabolic agent FR182877 (**Figure 1-21**).⁷⁸ Their total synthesis of (-)-spinosyn A also features a diastereoselective transannular Rauhut-Currier reaction (**Figure 1-22**).^{79, 80, 81, 82} The substrate for the Rauhut-Currier reaction was prepared from an intramolecular Horner-Wadsworth-Emmons macrolactonization followed by a transannular Diels-Alder reaction. PMe_3 provided in excess activated the enone to give an enolate, which proceeded with excellent diastereoselectivity to generate the perhydro-*as*-indacene core.

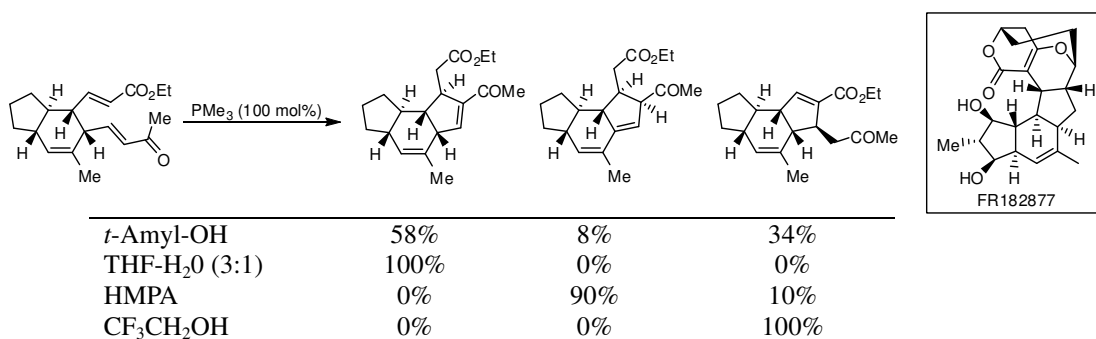


Figure 1-21. Intramolecular Rauhut-Currier cycloisomerization for the preparation of *as*-indacene ring in FR182877.

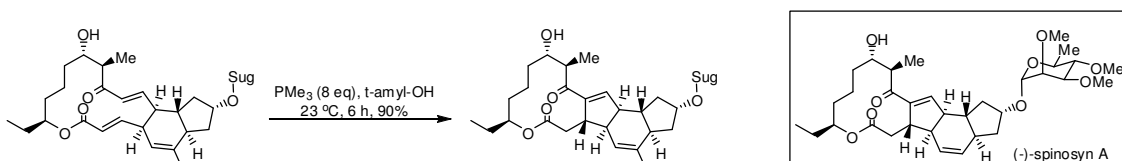


Figure 1-22. Diastereoselective synthesis of perhydro-as-indacene core in (-)-spinosyn A.

Although covalent catalysis is prevalent in enzymatic reactions, evidence to suggest that it is involved in generating an enolate to form a new C-C bond is rare. In nature, the closest example of the Rauhut-Currier type mechanism is the reaction catalyzed by thymidylate synthase (**Figure 1-23**),^{83, 84, 85, 86} which is regarded as a Baylis-Morita-Hillman reaction. The reaction is initiated by the nucleophilic addition of a cysteine residue in thymidylate synthase to the C-6 position of 2'-deoxyuridine-5'-monophosphate (dUMP) resulting in an activated enolate. The resulting enolate then attacks the positively charged activated imine of N^5,N^{10} -methylene-5,6,7,8-tetrahydrofolate to practically hijack a methyl group and eventually produce 2'-deoxythymidine-5'-monophosphate (TMP).

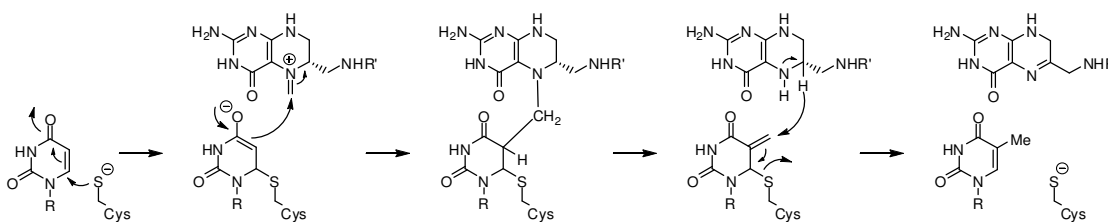


Figure 1-23. Proposed mechanism of the reaction catalyzed by thymidylate synthase (R = 2'-deoxyribose-5'-monophosphate, R' = (*para*-aminobenzoyl)-glutamate).

Utilization of the Rauhut-Currier reaction is an impressive step in the chemical synthesis of spinosyn A because it inspired the proposed mechanism of SpnL-catalyzed cyclization in the biosynthesis of spinosyn A.^{79, 80, 81, 82} While trimethylphosphine was the chemical reagent used as the nucleophile to initiate the Rauhut-Currier reaction in organic

synthesis, a nucleophilic side chain of an amino acid residue in SpnL such as cysteine or lysine, is expected to activate the enone component in the biosynthesis of spinosyn A, as shown in **Figure 1-6**. After activation, the C-C bond between C-3 and C-14 is made through Michael addition of the enolate to the C-3 position, followed by protonation at the C-2 position. Finally, the nucleophile covalently attached to the C-13 position is released by 1,2-elimination catalyzed by deprotonation at the C-14 position with an active site base to complete the synthesis of perhydro-as-indacene core in spinosyn A.

The second proposed mechanism is the Michael addition mechanism, which uses the base to activate the enone component.^{31, 32} The Michael reaction or Michael addition, was originally defined by Arthur Michael. It is an organic reaction describing the nucleophilic addition of a carbanion or nucleophile to an α,β -unsaturated carbonyl moiety to produce a 1,5-diketo-containing moiety (**Figure 1-24**). In general, the moiety containing an acidic hydrogen adjacent to electron-withdrawing groups, such as an acyl and cyano group, to produce a carbanion or nucleophile under basic conditions is called the Michael donor. The moiety containing an activated alkene adjacent to ketone which produces an enone by nucleophilic addition of the Michael donor is called the Michael acceptor. During the Michael addition, deprotonation of an acidic proton by base leads to formation of a carbanion, which is stabilized by its adjacent electron-withdrawing group as part of a resonance structure (namely, enolate). This nucleophile makes a C-C bond when coupled to the electrophilic alkene to form another carbanion or enolate. Protonation of this second carbanion by the protonated base or solvent finishes the Michael addition to give a 1,5-diketo-structure. The overall reaction is highly efficient

and is usually irreversible at ambient temperature. The energy coordination of the reaction is predominantly determined by orbital, rather than electrostatic, considerations. According to the frontier orbital theory, the highest occupied molecular orbital (HOMO) in a stabilized enolate is highly polarized by an electron-withdrawing group making the central carbon electron-deficient and the α -carbon electron-rich (highly nucleophilic). The energy of the lowest unoccupied molecular orbital (LUMO) in the α,β -unsaturated carbonyl moiety is lowered by an electron-withdrawing group, with the α -carbon becoming electron-rich and the β -carbon becoming electron-deficient (highly electrophilic). Both polarized frontier orbitals are of similar energy, and react efficiently to form a new C-C bond from one pair of in-phase overlap between HOMO in the Michael donor and LUMO in the Michael acceptor.

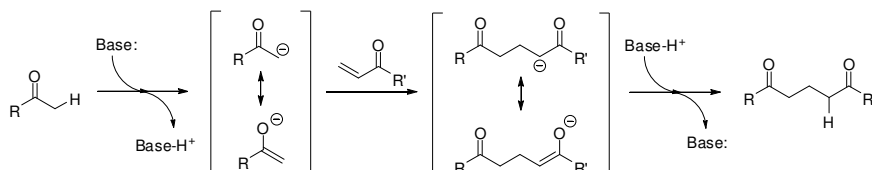


Figure 1-24. General mechanism of Michael addition.

Organic syntheses of natural products often rely on the Michael addition to make new C-C bonds between two α,β -unsaturated carbonyl-containing components. Indeed, Michael addition is considered one of the most powerful and reliable tools for the stereocontrolled formation of carbon-carbon and carbon-heteroatom bonds in natural product synthesis. In 2003, Halland and co-workers reported the synthesis of the anticoagulant (S)-warfarin by a one step intermolecular asymmetric Michael addition of

4-hydroxycoumarin and benzylideneacetone in the presence of an imidazolidine catalyst with an enantioselectivity of 82% ee (**Figure 1-25**).⁸⁷

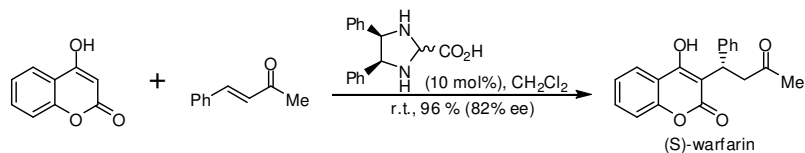


Figure 1-25. Asymmetric synthesis of (S)-warfarin using Michael addition.

Evans and co-workers reported the production of the synthetic intermediate of (-)-tetracycline and (-)-oxytetracycline through stereoselective transannular Michael addition (**Figure 1-26**).⁸⁸ Fukayama and co-workers also used Michael addition reaction in their synthesis of (-)-kainic acid, which was isolated from the Japanese marine algae *Digenea simplex*, and displays potent anthelmintic properties (**Figure 1-27**).^{89, 90, 91}

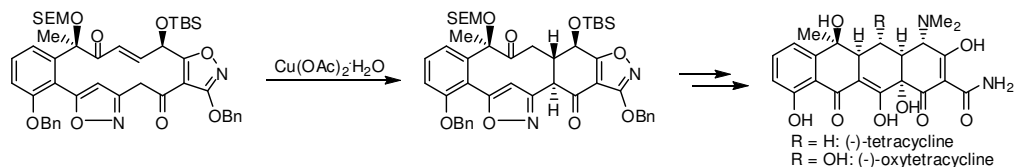


Figure 1-26. Preparation of synthetic intermediate for (-)-tetracycline and (-)-oxytetracycline.

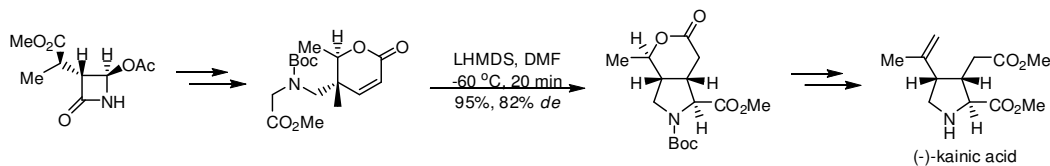


Figure 1-27. Preparation of synthetic intermediate for (-)-kainic acid.

Zalkow and co-workers demonstrated that the precursor of (+)-atisirene, an enantiomer of a diterpenoid isolated from *Erythroxylon monogynum*, could be synthesized from an optically active enone ester using an intramolecular double Michael reaction (**Figure 1-28**).^{92, 93} The Ihara group also demonstrated the use of an intramolecular

double Michael reaction to synthesize a precursor of atisine, a natural product found in *Aconitium heterophyllum* (**Figure 1-29**).^{93, 94, 95, 96, 97, 98, 99}

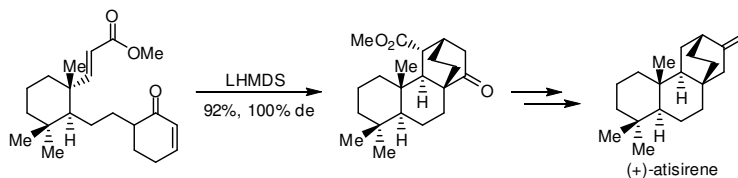


Figure 1-28. Preparation of synthetic precursor of (+)-atisirene using intramolecular double Michael reaction.

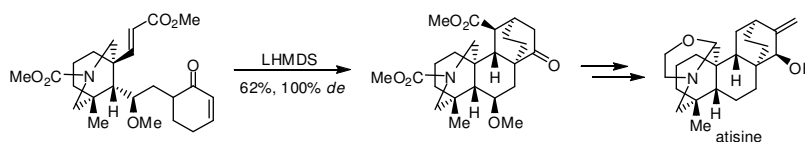


Figure 1-29. Preparation of synthetic precursor of atisine using intramolecular double Michael reaction.

SpnL-catalyzed cyclization through the Michael addition mechanism is obviously initiated by a simple deprotonation at C-12, although the source of the catalytic base is unknown. After Michael addition to make the C-C bond between C-3 and C-14, an isomerization of the double bond from $\Delta^{12,13}$ to $\Delta^{13,14}$ completes the perhydro-as-indacene core of spinosyn A (**Figure 1-6**).

1.4. DEUTERIUM-LABELED SUBSTRATE ANALOGS FOR MECHANISTIC STUDIES OF NATURAL PRODUCT BIOSYNTHESIS

In the biosynthesis of spinosyn A, the [4+2] cycloaddition by SpnF to produce the stereospecific cyclohexene moiety is consistent with a typical Diels-Alder reaction between a diene (C-4 to C-7) and a dienophile (C-11 to C-12) via the stereospecific *endo*-mode *syn*-addition through a pericyclic transition state. However, there is no experimental data to support this mechanism. In fact, there is no evidence to distinguish any of these three plausible mechanisms for this enzymatic reaction. To study the

mechanism of SpnF-catalyzed cycloaddition, a kinetic isotope effect study was proposed. We designed four mechanistic probes containing deuterium at the reaction centers, specifically, a [C4-²H] analog (C4-D analog), a [C7-²H] analog (C7-D analog), a [C11-²H] analog (C11-D analog), and a [C12-²H] analog (C12-D analog) (**Figure 1-30**).

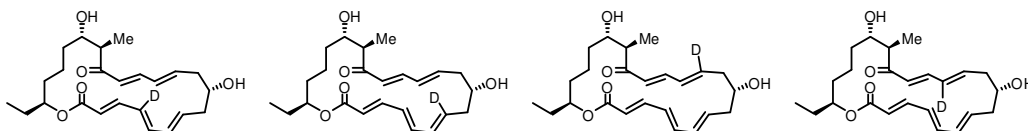


Figure 1-30. Mechanistic probes for SpnF-catalyzed cycloaddition (C4-D, C7-D, C11-D, and C12-D analogs).

The primary difference between the two proposed mechanisms for SpnL-catalyzed cyclization is the mode of activation of the conjugated enone component of C-12 to C-15, a nucleophilic attack at the C-13 position in the Rauhut-Currier type mechanism or a deprotonation at C-12 position in the Michael addition mechanism. Thus, several mechanistic probes, such as C12-D and C13-D analogs, were designed to distinguish between the two mechanisms (**Figure 1-31**), using the kinetic isotope effect.

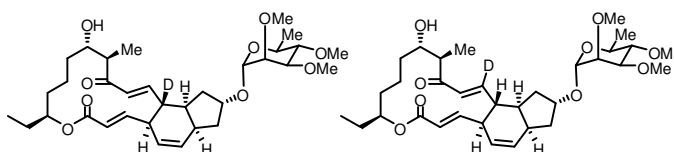


Figure 1-31. Mechanistic probes for SpnL-catalyzed cyclization (C12-D and C13-D).

Generally, an isotopic replacement involved in bond breakage or rehybridization leads to the change in the rate of reaction.¹⁰⁰ Substitution of hydrogen (H) with deuterium (D) affords a relatively large isotope effect when the bonds being broken or formed are connected with hydrogen, as compared to the isotope effect with other atoms. The magnitude of the isotope effect, expressed by k_H/k_D , can provide valuable information

about the reaction mechanism. Primary kinetic isotope effects are directly related to the bond breaking or bond forming event at the X-H/X-D bond, whereas secondary kinetic isotope effects arise from a rehybridization (α -) or an isotopic substitution remote from the bonds undergoing reaction (β -).

Basically, all isotope effects originate from the differences in the frequencies of the various vibrational modes of a molecule that arise by isotope substitution. For a bond breaking during the rate-determining step of a reaction (which is expected to be a primary kinetic isotope effect), the potential energy of the system does not change with isotope substitution. However, the shape of the potential wells on an energy surface is supposed to change with the vibrational modes undergoing the most change during the reaction. Zero-point energy (ZPE) for the lowest point in the potential energy well is expressed as $e_0 = \frac{1}{2} \cdot h\nu$, from the quantized energies, $e_n = (n + \frac{1}{2}) \cdot h\nu$, of the vibrational modes, where ν is the frequency of the vibrational mode being considered, expressed by $\nu = \frac{1}{2\pi} \sqrt{\frac{k}{m_r}}$, where $m_r = \frac{m_1 m_2}{m_1 + m_2}$. Thus, the frequency is directly proportional to the square root of the force constant for the bond, and inversely proportional to the square root of the reduced mass (m_r). The reduced mass for a bond between a heavy atom (carbon, nitrogen, or oxygen) and a light atom (H or D) is significantly affected by an H/D substitution. The stretching frequency for a bond with deuterium is lower, and the ZPE for a bond is also lower than that of hydrogen. Therefore, in the case of homolytic cleavage of a C-H or C-D bond, more activation energy is required for a C-D bond than a C-H bond (**Figure 1-32**). In other word, the difference between C-H ZPE and C-D ZPE defines the magnitude

of the isotope effect, and k_H/k_D is greater than 1. Mechanistically, the maximum value of the primary kinetic isotope effect is approximately $k_H/k_D = 6.5$, assuming that the bond is completely broken in the transition state. Most isotope effects are less than this value due to the partial cleavage of the bond in the transition state.

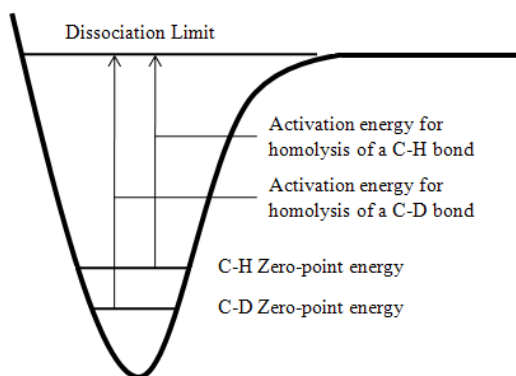


Figure 1-32. A Morse potential for a C-H bond showing that the activation energy for homolysis of a C-D bond is larger than for a C-H bond.

Secondary kinetic isotope effects occur from isotopic substitutions at a bond that is not being broken, and typically undergoes a change in bond hybridization or participation of the bond in hyperconjugation, as defined as an α or β secondary isotope effects. The α effect occurs when the atom undergoing the reaction has the associated isotope, while the β effect occurs when the neighboring atom has the isotope. When a C-H bond with sp^3 hybridization is changed to sp^2 hybridization, only a limited number of vibrational modes undergo a large change. These modes include stretches, as well as in-plane and out-of-plane bending motions (**Figure 1-33**). A change of sp^2 hybrid to sp gives a similar change of vibrational modes as well. Changes in the force constant for stretches of a bond undergoing hybridization are not large enough to make a significant isotope effects, although C-H bond strengths and force constants for the stretching

vibrations decrease in the order $sp > sp^2 > sp^3$. The difference in force constants for an in-plane bend is due in small part to the same frequency of the sp^3 and sp^2 hybridized carbons. The in-plane and out-of-plane bends for a sp^3 hybridized carbon are degenerate. However, the in-plane bend is a much stiffer motion for the sp^2 hybridized carbon than the out-of-plane bend due to the lower steric hindrance for the out-of-plane bend of a sp^2 hybridized carbon. Thus, there is a significant difference in zero potential energy difference between C-H and C-D bonds in reaction that involve rehybridization between sp^3 and sp^2 due to a large difference in force constant for the out-of-plane bend of an sp^3 hybrid versus an sp^2 hybrid, resulting in a measurable secondary isotope effect. A normal secondary kinetic isotope effect arises from the slower reaction due to the substitution of hydrogen with deuterium on the carbon undergoing rehybridization. An inverse secondary kinetic isotope effect occurs when the reaction proceeds faster with deuterium than with hydrogen.

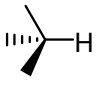
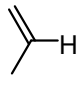
vibrational mode	Frequencies (cm^{-1}) for	
		
stretching	2900	2800
in-plane bending	1350	1350
out-of-plane bending	1350	800

Figure 1-33. Vibrational modes for C-H bonds on sp^3 and sp^2 hybridized carbons.

The flavoenzyme tryptophan 2-monooxygenase (TMO) from *Pseudomonas savastanoi* catalyzes the oxidative decarboxylation of L-tryptophan (**Figure 1-34A**) in the first step of a two-step biosynthetic pathway for the plant hormone indoleacetic acid.^{101,}

¹⁰² For the amine oxidation to imine, there are three mechanisms proposed with alanine

primary kinetic isotope effect.^{103, 104} Taken together with other biochemical results, the TMO oxidation of alanine was suggested to proceed through a hydride transfer mechanism.

In contrast, D-amino acid oxidase catalyzes the oxidation of D-amino acids to their respective imino acids by transfer of a hydride equivalent to the tightly bound FAD and subsequently transferring of electrons to molecular oxygen to form hydrogen peroxide. Previous results suggested two possible mechanisms, the direct nucleophilic attack mechanism and the radical mechanism (**Figure 1-36**).^{105, 106}

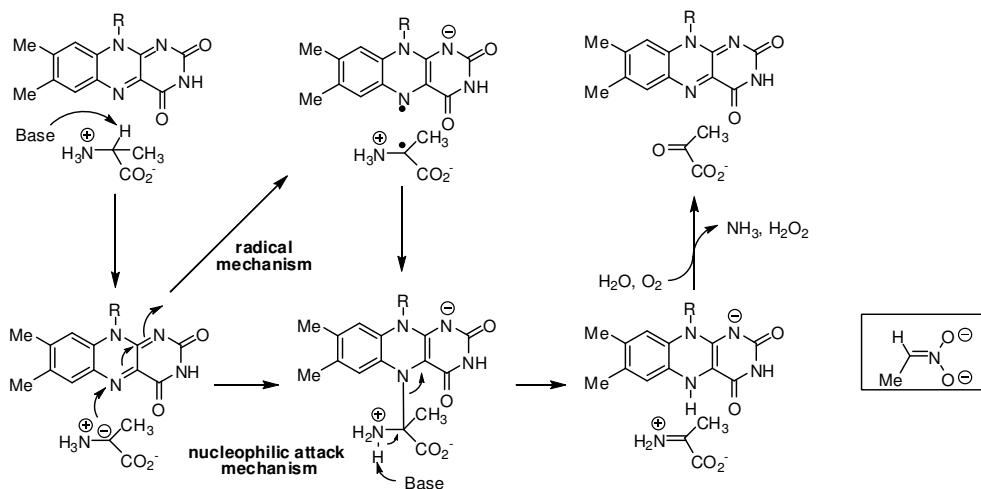


Figure 1-36. Proposed mechanisms of D-amino acid oxidase. Top) radical mechanism, and Bottom) nucleophilic attack mechanism.

Secondary kinetic isotope effect experiments using deuterated nitroethane and 1-nitropropane were performed over a pH range of 6-11, and an average value of $\alpha\text{-}^D V/K$ was determined to be 0.84 ± 0.02 , the inverse secondary kinetic isotope effect, indicating a significant sp^2 to sp^3 rehybridization in the transition state.^{105, 106} Assuming that deprotonation is very fast initially, only an anion intermediate can generate sp^2 -hybridized carbon at α -position. This strongly suggests that the reaction proceeds through

the direct nucleophilic attack mechanism rather than the two single electron transfers (biradical) mechanism.

In the case of SpnF-catalyzed [4+2] cycloaddition, the C-C bond formation connecting C-4 to C-12, and C-7 to C-11 may occur in a concerted or stepwise manner, depending on the mechanism. Measurement of a secondary kinetic isotope effect from the rehybridization of sp^2 to sp^3 at the reaction center is expected to be useful to differentiate among the three proposed reaction mechanisms. Likewise, the mechanism of SpnL-catalyzed cyclization can be differentiated by primary or secondary kinetic isotope effect depending on whether a C-H bond cleavage reaction is part of the rate limiting step.

1.5. FLUORINATED SUBSTRATE ANALOGS FOR MECHANISTIC STUDIES OF NATURAL PRODUCT BIOSYNTHESIS

As pointed out earlier, the only difference between the two mechanisms proposed for SpnL-catalyzed cyclization is the mode of activation of the conjugated enone component of C-12 to C-15, a nucleophilic attack at the C-13 position in the Rauhut-Currier type mechanism or deprotonation at the C-12 position in the Michael addition mechanism. In order to distinguish between these two mechanisms, a fluorinated mechanistic probe, C13-F analog, was also designed for the study of possible suicide inhibition and SpnL-covalent modification (**Figure 1-37**).

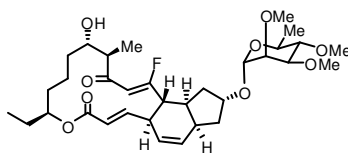


Figure 1-37. Mechanistic probes for SpnL-catalyzed cyclization (C13-F analogs).

Many mechanistic studies to determine enzymatic transformations rely on using fluoride-containing substrate analog as irreversible inhibitors.^{108, 109} The unique stereoelectronic properties of the fluorine atom make it an effective bioisostere for both hydrogen and oxygen atoms.^{110, 111, 112} Fluorine has a high electronegativity (4.0) and a van der Waals radii of 1.47 Å. This is comparable to hydrogen's van der Waals radii (1.2 Å) and oxygen's electronegativity (3.5). Thus, fluorine has been widely used to replace hydrogen or oxygen in designing mechanistic probes to study the mechanisms of enzymatic transformation. Some fluorine-containing substrate analogs have been demonstrated to make covalent modifications to target enzymes, which results in the inactivation of the target enzymes.

Thymidylate synthase is the enzyme used to catalyze the conversion of 2'-deoxyuridine monophosphate to 2'-deoxythymidine monophosphate (dTMP) with concomitant conversion of N^5, N^{10} -methylenetetrahydrofolate to 7,8-dihydrofolate (**Figure 1-38**).^{83, 84, 85, 86, 111, 112} 2'-Deoxythymidine monophosphate (dTMP) is subsequently phosphorylated to thymidine triphosphate (dTPP), which is then used for DNA synthesis and repair. If this enzyme is inhibited, DNA synthesis is blocked. These thymidylate synthase inhibitors are used clinically as antitumor and antimicrobial agents. When the mechanism-based inactivator, 5-fluoro-2'-deoxyuridylate, was used to facilitate

the elucidation of the structure of the inactivated thymidylate synthase complex (**Figure 1-39**), it was possible to propose a mechanism for the first part of the enzymatic transformation (**Figure 1-40, top**). The active site cysteine residue first attacks the C-6 position to afford a substrate-enzyme covalent adduct and to produce an enolate intermediate, which is then used to attack methylenetetrahydrofolate at the C-5 position. Due to the lack of a proton at the C-5' position, further transformation is inhibited, leading to a covalent inactivation of thymidylate synthase. Combined with other biochemical evidences, the mechanism of one carbon unit insertion catalyzed by thymidylate synthase was proposed, as shown in **Figure 1-40**.

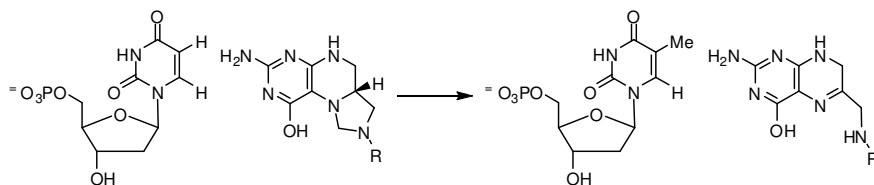


Figure 1-38. Reaction catalyzed by thymidylate synthase.

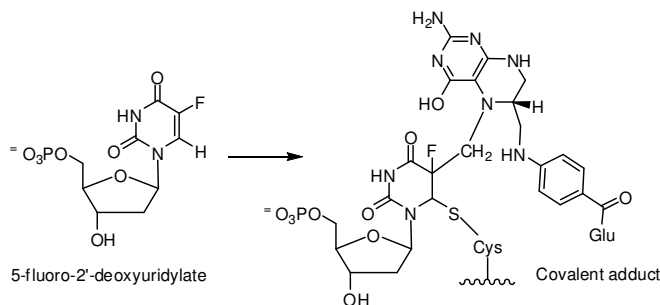


Figure 1-39. Inactivation of thymidylate synthase by 5-fluoro-2'-deoxyuridylyl.

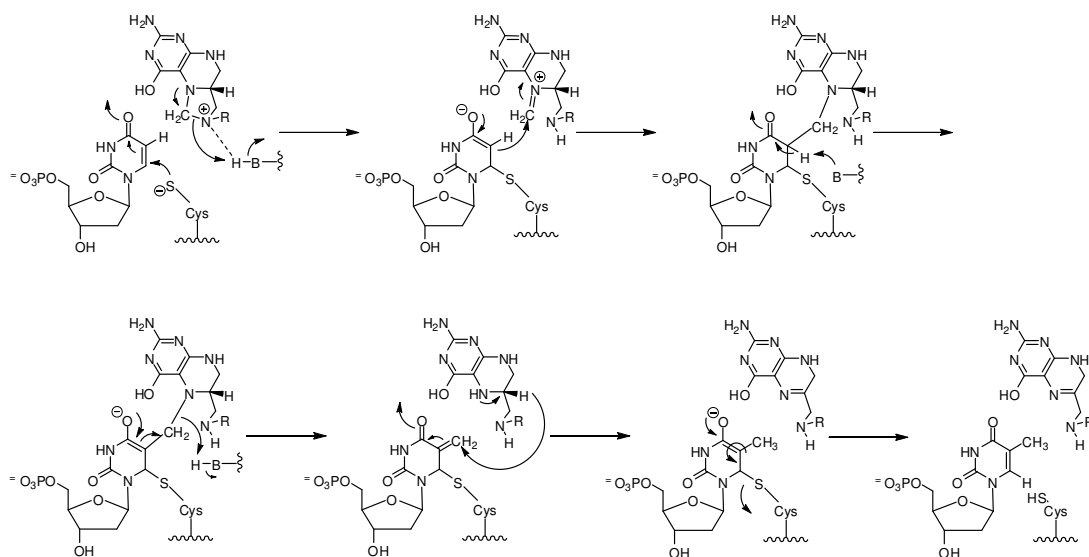


Figure 1-40. Proposed mechanism of thymidylate synthase.

The NAD^+ -dependent enzyme, CDP-D-glucose 4,6-dehydratase (E_{od}) catalyzes the conversion of CDP-D-glucose to CDP-4-keto-6-deoxyglucose (**Figure 1-41**). Labeling studies revealed that the C-4-H lost in the initial oxidation is transferred to the C-6-methyl group in the product. Incubation of difluoroglucose derivative with E_{od} led to the formation of a covalent adduct and inactivated the enzyme. The conclusion was supported by *in vitro* activity assay, ^{19}F NMR, and MS analysis (**Figure 1-42**).^{113, 114}

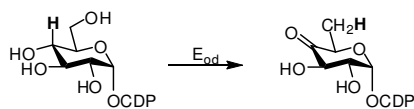


Figure 1-41. Reaction catalyzed by CDP-D-glucose 4,6-dehydratase (E_{od}).

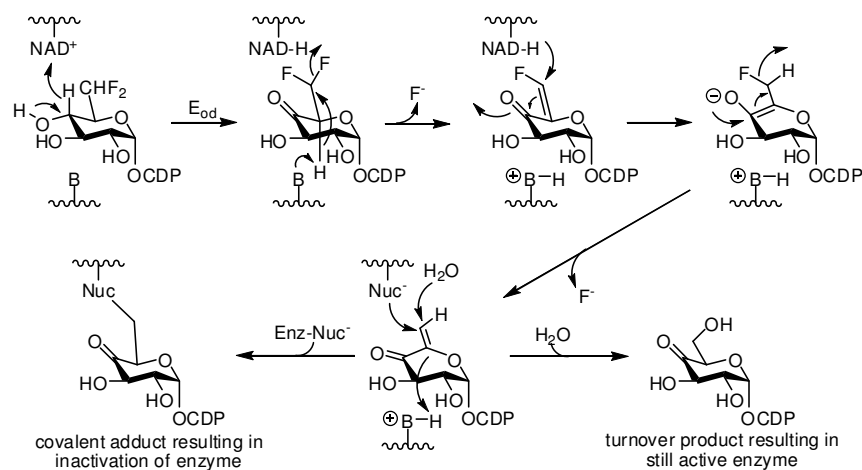


Figure 1-42. Proposed mechanism of E_{od} inactivation by difluoroglucose derivative.

A mechanistic probe, C13-F analog, was designed, which is predicted to form a covalent adduct with SpnL if the SpnL-catalyzed cyclization proceeds through the Rauhut-Currier type mechanism. First, the endogenous nucleophile of SpnL attacks the C-13 position to make a covalent bond, and the negative charge is stabilized by the keto group at the C-15 position to produce an enolate. Second, the enolate, as a Michael donor, undergoes the intramolecular cyclization connecting the C-14 and the C-3 position, the latter of which is a Michael acceptor. After protonation at the C-2 position, a proton at the C-14 position is abstracted by a base. If the nucleophile covalently bound at the C-14 position is removed by a 1,2-elimination, the turnover product will be the C13-F compound. However, if C-13-F, a good leaving group, is removed instead of the endogenous nucleophile, SpnL will be inactivated by irreversible inhibition to produce a covalent adduct with the inhibitor (**Figure 1-43, left**). Alternatively, if the SpnL reaction proceeds through the Michael addition mechanism and the C13-F analog is a substrate for SpnL, the product should be the C-13-F containing cyclized product, which is the same

compound produced when the enzyme nucleophile is removed at the last stage of the Rauhut-Currier type mechanism (**Figure 1-43, right**).

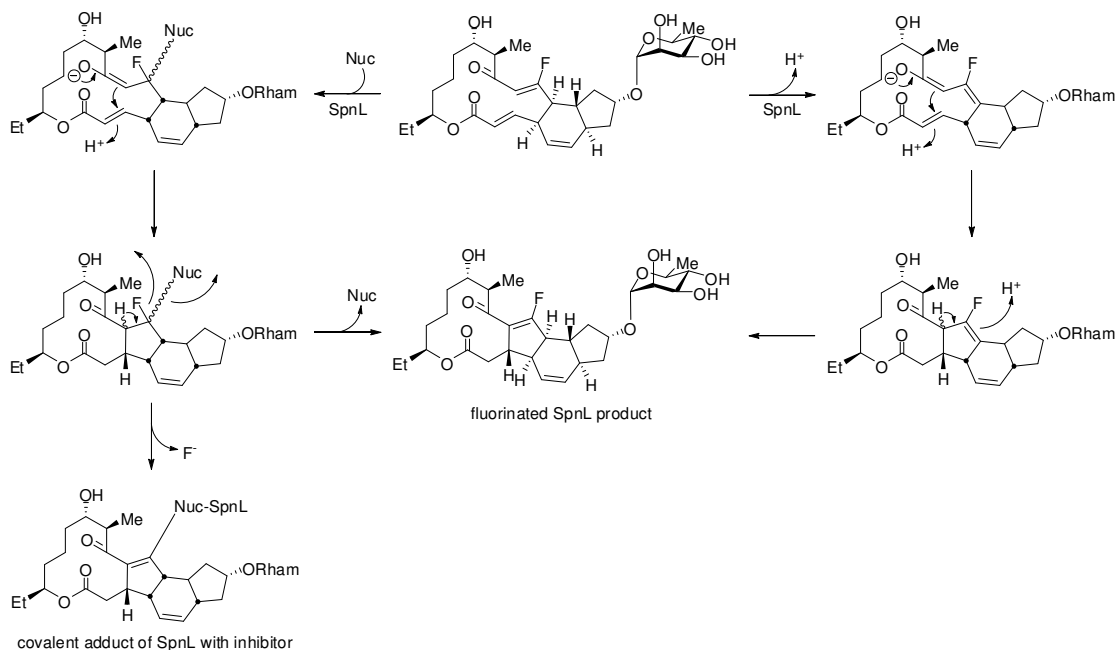


Figure 1-43. Proposed mechanism for SpnL reaction with C13-F analog through the Rauhut-Currier type mechanisms (left) and Michael addition mechanism (right).

1.6. DISSERTATION STATEMENT

Mechanistic studies of formation of polycyclic system in the biosynthesis of natural products have been an attractive area of research, particularly in the context of discovery and development since many unusual enzyme reactions must be involved. In order to study the mechanisms of enzymatic transformation, many biochemical tools have been developed over the years such as various spectroscopic methods, kinetic isotope effect measurement, and mechanism-based inhibition among others. Combined with organic chemistry to synthesize the novel enzyme substrates and mechanistic probes, mechanistic studies of many biosynthetic enzymes have expanded our understanding of

natural product biosynthesis. The biosynthetic pathway of spinosyn A is especially interesting, as it has two unusual features, the SpnF-catalyzed [4+2] cycloaddition and the SpnL-catalyzed cyclization to produce the perhydro-*as*-indacene core. Therefore, the aim of this dissertation is to investigate the detailed mechanistic aspects of the enzymatic transformations catalyzed by SpnF and SpnL. Chapter 2 describes the mechanistic investigation of SpnF-catalyzed [4+2] cycloaddition in the biosynthesis of spinosyn A. The first focus is to distinguish between the three proposed mechanisms: the Diels-Alder reaction mechanism, the ionic rearrangement mechanism, and the biradical cyclization mechanism. Chemical synthesis of the natural substrate and four deuterium-labeled substrate analogs for SpnF allows us to determine the secondary kinetic isotope effects, which are informative to differentiate the three proposed mechanisms. The second focus is to study the intrinsic properties of SpnF in terms of thermokinetics and thermodynamics using chemically synthesized cyclic and non-cyclic SpnF substrate analogs. Chapter 3 describes the mechanistic investigation of SpnL-catalyzed cyclization in the biosynthesis of spinosyn A. The Rauhut-Currier type mechanism and Michael addition mechanism are differentiated by kinetic isotope effect study using a competitive and direct comparison activity assay of SpnL with deuterium-labeled SpnL substrate analog. The mechanism-based inhibition study using a fluorinated SpnL substrate analog is also reported. Additionally, the roles of SAM in SpnF and SpnL are investigated.

Chapter 2. Mechanistic Investigation of SpnF-Catalyzed [4+2] Cycloaddition in the Biosynthesis of Spinosyn A

2.1. INTRODUCTION

SpnF-catalyzed [4+2] cycloaddition has attracted significant attention due to its mechanistic complexity in the biosynthesis of the perhydro-*as*-indacene core of spinosyn A and its potential as a “Diels-Alderase” reaction (**Figure 2-1**).^{37, 38, 39, 40} The substrate of SpnF, a keto component with an extended conjugated system spanning from C-11 to C-15, is biosynthesized through SpnJ-catalyzed oxidation of the C-15 hydroxyl group to form a ketone followed by SpnM-catalyzed dehydration of the hydroxyl group at C-11 to generate the dienophile moiety. The corresponding diene (C-4 to C-7), which is part of a well-conjugated ester, is derived directly from polyketide chain extension catalyzed by polyketide synthase (PKS). To explain how SpnF makes a cyclohexene, three plausible mechanisms have been proposed (**Figure 2-2**).

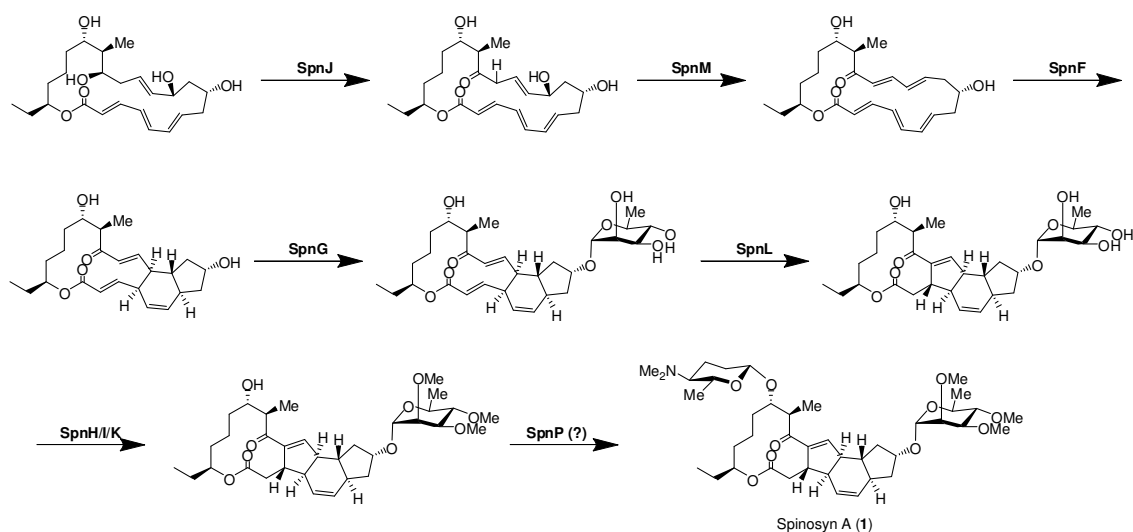


Figure 2-1. Established biosynthetic pathway of spinosyn A (1)

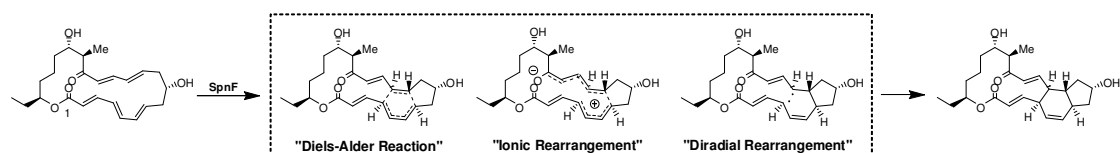


Figure 2-2. Proposed mechanisms for SpnF-catalyzed [4+2] cycloaddition in the biosynthesis of spinosyn A

The first proposed mechanism, the “Diels-Alder reaction mechanism”, describes the formation of the cyclohexene system through a [4+2] cycloaddition between a conjugated electron-rich 1,3-diene component and a substituted electron-deficient alkene (dienophile) via a concerted, pericyclic, and aromatic transition state.^{25, 26, 27, 28} Previously, several putative Diels-Alderases have been reported to catalyze [4+2] cycloaddition reactions in natural products biosynthesis such as the formation of solanapyrone, lovastatin, and macrophomate. However, the experimental evidence was inconclusive due to the fact that the putative cyclases such as solanapyrone synthase^{41, 42,}⁴³ and lovastatin nonaketide synthase (LovB)^{44, 45} are multifunctional enzymes which

catalyze more than one reaction, and macrophomate synthase (MPS)^{46, 47, 48, 49, 50, 51} has been shown to have a aldolase activity.⁵²

The second plausible mechanism to explain SpnF-catalyzed [4+2] cycloaddition is the “ionic rearrangement mechanism”. This mechanism describes that the cyclization involves a series of ionic rearrangements of the conjugated system by first connecting C-7 and C-11 in the macrolactone of spinosyn A. This mechanism is similar to those found in the biosynthesis of terpenoids.^{38, 39} Although the exact position of the carbocation in the conjugated system is unknown, the oxygen at C-15 should be negatively charged through an ionic rearrangement, and this may be a driving force stabilizing the di-ionic transition state during the SpnF reaction.

The third mechanism proposed for SpnF reaction is the “radical cyclization mechanism”, which explains the cyclization as a series of events starting with the generation of a biradical intermediate, followed by radical induced cyclization to yield a product with fixed stereochemistry. While radical cyclization is widely used in the area of organic synthesis, DNA photolyases^{68, 69} and (6-4) photolyase^{70, 71} are two rare enzymatic examples which use radical cyclization as part of their reaction mechanism. The Diels-Alder reaction is a concerted mechanism, while the ionic rearrangement reaction and radical cyclization reaction are stepwise mechanism.

In the biosynthesis of spinosyn A, the [4+2] cycloaddition to produce the stereospecific cyclohexene moiety is consistent with a typical Diels-Alder reaction between a diene (C-4 to C-7) and a dienophile (C-11 to C-12) via a stereospecific *endo*-mode *syn*-addition through a pericyclic transition state (**Figure 2-3**). However, there is no

experimental data to support this mechanism. In fact, none of the proposed mechanisms for this enzymatic reaction has ever been investigated. To differentiate the reaction mechanisms for SpnF-catalyzed cycloaddition, a kinetic isotope effect study is proposed.

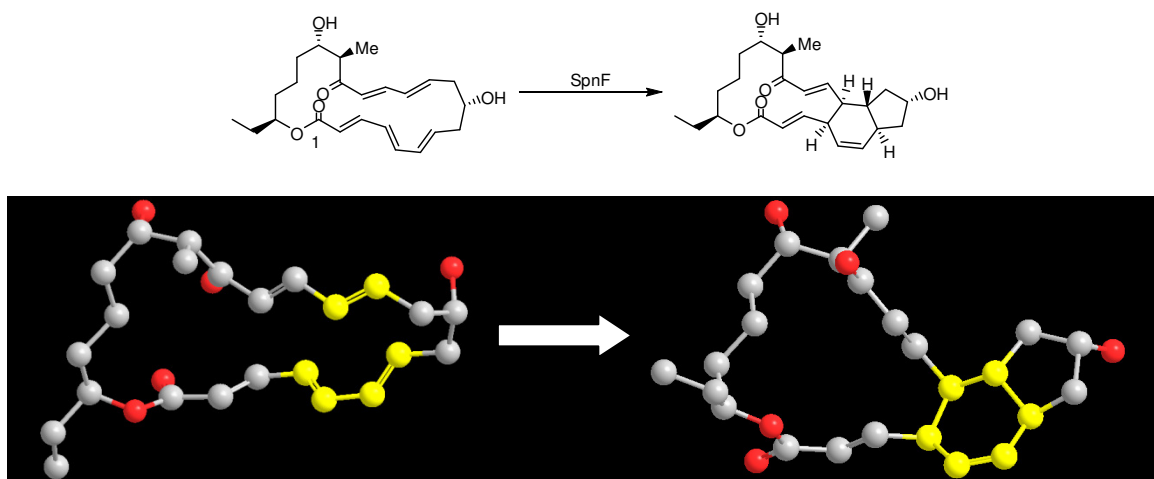


Figure 2-3. Diels-Alder reaction between diene (C-4 to C-7, bottom) and dienophile (C-11 to C-12, top) via the stereospecific *endo*-mode *syn*-addition.

The kinetic isotope effect deals with how an isotope substitution changes the rate of reaction.⁵⁸ A primary kinetic isotope effect is directly related to the bond breaking event at an X-H/X-D bond, whereas a secondary isotope effect arises from the change of rehybridization at the site of action (α -) or isotopic substitution at a site other the reactive bond (β -). Due to the change of vibrational mode during the rehybridization of a reaction center, measurement of the secondary kinetic isotope effect would provide useful information to determine the reaction mechanism. For the mechanistic study of SpnF-catalyzed [4+2] cycloaddition, four kinds of mechanistic probes are designed, each contains a deuterium instead of a hydrogen at one of the four reaction centers of interest, namely a C4-D analog, a C7-D analog, a C11-D analog, and a C12-D analog (**Figure 2-4**).

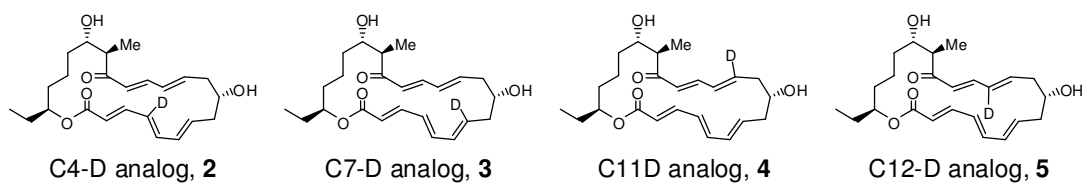


Figure 2-4. Mechanistic probes for SpnF-catalyzed cycloaddition (C4-D, C7-D, C11-D, and C12-D analogs).

No matter which reaction mechanism SpnF-catalyzed [4+2] cycloaddition follows, there are changes of hybridization from sp^2 to sp^3 at the C-4, C-7, C-11, and C-12 reaction centers, guiding to secondary kinetic isotope effects when the attached hydrogen at these sites is replaced by deuterium.^{115, 116, 117, 118, 119, 120, 121, 122, 134, 124} If the [4+2] cycloaddition undergoes the concerted Diels-Alder reaction mechanism, the kinetic isotope effects, $^D(V/K)$, are expected to be approximately 5% inverse at all reaction centers, because of an increased vibrational frequency of the C-H out-of-plane bending modes when each carbon is converted from sp^2 to sp^3 hybridized center.^{118, 119, 120, 121, 122} In the case of a stepwise ionic rearrangement mechanism, the C-7 and C-11 positions are expected to undergo C-C bond formation first due to the resonance stabilization of the ionic characters at the C-4 and the C-12 to C-15 positions of the intermediate, leading to around 5% inverse of the kinetic isotope effect for $^{C7D}(V/K)$ and $^{C11D}(V/K)$.^{123, 124} Previously, Houk and co-workers demonstrated that the $^{C4D}(V/K)$ effect is around 4% normal for a radical intermediate with an sp^2 carbon radical at the C-4 position.¹¹⁵ Since sp^2 carbocations and sp^2 carbon radicals have similar C-H vibrational frequencies, the secondary kinetic isotope effect at C-4, $^{C4D}(V/K)$, is expected to give a similar value of 4~5% normal for both the ionic rearrangement and biradical rearrangement mechanisms.^{116, 117} In contrast, the secondary kinetic isotope effect at C-12, $^{C12D}(V/K)$, is

expected to be an unity or slightly inverse because C-12 doesn't undergo a change of hybridization during the ionic rearrangement, but does undergo change of sp^2 to sp^3 hybridization during C-C bond formation between C-4 and C-12. Finally, study of the secondary kinetic isotope effect should be able to distinguish between the stepwise ionic rearrangement and biradical rearrangement mechanism according to the order of first C-C bond formation during the cyclization. If the C-C bond formation occurs first between C-4 and C-12 to leave biradical at C-7 and C-11, $^{C4D}(V/K)$ and $^{C12D}(V/K)$ are expected to be inverse due to the increased vibrational frequencies of the C-H out-of-plane bending modes in sp^3 versus sp^2 hybridized carbons. Formation of sp^2 hybridized carbon radicals at C-7 and C-11 are expected to give secondary kinetic isotope effect, $^{C7D}(V/K)$ and $^{C11D}(V/K)$, of unity. In contrast, if the C-C bond is formed first between C-7 and C-11, the secondary kinetic isotope effects for a biradical rearrangement mechanism will be the same as those of the ionic rearrangement mechanism, showing 4% normal for $^{C4D}(V/K)$, inverse for $^{C7D}(V/K)$ and $^{C11D}(V/K)$, and unity for $^{C12D}(V/K)$. The predicted secondary kinetic isotope effects are summarized in **Figure 2-5**. Experimentally, second kinetic isotope effects will be measured by LC-ESI-MS based on the competitive *in vitro* activity assay with a mixture of natural substrate and labeled probes.^{123, 124} The experiments to determine the secondary kinetic isotope effects will be repeated many times to ensure the results are reproducible.

	Diels-Alder reaction mechanism	Ionic rearrangement mechanism	Biradical rearrangement mechanism	
			Biradical at C-7 and C-11	Biradical at C-4 and C-12
$^{C4D}(V/K)$	0.95 (inverse)	1.04 (normal)	0.95 (inverse)	1.04 (normal)
$^{C7D}(V/K)$	0.95 (inverse)	0.95 (inverse)	1.00 (unity)	0.95 (inverse)
$^{C11D}(V/K)$	0.95 (inverse)	0.95 (inverse)	1.00 (unity)	0.95 (inverse)
$^{C12D}(V/K)$	0.95 (inverse)	1.00 (unity)	0.95 (inverse)	1.00 (unity)

Figure 2-5. The expected secondary kinetic isotope effect for the proposed mechanisms of SpnF-catalyzed [4+2] cycloaddition in the biosynthesis of spinosyn A.

Another interesting question concerning the SpnF reaction is how SpnF accelerates the reaction, whether it acts predominantly by an entropic preorganization or an enthalpic transition state stabilization.^{40, 125, 126, 127, 128, 129, 130} To investigate the intrinsic properties of the SpnF reaction, three SpnF substrate analogs are designed as shown in

Figure 2-6.

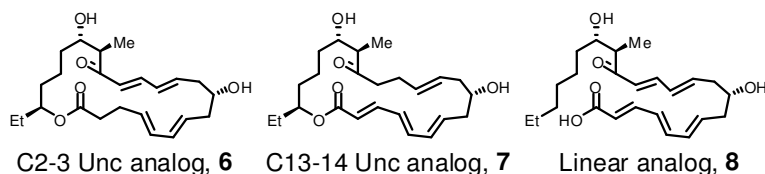


Figure 2-6. Analogs for studying the intrinsic property of SpnF

In order to differentiate between substrate modifications which specifically affect the SpnF reaction and those which simply retard cyclization, the concept of a relative rate enhancement is considered. First, rate enhancement is defined as the ability to accelerate the rate of SpnF reaction compared to non-enzymatic reaction, that is, $RE = k_{cat}/k_{non}$, accordingly, RE_{NS} is equal to $(k_{cat}/k_{non})_{NS}$ for the natural substrate, and RE_{analog} is equal to $(k_{cat}/k_{non})_{analog}$.¹³¹ Rate enhancement (RE) can be easily measured for the natural substrate or any substrate analog by an *in vitro* activity assay of SpnF. Second, if a substrate analog is modified, the relative rate enhancement is supposed to change in both the enzymatic

and non-enzymatic reaction. The relative rate enhancement is defined for natural substrate versus substrate analog as $RRE_{NS,analog} = \frac{RE_{NS}}{RE_{analog}} = \frac{(k_{cat}/k_{non})_{NS}}{(k_{cat}/k_{non})_{analog}}$. Thus, an $RRE_{NS,analog}$ of one means that the modification of the substrate doesn't affect the cyclization entropically and enthalpically when the substrate analog undergoes cycloaddition enzymatically or non-enzymatically. Two SpnF substrate analogs, C2-3 Unc and C13-14 Unc, were designed to study the contribution of enthalpic transition state stabilization by SpnF, assuming that the cyclic substrates are less affected by entropic preorganization. If the enthalpic transition state stabilization is dominant in SpnF reaction, $RRE_{NS,Unc}$ should be greater than one for C13-14 Unc and C2-3 Unc analogs, since there is no conjugation between the dienophile and ketone at the C-15 position in the C13-14 Unc analog and between the diene and ester at the C-1 position in the C2-3 Unc analog. Lacking of resonance stabilization through conjugation is expected to attenuate the rate of reaction. If rate increase of SpnF-catalyzed cyclization is observed for those two Unc analogs as compared to non-enzymatic reaction, one may hypothesis that the intact ketone at C-15 or the ester at C-1 may be more important for SpnF reaction. The possible enthalpic transition state stabilization may be achieved by coordination with a Lewis acid, or by accepting a proton in the transition state. If $RRE_{NS,Unc}$ is less than one, the enthalpic transition state stabilization may be less significant for the SpnF reaction. Contribution of entropic preorganization by SpnF can be measured with a non-cyclic Linear analog, which is less influenced by the enthalpic transition state stabilization since all the functional group are intact except for the lactone

ring. If entropic preorganization contributes more to the SpnF reaction, $RRE_{NS,Linear}$ should be less than one because the enzymatic transformation of the Linear analog is more affected by the entropic preorganization by SpnF, compared to the cyclic natural substrate. In the case of enthalpic transition state stabilization, $RRE_{NS,Linear}$ is expected to be slightly greater than one or equal to one because the Linear analog has the same conjugation system in its structure as the natural substrate. Along with the temperature dependence experiments, combined results will give insight into the SpnF reaction in terms of thermodynamics, assuming these substrate analogs are well behaved enzymatically and non-enzymatically.

This chapter summarizes the progress of our mechanistic study of SpnF-catalyzed [4+2] cycloaddition to differentiate the three plausible mechanisms: the Diels-Alder mechanism, the ionic rearrangement mechanism, and the biradical rearrangement mechanism. Also included are the experiments to determine the intrinsic properties of the SpnF reaction in terms of entropic preorganization and enthalpic transition state stabilization. Studies of the kinetic isotope effects are carried out using four mechanistic probes containing one deuterium at four different reaction centers (C4-D, C7-D, C11-D, and C12-D analogs). The intrinsic properties of the SpnF reaction are examined using two cyclic analogs (C2-3 Unc analog and C13-14 Unc analog) and one non-cyclic analog (Linear analog). Since the mechanistic studies are still in progress, no definite conclusions concerning the mechanism and intrinsic properties of SpnF can be drawn at this time. However, the experiments described in this chapter are the foundation of SpnF research. The completion of this project is already in sight.

2.2. EXPERIMENTAL PROCEDURES

2.2.1. Materials and Equipment

All chemicals were purchased from Sigma-Aldrich (St. Louis, MO, USA), Fisher Scientific (Pittsburgh, PA, USA), Tokyo Chemical Industry (TCI; Boston, MA, USA), Acros (Geel, Belgium), Alfar Aesar (Ward Hill, Ma, USA) and/or Chem-Impex (Wood Dale, IL, USA), and used without further purification unless otherwise specified. *Escherichia coli* DH5 α cells were obtained from Bethesda Research Laboratories (Muskegon, MI). The vector pEt28b(+) and enzyme KOD DNA polymerase were purchased from Novagen (Madison, WI, USA). DNA modifying enzymes (for restriction digestion and ligation), PCR primers, and the overexpression host *E. coli* BL21 star (DE3) were acquired from Invitrogen (Carlsbad, CA, USA) and New England Biolabs (NEB; Beverly, MA, USA). LB medium is a product of Difco (Detroit, MI, USA) or Fisher Scientific, and pre-stained protein markers are products of NEB. Ni-NTA agarose and kits for DNA gel extraction and spin miniprep were obtained from Qiagen (Valencia, CA, USA). All reagents for SDS-PAGE and Amicon YM-10 filtration products were purchased from Bio-Rad (Hercules, CA, USA) and Millipore (Billerica, MA, USA), respectively. Analytical thin layer chromatography (TLC) was carried out on pre-coated TLC glass plates (Silica gel, Grade 60, F₂₅₄, 0.25 mm layer thickness) obtained from EMD Chemicals (Madison, WI, USA). Flash column chromatography was performed (230-400 mesh, Grade 60) by elution with the specified solvents, using materials from Sorbent Technologies (Atlanta, GA, USA) or Silicycle (Quebec City, Canada). Protein

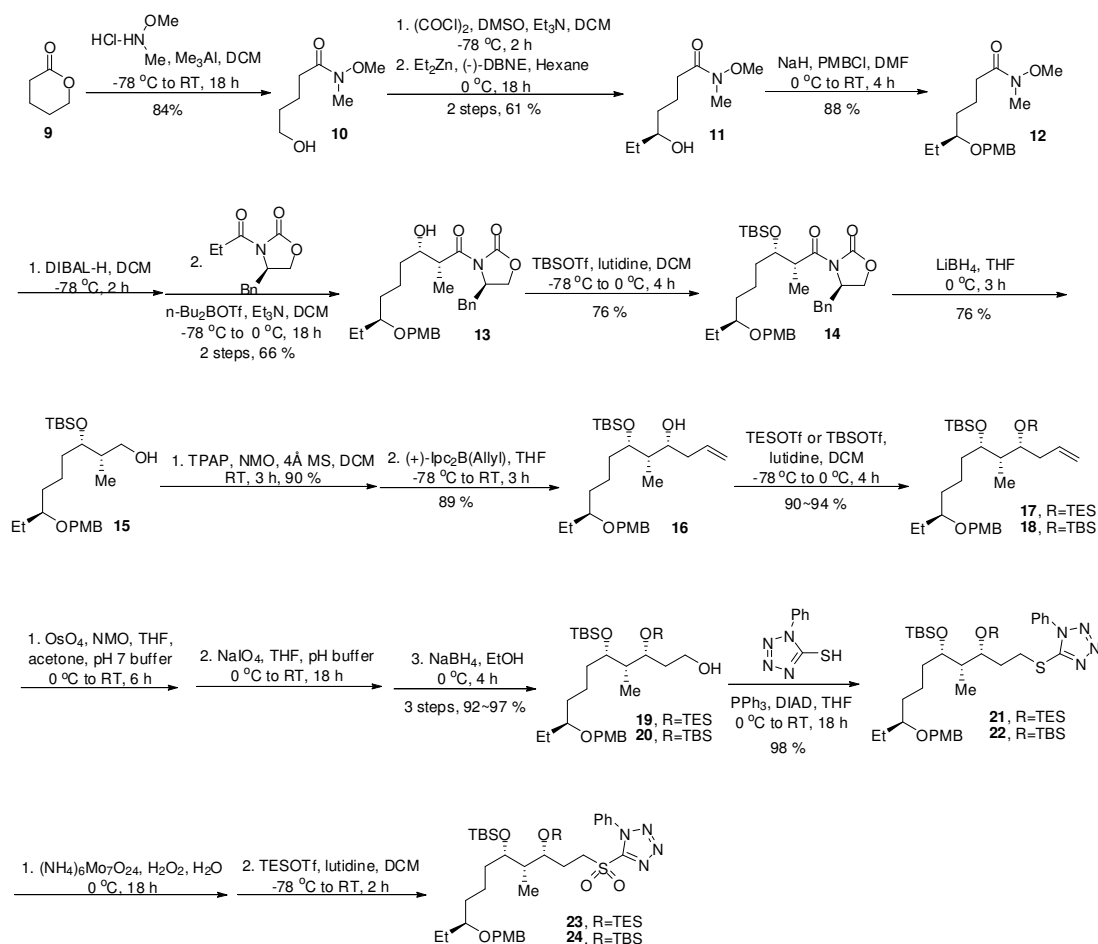
concentrations were determined by Bradford assay using bovine serum albumin as the standard, or measured by nanodrop, ND-1000 UV-VIS spectrophotometer from NanoDrop technologies (Wilmington, DE, USA). The relative molecular mass and purity of enzyme samples were determined using SDS-polyacrylamide gel electrophoresis as described. The general methods and protocols for recombinant DNA manipulations are as described by Sambrook and Russell. DNA sequencing was performed by the Core Facilities in the Institute of Cellular and Molecular Biology of the University of Texas at Austin. NMR spectra were acquired on a Varian Unity Inova 500 or 600 MHz spectrometer, housed in the NMR Facility of the Department of Chemistry and Biochemistry in the University of Texas at Austin. The Mass analyses were carried out at the Mass Spectrometry and Proteomics Facility of the Department of Chemistry and Biochemistry in the University of Texas at Austin.

2.2.2. Preparation of Enzymes

Cloning of *SpnJ*, *SpnM*, and *SpnF*, and the expression and purification of their products have already been reported.^{21, 22, 132}

2.2.3. Synthesis of the SpnM Natural Substrate

A. Preparation of Fragment A: The overall synthetic scheme is shown in **Scheme 2-1**.



Scheme 1. Preparation of Fragment A in the synthesis of natural substrate

5-hydroxy-*N*-methoxy-*N*-methylpentanamide (10): A solution of *N,O*-dimethylhydroxylamine hydrochloride (69.4 g, 0.71 mol) in dichloromethane (540 mL) was added dropwise over a period of three hours to a trimethylaluminum solution (356 mL, 2M, 711 mmol) under a nitrogen atmosphere at $-78\text{ }^\circ\text{C}$. This reaction mixture was stirred for 1 hour at $-78\text{ }^\circ\text{C}$ and slowly warmed to room temperature with stirring over 18 hours. Then, δ -valerolactone (30 ml, 323 mmol) in dichloromethane (356 mL) was added dropwise into the cool reaction mixture in an ice-bath over the course of 1 hour. This reaction mixture was slowly warmed to room temperature with stirring over the course of

3 hours. To quench the reaction mixture, cold Na⁺ K⁺ tartrate solution (Rochelle's salt, 75.8 g in water, 200 mL) was added to the reaction mixture in an ice-bath over 3 hours with vigorous mechanical stirring. After addition of celite (50 g), the solution was allowed to reaction with additional stirring for 1 hour. The liquid fraction was first filtered over paper filter, and the solid cake was washed with dichloromethane (200 mL x 5 times) until no product was detected in the solid cake. The organic fraction of the filtrate was extracted with dichloromethane (200 mL x 2 times). The collected organic fractions were washed with brine (200 mL) and dried over an anhydrous magnesium sulfate pad, before being filtered through a glass filter. The filtrate was concentrated, and chromatographed using EtOAc to elute unwanted substances and 10% methanol/dichloromethane solution to collect the target compound, 5-hydroxy-N-methoxy-N-methylpentanamide (51.3 g, 85%). All spectral data is identical to the literature reference.

(S)-5-hydroxy-N-methoxy-N-methylheptanamide (11): 1) DMSO was added to (73.8 mL, 0.95 mol) to a solution of oxalic chloride (41.7 mL, 0.48 mol) in dichloromethane (795 mL) at -78 °C dropwise over an hour. After addition of DMSO, this reaction mixture was stirred at -78 °C for an additional 10 min. Then, a solution of 5-hydroxy-N-methoxy-N-methylpentanamide (51.3 g, 0.32 mol) in dichloromethane (159 mL) was added dropwise into the reaction mixture over an hour at -78 °C, with vigorous stirring. The reaction mixture was stirred at -78 °C for additional 2 hours. The reaction was quenched by adding triethylamine (222 mL) dropwise for 3 hours with vigorous stirring. This reaction mixture was warmed to room temperature, and stirred for 18 hours. After

water (500 mL) was added, this the aqueous fraction was extracted with dichloromethane (500 mL x 3 times), and washed with brine (500 mL). The combined organic fractions were then dried over an anhydrous magnesium sulfate pad and concentrated under reduced pressure, resulting in a pale brown oil. This residue was purified using flash column chromatography, and unwanted compounds were eluted with the isocratic 70% EtOAc/Hexane solution first and then the target compound was eluted with EtOAc (47.9 g, 95 %) 2) Over a period of 3 hours, diethyl zinc solution (692 mL, 1.0 M, 0.69 mol) was added dropwise to a solution of aldehyde (47.9 g, 0.30 mol) and (-)-DBNE (4.8 mL, 0.018 mol) in anhydrous hexane (750 mL) at 0 °C under a nitrogen atmosphere. This solution was stirred at 0 °C for 18 hours, and then quenched with saturated the aqueous ammonium chloride solution (750 mL) for 2 hours. After filtering the liquid portion and the solid fraction with a celite pad with several washes with ethyl acetate (500 mL x 2 times), the organic and the aqueous layer of the filtrate were separated. Water fraction was extracted with ethyl acetate (300 mL x 4 times) and the combined organic fractions were washed with brine (400 mL), followed by drying over an anhydrous sodium sulfate pad and concentration under reduced pressure. The resulting residue was purified by flash column chromatography. The target compound was eluted with 80% of EtOAc/Hexane (34.6 g, 61% yield for 2 steps). All spectral data is identical to the literature reference.

(S)-N-methoxy-5-(4-methoxybenzyloxy)-N-methylheptanamide (12): To a solution of (S)-5-hydroxy-N-methoxy-N-methylheptanamide (34.0 g, 0.18 mol) and *p*-methoxybenzyl chloride (29.2 mL, 0.22 mol) in anhydrous DMF (360 mL), sodium hydride (8.6 g, 0.22 mol) was added portionwise over a period of 30 min at 0 °C with a

nitrogen atmosphere. Afterwards, the reaction mixture was slowly warmed to room temperature with vigorous stirring over 4 hours. After cooling to 0 °C in an ice-bath, water (360 mL) was added dropwise into the reaction mixture over the course of 1 hour to avoid a sudden gas eruption. The aqueous layer was extracted with ethyl acetate (200 mL x 3 times). The collected organic fractions were washed with brine (200 mL x 2 times), and dried over an anhydrous magnesium sulfate pad. After concentration under reduced pressure, the sticky residue was subjected to flash column chromatography. The target compound was eluted 30% EtOAc/Hexane solution (49.0 g, 88%). All spectral data is consistent with the literature reference.

(R)-4-benzyl-3-((2R,3S,7S)-3-hydroxy-7-(4-methoxybenzyloxy)-2-

methylnonanoyl)oxazolidin-2-one (13): 1) To a solution of (S)-N-methoxy-5-(4-methoxybenzyloxy)-N-methylheptanamide (20.0 g, 0.065 mol) in dichloromethane (323 mL) at -78 °C a DIBALH solution (97 mL, 1.0 M, 0.097 mol) was added over 30 min. The reaction mixture was stirred at -78 °C for 4 hours and at 0 °C for 1 hour. Methanol (64 mL) was slowly added with vigorous stirring at -78 °C, and the reaction mixture was then allowed to warm to room temperature. After 30 min, the aqueous 1 M solution of Rochelle's salt (64 mL) was slowly added to the reaction mixture over 30 min. After another 30 min, the reaction mixture was filtered with a celite pad and washed with dichloromethane (200 mL x 3 times). The separate organic fractions were washed with brine (200 mL), and dried over an anhydrous sodium sulfate. After filtration and concentration of the solution under reduced pressure, the resulting yellow residue was purified using flash column chromatography. The target compound was eluted, the target

aldehyde was eluted with 10% to 20% of EtOAc/Hexane solution (15.8 g, 97%). 2) Di-n-butylboryl trifluoromethanesulfonate (87 mL, 1.0 M, 0.087 mol) was added over the course of 30 min to a solution of (R)-4-benzyl-3-propionyloxazolidin-2-one (16.9 g, 0.73 mol) in dichloromethane (500 mL) at 0 °C, and the reaction mixture was stirred for 30 min. Triethylamine (14 mL, 0.098 mol) was added to the reaction mixture over 15 min, and the solution stirred at 0 °C for 30 min. After cooling to -78 °C, freshly prepared aldehyde (20 g, 0.080 mol) in dichloromethane (200 mL) was added slowly to the reaction mixture over 1 hour. The reaction mixture was stirred at -78 °C for 1 hour, and slowly warmed to 0 °C with stirring over 18 hours. To quench the reaction mixture, pH 7.0 phosphate buffer (100 mL), methanol (300 mL), and hydrogen peroxide solution (100 mL) were subsequently added to the reaction mixture with vigorous stirring at 0 °C over 2 hours. The aqueous fraction was extracted with dichloromethane (150 mL x 3 times), and the combined organic fractions were washed with brine (200 mL) and dried over an anhydrous sodium sulfate pad. The filtrate was concentrated under reduced pressure to give a yellow residue, which was subjected to flash column chromatography. The target compound was eluted with 20% to 30% EtOAc/Hexane solution (23.3 g, 66%). All spectral data is identical to the literature reference.

(R)-4-benzyl-3-((2R,3S,7S)-3-(tert-butyldimethylsilyloxy)-7-(4-methoxybenzyloxy)-2-methylnonanoyl)oxazolidin-2-one (14): TBSOTf (8.8 mL, 38.1 mmol) was added to a solution of alcohol compound (8.9 g, 25.4 mmol) and 2,6-lutidine (5.9 mL, 50.8 mmol) in dichloromethane (254 mL) at -78 °C over 15 min. The reaction mixture was stirred at -78 °C for 30 min and 0 °C for 30 min. When the starting material was no longer detectable

using TLC, the reaction mixture was quenched with a saturated the aqueous ammonium chloride solution (128 mL). After stirring for 30 min, the aqueous fraction was extracted with dichloromethane (100 mL x 3 times), which was then dried over an anhydrous sodium sulfate pad and concentrated under reduced pressure. The resulting residue was purified using flash column chromatography. The target compound was eluted with 10% EtOAc/Hexane solution (11.0 g, 93%). All spectral data is consistent with the literature reference.

(2S,3S,7S)-3-(tert-butyldimethylsilyloxy)-7-(4-methoxybenzyloxy)-2-methylnonan-1-ol (15): (R)-4-benzyl-3-((2R,3S,7S)-3-(tert-butyldimethylsilyloxy)-7-(4-methoxybenzyloxy)-2-methylnonanoyl)oxazolidin-2-one (11.0 g, 23.8 mmol) and reagent grade methanol (2.9 mL, 71.5 mmol) were dissolved in anhydrous THF (119 mL) at 0 °C. A lithium borohydride solution (17.8 mL, 35.7 mmol) was added to this reaction mixture over 20 min. After stirring at 0 °C for 6 hours, the reaction mixture was quenched with a cold the aqueous 15% sodium hydroxide solution (119 mL) with vigorous stirring. The aqueous fraction was extracted with ethyl acetate (100 mL x 3 times), and the combined organic fractions were washed with brine (100 mL) and dried over an anhydrous sodium sulfate pad and concentrated under reduced pressure. The residue was purified using flash column chromatography. The target compound was eluted the target compound with 10% EtOAc/Hexane solution (4.5 g, 66%). All spectral data is identical to the literature reference.

(4R,5S,6S,10S)-6-(tert-butyldimethylsilyloxy)-10-(4-methoxybenzyloxy)-5-methyldodec-1-en-4-ol (16): 1) At room temperature, (2S,3S,7S)-3-(tert-

butyldimethylsilyloxy)-7-(4-methoxybenzyloxy)-2-methylnonan-1-ol (4.8 g, 11 mmol), tetrapropylammonium perruthenate (TPAP, 200 mg, 0.57 mmol), N-methylmorpholine N-oxide (NMO, 2.66 g, 23 mmol) and activated 4 Å molecular sieve (0.96 g) were mixed together in dichloromethane (113 mL) with vigorous stirring over 3 hours. The reaction mixture was then quenched with the aqueous 10% sodium thiosulfate solution (23 mL). The aqueous fraction was extracted with dichloromethane (50 mL x 3 times), and the combined organic fractions were washed with brine (50 mL) and dried over an anhydrous sodium sulfate pad. The concentrated residue was purified using flash column chromatography. An aldehyde intermediate was eluted with 20% EtOAc/Hexane solution (4.4 g, 92%).

2) (+)-Ipc₂B(allyl) was prepared by mixing (+)-diisopinocampheylchloroborane (8.9 mL, 1.6 M, 14.2 mmol) and allyl magnesium bromide (13.6 mL, 1.0 M, 13.6 mmol) in anhydrous THF (32 mL) at 0 °C for 10 min. After cooling to -78 °C, the aldehyde (4.4 g, 10.4 mmol) in THF (10 mL) was added to the reaction mixture over 10 min, which was stirred at 0 °C for 1.5 hours, and allowed to warm to room temperature over the course of 1 hour with stirring. When the aldehyde was no longer detectable, the reaction mixture was quenched by subsequent addition of methanol (32 mL), the aqueous 1 N sodium hydroxide solution (32 mL), and hydrogen peroxide solution (11 mL) at 0 °C. This reaction mixture was stirred at 0 °C for 30 min. After filtration through paper filter, the filtrate was extracted with ethyl acetate (100 mL x 3 times), and the combined organic fractions were washed with brine (100 mL) and dried over an anhydrous sodium sulfate pad. After concentration under reduced pressure, the residue was purified using flash column chromatography. The target compound was

eluted with 10% to 20% EtOAc/Hexane solution (4.4 g, 90%). All spectral data is consistent with the literature reference.

(4R,5S,6S,10S)-6-(tert-butyldimethylsilyloxy)-10-(4-methoxybenzyloxy)-4-(triethylsilyloxy)-5-methyl-1-dodec-1-en-4-ol (17): TESOTf (3.2 mL, 14.1 mmol) was added dropwise to a solution of (4R,5S,6S,10S)-6-(tert-butyldimethylsilyloxy)-10-(4-methoxybenzyloxy)-5-methyldodec-1-en-4-ol (4.4 g, 9.4 mmol) and 2,6-lutidine (2.7 mL, 23.5 mmol) in anhydrous dichloromethane (141 mL) at -78 °C over 10 min. The reaction mixture was stirred at -78 °C for 2 hours and at 0 °C for 30 min, then quenched with saturated the aqueous ammonium chloride solution. The aqueous fraction was extracted with dichloromethane (50 mL x 3 times), and the combined organic fractions were washed with brine (50 mL) and dried over an anhydrous sodium sulfate pad. After concentration under reduced pressure, the resulting residue was subjected to flash column chromatography. The target compound was eluted with 2% to 5% EtOAc/Hexane (4.4 g, 89%). All spectral data is identical to the literature reference.

(5R,6R,7S)-5-allyl-7-((S)-4-(4-methoxybenzyloxy)hexyl)-2,2,3,3,6,9,9,10,10-nonamethyl-4,8-dioxa-3,9-disilaundecane (18): t-Butyldimethylsilyl trifluoromethanesulfonate (4.6 mL, 19.9 mmol) was added dropwise over 20 min to a solution of secondary alcohol compound (6.2 g, 13.3 mmol) and 2,6-lutidine (3.8 mL, 33.1 mmol) in anhydrous dichloromethane (100 mL) at -78 °C. The reaction mixture was stirred at -78 °C for 1 hour, at which time the dry ice bath was removed and the reaction mixture was stirred for additional 2 hours at room temperature. The reaction mixture was quenched with saturated the aqueous sodium bicarbonate solution (100 mL) and extracted

with dichloromethane (100 mL x 2 times). The combined organic fractions were washed with brine (100 mL), dried over an anhydrous sodium sulfate pad, and concentrated. The residue was purified by flash column chromatography. The target compound was eluted with 5% EtOAc/Hexane (7.0 g, 12.1 mmol, 91%).

^1H NMR (CDCl_3 , 600 MHz) δ (ppm) 7.28-7.25 (m, 2H, PhH of PMB), 6.88-6.85 (dt, 2H, $J = 8.7, 2.8, 2.1$ Hz, PhH of PMB), 5.84-5.76 (m, 1H, 2-CH), 5.05-5.00 (m, 2H, 1- CH_2), 4.45-4.40 (dd, 2H, $J = 18.6, 11.2$ Hz, CH_2 of PMB), 3.81-3.77 (m, 4H, OCH_3 of PMB+4-CH), 3.72-3.68 (m, 1H, 6-CH), 3.31-3.26 (m, 1H, 10-CH), 2.31-2.28 (m, 2H, 3- CH_2), 1.65-1.40 (m, 9H, 5-CH+7- CH_2 +8- CH_2 +9- CH_2 +11- CH_2), 0.94-0.88 (m, 24H, CH_3 of TBS+12- CH_3 +5- CH_3), 0.05-0.03 (m, 11H, CH_3 of TBS); ^{13}C NMR (CDCl_3 , 150 MHz) δ (ppm) 159.04, 135.04, 131.28, 129.24, 116.76, 113.71, 79.89, 72.66, 72.20, 70.50, 55.27, 40.55, 39.64, 35.04, 33.95, 26.31, 25.96, 20.95, 18.15, 9.50, 9.38, -3.80, -4.46; HRMS (ESI, positive) m/z for $\text{C}_{33}\text{H}_{62}\text{O}_4\text{Si}_2\text{Na}$ $[\text{M}+\text{Na}]^+$: calcd 601.4079, found 601.4078.

(4R,5S,6S,10S)-6-(tert-butyldimethylsilyloxy)-10-(4-methoxybenzyloxy)-4-

(triethylsilyloxy)-5-methyldodecane-1,4-diol (19): 1) (4R,5S,6S,10S)-6-(tert-butyldimethylsilyloxy)-10-(4-methoxybenzyloxy)-4-(tert-butyldimethylsilyloxy)-5-

methyl-1-dodec-1-en-4-ol (4.4 g, 7.6 mmol) was dissolved in a solution of THF (22.8 mL), acetone (22.8 mL), and pH 7 phosphate buffer (22.8 mL), and cooled to 0 °C with stirring for 10 min. Osmium tetroxide (0.10 g, 0.38 mmol) and N-methylmorpholine N-oxide (1.3 g, 11.4 mmol) were subsequently added to the reaction mixture, which was stirred at 0 °C for 30 min and at room temperature for 4 hours at which point the starting material was no longer visible. The reaction mixture was quenched with subsequent

addition of the aqueous 10% sodium thiosulfate solution (34.2 mL) and pH 7 phosphate buffer (34.2 mL) at 0 °C. After stirring at 0 °C for 30 min and at room temperature for 30 min, the aqueous fraction was extracted with ethyl acetate (50 mL x 3 times). The combined organic fractions were washed with brine (50 mL), dried over an anhydrous sodium sulfate pad, and concentrated to give a pale yellow residue, which was used in the next step without further purification. 2) The residue was dissolved in a solution of THF (159 mL) and pH 7 phosphate buffer (68 mL) at 0 °C. Sodium (meta)periodate (5.4 g, 25.1 mmol) was added portionwise to the reaction mixture over 1 hour at 0 °C, followed by stirring at room temperature for 18 hours. After quenching the reaction with saturated the aqueous ammonium chloride (76 mL), the organic fraction was isolated by extracting the aqueous fractions with ethyl acetate (50 mL x 3 times). The combined organic fractions were washed with brine (50 mL), dried over an anhydrous sodium sulfate pad, and concentrated under reduced pressure. The resulting residue was directly used for the next step without further purification. 3) Sodium borohydride (0.5 g, 12.2 mmol) was added to a solution of the residue from the previous reaction mixture dissolved in ethanol (38 mL) at 0 °C with vigorous stirring over 5 min. After stirring at 0 °C for 4 hours, the reaction mixture was quenched with saturated the aqueous ammonium chloride (38 mL). The aqueous fraction was extracted with ethyl acetate (50 mL x 4 times), and the combined organic fractions were washed with brine (50 mL), dried over an anhydrous sodium sulfate pad, and concentrated under reduced pressure. The residue was purified using flash column chromatography. The target compound was eluted with 5% to 10% EtOAc/Hexane (3.2 g, 74%). All spectral data is identical to the literature reference.

(3R,4R,5S,9S)-3,5-bis(tert-butyldimethylsilyloxy)-9-(4-methoxybenzyloxy)-4-methylundecan-1-ol (20) : 1) *N*-methylmorpholine oxide (NMO; 2.1 g, 18.1 mmol) was added to a solution of silyl ether compound (7.0 g, 12.1 mmol) in THF (48 mL), acetone (48 mL), and pH 7 phosphate buffer (48 mL) at room temperature, followed by the addition of osmium tetroxide (0.15 g, 0.60 mmol). The reaction mixture was stirred at room temperature for 18 hours. The reaction mixture was poured into an aqueous 10% sodium thiosulfate solution (50 mL), and the aqueous fraction was extracted with ethyl acetate (50 mL × 3 times). The combined organic fractions were washed with brine (40 mL), dried over an anhydrous sodium sulfate pad, and concentrated under reduced pressure. The resulting crude residue was used without further purification. 2) Sodium periodate (10.3 g, 48.4 mmol) was added to a clear solution of the above crude oil in THF (150 mL) and pH 7 phosphate buffer (50 mL) at room temperature. The reaction mixture was stirred for 3 hours at room temperature. Next, the reaction mixture was quenched with a saturated the aqueous sodium bicarbonate solution (50 mL). The aqueous fraction was extracted with ethyl acetate (50 mL × 3 times). The combined organic fractions was washed with brine (40 mL), dried over an anhydrous sodium sulfate pad, and concentrated under reduced pressure. The resulting residue was used in the next step without further purification. 3) Sodium borohydride (732 mg, 19.3 mmol) was added to the transparent solution of the crude aldehyde in ethyl alcohol (70 mL) at room temperature, and the reaction mixture was stirred for 1 hour, at which time the reaction was poured into saturated the aqueous ammonium chloride solution (50 mL). The aqueous fraction was extracted with ethyl acetate (50 mL × 3 times), and the combined

organic fractions were washed with brine (40 mL), dried over an anhydrous sodium sulfate pad, and concentrated under reduced pressure. The residue was subjected to flash column chromatography. The target compound was eluted with 5% EtOAc/Hexane (6.6 g, 11.3 mmol, 97% for 3 steps).

^1H NMR (CDCl_3 , 600 MHz) δ (ppm) 7.26-7.23 (m, 2H, PhH), 6.86-6.84 (m, 2H, PhH), 4.45-4.42 (dd, 1H, $J = 11.2, 5.0$ Hz, CH_2 of PMB), 4.40-4.37 (dd, 1H, $J = 11.2, 6.6$ Hz, CH_2 of PMB), 3.88-3.85 (m, 1H, 3-CH), 3.80-3.75 (m, 4H, 1- CH_2 +OCH₃ of PMB), 3.70-3.63 (m, 2H, 1- CH_2 +5-CH), 3.29-3.25 (m, 1H, 9-CH), 2.28 (br, 1H, 1-OH), 1.88-1.71 (m, 3H, 2- CH_2 +4-CH), 1.56-1.21 (m, 8H, 10- CH_2 +8- CH_2 +7- CH_2 +6- CH_2), 0.90-0.85 (m, 24H, CH_3 of TBS, 11- CH_3 , 4- CH_3), 0.077 (s, 3H, CH_3 of TBS), 0.039 (s, 3H, CH_3 of TBS), 0.016 (s, 3H, CH_3 of TBS), 0.005 (s, 3H, CH_3 of TBS); ^{13}C NMR (CDCl_3 , 150 MHz) δ (ppm) 159.07, 131.20, 129.30, 113.74, 79.84, 72.65, 72.40, 70.54, 70.39, 59.79, 55.27, 40.32, 35.55, 35.43, 33.93, 26.29, 25.94, 21.20, 18.13, 9.79, 9.47, -3.68, -4.13, -4.49; HRMS (ESI, positive) m/z for $\text{C}_{32}\text{H}_{62}\text{O}_5\text{Si}_2\text{Na}$ $[\text{M}+\text{Na}]^+$: calcd 605.4026, found 605.4026.

(4R, 5S, 6S, 10S)-6-(tert-butyldimethylsilyloxy)-10-(4-methoxybenzyloxy)-4-(triethylsilyloxy)-5-methyl-1-((1-Phenyl-1H-tetrazol-5-yl)thio)dodecan-4-ol (21): 1-Phenyl-1H-tetrazole-5-thiol (1.5 g, 8.4 mmol), triphenylphosphine (1.5 g, 8.4 mmol), and diisopropyl azodicarboxylate (DIAD; 2.2 g, 8.4 mmol) were added to a solution of a primary alcohol (3.2 g, 5.6 mmol) in THF at 0 °C. This reaction mixture was stirred at 0 °C for 3 hours, and allowed to warm to room temperature over 18 hours. Then, the reaction mixture was directly concentrated under reduced pressure, and purified using

flash column chromatography. The target compound was eluted with 10% EtOAc/Hexane (3.9 g, 93%). All spectral data is identical to the literature reference.

5-((3R,4R,5S,9S)-3,5-bis(tert-butyldimethylsilyloxy)-9-(4-methoxybenzyloxy)-4-methylundecylthio)-1-phenyl-1H-tetrazole (22): 1-Phenyl-1*H*-tetrazole-5-thiol (3.0 g, 16.9 mmol) was added to a solution of alcohol (6.6 g, 11.3 mmol) in anhydrous THF (30 mL) at 0 °C, followed by the addition of triphenylphosphine (4.5 g, 16.9 mmol) and diisopropyl azodicarboxylate (DIAD; 3.4 mL, 16.9 mmol). The resulting yellow suspension was stirred at 0 °C for 1 hour and then warmed to room temperature over the course of 1 hour. The reaction mixture was concentrated under reduced pressure and subjected to flash column chromatography, the target thioether compound was eluted with 10% EtOAc/Hexane (7.2 g, 9.6 mmol, 85%).

¹H NMR (CDCl₃, 600 MHz) δ (ppm) 7.56-7.52 (m, 5H, PhH), 7.26-7.23 (m, 2H, PhH of PMB), 6.86-6.83 (m, 2H, PhH of PMB), 4.45-4.39 (dd, 2H, *J* = 18.3, 11.1 Hz, CH₂ of PMB), 3.86-3.76 (m, 5H, OCH₃ of PMB, 3-CH, 5-CH), 3.40-3.29 (m, 3H, 1-CH₂, 9-CH), 2.20-1.95 (m, 2H, 2-CH₂), 1.70-1.65 (m, 1H, 4-CH), 1.59-1.26 (m, 8H, 6-CH₂+7-CH₂+8-CH₂+10-CH₂), 0.91-0.86 (m, 24H, CH₃ of TBS, 11-CH₃, 4-CH₃), 0.05-0.02 (m, 12H, CH₃ of TBS); ¹³C NMR (CDCl₃, 150 MHz) δ (ppm) 159.00, 154.29, 133.79, 131.25, 129.98, 129.72, 129.21, 123.78, 113.69, 79.75, 72.41, 72.14, 70.45, 55.23, 35.42, 33.85, 28.91, 26.27, 25.90, 21.20, 18.10, 9.76, 9.50, -3.66, -4.10, -4.38, -4.41; HRMS (ESI, positive) *m/z* for C₃₉H₆₇N₄O₄Si₂S [M+H]⁺: calcd 743.4416, found 743.4415.

(4R, 5S, 6S, 10S)-6-(tert-butyldimethylsilyloxy)-10-(4-methoxybenzyloxy)-4-(triethylsilyloxy)-5-methyl-1-((1-Phenyl-1H-tetrazol-5-yl)sulfonyl)dodecan-4-ol (23):

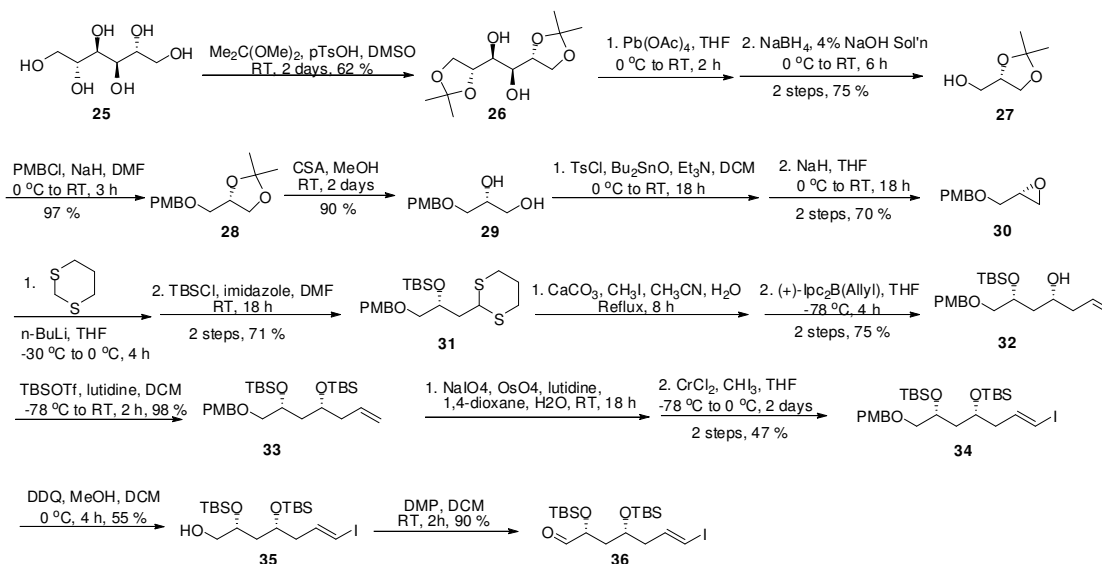
1) Ammonium heptamolybdate tetrahydrate (1.0 g, 0.8 mmol) was added to a solution of thioether (2.4 g, 3.2 mmol) in ethanol (126 mL) and hydrogen peroxide (3.9 mL) at 0 °C. This reaction mixture was stirred at 0 °C for 18 hours. The reaction mixture was quenched with brine (126 mL), and the aqueous fraction was extracted with ethyl acetate (100 mL x 3 times). The combined organic fractions were washed with brine (100 mL), and dried over an anhydrous sodium sulfate pad. The concentrated residue was purified using flash column chromatography, the target sulfonate compound was eluted with 10% EtOAc/Hexane (1.9 g, 91%). 2) TESOTf (1.0 mL, 4.3 mmol) was slowly added to a solution of this sulfonate (1.9 g, 2.9 mmol) and 2,6-lutidine (1.3 mL, 2.5 mmol) in dichloromethane (43.2 mL) at -78 °C. The reaction mixture was stirred at -78 °C for 1 hour and slowly warmed to room temperature with stirring for 30 min. After quenching with saturated the aqueous ammonium chloride (50 mL) and extraction with dichloromethane (50 mL x 3 times), combined organic fractions were washed with brine (50 mL) and dried over an anhydrous sodium sulfate pad, and concentrated under reduced pressure. The resulting residue was purified using flash column chromatography. The target compound was eluted with 5% EtOAc/Hexane (2.2 g, 98%). All spectral data is identical to the literature reference.

5-((3R,4R,5S,9S)-3,5-bis(tert-butyldimethylsilyloxy)-9-(4-methoxybenzyloxy)-4-methylundecylsulfonyl)-1-phenyl-1H-tetrazole (24): The premixed oxidant (ammonium heptamolybdate, 2.7 g; 30% H₂O₂, 10.7 mL) was added to a solution of thioether (6.5 g, 8.8 mmol) in ethyl alcohol (50 mL) at 0 °C, and the reaction mixture was stirred at 0 °C for 18 hours, at which time the mixture was poured into water (30 mL).

The aqueous fraction was extracted with EtOAc (50 mL × 3 times), and the combined organic fractions were washed with brine (50 mL), dried over an anhydrous sodium sulfate pad, and concentrated under reduced pressure. The residue was subjected to flash column chromatography. The target compound was eluted with 2% EtOAc/Hexane (6.0 g, 7.7 mmol, 89%).

^1H NMR (CDCl_3 , 500 MHz) δ (ppm) 7.71-7.69 (m, 2H, PhH), 7.62-7.57 (m, 3H, PhH), 7.26 (d, 2H, $J = 9.4$ Hz, PhH of PMB), 6.86-6.84 (dd, 2H, $J = 8.8, 2.1$ Hz, PhH of PMB), 4.46-4.39 (m, 2H, CH_2 of PMB), 3.90-3.74 (m, 7H, OCH_3 of PMB+3-CH+5-CH+1- CH_2), 3.31-3.29 (m, 1H, 9-CH), 2.31-2.13 (m, 2H, 2- CH_2), 1.61-1.24 (m, 9H, 4- CH_4 +6- CH_2 +7- CH_2 +8- CH_2 +10- CH_2), 0.91-0.85 (m, 24H, CH_3 of TBS+12- CH_3 +4- CH_3), 0.086 (s, 3H, CH_3 of TBS), 0.067 (s, 3H, CH_3 of TBS), 0.053 (s, 3H, CH_3 of TBS), 0.019 (s, 3H, CH_3 of TBS); ^{13}C NMR (CDCl_3 , 125 MHz) δ (ppm) 159.03, 153.48, 133.09, 131.37, 131.20, 129.68, 129.23, 125.00, 113.72, 79.63, 71.68, 71.53, 70.49, 55.24, 52.11, 40.69, 35.45, 33.71, 26.34, 25.90, 21.43, 18.09, 18.05, 9.62, 9.49, -3.57, -4.27, -4.48; HRMS (ESI, positive) m/z for $\text{C}_{39}\text{H}_{66}\text{N}_4\text{O}_6\text{Si}_2\text{SNa}$ $[\text{M}+\text{Na}]^+$: calcd 797.4134, found 797.4143.

B. Preparation of Fragment B: The overall synthetic scheme is depicted in **Scheme 2-2**.



Scheme 2-2. Preparation of Fragment B in the synthesis of natural substrate

(1S,2S)-1,2-bis((R)-2,2-dimethyl-1,3-dioxolan-4-yl)ethane-1,2-diol (26): D-Mannitol (109.3 g, 0.60 mol) and p-toluenesulfonic acid (0.6 g, 3.2 mmol) were stirred in a solution of 2,2-dimethoxypropane (180 mL, 1.50 mol) and DMSO (180 mL) at room temperature for 2 days. Aqueous 3% sodium bicarbonate solution (360 mL) was slowly added to the reaction mixture, and the aqueous fraction was extracted with ethyl acetate (1,000 mL x 3 times). The combined organic fractions were washed with water (300 mL x 3 times), dried over an anhydrous sodium sulfate pad, and concentrated under reduced pressure. The resulting residue was refluxed in hexane solution (1,800 mL) for 1 hour, then allowed to cool to 0 °C over 18 hours. White precipitate was filtered through glass filter and air-dried to afford a white solid as the target compound (99.1 g, 63%). All spectral data is identical to the literature reference.

(S)-(2,2-dimethyl-1,3-dioxolan-4-yl)methanol (27): Lead (IV) acetate (200.0 g, 0.92 mol) was slowly added portionwise to a solution of (1S,2S)-1,2-bis((R)-2,2-dimethyl-1,3-

dioxolan-4-yl)ethane-1,2-diol (120.2 g, 0.46 mol) in THF (600 mL) at 0 °C with maintaining the inner temperature below 10 °C for 2 hours. Then, the reaction mixture was stirred at 0 °C for 30 min and at room temperature for 30 min, followed by filtering through a celite pad and washing with THF. The sodium borohydride (35.2 g, 0.90 mol) in the aqueous 4% sodium hydroxide solution was slowly added to the resulting filtrate at 0 °C for 3 hours while maintaining an inner temperature below 10 °C. The reaction mixture was stirred at 0 °C for 30 min and at room temperature for 1.5 hours. The reaction mixture was quenched with solid ammonium chloride to adjust the pH to 8.0. The reaction mixture was then filtered through celite and separated into an organic fraction and aqueous fraction. The aqueous fraction was saturated with solid sodium chloride and extracted with ethyl acetate (300 mL x 3 times). The combined organic fractions were washed with the aqueous 5% sodium hydroxide in saturated sodium chloride solution (1,000 mL), dried over an anhydrous sodium sulfate pad, and concentrated under reduced pressure. The resulting residue was vacuum-distilled at 90 °C (91.9 g, 76%). All spectral data is consistent with the literature reference.

(S)-4-((4-methoxybenzyloxy)methyl)-2,2-dimethyl-1,3-dioxolane (28): Sodium hydride (33.2 g, 0.83 mol) was added portionwise to a solution of (S)-(2,2-dimethyl-1,3-dioxolan-4-yl)methanol (91.5 g, 0.69 mol) in anhydrous DMF (1,000 mL) at 0 °C over 30 min. After stirring for 30 min at 0 °C, PMPCl (124.1 g, 0.79 mol) was added to the reaction mixture for 30 min. The reaction mixture was allowed to warm to room temperature with vigorous stirring over 18 hours. After quenching this reaction mixture in ice-bath with water (1,000 mL), the aqueous fraction was extracted with ethyl acetate

(500 mL x 3 times). The combined organic fractions were washed with brine (500 mL), dried over an anhydrous sodium sulfate pad, and concentrated under reduced pressure to dryness to afford the target compound (174 g, quantitative) with no further purification. All spectral data is identical to the literature reference.

(R)-3-(4-methoxybenzyloxy)propane-1,2-diol (29): Crude starting material (174 g, 0.69 mol) gained from previous step was stirred in methanol (1,750 mL) with (±)-camphorsulfonic acid (8.0 g, 34.6 mmol) at room temperature for 2 days. The reaction mixture was concentrated under reduced pressure, and mixed with water (1,000 mL) and ethyl acetate (1,000 mL). The organic fraction was separated by additional extraction with ethyl acetate (500 mL x 2 times), and washed out with brine (500 mL). After drying over an anhydrous sodium sulfate pad and concentrating under reduced pressure, the resulting residue was subjected to flash column chromatography. The target compound was eluted with 50% EtOAc/Hexane solution (132.0 g, 90%). All spectral data is identical to the literature reference.

(R)-2-((4-methoxybenzyloxy)methyl)oxirane (30): 1) p-Toluenesulfonyl chloride (148.0 g, 0.78 mol) was added to a solution of diol (132.0 g, 0.62 mol), triethylamine (121.4 mL, 0.87 mol), and di-n-butyltin oxide (7.7 g, 31.1 mmol) in dichloromethane (1,580 mL) at 0 °C. The reaction mixture was stirred at 0 °C for 30 min, and allowed to warm to room temperature with stirring over 18 hours. The reaction mixture was quenched with dilute hydrochloric acid solution (0.1 N, 400 mL), and extracted with dichloromethane (200 mL x 2 times). The combined organic fractions were washed with brine (500 mL), dried over an anhydrous sodium sulfate pad, and concentrated under

reduced pressure. The resulting residue was directly used for the epoxidation without further purification. 2) Sodium hydride (29.9 g, 0.75 mol) was added to a solution of the dried residue from the previous step in THF (1,320 mL) at 0 °C over 30 min under a nitrogen atmosphere. The reaction mixture was stirred at 0 °C for 2 hours, and allowed to warm to room temperature with stirring over 18 hours. After quenching with saturated the aqueous ammonium chloride solution (500 mL) at 0 °C, the aqueous fraction was extracted with ethyl acetate (500 mL x 2 times). The combined organic fractions were washed with brine (300 mL), dried over an anhydrous sodium sulfate pad, and concentrated under reduced pressure. The resulting residue was purified using flash column chromatography. The target compound was eluted with 20% to 30% EtOAc/Hexane solution (83 g, 69%). All spectral data was identical to the literature reference.

(R)-(1-(1,3-dithian-2-yl)-3-(4-methoxybenzyloxy)propan-2-yloxy)(tert-butyl)dimethylsilane (31): 1) n-Butyllithium (239 mL, 2.5 M, 0.60 mol) was added to a solution of 1,3-dithiane (65.0 g, 0.54 mol) in THF (980 mL) at -30 °C over 30 min with vigorous stirring. After stirring at -30 °C for 2 hours, an epoxide (96.0 g, 0.49 mol) in THF (250 mL) was added to the reaction mixture at -30 °C over 30 min, the solution was then allowed to warm to 0 °C with stirring over 2 hours. The reaction mixture was quenched with saturated the aqueous ammonium chloride solution (500 mL), and the aqueous fraction was extracted with ethyl acetate (400 mL x 3 times). The combined organic fractions were washed with brine (300 mL), dried over an anhydrous sodium

sulfate pad, and concentrated under reduced pressure. The resulting residue was subjected to the next step without further purification.

^1H NMR (CDCl_3 , 400 MHz) δ (ppm) 7.25 (m, 2H, PMB), 6.88 (m, 2H, PMB), 4.48 (d, $J = 1.7$ Hz, 2H, PMB), 4.25 (dd, $J = 9.6, 4.9$ Hz, 1H, 2-H), 4.10 (m, 1H, 2'-H), 3.80 (s, 3H, PMB), 3.48 (dd, $J = 9.5, 3.4$ Hz, 1H, 3-H), 3.34 (dd, $J = 9.5, 6.9$ Hz, 1H, 3-H), 2.94-2.79 (m, 4H, 3'-H, 5'-H), 2.50 (d, $J = 4.2$ Hz, 1H, OH), 2.14-1.78 (m, 4H, 1-H, 4'-H); ^{13}C NMR (CDCl_3 , 100 MHz) δ (ppm) 159.3, 129.8, 129.3, 113.8, 73.6, 73.0, 67.1, 55.2, 43.7, 38.9, 30.3, 30.0, 25.9; HRMS (CI, positive) m/z for $\text{C}_{15}\text{H}_{22}\text{NaO}_3\text{S}_2$ $[\text{M}+\text{Na}]^+$: calcd 337.0904, found 337.0903.

2) The residue was dissolved in a solution of imidazole (66.6 g, 0.98 mol) in DMF (1,110 mL) at room temperature. TBSCl (76.0 g, 0.49 mol) was then added to the reaction mixture with vigorous stirring. After 18 hours of stirring at ambient temperature, the reaction mixture was quenched with saturated the aqueous ammonium chloride solution (500 mL), and the aqueous fraction was extracted with ethyl acetate (500 mL x 4 times). The combined organic fractions were washed with brine (400 mL), dried over an anhydrous sodium sulfate pad, and concentrated under reduced pressure. The resulting residue was purified using flash column chromatography. The target compound was eluted with 10% to 20% EtOAc/Hexane (110 g, 58% for 2 steps).

^1H NMR (CDCl_3 , 400 MHz) δ (ppm) 7.28 (m, 2H, PMB), 6.89 (m, 2H, PMB), 4.47 (s, 2H, PMB), 4.17-4.09 (m, 2H, 2-H, 2'-H), 3.83 (s, 3H, PMB), 3.30 (m, 1H, 3-H), 2.89-2.75 (m, 4H, 4''-H, 6''-H), 2.15-1.62 (m, 4H, 1-H, 5''-H), 0.91 (s, 9H, TBS), 0.13 (s, 3H, TBS), 0.09 (s, 3H, TBS); ^{13}C NMR (CDCl_3 , 100 MHz) δ (ppm) 159.1, 130.3, 129.2,

113.7, 74.3, 72.9, 67.9, 55.3, 43.6, 40.3, 30.5, 29.9, 26.0, 25.9, 18.1, -4.4, -4.8; HRMS (CI, positive) m/z for $C_{21}H_{37}O_3S_2Si$ $[M+H]^+$: calcd 429.1955, found 429.1948.

(4R,6R)-6-(tert-butyldimethylsilyloxy)-7-(4-methoxybenzyloxy)hept-1-en-4-ol (32):

1) A solution of (R)-(1-(1,3-dithian-2-yl)-3-(4-methoxybenzyloxy)propan-2-yloxy)(tert-butyl)dimethylsilane (50.0 g, 0.12 mol), iodomethane (72.6 mL, 1.17 mol) and calcium carbonate (70.0 g, 0.70 mol) in acetonitrile (700 mL) and water (175 mL) was refluxed for 8 hours. After cooling and filtering over a celite pad, the filtrate was concentrated under reduced pressure to 200 ml to remove the acetonitrile, and extracted with ethyl acetate (300 mL x 4 times). The combined organic fractions were dried over an anhydrous sodium sulfate pad, and concentrated under reduced pressure. The residue was purified using short-pass over a silica gel pad, an aldehyde was eluted with 10% EtOAc/Hexane (31.0 g, 79%).

1H NMR ($CDCl_3$, 400 MHz) δ (ppm) 9.72 (t, $J = 2.4$ Hz, 1H, 1-H), 7.17 (m, 2H, PMB), 6.82 (m, 2H, PMB), 4.39 (s, 2H, PMB), 4.28 (tt, $J = 6.4, 5.1$ Hz, 1H, 3-H), 3.75 (s, 3H, PMB), 3.41 (dd, $J = 9.5, 5.1$ Hz, 1H, 4-H), 3.30 (dd, $J = 9.5, 6.4$ Hz, 1H, 4-H), 2.58 (ddd, $J = 15.9, 5.1, 2.1$ Hz, 1H, 2-H), 2.50 (ddd, $J = 15.9, 6.7, 2.7$ Hz, 1H, 2-H), 0.80 (s, 9H, TBS), 0.00 (s, 6H, TBS); ^{13}C NMR ($CDCl_3$, 100 MHz) δ (ppm) 201.5, 159.2, 123.0, 119.3, 113.8, 73.7, 73.0, 67.3, 55.3, 49.0, 25.7, 18.0, -4.5, -5.0; HRMS (CI, positive) m/z for $C_{18}H_{31}O_4Si$ $[M+H]^+$: calcd 339.1986, found 339.1984.

2) (+)-Ipc₂B(allyl) was prepared by mixing of (+)-diisopinocampheylchloroborane (77.8 mL, 1.6 M, 0.13 mol) and allyl magnesium bromide (119.1 mL, 1.0 M, 0.12 mol) in anhydrous THF (274 mL) at 0 °C for 1 hour. After cooling to -78 °C, the aldehyde from

the previous step (31.0 g, 0.09 mol) in THF (92 mL) was added to the reaction mixture over 1 hour, which was stirred at -78 °C for 2 hours, and allowed to warm to room temperature for 1 hour with stirring. When the aldehyde was no longer detectable, the reaction mixture was quenched by subsequent addition of methanol (274 mL), the aqueous 1 N sodium hydroxide solution (274 mL), and hydrogen peroxide solution (92 mL) at 0 °C. This reaction mixture was stirred at 0 °C for 3 hours. After filtration through a paper filter, the filtrate was extracted with ethyl acetate (300 mL x 4 times), and the combined organic fractions were washed with brine (500 mL) and dried over an anhydrous sodium sulfate pad. After concentration under reduced pressure, the residue was purified using flash column chromatography. The target compound was eluted with 10% EtOAc/Hexane solution (35.2 g, 91%). Spectral data was not collected.

(5R,7R)-5-allyl-7-((4-methoxybenzyloxy)methyl)-2,2,3,3,9,9,10,10-octamethyl-4,8-dioxa-3,9-disilaundecane (33): TBSOTf (21.0 mL, 0.09 mol) was added over 20 min to a solution of (4R,6R)-6-(tert-butyldimethylsilyloxy)-7-(4-methoxybenzyloxy)hept-1-en-4-ol (29.0 g, 0.08 mol) and 2,6-lutidine (21.3 mL, 0.18 mol) in dichloromethane (381 mL) at -78 °C. The reaction mixture was stirred at -78 °C for 2 hours, and allowed to warm to 0 °C over 18 hours. After quenching with saturated the aqueous ammonium chloride solution (200 mL), the aqueous fraction was extracted with dichloromethane (200 mL x 4 times). The combined organic fractions were washed with brine (200 mL), dried over an anhydrous sodium sulfate pad, and concentrated under reduced pressure. The resulting residue was purified using flash column chromatograph by eluting with 5% EtOAc/Hexane (34.1 g, 98%).

^1H NMR (CDCl_3 , 300 MHz) δ (ppm) 7.26 (d, $J = 8.7$ Hz, 2H, PMB-aromatic H), 6.89 (d, $J = 8.5$ Hz, 2H, PMP-aromatic H), 5.81 (m, 1H, 6-H), 5.05 (app d, $J = 14$ Hz, 2H, 7-H), 4.46 (s, 2H, PMB-CH₂), 3.97-3.83 (m, 2H, 2-H, 4-H), 3.80 (s, 3H, PMB-Me), 3.38 (d, $J = 4.9$ Hz, 2H, 1-H), 2.34-2.12 (m, 2H, 5-H), 1.78-1.58 (m, 2H, 3-H), 0.91 (s, 9H, TBS), 0.90 (s, 9H, TBS), 0.08 (s, 3H, TBS), 0.07 (s, 3H, TBS), 0.05 (s, 3H, TBS), 0.04 (s, 3H, TBS); ^{13}C NMR (CDCl_3 , 75 MHz) δ (ppm) 159.0, 135.1, 130.5, 129.2, 116.9, 113.6, 74.6, 72.8, 69.1, 68.8, 55.2, 42.1, 41.6, 25.9, 25.9, 18.1, 18.0, -4.23, -4.41, -4.54, -4.82; HRMS (CI, positive) m/z for $\text{C}_{27}\text{H}_{49}\text{O}_4\text{Si}_2$ $[\text{M}+\text{H}]^+$: calcd 493.3169, found 493.3149.

(5R,7R)-5-((E)-3-iodoallyl)-7-((4-methoxybenzyloxy)methyl)-2,2,3,3,9,9,10,10-octamethyl-4,8-dioxa-3,9-disilaundecane (34): 1) Allyl compound (10.0 g, 0.02 mol) was mixed with water and a solution of sodium (meta)periodate (13.0 g, 0.06 mol), osmium (VIII) oxide (0.12 g, 0.48 mmol), and 2,6-lutidine (3.5 mL, 0.03 mol) in 1,4-dioxane (61 mL) at 0 °C over 18 hours. After quenching with the aqueous 1 N sodium thiosulfate solution (40 mL) with stirring for 1 hour, the reaction mixture was filtered through a paper filter, and extracted with dichloromethane (100 mL x 3 times). The combined organic fractions were washed with brine (150 mL), dried over an anhydrous sodium sulfate pad, and concentrated under reduced pressure. The resulting residue was purified using flash column chromatography. The target compound was eluted with 5% to 10% EtOAc/Hexane (9.8 g, 99%).

^1H NMR (CDCl_3 , 300 MHz) δ (ppm) 9.77 (t, $J = 2.4$ Hz, 1H, 1-H), 7.22 (d, $J = 9.6$ Hz, 2H, PMB-aromatic H), 6.85 (d, $J = 8.4$ Hz, 2H, PMB-aromatic H), 4.42 (s, 2H,

PMB-CH₂), 4.34 (m, 1H, 3-H), 3.84 (m, 1H, 5-H), 3.79 (s, 3H, PMB-Me), 3.34 (m, 2H, 6-H), 2.50 (m, 2H, 2-H), 1.74 (t, J = 6.3 Hz, 2H, 4-H), 0.85 (s, 9H, TBS), 0.84 (s, 9H, TBS), 0.03-0.02 (m, 12H, TBS); ¹³C NMR (CDCl₃, 75 MHz) δ (ppm) 202.2, 159.1, 130.3, 129.2, 113.7, 74.3, 72.9, 68.7, 65.6, 55.2, 50.4, 42.7, 25.8, 25.7, 18.1, 17.9, -4.23, -4.41, -4.82, -4.87; HRMS (CI, positive) *m/z* for C₂₆H₄₇O₅Si₂ [M+H]⁺: calcd 495.2962, found 495.2970.

2) A solution of the resulting aldehyde (9.8 g, 18 mmol) and chromium (II) chloride (11.1 g, 91 mmol) in anhydrous THF (217 mL) was stirred at 0 °C for 30 min. Then, a solution of iodoform (14.3 g, 36 mmol) in anhydrous THF (36 mL) was added at 0 °C for 15 min under a nitrogen atmosphere. This reaction mixture was stirred at 0 °C for 2 days. The reaction mixture was then added to water (150 mL), and filtered through a paper filter and washed with ethyl acetate (300 mL x 2 times). The aqueous fraction was extracted with ethyl acetate (300 mL x 3 times). The combined organic fractions were washed with brine (300 mL), dried over an anhydrous sodium sulfate pad, and concentrated under reduced pressure in a bath which was kept below 30 °C. The resulting residue was purified twice using flash column chromatography to remove excess amount of iodine, the target compound was eluted with a gradient of hexane alone to a 5% EtOAc/Hexane solution (10.4 g, 83%).

¹H NMR (CDCl₃, 300 MHz) δ (ppm) 7.23 (d, J = 8.7 Hz, 2H, PMB-aromatic H), 6.86 (d, J = 8.7 Hz, 2H, PMB-aromatic H), 6.53-6.43 (m, 1H, 6-H), 5.99 (d, J = 14.0 Hz, 1H, 7-H), 4.42 (s, 2H, PMB-CH₂), 3.87-3.81 (m, 2H, 2-H, 4-H), 3.79 (s, 3H, PMB-Me), 3.37-3.27 (m, 2H, 1-H), 2.28-2.20 (m, 1H, 5-H), 2.14-2.04 (m, 1H, 5-H), 1.72-1.54 (m,

2H, 3-H), 0.86 (s, 9H, TBS), 0.85 (s, 9H, TBS), 0.03-0.00 (m, 12H, TBS); ^{13}C NMR (CDCl_3 , 75 MHz) δ (ppm) 159.0, 143.2, 130.4, 129.2, 113.7, 74.5, 72.9, 68.9, 68.0, 55.3, 43.3, 32.3, 25.9, 25.8, 18.1, 18.0, -4.20, -4.48, -4.56, -4.79; HRMS (CI, positive) m/z for $\text{C}_{27}\text{H}_{48}\text{IO}_4\text{Si}_2$ $[\text{M}+\text{H}]^+$: calcd 619.2136, found 619.2136.

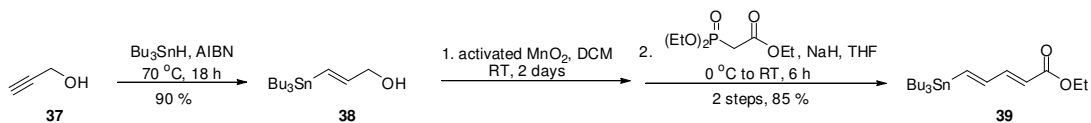
(2R,4R,E)-2,4-bis(tert-butyldimethylsilyloxy)-7-iodohept-6-en-1-ol (35): 2,3-Dichloro-5,6-dicyano-p-benzoquinone (DDQ; 1.4 g, 6.2 mmol) was added to a solution of (5R,7R)-5-((E)-3-iodoallyl)-7-((4-methoxybenzyloxy)methyl)-2,2,3,3,9,9,10,10-octamethyl-4,8-dioxa-3,9-disilaundecane (3.2 g, 5.2 mmol) in dichloromethane (15.5 mL) and methanol (1.5 mL) 0 °C, and the reaction mixture was stirred 0 °C for 18 hours. The reaction mixture was quenched with saturate the aqueous sodium bicarbonate (25 mL) at 0 °C, and the aqueous fraction was extracted with dichloromethane (30 mL x 4 times). The combined organic fractions were washed with brine (30 mL), dried over an anhydrous sodium sulfate pad, and concentrated under reduced pressure. The resulting residue was subjected to flash column chromatography. The target compound was eluted with 5% EtOAc/Hexane (1.42 g, 55%).

^1H NMR (CDCl_3 , 300 MHz) δ (ppm) 6.46 (dt, $J = 14.4, 7.5$ Hz, 1H, 6-H), 5.99 (dt, $J = 14.7, 1.2$ Hz, 1H, 7-H), 3.89-3.76 (m, 2H, 2-H, 4-H), 3.58-3.51 (m, 1H, 1-H), 3.48-3.40 (m, 1H, 1-H), 2.30-2.12 (m, 2H, 3-H), 1.73-1.58 (m, 2H, 5-H), 0.87 (s, 9H, TBS), 0.86 (s, 9H, TBS), 0.06-0.03 (m, 12H, TBS); ^{13}C NMR (CDCl_3 , 75 MHz) δ (ppm) 142.6, 77.0, 69.8, 68.2, 66.1, 43.7, 41.3, 25.79, 25.77, 18.0, 17.9, -4.36, -4.55, -4.64; HRMS (CI, positive) m/z for $\text{C}_{19}\text{H}_{42}\text{IO}_3\text{Si}_2$ $[\text{M}+\text{H}]^+$: calcd 501.1717, found 501.1703.

(2R,4R,E)-2,4-Bis(tert-butyldimethylsilyloxy)-7-iodohept-6-enal (36): An alcohol (2.2 g, 4.4 mmol) and Dess-Martin periodinane (DMP; 2.2 g, 5.3 mmol) was dissolved in dichloromethane (53 mL) at room temperature with stirring for 3 hours. The reaction mixture was then quenched with 10% the aqueous sodium thiosulfate (53 mL) and saturated the aqueous sodium bicarbonate (53 mL), and the aqueous fraction was extracted with dichloromethane (30 mL x 3 times). The combined organic fractions were washed with brine (30 mL), dried over an anhydrous sodium sulfate pad, and concentrated. The resulting residue was short-pass chromatographed by eluting with 2% to 5% EtOAc/Hexane solution (2.1 g, 90%). No spectral data was collected.

^1H NMR (CDCl_3 , 300 MHz) δ (ppm) 9.57 (d, $J = 1.2$ Hz, 1H, 1-H), 6.46 (dt, $J = 14.4, 7.5$ Hz, 1H, 6-H), 6.04 (d, $J = 14.7$ Hz, 1H, 7-H), 4.08-4.03 (m, 1H, 2-H), 3.95 (m, 1H, 4-H), 2.26-2.18 (m, 2H, 5-H), 1.81-1.76 (m, 2H, 3-H), 0.90 (s, 9H, TBS), 0.85 (s, 9H, TBS), 0.07-0.04 (m, 12H, TBS); ^{13}C NMR (CDCl_3 , 75 MHz) δ (ppm) 203.4, 142.3, 77.1, 74.7, 66.8, 43.5, 40.2, 25.8, 25.7, 18.1, 17.9, -4.36, -4.51, -4.64, -4.95; HRMS (CI, positive) m/z for $\text{C}_{19}\text{H}_{40}\text{IO}_3\text{Si}_2$ $[\text{M}+\text{H}]^+$: calcd 499.1561, found 499.1572.

C. Preparation of Fragment C: The overall synthetic scheme is figured in **Scheme 2-3**.



Scheme 2-3. Preparation of Fragment C in the synthesis of natural substrate

(E)-3-(Tributylstannyl)prop-2-en-1-ol (38): Propargyl alcohol (1.5 g, 26.7 mmol) was mixed with tributyltin hydride (9.2 mL, 34.7 mmol), to which 2,2'-azobis(2-methylpropionitrile) (AIBN; 43.8 mg, 0.3 mmol) was added at room temperature. The

reaction was gradually heated up to 80 °C over 1 hour and this temperature was maintained for 18 hours under reflux. After completion of the reaction was confirmed by TLC analysis, the crude product was directly subjected to flash column chromatography. The target compound was eluted with Hexane (4.6 g, 13.1 mmol, 50%).

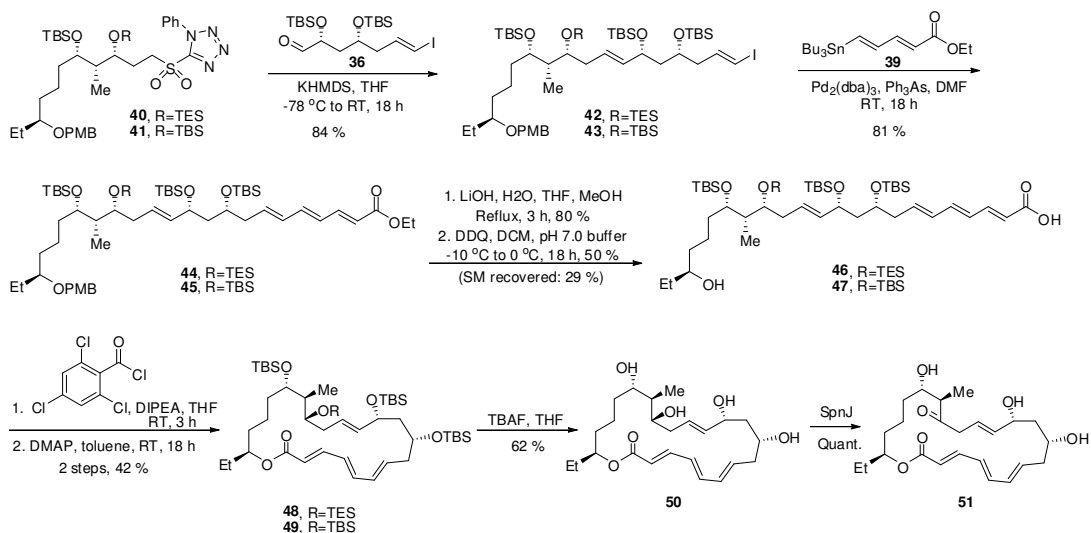
^1H NMR (CDCl_3 , 400 MHz) δ 6.24-6.11 (m, 2H, 1-H, 2-H), 4.15 (*br d*, $J = 3.1$ Hz, 2H, 3-H), 1.58-1.43 (m, 6H, Bu_3Sn), 1.40-1.1.26 (m, 6H, Bu_3Sn), 0.98-0.80 (m, 15H, Bu_3Sn); ^{13}C NMR (CDCl_3 , 100 MHz) δ 147.0, 128.3, 66.4, 29.1, 27.3, 13.7, 9.4; HRMS (CI, positive) m/z for $\text{C}_{15}\text{H}_{33}\text{OSn}$ $[\text{M}+\text{H}]^+$: calcd 349.1548, found 139.1550.

(2E,4Z)-Ethyl 5-(tributylstannyl)penta-2,4-dienoate (39): 1) Activated manganese oxide (3.9 g, 44.3 mmol) was added to a solution of alcohol **72** (1.5 g, 4.4 mmol) in acetone (50 mL) at room temperature. After stirring for 18 hours, the reaction mixture was filtered through a pad of celite to remove the manganese oxide. The filtrate was then concentrated under reduced pressure. The crude residue was briefly purified using flash column chromatography, the target aldehyde compound was eluted with Hexane (1.3 g, 3.8 mmol, 85%). The resulting aldehyde was immediately used for the next step, a Horner-Wadsworth-Emmons reaction. 2) Sodium hydride (60% in mineral oil, 0.3 g, 5.5 mmol) was added to a solution of triethylphosphonoacetate (1.1 mL, 5.5 mmol) in THF (15 mL) at 0 °C. Aldehyde **73** (1.3 g, 3.6 mmol) was added to the resulting suspension. After 4 hours, the reaction was quenched by adding a saturated the aqueous ammonium chloride solution (15 mL), and the mixture was extracted with ethyl acetate (20 mL x 3 times). The combined organic fractions were washed with a brine solution (30 mL), dried over an anhydrous magnesium sulfate pad, and concentrated under reduced pressure. The

crude residue was subjected to flash column chromatography. The target compound was eluted with 2% EtOAc/Hexane solution (1.1 g, 74%).

^1H NMR (CDCl_3 , 400 MHz) δ 7.18 (dd, $J = 15.4, 10.2$ Hz, 1H, 3-H), 6.81 (d, $J = 18.7$ Hz, 1H, 1-H), 6.64 (dd, $J = 10.2$ Hz, 1H, 2-H), 5.79 (d, $J = 15.4$ Hz, 1H, 4-H), 4.20 (q, $J = 7.1$ Hz, 1H, $\text{CH}_3\text{CH}_2\text{ocO}$), 1.56-1.41 (m, 6H, Bu_3Sn), 1.30-1.26 (m, 9H, Bu_3Sn), 0.95-0.78 (m, 15H, Bu_3Sn , $\text{CH}_3\text{CH}_2\text{OCO}$); ^{13}C NMR (CDCl_3 , 100 MHz) δ 167.4, 147.2, 146.3, 144.2, 119.9, 60.2, 29.0, 27.2, 13.7, 9.6; HRMS (CI, positive) m/z for $\text{C}_{19}\text{H}_{37}\text{O}_2\text{Sn}$ $[\text{M}+\text{H}]^+$: calcd 417.1816, found 417.1821.

D. Synthesis of Natural SpnM Substrate by Coupling Reactions and Enzymatic Conversion: The overall synthetic scheme is pictured in **Scheme 2-4**.



Scheme 2-4. Preparation of natural SpnM substrate.

(5S,6S,7R,11R,13R,E)-11-(tert-butyldimethylsilyloxy)-13-((E)-3-iodoallyl)-7-(triethylsilyloxy)-5-((S)-4-(4-methoxybenzyloxy)hexyl)-2,2,3,3,6,15,15,16,16-

nonamethyl-4,14-dioxa-3,15-disilaheptadec-9-en (42): Compound (42) was prepared following the literature reference.

(1E,4R,6R,7E,10R,11R,12S,16S)-4,6,10,12-Tetrakis(tert-butyldimethylsilyloxy)-11-methyl-16-(4-methoxybenzyloxy)octadeca-1,7-diene (43): Potassium hexamethyldisilazide (KHMDs; 0.5 M in toluene, 5.8 mL, 2.9 mmol) was added dropwise over ten min to a solution of fragment A (41) (1.5 g, 1.9 mmol) in THF (19 mL) at -78 °C. The reaction mixture was kept stirring at -78 °C for 1 hour, at which time fragment B (36) (1.1 g, 2.1 mmol) in THF (10 mL) was added to the resulting yellow solution at -78 °C over 30 min. After 4 hours, the temperature was slowly raised to room temperature over 1 hour, at which time the mixture was poured into a saturated the aqueous sodium bicarbonate solution (20 mL). After stirring for 10 min, the aqueous fraction was extracted with ethyl acetate (20 mL × 3 times), dried over an anhydrous sodium sulfate pad, filtered, and concentrated under reduced pressure. The residue was subjected to flash column chromatography. The target compound was eluted with 2% EtOAc/Hexane (1.6 g, 1.5 mmol, 80%).

¹H NMR (CDCl₃, 500 MHz) δ (ppm) 7.27-7.25 (t, 2H, *J* = 4.4 Hz, PhH of PMB), 6.87-6.85 (dt, 2H, *J* = 8.7, 2.8 Hz, PhH of PMB), 6.53-6.47 (m, 1H, 2-CH), 6.09-5.98 (ddt, 1H, *J* = 34.4, 14.4, 1.3 Hz, 1-CH), 5.57-5.51 (m, 1H, 8-CH), 5.43-5.38 (dd, 1H, *J* = 15.4, 6.8 Hz, 7-CH), 4.43 (s, 2H, CH₂ of PMB), 4.12-4.08 (m, 1H, 6-CH), 3.84-3.80 (m, 1H, 4-CH), 3.80 (s, 3H, OCH₃ of PMB), 3.77-3.74 (q, 1H, *J* = 5.6 Hz, 10-CH), 3.70-3.65 (q, 1H, *J* = 5.6 Hz, 12-CH), 3.32-3.27 (quint, 1H, *J* = 5.7 Hz, 16-CH), 2.31-2.21 (m, 3H, 3-CH₂ and 9-CH₂), 2.15-2.08 (m, 1H, 3-CH₂), 1.74-1.69 (m, 1H, 5-CH₂), 1.62-1.25 (m,

10H, 5-CH₂, 11-CH, 13-CH₂, 14-CH₂, 15-CH₂ and 17-CH₂), 0.93-0.84 (m, 42H, 11-C-CH₃, 18-CH₃ and CH₃ of TBS), 0.10-0.01 (m, 24H, CH₃ of TBS); ¹³C NMR (CDCl₃, 125 MHz) δ (ppm) 143.31, 135.54, 129.17, 126.81, 113.71, 79.79, 72.90, 72.25, 70.74, 70.45, 68.22, 55.26, 46.03, 43.47, 41.26, 37.87, 35.40, 33.91, 26.25, 25.99, 25.90, 25.85, 21.30, 18.18, 18.14, 18.12, 18.01, 9.52, -4.24, -4.35, -4.42, -4.49, -4.61, -4.71; HRMS (ESI, positive) *m/z* for C₅₁H₉₉IO₆Si₄Na [M+Na]⁺: 1069.5461, found 1069.5460.

(2E,4E,6E,9R,11R,12E,15R,16S,17S,21S)-Ethyl 9,11,17-tris(tert-butyltrimethylsilyloxy)-15-(triethylsilyloxy)-21-(4-methoxybenzyloxy)-16-methyltricoso-2,4,6,12-tetraenoate (44): Compound (44) was prepared following the literature reference.

(2E,4E,6E,9R,11R,12E,15R,16R,17S,21S)-Ethyl 9,11,15,17-Tetrakis(tert-butyltrimethylsilyloxy)-16-methyl-21-(4-methoxybenzyloxy)tricoso-2,4,6,12-tetraenoate (45): Tris(dibenzylideneacetone) dipalladium (Pd₂(dba)₃; 71 mg, 0.08 mmol) and triphenylarsine (71 mg, 0.23 mmol) was added to a solution of vinyl iodide (43, 1.6 g, 1.5 mmol) and fragment C (39) (1.0 g, 2.3 mmol) in anhydrous *N,N*-dimethylformamide (30 mL) at room temperature. The reaction mixture was stirred for 18 hours at room temperature, at which time ethyl acetate (150 mL) was added. The reaction mixture was washed with water (50 mL × 4 times), and resulting organic fraction was dried over an anhydrous sodium sulfate pad, filtered, and concentrated under reduced pressure. The residue was subjected to flash column chromatography. The target compound was eluted with 2% EtOAc/Hexane (1.2 g, 1.2 mmol, 76%).

^1H NMR (CDCl_3 , 500 MHz) δ (ppm) 7.32-7.25 (m, 3H, 3-CH and PhH of PMB), 6.87-6.85 (d, 2H, $J = 8.6$ Hz, PhH of PMB), 6.54-6.49 (m, 1H, 5-CH), 6.23-6.18 (m, 1H, 4-CH), 6.15-6.10 (m, 1H, 6-CH), 5.94-5.88 (m, 1H, 7-CH), 5.86-5.83 (d, 1H, $J = 15.4$ Hz, 2-CH), 5.57-5.51 (m, 1H, 13-CH), 5.43-5.38 (m, 1H, 7-CH), 4.43 (s, 2H, CH_2 of PMB), 4.22-4.18 (q, 2H, $J = 7.1$ Hz, CH_2CH_3 of OEt), 4.15-4.11 (m, 1H, 11-CH), 3.86-3.82 (m, 1H, 9-CH), 3.79 (s, 3H, OCH_3 of PMB), 3.76-3.75 (m, 1H, 15-CH), 3.69-3.68 (m, 1H, 17-CH), 3.30-3.28 (m, 1H, 21-CH), 2.39-2.36 (m, 1H, 8- CH_2), 2.27-2.17 (m, 3H, 14- CH_2 and 8- CH_2), 1.74-1.69 (m, 1H, 10- CH_2), 1.63-1.26 (m, 13H, 10- CH_2 , 16-CH, 18- CH_2 , 19- CH_2 , 20- CH_2 , 22- CH_2 and CH_2CH_3 of OEt), 0.93-0.84 (m, 42H, 16-C- CH_3 , 23- CH_3 and CH_3 of TBS), 0.04-0.01 (m, 24H, CH_3 of TBS); ^{13}C NMR (CDCl_3 , 125 MHz) δ (ppm) 167.17, 159.02, 144.72, 140.89, 136.54, 135.62, 132.03, 129.18, 128.13, 126.76, 120.27, 113.71, 79.79, 72.89, 72.27, 70.81, 70.46, 68.95, 60.19, 55.25, 46.16, 41.26, 40.76, 37.89, 35.42, 33.91, 26.26, 25.99, 25.98, 25.91, 25.86, 21.30, 18.18, 18.14, 18.04, 14.32, 9.52, -3.72, -3.93, -4.26, -4.31, -4.37, -4.51, -4.72; HRMS (ESI, positive) m/z for $\text{C}_{58}\text{H}_{108}\text{O}_8\text{Si}_4$ [$\text{M}+\text{Na}$] $^+$: calcd 1067.7019, found 1067.7005.

(2E,4E,6E,9R,11R,12E,15R,16S,17S,21S)-9,11,17-tris(tert-butyldimethylsilyloxy)-15,21-dihydroxy-16-methyltricoso-2,4,6,12-tetraenoic acid (46): Compound (46) was prepared following the literature reference.

(2E,4E,6E,9R,11R,12E,15R,16R,17S,21S)-9,11,15,17-Tetrakis(tert-butyldimethylsilyloxy)-21-hydroxy-16-methyltricoso-2,4,6,12-tetraenoic acid (47): 1) 0.5 N Lithium hydroxide solution (8 mL) was added to a solution of long-chain compound (45, 0.31 g, 0.30 mmol) in THF (8 mL) and methanol (8 mL) at room

temperature. The reaction mixture was stirred under reflux for 3 hours, at which time volatile solvents were concentrated under reduced pressure. The pH of the aqueous solution was adjusted to approximately 7, and the mixture was extracted with ethyl acetate (20 mL \times 3 times). The organic fractions were pooled, washed with brine (20 mL), dried over an anhydrous sodium sulfate, and concentrated under reduced pressure. The residue was subjected to flash column chromatography, a carboxylic acid compound was eluted with 20% EtOAc/Hexane (0.24 g, 0.24 mmol, 80%).

^1H NMR (CDCl_3 , 500 MHz) δ (ppm) 7.40-7.34 (dd, 1H, $J = 15.1, 11.5$ Hz 3-CH), 7.27-7.25 (m, 2H, PhH of PMB), 6.87-6.84 (dt, 2H, $J = 8.7, 2.8, 2.1$ Hz, PhH of PMB), 6.58-6.53 (dd, 1H, $J = 14.8, 10.9$ Hz, 5-CH), 6.26-6.20 (dd, 1H, $J = 14.8, 11.6$ Hz, 4-CH), 6.17-6.12 (m, 1H, 6-CH), 5.98-5.92 (m, 1H, 7-CH), 5.88-5.83 (dd, 1H, $J = 15.1, 10.3$ Hz, 2-CH), 5.57-5.51 (m, 1H, 13-CH), 5.43-5.38 (dd, 1H, $J = 15.4, 6.8$ Hz, 7-CH), 4.43 (s, 2H, CH_2 of PMB), 4.14-4.11 (q, 1H, $J = 6.2$ Hz, 11-CH), 3.85-3.83 (m, 1H, 9-CH), 3.79 (s, 3H, OCH_3 of PMB), 3.77-3.73 (q, 1H, $J = 5.6$ Hz, 15-CH), 3.70-3.67 (m, 1H, 17-CH), 3.30-3.27 (m, 1H, 21-CH), 2.41-2.37 (m, 1H, 8- CH_2), 2.27-2.17 (m, 3H, 14- CH_2 and 8- CH_2), 1.75-1.26 (m, 11H, 10- CH_2 , 16-CH, 18- CH_2 , 19- CH_2 , 20- CH_2 and 22- CH_2), 0.90-0.84 (m, 42H, 16-C- CH_3 , 23- CH_3 and CH_3 of TBS), 0.04-0.01 (m, 24H, CH_3 of TBS); ^{13}C NMR (CDCl_3 , 125 MHz) δ (ppm) 159.03, 147.05, 142.06, 135.60, 131.94, 129.19, 127.86, 126.80, 118.65, 113.72, 79.80, 72.90, 72.27, 70.82, 70.47, 68.92, 55.26, 46.17, 41.27, 40.77, 37.89, 35.42, 33.92, 26.26, 25.98, 25.91, 25.86, 21.31, 18.18, 18.15, 18.05, 9.51, -3.72, -3.75, -3.91, -4.25, -4.31, -4.37, -4.50, -4.71; HRMS (ESI, negative) m/z for $\text{C}_{56}\text{H}_{103}\text{O}_8\text{Si}_4$ $[\text{M}-\text{H}]^-$: 1015.6736, found 1015.6731.

2) 2,3-Dichloro-5,6-dicyano-*p*-benzoquinone (DDQ; 107 mg, 0.47 mmol) was added to a solution of the carboxylic acid from the previous step (0.24 g, 0.24 mmol) in dichloromethane (22 mL) and pH 7 phosphate buffer (2.4 mL) at 0 °C. The reaction mixture was stirred at 0 °C for 6 hours, at which time saturated the aqueous sodium bicarbonate solution (6 mL) was added. The organic and aqueous fractions were separated, and the aqueous fraction was extracted with ethyl acetate (40 mL × 3 times). The combined organic fractions were washed with brine (20 mL), dried over an anhydrous sodium sulfate, and concentrated under reduced pressure. The residue was subjected to flash column chromatography. The target compound was eluted with 20% to 50% EtOAc/Hexane (0.16 g, 0.18 mmol, 75%).

¹H NMR (CDCl₃, 500 MHz) δ (ppm) 7.36 (dd, J = 15.3, 11.3 Hz, 1H, 3-H), 6.55 (dd, J = 14.8, 10.5 Hz, 1H, 5-H), 6.22 (dd, J = 14.8, 11.3 Hz, 1H, 4-H), 6.14 (dd, J = 15.3, 10.5 Hz, 1H, 6-H), 5.94 (dt, J = 15.3, 7.4 Hz, 1H, 7-H), 5.82 (d, J = 15.1 Hz, 1H, 2-H), 5.54 (dt, J = 15.5, 7.2 Hz, 1H, 13-H), 5.39 (dd, J = 15.5, 6.8 Hz, 1H, 12-H), 4.12 (br q, J = 12.6, 7.1 Hz, 1H, 11-H), 3.81 (br quint, J = 17.0, 11.8, 6.6 Hz, 1H, 9-H), 3.73 (q, J = 11.0, 5.5 Hz, 1H, 15-H), 3.67 (q, J = 10.5, 5.5 Hz, 1H, 17-H), 3.48 (m, 1H, 21-H), 2.39-2.34 (m, 1H, 8-H), 2.24-2.18 (m, 3H, 8-H, 14-H), 1.70 (ddd, J = 13.5, 7.7, 5.5 Hz, 1H, 10-H), 1.61-1.18 (m, 10H, 10-H, 16-H, 18-H, 19-H, 20-H, 22-H), 0.92 (t, J = 7.5 Hz, 3H, 23-H), 0.87-0.83 (m, 36H, TBS), 0.83 (d, J=7 Hz, 3H, 16-Me), 0.04-(-0.01) (m, 24H, TBS); ¹³C NMR (CDCl₃, 125 MHz) δ (ppm) 171.3, 147.0, 142.0, 137.4, 135.8, 132.0, 127.9, 126.9, 120.0, 73.1, 72.6, 72.2, 70.9, 69.0, 60.2, 46.2, 40.8, 40.6, 37.7, 37.4, 35.1, 30.1, 25.95, 25.93, 25.87, 21.3, 18.2, 18.16, 18.13, 18.0, 9.9, 9.3, -3.77, -3.82, -3.99, -

4.28, -4.37, -4.38, -4.59, -4.71; HRMS (CI, negative) m/z for $C_{48}H_{96}O_7Si_4$ $[M-H]^-$: calcd 896.6233, found 896.6230.

(3E,5E,7E,10R,12R,13E,16R,17S,18S,22S)-10,12,18-tris(tert-butyldimethylsilyloxy)-22-ethyl-16-(triethylsilyloxy)-17-methyloxacyclodocosa-3,5,7,13-tetraen-2-one (48):

Compound (48) was prepared following the literature reference.

(3E,5E,7E,10R,12R,13E,16R,17R,18S,22S)-10,12,16,18-tetrakis(tert-butyldimethylsilyloxy)-22-ethyl-17-methyloxacyclodocosa-3,5,7,13-tetraen-2-one

(49): A solution of *N,N*-diisopropylethylamine (0.92 mL, 0.4 M, 0.37 mmol) and activated 4 Å molecular sieve (164 mg) was mixed with acid compound (**47**, 164 mg, 0.18 mmol) in THF (36 mL). 2,4,6-Trichlorobenzoyl chloride solution (0.50 mL, 0.4 M, 0.20 mmol) was added to the mixture at room temperature. The reaction mixture was stirred at room temperature for 3 hours, and concentrated under reduced pressure to afford the crude anhydride intermediate. A solution of the obtained anhydride in toluene (20 mL) was added to a solution of *N,N*-dimethylaminopyridine (DMAP; 67 mg, 0.55 mmol) in toluene (30 mL) using a syringe pump over 3 hours. At the end of the addition, the syringe was rinsed with additional toluene (2 mL). After stirring for 18 hours, the mixture was quenched with a saturated aqueous sodium bicarbonate solution (20 mL), and the aqueous fraction was extracted with ethyl acetate (40 mL x 3 times). The combined organic fractions were washed with brine (20 mL), dried over an anhydrous sodium sulfate pad, and concentrated under reduced pressure. The crude residue was purified using flash column chromatography. The target compound was eluted with 2% EtOAc/Hexane (141 mg, 0.16 mmol, 88%).

^1H NMR (CDCl_3 , 500 MHz) δ (ppm) 7.24 (dd, $J = 15.3, 11.3$ Hz, 1H, 3-H), 6.47 (dd, $J = 14.8, 10.5$ Hz, 1H, 5-H), 6.21 (dd, $J = 14.8, 11.3$ Hz, 1H, 4-H), 6.11 (dd, $J = 15.3, 10.5$ Hz, 1H, 6-H), 5.79 (d, $J = 15.1$ Hz, 1H, 2-H), 5.77 (dt, $J = 15.3, 7.4$ Hz, 1H, 7-H), 5.38 (dt, $J = 15.5, 7.2$ Hz, 1H, 13-H), 5.27 (dd, $J = 15.5, 6.8$ Hz, 1H, 12-H), 4.85 (m, 1H, 21-H), 4.01 (br dd, $J = 13.4, 6.7$ Hz, 1H, 11-H), 3.75 (br ddd, $J = 13.0, 9.0, 5.0$ Hz, 1H, 9-H), 3.67 (br dd, $J = 9.0, 5.5$ Hz, 1H, 15-H), 3.57 (br dd, $J = 10.0, 6.0$ Hz, 1H, 17-H), 2.46-2.42 (m, 1H, 8-H), 2.24-2.18 (m, 2H, 14-H, 8-H), 2.12-2.08 (m, 1H, 14-H), 1.42-1.17 (m, 11H, 10-H, 16-H, 18-H, 19-H, 20-H, 22-H), 0.91 (t, $J = 7.5$ Hz, 3H, 23-H), 0.874 (s, 9H, TBS), 0.897 (s, 9H, TBS), 0.85 (s, 9H, TBS), 0.93 (s, 9H, TBS), 0.74 (d, 3H, $J = 7.0$ Hz, 16-Me), 0.04-(-0.01) (m, 24H, TBS); ^{13}C NMR (CDCl_3 , 125 MHz) δ (ppm) 167.0, 144.8, 140.9, 136.0, 135.2, 132.0, 128.0, 127.0, 120.8, 75.2, 73.2, 72.1, 71.1, 69.1, 46.6, 42.3, 42.1, 38.4, 34.4, 33.4, 29.7, 27.8, 26.04, 25.99, 25.91, 25.8, 21.1, 18.18, 18.14, 18.08, 18.02, 10.2, 9.9, -3.47, -3.87, -3.97, -4.33, -4.41, -4.53, -4.62; HRMS (CI, negative) m/z for $\text{C}_{48}\text{H}_{94}\text{O}_6\text{Si}_4$ [$\text{M}-\text{H}$] $^-$: calcd 878.6128, found 878.6128.

(3E,5E,7E,10R,12R,13E,16R,17R,18S,22S)-22-ethyl-10,12,16,18-tetrahydroxy-17-methyloxacyclodocosa-3,5,7,13-tetraen-2-one (50): A solution of the macrolactone (141 mg, 0.16 mmol) in hydrogen fluoride-pyridine complex (1.4 mL) was stirred at 0 °C for 4 days until the starting material was no longer detectable. After quenching with a saturated the aqueous sodium bicarbonate solution (20 mL) at 0 °C, the aqueous fraction was extracted with dichloromethane (30 mL x 3 times). The combined organic fractions were dried over an anhydrous sodium sulfate pad, and concentrated under reduced

pressure. The resulting residue was purified using flash column chromatography. The target compound was eluted with 5% MeOH/DCM solution (41 mg, 0.097 mmol, 62%).

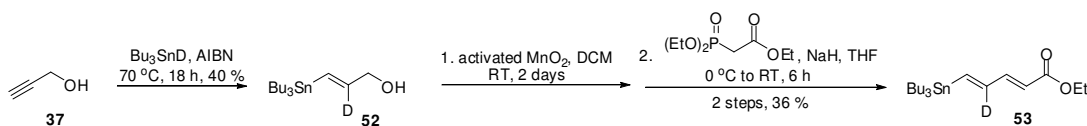
^1H NMR (DMSO- d_6 , 500 MHz) δ (ppm) 7.25 (dd, $J = 15.2, 11.3$ Hz, 1H, 3-H), 6.70 (dd, $J = 14.9, 10.9$ Hz, 1H, 5-H), 6.35 (dd, $J = 14.9, 11.3$ Hz, 1H, 4-H), 6.18 (dd, $J = 15.2, 10.9$ Hz, 1H, 6-H), 5.89 (ddd, $J = 15.2, 10.3, 5.4$ Hz, 1H, 7-H), 5.85 (d, $J = 15.2$ Hz, 1H, 2-H), 5.29 (app dd, $J = 15.4, 7.2$ Hz, 1H, 12-H), 5.18 (ddd, $J = 15.4, 7.6, 5.9$ Hz, 1H, 13-H), 4.75 (quint, $J = 6.2$ Hz, 1H, 21-H), 4.64 (br s, 1H, OH), 4.51 (br s, 1H, OH), 4.38 (br m, 2H, OH), 3.78 (br s, 1H, 11-H), 3.69 (br s, 1H, 9-H), 3.50 (br s, 1H, 15-H), 3.45 (br s, 1H, 17-H), 2.52-2.50 (m, 1H, 8-H), 2.08-1.86 (m, 3H, 8-H, 14-H), 1.60-1.45 (m, 5H, 10-H, 19-H, 22-H), 1.40-1.21 (m, 5H, 10-H, 18-H, 20-H), 1.19-1.54 (m, 1H, 16-H), 0.84 (t, $J = 7.3$ Hz, 3H, 23-H), 0.67 (d, $J = 7.1$ Hz, 3H, 16-Me); ^{13}C NMR (DMSO- d_6 , 125 MHz) δ (ppm) 165.9, 144.7, 141.5, 137.0, 136.2, 131.7, 127.8, 126.0, 120.2, 74.7, 74.4, 73.3, 69.4, 66.9, 54.9, 45.8, 42.8, 38.4, 33.8, 32.8, 27.3, 21.3, 9.72, 6.06; HRMS (CI, negative) m/z for $\text{C}_{24}\text{H}_{38}\text{O}_6$ $[\text{M}-\text{H}]^-$: calcd 422.2668, found 422.2664.

SpnM Natural substrate (51): SpnJ (7.0 mL of 50 μM in 50 mM Tris·HCl buffer) was added to a solution of macrolactone (20.7 mg, 4 mM in DMSO) in Tris·HCl buffer (2.63 mL of 100 mM Tris·HCl, pH 8.0 and 1.40 mL of water) at 30 $^\circ\text{C}$ to initiate the enzymatic reaction (total volume 12.25 mL, DMSO 10% v/v). Through the incubation, the reaction was monitored by HPLC using a 4 x 250 mm Econosil C18 column (Alltech). The detector was set at 254 nm, and the solution was eluted from the column at 1 mL/min using the following gradient: initially 30% acetonitrile, the concentration of acetonitrile was increased linearly to 45% over 30 min, then increased linearly to 80% over 3 min,

and finally decreased linearly back to 30% over 3 min. After 2.5 hours of incubation at 30 °C the reaction appeared to have reached completion, the reaction mixture was then directly filtered through a YM-10 filter by centrifugation at 4,000 rpm over 40 min. The clear filtrate was purified by semi-preparative HPLC using a 10 x 250 mm Econosil C18 column (254 nm, Alltech). The solution was eluted from the column at a rate of 4 mL/min with water versus acetonitrile by following gradient: initially 30% acetonitrile, concentration of acetonitrile was increased linearly to 45% over 30 min, and again increased linearly to 80% over 3 min, and finally decreased linearly back to 30% over 3 min. The collected fractions were pooled, extracted with EtOAc (50 mL x 3 times), dried over an anhydrous sodium sulfate pad, and concentrated under reduce pressure (19.0 mg, 92%). All spectral data is identical to the literature reference.

2.2.4. Synthesis of the [C4-²H] SpnM Substrate Analog (C4-D analog)

A. Preparation of Fragment C: The overall synthetic scheme is figured in **Scheme 2-5**.



Scheme 2-5. Preparation of Fragment C for in the synthesis of [C4-²H] substrate analog.

(E)-3-(Tributylstannyl)prop-2-en-1-ol (52): Compound (**52**) was prepared following the same procedure as compound (**38**) using tributyltin deuteride instead of tributyltin hydride with a yield of 40%.

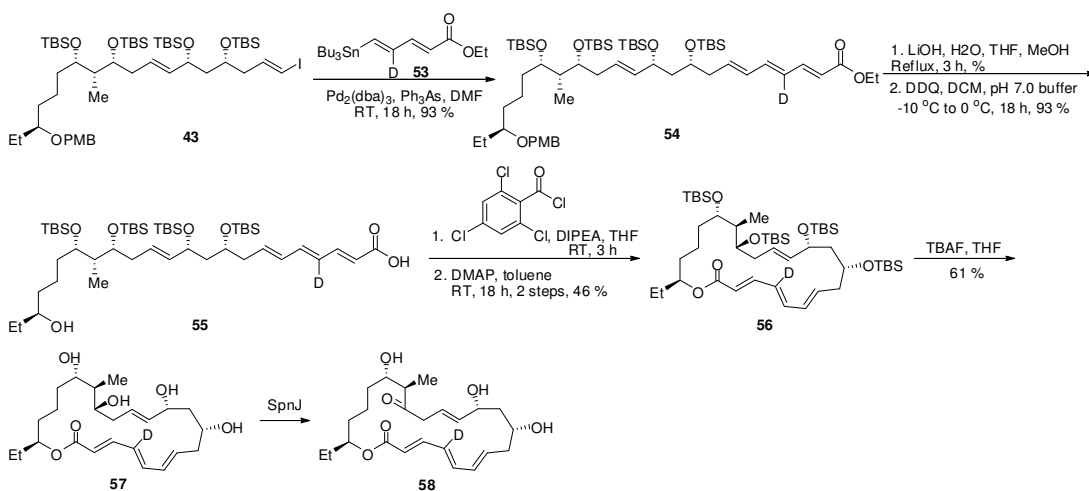
¹H NMR (CDCl₃, 400 MHz) δ (ppm) 6.27-6.13 (m, 1H, 3-H), 4.18-4.16 (m, 2H, 1-CH₂), 1.57-1.47 (m, 6H, Bu₃Sn), 1.41-1.27 (m, 6H, Bu₃Sn), 1.02-0.82 (m, 15H, Bu₃Sn); ¹³C NMR (CDCl₃, 100 MHz) δ (ppm) 146.86, 146.67, 146.48, 128.20, 66.32,

29.06, 27.27, 13.68, 9.44; HRMS (CI, positive) m/z for $C_{15}H_{31}DOSn$ $[M+H]^+$: calcd 350.1616, found 350.1618.

(2E,4Z)-Ethyl 5-(tributylstannyl)penta-2,4-dienoate (53): Compound **(53)** was prepared following the same procedure as compound **(39)** with a yield of 36% for 2 steps.

1H NMR ($CDCl_3$, 400 MHz) δ (ppm) 7.19 (d, 1H, $J = 15.4$ Hz, 3-H), 6.80 (s, 1H, 5-H), 5.82 (d, 1H, $J = 15.4$ Hz, 2-H), 4.23-4.18 (q, 2H, $J = 7.1$ Hz, $\underline{CH_2-CH_3}$), 1.55-1.47 (m, 6H, Bu_3Sn), 1.35-1.27 (m, 9H, $Bu_3Sn+CH_2-\underline{CH_3}$), 0.96-0.87 (m, 15H, Bu_3Sn); ^{13}C NMR ($CDCl_3$, 100 MHz) δ (ppm) 167.41, 147.01, 146.25, 144.08, 119.88, 60.26, 29.03, 27.22, 14.30, 13.66, 9.63; HRMS (CI, positive) m/z for $C_{19}H_{36}DO_2Sn$ $[M+H]^+$: 418.1878, found 418.1882

B. Synthesis of $[C4-^2H]$ SpnM Substrate by Coupling Reactions and Enzymatic Conversion: The overall synthetic scheme is pictured in **Scheme 2-6**.



Scheme 2-6. Preparation of $[C4-^2H]$ SpnM substrate

(2E,4E,6E,9R,11R,12E,15R,16R,17S,21S)-Ethyl 9,11,15,17-Tetrakis(tert-butyltrimethylsilyloxy)-16-methyl-21-(4-methoxybenzyloxy)tricos-2,4,6,12-

tetraenoate (54): Compound (**54**) was prepared following the same procedure as compound (**45**) using compound (**53**) instead of compound (**39**) with a yield of 93%.

^1H NMR (CDCl_3 , 500 MHz) δ (ppm) 7.31-7.25 (m, 3H, Ph of PMB+3-CH), 6.87-6.84 (m, 2H, Ph of PMB), 6.52 (d, 1H, $J = 10.8$ Hz, 5-CH), 6.17-6.10 (m, 1H, 6-CH), 5.94-5.89 (m, 1H, 7-CH), 5.86 (d, 1H, $J = 15.3$ Hz, 2-CH), 5.57-5.51 (m, 1H, 13-CH), 5.43-5.39 (dd, 1H, $J = 15.4, 6.8$ Hz, 12-CH), 4.43 (s, 2H, CH_2 of PMB), 4.22-4.18 (q, 2H, $J = 7.1$ Hz, $\text{CH}_3\text{CH}_2\text{CO}(\text{O})$), 4.15-4.11 (q, 1H, $J = 6.6$ Hz, 11-CH), 3.86-3.81 (m, 1H, 9-CH), 3.79 (s, 3H, OCH_3 of PMB), 3.77-3.74 (m, 1H, 15-CH), 3.70-3.67 (m, 1H, 17-CH), 3.30-3.27 (m, 1H, 21-CH) 2.40-2.35 (m, 1H, 8- CH_2), 2.27-2.20 (m, 3H, 8- CH_2 +14-CH), 1.75-1.69 (m, 1H, 10- CH_2), 1.62-1.25 (m, 13H, 10- CH_2 +16-CH +18- CH_2 +19- CH_2 +20- CH_2 +22- CH_2 + $\text{CH}_3\text{CH}_2\text{CO}(\text{O})$), 0.92-0.84 (m, 42H, CH_3 of TBS+16- CH_3 +23- CH_3), 0.04-0.01 (m, 24H, CH_3 of TBS); ^{13}C NMR (CDCl_3 , 125 MHz) δ (ppm) 167.15, 159.01, 144.64, 140.78, 136.49, 135.61, 131.99, 131.29, 129.17, 126.75, 120.23, 113.70, 79.78, 72.88, 72.25, 70.80, 70.45, 68.94, 60.17, 55.24, 46.15, 41.23, 40.75, 37.87, 35.41, 33.90, 25.98, 25.90, 25.86, 21.29, 18.16, 18.13, 18.03, 14.31, 9.50, -3.74, -3.76, -3.94, -4.27, -4.32, -4.38, -4.52, -4.73; HRMS (ESI, positive) m/z for $\text{C}_{58}\text{H}_{107}\text{DO}_8\text{Si}_4 \text{Na}$ $[\text{M}+\text{Na}]^+$: calcd 1068.7076, found 1068.7065.

(2E,4E,6E,9R,11R,12E,15R,16R,17S,21S)-9,11,15,17-Tetrakis(tert-butyltrimethylsilyloxy)-21-hydroxy-16-methyltricoso-2,4,6,12-tetraenoic acid (55): Compound (**55**) was prepared following the same procedure as compound (**47**) with a yield of 43% for 2 steps.

^1H NMR (CDCl_3 , 500 MHz) δ (ppm) 7.38 (d, 1H, 3-CH), 6.56 (d, 1H, 5-CH), 6.18-6.13 (dd, 1H, $J = 14.8, 11.0$ Hz, 6-CH), 5.96-5.95 (m, 1H, 7-CH), 5.87 (d, 1H, $J = 15.1$ Hz, 2-CH), 5.59-5.52 (m, 1H, 13-CH), 5.44-5.40 (dd, 1H, $J = 15.4, 6.7$ Hz, 12-CH), 4.16-4.12 (q, 1H, $J = 6.6$ Hz, 11-CH), 3.85-3.82 (q, 1H, $J = 5.6$ Hz, 9-CH), 3.76-3.73 (q, 1H, $J = 5.3$ Hz, 15-CH), 3.71-3.68 (q, 1H, $J = 5.1$ Hz, 17-CH), 3.51-3.48 (m, 1H, 21-CH) 2.40-2.38 (m, 1H, 8- CH_2), 2.27-2.22 (m, 3H, 8- CH_2 +14-CH), 1.75-1.26 (m, 11H, 10- CH_2 +16-CH +18- CH_2 +19- CH_2 +20- CH_2 +22- CH_2), 0.95-0.84 (m, 42H, CH_3 of TBS+16- CH_3 +23- CH_3), 0.04-0.02 (m, 24H, CH_3 of TBS); ^{13}C NMR (CDCl_3 , 125 MHz) δ (ppm) 171.93, 146.90, 141.89, 137.30, 135.64, 132.00, 127.58, 126.87, 126.68, 119.23, 73.12, 73.09, 72.77, 72.64, 72.18, 70.79, 68.99, 46.14, 40.90, 40.81, 40.63, 37.80, 37.67, 37.41, 35.05, 30.09, 29.69, 27.84, 27.03, 21.32, 21.26, 18.19, 18.15, 18.12, 18.04, 16.49, 9.87, 9.31, -3.78, -3.82, -3.96, -4.00, -4.28, -4.31, -4.32, -4.38, -4.60, -4.71; HRMS (ESI, positive) m/z for $\text{C}_{48}\text{H}_{95}\text{DO}_7\text{Si}_4$ $[\text{M}-\text{H}]^-$: calcd 896.6223, found 896.6215.

(3E,5E,7E,10R,12R,13E,16R,17R,18S,22S)-10,12,16,18-tetrakis(tert-butyltrimethylsilyloxy)-22-ethyl-17-methyloxacyclodocosa-3,5,7,13-tetraen-2-one
(56): Compound **(56)** was prepared following the same procedure as compound **(49)** with a yield of 72%.

^1H NMR (CDCl_3 , 500 MHz) δ (ppm) 7.24 (d, $J = 15.0$, 1H, C3-H), 6.45 (d, $J = 10.5$ Hz, 1H, C5-H), 6.11 (dd, $J = 15.5, 10.5$ Hz, 1H, C6-H), 5.80 (d, $J = 15.0$ Hz, 1H, C2-H), 5.78 (dt, $J = 15.5, 8.0$ Hz, 1H, C7-H), 5.42-5.22 (m, 2H, C12-H and C13-H), 4.90-4.80 (m, 1H, C21-H), 4.01 (q, $J = 7.0$ Hz, 1H, C11-H), 3.80-3.72 (m, 1H, C9-H), 3.71-3.64 (m, 1H, C15-H), 3.61-3.52 (m, 1H, C17-H), 2.50-2.06 (m, 4H, C8H and C14-

H), 1.781.16 (m, 11H, C10-H, C16-H, C18H, C19-H, C20-H, C22-H), 0.91-0.80 (m, 39H, *t*-Bu of TBS and C23-H), 0.75 (d, $J = 7.0$ Hz, 3H, C16-Me), 0.08-0.06 (m, 24H, CH₃ of TBS); ¹³C NMR (CDCl₃, 125 MHz) δ (ppm) 166.9, 144.7, 140.8, 136.0, 135.2, 131.9, 128.0, 127.1, 120.8, 75.2, 73.2, 71.1, 69.1, 46.6, 42.3, 42.1, 38.4, 34.4, 33.4, 27.8, 26.1, 26.0, 26.0, 25.9, 25.9, 25.8, 21.1, 18.2, 18.2, 18.1, 18.1, 18.1, 18.1, 18.1, 18.0, 10.2, 9.9, -3.5, -3.8, -4.0, -4.3, -4.4, -4.5, -4.5, -4.6, -4.6, -4.7, -4.7; HRMS (ESI) m/z for C₄₈H₉₃DO₆Si₄ [M+Na]⁺: calcd 902.60824, found 902.60711.

(3E,5E,7E,10R,12R,13E,16R,17R,18S,22S)-22-ethyl-10,12,16,18-tetrahydroxy-17-methyloxacyclodocosa-3,5,7,13-tetraen-2-one with [C4-²H] (57): Compound (**57**) was prepared following the same procedure as compound (**50**) with a yield of 61%.

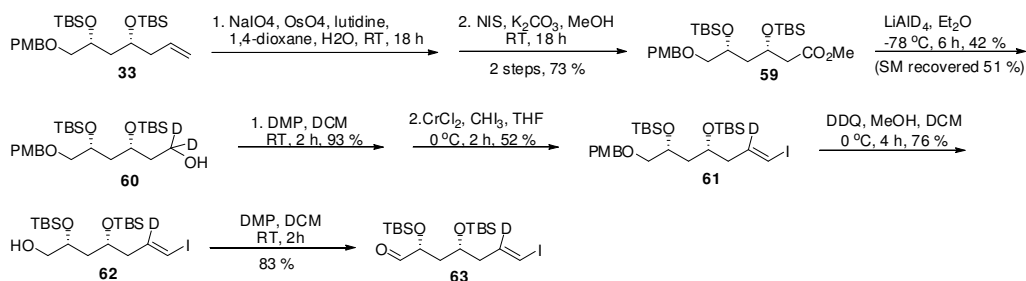
¹H NMR (CDCl₃, 500 MHz) δ (ppm); ¹³C NMR (CDCl₃, 125 MHz) δ (ppm); HRMS (ESI, positive) m/z for C₂₄H₃₇DO₆ Na [M+Na]⁺: calcd 446.2623, found 446.2625.

[C4-²H] SpnM substrate analog (58): [C4-²H] SpnM substrate (**58**) was prepared following the same procedure as SpnM natural substrate (**51**) quantitatively.

HRMS (ESI, positive) m/z for C₂₄H₃₅DO₆ Na [M+Na]⁺: calcd 444.2467, found 444.2461.

2.2.5. Synthesis of the [C7-²H] SpnM Substrate Analog (C7-D analog)

A. Preparation of Fragment B: The overall synthetic scheme is depicted in **Scheme 2-7**.



Scheme 2-7. Preparation of fragment B for the synthesis of [C7-2H] substrate analog

(5R,7R)-5-((E)-3-iodoallyl)-7-((4-methoxybenzyloxy)methyl)-2,2,3,3,9,9,10,10-

octamethyl-4,8-dioxa-3,9-disilaundecane (59): 1) Allyl compound (10.0 g, 0.02 mol) was mixed with water (20 mL) and a solution sodium (meta)periodate (13.0 g, 0.06 mol), osmium (VIII) oxide (0.12 g, 0.48 mmol), 2,6-lutidine (3.5 mL, 0.03 mol) in 1,4-dioxane (61 mL) at 0 °C with stirring for 18 hours. After quenching with the aqueous 1 N sodium thiosulfate solution (40 mL) with stirring for 1 hour, the reaction mixture was filtered through a paper filter, and extracted with dichloromethane (100 mL x 3 times). The combined organic fractions were washed with brine (150 mL), dried over an anhydrous sodium sulfate pad, and concentrated under reduced pressure. The resulting residue was purified using flash column chromatography, an aldehyde compound was eluted with 5% to 10% EtOAc/Hexane with a quantitative yield. 2) N-Iodosuccinimide (NIS; 11.3 g, 0.05 mol) and potassium carbonate (6.9 g, 0.05 mol) was added to a solution of aldehyde from previous step in methanol (100 mL) at room temperature. The reaction mixture was stirred at room temperature for 18 hours, and quenched with saturated the aqueous sodium thiosulfate solution (200 mL). The aqueous fraction was extracted with dichloromethane (150 mL x 3 times), and collected organic fractions were dried over an anhydrous sodium sulfate pad, filtered and concentrated under the reduced pressure. The

resulting residue was subjected to flash column chromatography. The target compound was eluted with EtOAc/Hexane (7.2 g, 73%). Spectral data was not collected.

(3R,5R)-3,5-bis(tert-butyldimethylsilyloxy)-6-(4-methoxybenzyloxy)hexan-1-ol with 1,1-dideuteride (60): Lithium aluminum deuteride (144 mg, 3.4 mmol) was added to a solution of ester compound (3.0 g, 5.7 mmol) in anhydrous diethylether (40 mL) at -78 °C, and the reaction mixture was stirred at -78 °C for 6 hours. Rochelle's salt solution (10 mL) was slowly added to quench the reaction. The organic fraction was separated and the aqueous fraction was extracted with ethyl acetate (100 mL \times 3 times). The combined organic fractions were dried over an anhydrous magnesium sulfate pad, concentrated under reduced pressure, and purified using flash column chromatography, 1,1-dideuterated alcohol was eluted with 10% to 20% EtOAc/Hexane (1.2 g, 2.4 mmol, 42%). Some of the starting material was recovered (1.5 g, 2.9 mmol, 51%).

^1H NMR (CDCl_3 , 500 MHz) δ (ppm) 7.23-7.21 (dt, 2H, $J = 8.7, 2.8, 2.1$ Hz, PhH of PMB), 6.86-6.84 (dt, 2H, $J = 8.7, 2.8, 2.1$ Hz, PhH of PMB), 4.42 (s, 2-H, CH2 of PMB), 4.10-4.04 (m, 1H, 5-CH), 3.83-3.79 (m, 1H, 3-CH), 3.77 (s, 3H, OCH3 of PMB), 3.36-3.29 (m, 2H, 6-CH2), 1.85-1.76 (m, 2H, 2-CH2), 1.71-1.59 (m, 2H, 4-CH2), 0.87 (s, 9H, CH3 of TBS), 0.86 (s, 9H, CH3 of TBS), 0.06 (d, 6H, $J = 7.0$ Hz, CH3 of TBS), 0.02 (s, 6H, CH3 of TBS); ^{13}C NMR (CDCl_3 , 125 MHz) δ (ppm) 159.09, 130.30, 129.15, 113.65, 74.66, 72.89, 68.93, 55.14, 51.31, 41.78, 37.15, 25.80, 25.77, 18.02, 17.84, -4.21, -4.49, -4.83, -4.90; HRMS (ESI, positive) m/z for $\text{C}_{26}\text{H}_{48}\text{D}_2\text{O}_5\text{Si}_2$ $[\text{M}+\text{Na}]^+$: calcd 523.3215, found 523.3206.

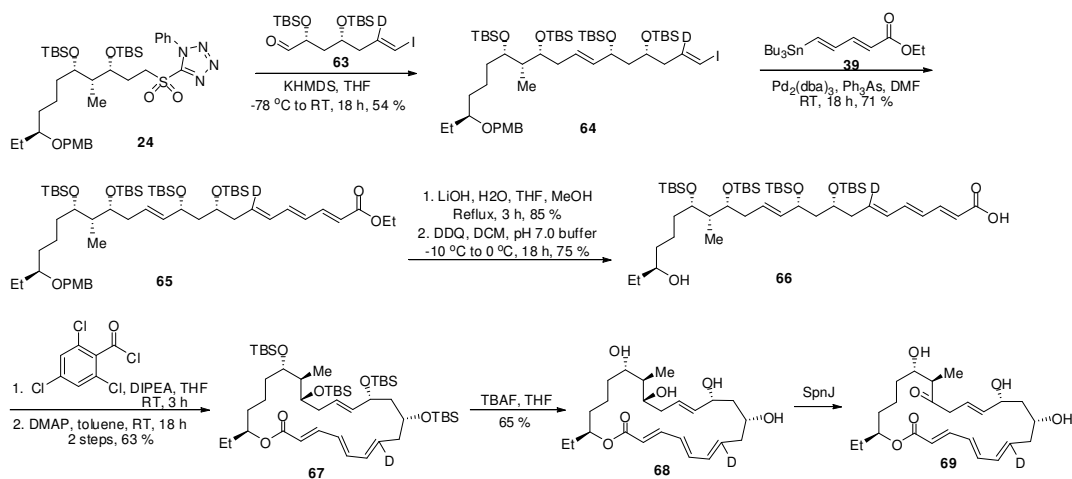
(5R,7R)-5-((E)-3-iodoallyl)-7-((4-methoxybenzyloxy)methyl)-2,2,3,3,9,9,10,10-octamethyl-4,8-dioxo-3,9-disilaundecane with mono-deuteride (61): 1) Dess-Martin periodinane (3.2 g, 7.5 mmol) was added to a solution of alcohol compound (3.1 g, 6.3 mmol) in dichloromethane (150 mL) at room temperature, and the reaction mixture was stirred at room temperature for 2 hours. The reaction mixture was washed sequentially with saturated the aqueous sodium bicarbonate solution (70 mL), sodium thiosulfate solution (50 mL), and brine (80 mL). The organic fraction was dried over an anhydrous sodium sulfate pad and concentrated. The residue was purified using flash column chromatography, the aldehyde compound was eluted with 5% EtOAc/Hexane (2.9 g, 5.8 mmol, 93%). 2) The aldehyde was not stable enough for spectroscopic analysis, so it was used for the next step directly. A THF (20 mL) solution of compound (2.9 g, 5.8 mmol) and iodoform (4.6 g, 11.7 mmol) was added to a mixture of chromium (II) chloride (3.6 g, 29.1 mmol) in THF (70 mL) over 70 min at 0 °C. The reaction mixture was stirred for 14 hours at 4 °C and stirred for additional 2 hours at room temperature. The reaction mixture was diluted with ethyl acetate (200 mL) and washed with brine (250 mL) and water (200 mL). The organic fraction was dried over a magnesium sulfate pad and concentrated. The residue was purified using flash column chromatography, the vinyl iodide compound was eluted with 2% EtOAc/Hexane (1.9 g, 3.0 mmol, 52%). No spectral data was collected.

(2R,4R,E)-2,4-bis(tert-butyldimethylsilyloxy)-7-iodohept-6-en-1-ol with 6-mono-deuteride (62): Compound (62) was prepared following the same procedure as compound (35) with a yield of 76%.

^1H NMR (CDCl_3 , 500 MHz) δ (ppm) 6.05 (s, 1H, 1-CH), 3.90-3.81 (m, 2H, 4-CH+6-CH), 3.60-3.57 (m, 1H, 7-CH₂), 3.49-3.44 (m, 1H, 7-CH₂), 2.29-2.25 (m, 1H, 3-CH₂), 2.21-2.16 (m, 1H, 3-CH₂), 1.74-1.63 (m, 2H, 5-CH₂), 0.90 (s, 9H, CH₃ of TBS), 0.89 (s, 9H, CH₃ of TBS), 0.09 (s, 6H, CH₃ of TBS), 0.06 (d, 6H, $J = 4.4$ Hz, CH₃ of TBS); ^{13}C NMR (CDCl_3 , 125 MHz) δ (ppm) 142.47, 142.27, 142.08, 69.81, 68.26, 66.19, 43.58, 41.36, 25.82, 18.06, 17.98, -4.34, -4.50, -4.61; HRMS (ESI, positive) m/z for $\text{C}_{19}\text{H}_{40}\text{DIO}_3\text{Si}_2$ $[\text{M}+\text{H}]^+$: 502.1771, found 502.1774.

(2R,4R,E)-2,4-bis(tert-butyldimethylsilyloxy)-7-iodohept-6-enal with 6-mono-deuteride (63): Compound **(63)** was prepared following the same procedure as compound **(36)** with a quantitative yield.

B. Synthesis of C7-D analog by Coupling Reactions and Enzymatic Conversion: The overall synthetic scheme is pictured in **Scheme 2-8**.



Scheme 2-8. Preparation of C7-D SpnM substrate analog.

(5R,7R,11R,12R,13S,E)-7,11-bis(tert-butyldimethylsilyloxy)-5-((E)-3-iodoallyl)-13-(4-(4-methoxybenzyloxy)hexyl)-2,2,3,3,12,15,15,16,16-nonamethyl-4,14-dioxa-3,15-

disilaheptadec-8-ene with mono-deuteride (64): Compound (64) was prepared following the same procedure as compound (43) using compound (63) instead of compound (36) with a yield of 54%.

^1H NMR (CDCl_3 , 500 MHz) δ (ppm) 7.27-7.25 (m, 2H, Ph of PMB), 6.87-6.85 (m, 2H, Ph of PMB), 5.99 (s, 1H, 1-CH), 5.57-5.51 (m, 1H, 8-CH), 5.43-5.38 (dd, 1H, $J = 15.4, 6.8$ Hz, 7-CH), 4.43 (s, 2H, CH_2 of PMB), 4.12-4.08 (m, 1H, 6-CH), 3.84-3.81 (m, 1H, 4-CH), 3.80 (s, 3H, OCH_3 of PMB), 3.77-3.74 (m, 1H, 10-CH), 3.70-3.65 (m, 1H, 12-CH), 3.32-3.27 (m, 1H, 16-CH) 2.31-2.21 (m, 3H, 3- CH_2 +9- CH_2), 2.15-2.08 (m, 1H, 3- CH_2), 1.74-1.69 (m, 1H, 5- CH_2), 1.62-1.25 (m, 10H, 5- CH_2 +11-CH +13- CH_2 +14- CH_2 +15- CH_2 +17- CH_2), 0.93-0.84 (m, 42H, CH_3 of TBS +11- CH_3 +18- CH_3), 0.10-0.01 (m, 24H, CH_3 of TBS); ^{13}C NMR (CDCl_3 , 125 MHz) δ (ppm) 159.01, 143.31, 143.33, 135.54, 131.31, 129.17, 126.81, 113.71, 79.79, 76.45, 74.78, 72.90, 72.25, 70.74, 70.45, 68.22, 55.26, 46.03, 43.37, 41.26, 37.84, 35.40, 33.91, 25.99, 25.90, 25.85, 21.30, 18.18, 18.14, 18.12, 18.01, 9.52, -3.72, -3.90, -4.24, -4.35, -4.42, -4.49, -4.61, -4.71; HRMS (ESI, negative) m/z for $\text{C}_{51}\text{H}_{98}\text{DIO}_6\text{Si}_4\text{Cl}$ [$\text{M}+\text{Cl}$]: calcd 1082.5320, found 1082.5324.

(2E,4E,6E,9R,11R,12E,15R,16R,17S)-ethyl 9,11,15,17-tetrakis(tert-butyltrimethylsilyloxy)-21-(4-methoxybenzyloxy)-16-methyltricoso-2,4,6,12-

tetraenoate with mono-deuteride (65): Compound (65) was prepared following the same procedure as compound (45) with a yield of 71%.

^1H NMR (CDCl_3 , 500 MHz) δ (ppm) 7.31-7.25 (m, 3H, Ph of PMB+3-CH), 6.87-6.84 (m, 2H, Ph of PMB), 6.52 (d, 1H, $J = 10.8$ Hz, 5-CH), 6.23-6.18 (m, 1H, 4-CH),

6.17-6.10 (m, 1H, 6-CH), 5.86 (d, 1H, $J = 15.3$ Hz, 2-CH), 5.57-5.51 (m, 1H, 13-CH), 5.43-5.39 (dd, 1H, $J = 15.4, 6.8$ Hz, 12-CH), 4.43 (s, 2H, CH₂ of PMB), 4.22-4.18 (q, 2H, $J = 7.1$ Hz, CH₃CH₂CO(O)), 4.15-4.11 (q, 1H, $J = 6.6$ Hz, 11-CH), 3.86-3.81 (m, 1H, 9-CH), 3.79 (s, 3H, OCH₃ of PMB), 3.77-3.74 (m, 1H, 15-CH), 3.70-3.67 (m, 1H, 17-CH), 3.30-3.27 (m, 1H, 21-CH) 2.40-2.35 (m, 1H, 8-CH₂), 2.27-2.20 (m, 3H, 8-CH₂+14-CH), 1.75-1.69 (m, 1H, 10-CH₂), 1.62-1.25 (m, 13H, 10-CH₂, 16-CH, 18-CH₂, 19-CH₂, 20-CH₂, 22-CH₂, CH₃CH₂CO(O)), 0.92-0.84 (m, 42H, CH₃ of TBS, 16-CH₃, 23-CH₃), 0.04-0.01 (m, 24H, CH₃ of TBS); ¹³C NMR (CDCl₃, 125 MHz) δ (ppm) 167.17, 159.02, 144.72, 140.89, 136.54, 135.62, 132.03, 131.31, 129.18, 128.13, 120.23, 113.70, 79.79, 72.89, 72.25, 70.80, 70.46, 68.94, 60.17, 55.24, 46.15, 41.23, 40.75, 37.87, 35.41, 33.90, 25.98, 25.90, 25.86, 21.29, 18.16, 18.13, 18.03, 14.31, 9.50, -3.74, -3.76, -3.94, -4.27, -4.32, -4.38, -4.52, -4.73; HRMS (ESI, positive) m/z for C₅₈H₁₀₇DO₈Si₄ [M+Na]⁺: calcd 1068.7076, found 1068.7065.

(2E,4E,6E,9R,11R,12E,15R,16R,17S,21S)-9,11,15,17-tetrakis(tert-butyltrimethylsilyloxy)-21-hydroxy-16-methyltricoso-2,4,6,12-tetraenoic acid (66):

Compound (66) was prepared following the same procedure as compound (47) with a yield of 60% for 2 steps. No spectral data was collected.

(3E,5E,7E,10R,12R,13E,16R,17R,18S,22S)-10,12,16,18-tetrakis(tert-butyltrimethylsilyloxy)-22-ethyl-17-methyloxacyclodocosa-3,5,7,13-tetraen-2-one (67):

Compound (67) was prepared following the same procedure as compound (48) with a yield of 57% for 2 steps.

^1H NMR (CDCl_3 , 500 MHz) δ (ppm) 7.30-7.24 (m, 1H, 3-H), 6.48 (dd, $J = 15.0$, 10.5 Hz, 1H, 5-H), 6.25-6.20 (m, 1H, 4-H), 6.13 (d, $J = 10.5$ Hz, 1H, 6-H), 5.82 (d, $J = 15.0$ Hz, 1H, 2-H), 5.43-5.27 (m, 2H, 12-H, 13-H), 4.87 (m, 1H, 21-H), 4.02 (m, 1H, 11-H), 3.76 (m, 1H, 9-H), 3.68 (m, 1H, 15-H), 3.58 (m, 1H, 17-H), 2.46 (d, $J = 10.0$ Hz, 1H, 8-H), 2.37-2.20 (m, 2H, 14-H, 8-H), 2.14-2.04 (m, 1H, 14-H), 1.71-1.20 (m, 11H, 10-H, 16-H, 18-H, 19-H, 20-H, 22-H), 0.90-0.83 (m, 39H, 23-H, 12 x CH_3 of TBS), 0.08-(-0.02) (m, 24H, 8 x CH_3 of TBS); ^{13}C NMR (CDCl_3 , 125 MHz) δ (ppm) 144.8, 140.9, 135.2, 131.9, 128.0, 127.1, 120.8, 75.2, 73.2, 72.1, 71.1, 69.1, 46.6, 42.4, 42.0, 38.4, 34.4, 33.4, 27.9, 27.8, 26.1, 26.0, 25.9, 25.8, 21.1, 18.25, 18.11, 18.08, 18.01, 10.2, 9.9, -3.47, -3.86, -3.96, -4.32, -4.39, -4.52, -4.56, -4.62; HRMS (ESI, positive) m/z for $\text{C}_{48}\text{H}_{93}\text{DO}_6\text{Si}_4$ $[\text{M}+\text{Na}]^+$: calcd 902.6082, found 902.6082.

(3E,5E,7E,10R,12R,13E,16R,17R,18S,22S)-22-ethyl-10,12,16,18-tetrahydroxy-17-methyloxacyclodocosa-3,5,7,13-tetraen-2-one (68): Compound **(68)** was prepared following the same procedure as compound **(50)** with a yield of 65%.

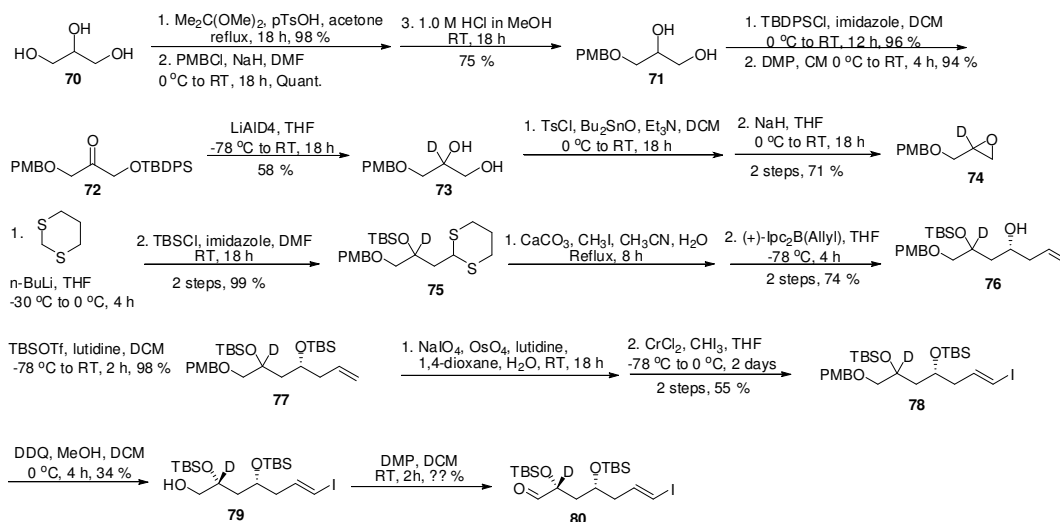
^1H NMR (CDCl_3 , 500 MHz) δ (ppm); ^{13}C NMR (CDCl_3 , 125 MHz) δ (ppm); HRMS (ESI, positive) m/z for $\text{C}_{24}\text{H}_{37}\text{DO}_6$ Na $[\text{M}+\text{Na}]^+$: 446.2623, found 446.2625.

[C7- ^2H] SpnM substrate analog (69): Compound **(69)** was prepared following the same procedure as compound **(38)** with a quantitative yield.

HRMS (ESI, positive) m/z for $\text{C}_{24}\text{H}_{35}\text{DO}_6$ $[\text{M}+\text{Na}]^+$: calcd 444.2465, found 444.2467.

2.2.6. Synthesis of the [C11- ^2H] SpnM Substrate Analog (C11-D analog)

A. Preparation of Fragment B: The overall synthetic scheme is depicted in **Scheme 2-9**.



Scheme 2-9. Preparation of fragment B for the synthesis of [C11-2H] SpnM substrate analog.

3-(4-methoxybenzyloxy)propane-1,2-diol (71): 1) Glycerol (92.0 g, 1.0 mol) was mixed with 2,2-dimethoxypropane (136 mL, 1.1 mol) in acetone (500 mL) containing a catalytic amount of p-toluenesulfonic acid (1.9 g, 10 mmol) at room temperature over 18 hours. After the solvent was concentrated under reduced pressure, the residue was vacuum-distilled at 70-80 °C to afford the intermediate (boiling point 188 °C at 760 torr; 129 g, 98%). 2) Sodium hydride (60% in mineral oil; 39.2 g, 1.18 mol) was added portionwise over 30 min to a solution of above intermediate (129 g, 0.98 mol) in DMF (0.98 L) at 0 °C with mechanical stirring. After stirring for an additional 30 min, p-methoxybenzyl chloride (freshly prepared from the reaction of p-methoxybenzyl alcohol (154.7 g, 1.12 mol) and thionyl chloride (SOCl₂; 233.0 g, 1.96 mol) in diethyl ether (1.12 L)) was added to the reaction mixture at 0 °C over 1 hour. The reaction mixture was allowed to warm to room temperature with vigorous stirring for 18 hours. After quenching the reaction with addition of water (0.98 L) at 0 °C for 30 min, the aqueous fraction was extracted with

ethyl acetate (500 mL x 4 times). The combined organic fractions were washed out with brine (500 mL), dried over an anhydrous sodium sulfate pad, and concentrated under reduced pressure. The resulting residue was concentrated further under high vacuum to produce a quantitative amount of an intermediate, which was used directly to the next step without further purification. 3) The above intermediate was directly dissolved in a solution of the aqueous 1.0 M hydrochloric acid solution (250 mL) and methanol (375 mL) at room temperature, and stirred at room temperature for 18 hours. After partially evaporating methanol under reduced pressure, the organic phase was repeatedly separated by the addition of water (400 mL) and ethyl acetate (250 mL x 4 times). The combined organic fractions were washed with brine (250 mL), dried over an anhydrous sodium sulfate pad, and concentrated under reduced pressure. The resulting residue was subjected to the flash column chromatography. The target compound was eluted with 30% to 50% of EtOAc/Hexane solution (152 g, 75%). All spectral data was identical to the literature reference.

1-(tert-butyldiphenylsilyloxy)-3-(4-methoxybenzyloxy)propan-2-one (72): 1) tert-Butyl(chloro)diphenylsilane (80.0 g, 0.29 mol) was added dropwise over 30 min to a solution of diol compound (62.0 g, 0.29 mol) and imidazole (39.5 g, 0.58 mol) in anhydrous dichloromethane (580 mL) at 0 °C. The reaction mixture was stirred at room temperature for 12 hours, and subsequently washed with the aqueous 1.0 M hydrochloric acid solution (500 mL x 2 times), water (500 mL), and brine (500 mL). The resulting organic fraction was dried over an anhydrous sodium sulfate pad, and concentrated under reduced pressure. The residue was purified using flash column chromatography. The

target compound was eluted with 10% of EtOAc/Hexane solution (125 g, 96%). 2) Dess-Martin periodinane (47.0 g, 0.11 mol) was added portionwise to a solution of the above compound (100.0 g, 0.10 mol) in anhydrous dichloromethane (500 mL) at 0 °C over 10 min with vigorous stirring. The reaction mixture was allowed to warm to room temperature for 4 hours with stirring. Aqueous 10% sodium thiosulfate solution (500 mL) was added to the reaction mixture, and stirred for additional 30 min. The organic phase was then separated by extracting the aqueous phase with dichloromethane (200 mL x 3 times), and dried over an anhydrous sodium sulfate pad. The concentrated residue was subjected to the flash column chromatography. The target compound was eluted with 10% EtOAc/Hexane solution (95 g, 94%). All spectral data is identical to the literature reference.

3-(4-methoxybenzyloxy)propane-1,2-diol with 2-deuteride or 2-deuteride-3-(4-methoxybenzyloxy)propane-1,2-diol (73): Lithiumaluminum deuteride (10.6 g, 254 mmol) was added to a solution of the keto compound (95.0 g, 212 mmol) in anhydrous THF (1.05 L) at -78 °C over 20 min. The reaction mixture was kept stirring at -78 °C for 2 hours, and allowed to warm to room temperature for 18 hours with stirring. After quenching the reaction at 0 °C with the aqueous 10% sodium hydroxide solution (420 mL) added dropwise and saturated the aqueous sodium potassium tartrate solution (420 mL), the reaction mixture was stirred for an additional 1 hour, and filtered through filter paper with several washings with ethyl acetate (200 mL x 3 times). The organic fraction was separated by extracting the aqueous fraction with ethyl acetate (300 mL x 3 times), dried over an anhydrous sodium sulfate pad, and concentrated under reduced pressure.

The resulting residue was chromatographed. The target compound was eluted with a gradient of 50% EtOAc/Hexane to 100% EtOAc (26.0 g, 58%). All spectral data is identical to the literature reference.

(R)-2-((4-methoxybenzyloxy)methyl)oxirane (74): Compound **(74)** was prepared following the same procedure as compound **(30)** with a yield of 71% for 2 steps.

¹H NMR (CDCl₃, 400 MHz) δ (ppm) 7.25-7.20 (m, 2H, Ph-H), 6.86-6.81 (m, 2H, Ph-H), 4.49 (d, J = 11.4 Hz, 1H, CH₂ of PMB), 4.44 (d, J = 11.4 Hz, 1H, CH₂ of PMB), 3.75 (s, 3H, CH₃-OPh), 3.69 (d, J = 11.6 Hz, 1H, 3-H), 3.36 (d, J = 11.6 Hz, 1H, 3-H), 2.73 (d, J = 5.2 Hz, 1H, 1-H), 2.55 (d, J = 5.2 Hz, 1H, 1-H); ¹³C NMR (CDCl₃, 100 MHz) δ (ppm) 159.2 (C-1''), 129.8 (C-4''), 129.3 (C-2'', C-6''), 113.7 (C-3'', C-5''), 72.8 (CH₂ of PMB), 70.3 (C-1), 55.1 (C-OPh), 50.4 (t, J = 26.8 Hz, C-2), 44.1 (C-3); HRMS (CI, positive) *m/z* for C₁₁H₁₃DO₃ [M+H]⁺: calcd 195.1006, found 195.1003.

(R)-(1-(1,3-dithian-2-yl)-3-(4-methoxybenzyloxy)propan-2-yloxy)(tert-butyl)dimethylsilane (75): Compound **(75)** was prepared following the same procedure as compound **(31)** with a yield of 99% for 2 steps.

¹H NMR (CDCl₃, 400 MHz) δ (ppm) 7.26-7.20 (m, 2H, Ph-H), 6.88-6.81 (m, 2H, Ph-H), 4.42 (s, 2H, CH₂ of PMB), 4.10 (dd, J = 9.6, 4.8 Hz, 1H, 4-H), 3.78 (s, 3H, CH₃-OPh), 3.38 (d, J = 9.8 Hz, 1H, 1-H), 3.31 (d, J = 9.8 Hz, 1H, 1-H), 2.69-2.90 (m, 4H, 2'-H, 4'-H), 2.02-2.12 (m, 1H, 3'-H), 1.94 (dd, J = 14.2, 9.6 Hz, 1H, 3-H), 1.79-1.92 (m, 2H, 3-H, 3'H), 0.87 (s, 9H, TBS), 0.08 (s, 3H, TBS), 0.04 (s, 3H, TBS); ¹³C NMR (CDCl₃, 100 MHz) δ (ppm) 159.1 (C-1''), 130.3 (C-4''), 129.2 (C-2'', C-6''), 113.7 (C-3'', C-5''), 74.2 (CH₂ of PMB), 72.9 (C-4), 67.5 (t, J = 21.2 Hz, C-3), 55.2 (C-OPhH), 43.6

(C-1), 40.2 (C-2), 30.4 (C-S), 29.8 (C-S), 26.0 (3 x CH₃-C-Si of TBS), 25.9 (C-C-S), 18.1 (C-Si of TBS), -4.4 (CH₃-Si of TBS), -4.9 (CH₃-Si of TBS); HRMS (ESI, positive) *m/z* for C₂₁H₃₅DO₃S₂Si [M+Na]⁺: calcd 452.1830, found 452.1838.

(4R,6R)-6-(tert-butyldimethylsilyloxy)-7-(4-methoxybenzyloxy)hept-1-en-4-ol (76):

Compound **(76)** was prepared following the same procedure as compound **(32)** with a yield of 65% for 2 steps.

¹H NMR (CDCl₃, 400 MHz) δ (ppm) 7.24-7.18 (m, 2H, Ph-H), 6.90-6.80 (m, 2H, Ph-H), 5.72-5.88 (m, 1H, 6-H), 5.13-5.03 (m, 2H, 7-H), 4.46 (d, J = 11.6 Hz, 1H, CH₂ of PMB), 4.43 (s, 1H, CH₂ of PMB), 3.92-3.78 (m, 1H, 4-H), 3.79 (s, 3H, CH₃-OPh), 3.44 and 3.41 (dd, J = 9.6 Hz, 1H, 1-H), 3.40 and 3.37 (dd, J = 9.6 Hz, 1H, 1-H), 3.22 (br s, 1H, OH), 3.13 (br s, 1H, OH), 2.21 (br t, J = 6.4 Hz, 2H, 5-H), 1.73 (ddd, J = 20.0, 14.4, 2.4 Hz, 1H, 3-H), 1.58 (ddd, J = 16.0, 14.4, 8.8 Hz, 1H, 3-H), 0.85 (s, 9H, TBS), 0.06 (s, 3H, TBS), 0.04 (s, 3H, TBS); ¹³C NMR (CDCl₃, 100 MHz) δ (ppm) 159.2 (C-1''), 134.5 (C-6), 130.05 (C-4''), 129.35 (C-2''), 129.33 (C-6''), 117.4 (C-7), 113.7 (C-3'', C-5''), 74.7 (CH₂ of PMB), 73.0 (C-1), 69.1 (C-4), 67.7 (C-2), 55.2 (C-OPhH), 42.4 (C-5), 40.9 (C-3), 25.8 (3 x CH₃-C-Si of TBS), 18.0 (C-Si of TBS), -4.2 and -4.6 (CH₃-Si of TBS), -4.8 and -5.0 (CH₃-Si of TBS); HRMS (ESI, positive) *m/z* for C₂₁H₃₅DO₄Si [M+Na]⁺: calcd 404.23378, found 404.23305.

(5R,7R)-5-allyl-7-((4-methoxybenzyloxy)methyl)-2,2,3,3,9,9,10,10-octamethyl-4,8-dioxa-3,9-disilaundecane (77): Compound **(77)** was prepared following the same procedure as compound **(33)** with a yield of 98%.

^1H NMR (CDCl_3 , 400 MHz) δ (ppm) 7.25-7.21 (m, 2H, Ph-H), 6.87-6.83 (m, 2H, Ph-H), 5.85-5.72 (m, 1H, 6-H), 5.05-4.98 (m, 2H, 7-H), 4.44 (d, $J = 11.8$ Hz, 1H, CH_2 of PMB), 4.41 (d, $J = 11.8$ Hz, 1H, CH_2 of PMB), 3.90-3.80 (m, 1H, 4-H), 3.79 (s, 3H, $\text{CH}_3\text{-OPh}$), 3.37-3.30 (m, 2H, 1-H), 2.30-2.09 (m, 2H, 5-H), 1.69 (dd, $J = 13.8, 6.8$ Hz, 1H, 3-H), 1.62-1.55 (m, 1H, 3-H), 0.86-0.85 (m, 18H, 3 x 2 x $\text{CH}_3\text{-C-Si}$ of TBS), 0.05-0.00 (m, 12 H, 2 x 2 x $\text{CH}_3\text{-Si}$ of TBS); ^{13}C NMR (CDCl_3 , 100 MHz) δ (ppm) 159.1 (C-1''), 135.1 (C-6), 130.6 (C-4''), 129.2 (C-2'', C-6''), 116.9 (C-7), 113.7 (C-3'', C-5''), 75.1 (CH_2 of PMB), 72.9 (C-1), 69.5 (C-4), 68.9 (t, $J = 20.3$ Hz, C-2), 55.3 (C-OPhH), 42.7 (C-5), 42.0 (C-3), 26.05 (3 x $\text{CH}_3\text{-C-Si}$ of TBS), 25.90 (3 x $\text{CH}_3\text{-C-Si}$ of TBS), 18.26 (C-Si of TBS), 18.14 (C-Si of TBS), -3.9 ($\text{CH}_3\text{-Si}$ of TBS), -4.0 ($\text{CH}_3\text{-Si}$ of TBS), -4.2 ($\text{CH}_3\text{-Si}$ of TBS), -4.2 ($\text{CH}_3\text{-Si}$ of TBS); HRMS (ESI, positive) m/z for $\text{C}_{21}\text{H}_{35}\text{DO}_4\text{Si}$ $[\text{M}+\text{Na}]^+$: calcd 404.23378, found 404.23305.

(5R,7R)-5-((E)-3-iodoallyl)-7-((4-methoxybenzyloxy)methyl)-2,2,3,3,9,9,10,10-octamethyl-4,8-dioxa-3,9-disilaundecane (78): Compound (78) was prepared following the same procedure as compound (34) with a yield of 55% for 2 steps.

^1H NMR (CDCl_3 , 400 MHz) δ (ppm) 7.26-7.19 (m, 2H, Ph-H), 6.89-6.83 (m, 2H, Ph-H), 6.48 (dt, $J = 14.4, 7.2$ Hz, 1H, 2-H), 6.04-5.95 (dt, $J = 14.4, 1.2$ Hz, 1H, 1-H), 4.48-4.36 (m, 2H, CH_2 of PMB), 4.00-3.76 (m, 1H, 4-H), 3.79 (s, 3H, $\text{CH}_3\text{-OPhH}$), 3.37-3.27 (m, 2H, 7-H), 2.38-2.02 (m, 2H, 3-H), 1.72-1.51 (m, 2H, 5-H), 0.89-0.84 (m, 18 H, 3 x 2 x $\text{CH}_3\text{-C-Si}$ of TBS), 0.08-0.00 (m, 12H, 2 x 2 x $\text{CH}_3\text{-Si}$ of TBS); ^{13}C NMR (CDCl_3 , 100 MHz) δ (ppm) 159.1 (C-1''), 143.2 (C-2), 130.4 (C-4''), 129.2 (C-2'', C-6''), 113.7 (C-3'', C-5''), 76.6 (C-1), 74.5 (CH_2 of PMB), 72.9 (C-7), 68.7 (C-6), 68.0 (C-4), 55.2

(C-OPhH), 44.4 (C-3), 42.9 (C-5), 25.9 and 25.8 (3 x 2 x CH₃-C-Si of TBS), 18.2 and 18.0 (2 x C-Si of TBS), -4.0, -4.2, -4.5, and -4.6 (2 x 2 x CH₃-Si of TBS); HRMS (ESI, positive) *m/z* for C₂₇H₄₈DIO₄Si₂ [M+Na]⁺: calcd 644.21690, found 644.21675.

(2R,4R,E)-2,4-bis(tert-butyldimethylsilyloxy)-7-iodohept-6-en-1-ol (79): Compound **(79)** was prepared following the same procedure as compound **(35)** with a yield of 39%.

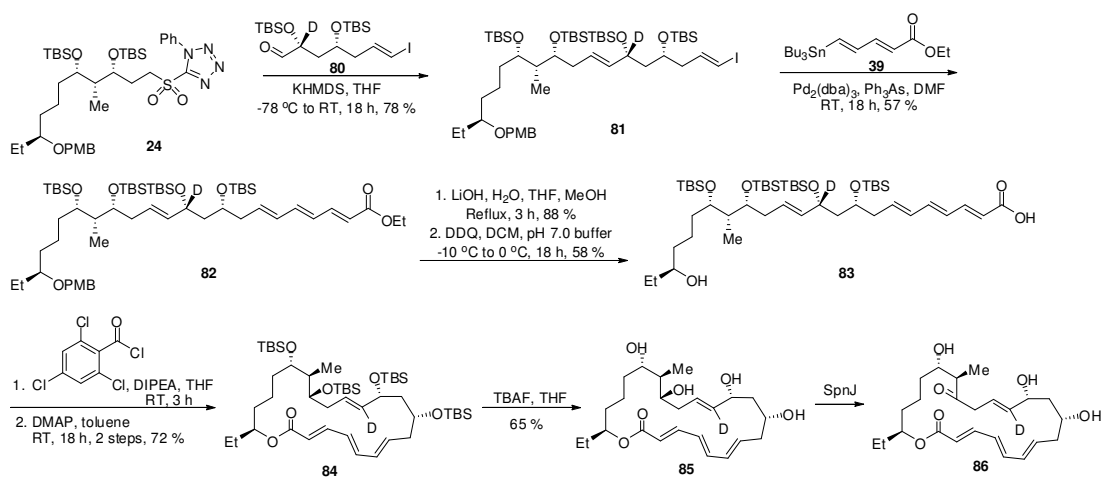
¹H NMR (CDCl₃, 400 MHz) δ (ppm) 6.48 (dt, J = 14.6, 7.4 Hz, 1H, 2-H), 6.04 (dt, J = 14.6, 1.2 Hz, 1H, 1-H), 3.80 (quint, J = 6.0 Hz, 1H, 4-H), 3.55 (dd, J = 11.2, 4.8 Hz, 1H, 7-Ha), 3.44 (dd, J = 11.2 7.8 Hz, 1H, 7-Hb), 2.30-2.12 (m, 3H, 3-H, OH), 1.68 (dd, J = 14.0, 6.8 Hz, 1H, 5-Ha), 1.62 (dd, J = 14.0, 5.2 Hz, 1H, 5-Hb), 0.88 (s, 9H, 3 x CH₃-C-Si of TBS), 0.87 (s, 9H, 3 x CH₃-C-Si of TBS), 0.06 (s, 6H, 2 x CH₃-Si of TBS), 0.04 (s, 3H, CH₃-Si of TBS), 0.03 (s, 3H, CH₃-Si of TBS); ¹³C NMR (CDCl₃, 100 MHz) δ (ppm) 142.6 (C-2), 77.1 (C-1), 69.3 (t, J = 21.0 Hz, C-6), 68.2 (C-4), 66.1 (C-7), 43.7 (C-3), 41.2 (C-5), 25.80 and 25.77 (3 x 2 x CH₃-C-Si of TBS), 18.04 and 17.95 (2 x C-Si of TBS), -4.35, -4.51, -4.53, -4.63 (2 x 2 x CH₃-Si of TBS); HRMS (ESI, positive) *m/z* for C₁₉H₄₀DIO₃Si₂ [M+Na]⁺ : calcd 524.1594, found 524.1601.

(2R,4R,E)-2,4-bis(tert-butyldimethylsilyloxy)-7-iodohept-6-enal (80): Compound **(80)** was prepared following the same procedure as compound **(36)** with a yield of 96%.

¹H NMR (CDCl₃, 400 MHz) δ (ppm) 9.56 (s, 1H, 7-H), 6.45 (dt, J = 14.4, 7.6 Hz, 1H, 2-H), 6.03 (dt, J = 14.4, 1.2 Hz, 1H, 1-H), 3.94 (quint, J = 6.0 Hz, 1H, 4-H), 2.30-2.12 (m, 2H, 3-H), 1.83-1.72 (m, 2H, 5-H), 0.89 (s, 9H, 3 x CH₃-C-Si of TBS), 0.85 (s, 9H, 3 x CH₃-C-Si of TBS), 0.06 (s, 3H, CH₃-Si of TBS), 0.04 (s, 3H, CH₃-Si of TBS), 0.03 (s, 6H, 2 x CH₃-Si of TBS); ¹³C NMR (CDCl₃, 100 MHz) δ (ppm) 203.5 (C-7),

142.3 (C-2), 77.1 (C-1), 74.3 (t, $J = 21.3$ Hz, C-6), 66.7 (C-4), 43.5 (C-3), 40.1 (C-5), 25.80 and 25.72 (3 x 2 x CH₃-C-Si of TBS), 18.07 and 18.01 (2 x C-Si of TBS), -4.36, -4.51, -4.63, -4.93 (2 x 2 x CH₃-Si of TBS); HRMS (ESI, positive) m/z for C₁₉H₃₈DIO₃Si₂ [M+H]⁺: calcd 500.1618, found 500.1609.

B. Synthesis of [C11-²H] SpnM Substrate by Coupling Reactions and Enzymatic Conversion: The overall synthetic scheme is pictured in **Scheme 2-10**.



Scheme 2-10. Preparation of [C11-²H] SpnM substrate analog.

(2E,4E,6E,9R,11R,12E,15R,16R,17S)-ethyl 9,11,15,17-tetrakis(tert-butyltrimethylsilyloxy)-21-(4-methoxybenzyloxy)-16-methyltricoso-2,4,6,12-tetraenoate with 11-deuteride (81): Compound (**81**) was prepared following the same procedure as compound (**43**) using compound (**80**) instead of compound (**36**) with a yield of 78%.

¹H NMR (CDCl₃, 400 MHz) δ (ppm) 7.287.21 (m, 2H, CH of PMB), 6.87-6.81 (m, 2H, CH of PMB), 6.47 (dt, $J = 14.6, 7.4$ Hz, 1H, C2H), 5.98 (brd, $J = 14.6$ Hz, 1H, C1-H), 5.59-5.43 (m, 1H, C8-H), 5.38 (brd, $J = 15.6$ Hz, 1H, C7-H), 4.41 (s, 2H, CH₂ of

PMB), 3.78 (s, 3H, OCH₃ of PMB), 3.86-3.70 (m, 2H, C4-H and C10-H), 3.70-3.56 (m, 1H, C12-H), 3.27 (quint, *J* = 5.6 Hz, 1H, C16-H), 2.32-2.18 (m, 3H, two C9-H and one C3-H), 2.18 and -2.02 (m, 1H, C3-H), 1.75-1.64 (m, 1H, C11-H), 1.64-1.18 (m, 10H, C5-H, C13-H, C14-H, C15-H and C17-H), 0.96-0.74 (m, 42H, *t*-Bu of TBS, C11-Me and C18H), 0.04-0.01 (m, 24H, CH₃ of TBS); ¹³C NMR (CDCl₃, 100 MHz) δ (ppm) 159.0, 143.3, 135.4, 131.2, 129.2, 126.8, 113.7, 79.8, 72.9, 72.2, 70.4, 68.2, 55.2, 45.9, 43.5, 41.2, 37.8, 35.4, 33.9, 26.2, 26.0, 26.0, 25.9, 25.8, 25.8, 21.3, 18.2, 18.1, 18.1, 18.0, 4.7, 4.5, 4.4, 4.4, 4.3, 4.0, 3.9, 3.7, 3.7, 3.6; HRMS (ESI, positive) *m/z* for C₅₁H₉₈DIO₆Si₄ [M+Na]⁺: calcd 1070.5518, found 1070.5546.

(2E,4E,6E,9R,11R,12E,15R,16R,17S)-ethyl 9,11,15,17-tetrakis(tert-butyltrimethylsilyloxy)-21-(4-methoxybenzyloxy)-16-methyltricosanoate with 11-deutride (82)

Compound (**82**) was prepared following the same procedure as compound (**45**) with a yield of 57%.

¹H NMR (CDCl₃, 400 MHz) δ (ppm) 7.28 (dd, *J* = 15.2, 11.2 Hz, 1H, C3-H), 7.287.21 (m, 2H, CH of PMB), 6.87-6.81 (m, 2H, CH of PMB), 6.50 (dd, *J* = 14.6, 11.0 Hz, 1H, C5-H), 6.18 (dd, *J* = 14.6, 11.2 Hz, 1H, C4-H), 6.11 (dd, *J* = 15.0, 11.0 Hz, 1H, C6-H), 6.00-5.78 (m, 1H, C7-H), 5.82 (d, *J* = 15.2 Hz, 1H, C2-H), 5.585.44 (m, 1H, C13-H), 5.38 (brd, *J* = 15.6 Hz, 1H, C12-H), 4.40 (s, 2H, CH₂ of PMB), 4.18 (q, *J* = 7.2 Hz, 2H, CH₂ of OEt), 3.77 (s, 3H, OCH₃ of PMB), 3.883.70 (m, 2H, C9-H and C15-H), 3.70-3.56 (m, 1H, C17-H), 3.27 (quint, *J* = 5.6 Hz, 1H, C21-H), 2.54-2.12 (m, 4H, C8H and C14-H), 1.781.20 (m, 11H, C10-H, C16-H, C18H, C19-H, C20-H and C22-H), 1.27 (t, *J* = 7.2 Hz, 3H, CH₃ of OEt), 0.94-0.78 (m, 42H, *t*-Bu of TBS, C16-Me and C23-H), 0.08-

0.04) (m, 24H, CH₃ of TBS); ¹³C NMR (CDCl₃, 100 MHz) δ (ppm) 167.2, 159.0, 144.7, 140.9, 136.5, 135.5, 132.0, 131.2, 129.2, 128.1, 126.8, 120.2, 113.7, 79.8, 72.2, 70.4, 68.9, 60.2, 55.2, 46.0, 41.2, 40.8, 35.4, 33.9, 26.2, 26.0, 26.0, 25.9, 25.8, 25.8, 21.3, 18.2, 18.1, 18.0, 14.3, 9.5, -3.7, -3.8, -3.9, -4.3, -4.3, -4.4, -4.5, -4.7; HRMS (ESI, positive) *m/z* for C₅₈H₁₀₇DO₈Si₄ [M+Na]⁺: calcd 1068.7076, found 1068.7078.

(2E,4E,6E,9R,11R,12E,15R,16R,17S,21S)-9,11,15,17-tetrakis(tert-butyltrimethylsilyloxy)-21-hydroxy-16-methyltricoso-2,4,6,12-tetraenoic acid with 11-deuteride (83): Compound **(83)** was prepared following the same procedure as compound **(47)** with a yield of 51% for 2 steps.

¹H NMR (CDCl₃, 500 MHz) δ (ppm) 7.36 (dd, *J* = 15.3, 11.5 Hz, 1H, C3-H), 6.55 (dd, *J* = 15.0, 10.8 Hz, 1H, C5-H), 6.22 (dd, *J* = 15.0, 11.5 Hz, 1H, C4-H), 6.14 (dd, *J* = 15.0, 10.8 Hz, 1H, C6-H), 5.94 (dt, *J* = 15.0, 7.5 Hz, 1H, C7-H), 5.83 (d, *J* = 15.3 Hz, 1H, C2-H), 5.55 (dt, *J* = 15.0, 7.5 Hz, 1H, C13-H), 5.40 (brd, *J* = 15.0 Hz, 1H, C12-H), 3.81 (quint, 1H, *J* = 6.0 Hz, C9-H), 3.73 (q, 1H, *J* = 5.5 Hz, C15-H), 3.67 (q, 1H, *J* = 5.5 Hz, C17-H), 3.54-3.44 (m, 1H, C21-H), 2.482.32 (m, 1H, C8H), 2.32-2.16 (m, 3H, one C8H and two C14-H), 1.70 (dd, *J* = 13.5, 6.0 Hz, 1H, C10-H), 1.65-1.16 (m, 11H, one C10-H, C16-H, C18H, C19-H, C20-H, C22-H and OH), 0.92 (t, *J* = 7.5 Hz, 3H, C23-H), 0.90-0.84 (m, 36H, *t*Bu of TBS), 0.83 (d, *J* = 7.0 Hz, 3H, C16-Me), 0.07-0.02) (m, 24H, CH₃ of TBS); ¹³C NMR (CDCl₃, 125 MHz) δ (ppm) 171.1, 147.0, 142.0, 137.4, 135.6, 132.0, 127.9, 126.9, 119.0, 73.1, 72.6, 72.2, 69.0, 46.0, 40.8, 40.6, 37.7, 37.4, 35.1, 30.1, 26.0, 26.0, 25.9, 25.9, 21.3, 18.2, 18.2, 18.1, 18.1, 9.9, 9.3, -3.8, -3.8, -4.0, -4.3, -4.4, -4.6, -4.7; HRMS (ESI, positive) *m/z* for C₄₈H₉₅DO₇Si₄ [M+Na]⁺: calcd 920.6188, found 920.6179.

(3E,5E,7E,10R,12R,13E,16R,17R,18S,22S)-10,12,16,18-tetrakis(tert-butyltrimethylsilyloxy)-22-ethyl-17-methyloxacyclodocosa-3,5,7,13-tetraen-2-one

with 11-deuteride (84): Compound (84) was prepared following the same procedure as compound (49) with a yield of 72%.

^1H NMR (CDCl_3 , 500 MHz) δ (ppm) 7.24 (dd, $J = 15.0, 11.0$ Hz, 1H, C3-H), 6.47 (dd, $J = 15.0, 10.5$ Hz, 1H, C5-H), 6.21 (dd, $J = 15.0, 11.0$ Hz, 1H, C4-H), 6.12 (dd, $J = 15.5, 10.5$ Hz, 1H, C6-H), 5.80 (d, $J = 15.0$ Hz, 1H, C2-H), 5.78 (dt, $J = 15.0, 7.5$ Hz, 1H, C7-H), 5.42-5.22 (m, 1H, C12-H and C13-H), 4.90-4.80 (m, 1H, C21-H), 3.80-3.72 (m, 1H, C9-H), 3.71-3.64 (m, 1H, C15-H), 3.61-3.52 (m, 1H, C17-H), 2.50-2.06 (m, 4H, C8H and C14-H), 1.781.16 (m, 11H, C10-H, C16-H, C18H, C19-H, C20-H, C22-H), 0.91 (t, $J = 7.5$ Hz, 3H, C23-H), 0.90-0.80 (m, 36H, *t*Bu of TBS), 0.75 (d, $J = 7.0$ Hz, 3H, C16-Me), 0.08 -0.08 (m, 24H, CH_3 of TBS); ^{13}C NMR (CDCl_3 , 125 MHz) δ (ppm) 166.9, 144.7, 140.9, 136.0, 135.2, 132.0, 128.0, 127.1, 120.8, 75.2, 73.2, 69.1, 46.5, 42.3, 42.1, 38.3, 34.4, 33.4, 27.8, 26.0, 26.0, 26.0, 25.9, 25.8, 25.8, 21.1, 18.2, 18.2, 18.1, 18.1, 18.1, 18.0, 18.0, 10.2, 9.8, -3.5, -3.8, -4.0, -4.3, -4.4, -4.5, -4.5, -4.6, -4.6, -4.7; HRMS (ESI, positive) m/z for $\text{C}_{48}\text{H}_{93}\text{DO}_6\text{Si}_4$ $[\text{M}+\text{Na}]^+$: calcd 902.6082, found 902.6086.

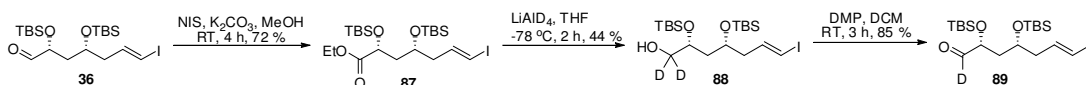
(3E,5E,7E,10R,12R,13E,16R,17R,18S,22S)-22-ethyl-10,12,16,18-tetrahydroxy-17-methyloxacyclodocosa-3,5,7,13-tetraen-2-one with 11-deuteride (85): Compound (85) was prepared following the same procedure as compound (50) with a yield of 65%.

^1H NMR (CDCl_3 , 500 MHz) δ (ppm); ^{13}C NMR (CDCl_3 , 125 MHz) δ (ppm); HRMS (ESI, positive) m/z for $\text{C}_{24}\text{H}_{37}\text{DO}_6$ $[\text{M}+\text{Na}]^+$: calcd 446.2623, found 446.2635.

[C11-²H] SpnM substrate analog (86): [C11-²H] SpnM substrate analog (**86**) was prepared following the same procedure as compound (**51**) quantitatively. MS data was not collected.

2.2.7. Synthesis of the [C12-²H] SpnM Substrate Analog (C12-D analog)

A. Preparation of Fragment B: The overall synthetic scheme is depicted in **Scheme 2-11**.



Scheme 2-11. Preparation of fragment B for the synthesis of [C12-²H] SpnM substrate analog.

(2R,4R,E)-ethyl 2,4-bis(tert-butyldimethylsilyloxy)-7-iodohept-6-enoate (87): N-Iodosuccinimide (NIS; 2.3 g, 10 mmol) and potassium carbonate (1.4 g, 10 mmol) were each added subsequently to a solution of aldehyde (freshly prepared; 2.0 g, 4 mmol) in methanol (20 mL) at room temperature. The reaction mixture was stirred at room temperature for 18 hours. After quenching with saturated the aqueous sodium thiosulfate solution (20 mL), the aqueous fraction was extracted with dichloromethane (50 mL x 3 times). The combined organic fractions were dried over an anhydrous sodium sulfate pad, filtered, and concentrated under reduced pressure. The resulting residue was purified using flash column chromatography. The target compound was eluted with 5% EtOAc/Hexane (1.5 g, 72%).

¹H NMR (CDCl₃, 500 MHz) δ (ppm) 6.50 (ddd, 1H, *J* = 7.1, 8.0, 14.5 Hz, 6-H), 6.05 (d, 1H, *J* = 14.5 Hz, 7-H), 4.28 (dd, *J* = 5.6, 7.1 Hz, 2-H), 3.90-3.85 (m, 1H, 4-H), 3.71 (s, 3H, OCH₃), 2.34-2.29 (m, 1H, 5-H), 2.23-2.17 (m, 1H, 5-H), 1.91-1.80 (m, 2H, 3-Hs), 0.90 (s, 9H, CH₃ of TBS), 0.88 (s, 9H, tBu of TBS), 0.073 (CH₃ of TBS), 0.052

(CH3 of TBS), 0.047 (CH3 of TBS), 0.045 (CH3 of TBS); ^{13}C NMR (CDCl_3 , 125 MHz) δ (ppm) 173.77 (1-C=O), 142.83 (C-6), 137.46 (C-7), 69.38 (C-2), 67.82 (C-4), 51.78 (OCH3), 43.33 (C-5), 42.20 (C-3), 25.81 (CH3 of tBu), 25.70 (CH3 of tBu), 18.19 (Me3-C-Si), 17.99 (Me3-C-Si), -4.55 (CH3 of TBS), -4.70 (CH3 of TBS), -4.70 (CH3 of TBS), -5.28 (CH3 of TBS); HRMS (ESI, positive) m/z for $\text{C}_{20}\text{H}_{41}\text{IO}_4\text{Si}_2$ $[\text{M}+\text{Na}]^+$: calcd 551.1480, found 551.1484.

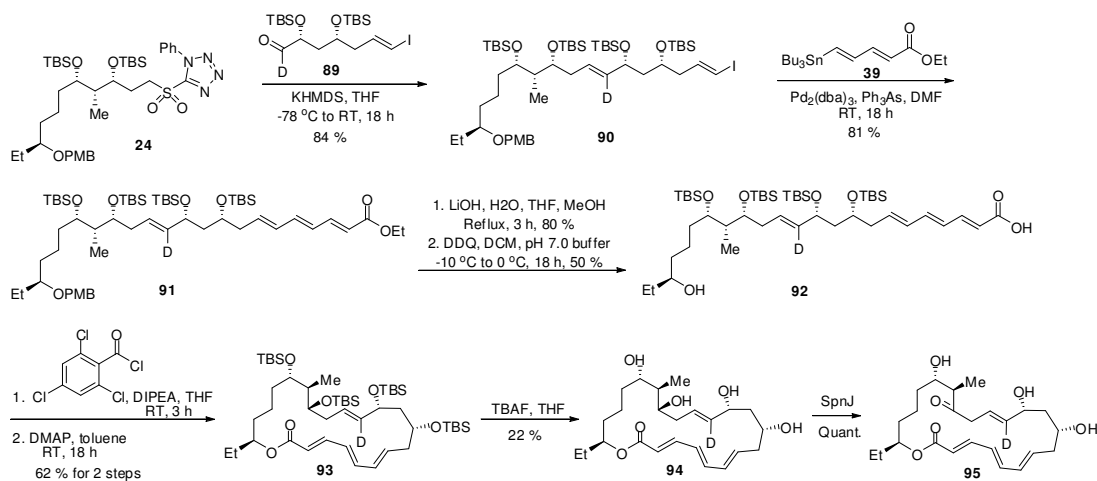
(2R,4R,E)-2,4-bis(tert-butyldimethylsilyloxy)-7-iodohept-6-en-1-ol with 1-deuteride (88): Lithium aluminum deuteride (LiAlD_4 ; 265 mg, 5.6 mol) was added portionwise to a solution of ester compound (2.0 g, 3.8 mmol) in anhydrous THF (37 mL) at $-78\text{ }^\circ\text{C}$. The reaction mixture was stirred at $-78\text{ }^\circ\text{C}$ for 2 hours, and quenched with saturated the aqueous ammonium chloride solution (37 mL). After filtration and washing with ethylacetate (30 mL), the aqueous fraction was extracted with ethyl acetate (50 mL x 5 times). The combined organic fractions were then dried over an anhydrous sodium sulfate pad and concentrated under reduced pressure. The resulting residue was subjected with flash column chromatography. The target compound was eluted with 5% to 10% EtOAc/Hexane (0.84 g, 44%) with a portion of starting material also recovered (0.92 g, 46%).

^1H NMR (CDCl_3 , 600 MHz) δ (ppm) 6.46 (ddd, 1H, $J = 7.1, 8.0, 14.5$ Hz, 6-H), 6.04 (d, 1H, $J = 14.7$ Hz, 7-H), 3.85 (dd, $J = 5.7, 7.6$ Hz, 2-H), 3.83-3.79 (m, 1H, 4-H), 2.27-2.22 (m, 1H, 5-H), 2.20-2.15 (m, 1H, 5-H), 1.71-1.61 (m, 2H, 3-Hs), 0.88 (s, 9H, CH3 of TBS), 0.87 (s, 9H, tBu of TBS), 0.066 (CH3 of TBS), 0.062 (CH3 of TBS), 0.041 (CH3 of TBS), 0.032 (CH3 of TBS); ^{13}C NMR (CDCl_3 , 150 MHz) δ (ppm) 173.77 (1-

C=O), 142.60 (C-6), 137.30 (C-7), 69.66 (C-2), 68.30 (C-4), 65.44 (quint, $J = 20.4$ Hz, C-1), 43.68 (C-5), 41.29 (C-3), 25.81 (CH₃ of tBu), 25.78 (CH₃ of tBu), 18.04 (Me₃-C-Si), 17.96 (Me₃-C-Si), -4.35 (CH₃ of TBS), -4.46 (CH₃ of TBS), -4.52 (CH₃ of TBS), -4.63 (CH₃ of TBS); HRMS (ESI, positive) m/z for C₁₉H₃₉D₂IO₃Si₂ [M+Na]⁺: calcd 525.1657, found 525.1657.

(2R,4R,E)-2,4-bis(tert-butyldimethylsilyloxy)-7-iodohept-6-enal with 1-deuteriude (89): Compound (89) was prepared following the same procedure as compound (36) quantitatively. Spectral data was not collected.

B. Synthesis of [C12-²H] SpnM Substrate analog by Coupling Reactions and Enzymatic Conversion: The overall synthetic scheme is pictured in **Scheme 2-12**.



Scheme 2-12. Preparation of [C12-²H] SpnM substrate analog.

(5R,7R,11R,12R,13S,E)-7,11-bis(tert-butyldimethylsilyloxy)-5-((E)-3-iodoallyl)-13-(4-(4-methoxybenzyloxy)hexyl)-2,2,3,3,12,15,15,16,16-nonamethyl-4,14-dioxa-3,15-disilaheptadec-8-ene with mono-deuteride (90): Compound (90) was prepared

following the same procedure as compound (43) using compound (89) instead of compound (36) with a yield of 84%.

¹H NMR (CDCl₃, 500 MHz) δ (ppm) 7.27 (d, 2H, *J* = 8.8 Hz, PhH of PMB), 6.87 (d, 2H, *J* = 8.5 Hz, PhH of PMB), 6.54-6.48 (m, 1H, 2-H), 6.01 (d, 1H, *J* = 14.4 Hz, 1-H), 5.54 (t, 1H, *J* = 7.1 Hz, 7-H), 4.44 (s, 2H, CH₂ of PMB), 4.11 (t, 1H, *J* = 5.9 Hz, 6-H), 3.84-3.81 (m, 4H, 4-H+OCH₃ of PMB), 3.79-3.75 (m, 1H, 10-H), 3.72-3.69 (m, 1H, 12-H), 3.31-3.28 (m, 1H, 16-H), 2.32-2.24 (m, 3H, 3-H₂+9-Hs), 2.16-2.10 (m, 1H, 3-H), 1.77-1.70 (m, 1H, 11-H), 1.65-1.27 (m, 10H, 5-Hs+13-Hs+14-Hs+15-Hs+17-Hs), 0.94-0.86 (m, 42H, 4 x *t*Bu of TBS+11-CH₃+18-Hs), 0.075-0.022 (m, 24H, 8 x CH₃ of TBS); ¹³C NMR (CDCl₃, 125 MHz) δ (ppm) 159.01, 143.30, 135.17 (t, *J* = 19.1 Hz, C-7), 131.30, 129.17, 126.69, 113.71, 79.78, 76.45, 72.89, 72.24, 70.65, 70.45, 68.21, 55.25, 46.01, 43.46, 41.25, 37.82, 35.39, 33.90, 26.34, 26.25, 25.99, 25.90, 25.85, 21.28, 18.17, 18.14, 18.11, 18.01, 9.51, 3.73, 3.91, 4.25, 4.35, 4.43, 4.50, 4.62, 4.72; HRMS (ESI, positive) *m/z* for C₅₁H₉₈DIO₆Si₄ [M+Na]⁺: calcd 1070.5518, found 1070.5506.

(2E,4E,6E,9R,11R,12E,15R,16R,17S)-ethyl 9,11,15,17-tetrakis(tert-butyltrimethylsilyloxy)-21-(4-methoxybenzyloxy)-16-methyltricoso-2,4,6,12-

tetraenoate with 12-deuteride (91): Compound (91) was prepared following the same procedure as compound (45) with a yield of 81%.

¹H NMR (CDCl₃, 500 MHz) δ (ppm) 7.40 (dd, 1H, *J* = 11.3, 14.1 Hz, 3-H), 7.24 (d, 2H, *J* = 8.6 Hz, PhH of PMB), 6.84 (d, 2H, *J* = 8.7 Hz, PhH of PMB), 6.50 (dd, 1H, *J* = 10.8, 14.5 Hz, 5-H), 6.18 (dd, 1H, *J* = 11.5, 14.8 Hz, 4-H), 6.11 (dd, 1H, *J* = 11.1, 15.3 Hz, 6-H), 5.91-5.84 (m, 1H, 7-H), 5.82 (d, 1H, *J* = 15.3 Hz, 2-H), 5.51 (dd, 1H, *J* = 6.8,

7.2 Hz, 13-H), 4.44 (s, 2H, CH₂ of PMB), 4.18 (q, 2H, $J = 7.1$ Hz, CH₂ of Et), 4.13-4.10 (m, 1H, 21-H), 3.84-3.80 (m, 1H, 11-H), 3.77 (s, 3H, OCH₃ of PMB), 3.75-3.72 (m, 1H, 9-H), 3.68-3.65 (m, 1H, 15-H), 3.28-3.26 (m, 1H, 17-H), 2.38-2.20 (m, 4H, 8-Hs+14-CH₂), 1.72-1.21 (m, 11H, 10-CH₂,16-CH+18-CH₂+19-CH₂+20-CH₂+22-CH₂), 0.95-0.82 (m, 45H, 23-CH₂+CH₃ of Et, 4 x *t*Bu of TBS+16-CH₃), 0.030-0.010 (m, 24H, 8 x CH₃ of TBS); ¹³C NMR (CDCl₃, 125 MHz) δ (ppm) 167.16, 159.02, 147.15, 144.71, 140.89, 140.27, 136.97, 136.53, 135.21 (t, $J = 19.5$ Hz, 12-C), 132.02, 131.30, 129.17, 129.16, 128.13, 126.65, 120.27, 114.31, 113.71, 79.78, 72.89, 72.26, 70.72, 70.46, 70.43, 68.95, 60.17, 55.24, 46.13, 41.24, 40.75, 37.84, 37.77, 35.41, 33.91, 29.14, 27.84, 26.83, 26.62, 25.98, 25.90, 25.86, 21.29, 18.17, 18.13, 18.08, 18.05, 18.03, 17.52, 16.42, 14.31, 13.58, 13.55, 9.51, 9.50, 4.72, 4.52, 4.38, 4.30, 4.26, 3.94, 3.76, 3.73; HRMS (ESI, positive) m/z for C₅₈H₁₀₇DO₈Si₄ [M+Na]⁺: calcd 1068.7076, found 1068.7075.

(2E,4E,6E,9R,11R,12E,15R,16R,17S,21S)-9,11,15,17-tetrakis(tert-butyltrimethylsilyloxy)-21-hydroxy-16-methyltricoso-2,4,6,12-tetraenoic acid with 12-deuteride (92): Compound (92) was prepared following the same procedure as compound (47) with a yield of 40% for 2 steps.

¹H NMR (CDCl₃, 500 MHz) δ (ppm) 7.38 (dd, 1H, $J = 11.2, 14.9$ Hz, 3-H), 6.57 (dd, 1H, $J = 10.4, 14.6$ Hz, 5-H), 6.24 (dd, 1H, $J = 11.5, 14.8$ Hz, 4-H), 6.16 (dd, 1H, $J = 11.1, 15.1$ Hz, 6-H), 5.99-5.93 (m, 1H, 7-H), 5.85 (d, 1H, $J = 15.2$ Hz, 2-H), 5.55 (dd, 1H, $J = 7.0, 7.1$ Hz, 13-H), 4.14-4.11 (m, 1H, 21-H), 3.86-3.81 (m, 1H, 11-H), 3.76-3.73 (m, 1H, 9-H), 3.71-3.68 (m, 1H, 15-H), 3.26-3.18 (m, 1H, 17-H), 2.42-2.33 (m, 1H, 8-H), 2.27-2.22 (m, 3H, 8-H+14-Hs), 1.75-1.09 (m, 11H, 10-Hs+16-H+18-Hs+19-Hs+20-

Hs+22-Hs), 0.94 (t, 3H, $J = 7.4$ Hz, 23-Hs), 0.887–0.881 (m, 36H, 4 x *t*Bu of TBS), 0.94 (d, 3H, $J = 6.8$ Hz, 16-CH₃), 0.045-0.017 (m, 24H, 8 x CH₃ of TBS); ¹³C NMR (CDCl₃, 125 MHz) δ (ppm) 171.37, 147.04, 142.05, 137.37, 135.15 (t, $J = 19.5$ Hz, C-12), 131.99, 129.25, 128.62, 127.90, 126.77, 119.06, 113.71, 73.08, 72.63, 72.18, 70.77, 68.97, 46.12, 40.81, 40.64, 37.63, 37.42, 35.05, 30.11, 27.84, 26.83, 25.95, 25.93, 25.86, 21.32, 18.19, 18.15, 18.12, 18.05, 17.52, 13.58, 9.87, 9.31, -3.78, -3.82, -4.00, -4.29, -4.35, -4.38, -4.59, -4.71; HRMS (ESI, positive) m/z for C₄₈H₉₅DO₇Si₄ [M+Na]⁺: calcd 920.6188, found 920.6178.

(3E,5E,7E,10R,12R,13E,16R,17R,18S,22S)-10,12,16,18-tetrakis(tert-butyltrimethylsilyloxy)-22-ethyl-17-methyloxacyclodocosa-3,5,7,13-tetraen-2-one

with 12-deuteride (93): Compound (93) was prepared following the same procedure as compound (49) with a yield of 62% for 2 steps. No spectral data was collected.

(3E,5E,7E,10R,12R,13E,16R,17R,18S,22S)-22-ethyl-10,12,16,18-tetrahydroxy-17-methyloxacyclodocosa-3,5,7,13-tetraen-2-one with 12-deuteride (94): Compound (94) was prepared following the same procedure as compound (50) with a yield of 22%.

¹H NMR (CDCl₃, 500 MHz) δ (ppm) 7.25 (dd, 1H, $J = 10.7, 14.8$ Hz, 3-H), 6.70 (dd, 1H, $J = 11.1, 14.9$ Hz, 5-H), 6.35 (dd, 1H, $J = 11.0, 14.8$ Hz, 4-H), 6.18 (dd, 1H, $J = 10.6, 15.0$ Hz, 6-H), 5.92-5.88 (m, 1H, 7-H), 5.85 (d, 1H, $J = 15.6$ Hz, 2-H), 5.18 (dd, 1H, $J = 6.6, 7.4$ Hz, 13-H), 4.76-4.73 (m, 1H, 21-H), 3.79-3.75 (m, 1H, 11-H), 3.71-3.64 (m, 1H, 9-H), 3.57-3.51 (m, 1H, 15-H), 3.49-3.43 (m, 1H, 17-H), 2.48-2.09 (m, 4H, 8-Hs+14-Hs), 1.73-1.22 (m, 11H, 10-Hs+16-H+18-Hs+19-Hs+20-Hs+22-Hs), 0.88-0.81 (m, 6H, 23-Hs+16-CH₃); ¹³C NMR (CDCl₃, 150 MHz) δ (ppm) 166.62 (1-C=O), 145.47 (C-3),

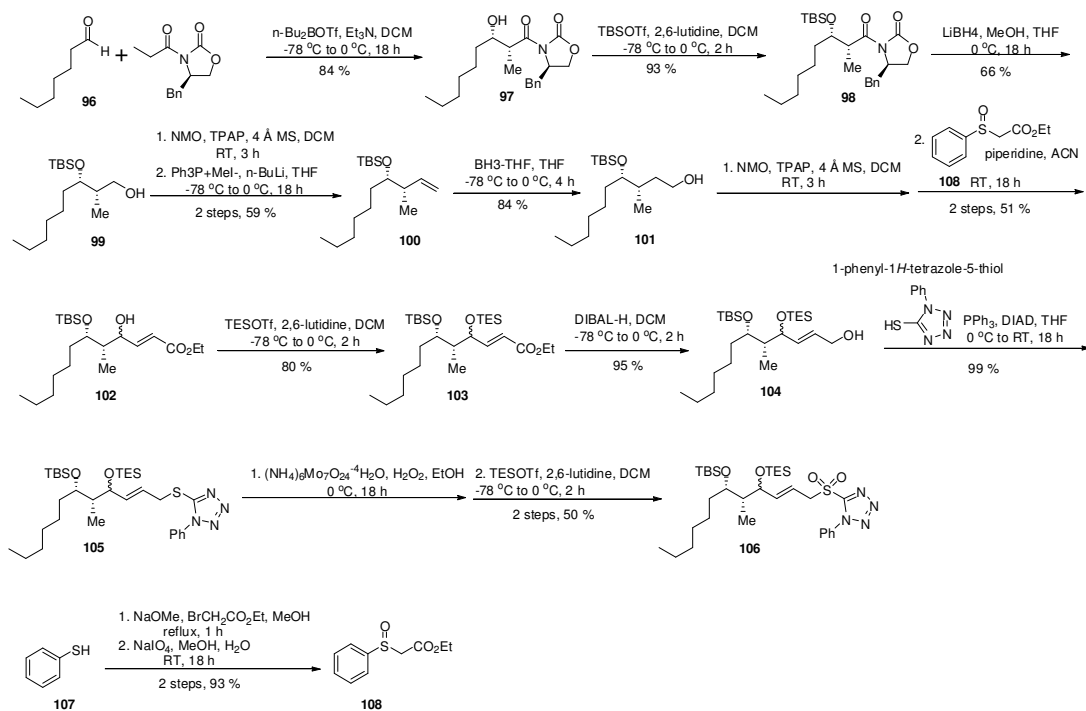
142.22 (C-5), 137.68 (C-7), 132.39 (C-6), 128.47 (C-4), 126.57 (C-13), 120.92 (C-2), 75.46, 75.12, 74.07, 70.07, 67.64, 60.44, 46.52, 43.51, 34.57, 27.98, 22.02, 10.43, 6.78; HRMS (ESI, positive) m/z for $C_{24}H_{37}DO_6$ $[M+Na]^+$: calcd 446.2623, found 446.2626.

[C12-²H] SpnM substrate analog (95): Compound (95) was prepared following the same procedure as compound (51) quantitatively.

HRMS (ESI, positive) m/z for $C_{24}H_{35}DO_6$ $[M+Na]^+$: calcd 444.2467, found 444.2479.

2.2.8. Synthesis of the Linear SpnF Substrate Analog (Linear analog)

A. Preparation of Fragment A: The overall synthetic scheme is shown in **Scheme 2-13**.



Scheme 2-13. Preparation of fragment A for the synthesis of Linear SpnF substrate analog.

(R)-4-benzyl-3-((2R,3S)-3-hydroxy-2-methylnonanoyl)oxazolidin-2-one (97): Di-n-butylboron trifluoromethanesulfonate (107.4 mL, 1.0 M in DCM, 107.4 mmol) was

added over 10 min to a solution of chiral auxiliary (25.1 g, 107 mmol) in dichloromethane (600 mL) at 0 °C, and the reaction mixture was stirred at the same temperature for 10 min. Triethylamine (19.2 mL, 137 mmol) was slowly added to the reaction mixture at 0 °C for 10 min, which was then stirred at 0 °C for an additional 30 min. After cooling the above reaction mixture to -78 °C, heptanal (15.0 g, 131 mmol) in dichloromethane (120 mL) was added dropwise to the reaction mixture over 10 min with vigorous stirring. The reaction mixture was kept stirring at -78 °C for 1 hour and allowed to warm to 0 °C over 18 hours. After sequential quenching with pH 7 phosphate buffer (120 mL), methanol (240 mL), and 30% hydrogen peroxide solution (120 mL) at 0 °C over 1 hour, the reaction mixture was stirred at room temperature for an additional 1 hour. The aqueous fraction was extracted with ethyl acetate (200 mL x 4 times), and the combined organic fractions were washed with brine (200 mL), dried over an anhydrous sodium sulfate pad, and concentrated under reduced pressure. The resulting residue was purified using flash column chromatography. The target compound was eluted with 20% EtOAc/Hexane (31.2 g, 84%).

^1H NMR (CDCl_3 , 500 MHz) δ (ppm) 7.33-7.30 (m, 2H, Ph-H), 7.27-7.24 (m, 1H, Ph-H), 7.20-7.17 (m, 2H, Ph-H), 4.71-4.66 (m, 1H, 4'-H), 4.23-4.15 (dd, $J = 17.0, 9.0$ Hz, 2H, 3'-H), 3.94-3.90 (m, 1H, 3-H), 3.75 (ddd, $J = 15.0, 7.0, 2.5$ Hz, 1H, 2-H), 3.23 (dd, $J = 13.5, 3.5$ Hz, 1H, 5'-Ha), 2.77 (dd, $J = 13.5, 9.5$ Hz, 1H, 5'-Hb), 1.53-1.38 (m, 2H, 4-H), 1.31-1.25 (m, 8H, 5-H, 6-H, 7-H, 8-H), 1.24 (d, $J = 7.0$ Hz, 3H, 10-H), 0.87-0.84 (t, $J = 7.0$ Hz, 3H, 9-H); ^{13}C NMR (CDCl_3 , 125 MHz) δ (ppm) 177.6 (C-1), 153.0 (1'-C=O), 135.0 (C1 of Ph), 129.4 (C2, C5 of Ph), 129.0 (C3, C5 of Ph), 127.4 (C4 of Ph), 71.5 (C-

3), 66.2 (C-3'), 55.1 (4'-CH₂), 42.1 (C-2), 37.8 (C-5'), 33.8 (C-4), 31.8 (C-7), 29.2 (C-8), 26.0 (C-6), 22.6 (C-5), 14.0 (C-10), 10.4 (C-9); HRMS (ESI, positive) *m/z* for C₂₀H₂₉NO₄ [M+Na]⁺: calcd 370.1994, found 370.1989.

(R)-4-benzyl-3-((2R,3S)-3-(tert-butyldimethylsilyloxy)-2-

methylnonanoyl)oxazolidin-2-one (98): Compound **(98)** was prepared following the same procedure as compound **(14)** with a yield of 93%.

¹H NMR (CDCl₃, 500 MHz) δ (ppm) 7.35-7.30 (m, 2H, Ph-H), 7.29-7.25 (m, 1H, Ph-H), 7.22-7.18 (m, 1H, Ph-H), 4.66-4.57 (m, 1H, 4'-H), 4.18-4.09 (m, 2H, 3'-H), 3.98 (dd, J = 11.0, 6.0 Hz, 1H, 3-H), 3.86 (ddd, J = 13.5, 7.0, 5.0 Hz, 1H, 2-H), 3.29 (dd, J = 13.0, 3.0 Hz, 1H, 5'-Ha), 2.77 (dd, J = 13.5, 10.0 Hz, 1H, 5'-Hb), 1.56-1.59 (m, 2H, 4-H), 1.31-1.25 (m, 8H, 5-H, 6-H, 7-H, 8-H), 1.20 (d, J = 7.0 Hz, 3H, 10-H), 0.88 (t, J = 3.0 Hz, 3H, 9-H), 0.87 (s, 9H, TBS), 0.04 (s, 3H, TBS), -0.01 (s, 3H, TBS); ¹³C NMR (CDCl₃, 125 MHz) δ (ppm) 175.3 (C-1), 153.1 (C-1'), 135.4 (C1 of Ph), 129.5 (C2, C6 of Ph), 128.9 (C3, C5 of Ph), 127.3 (C4 of Ph), 72.9 (C-3), 66.0 (C-3'), 55.8 (C-4'), 42.8 (C-2), 37.6 (C-5'), 35.6 (C-4), 31.7 (C-7), 29.5 (C-8), 25.8 (3 x CH₃-C-Si), 24.9 (C-6), 22.6 (C-5), 18.0 (CH₃-C-Si), 14.1 (C-9), 11.5 (C-10), -4.1 (CH₃-Si), -4.8 (CH₃-Si); HRMS (ESI, positive) *m/z* for C₂₆H₄₃NO₄Si [M+Na]⁺: calcd 484.2859, found 484.2854.

(2S,3S)-3-(tert-butyldimethylsilyloxy)-2-methylnonan-1-ol (99): Compound **(99)** was prepared following the same procedure as compound **(15)** with a yield of 66%.

¹H NMR (CDCl₃, 500 MHz) δ (ppm) 3.76-3.73 (m, 1H, 3-H), 3.69 (dd, J = 10.5, 8.5 Hz, 1H, 1-Ha), 3.51 (dd, J = 10.5, 5.0 Hz, 1H, 1-Hb), 2.47 (br s, 1H, OH), 2.04-1.91 (m, 1H, 2-H), 1.49-1.43 (m, 2H, 4-H), 1.32-1.24 (m, 8H, 5-H, 6-H, 7-H, 8-H), 0.92 (s,

9H, TBS), 0.90 (t, $J = 5.5$ Hz, 3H, 9-H), 0.81 (d, $J = 7.0$ Hz, 3H, 10-H), 0.09 (s, 3H, TBS), 0.07 (s, 3H, TBS); ^{13}C NMR (CDCl_3 , 125 MHz) δ (ppm) 75.9 (C-3), 66.1 (C-1), 39.5 (C-2), 32.4 (C-4), 31.8 (C-7), 29.5 (C-9), 26.2 (C-6), 25.9 (3 x $\text{CH}_3\text{-C-Si}$), 22.6 (C-5), 18.0 (C-Si), 14.1 (C-9), 11.9 (C-10), -4.4 ($\text{CH}_3\text{-Si}$), -4.5 ($\text{CH}_3\text{-Si}$); HRMS (ESI, positive) m/z for $\text{C}_{16}\text{H}_{36}\text{O}_2\text{Si}$ $[\text{M}+\text{Na}]^+$: calcd 311.2382, found 311.2377.

Tert-butyldimethyl((3S,4S)-3-methyldec-1-en-4-yloxy)silane (100): Compound (100) was prepared following the same procedure as compound (16) with a yield of 59% for 2 steps.

^1H NMR (CDCl_3 , 500 MHz) δ (ppm) 5.86 (ddd, $J = 17.5, 10.0, 7.0$ Hz, 1H, 2-H), 5.00 (ddd, $J = 8.5, 2.0, 1.5$ Hz, 1H, 1-Ha), 4.97 (dd, $J = 3.5, 2.0$ Hz, 1H, 1-Hb), 3.52 (dd, $J = 10.5, 5.0$ Hz, 1H, 4-H), 2.33-2.26 (m, 1H, 3-H), 1.40-1.33 (m, 2H, 5-H), 1.29-1.20 (m, 8H, 6-H, 7-H, 8-H, 9-H), 0.96 (d, $J = 6.5$ Hz, 3H, 11-H), 0.90 (s, 9H, TBS), 0.89 (t, $J = 2.5$ Hz, 3H, 10-H), 0.04 (s, 6H, TBS); ^{13}C NMR (CDCl_3 , 125 MHz) δ (ppm) 141.8 (C-2), 113.6 (C-1), 76.0 (C-4), 42.7 (C-3), 33.8 (C-5), 31.9 (C-8), 29.6 (C-7), 26.0 (3 x $\text{CH}_3\text{-C-Si}$), 25.2 (C-6), 22.6 (C-9), 18.2 (C-Si), 14.8 (C-11), 14.1 (C-10), -4.3 ($\text{CH}_3\text{-Si}$), -4.4 ($\text{CH}_3\text{-Si}$); HRMS (ESI, positive) m/z for $\text{C}_{17}\text{H}_{36}\text{OSi}$ $[\text{M}+\text{Na}]^+$: calcd 307.2433, found 307.2428.

(3S,4S)-4-(tert-butyldimethylsilyloxy)-3-methyldec-1-ol (101): Borane-THF solution (62.2 mL, 1.0 M in THF, 62.2 mmol) was added dropwise to a solution of allyl compound (11.8 g, 41.5 mmol) in anhydrous THF (414 mL) at -78 °C over 20 min with vigorous stirring. The reaction mixture was kept stirring at -78 °C for 1 hour, and allowed to warm to 0 °C for 3 hours. Then, the reaction mixture was quenched with the aqueous 3

N sodium hydroxide solution (207 mL) and the aqueous 30% hydrogen peroxide solution (207 mL) over 1 hour at 0 °C. The organic fraction was isolated, and the aqueous fraction was extracted with ethyl acetate (100 mL x 4 times). The combined organic fractions were washed with brine (200 mL), dried over an anhydrous sodium sulfate pad, and concentrated under reduced pressure. The resulting residue was subjected to the flash column chromatography. The target compound was eluted with 20% EtOAc/Hexane (10.5 g, 84%).

¹H NMR (CDCl₃, 500 MHz) δ (ppm) 3.69-3.64 (m, 1H, 1-Ha), 3.63-4.57 (m, 1H, 1-Hb), 3.54-3.50 (m, 1H, 4-H), 1.74-1.68 (m, 2H, 3-H, 2-Ha), 1.46-1.38 (m, 1H, 5-Ha), 1.37-1.33 (m, 3H, 2-Hb, 5-Hb, 6-Ha), 1.30-1.22 (m, 6H, 7-H, 8-H, 9-H), 1.18-1.14 (m, 1H, 6-Hb), 0.88 (s, 9H, TBS), 0.86 (t, J = 5.0 Hz, 3H, 10-H), 0.85 (d, J = 4.5 Hz, 3H, 11-H), 0.05 (s, 6H, TBS); ¹³C NMR (CDCl₃, 125 MHz) δ (ppm) 76.8 (C-4), 62.1 (C-1), 37.1 (C-3), 35.6 (C-2), 32.2 (C-5), 31.9 (C-8), 29.5 (C-7), 26.4 (C-6), 25.9 (CH₃-C-Si), 22.6 (C-9), 18.1 (C-Si), 16.9 (C-11), 14.1 (C-10), -4.3 (CH₃-Si), -4.4 (CH₃-Si).

(5S,6S,E)-ethyl 6-(tert-butyldimethylsilyloxy)-4-hydroxy-5-methyldodec-2-enoate (102): 1) The reaction mixture of alcohol compound (11.5 g, 38.0 mmol), 4-methylmorpholine N-oxide (NMO; 8.9 g, 76.0 mmol), tetrapropylammonium perruthenate (TPAP; 599 mg, 1.9 mmol) and activated 4 Å molecular sieve (1.2 g) in dichloromethane (380 mL) was stirred at room temperature for 3 hours. After filtering through a paper filter and washing with dichloromethane (100 mL x 2 times), the filtrate was directly concentrated and used for the next reaction without further purification. 2) Ethyl 2-(phenylsulfinyl)acetate (**108**, 16.1 g, 76.0 mmol) and piperidine (9.4 mL, 95.3

mmol) were pre-mixed in anhydrous acetonitrile (76 mL) with stirring at room temperature for 30 min. A solution of the above aldehyde in acetonitrile (38 mL) was very slowly added to the reaction mixture via cannular at room temperature over 60 min. The reaction mixture was kept stirring at room temperature for 18 hours, and quenched with saturated the aqueous sodium bicarbonate solution (114 mL). Organic phase was separated, and the aqueous fraction was extracted with ethyl acetate (100 mL x 5 times). The combined organic fractions were washed with brine (200 mL), dried over an anhydrous sodium sulfate pad, and concentrated. The resulting residue was purified using flash column chromatography. The target compound was eluted with 5% EtOAc/Hexane (7.5 g, 51% for 2 steps).

^1H NMR (CDCl_3 , 600 MHz) δ (ppm) 6.87 (dd, $J = 15.6, 3.6$ Hz, 1H, 3-H), 6.09 (dd, $J = 5.6, 3.6$ Hz, 1H, 2-H), 4.91 (quint, $J = 2.4$ Hz, 1H, 4-H), 4.18 (q, $J = 7.2$ Hz, 2H, 14-H), 3.90 (ddd, $J = 9.0, 5.4, 3.0$ Hz, 1H, 6-H), 1.7601.74 (m, 1H, 5-H), 1.58-1.55 (m, 1H, 7-Ha), 1.50-1.46 (m, 1H, 7-Hb), 1.29-1.22 (m, 9H, 8-Ha, 9-H, 10-H, 11-H), 1.23 (t, $J = 7.2$ Hz, 3H, 15-H), 1.22-1.17 (m, 1H, 8-Hb), 0.89 (s, 9H, TBS), 0.87 (t, $J = 7.2$ Hz, 3H, 12-H), 0.82 (d, $J = 7.2$ Hz, 3H, 13-H), 0.099 (s, 3 H, TBS), 0.095 (s, 3H, TBS); ^{13}C NMR (CDCl_3 , 150 MHz) δ (ppm) 171.1 (C-1), 166.7 (C-3), 149.4 (C-2), 77.8 (C-6), 74.5 (C-4), 60.2 (C-14), 39.7 (C-5), 34.7 (C-7), 31.8 (C-10), 29.4 (C-9), 25.9 (3 x $\text{CH}_3\text{-C-Si}$), 25.6 (C-8), 22.6 (C-11), 18.0 (C-Si), 14.2 (C-12), 14.0 (C-15), 5.6 (C-13), -3.6 ($\text{CH}_3\text{-Si}$), -4.5 ($\text{CH}_3\text{-Si}$); LRMS (ESI, positive) m/z for $\text{C}_{21}\text{H}_{42}\text{O}_4\text{Si}$ $[\text{M}+\text{Na}]^+$: calcd 409.3, found 409.3.

(5R,6S,E)-ethyl 6-(tert-butyldimethylsilyloxy)-5-methyl-4-(triethylsilyloxy)dodec-2-enoate (103): TESOTf (5.3 mL, 23.3 mmol) was added over 10 min to a solution of

secondary alcohol compound (7.5 g, 19.4 mmol) and 2,6-lutidine (4.5 mL, 38.8 mmol) in dichloromethane (193 mL) at -78 °C. The reaction mixture was subsequently kept stirring at -78 °C for 30 min and at 0 °C for 1 hour. After quenching the reaction mixture with saturated the aqueous ammonium chloride solution (193 mL) over 30 min, the aqueous fraction was extracted with dichloromethane (100 mL x 5 times). The combined organic fractions were washed with brine (100 mL), dried over an anhydrous sodium sulfate pad, and concentrated. The resulting residue was subjected to flash column chromatography. The target compound was eluted with 5% EtOAc/Hexane (7.8 g, 80%).

¹H NMR (CDCl₃, 500 MHz) δ (ppm) 6.94 (dd, J = 15.5, 6.0 Hz, 1H, 3-H), 5.91 (dd, J = 15.5, 1.5 Hz, 1H, 2-H), 4.30 (td, J = 6.0, 1.5 Hz, 1H, C-4), 4.18 (q, J = 7.0 Hz, 2H, 14-H), 3.64 (td, J = 6.0, 4.0 Hz, 1H, 6-H), 1.64-1.60 (m, 1H, 5-H), 1.48-1.43 (m, 2H, 7-H), 1.27 (t, J = 7.5 Hz, 3H, 15-H), 1.26-1.22 (m, 8H, 8-H, 9-H, 10-H, 11-H), 0.93 (t, J = 8.0 Hz, 9H, TES), 0.89 (d, J = 7.0 Hz, 3H, 13-H), 0.87 (m, 3H, C-12), 0.865 (m, 9H, TBS), 0.57 (q, J = 5.7 Hz, 6H, TES), 0.02 (s, 3H, TBS), 0.01 (s, 3H, TBS); ¹³C NMR (CDCl₃, 125 MHz) δ (ppm) 166.6 (C-1), 150.6 (C-3), 120.6 (C-2), 73.0 (C-4), 72.6 (C-6), 60.3 (C-14), 43.9 (C-5), 34.6 (C-7), 31.8 (C-10), 29.5 (C-9), 25.9 (3 x CH₃-C-Si), 25.4 (C-8), 22.6 (C-11), 18.2 (C-Si), 14.2 (C-15), 14.1 (C-12), 0.8 (C-13), 6.8 (3 x CH₃-CH₂-Si), 5.0 (3 x CH₂-Si), -3.7 (CH₃-Si), -4.4 (CH₃-Si).

(5R,6S,E)-6-(tert-butyl dimethylsilyloxy)-5-methyl-4-(triethylsilyloxy)dodec-2-en-1-ol (104): Diisobutylaluminium hydride (DIBAL-H; 18.5 mL, 1.0 M in DCM, 18.5 mmol) was added dropwise to a solution of ester compound (7.7 g, 15.4 mmol) in dichloromethane (154 mL) at -78 °C over 10 min. The reaction mixture was stirred at -78 °C for 30 min

and at 0 °C for 1 hour, then quenched with saturated the aqueous Na⁺K⁺ tartrate (100 mL) at room temperature over 2 hours. After filtering through celite and washing with dichloromethane (100 mL x 2 times), the filtrate was extracted with dichloromethane (100 mL x 3 times). The combined organic fractions were washed with brine (100 mL), dried over an anhydrous sodium sulfate pad, and concentrated under reduced pressure. The resulting residue was purified using flash column chromatography. The target compound was eluted with 10% EtOAc/Hexane (6.7 g, 95%).

¹H NMR (CDCl₃, 500 MHz) δ (ppm) 5.76-5.70 (m, 1H, 3-H), 5.68-5.58 (m, 1H, 2-H), 4.12 (dd, J = 10.0, 6.0 Hz, 2H, 1-H), 4.11-4.01 (dt, J = 39.0, 6.0 Hz, 1H, 4-H), 3.86-3.62 (tdt, J = 107.0, 5.0, 3.0 Hz, 1H, 6-H), 1.57-1.52 (m, 1H, 5-H), 1.47-1.42 (m, 2H, 7-H), 1.29-1.16 (m, 8H, 8-H, 9-H, 10-H, 11-H), 0.94-0.91 (m, 9H, TES), 0.86 (s, 9H, TBS), 0.85 (m, 3H, 12-H), 0.70 (d, J = 6.0 Hz, 3H, 13-H), 0.58-0.53 (m, 6H, TES), 0.03 (s, 3H, TBS), -0.01 (s, 3H, TBS); ¹³C NMR (CDCl₃, 125 MHz) δ (ppm) 134.8 (C-2), 129.7 (C-3), 74.2 (C-4), 72.6 (C-6), 63.4 (C-1), 43.8 (C-5), 34.9 (C-7), 31.8 (C-10), 29.5 (C-9), 25.4 (C-8), 22.6 (C-11), 18.2 (C-Si), 9.4 (C-13), 6.9 (3 x CH3-C-Si), 5.2 (3 x CH2-Si), -3.6 (CH3-Si), -4.4 (CH3-Si).

5-((5R,6S,E)-6-(tert-butyldimethylsilyloxy)-5-methyl-4-(triethylsilyloxy)dodec-2-enylthio)-1-phenyl-1H-tetrazole (105): Compound (105) was prepared following the same procedure as compound (22) with a yield of 99%.

¹H NMR (CDCl₃, 500 MHz) δ (ppm) 7.54-7.51 (m, 5H, Ph-H), 5.85-5.79 (m, 1H, 3-H), 5.77-5.71 (m, 1H, 2-H), 4.11-4.02 (m, 2H, 1-H), 4.00-3.83 (m, 1H, 4-H), 3.81-3.56 (m, 1H, 6-H), 1.55-1.47 (m, 1H, 5-H), 1.45-1.39 (m, 2H, 7-H), 1.29-1.20 (m, 8H, 8-H, 9-

H, 10-H, 11-H), 0.88-0.84 (m, 20H, TBS, TES, 12-H, 13-H), 0.53-0.49 (m, 6H, TES), -0.20 (s, 3H, TBS), -0.06 (s, 3H, TBS); ^{13}C NMR (CDCl_3 , 125 MHz) δ (ppm) 153.8 (C-1' of tetrazole), 139.3 (C-3), 130.0 (C-1'' of PhH), 129.8 (C-3'', 4'', 5'' of PhH), 123.9 (C-2'' of PhH), 123.8 (C-6'' of PhH), 123.7 (C-2), 73.9 (C-4), 72.5 (C-6), 43.8 (C-5), 35.0 (C-7), 34.8 (C-1), 31.8 (C-10), 29.5 (C-9), 25.4 (C-8), 22.6 (C-11), 18.1 (C-Si), 14.1 (C-12), 9.3 (C-13), 6.8 (3 x $\text{CH}_3\text{-C-Si}$), 5.1 (3 x $\text{CH}_2\text{-Si}$), -3.7 ($\text{CH}_3\text{-Si}$), -4.4 ($\text{CH}_3\text{-Si}$).

5-((5R,6S,E)-6-(tert-butyldimethylsilyloxy)-5-methyl-4-(triethylsilyloxy)dodec-2-enylsulfonyl)-1-phenyl-1H-tetrazole (106): 1) The pre-mixed solution of ammonium heptamolybdate (2.4 g, 1.9 mmol) in the aqueous 30% hydrogen peroxide (9.5 mL, 93.0 mmol) was added over 10 min to a solution of thioether compound (4.8 g, 7.8 mmol) in ethanol (62 mL) at 0 °C, and the reaction mixture was stirred at 4 °C for 18 hours. After dilution with brine (62 mL) at 0 °C, the aqueous fraction was extracted with ethyl acetate (50 mL x 5 times). The combined organic fractions were dried over an anhydrous sodium sulfate pad and concentrated under reduced pressure. The residue was subjected to flash column chromatography. The intermediate compound was eluted with 10% to 20% EtOAc/Hexane (4.0 g, 96%). 2) TESOTf (2.1 mL, 8.9 mmol) was added dropwise over 20 min to a solution of above compound (4.0 g, 7.5 mmol) and 2,6-lutidine (1.7 mL, 8.9 mmol) in dichloromethane (75 mL) at -78 °C. The reaction mixture was stirred at -78 °C for 1 hour and at 0 °C for 1 hour. After quenching with saturated the aqueous ammonium chloride solution (75 mL), the aqueous fraction was extracted with dichloromethane (50 mL x 4 times). The combined organic fractions were washed with brine (50 mL), dried over an anhydrous sodium sulfate pad, and concentrated under reduced pressure. The

resulting residue was purified using flash column chromatography. The target compound was eluted with 10% EtOAc/Hexane (2.5 g, 50% for 2 steps).

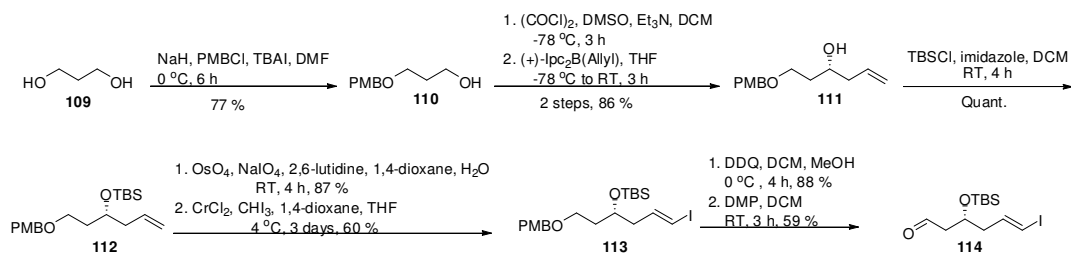
^1H NMR (CDCl_3 , 500 MHz) δ (ppm) 7.66-7.55 (m, 5H, Ph-H), 6.13 (dd, $J = 11.4$, 4.8 Hz, 1H, 3-H), 5.66 (ddd, $J = 26.0$, 12.5, 7.0 Hz, 1H, 2-H), 4.49-4.37 (m, 2H, 1-H), 4.18-4.05 (m, 1H, 4-H), 3.66 (m, 1H, 6-H), 1.61-1.54 (m, 1H, 5-H), 1.51-1.43 (m, 2H, 7-H), 1.34-1.19 (m, 8H, 8-H, 9-H, 10-H, 11-H), 0.95-0.81 (m, 20H, TBS, TES, 12-H, 13-H), 0.53-0.47 (m, 6H, TES), 0.00 (s, 3H, TBS), -0.11 (s, 3H, TBS); ^{13}C NMR (CDCl_3 , 125 MHz) δ (ppm) 154.2 (C-1' of tetrazole), 133.0 (C-3), 131.4 (C-1' of PhH), 129.7 (C-3' of PhH), 129.7 (C-4' of PhH), 129.7 (C-5' of PhH), 125.04 (C-2' of PhH), 124.95 (C-6' of PhH), 74.1 (C-4), 73.6 (C-6), 43.7 (C-5), 35.1 (C-7), 34.8 (C-1), 31.9 (C-10), 29.4 (C-9), 25.3 (C-8), 22.6 (C-11), 18.1 (C-Si), 14.1 (C-12), 9.4 (C-13), 6.8 (3 x $\text{CH}_3\text{-C-Si}$), 5.5 (3 x $\text{CH}_2\text{-Si}$), -3.0 ($\text{CH}_3\text{-Si}$), -3.7 ($\text{CH}_3\text{-Si}$); LRMS (ESI, positive) m/z for $\text{C}_{32}\text{H}_{58}\text{N}_4\text{O}_4\text{SSi}_2$ [$\text{M}+\text{Na}$] $^+$: calcd 674.3633, found 674.3643.

Ethyl 2-(phenylsulfinyl)acetate (108): 1) Thiophenol (**107**, 5.5 g, 50 mmol) was dissolved in a sodium methoxide solution (100 mL, 0.5 N in methanol, 50 mmol) at room temperature, and cooled to 0 °C. Ethyl bromoacetate (8.4 g, 50 mmol) was added dropwise to the reaction mixture at 0 °C with vigorous stirring over 30 min. The reaction mixture was then refluxed for 1 hour, and cooled to room temperature, followed by dilution with water (100 mL). The aqueous fraction was extracted with dichloromethane (100 mL x 4 times), which was washed with brine (50 mL), dried over an anhydrous sodium sulfate pad, and concentrated. The resulting residue was purified using flash column chromatography. A quantitative amount of sulfide compound was eluted with 2%

to 5% EtOAc/Hexane. 2) A solution of above sulfide compound and sodium periodate (12.8 g, 60 mmol) in methanol (10 mL) and water (40 mL) was stirred at room temperature for 18 hours. After filtering through paper filter and washing with dichloromethane (50 mL x 2 times), the aqueous fraction was extracted with dichloromethane (50 mL x 3 times). The combined organic fractions were washed with brine (100 mL), dried over an anhydrous sodium sulfate pad, and concentrated. The resulting residue was flash column chromatographed, and the target sulfoxide compound was eluted with 50% EtOAc/Hexane (9.8 g, 93%).

^1H NMR (CDCl_3 , 500 MHz) δ (ppm) 7.68-7.64 (m, 2H, C-2', C-5' of Ph-H), 7.53-7.50 (m, 3H, C-3', C-4', C-5' of Ph-H), 4.12 (q, $J = 7.0$ Hz, 2H, C-3), 3.73 (dd, $J = 86.0, 13.5$ Hz, 2H, C-2), 1.18 (t, $J = 7.0$ Hz, 3H, C-4); ^{13}C NMR (CDCl_3 , 125 MHz) δ (ppm) 164.6 (C-1), 143.1 (C-1' of Ph-H), 131.6 (C-4' of Ph-H), 129.3 (C-3', C-5' of Ph-H), 124.1 (C-2', C-5' of Ph-H), 61.9 (C-3), 61.6 (C-2), 13.9 (C-4); LRMS (ESI, positive) m/z for $\text{C}_{10}\text{H}_{12}\text{O}_3\text{S}$ $[\text{M}+\text{Na}]^+$: calcd 235.0, found 235.0.

B. Preparation of Fragment B: The overall synthetic scheme is depicted in **Scheme 2-14**.



Scheme 2-14. Preparation of fragment B for the synthesis of Linear SpnF substrate analog.

3-(4-methoxybenzyloxy)propan-1-ol (110): Sodium hydride (8.7 g, 60% in mineral oil, 0.22 mol) was added to a solution of 1,3-propanediol (**109**, 15.0 g, 0.20 mol) in

anhydrous DMF (591 mL) at 0 °C. The reaction mixture was stirred at room temperature for 30 min, and cooled to 0 °C. p-Methoxybenzyl chloride (29.4 mL, 0.22 mol) and tetrabutylammonium iodide (8.1 g, 0.02 mol) were subsequently added to the reaction mixture with vigorous stirring at 0 °C for 30 min. The reaction mixture was stirred at 0 °C for 6 hours. After quenching by the addition of cold water (197 mL), the aqueous fraction was extracted with ethyl acetate (300 mL x 3 times, 200 mL x 2 times). The combined organic fractions were washed with water (200 mL x 3 times) and brine (200 mL), then dried over an anhydrous sodium sulfate, filtered, and concentrated under reduced pressure. The resulting residue was purified using flash column chromatography. The target compound was eluted with 10% to 30% EtOAc/Hexane solution (30.0 g, 0.17 mol, 77%). All spectra data is identical to the literature reference.

(R)-1-(4-methoxybenzyloxy)hex-5-en-3-ol (111): 1) DMSO (35.5 mL, 0.46 mol) in dichloromethane (153 mL) was added to a solution of oxalyl chloride (20.0 mL, 0.23 mol) in dichloromethane (305 mL) at -78 °C with vigorous stirring for 30 min. The reaction mixture was stirred for 30 min at -78 °C. The alcohol compound (30.0 g, 0.15 mol) in dichloromethane (153 mL) was added to the reaction mixture via cannular at -78 °C for 10 min. After 1 hour, the reaction mixture was slightly warmed to -60 °C, and triethylamine (96 mL, 0.69 mol) was added to the reaction mixture over 10 min. After slowly warming the solution to room temperature for 30 min, the reaction mixture was quenched with water (611 mL), and the aqueous fraction was extracted with dichloromethane (200 mL x 3 times). The combined organic fractions were washed with brine (300 mL), dried over an anhydrous sodium sulfate, filtered, and concentrated under

reduced pressure. After passing through a celite pad, the filtrate was again concentrated and used for the next reaction without further purification. 2) (+)-Ipc₂BCl (123.5 mL, 1.6 M, 0.20 mol) and allylmagnesium bromide (189 mL, 1.0 M, 0.19 mol) were mixed with vigorous stirring in THF (435 mL) for 10 min at 0 °C, and then cooled to -78 °C. Freshly prepared aldehyde from the previous step in THF (145 mL) was added to the reaction mixture at -78 °C over 1 hour. The reaction mixture was stirred at -78 °C for 1.5 hour, and allowed to warm to room temperature for 3 hours with stirring. Cold methanol (435 mL), aqueous 1 N sodium hydroxide solution (435 mL), and aqueous 30% hydrogen peroxide solution were subsequently added to the reaction mixture while maintaining the temperature of the reaction mixture below 5~10 °C. After stirring at room temperature for additional 1.5 hours, the reaction mixture was filtered through paper filter, and washed with ethyl acetate (500 mL). The filtrate was phase-separated, and the aqueous fraction was extracted with ethylacetate (400 mL x 3 times). The combined organic fractions were washed with brine (300 mL), and dried over an anhydrous sodium sulfate pad, filtered, and concentrated. The resulting residue was subjected to flash column chromatography. The target compound was eluted with 20% EtOAc/Hexane (20.4 g, 60%). All spectral data was identical to the literature reference.

(R)-tert-butyl(1-(4-methoxybenzyloxy)hex-5-en-3-yloxy)dimethylsilane (112): TBSCl (14.3 g, 95 mmol) was added to a solution of the alcohol compound (20.4 g, 86 mmol) and imidazole (12.9 g, 190 mmol) in DMF (432 mL) at 0 °C. The reaction mixture was allowed to warm to room temperature for 18 hours with stirring. Then, the reaction mixture was directly concentrated under reduced pressure. The residue was diluted with

water (200 mL), and extracted with ethyl acetate (200 mL x 4 times). The combined organic fractions were washed with brine (200 mL), dried over an anhydrous sodium sulfate pad, and concentrated under reduced pressure. The resulting residue was purified using flash column chromatography. The target compound was eluted with 5% EtOAc/Hexane with a quantitative yield. Spectral data was not collected.

(R,E)-tert-butyl(6-iodo-1-(4-methoxybenzyloxy)hex-5-en-3-yloxy)dimethylsilane

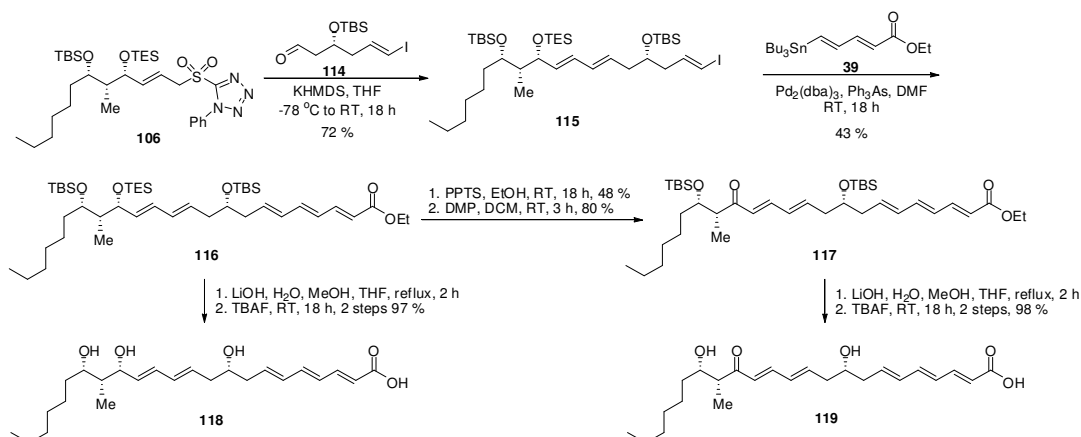
(113): Compound **(113)** was prepared following the same procedure as compound **(34)** with a yield of 52% for 2 steps. All spectral data was identical to the literature reference.

(R,E)-tert-butyl(6-iodo-1-(4-methoxybenzyloxy)hex-5-en-3-yloxy)dimethylsilane

(113): Compound **(113)** was prepared following the same procedure as compound **(35)** with a yield of 88%. All spectral data was identical to the literature reference.

(R,E)-3-(tert-butyldimethylsilyloxy)-6-iodohex-5-enal (114): Compound **(114)** was prepared following the same procedure as compound **(36)** quantitatively. All spectral data was consistent with the literature reference.

C. Synthesis of Linear SpnF Substrate Analog by Coupling Reactions and Enzymatic Conversion: The overall synthetic scheme is pictured in **Scheme 2-15**.



Scheme 2-15. Preparation of Linear SpnF substrate analog.

(5S,7E,9E,11R,12R,13S)-13-hexyl-5-((E)-3-iodoallyl)-2,2,3,3,12,15,15,16,16-nonamethyl-11-(triethylsilyloxy)-4,14-dioxa-3,15-disilaheptadeca-7,9-diene (115):

Potassium bis(trimethylsilyl)amide (KHMDS; 12.4 mL, 0.5 M in toluene, 6.2 mmol) was added to a solution of sulfone compound (2.4 g, 3.8 mmol) in anhydrous THF (75 mL) at $-78\text{ }^{\circ}\text{C}$ using a syringe pump over 30 min. The reaction mixture was kept stirring at $-78\text{ }^{\circ}\text{C}$ for 30 min. The aldehyde compound (2.0 g, 5.6 mmol) in anhydrous THF (18 mL) was added to the reaction mixture at $-78\text{ }^{\circ}\text{C}$ with a syringe pump over 30 min. The reaction mixture was stirred at $-78\text{ }^{\circ}\text{C}$ for 2 hours, and allowed to slowly warm to room temperature for 18 hours with stirring. After quenching with a saturated the aqueous sodium bicarbonate solution (2.3 mL), the aqueous fraction was extracted with ethyl acetate (60 mL x 3 times). The combined organic fractions were washed with brine (30 mL), dried over an anhydrous sodium sulfate pad, and concentrated under reduced pressure. The resulting dark brown residue was purified using flash column chromatography. The target compound was eluted with 5% EtOAc/Hexane (1.5 g, 52%).

^1H NMR (CDCl_3 , 500 MHz) δ 6.49 (td, $J = 12.0, 6.0$ Hz, 1H, 2-H), 6.31 (dd, $J = 22.0, 13.0$, 1H, 8-H), 6.03 (dd, $J = 15.0, 12.0$ Hz, 1H, 7-H), 6.00 (d, $J = 12.0$ Hz, 1H, 1-H), 5.60 (ddd, $J = 38.0, 13.0, 6.0$ Hz, 1H, 9-H), 5.38 (ddd, $J = 15.0, 6.0, 2.5$ Hz, 1H, 6-H), 4.10 (dt, $J = 29.0, 6.0$ Hz, 1H, 10-H), 3.88-3.61 (m, 1H, 12-H), 3.75-3.69 (m, 1H, 4-H), 2.38-2.22 (m, 2H, 5-H), 2.21-2.09 (m, 2H, 3-H), 1.60-1.53 (m, 1H, 11-H), 1.48-1.42 (m, 2H, 13-H), 1.29-1.22 (m, 8H, 14-H, 15-H, 16-H, 17-H), 0.96-0.84 (m, 17H, 9H of TBS, 6H of TES, 18-H), 0.57-0.53 (m, 9H, 9H of TES), 0.04-(-0.01) (m, 6H, 6H of TBS); ^{13}C NMR (CDCl_3 , 125 MHz) δ 143.3 (C-2), 137.1 (C-9), 130.0 (C-7), 126.9 (C-6), 125.7 (C-8), 76.6 (C-1), 74.7 (C-10), 72.5 (C-12), 71.1 (C-4), 44.0 (C-11), 43.5 (C-3), 35.5 (C-5), 35.0 (C-13), 31.9 (C-16), 29.5 (C-15), 26.1 (C-14), 26.0 (3 x $\text{CH}_3\text{-C-Si}$), 25.8 (3 x $\text{CH}_3\text{-C-Si}$), 22.6 (C-17), 18.2 (C-Si of TBS), 18.1 (C-Si of TBS), 14.1 (C-18), 9.4 (C-19), 6.9 (3 x $\text{CH}_3\text{-CH}_2\text{-Si}$ of TES), 5.5 (3 x $\text{CH}_2\text{-Si}$ of TES), -3.6 ($\text{CH}_3\text{-Si}$ of TBS), -4.5 ($\text{CH}_3\text{-Si}$ of TBS).

(2E,4E,6E,9R,11E,13E,15R,16R,17S)-ethyl 9,17-bis(tert-butyltrimethylsilyloxy)-16-methyl-15-(triethylsilyloxy)tricoso-2,4,6,11,13-pentaenoate (116): A vinyl iodide compound (1.5 g, 2.0 mmol) and tinylated compound (1.2 g, 2.9 mmol) were mixed in anhydrous deoxygenated DMF (39 mL) at room temperature. Tris(dibenzylideneacetone)dipalladium (0) ($\text{Pd}_2(\text{dba})_3$; 89 mg, 0.10 mmol) and triphenylarsine (AsPh_3 ; 120 mg, 0.39 mmol) were added to the reaction mixture under a nitrogen atmosphere with stirring at room temperature. The reaction mixture was kept stirring at room temperature for 18 hours, and then diluted with water (150 mL). Organic phase was separated by extracting the aqueous fraction with ethyl acetate (50 mL x 4

times), and washing with brine (100 mL). After drying over an anhydrous sodium sulfate pad and concentration under reduced pressure, the resulting residue was subjected to flash column chromatography. The target compound was eluted with 5% EtOAc/Hexane (0.97 g, 1.25 mmol, 64%).

^1H NMR (CDCl_3 , 500 MHz) δ 7.31 (dt, $J = 17.5, 3.0$ Hz, 1H, 3-H), 6.51 (ddd, $J = 20.0, 10.5, 5.0$ Hz, 1H, 5-H), 6.35 (dd, $J = 15.0, 11.5$ Hz, 1H, 13-H), 6.24-6.11 (m, 2H, 4-H, 6-H), 6.08-5.98 (m, 1H, 12-H), 5.95-5.89 (m, 1H, 7-H), 5.84 (dd, $J = 15.0, 3.0$ Hz, 1H, 2-H), 5.66-5.55 (m, 1H, 14-H), 5.53-5.42 (m, 1H, 11-H), 4.22 (q, $J = 6.0$ Hz, 2H, 25-H), 4.11 (dt, $J = 24.5, 8.0$ Hz, 1H, 15-H), 3.82-3.75 (m, 1H, 9-H), 3.74-3.63 (m, 1H, 17-H), 2.42-2.22 (m, 4H, 8-H, 10-H), 1.54-1.47 (m, 3H, 16-H, 18-H), 1.31-1.25 (m, 11H, 19-H, 20-H, 21-H, 22-H, 26-H), 0.96-0.86 (m, 33H, 3 x $\text{CH}_3\text{-C-Si}$ of TBS at C-9, 3 x $\text{CH}_3\text{-C-Si}$ of TBS at C-17, 3 x $\text{CH}_3\text{-CH}_2\text{-Si}$ of TES, 23-H, 24-H), 0.59-0.52 (m, 6H, 3 x $\text{CH}_3\text{-CH}_2\text{-Si}$ of TES), 0.05-0.00 (m, 12H, 2 x $\text{CH}_3\text{-Si}$ of TBS at C-9, 2 x $\text{CH}_3\text{-Si}$ of TBS at C-17); ^{13}C NMR (CDCl_3 , 125 MHz) δ 167.2 (C-1), 147.2 (C-3), 140.8 (C-5), 136.4 (C-7), 132.1 (C-6), 130.8 (C-14), 129.9 (C-12), 128.2 (C-4), 127.4 (C-11), 125.8 (C-13), 119.9 (C-2), 74.8 (C-15), 72.5 (C-17), 71.9 (C-9), 60.3 (C-25), 44.0 (C-16), 40.8 (C-8), 40.7 (C-10), 31.9 (C-21), 29.7 (C-20), 29.0 (C-18), 27.2 (C-19), 25.99 (3 x $\text{CH}_3\text{-C-Si}$ of TBS), 25.83 (3 x $\text{CH}_3\text{-C-Si}$ of TBS), 22.6 (C-22), 18.19 ($\text{CH}_3\text{-C-Si}$ of TBS), 18.09 ($\text{CH}_3\text{-C-Si}$ of TBS), 6.97 (3 x $\text{CH}_3\text{-CH}_2\text{-Si}$ of TES), 14.3 (C-26), 13.7 (C-23), 9.6 (C-24), 5.15 (3 x $\text{CH}_3\text{-CH}_2\text{-Si}$ of TES), -4.34 (2 x $\text{CH}_3\text{-Si}$ of TBS), -4.51 (2 x $\text{CH}_3\text{-Si}$ of TBS). HRMS (ESI, positive) m/z for $\text{C}_{44}\text{H}_{84}\text{O}_5\text{Si}_3$ $[\text{M}+\text{Na}]^+$: calcd 799.5524, found 799.5500.

(2E,4E,6E,9R,11E,13E,16R,17S)-ethyl 9,17-bis(tert-butyldimethylsilyloxy)-16-methyl-15-oxotricos-2,4,6,11,13-pentaenoate (117): 1) Pyridinium p-toluenesulfonate (PPTS; 646 mg, 2.57 mmol) was added to a solution of 15-OTES compound (800 mg, 1.03 mmol) in ethanol (21 mL) at room temperature, and the suspended reaction mixture was stirred for 18 hours. After dilution with saturated the aqueous sodium bicarbonate solution (21 mL), the aqueous fraction was extracted with dichloromethane (20 mL x 5 times). The combined organic fractions were dried over an anhydrous sodium sulfate pad and concentrated. The resulting residue was purified using flash column chromatography. The target compound was eluted with 10% EtOAc/Hexane (325 mg, 48%), and a portion of the starting material was also recovered (300 mg, 39%). 2) Dess-Martin periodinane (DMP; 32 mg, 74 μ mol) was added to a solution of secondary-alcohol compound (45 mg, 68 μ mol) in dichloromethane (2 mL) at room temperature. The reaction mixture was stirred for 3 hours, and then quenched with saturated the aqueous sodium thiosulfate (2 mL) and saturated the aqueous sodium bicarbonate (2 mL). The aqueous fraction was extracted with dichloromethane (5 mL x 3 times), and the combined organic fractions were washed with brine (5 mL), dried over an anhydrous sodium sulfate pad, and concentrated under reduced pressure. The resulting residue was subjected to the flash column chromatography. The target compound was eluted with 30% EtOAc/Hexane (36 mg, 80%).

$^1\text{H NMR}$ (CDCl_3 , 500 MHz) δ (ppm) 7.30 (dd, $J = 30.0, 11.5$ Hz, 1H, 3-H), 7.14 (dd, $J = 15.0, 10.0$ Hz, 1H, 13-H), 6.52 (dd, $J = 14.5, 11.0$ Hz, 1H, 5-H), 6.25-6.11 (m, 5H, 4-H, 6-H, 7-H, 12-H, 14-H), 5.91-5.82 (m, 1H, 11-H), 5.85 (d, $J = 15.5$ Hz, 1H, 2-H),

4.20 (q, J = 7.0 Hz, 2H, 25-H), 3.93-3.89 (m, 1H, 17-H), 3.84-3.79 (m, 1H, 9-H), 2.82 (dd, J = 7.0, 5.5 Hz, 1H, 16-H), 2.36-2.26 (m, 4H, 8-H, 10-H), 1.44-1.33 (m, 2H, 18-H), 1.31-1.20 (m, 8H, 19-H, 20-H, 21-H, 22-H), 1.29 (t, J = 7.0 Hz, 3H, 26-H), 1.08 (d, J = 7.0 Hz, 3H, 24-H), 0.91-0.80 (m, 21H, 3 x 2 x CH₃-C-Si of TBS, 23-H), 0.04-0.00 (m, 12H, 3 x 2 x CH₃-Si of TBS); ¹³C NMR (CDCl₃, 125 MHz) δ (ppm) 202.8 (C-15), 167.1 (C-1), 144.5 (C-3), 142.0 (C-13), 141.1 (C-6), 140.5 (C-5), 135.7 (C-11), 132.4 (C-12), 131.4 (C-7), 128.5 (C-4), 127.8 (C-14), 120.6 (C-2), 73.8 (C-17), 71.3 (C-9), 60.2 (C-25), 49.8 (C-16), 40.9 (C-8, C-10), 36.2 (C-18), 31.8 (C-19), 29.4 (C-20), 25.89 (3 x CH₃-C-Si of TBS), 25.77 (3 x CH₃-C-Si of TBS), 25.1 (C-21), 22.6 (C-22), 18.08 (3 x CH₃-C-Si of TBS), 18.03 (3 x CH₃-C-Si of TBS), 14.3 (C-26), 14.0 (C-23), 12.3 (C-24), -4.29 (3 x CH₃-Si of TBS), -4.51 (3 x CH₃-Si of TBS); MS data was not collected.

(2E,4E,6E,9R,11E,13E,15R,16R,17S)-9,15,17-trihydroxy-16-methyltriosa-

2,4,6,11,13-pentaenoic acid (118): 1) A long chain compound (30 mg, 45 μmol) was dissolved in a solution of the aqueous 0.5 N lithium hydroxide solution (0.91 mL), methanol (0.91 mL), and THF (0.91 mL). The reaction mixture was then refluxed for 2 hours. After cooling to room temperature, the pH of the aqueous solution was adjusted to around 7.0 with the aqueous 1 N hydrochloric acid solution, and then the aqueous fraction was extracted with ethyl acetate (5 mL × 3 times). The combined organic fractions were dried over an anhydrous sodium sulfate pad and concentrated under reduced pressure. The resulting residue was short pass chromatographed through a silica gel pad by washing with 30% EtOAc/Hexane solution. The filtrate was concentrated and used for the next reaction without further purification. 2) A reaction mixture of the above

acid compound was dissolved in tetra-n-butylammonium fluoride solution (2 mL, 1.0 M in THF, 2.0 mmol) and was stirred for 18 hours at room temperature. After quenching with saturated the aqueous sodium bicarbonate solution (8 mL), the aqueous fraction was extracted with ethyl acetate (5 mL x 5 times). The combined organic fractions were dried over an anhydrous sodium sulfate pad and concentrated under reduced pressure. The resulting residue was purified using flash column chromatography. The target compound was eluted with EtOAc added linearly to a 10% MeOH/EtOAc solution (17 mg, 97%).

^1H NMR (CDCl_3 , 500 MHz) δ (ppm); ^{13}C NMR (CDCl_3 , 125 MHz) δ (ppm);;
HRMS (ESI, negative) m/z for $\text{C}_{24}\text{H}_{38}\text{O}_5$ $[\text{M}-\text{H}]^-$: calcd 405.2641 , found 405.2701.

(2E,4E,6E,9R,11E,13E,16R,17S)-9,17-dihydroxy-16-methyl-15-oxotricosa-

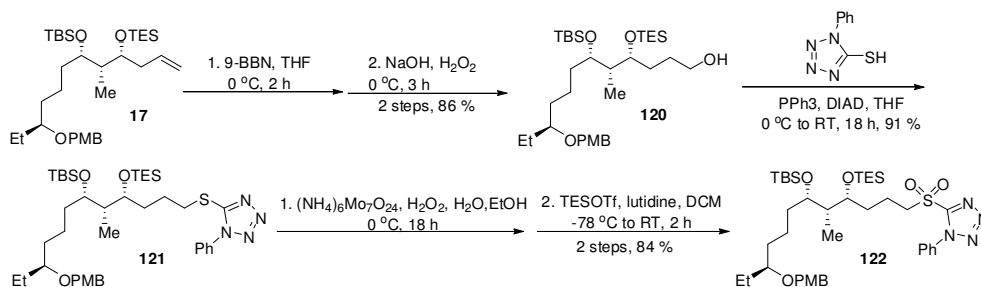
2,4,6,11,13-pentaenoic acid (119): 1) A keto-compound (30 mg, 45 μmol) was dissolved in a solution of the aqueous 0.5 N lithium hydroxide solution (0.91 mL), methanol (0.91 mL), and THF (0.91 mL), and the reaction mixture was refluxed for 2 hours. After cooling to room temperature, the pH of the aqueous solution was adjusted to around 7 with the aqueous 1 N hydrochloric acid solution, and then the aqueous fraction was then extracted with ethyl acetate (5 mL \times 3 times). The combined organic fractions were dried over an anhydrous sodium sulfate pad and concentrated under reduced pressure. The resulting residue was short-passed through a silica gel pad by washing with 30% EtOAc/Hexane solution. The filtrate was concentrated and used for the next reaction without further purification. 2) A reaction mixture of the above acid compound dissolved in tetra-n-butylammonium fluoride solution (2 mL, 1.0 M in THF, 2.0 mmol) was stirred for 18 hours at room temperature. After quenching with saturated the aqueous sodium

bicarbonate solution (8 mL), the aqueous fraction was extracted with ethyl acetate (5 mL x 5 times). The combined organic fractions were dried over an anhydrous sodium sulfate pad and concentrated under reduced pressure. The resulting residue was purified using flash column chromatography. The target compound was eluted with a changing concentration of pure EtOAc to 10% MeOH/EtOAc solution (18 mg, quantitatively).

^1H NMR (CDCl_3 , 500 MHz) δ (ppm); 7.36-7.31 (m, 1H, 3-H), 7.04-6.88 (m, 1H, 13-H), 6.57-6.49 (m, 1H, 5-H), 6.31-6.12 (m, 5H, 14-H, 4-H, 6-H, 7-H, 12-H), 5.98-5.72 (m, 2H, 11-H, 2-H), 3.83-3.81 (m, 1H, 17-H), 3.67-3.62 (m, 1H, 9-H), 3.04-2.97 (m, 1H, 16-H), 2.66-2.60 (m, 2H, 8-H), 2.34-2.31 (m, 2H, 10-H), 1.80-1.20 (m, 14H, 19-H's, 20-H's, 21-H's, 22-H's, 23-H's, 24-CH₃); ^{13}C NMR (CDCl_3 , 125 MHz) δ (ppm) 198.2 (C-15), 174.1 (C-1), 158.2 (C-3), 154.2 (C-13), 153.1 (C-6), 145.5 (C-5), 135.4 (C-11), 124.5 (C-12), 122.7 (C-4), 121.6 (C-4), 120.3 (C-14), 118.7 (C-2), 60.1 (C-17), 56.4 (C-9), 51.5 (C-16), 39.1 (C-10), 38.6 (C-8), 33.1 (C-18), 31.1 (C-19), 30.0 (C-20), 24.2 (C-19), 23.7 (C-22), 15.4 (C-23), 14.1 (C-24); HRMS (ESI, negative) m/z for $[\text{M}-\text{H}]^-$: calcd 403.2483, found 403.2494.

2.2.9. Synthesis of the C13-14 Unc SpnF Substrate Analog (C13-14 Unc analog)

A. Preparation of Fragment A: The overall synthetic scheme is shown in **Scheme 2-16**.



Scheme 2-16. Preparation of fragment A in the synthesis of C13-14 Unc SpnF substrate analog.

(4R,S,6S,10S)-6-(tert-butyldimethylsilyloxy)-10-(4-methoxybenzyloxy)-5-methyl-4-(triethylsilyloxy)dodecan-1-ol (120): 9-BBN (28 mL, 0.5 M, 14.0 mmol) was added dropwise to a solution of allyl compound (2.7 g, 4.7 mmol) in THF (100 mL) over 45 min at 0 °C. After the reaction mixture was stirred for 1.5 hours, water (2.7 mL) and an the aqueous 2 N sodium hydroxide solution (26 mL, 56 mmol) were subsequently added over 20 min. The reaction mixture was stirred for 10 min, and a hydrogen peroxide solution (5.4 mL, the aqueous 30% solution) was added over 10 min at 0 °C. After stirring for 3 hours, the reaction mixture was extracted with ethyl acetate (40 mL x 3 times), and the combined organic fractions were dried over an anhydrous sodium sulfate, filtered, and concentrated under reduced pressure. The resulting residue was purified using flash column chromatography. The target compound was eluted with 10% EtOAc/Hexane solution (2.4 g, 4.0 mmol).

¹H NMR (CDCl₃, 500 MHz) δ (ppm) 7.24 (d, 2H, J = 8.7 Hz, PhH of PMB), 6.85 (d, 2H, J = 8.7 Hz, PhH of PMB), 4.44 (d, 1H, J = 11.1 Hz, CH₂ of PMB), 4.38 (d, 1H, J = 11.1 Hz, CH₂ of PMB), 3.78-3.75 (m, 4H, OCH₃ of PMB+4-H), 3.67-3.63 (m, 1H, 6-H), 3.60-3.52 (m, 2H, 1-Hs), 3.29-3.24 (m, 1H, 10-H), 2.14-2.11 (m, 1H, 1-OH), 1.71-1.19 (m, 13H, 2-Hs+3-Hs+5-H+7-Hs 2+8-Hs+9-Hs+11-Hs), 0.95 (t, 9H, J = 8.1 Hz, CH₃ of TES), 0.87 (t, 3H, J = 7.0 Hz, 12-CH₃), 0.85 (s, 9H, CH₃ of tBu of TBS), 0.84 (t, 3H, J = 7.0 Hz, 5-CH₃), 0.60 (q, 6H, J = 7.8 Hz, CH₂ of TES), 0.014 (s, 3H, CH₃ of TBS), -0.001 (s, 3H, CH₃ of TBS); ¹³C NMR (CDCl₃, 125 MHz) δ (ppm) 159.07 (Ph(C) of PMB), 131.19 (Ph(C) of PMB), 129.31 (Ph of PMB), 113.74 (Ph of PMB), 79.97 (C-10),

72.96 (C-6), 72.47 (C-4), 70.61 (CH₂ of PMB), 63.30 (C-1), 55.28 (OCH₃ of PMB), 40.16 (C-11), 35.32 (C-5), 33.98 (C-7), 31.40 (C-3), 26.35 (C-9), 25.90 (CH₃ of *t*Bu of TBS), 21.36 (C-8), 18.12 (Me₃(C)-Si), 9.46 (C-12), 9.43 (5-CH₃), 6.99 (CH₃ of TES), 5.25 (CH₂ of TES), -3.74 (CH₃ of TBS), -4.50 (CH₃ of TBS); HRMS (CI, positive) *m/z* for C₃₃H₆₅O₅Si₂ [M+H]⁺: calcd 597.4371, found 597.4367.

5-((4R,5S,6S,10S)-6-(tert-butyldimethylsilyloxy)-10-(4-methoxybenzyloxy)-5-methyl-4-(triethylsilyloxy)dodecylthio)-1-phenyl-1H-tetrazole (121): Compound (121) was prepared following the same procedure as compound (22) with a yield of 91%.

¹H NMR (CDCl₃, 600 MHz) δ (ppm) 7.56-7.50 (m, 5H, PhH), 7.23 (d, 2H, *J* = 8.7 Hz, PhH of PMB), 6.83 (d, 2H, *J* = 8.7 Hz, PhH of PMB), 4.41 (d, 1H, *J* = 11.1 Hz, CH₂ of PMB), 4.38 (d, 1H, *J* = 11.1 Hz, CH₂ of PMB), 3.76 (s, 3H, OCH₃ of PMB), 3.74-3.71 (m, 1H, 4-H), 3.66-3.64 (m, 1H, 6-H), 3.41-3.67 (m, 2H, 1-Hs), 3.28-3.24 (m, 1H, 10-H), 1.87-1.76 (m, 2H, 2-Hs), 1.66-1.62 (m, 2H, 3-Hs), 1.57-1.38 (m, 7H, 5-H+7-Hs+9-Hs+11-Hs), 1.33-1.19 (m, 2H, 8-Hs), 0.92 (t, 9H, *J* = 8.1 Hz, CH₃ of TES), 0.87 (t, 3H, *J* = 7.4 Hz, 12-Hs), 0.84 (s, 9H, CH₃ of *t*Bu of TBS), 0.83 (t, 3H, *J* = 7.0 Hz, 5-CH₃), 0.55 (q, 6H, *J* = 7.9 Hz, CH₂ of TES), 0.00 (s, 3H, CH₃ of TBS), -0.031 (s, 3H, CH₃ of TBS); ¹³C NMR (CDCl₃, 150 MHz) δ (ppm) 159.05 (Ph(C) of PMB), 154.33 (C=N of tetrazole), 133.78 (Ph(C) of Ph), 131.26 (Ph of Ph), 130.02 (Ph(C) of PMB), 129.74 (Ph of Ph), 129.23 (Ph of PMB), 123.80 (Ph of Ph), 113.72 (Ph of PMB), 79.78 (C-10), 72.74 (C-4), 72.72 (C-6), 70.50 (CH₂ of PMB), 55.26 (OCH₃ of PMB), 41.00 (C-11), 35.21 (C-5), 33.88 (C-1), 33.82 (C-7), 33.76 (C-3), 26.29 (C-9), 25.91 (CH₃ of *t*Bu of TBS), 24.33 (C-2), 21.21 (C-8), 18.12 (Me₃(C)-Si), 9.68 (C-12), 9.50 (5-CH₃),

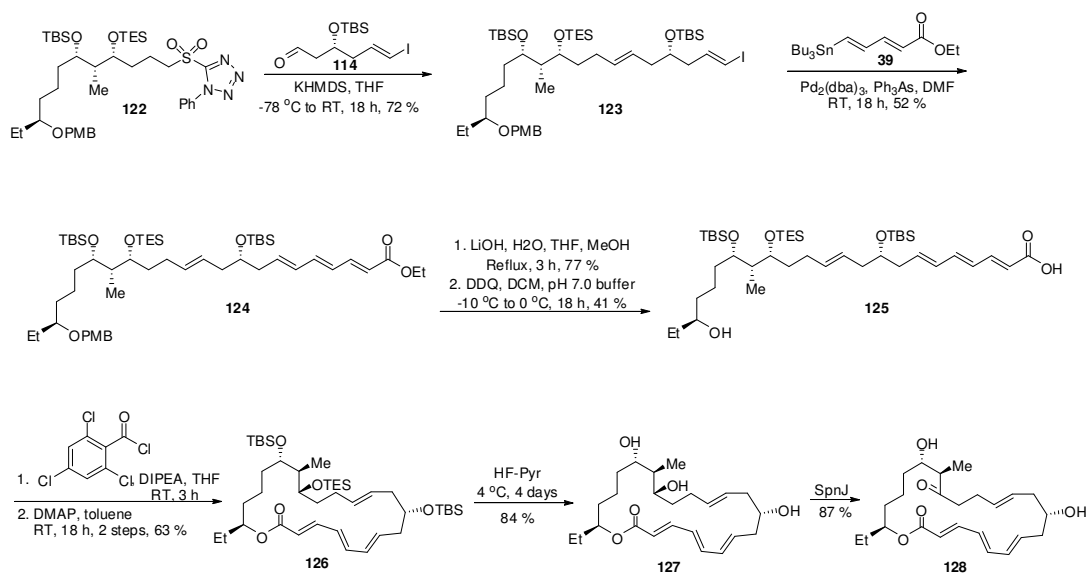
7.02 (CH₃ of TES), 5.34 (CH₂ of TES), -3.74 (CH₃ of TBS), -4.44 (CH₃ of TBS); HRMS (CI, positive) *m/z* for C₄₀H₆₉O₄Si₂S [M+H]⁺: calcd 757.4578, found 757.4582.

5-((4R,5S,6S,10S)-6-(tert-butyldimethylsilyloxy)-10-(4-methoxybenzyloxy)-5-methyl-4-(triethylsilyloxy)dodecylsulfonyl)-1-phenyl-1H-tetrazole (122): 1) Ammonium heptamolybdate tetrahydrate (0.53 g, 0.41 mmol) was added to a solution of thioether (2.8 g, 3.7 mmol) in ethanol (10 mL) and hydrogen peroxide (2.4 mL) at 0 °C. This reaction mixture was stirred at 0°C for 24 hours. The reaction mixture was quenched with water (30 mL), and the aqueous fraction was extracted with ethyl acetate (30 mL x 3 times). The combined organic fractions were dried over an anhydrous sodium sulfate pad. The concentrated residue was directly used for TES-protection without further purification. 2) TESOTf (1.2 mL, 5.5 mmol) was added to a solution of the above sulfonate and 2,6-lutidine (1.1 mL, 9.15 mmol) in dichloromethane (70 mL) at -78 °C. The reaction mixture was stirred at -78 °C for 1 hour and slowly warmed to room temperature with stirring for 30 min. After quenching with saturated the aqueous ammonium chloride (30 mL) and extraction with dichloromethane (15 mL x 3 times), the combined organic fractions were washed with brine (20 mL), dried over an anhydrous sodium sulfate pad, and concentrated under reduced pressure. The resulting residue was purified using flash column chromatography. The target compound was eluted with 5% EtOAc/Hexane (2.4 g, 3.1 mmol).

¹H NMR (CDCl₃, 500 MHz) δ (ppm) 7.67-7.64 (m, 2H, PhH), 7.61-7.56 (m, 3H, PhH), 7.22 (d, 2H, *J* = 8.8 Hz, PhH of PMB), 6.82 (d, 2H, *J* = 8.8 Hz, PhH of PMB), 4.41 (d, 1H, *J* = 11.2 Hz, CH₂ of PMB), 4.38 (d, 1H, *J* = 11.2 Hz, CH₂ of PMB), 3.76 (s, 3H,

OCH₃ of PMB), 3.75-3.52 (m, 4H, 4-H+6-H+1-Hs), 3.29-3.24 (m, 1H, 10-H), 2.00-1.93 (m, 2H, 2-Hs), 1.76-1.55 (m, 2H, 3-Hs), 1.60-1.55 (m, 2H, 11-Hs), 1.54-1.38 (m, 5H, 5-H+7-Hs+9-Hs), 1.34-1.18 (m, 2H, 8-Hs), 0.92 (t, 9H, *J* = 8.1 Hz, CH₃ of TES), 0.87 (t, 3H, *J* = 7.4 Hz, 12-CH₃), 0.84 (s, 9H, CH₃ of *t*Bu of TBS), 0.83 (t, 3H, *J* = 7.0 Hz, 5-CH₃), 0.57 (q, 6H, *J* = 7.9 Hz, CH₂ of TES), 0.016 (s, 3H, CH₃ of TBS), -0.009 (s, 3H, CH₃ of TBS); ¹³C NMR (CDCl₃, 125 MHz) δ (ppm) 159.02 (Ph(C) of PMB), 153.50 (C=N of tetrazole), 133.07 (Ph(C) of Ph), 131.39 (Ph of Ph), 131.26 (Ph(C) of PMB), 129.67 (Ph of Ph), 129.23 (Ph of PMB), 125.03 (Ph of Ph), 113.71 (Ph of PMB), 79.73 (C-10), 72.66 (C-4), 72.60 (C-6), 70.49 (CH₂ of PMB), 56.37 (C-1), 55.25 (OCH₃ of PMB), 40.99 (C-11), 35.25 (C-5), 33.86 (C-7), 33.07 (C-3), 26.27 (C-9), 25.89 (CH₃ of *t*-Bu of TBS), 21.36 (C-8), 18.11 (Me₃(C)-Si), 17.68 (C-2), 9.82 (C-12), 9.50 (5-CH₃), 6.99 (CH₃ of TES), 5.27 (CH₂ of TES), -3.72 (CH₃ of TBS), -4.41 (CH₃ of TBS); HRMS (CI, positive) *m/z* for C₄₀H₆₉N₄O₆Si₂S [M+H]⁺: calcd 789.4476, found 789.4474.

B. Synthesis of C13-14 Unc SpnF Substrate Analog by Coupling Reactions and Enzymatic Conversion: The overall synthetic scheme is pictured in **Scheme 2-17**.



Scheme 2-17. Preparation of Linear C13-14 Unc SpnF substrate analog.

(5S,6S,7R,13S,E)-13-((E)-3-iodoallyl)-5-(4-(4-methoxybenzyloxy)hexyl)-7-

(triethylsilyloxy)-2,2,3,3,6,15,15,16,16-nonamethyl-4,14-dioxa-3,15-disilaheptadec-

10-en (123): Compound (123) was prepared following the same procedure as compound (43) using compound (122) and compound (114) instead of compound (41) and compound (36) with a yield of 71%.

$^1\text{H NMR}$ (CDCl_3 , 500 MHz) δ (ppm) 7.24 (d, 2H, $J = 8.7$ Hz, PhH of PMB), 6.84 (d, 2H, $J = 8.7$ Hz, PhH of PMB), 6.51-6.45 (m, 1H, 2-H), 5.98 (d, 1H, $J = 14.4$ Hz, 1-H), 5.45-5.39 (m, 1H, 7-H), 5.36-5.31 (m, 1H, 6-H), 4.43 (d, 1H, $J = 11.1$ Hz, CH₂ of PMB), 4.39 (d, 1H, $J = 11.1$ Hz, CH₂ of PMB), 3.78 (s, 3H, OCH₃ of PMB), 3.74-3.70 (m, 1H, 10-CH), 3.68-3.63 (m, 2H, 4-H+12-H), 3.29-3.25 (m, 1H, 16-H), 2.21-2.15 (m, 2H, 3-Hs), 2.13-2.07 (m, 2H, 5-Hs), 2.02-1.92 (m, 2H, 8-Hs), 1.59-1.23 (m, 11H, 9-Hs+11-H+13-Hs+14-Hs+15-Hs+17-Hs), 0.94 (t, 9H, $J = 8.1$ Hz, CH₃ of TES), 0.89 (t, 3H, $J = 7.4$ Hz, 18-CH₃), 0.87 (s, 9H, CH₃ of *t*Bu of TBS), 0.85 (s, 9H, CH₃ of *t*Bu of TBS), 0.847 (d,

3H, $J = 6.9$ Hz, 11-CH₃), 0.58 (q, 6H, $J = 7.8$ Hz, CH₂ of TES), 0.024 (s, 3H, CH₃ of TBS), 0.021 (s, 3H, CH₃ of TBS), 0.016 (s, 3H, CH₃ of TBS), 0.002 (s, 3H, CH₃ of TBS); ¹³C NMR (CDCl₃, 125 MHz) δ (ppm) 159.04 (Ph(C) of PMB), 143.45 (C-2), 133.30 (C-7), 131.269 (Ph(C) of PMB), 129.22 (Ph of PMB), 125.82 (C-6), 113.72 (Ph of PMB), 79.83 (C-16), 76.41 (C-1), 72.94 (C-12), 72.83 (C-10), 71.21 (C-4), 70.50 (CH₂ of PMB), 55.26 (OCH₃ of PMB), 43.29 (C-3), 40.87 (C-11), 40.56 (C-5), 35.11 (C-15), 34.79 (C-9), 33.92 (C-13), 27.97 (C-8), 26.30 (C-17), 25.94 (CH₃ of *t*Bu of TBS), 25.83 (CH₃ of *t*Bu of TBS), 21.09 (C-14), 18.13 (Me₃(C)-Si), 18.07 (Me₃(C)-Si), 9.69 (11-CH₃), 9.52 (C-18), 7.05 (CH₃ of TES), 5.41 (CH₂ of TES), -3.80 (CH₃ of TBS), -4.41 (CH₃ of TBS), -4.48 (CH₃ of TBS), -4.52 (CH₃ of TBS); HRMS (CI, positive) m/z for C₄₅H₈₄O₅Si₃I [M+H]⁺: calcd 915.4671, found 915.4674.

(2E,4E,6E,9S,11E,15R,16S,17S)-ethyl 9,17-bis(tert-butyldimethylsilyloxy)-21-(4-methoxybenzyloxy)-16-methyl-15-(triethylsilyloxy)tricoso-2,4,6,11-tetraenoate (124):

Compound (124) was prepared following the same procedure as compound (45) with a yield of 34%.

¹H NMR (CDCl₃, 500 MHz) δ (ppm) 7.30 (dd, 1H, $J = 11.5, 15.4$ Hz, 3-H), 7.25 (d, 2H, $J = 8.8$ Hz, PhH of PMB), 6.86 (d, 2H, $J = 8.8$ Hz, PhH of PMB), 6.52 (dd, 1H, $J = 10.7, 14.9$ Hz, 5-H), 6.21 (dd, 1H, $J = 11.5, 14.9$ Hz, 4-H), 6.13 (dd, 1H, $J = 11.0, 15.1$ Hz, 6-H), 5.96-5.88 (m, 1H, 7-H), 5.84 (d, 1H, $J = 15.4$ Hz, 2-H), 5.46-5.36 (m, 2H, 12-H+11-H), 4.43 (dd, 2H, $J = 11.2, 15.9$ Hz, CH₂ of PMB), 4.20 (q, 2H, $J = 7.1$ Hz, CH₂ of OEt), 3.79 (s, 3H, OCH₃ of PMB), 3.74-3.66 (m, 3H, 15-H+9-H+17-H), 3.30-3.27 (m, 1H, 21-H), 2.30-2.17 (m, 2H, 8-Hs), 2.13-2.10 (m, 2H, 10-Hs), 2.00-1.92 (m, 2H, 13-Hs),

1.59-1.21 (m, 11H, 16-H+14-Hs+22-Hs+20-Hs+18-Hs+19-Hs), 1.26 (t, 3H, $J = 7.1$ Hz, CH₃ of OEt), 0.96 (t, 9H, $J = 8.1$ Hz, CH₃ of TES), 0.91 (t, 3H, $J = 7.3$ Hz, 23-Hs), 0.88 (s, 9H, CH₃ of *t*Bu of TBS), 0.87 (s, 9H, CH₃ of *t*Bu of TBS), 0.86 (d, 3H, $J = 6.9$ Hz, 16-CH₃), 0.59 (q, 6H, $J = 8.1$ Hz, CH₂ of TES), 0.035 (s, 3H, CH₃ of TBS), 0.032 (s, 3H, CH₃ of TBS), 0.019 (s, 6H, CH₃ of TBS); ¹³C NMR (CDCl₃, 125 MHz) δ (ppm) 167.19 (1-C=O), 159.05 (Ph(C) of PMB), 144.72 (C-3), 140.92 (C-5), 136.77 (C-7), 133.11 (C-12), 131.97 (C-6), 131.27 (Ph(C) of PMB), 129.23 (Ph of PMB), 128.10 (C-4), 126.13 (C-11), 120.26 (C-2), 113.73 (Ph of PMB), 79.83 (C-21), 72.96 (C-17), 72.85 (C-15), 72.09 (C-9), 70.51 (CH₂ of PMB), 60.20 (CH₂ of OEt), 55.25 (OCH₃ of PMB), 40.98 (C-16), 40.66 (C-10), 40.59 (C-8), 35.12 (C-20), 34.82 (C-14), 33.92 (C-18), 28.03 (C-13), 26.31 (C-22), 25.95 (CH₃ of *t*Bu of TBS), 25.84 (CH₃ of *t*Bu of TBS), 21.09 (C-19), 18.14 (Me₃(C)-Si), 18.11 (Me₃(C)-Si), 14.31 (CH₃ of OEt), 9.64 (16-CH₃), 9.52 (C-23), 7.05 (CH₃ of TES), 5.42 (CH₂ of TES), -3.80 (CH₃ of TBS), -4.41 (CH₃ of TBS), -4.39 (CH₃ of TBS), -4.51 (CH₃ of TBS); HRMS (ESI, positive) m/z for C₅₂H₉₄O₇Si₃ [M+Na]⁺: calcd 937.6205, found 937.6204.

(2E,4E,6E,9S,11E,15R,16S,17S,21S)-9,17-bis(tert-butyldimethylsilyloxy)-21-hydroxy-16-methyl-15-(triethylsilyloxy)tricoso-2,4,6,11-tetraenoic acid (125):

Compound **(125)** was prepared following the same procedure as compound **(47)** with a yield of 32% for 2 steps.

¹H NMR (CDCl₃, 500 MHz) δ (ppm) 7.37 (dd, 1H, $J = 11.3, 14.6$ Hz, 3-H), 6.57 (dd, 1H, $J = 11.2, 15.1$ Hz, 5-H), 6.24 (dd, 1H, $J = 11.4, 14.8$ Hz, 4-H), 6.16 (dd, 1H, $J = 11.0, 15.3$ Hz, 6-H), 5.99-5.93 (m, 1H, 7-H), 5.85 (d, 1H, $J = 15.3$ Hz, 2-H), 5.45-5.36 (m,

2H, 12-H+11-H), 3.77-3.67 (m, 3H, 15-H+9-H+17-H), 3.54-3.51 (m, 1H, 21-H), 2.34-2.19 (m, 2H, 8-Hs), 2.14 (d, 2H, $J = 5.9, 6.1$ Hz, 10-Hs), 2.05-1.93 (m, 2H, 13-Hs), 1.61-1.25 (m, 11H, 16-H+14-Hs+22-Hs+20-Hs+18-Hs+19-Hs), 0.96 (t, 9H, $J = 8.0$ Hz, CH₃ of TES), 0.91 (t, 3H, $J = 7.3$ Hz, 23-Hs), 0.883 (s, 9H, CH₃ of *t*Bu of TBS), 0.882 (s, 9H, CH₃ of *t*Bu of TBS), 0.86 (d, 3H, $J = 6.9$ Hz, 16-CH₃), 0.59 (q, 6H, $J = 7.9$ Hz, CH₂ of TES), 0.039 (s, 6H, CH₃ of TBS), 0.026 (s, 6H, CH₃ of TBS); ¹³C NMR (CDCl₃, 125 MHz) δ (ppm) 170.01 (1-C=O), 147.04 (C-3), 142.08 (C-5), 137.70 (C-7), 133.12 (C-12), 131.88 (C-6), 127.83 (C-4), 126.12 (C-11), 118.62 (C-2), 73.22 (C-21), 72.86 (C-17), 72.81 (C-15), 72.04 (C-9), 40.84 (C-16), 40.65 (C-10), 40.61 (C-8), 37.34 (C-20), 34.90 (C-14), 34.79 (C-18), 30.14 (C-13), 28.06 (C-22), 25.95 (CH₃ of *t*Bu of TBS), 25.85 (CH₃ of *t*Bu of TBS), 21.18 (C-19), 18.15 (Me₃(C)-Si), 9.85 (C-23), 9.67 (16-CH₃), 7.05 (CH₃ of TES), 5.42 (CH₂ of TES), -3.82 (CH₃ of TBS), -4.41 (CH₃ of TBS); HRMS (ESI, positive) m/z for C₄₂H₈₂O₆Si₃ [M+Na]⁺: calcd 789.5309, found 789.5311.

(3E,5E,7E,10S,12E,16R,17S,18S,22S)-10,18-bis(tert-butyldimethylsilyloxy)-22-ethyl-17-methyl-16-(triethylsilyloxy)oxacyclodocosa-3,5,7,12-tetraen-2-one (126):

Compound (126) was prepared following the same procedure as compound (49) with a yield of 63% for 2 steps.

¹H NMR (CDCl₃, 500 MHz) δ (ppm) 7.20 (dd, 1H, $J = 10.7, 14.9$ Hz, 3-H), 6.40 (dd, 1H, $J = 10.9, 14.9$ Hz, 5-H), 6.19 (dd, 1H, $J = 11.2, 14.9$ Hz, 4-H), 6.06 (dd, 1H, $J = 10.9, 15.4$ Hz, 6-H), 5.79-5.74 (m, 1H, 7-H), 5.78 (d, 1H, $J = 15.3$ Hz, 2-H), 5.29-5.18 (m, 2H, 12-H+11-H), 4.84-4.79 (m, 1H, 21-H), 3.85-3.81 (m, 1H, 9-H), 3.67-3.63 (m, 2H, 15-H+17-H), 2.58-2.54 (m, 1H, 8-H), 2.35-2.31 (m, 1H, 8-H), 2.32-2.26 (m, 2H, 10-Hs),

1.86-1.81 (m, 2H, 13-Hs), 1.70-1.23 (m, 11H, 16-H+14-Hs+22-Hs+20-Hs+18-Hs+19-Hs), 0.98 (t, 9H, $J = 8.1$ Hz, CH₃ of TES), 0.91 (t, 3H, $J = 7.5$ Hz, 23-Hs), 0.90 (s, 9H, CH₃ of *t*Bu of TBS), 0.87 (s, 9H, CH₃ of *t*Bu of TBS), 0.83 (d, 3H, $J = 6.9$ Hz, 16-CH₃), 0.603 (q, 6H, $J = 7.6$ Hz, CH₂ of TES), 0.601 (q, 6H, $J = 8.0$ Hz, CH₂ of TES), 0.079 (s, 6H, CH₃ of TBS), 0.028 (s, 3H, CH₃ of TBS), 0.023 (s, 3H, CH₃ of TBS); ¹³C NMR (CDCl₃, 125 MHz) δ (ppm) 166.71 (1-C=O), 144.47 (C-3), 141.65 (C-5), 137.51 (C-7), 132.83 (C-12), 130.66 (C-6), 127.13 (C-4), 126.30 (C-11), 120.40 (C-2), 75.91 (C-21), 73.14 (C-17), 72.96 (C-15), 71.18 (C-9), 43.61 (C-8), 42.39 (C-10), 40.75 (C-16), 35.31 (C-20), 35.02 (C-14), 34.70 (C-18), 28.24 (C-13), 27.99 (C-22), 25.96 (CH₃ of *t*Bu of TBS), 25.83 (CH₃ of *t*Bu of TBS), 19.79 (C-19), 18.16 (Me₃(C)-Si), 9.62 (C-23), 9.52 (16-CH₃), 7.08 (CH₃ of TES), 5.59 (CH₂ of TES), -4.02 (CH₃ of TBS), -4.56 (CH₃ of TBS), -4.77 (CH₃ of TBS); LRMS (ESI, positive) m/z for C₄₂H₈₀O₅Si₃ [M+Na]⁺: calcd 771.5211, found 771.67.

(3E,5E,7E,10S,12E,16R,17R,18S,22S)-22-ethyl-10,16,18-trihydroxy-17-

methyloxacyclodocosa-3,5,7,12-tetraen-2-one (127): Compound (127) was prepared following the same procedure as compound (50) with a yield of 84%.

¹H NMR (CDCl₃, 500 MHz) δ (ppm) 7.17 (dd, 1H, $J = 11.2, 15.3$ Hz, 3-H), 6.59 (dd, 1H, $J = 10.8, 14.9$ Hz, 5-H), 6.20 (dd, 1H, $J = 11.2, 14.8$ Hz, 4-H), 6.11 (dd, 1H, $J = 10.9, 15.0$ Hz, 6-H), 5.86-5.81 (m, 1H, 7-H), 5.81 (d, 1H, $J = 15.3$ Hz, 2-H), 5.31-5.21 (m, 2H, 12-H+11-H), 4.73-4.70 (m, 1H, 21-H), 3.79-3.55 (m, 2H, 9-H+17-H), 3.39-3.32 (m, 1H, 15-H), 2.57-2.52 (m, 2H, 8-H+10-H), 2.35-2.23 (m, 1H, 14-H), 2.22-1.99 (m, 4H, 8-H+10-H+13-H+14-H), 1.78-1.67 (m, 1H, 13-H), 1.60-1.09 (m, 9H, 16-H+18-Hs+19-

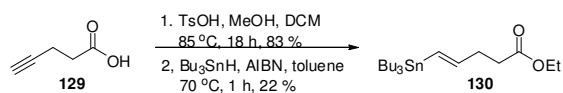
Hs+20-Hs+22-Hs), 0.83 (t, 3H, $J = 7.4$ Hz, 23-Hs), 0.61 (d, 3H, $J = 6.9$ Hz, 16-CH₃); ¹³C NMR (CDCl₃, 125 MHz) δ (ppm) 165.77 (1-C=O), 144.56 (C-3), 141.97 (C-5), 138.52 (C-7), 131.73 (C-12), 129.65 (C-6), 127.04 (C-4), 126.29 (C-11), 119.98 (C-2), 75.00 (C-21), 74.61 (C-15), 73.90 (C-17), 69.08 (C-16), 34.55 (C-14), 33.15 (C-20), 31.96 (C-18), 29.17 (C-13), 27.00 (C-22), 20.39 (C-19), 9.52 (C-23), 4.95 (16-CH₃); HRMS (ESI, positive) m/z for C₂₄H₃₉O₅ [M+H]⁺: calcd 407.2792, found 407.2794.

C13-14 Unc SpnF substrate analog (128): Compound (**128**) was prepared following the same procedure as compound (**51**) with a yield of 87%.

¹H NMR (CDCl₃, 500 MHz) δ (ppm) 7.24 (dd, 1H, $J = 11.2, 15.2$ Hz, 3-H), 6.65 (dd, 1H, $J = 10.7, 15.0$ Hz, 5-H), 6.31 (dd, 1H, $J = 10.9, 14.5$ Hz, 4-H), 6.12 (dd, 1H, $J = 11.0, 14.7$ Hz, 6-H), 5.86-5.82 (m, 1H, 7-H), 5.82 (d, 1H, $J = 15.3$ Hz, 2-H), 5.31-5.18 (m, 2H, 12-H+11-H), 4.73-4.70 (m, 1H, 21-H), 3.69-3.55 (m, 2H, 15-H, 17-H), 3.39-3.31 (m, 1H, 9-H), 2.57-2.54 (m, 1H, 8-H), 2.44-2.35 (m, 1H, 16-H), 2.32-2.30 (m, 2H, 10-Hs), 2.21-2.14 (m, 1H, 8-H), 2.10-2.00 (m, 4H, 14-Hs+13-Hs), 1.59-1.50 (m, 2H, 22-Hs), 1.39-1.22 (m, 6H, 20-Hs+18-Hs+19-Hs), 0.88 (d, 3H, $J = 7.1$ Hz, 16-CH₃), 0.83 (t, 3H, $J = 7.5$ Hz, 23-Hs); ¹³C NMR (CDCl₃, 125 MHz) δ (ppm) 212.11 (15-C=O), 165.84 (1-C=O), 144.92 (C-3), 142.25 (C-5), 138.33 (C-7), 130.23 (C-12), 129.77 (C-6), 127.25 (C-4), 127.06 (C-11), 119.93 (C-2), 74.88 (C-21), 70.00 (C-17), 69.45 (C-9), 50.41 (C-16), 43.10 (C-8), 42.21 (C-10), 40.08 (C-14), 34.08 (C-20), 32.14 (C-18), 27.11 (C-13), 26.41 (C-22), 21.75 (C-19), 10.34 (C-23), 9.52 (16-CH₃); HRMS (ESI, positive) m/z for C₂₄H₃₆O₅ [M+Na]⁺: calcd 427.2455, found 427.2451.

2.2.10. Synthesis of the C2-3 Unc SpnF Substrate Analog (C2-3 Unc analog)

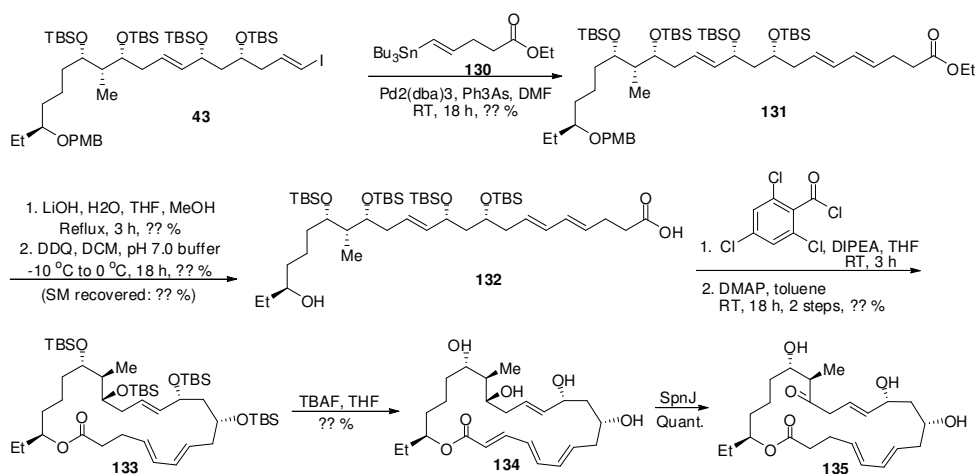
A. Preparation of Fragment C: The overall synthetic scheme is figured in **Scheme 2-18**.



Scheme 2-18. Preparation of fragment C for the synthesis of C2-3 Unc SpnF substrate analog

(E)-ethyl 5-(tributylstannyl)pent-4-enoate (130): 1) A solution of pent-4-ynoic acid (5.0 g, 51.0 mmol) and p-toluenesulfonic acid monohydrate (0.97 g, 5.1 mmol) in methanol (30 mL) and dichloromethane (60 mL) was refluxed at 85 °C for 18 hours, and then diluted with saturated the aqueous ammonium chloride solution (20 mL) at room temperature. The aqueous fraction was extracted with dichloromethane (50 mL x 4 times). The combined organic fraction were dried over an anhydrous sodium sulfate pad, and concentrated under reduced pressure. The residue was purified using flash column chromatography. The target compound was eluted with 10% of EtOAc/Hexane solution (4.7 g, 83%). 2) A suspension of the above ester compound (4.7 g, 42.0 mmol) and n-butyltin hydride (15.9 g, 55.0 mmol) in toluene was refluxed at 70 °C for 1 hour, and concentrated under reduced pressure. The residue was directly subjected to flash column chromatography. The target compound was eluted with 10% EtOAc/Hexane solution (3.6 g, 22%). All spectral data was identical to the literature reference.

B. Synthesis of C2-3 Unc SpnF Substrate Analog by Coupling Reactions and Enzymatic Conversion: The overall synthetic scheme is pictured in **Scheme 2-19**.



Scheme 2-19. Preparation of C2-3 Unc SpnF substrate analog

(4E,6E,9R,11R,12E,15R,16R,17S)-ethyl 9,11,15,17-tetrakis(tert-butyltrimethylsilyloxy)-21-(4-methoxybenzyloxy)-16-methyltricos-4,6,12-trienoate

(131): Compound **(131)** was prepared following the same procedure as **(43)** with a yield of ??%.

^1H NMR (CDCl_3 , 500 MHz) δ (ppm); ^{13}C NMR (CDCl_3 , 125 MHz) δ (ppm);
HRMS (ESI, positive) m/z for $[\text{M}+\text{Na}]^+$: calcd , found .

(4E,6E,9R,11R,12E,15R,16R,17S,21S)-9,11,15,17-tetrakis(tert-butyltrimethylsilyloxy)-21-hydroxy-16-methyltricos-4,6,12-trienoic acid **(132)**:

Compound **(132)** was prepared following the same procedure as **(45)** with a yield of ??%.

^1H NMR (CDCl_3 , 500 MHz) δ (ppm); ^{13}C NMR (CDCl_3 , 125 MHz) δ (ppm);
HRMS (ESI, positive) m/z for $[\text{M}+\text{Na}]^+$: calcd , found .

(5E,7E,10R,12R,13E,16R,17R,18S,22S)-10,12,16,18-tetrakis(tert-butyltrimethylsilyloxy)-22-ethyl-17-methyloxacyclodocosa-5,7,13-trien-2-one **(133)**:

Compound (**133**) was prepared following the same procedure as compound (**49**) with a yield of ??%.

^1H NMR (CDCl_3 , 500 MHz) δ (ppm); ^{13}C NMR (CDCl_3 , 125 MHz) δ (ppm); HRMS (ESI, positive) m/z for $[\text{M}+\text{Na}]^+$: calcd , found .

(3E,5E,7E,10R,12R,13E,16R,17R,18S,22S)-22-ethyl-10,12,16,18-tetrahydroxy-17-methyloxacyclodocosa-3,5,7,13-tetraen-2-one (134): Compound (**134**) was prepared following the same procedure as compound (**50**) with a yield of ??%.

^1H NMR (CDCl_3 , 500 MHz) δ (ppm); ^{13}C NMR (CDCl_3 , 125 MHz) δ (ppm); HRMS (ESI, positive) m/z for $[\text{M}+\text{Na}]^+$: calcd , found .

C2-3 Unc SpnF substrate analog (135): Compound (**135**) was prepared following the same procedure as compound (**51**) with a yield of ??%.

^1H NMR (CDCl_3 , 500 MHz) δ (ppm); ^{13}C NMR (CDCl_3 , 125 MHz) δ (ppm); HRMS (ESI, positive) m/z for $[\text{M}+\text{Na}]^+$: calcd , found .

2.2.11. *In vitro* activity assay of SpnM and SpnF

Prior to the kinetic isotope effect studies, the activity of SpnM and SpnF was verified as follows.

As a control for SpnM and SpnF, a solution containing SpnM natural substrate (100 μM) in pH 8.0 Tris buffer was incubated without SpnM and SpnF at 30 $^\circ\text{C}$ for 1 min, 2 min, 5 min, and 30 min, at which times an aliquat was quenched with half its volume of 1:1 DMSO/acetonitrile solution at 0 $^\circ\text{C}$, and subjected to HPLC analysis.

As a control for SpnF, a solution containing SpnM natural substrate (100 μM) and SpnM (10 μM) in pH 8.0 Tris buffer was incubated without SpnF at 30 $^\circ\text{C}$ for 1 min, 2

min, 5 min, and 30 min, at which times an aliquat was quenched with half its volume of 1:1 DMSO/acetonitrile at 0 °C, and the protein was precipitated by centrifugation. The resulting supernatant was subjected to HPLC analysis.

For the verification of SpnF activity, a solution containing SpnM natural substrate (100 µM), SpnM (10 µM), and SpnF (3 µM) in pH 8.0 Tris buffer was incubated at 30 °C for 1 min, 2 min, 5 min, and 30 min, at which times an aliquat was quenched with half its volume of 1:1 DMSO/acetonitrile at 0 °C, and protein was precipitated by centrifugation. The resulting supernatant was subjected to HPLC analysis.

2.2.12. *In vitro* activity assay of SpnF-Catalyzed Cycloaddition by Competitive Reaction Using SpnM Natural Substrate and Deuterium-Labeled SpnM Substrate Analog

2.2.12.1. Determination of the kinetic parameters for the SpnM reaction for SpnM natural substrate and deuterium-labeled SpnM substrate analog

In order to determine kinetic parameters for SpnM reaction, SpnM natural substrate (62.5, 125, 250, 500, 800, and 1000 µM) and *para*-methoxyacetophenone (100 µM) was incubated with SpnM (0.1 µM) in pH 8.0 Tris buffer (50 mM) containing DMSO (10% v/v) at 30 °C for several time periods, which were selected to measure the rate of substrate consumption and product formation. After quenching with an equal volume of 1:1 DMSO/acetonitrile solution and precipitating the proteins by centrifugation, the supernatant was subjected to HPLC analysis. HPLC conditions were as follows: C18 analytical column (250 x 4.6 mm, 5 µm), gradient was from 30% to 45% acetonitrile in water for 30 min at a rate of 1 mL/min, compounds were detected using

absorbance at 254 nm. The same procedure was conducted with deuterium-labeled SpnM substrate analog.

2.2.12.2. Determination of $^Dk_{\text{non}}$ from competitive *in vitro* activity assay

A mixture of SpnM natural substrate, C4-D SpnM substrate analog (250 μM , respectively) and *para*-methoxyacetophenone (100 μM) was incubated with SpnM (1 μM) in pH 8.0 Tris buffer (50 mM) containing DMSO (10% v/v) at 30 °C. After 5 min, 15 min, 30 min, 60 min, and 90 min (variable dependant on the reaction progress), a reaction aliquot was quenched with an equal volume of 1:1 DMSO/acetonitrile solution and the protein was precipitated by centrifugation. The supernatant was subjected to HPLC analysis to isolate SpnM product (= identical to SpnF substrate) and SpnF product. After evaporation under reduced pressure and a purity check for each collection by HPLC analysis, each collection was subjected to Q-ToF-LC-MS. The same experiments were performed for a mixture of SpnM natural substrate and each of the other SpnM substrate analog (C7-D, C11-D, and C12-D).

2.2.12.3. Determination of $^Dk_{\text{enz}}$ from competitive *in vitro* activity assay

A mixture of SpnM natural substrate and C4-D SpnM substrate analog (250 μM , each) and *para*-methoxyacetophenone (100 μM) was incubated with SpnM (15.8 μM) in pH 8.0 Tris buffer (50 mM) containing DMSO (10% v/v) at 30 °C. After a 2 min-incubation, SpnF (5 μM) was added to initiate the enzymatic conversion of SpnF substrate to SpnF product. After several time periods (10 seconds, 50 seconds, 105 seconds, 165 seconds, 225 seconds, and 290 seconds; 6 points), which were selected to measure the rate of reaction progress, a reaction aliquot was quenched with an equal

volume of 1:1 DMSO/acetonitrile solution and the proteins was precipitated by centrifugation. The supernatant was subjected to HPLC analysis to isolate the SpnM product (= identical to the SpnF substrate) and the SpnF product. After evaporation under reduced pressure and a purity check for each collection by HPLC analysis, each collection was subjected to Q-ToF-LC-MS. The same experiments were performed for a mixture of SpnM natural substrate and each of the SpnM substrate analogs (C7-D, C11-D, and C12-D).

2.2.13. *In vitro* activity assay of SpnF-Catalyzed Cycloaddition Reaction Using the Linear, C13-14 Unc, and C2-3 Unc SpnF Substrate Analog

2.2.13.1. Test for non-enzymatic [4+2] cycloaddition of Linear, C13-14 Unc, and C2-3 Unc SpnF substrate analog

In order to measure a rate of non-enzymatic [4+2] cycloaddition, Linear, C13-14 Unc, and C2-3 Unc SpnF substrate analog (250 μ M) were each incubated in pH 8.0 Tris buffer (50 mM) at 30, 40, 50, 60, and 80 °C for 2 hours or 24 hours (30 reactions total). Additionally, the reaction mixtures were refluxed for 24 hours. The reaction mixtures were subjected to HPLC analysis to analyze non-enzymatic conversion. HPLC conditions were as follows: C18 analytical column (250 x 4.6 mm, 5 μ m), elution gradient was increased linearly from 30% to 60% acetonitrile in water for 60 min at a rate of 1 mL/min, compounds detected by their absorbance at 254 nm.

2.2.13.2. Test for SpnF-catalyzed enzymatic [4+2] cycloaddition of the Linear, C13-14 Unc, and C2-3 Unc SpnF substrate analog

A solution containing Linear SpnF substrate analog (250 μM) in pH 8.0 Tris buffer (50 mM) was incubated with SpnF (50 μM , 250 μM , or 500 μM) at 30, 40, 50, and 60 $^{\circ}\text{C}$ for 2 hours or 24 hours (24 reactions total). The reaction mixtures were quenched with an equal volume of 1:1 DMSO/acetonitrile solution and the proteins were precipitated by centrifugation. The supernatant was subjected to HPLC analysis to analyze the conversion of Linear SpnM substrate analog to product, assuming conversion occurred. HPLC conditions were the same as those described in Section 2. 2.13.1.

2.2.13.3. *In vitro* inhibition assay of SpnF using Linear, C13-14 Unc, and C2-3 Unc SpnF substrate analog

2.2.13.3.1. Inhibition effect on SpnM by Linear, C13-14 Unc, C2-3 Unc SpnF substrate analog

For the control reaction, a solution containing SpnM natural substrate (100 μM) in pH 8.0 Tris buffer (50 mM) containing DMSO (10% v/v) was incubated with SpnM (5 μM) at 30 $^{\circ}\text{C}$. At 1 min, 2 min, and 10 min an aliquots was transferred into a solution of 1:1 DMSO/acetonitrile solution at 0 $^{\circ}\text{C}$. After precipitation of the proteins by centrifugation, the supernatant was subjected to HPLC analysis to show the conversion rate of SpnM natural substrate into SpnM product and non-enzymatic cycloaddition product. HPLC conditions were the same as described in Section 2.2.13.1.

For the inhibition assay, a solution containing SpnM natural substrate (100 μM) in pH 8.0 Tris buffer (50 mM) containing DMSO (10% v/v) was pre-incubated with Linear SpnF substrate analog at variable concentrations (50 μM , and 200 μM) at 30 $^{\circ}\text{C}$ for 2 min, and then incubated with SpnM (5 μM) at 30 $^{\circ}\text{C}$. At 1 min, 2 min, and 10 min an

aliquot was transferred into a solution of 1:1 DMSO/acetonitrile solution at 0 °C. After precipitation of the proteins by centrifugation, the supernatant was subjected to HPLC analysis to show the conversion rate of SpnM natural substrate into SpnM product and non-enzymatic cycloaddition product. HPLC conditions were the same as described in Section 2.2.13.1.

2.2.13.3.2. Inhibition effect on SpnF by Linear, C13-14 Unc, C2-3 Unc SpnF substrate analog

For the control reaction, a solution containing SpnM natural substrate (300 μM) in pH 8.0 Tris buffer (50 mM) containing DMSO (10% v/v) was incubated with SpnM (10 μM) and SpnF (3 μM) at 30 °C, and at 30 seconds, 60 seconds, 120 seconds, and 180 seconds an aliquot was transferred into a solution of 1:1 DMSO/acetonitrile solution at 0 °C. After precipitation of the proteins by centrifugation, the supernatant was subjected to HPLC analysis to show the conversion rate of SpnM natural substrate into SpnM product and non-enzymatic cycloaddition product. HPLC conditions were the same as described in Section 2.2.13.1.

For the inhibition assay, a solution containing SpnM natural substrate (300 μM) in pH 8.0 Tris buffer (50 mM) containing DMSO (10% v/v) was pre-incubated with Linear SpnF substrate analog at various concentrations (150 μM , and 450 μM) at 30 °C for 2 min, and incubated with SpnM (10 μM) and SpnF (3 μM) at 30 °C. At 30 seconds, 60 seconds, 120 seconds, and 180 seconds an aliquot was transferred into a solution of 1:1 DMSO/acetonitrile solution at 0 °C. After precipitation of the proteins by centrifugation, the supernatant was subjected to HPLC analysis to show the conversion rate of SpnM

natural substrate into SpnM product and non-enzymatic cycloaddition product. HPLC conditions were the same as described in Section 2.2.13.1.

2.3. RESULTS AND DISCUSSION

2.3.1. Synthesis of the SpnM Natural Substrate & Deuterium-Labeled SpnM Substrate Analogs

For the SpnF-catalyzed [4+2] cycloaddition, three possible mechanisms are proposed, the Diels-Alder reaction mechanism, the ionic rearrangement mechanism, and the biradical rearrangement mechanism, shown in **Figure 2-7**.

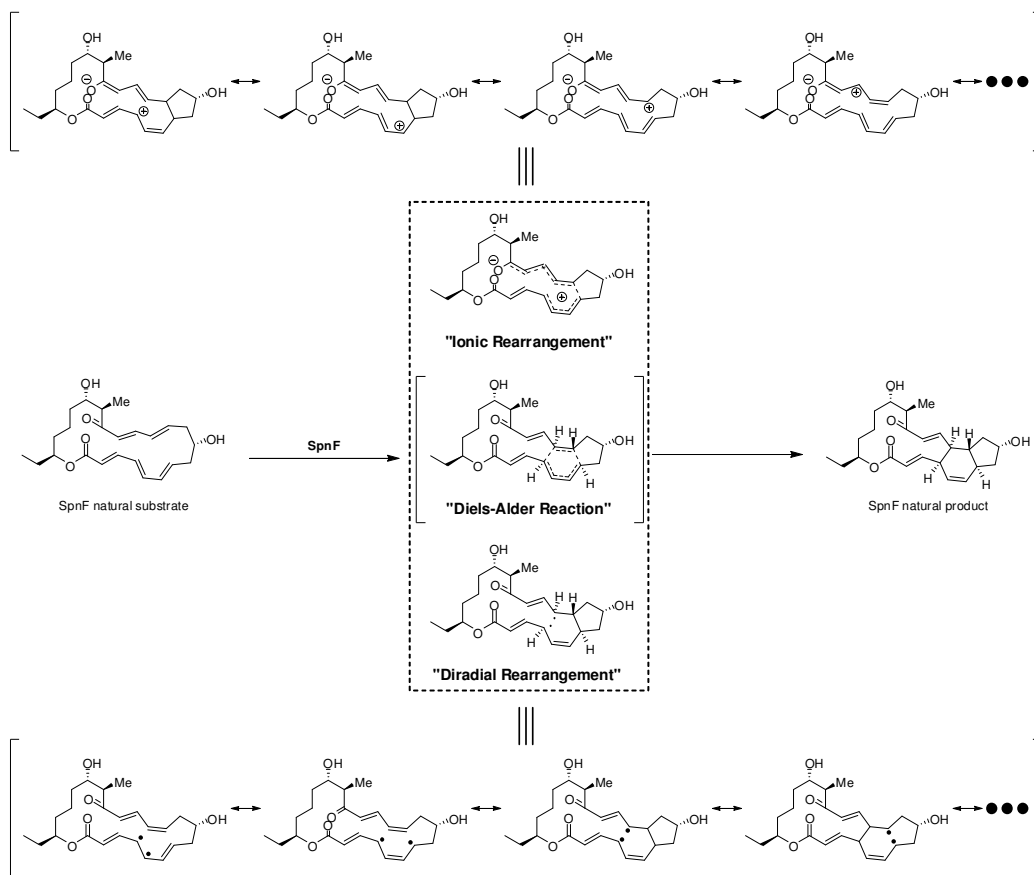


Figure 2-7. Proposed mechanisms for SpnF reaction.

During enzymatic conversion by SpnF, the Diels-Alder reaction mechanism is believed to proceed via a concerted, pericyclic, and aromatic transition state leading to an inverse kinetic isotope effect at the C-4, C-7, C-11, and C-12 positions when the corresponding deuterated compound are used as substrates.^{118, 119, 120, 121, 122} In contrast, the ionic rearrangement mechanism and the biradical rearrangement mechanism are expected to proceed in a stepwise manner, where many resonance structures are possible for the putative reaction intermediate.^{123, 124} The ionic rearrangement mechanism predicts that the reaction is initiated by a charge separation with a negative charge on the oxygen at the C-15 position and a positive charge on a carbon in the conjugated system. Subsequent C-C bond formation between C-7 and C-11 will give an inverse kinetic isotope effect at both C-7 and C-11 positions. The biradical rearrangement mechanism predicts that the biradical can occur on any two carbons in the reaction centers in the diene of C-4 to C-7 and the alkene of C-11 to C-12, and that the timing and position of C-C bond formation may lead to two different sets of kinetic isotope effects, as listed in **Figure 2-5**. However, the secondary kinetic isotope effect between the natural substrate and a deuterium-labeled substrate analog is relatively small, less than ten percent, making it difficult to determine.^{115, 116, 117, 118, 119, 120, 121, 122, 123, 124} High accuracy of the measurement is essential for the proposed kinetic isotope effects study. Additionally, SpnF natural substrate is known to undergo a non-enzymatic [4+2] cycloaddition to generate the same product.²² It is important to uncouple the enzymatic and non-enzymatic results in the kinetic experiments. In order to overcome these limitations, the SpnM and

SpnF coupled competitive kinetic experiments were designed, where SpnF substrates are biosynthesized in situ by SpnM, and the kinetic isotope effect is measured based on the competitive activity assay of SpnF by incubating SpnF natural substrate and deuterium-labeled substrate analog in one solution. To accomplish this, SpnM natural substrate and its deuterium-labeled derivatives were synthesized.

Retrosynthetic analysis was applied to design the synthetic schemes for SpnM natural substrate and the deuterium-labeled SpnM substrate analogs (**Figure 2-8**). Yamaguchi macrolactonization¹³³ was selected for the preparation of SpnM natural substrate after coupling of the three fragments A, B, and C by Julia-Kocienski olefination^{134, 135} and Stille cross-coupling,¹³⁶ sequentially. Modifications of fragment B and C were envisioned for the synthesis of the deuterium-labeled SpnM substrate analogs.

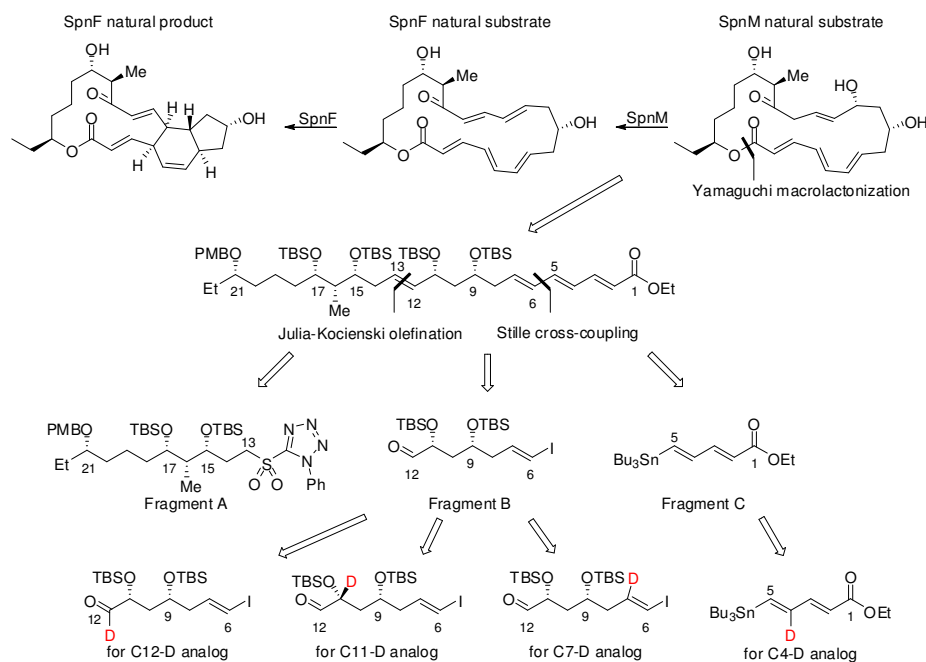


Figure 2-8. Retrosynthetic analysis for the synthesis of SpnM natural substrate and its deuterium-labeled derivatives

Starting with δ -valerolactone, fragment A was prepared through the introductions of three chiral centers by Soai ethylation¹³⁷ at C-15, Evans asymmetric aldolation¹³⁸ at C-16, and Brown's asymmetric allylation^{139, 140, 141} at C-17 position (**Scheme 2-1**). The TES protecting group at the C-15 position of compound (**48**) could be selectively deprotected allowing chemical oxidation of the C-15 hydroxy group with mild acid such as pyridinium *para*-toluenesulfonic acid (PPTS). A global deprotection of the rest of the TBS protecting groups should yield the SpnM natural substrate. However, there were concerns that the methyl group at C-16 position may epimerize during the global deprotection of the TBS's. Since SpnJ can selectively oxidize the alcohol at the C-15 position, preparation of alcohol (**51**) was eventually accomplished by global deprotection of compound (**48**) followed by incubation of compound (**50**) with SpnJ (**Figure 2-9**).

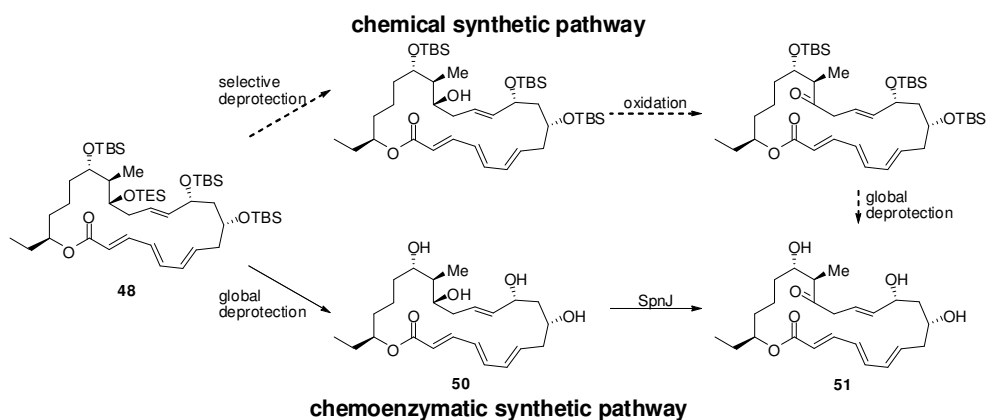


Figure 2-9. Two synthetic pathways for the preparation of SpnM natural substrate (**51**)

Fragment B of the natural substrate was prepared from D-mannitol through Corey-Seabach reaction,^{142, 143} Brown's asymmetric allylation,^{139, 140, 141} Lemieux-Johnson oxidation,¹⁴⁴ and Takai olefination¹⁴⁵ (**Scheme 2-2**). The deuterium in fragment B for the C7-D and C12-D analogs was introduced using lithiumaluminum deuteride (LiAlD₄) to

reduce a methyl ester intermediate (**59** or **87**) which was prepared by a NIS-mediated esterification, as shown in **Scheme 2-8** (C7-D analog) and **Scheme 2-11** (C12-D analog), respectively. The deuterium in fragment B for C11-D analog was achirally introduced using LiAlD₄ to compound **72**, resulting in a racemic product **73**, which was then subjected to a series of transformation to give compound **78**. The designed isomer (**79**) was obtained after deprotection of the PMB group with DDQ, as shown in **Scheme 2-9**. Fragment C was prepared from propargyl alcohol (**37**) by tinnylation and then Horner-Wadsworth-Emmons olefination,^{146, 147} where tri-n-butyltin hydride was used for making the component for SpnM natural substrate and tri-n-butyltin deuteride was used for making the C4-D analog, as shown in **Scheme 2-3** and **Scheme 2-5**, respectively. After Yamaguchi macrolactonization¹³³ of an intermediate (**47**), which was produced through Julia-Kocienski olefination^{134, 135} between fragments A and B, and Stille cross-coupling¹³⁶ between fragments A+B and C, the resulting cyclized intermediate (**49**) was global deprotected to yield the SpnJ natural substrate (**50**, see **Scheme 2-4**). SpnJ-catalyzed oxidation of C15-OH produced the desired compound (**51**),²⁰ the SpnM natural substrate (**Figure 2-10**). Other deuterium-labeled SpnM natural substrate analogs (**58**, **69**, **86**, and **95**) were prepared in the same manner with similar yields.

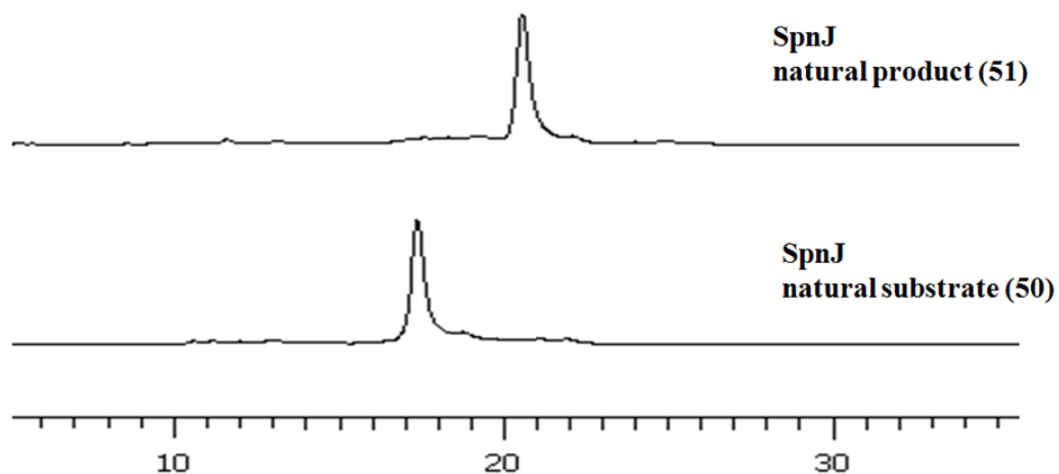


Figure 2-10. HPLC trace of SpnJ-catalyzed oxidation of its natural substrate (**50**) into product (**51**)

2.3.2. Synthesis of the Linear, C13-14 Unc, and C2-3 Unc SpnF Substrate Analogs

It is interesting to investigate what affects the enzymatic acceleration of SpnF-catalyzed [4+2] cycloaddition as compared to non-enzymatic reaction. Two factors need to be considered, an entropic preorganization and enthalpic transition state stabilization. To study the relative rate enhancement (RRE),¹³¹ three SpnF substrate analogs were designed, as shown in **Figure 2-6**.

Synthesis of the Linear SpnF substrate analog is slightly different from that of the natural substrate (**Figure 2-11**). Considering the possibility that SpnJ and SpnM may not accept the Linear analog as a substrate, the ketone at the C-15 position and the olefin through C-11 and C-14 were chemically introduced in fragments A and B. Preparation of fragment A from heptanal (**96**) began with Evans asymmetric aldolization,¹³⁸ followed by TBS protection and one-carbon extension by Wittig reaction^{148, 149} to give an alcohol intermediate (**101**, see **Scheme 2-13**). After olefination with sulfoxide reagent and TBS protection of resulting C-15-OH, intermediate **103** was reduced to give an alcohol (**104**),

which was transformed into fragment A by the same procedure that was used in the production of the natural substrate. Fragment B is one-carbon shorter than the natural substrate, and contains one chiral center at C-9 position, which was introduced by Brown's asymmetric allylation.^{139, 140, 141} After Julia-Kocienski olefination^{134, 135} and Stille cross-coupling,¹³⁶ the C-15-OH of compound **116** was ketonized by selective deprotection and oxidation to give intermediate (**117**). Following hydrolysis and global deprotection the Linear SpnF substrate analog (**119**) was obtained. In contrast, when intermediate (**116**) was directly hydrolyzed and deprotected globally the Linear SpnJ substrate analog (**118**) was obtained as the product.

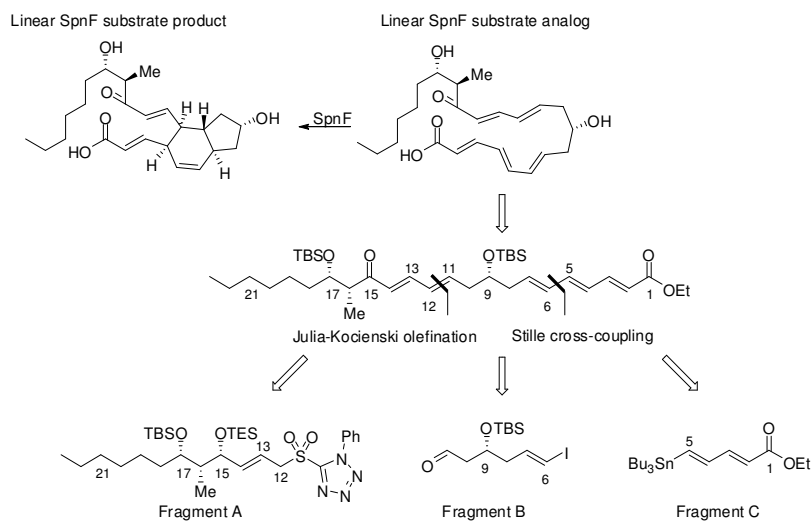


Figure 2-11. Retrosynthetic analysis for the synthesis of Linear SpnF substrate analog

The C13-14 Unc and C2-3 Unc SpnF substrate analogs were also designed based on the assumption that SpnJ and SpnM may not recognize the precursors of these analogs. Retrosynthetic analysis of C13-14 Unc SpnF substrate analog suggested that fragment A and fragment B should be modified to uncouple the olefin at C13 and C14 by preparing the C13-14 saturated fragment A (**122**) and modified fragment B (**114**), which

were already used in the preparation of Linear SpnF substrate analog (**Figure 2-12**). The modified fragment A (**122**) for C13-14 Unc analog was prepared from the intermediate (**17**) by hydroboration¹⁵⁰ and oxidation as the key reactions. Retrosynthesis of the C2-3 Unc SpnF substrate analog indicated that only C2-3 saturated fragment C is required (**Figure 2-13**). The macrolactone for C13-14 Unc and C2-3 Unc SpnF substrate analogs were prepared following the same procedures used to produce the natural substrate.

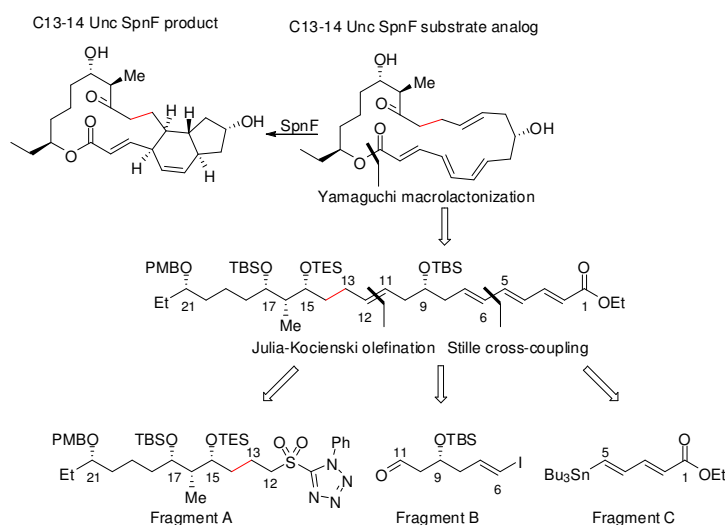


Figure 2-12. Retrosynthetic analysis for the synthesis of C13-14 Unc SpnF substrate analog

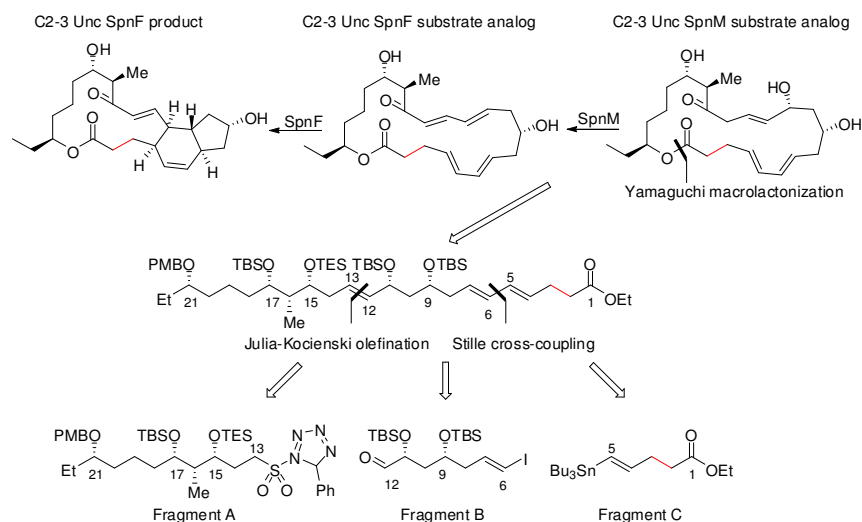


Figure 2-13. Retrosynthetic analysis for the synthesis of C2-3 Unc SpnF substrate analog

2.3.3. *In vitro* activity assay of SpnM and SpnF

Prior to the kinetic isotope effect study of SpnF, the activities of SpnM and SpnF were verified using SpnM natural substrate. SpnM natural substrate was incubated with SpnM and/or SpnF at 30 °C for 1 min, 2 min, 5 min, and 30 min, and the substrate/product ratio (% of conversion) was determined by HPLC analysis. It was found that SpnM-catalyzed dehydration was complete in 5 min, and SpnF-catalyzed [4+2] cycloaddition was complete in 30 min. It is notable that SpnF product is also produced during SpnM reaction, although not in significant quantities (data not shown). The HPLC trace of SpnM natural substrate is shown in **Figure 2-14** after completion of each enzymatic conversion.

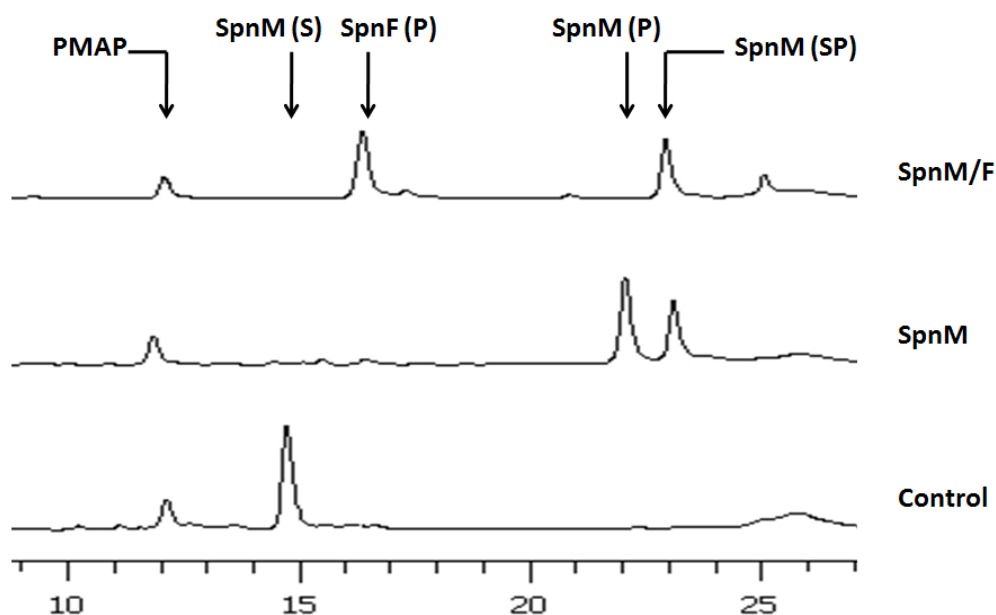


Figure 2-14. HPLC trace of SpnM and SpnF reactions. (SpnM (S) = SpnM natural substrate, SpnM (P) = SpnM product, SpnF (P) = SpnF product, SpnM (SP) = unknown SpnM side product, PMAP = para-methoxyacetophenone as internal standard)

2.3.4. *In vitro* Activity Assay of SpnF-Catalyzed [4+2] Cycloaddition by Competitive Reaction using SpnM Natural Substrate and Deuterium-Labeled SpnM Substrate Analog

SpnF-catalyzed [4+2] cycloaddition is an interesting reaction which makes the cyclohexene moiety in the biosynthesis of spinosyn A. The [4+2] cycloaddition is typically achieved using Diels-Alder reaction in organic synthesis.^{25, 26, 27, 28} However, there is no natural enzyme reported to be a true “Diels-Alderase” although several enzymes have been investigated with the intention of finding a “Diels-Alderase.”^{37, 38, 39, 40, 41, 42, 43, 44, 45, 46, 47, 48, 49, 50, 51, 52} Three plausible mechanisms have been proposed to explain SpnF reaction, as shown in Chapter 1, and α -secondary deuterium kinetic isotope effect (KIE) studies are designed to determine the actual mechanism used. The following

kinetic isotope effect studies were performed using the C4-D and the C7-D analog as substrates. Additional kinetic isotope effect studies are currently in progress, therefore this section will be restricted to the results from these two C4-D and C7-D analogs. These kinetic studies were collaborate efforts with Dr. Mark Ruszczycky and Byung-sun Jeon, a graduate student.

2.3.4.1. Determination of the kinetic parameters for SpnM reaction for SpnM natural substrate and deuterium-labeled SpnM substrate analog

Using the data from the kinetic experiment, and assuming a zero-order reaction, the kinetic parameters for the SpnM reaction at 30 °C at pH 8.0 were determined based on the Michaelis-Menten equation. All of kinetic data are comparable to that reported by Dr. Kim, a former graduate student in Liu lab. Specifically, he found K_M to be 380 ± 51 uM, and k_{cat}/K_M to be 2.6 ± 0.42 uM⁻¹s⁻¹.²²

2.3.4.2. Determination of $^Dk_{non}$ from competitive reaction

A competitive reaction using SpnM natural substrate and deuterium-labeled SpnM substrate analog was designed to differentiate the three proposed SpnF reaction mechanisms, as described in **Section 2.1**.

To determine the kinetic constant, $^Dk_{non}$ for the non-enzymatic [4+2] cycloaddition in a competitive reaction using SpnM natural substrate and C7-D SpnM substrate analog was measured. The reaction mixture was prepared by mixing the unlabeled (natural substrate) and deuterium labeled substrates together. As the reaction progresses, the unlabeled material becomes “enriched” in the substrate or in the product beyond natural abundance. The enrichment ratio is defined as the ratio of the

concentration of the labeled material divided by the concentration of the unlabeled material, denoted by $R_X = \frac{\text{Concentration}_{\text{C}_{\text{X-D}}}}{\text{Concentration}_{\text{C}_{\text{X-H}}}}$ where X is the position of reaction center.

So, enrichment ratios during the SpnM reaction are expected to change between SpnM substrate and SpnM product depending on the mechanism, which can be used to determine the KIE of the SpnM reactions. For example, if the enrichment ratio of substrate becomes smaller (i.e., more depleted compared to the starting material), accompanied by increased enrichment ratio of product, it indicates the labeled material reacts faster and there is an inverse kinetic isotope effect. Alternatively, if the enrichment ratio of a substrate becomes greater (i.e., more enriched in labeled material), it means the unlabeled material reacts faster and there is a normal kinetic isotope effect. A mixture prepared as outlined above was incubated with SpnM at 30 °C for several time periods (5 min, 15 min, 25 min, 40 min, 60 min, and 90 min) to allow the non-enzymatic [4+2] cycloaddition of the SpnM product (identical to SpnF substrate) into SpnF product to take place. The reaction was then quenched. The kinetic isotope effect can be calculated from the enrichment ratios, derived from the MS results of the substrates and products, which were isolated from the quenching reaction mixture at various time points. Here, it is assumed that the SpnM reaction is less likely to affect the change of enrichment ratio, although it is predicted to slightly affect the enrichment ratio in the cases of C11-D analog and C12-D analog. In addition, the enrichment ratio is calculated from the MS results of SpnM product (identical to SpnF substrate) due to the ease of performing the experiment. It is apparent that the concentration of SpnF product is at much lower

concentrations than the SpnF substrate in the initial time point, making it difficult to conduct MS analysis. To avoid this problem, the MS analysis was mainly performed with SpnF substrate when both of substrate and product were isolated. **Figure 2-15** shows a representative result from the competition assays of SpnM natural substrate and the C7-D SpnM substrate analog, showing several ionic states of the sample.

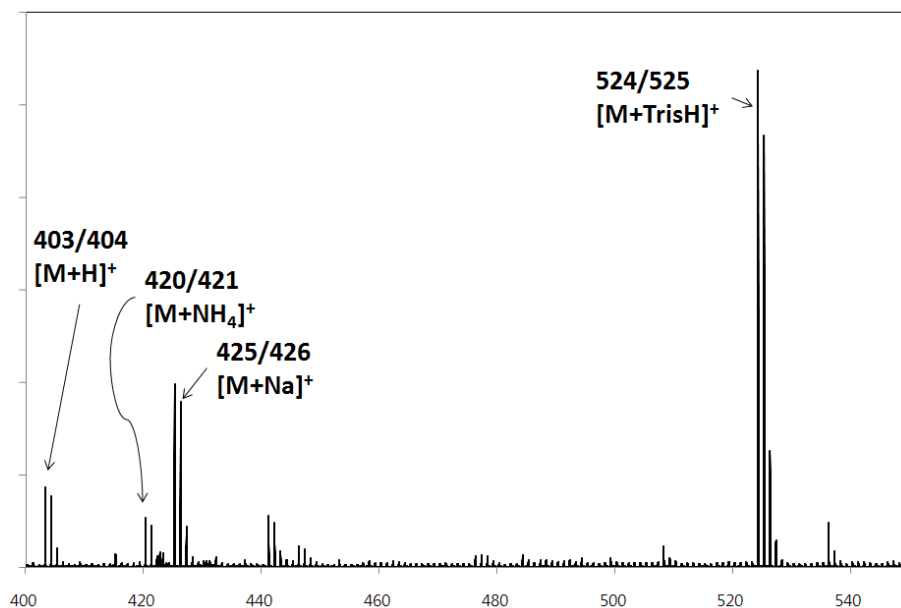


Figure 2-15. Representative MS results from the competition reaction of SpnM natural substrate and C7-D SpnM substrate analog.

Based on the statistical analysis of the MS results, the non-enzymatic kinetic isotope effects for C-4 and C-7 positions were determined to be $^{C4D}k_{\text{non}} = 0.9975 \pm 0.0033$, and $^{C7D}k_{\text{non}} = 0.9676 \pm 0.0031$, respectively (**Figure 2-16**). The value for $^{C7D}k_{\text{non}}$ is within the expected range of 0.97-0.99, which is based on computational models and experimental observations for Diels-Alder reaction mechanism.^{115, 117, 118, 119} The value of $^{C4D}k_{\text{non}}$ is not significantly different from unity, and means that there is relatively little change in hybridization of the carbon at the C-4 position during the isotopically sensitive

step of the non-enzymatic cycloaddition. In other word, the C-C bond formation at C-4 is less likely to occur at an early stage. If the reaction follows the Diels-Alder type mechanism, it can be inferred that the non-enzymatic reaction adopts highly or very early asynchronous transition state. On the other hand, it may still proceed via a stepwise mechanism. However, the non-enzymatic reaction is unlikely to proceed through the ionic rearrangement or biradical rearrangement mechanism, which should show a value greater than unity for the kinetic isotope effect at the C-4 position, because the inverse kinetic isotope effect is observed at the C-7 position. Another possible mechanism is a [6+4] cycloaddition followed by a [3,3] sigmatropic rearrangement, suggested by Ken Houk to Dr. Liu (not published; **Figure 2-17**). In this mechanism, a small kinetic isotope effect on C-4 position can be explained since a sp^2 hybridized carbon at the C-4 position does not undergo a significant hybridal change at the initial stage, considered as the rate determining step. Additionally, an inverse kinetic isotope effect at C-7 is also well explained. The kinetic isotope effect study with C11-D and C12-D analogs will help to determine the non-enzymatic reaction mechanism.

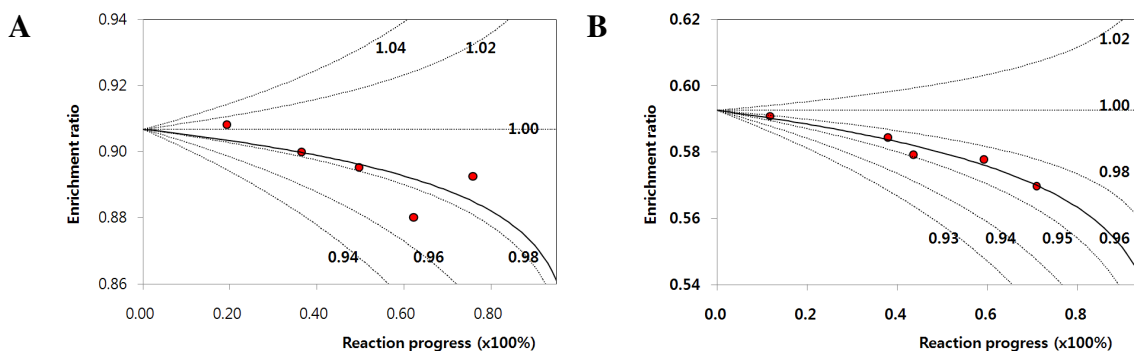


Figure 2-16. Plots of enrichment (R_x) versus reaction progress for (A) C4-D and (B) C7-D kinetic isotope effect in the non-enzymatic reaction.

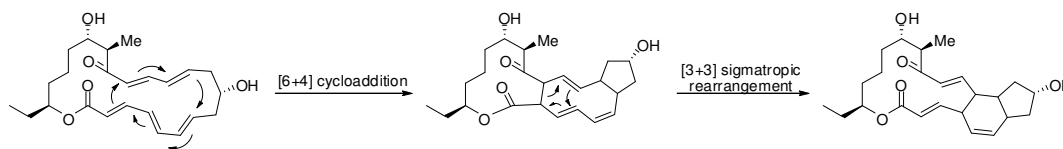


Figure 2-17. Alternative mechanism describing a [6+4] cycloaddition followed by a [3+3] sigmatropic rearrangement, suggested by Ken Houk

2.3.4.3. Determination of Dk_{enz} from the competitive reaction

To determine the Dk_{enz} for the SpnF-catalyzed [4+2] cycloaddition, another competition reaction was performed using SpnM natural substrate and the deuterium-labeled SpnM substrate analog by a coupled assay with SpnM and SpnF. Unlike the determination of the non-enzymatic kinetic isotope effect, the timing of the SpnF reaction should be considered because SpnF product is being formed as soon as SpnF substrate formed by the SpnM reaction. If SpnF is added too early, it become difficult to measure the initial enrichment ratio of SpnF substrate due to the rapid turnover of SpnF substrate into SpnF product, a reaction that is approximately 500 times faster than the non-enzymatic reaction. If SpnF is added too late, the initial non-enzymatic turnover of SpnF substrate into product prior to SpnF addition will be problematic. Fortunately, these problems were solved by using only the observed fractions of the reaction or readjustment of the data to the SpnF addition point. Essentially, the best time to add SpnF is right before taking the first aliquot. In other words, the initial enrichment ratio can be extrapolated from the enrichment ratio of the first aliquot. The interval between SpnF addition and the first aliquot was therefore minimized, to a range of several seconds. Next, the concentration of SpnF added must be considered to keep the kinetic isotope effect from the non-enzymatic reaction within the margin of error of the kinetic isotope

effect from the enzymatic reaction. In addition, the overall reaction time which would be adequate to determine the kinetic isotope effect was also considered. Based on the enzymatic kinetics and statistic analysis, all of reaction conditions, including the concentration of substrates and enzymes, SpnM preincubation time, SpnF addition time and quenching time, were determined as described in Section 2.2.12.3.

From the statistical analysis of the MS results, the kinetic isotope effects of the enzymatic reaction were determined in the same manner as the non-enzymatic reaction. The results shows that $^{C4D}k_{enz} = 0.9287 \pm 0.0087$, and $^{C7D}k_{enz} = 1.0033 \pm 0.0084$ (**Figure 2-18**).

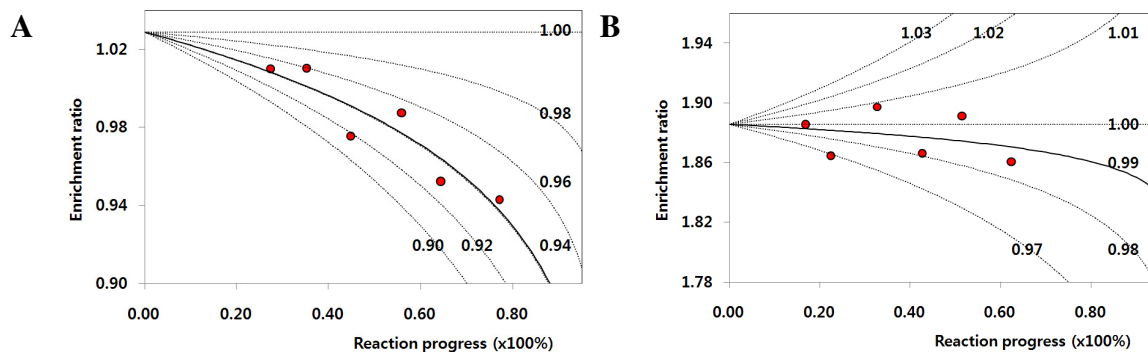


Figure 2-18. Plots of enrichment (R_x) versus fraction of reaction (f) for (A) C4-D and (B) C7-D kinetic isotope effect in the enzymatic reaction.

The inverse kinetic isotope effect for C-4 positions is consistent with an sp^2 to sp^3 rehybridization in the early stage of the SpnF reaction, and consistent with the Diels-Alder reaction mechanism. However, the normal or unity kinetic isotope effect for the C-7 position does not match the expected kinetic isotope effect (inverse) for the Diels-Alder reaction mechanism and the ionic rearrangement mechanism, in which the C-C bond between the C-7 and C-11 positions form either concurrently with or prior to the

formation of the C-4-C-12 bond. Rather, this normal value is consistent with the biradical rearrangement mechanism. If the SpnF reaction proceeds through a highly asynchronous transition state, similar to the non-enzymatic kinetic isotope effect at the C-4 position, a normal kinetic isotope effect may be possible for the Diels-Alder reaction mechanism. For the ionic rearrangement, the kinetic isotope effect at the C-7 position must be “inverse” due to the early formation of the C-7-C-11 bond during a stepwise reaction with a dipolar intermediate, for which the charges are most stabilized along the π -electron conjugated systems for both C-4-C-7 and C-11-C-15-Oxygen. Therefore, the normal kinetic isotope effect at the C-7 position should rule out the ionic rearrangement mechanism. In the case of the biradical rearrangement mechanism, the kinetic isotope effect at the C-4 position depends on the timing of the C-C bond formation between the C-4 and C-12 positions and the C-7 and C-11 positions is opposite to the order of biradical formation. The normal kinetic isotope effect at the C-4 position and the inverse kinetic isotope effect at the C-7 position is completely consistent with the biradical rearrangement mechanism, where the early biradical formation at C-7 and C-11 positions and the early C-C bond formation between C-4 and C-12 positions are involved during the SpnF-catalyzed [4+2] cycloaddition (**Figure 2-19**). This interpretation is consistent with the computational results of a simplified model system from the Houk group, which suggest that $^{C4D}(V/K)$ would be approximately 0.90-0.96, and $^{C7D}(V/K)$ is expected to be 1.03-1.15.

It is conceivable that there is an unusual ionic rearrangement where the charge separation happens at the C-7 and C-11 positions without conjugation (**Figure 2-20**),

which was suggested by Dr. Rusczychy, the post-doc in the Liu Lab. Although the kinetic isotope effects from this unusual intermediate may be consistent with the above observations, this mechanism seems very unlikely due to the lack of charge stabilization at the C-7 and C-11 positions.

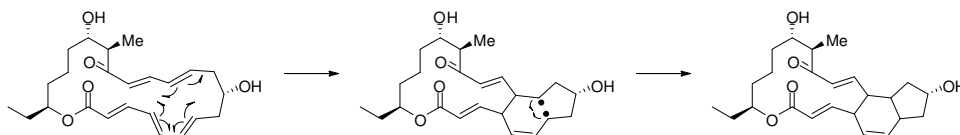


Figure 2-19. The most likely mechanism for the SpnF-catalyzed cycloaddition based on the current estimation of kinetic isotope effects at the C-4 and C-7 positions.

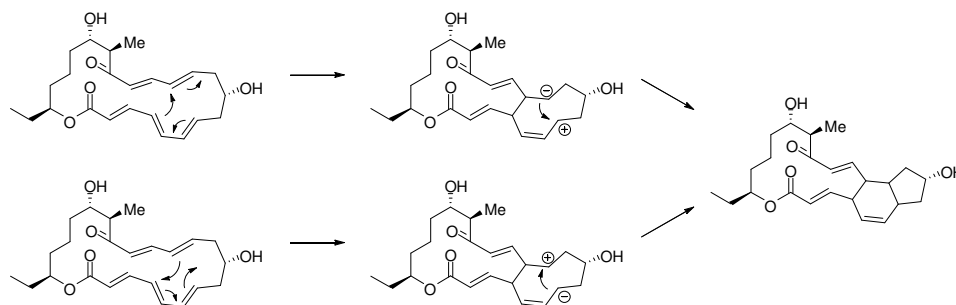


Figure 2-20. The ionic rearrangement mechanism via the unusual zwitterion intermediates.

Based on the kinetic isotope effect at the C-4 and C-7 positions for the enzymatic SpnF reaction, it is hard to say which mechanism most accurately models the SpnF-catalyzed [4+2] cycloaddition. However, at least the ionic rearrangement mechanism can be ruled out as a possible mechanism. Future kinetic isotope effect studies using the C11-D and C12-D analog are expected to help further elucidate the reaction mechanism. The summary of the current values for the non-enzymatic and enzymatic kinetic isotope effect for the [4+2] cycloaddition is shown in **Figure 2-21**.

Secondary kinetic isotope effect	Current estimation
$^{13}\text{C} k_{\text{non}}$	0.9975 ± 0.0033
$^{15}\text{N} k_{\text{non}}$	0.9676 ± 0.0031
$^{13}\text{C} k_{\text{enz}} = ^{13}\text{C}(V/K)$	0.9287 ± 0.0087
$^{15}\text{N} k_{\text{enz}} = ^{15}\text{N}(V/K)$	1.0033 ± 0.0084

Figure 2-21. Current estimations for non-enzymatic and enzymatic kinetic isotope effects for the [4+2] cycloaddition in the biosynthesis of spinosyn A.

2.3.5. *In vitro* Activity Assay of SpnF-Catalyzed [4+2] Cycloaddition using the Linear, C13-14 Unc, and C2-3 Unc SpnF Substrate Analogs

In vitro activity assays of SpnF-catalyzed [4+2] cycloaddition were first performed using the Linear SpnF substrate analog and C13-14 Unc SpnF substrate analog, described as follows. The experiments for the C2-3 Unc SpnF substrate analog are still in progress.

2.3.5.1. Test for non-enzymatic and enzymatic [4+2] cycloaddition of Linear, C13-14 Unc, and C2-3 Unc SpnF Substrate Analog

It is worthwhile to investigate how SpnF accelerates the [4+2] cycloaddition in the biosynthesis of spinosyn A, to approximately 500-fold the rate of the non-enzymatic from the view of thermokinetics and thermodynamic perspective.²² The two proposed hypotheses are the entropic preorganization and enthalpic transition state stabilization. The Linear analog is designed to determine the contribution of entropic preorganization^{125, 126, 127, 128, 129, 130} and the two Unc analogs are designed to examine the contribution of enthalpic transition state stabilization.

In terms of entropy, it is likely that an entropic preorganization effect on the Linear analog will be more significant than for SpnF natural substrate, due to the fixation of the relatively free long chain into the rigid cyclic core and a decrease of the overall

entropy after [4+2] cycloaddition. In terms of enthalpy, since the Linear analog has the ready [4+2] components to form both the C-1 to C-7 and the C-11 to C-15-ketone conjugation systems, same as those in SpnF natural substrate, the difference in the stabilization effect is expected to be small or nonexistent, compared to the SpnF natural substrate. Thus, the relative rate enhancement for the natural substrate compared to the Linear analog ($RRE_{NS,Linear}$) should predominantly be due to the entropic preorganization effect rather than the enthalpic transition state stabilization effect .

The C13-14 Unc and C2-3 Unc analogs may have different enthalpic states compared to that of SpnF natural substrate, because the activating groups adjacent to the reaction centers of the diene and dienophile have been modified. Entropically, these two analogs seem to be similar with SpnF natural substrate due to their structural resemblance as a macrolactone ring, although there may still be small entropic differences. Thus, any relative rate enhancement for natural substrate compared to the unconjugated analogs ($RRE_{NS,Unc}$) is expected to arise predominantly from the enthalpic transition state stabilization effect rather than the entropic preorganization effect (**Figure 2-22**).

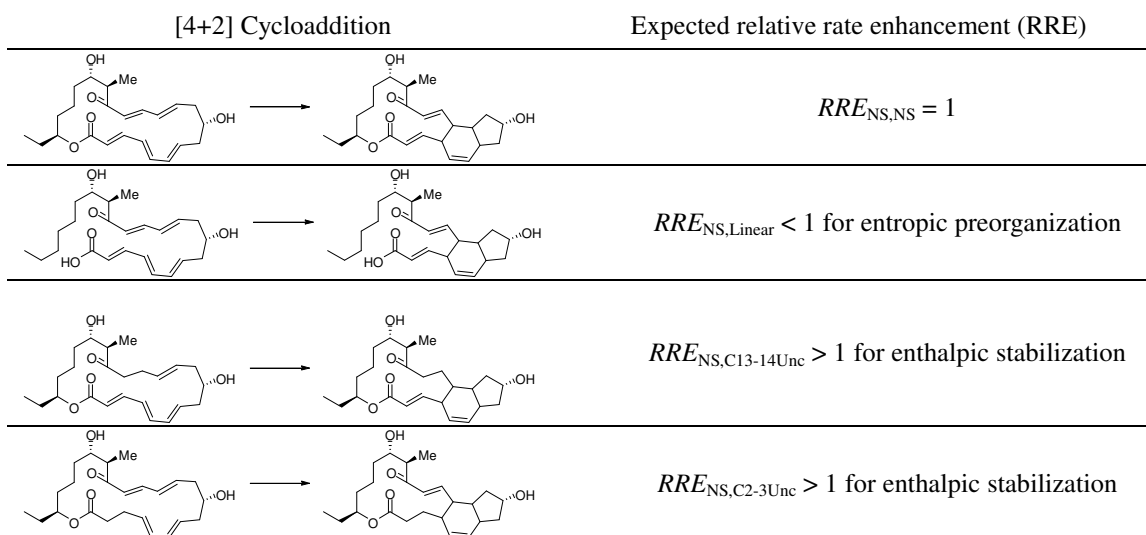


Figure 2-22. Expected $RRE_{NS,Analog}$ for [4+2] cycloaddition.

In order to investigate the SpnF intrinsic properties, it is necessary to observe the mechanistic probes undergoing both the enzymatic and non-enzymatic [4+2] cycloadditions, since rate enhancement (RE) is defined as the ratio of enzymatic reaction rate divided by non-enzymatic reaction rate. Non-enzymatic conversion of the Linear analog and C13-14 Unc analog did not occur even under the reflux condition for 24 hr. Moreover, the enzymatic turnover for these two analogs was not observed, even with a high concentration of SpnF at the elevated temperature (up to 60 °C) for an extended period (up to 24 hr) (**Figure 2-23** and **Figure 2-24**).

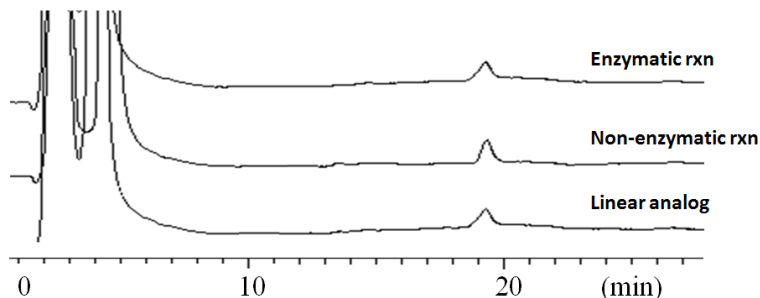


Figure 2-23. HPLC trace of Linear SpnF substrate analog for [4+2] cycloaddition. HPLC condition: 50% to 70% aqueous acetonitrile with a flow rate of 1 mL/min over 30 min.

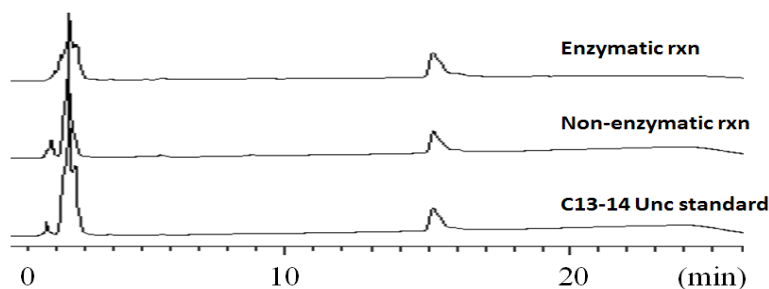


Figure 2-24. HPLC trace of C13-14 Unc SpnF substrate analog for [4+2] cycloaddition. HPLC condition: 40% to 60% aqueous acetonitrile with a flow rate of 1 mL/min over 30 min.

Based on the molecular orbital theory for the [4+2] cycloaddition, the collision of a diene and dienophile in a face-to-face manner should happen prior to the alignment of the “allowed” geometries for the diene and dienophile. After collision of the two moieties, the π molecular orbitals of the diene and dienophile are rearranged to match each other to make a partial C-C bond if the energy difference is between the highest occupied molecular orbital (HOMO) of the diene and the lowest unoccupied molecular orbital (LUMO) of the dienophile. This is the general process for the [4+2] cycloaddition (**Figure 2-25**).^{34, 100}

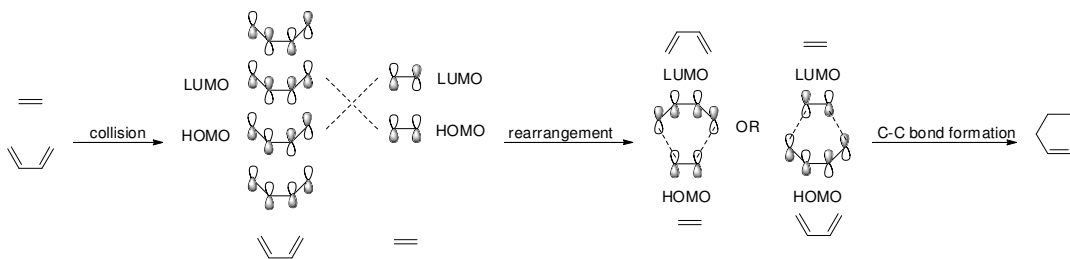


Figure 2-25. General procedure for the [4+2] cycloaddition through the collision of diene and dienophile, rearrangement, and C-C bond formation.

For the Linear analog, the energy difference between HOMO and LUMO seems to be similar to that of SpnF natural substrate. So, the collision of the diene and dienophile in the Linear analog should lead to the formation of a [4+2] cycloaddition only

if the orientation of the molecular orbitals is correct. However, the higher structural flexibility of the Linear analog may have prevented the collision of two reaction centers in the proper orientation of diene and dienophile, where the molecular orbitals are in different phases. In other word, the Linear analog cannot overcome the higher barrier of entropy and facilitate the [4+2] cycloaddition, even though the energy level of HOMO and LUMO is comparable to that of SpnF natural substrate. This appears to be the same for the enzymatic reaction for several reasons. One possible reason is that SpnF cannot accommodate the Linear analog due to its high flexibility. Another plausible reason is that SpnF cannot preorganize the Linear analog although SpnF can accommodate the Linear analog in its active site. To test this hypothesis, the inhibition assay was performed, as described in the next section.

For the C13-14 Unc analog, the collision of the diene and dienophile is facilitated by the structure to a higher degree than the Linear analog, and is probably to a comparable degree as the SpnF natural substrate, due to their structural similarity, except for one less C-C bond conjugation at the C-13 to C-14 position. One possible explanation for the observed data is the incorrect direction of molecular orbitals for HOMO and LUMO in the C13-14 Unc analog, a situation similar to the Linear analog. If the direction is correct for the [4+2] cycloaddition, the remaining explanation lies in the energy difference between HOMO and LUMO. For the [4+2] cycloaddition, the moiety adjacent to the diene or dienophile is most critical to the success or failure of the reaction, since it can change energy of HOMO and LUMO. SpnF natural substrate has two activated conjugations for the diene and dienophile to facilitate even the non-enzymatic

cycloaddition. These two conjugations could increase the energy level of HOMO of the diene by donating electrons, and lower the energy level of LUMO of the dienophile by withdrawing electrons (**Figure 2-26**). The C13-14 Unc analog is deficient in one of conjugation on the C-13 to C-14 position, which does not affect the LUMO of the dienophile. Although the energy gap between the LUMO activated by conjugation and the original LUMO of the C13-14 Unc analog is unknown, it seems that this gap cannot be overcome by SpnF to facilitate the [4+2] cycloaddition of C13-14 Unc analog. In other word, the C13-14 Unc analog does not transform due to the lack of enthalpic stabilization in the initial collision stage, not in the transition state. Even enzymatic assistance seems unable to overcome this energy gap derived from the lack of conjugation at the C-13 to C-14 position. As mentioned above, the issue may also be the inability of SpnF to receive the C13-14 Unc analog into its active site. To verify the hypothesis that the entropic or enthalpic difference may lead to the lack of conversion of the Linear analog and the C13-14 Unc analog into the [4+2] cycloaddition product, the *in vitro* inhibition assay was performed, as described in next section.

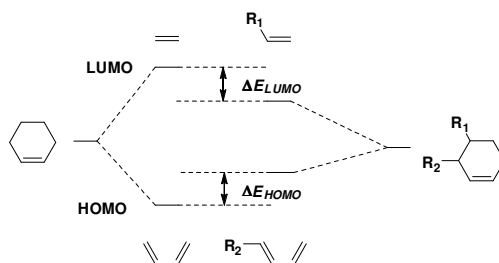


Figure 2-26. The change of HOMO and LUMO by the adjacent conjugation in the [4+2] cycloaddition, where R_1 is electron-withdrawing from dienophile, and R_2 is electron-donating to diene.

2.3.5.2. *In vitro* inhibition assay of SpnF using the Linear, the C13-14 Unc, and the C2-3 Unc SpnF substrate analog

Since the Linear SpnF substrate analog and the C13-14 Unc SpnF substrate analog were not transformed into any product under non-enzymatic and enzymatic conditions, several questions need to be addressed to understand the reaction. The first is why the [4+2] cycloaddition does not happen under non-enzymatic and enzymatic condition, for which some possible explanations were described in previous section in terms of entropy and enthalpy. The next question is whether SpnF can accommodate the Linear analog or the C13-14 Unc analog in its active site. To verify this, the inhibition assay of SpnF is designed to measure the conversion rate of SpnF natural substrate into SpnF product in the presence of various concentrations of analog. It is also important to confirm that the activity of SpnM is not affected by the Linear and the C13-14 Unc analog. Inhibition assays of SpnM with the Linear analog and the C13-14 Unc analog showed that these analogs do not affect the activity of SpnM even in the high concentration conditions in amount of 40 equivalences to enzyme. Inhibition assays of SpnF were performed under two sets of conditions, where a half equivalent or double equivalents of SpnM natural substrate was used in competition with one equivalent of inhibitor. As reaction proceeded, all SpnM natural substrate was converted to SpnF product in the presence of other substrate analogs. The results are shown in **Figure 2-27** and **Figure 2-28**.

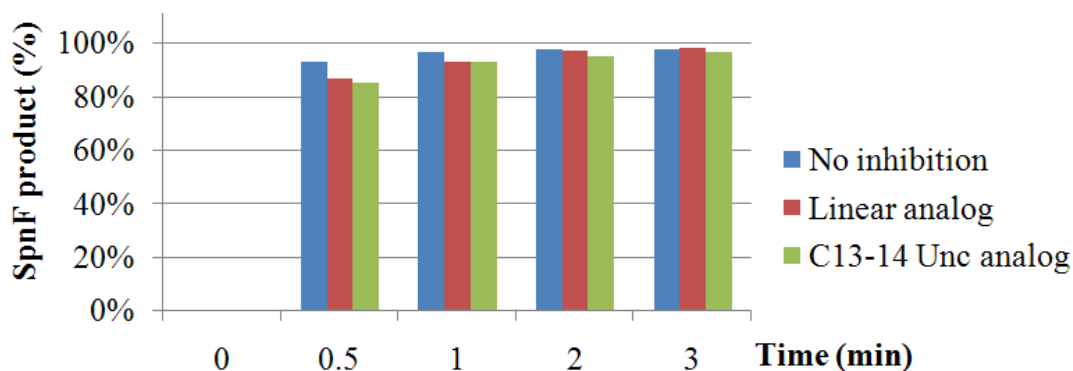


Figure 2-27. Inhibition assay of SpnF with the Linear analog and C13-14 Unc analog in the presence of half equivalent of SpnM natural substrate.

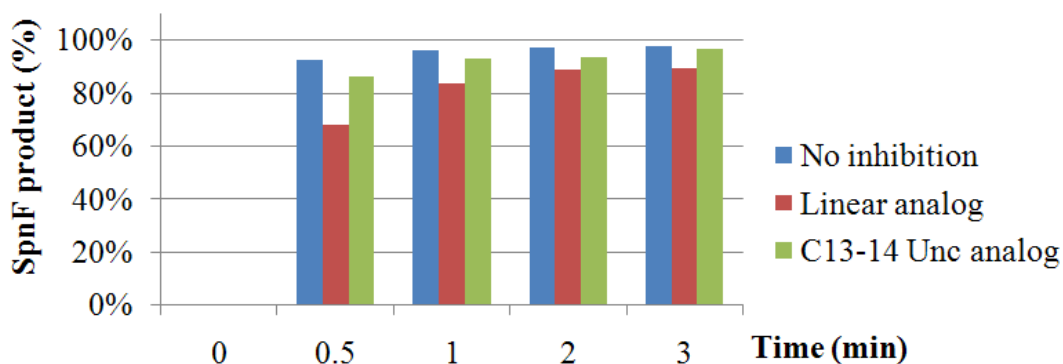


Figure 2-28. Inhibition assay of SpnF with the Linear analog and C13-14 Unc analog in the presence of double equivalents of SpnM natural substrate.

The Linear analog seems not to affect the activity of SpnF at low or high concentrations while the C13-14 Unc analog shows inhibition of SpnF, at high concentrations by around 20% of the initial reaction progress and at low concentrations by around 5% (possibly within the margin of error). This observation demonstrated that the Linear analog may be not accommodated into the active site of SpnF, and therefore does not compete with SpnF natural substrate during the SpnF reaction. In contrast, the C13-14 Unc analog competes with SpnF natural substrate to occupy the active site of SpnF during the SpnF reaction. Based on the observation that the SpnF product is

produced as time goes on in the inhibition assay with the C13-14 Unc analog, the binding of C13-14 Unc analog to the active site of SpnF is not tight, and rather reversible.

The purpose of synthesizing the Linear SpnF substrate analog and the C13-14 Unc SpnF substrate analog was to address the intrinsic properties of SpnF, specifically how SpnF accelerates the enzymatic transformation of [4+2] cycloaddition based on the concept of relative rate enhancement. It was assumed that the Linear analog and C13-14 Unc analog undergo the [4+2] cycloaddition under non-enzymatic and enzymatic conditions. However, these two analogs turned out not to undergo the [4+2] cycloaddition, even under the somewhat extreme conditions of high temperature or high concentration of enzyme. Thus, the reason why these two analogs are not able to undergo the [4+2] cycloaddition is pursued in terms of entropy and enthalpy. The inhibition assay simply demonstrated that the C13-14 Unc analog may be a reversible inhibitor, but the Linear analog is not. Additional experiments will be pursued in order to verify the hypothesis that the high entropy of the Linear analog and the low activation of HOMO and LUMO of the C13-14 Unc analog block the [4+2] cycloaddition. In addition, the C2-3 Unc SpnF substrate analog will be used to expand the understanding of SpnF intrinsic properties.

2.4. CONCLUSION

For a long time, many biochemical studies have been devoted to finding a “Diels-Alderase” in nature. Although solanapyrone synthase^{41, 42, 43} and lovastatin synthase (LovB)^{44, 45} have shown to catalyze a [4+2] cycloaddition, they turned out to be multi-

functional enzymes. Thus, conclusive evidence for a naturally occurring Diels-Alderase is still lacking.^{37, 38, 39, 40}

SpnF, the enzyme which catalyzes the [4+2] cycloaddition in the biosynthesis of spinosyn A, has attracted significant interest as a real Diels-Alderase. For this interesting [4+2] cycloaddition by SpnF, three possible mechanisms have been suggested, the Diels-Alder reaction mechanism, the ionic rearrangement mechanism, and the biradical rearrangement mechanism. In order to distinguish among these three mechanisms, experiments to measure the secondary kinetic isotope effects were designed, and mechanistic probes containing deuterium at appropriate reaction centers were prepared through chemoenzymatic syntheses. These include a C4-D, a C7-D, a C11-D, and a C12-D analog. So far, the ionic rearrangement mechanism has been disproven, based on the results of the kinetic isotope effects studies using the C4-D and C7-D analogs. Additional experiments in progress using the C11-D and C12-D analogs will provide more details about the SpnF-catalyzed [4+2] cycloaddition in the future.

Another interesting question concerning the SpnF reaction is the way it accelerates the [4+2] cycloaddition of SpnF substrate into SpnF product in terms of thermokinetics and thermodynamics. Two hypotheses have been proposed. The SpnF catalysis may be facilitated either by an entropic preorganization or an enthalpic transition state stabilization during the enzymatic reaction. To measure the relative rate enhancements¹³¹ due to structural perturbations, three mechanistic probes were designed: namely, the Linear analog, the C13-14 Unc analog, and the C2-3 Unc analog. So far, the Linear analog and C13-14 Unc analog didn't show any turnover activity under either

non-enzymatic or enzymatic conditions, resulting in no further progress concerning determination of relative rate enhancement. The C13-14 Unc analog shows inhibition of SpnF, probably by competing with SpnF natural substrate for the active site in SpnF, while the Linear analog does not inhibit the SpnF reaction. In spite of the limited experimental results, it is proposed that SpnF may accommodate the macrolactone structure as its adequate substrate rather than the linear structure. Additional experiments using the C2-3 Unc analog are expected to expand our understanding of SpnF.

It is hard to draw any conclusion about the mechanism and intrinsic properties of SpnF catalysis based on the results available at this stage. Additional experimental data on SpnF reaction are being collected and will provide more insights into the mechanism and intrinsic properties of this intriguing enzyme.

Chapter 3. Mechanistic Investigation of SpnL-Catalyzed Cyclization In the Biosynthesis of Spinosyn A

3.1. INTRODUCTION

SpnL-catalyzed cyclization is a key reaction to complete the formation of a perhydro-*as*-indacene core in the biosynthesis of spinosyn A (**Figure 3-1**).^{20, 21, 22} Specifically, it is the point where a new C-C bond is formed between C-3 and C-14 to produce a cyclopentene moiety with a well controlled stereospecificity.

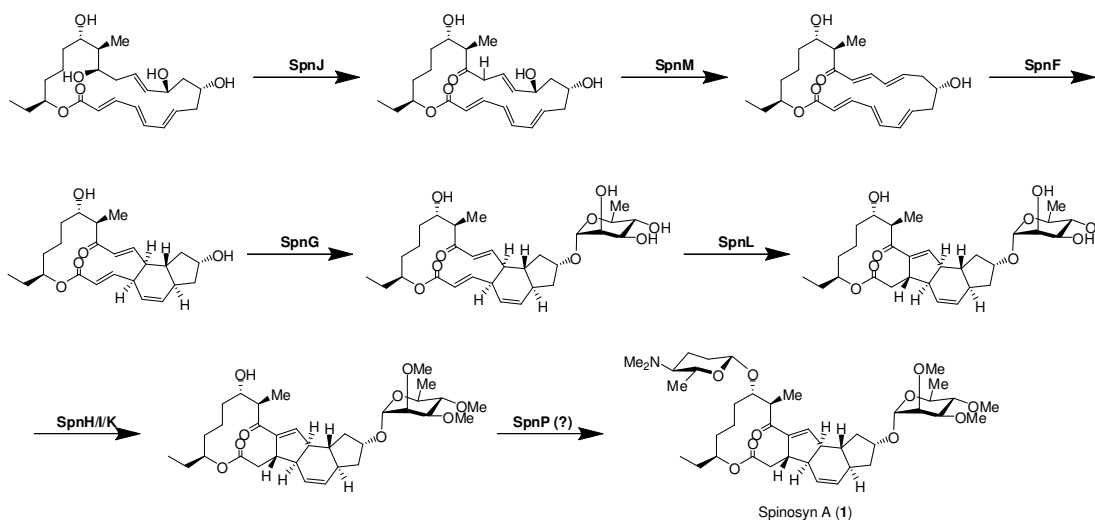


Figure 3-1. Established biosynthetic pathway of spinosyn A (1)

Two suggested mechanisms for SpnL are the Rauhut-Currier type mechanism and the Michael addition mechanism (**Figure 3-2**).^{29, 30, 31, 132} The Rauhut-Currier reaction describes the dimerization or isomerization of alkenes activated by adjacent to an electron-withdrawing functional group such as ketone, ester, or nitrile, in the presence of an organophosphine of the type R_3P as a nucleophile.^{29, 30} In the SpnL-reaction, one

component is the alkene at C-13 and C-14, which is adjacent to an electron-withdrawing ketone, and the other component the alkene at C-2 and C-3 connected to an electron-withdrawing ester. The Rauhut-Currier type mechanism of the SpnL reaction is believed to be initiated by the addition of a nucleophile such as cysteine or lysine in SpnL to the C-13 position of its substrate to produce an enolate intermediate, which may be stabilized by a positively charged residue or metal ion, such as magnesium. The following formation of the C-C bond between C-3 and C-14 occurs through a Michael addition, followed by a protonation at the C-2 position. Finally, the nucleophile bound to the C-13 position is released in a 1,2-elimination triggered by the deprotonation at the C-14 position. During the Rauhut-Currier type mechanism, the sp^2 -hybridized carbon at C-13 undergoes two rounds of rehybridization to sp^3 by nucleophilic addition, and then back to sp^2 by release of the nucleophile. Of note, if the nucleophilic amino acid residue of SpnL can be made irreversibly bound to the substrate, SpnL's enzymatic activity would be expected to be shut down, resulting in a suicide inhibition.

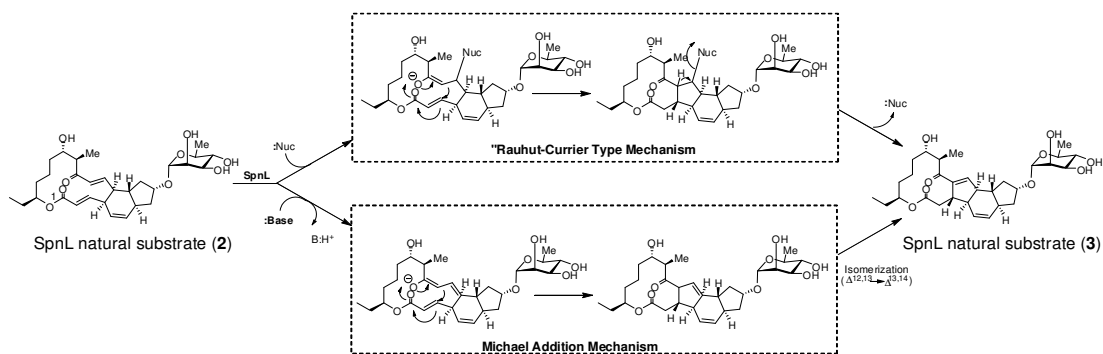


Figure 3-2. Plausible mechanisms for SpnL-catalyzed cyclization in the biosynthesis of spinosyn A

Another conceivable mechanism for SpnL-catalyzed cyclization is simply a Michael addition initiated by deprotonation at the C-12 position.³¹ The Michael addition

is defined as the organic reaction in which a nucleophilic addition of a carbanion to an α,β -unsaturated carbonyl moiety produces a 1,5-diketo-containing moiety. It is proposed that at the initial stage of the SpnL reaction, deprotonation of an acidic proton (allylic proton) at the C-12 position leads to the production of a long conjugated enolate, which may be stabilized by a positively charged residue or a metal ion. The C-C bond is subsequently formed between C-13 and C-14, followed by protonation at the C-2 position. Finally, the desired cyclopentene is produced through the isomerization by deprotonation at C-14 and protonation of C-12. While the sp^2 -hybridized carbon at the C-13 position undergoes the rehybridization to sp^3 through the Rauhut-Currier type mechanisms, sp^2 -hybridization of C-13 don't rehybridize in the Michael addition mechanism. Rather, the C-H bond breaking at the C-12 position in the first stage is more significant in terms of the kinetic isotope effect.

In other word, the only difference between the two proposed mechanisms is the way they activate the conjugated enone component of C-12 to C-15-ketone. The Rauhut-Currier mechanism utilizes a nucleophilic attack, with an amino acid residue as the nucleophile, at the C-13 position, whereas the Michael addition mechanism employs a deprotonation at C-12 position.^{29, 30, 31} Several mechanistic probes were designed to distinguish between these two mechanisms, including the C12-D, C13-D, and C13-F analogs (**Figure 3-3**),¹⁵¹ of which the two isotopologs (**4** and **5**) are used for the study of the kinetic isotope effect and the fluoride-containing analog (**6**) is used for the study of SpnL-covalent modification by suicide inhibition (mechanism-based inhibition).

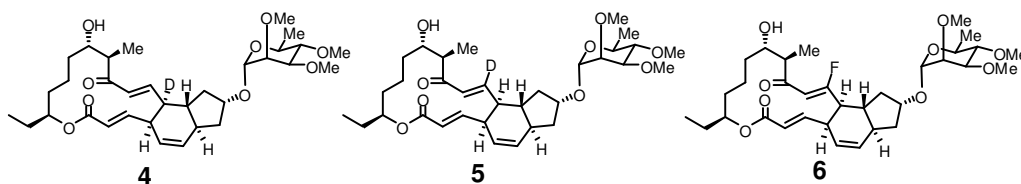


Figure 3-3. Mechanistic probes for SpnL-catalyzed cyclization (C12-D, C13-D, and C13-F analogs)

Through the Rauhut-Currier type mechanism, SpnL-catalyzed cyclization is prompted by nucleophilic addition, resulting in the rehybridization of the carbon at the C-13 position from sp^2 hybrid to sp^3 hybrid, which should give an inverse α -secondary kinetic isotope effect.⁵⁸ The sp^2 hybridization of the carbon at C-12 is unaffected throughout the reaction, resulting in a unity kinetic isotope effect. Alternatively, if the SpnL reaction proceeds via the Michael addition mechanism and undergoes C-H bond breaking at the C-12 position, a primary kinetic isotope effect would be observed for mechanistic probe **4**. The sp^2 hybridization at C-13 is unchanged during the reaction and an unity kinetic isotope effect for mechanistic probe **5** is expected. Therefore, a kinetic isotope effect study, using two deuterium-containing isotopologs, C12-D and C13-D analog, will give valuable information which can be used to distinguish between these two plausible mechanisms (**Figure 3-4**).

	Rauhut-Currier type mechanism	Michael addition mechanism
C12-D analog	Unity KIE	Primary KIE
C13-D analog	Inverse secondary KIE	Unity KIE

Figure 3-4. The expected kinetic isotope effect for C12-D and C13-D analogs during SpnL reaction

A mechanistic probe, C13-F analog, was also designed as a mechanism-based inhibitor to form a covalent adduct with SpnL as a mechanism-based inhibitor, assuming that the SpnL-catalyzed cyclization undergoes the Rauhut-Currier type mechanism

(Figure 3-5).¹⁵² However, there is a possibility that a C13-F containing turnover product may be produced no matter which mechanism the SpnL reaction follows.

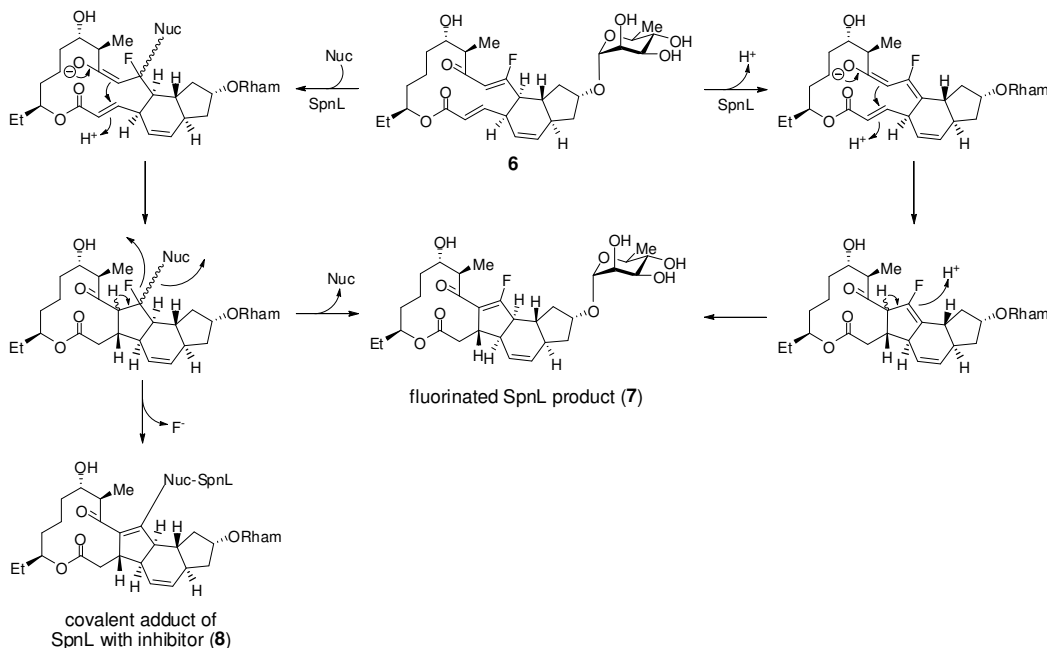


Figure 3-5. Proposed mechanism for SpnL reaction with C13-F analog through the Rauhut-Currier type mechanisms (left) and Michael addition mechanism (right).

Curiously, SpnF and SpnL show high sequence homology to *S*-adenosyl-L-methionine (SAM) dependent methyltransferases even though their functions in the biosynthesis of spinosyn A are not related to a methyl transfer reaction but rather a cycloaddition and cyclization reaction, respectively.^{15, 19, 151} Thus, a question arose about the possible function of SAM in the catalytic activity of SpnF and SpnL. Biochemical approaches have been used to characterize the relationship of SAM with SpnF and SpnL.

The purpose of Chapter 3 is to differentiate the reaction mechanisms between the Rauhut-Currier type mechanism and Michael addition mechanism using the mechanistic probes, C12-D, C13-D, and C13-F analogs, and to study SpnF and SpnL dependency on

SAM. First, measurement of the kinetic isotope effect is conducted with the C12-D and C13-D analogs. Second, if C13-F analog is covalently bound to SpnL, the Rauhut-Currier type mechanism is more likely. However, if the C13-F containing turnover product is isolated, one cannot distinguish the Rauhut-Currier mechanism from the Michael addition mechanism. Additionally, several biochemical experiments related to SpnL are presented in this Chapter, such as the activity assay to determine SAM dependency and the activity of several SpnL mutants. On-going biochemical experiments with SpnF and SpnL reaction will further verify the reaction mechanism and characterize the enzymes' relationship with SAM in near future.

3.2. EXPERIMENTAL PROCEDURES

3.2.1. Materials and Equipment

All chemicals were purchased from Sigma-Aldrich (St. Louis, MO, USA), Fisher Scientific (Pittsburgh, PA, USA), Tokyo Chemical Industry (TCI; Boston, MA, USA), Acros (Geel, Belgium), Alfar Aesar (Ward Hill, Ma, USA) and/or Chem-Impex (Wood Dale, IL, USA), and used without further purification unless otherwise specified. *Escherichia coli* DH5 α cells were obtained from Bethesda Research Laboratories (Muskegon, MI). The vector pEt28b(+) and enzyme KOD DNA polymerase were purchased from Novagen (Madison, WI, USA). DNA modifying enzymes (for restriction digestion and ligation), PCR primers, and the overexpression host *E. coli* BL21 star (DE3) were acquired from Invitrogen (Carlsbad, CA, USA) and New England Biolabs (NEB; Beverly, MA, USA). LB medium is a product of Difco (Detroit, MI, USA) or

Fisher Scientific, and pre-stained protein markers are products of NEB. Ni-NTA agarose and kits for DNA gel extraction and spin miniprep were obtained from Qiagen (Valencia, CA, USA). All reagents for SDS-PAGE and Amicon YM-10 filtration products were purchased from Bio-Rad (Hercules, CA, USA) and Millipore (Billerica, MA, USA), respectively. Analytical thin layer chromatography (TLC) was carried out on pre-coated TLC glass plates (Silica gel, Grade 60, F₂₅₄, 0.25 mm layer thickness) obtained from EMD Chemicals (Madison, WI, USA). Flash column chromatography was performed (230-400 mesh, Grade 60) by elution with the specified solvents, using materials from Sorbent Technologies (Atlanta, GA, USA) or Silicycle (Quebec City, Canada). Protein concentrations were determined by Bradford assay using bovine serum albumin as the standard, or measured by nanodrop, ND-1000 UV-VIS spectrophotometer from NanoDrop technologies (Wilmington, DE, USA). The relative molecular mass and purity of enzyme samples were determined using SDS-polyacrylamide gel electrophoresis as described. The general methods and protocols for recombinant DNA manipulations are as described by Sanbrook and Russell. DNA sequencing was performed by the Core Facilities in the Institute of Cellular and Molecular Biology of the University of Texas at Austin. NMR spectra were acquired on a Varian Unity Inova 500 or 600 MHz spectrometer, housed in the NMR Facility of the Department of Chemistry and Biochemistry in the University of Texas at Austin. The Mass analyses were carried out at the Mass Spectrometry and Proteomics Facility of the Department of Chemistry and Biochemistry in the University of Texas at Austin.

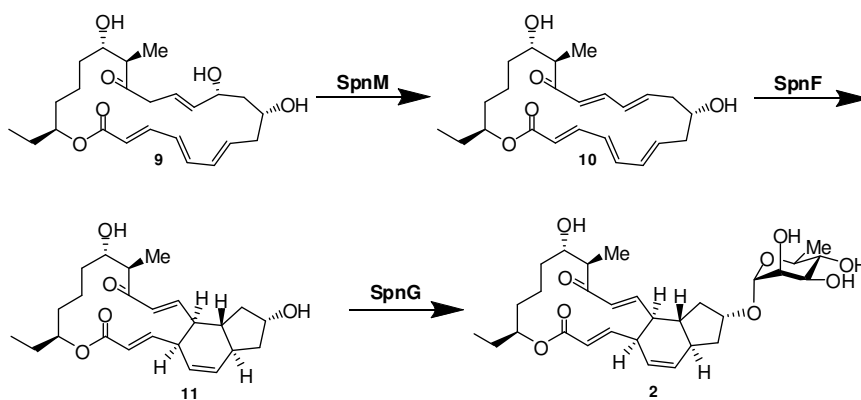
3.2.2. Preparation of Enzymes

Cloning of *SpnJ*, *SpnM*, and *SpnF*, and the expression and purification of their products have already been reported.

3.2.3. Synthesis of the SpnL Natural Substrates

A. Enzymatic conversions: The overall scheme of the enzymatic conversions is shown in

Scheme 3-1.



Scheme 3-1. Preparation of SpnL natural substrate

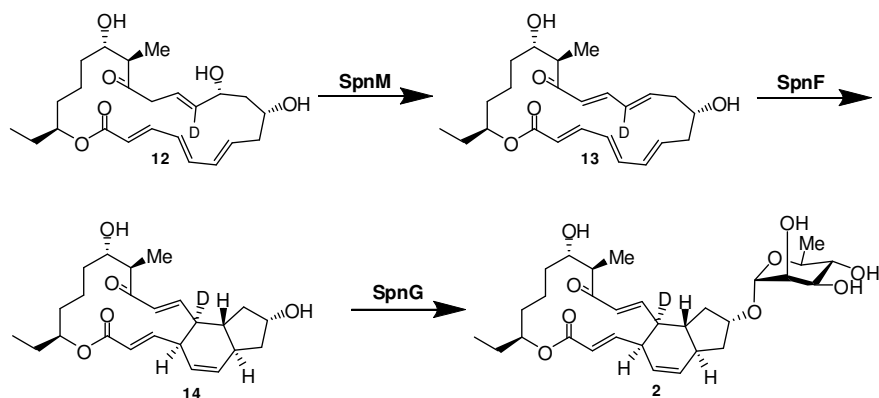
SpnG natural substrate (11): A solution containing SpnM natural substrate (**3**; 1.4 mg, 0.4 mM) in pH 8.0 Tris buffer (50 mM) was incubated with SpnM (10 μ M) and SpnF (30 μ M) at 30 °C with stirring. Through the incubation, the reaction was monitored by HPLC using a 4 x 250 mm Econosil C18 column (Alltech). Product was detected by absorbance at 254 nm, and the column eluted at 1 mL/min with water (A) and acetonitrile (B) using the following gradient. Initially 30% B, concentration of B was raised linearly to 45% over 30 min, then increased 80% linearly over 3 min, and finally decreased to 30% linearly over 3 min. After incubation for 6 hr, at which point the reaction was complete, the reaction mixture was directly filtered through a YM-10 membrane filter by centrifugation at 4,000 rpm for 40 min. The clear filtrate was purified by semi-

preparative HPLC using a 10 x 250 mm Econosil C18 column (Alltech). The column was eluted at 4 mL/min with water (A) and acetonitrile (B) using the same gradient as that of the above analytic HPLC. Collected fractions were pooled, extracted with ethylacetate (50 mL x 3 times), dried over an anhydrous sodium sulfate, and concentrated under reduced pressure to afford the target compound (1.0 mg, 72%). All spectral data was identical to the literature reference.

SpnL natural substrate (2): SpnG (80 μ M) was added to a solution containing SpnG natural substrate (**11**; 2.4 mg, 0.85 mM) and TDP-L-rhamnose (4.0 mg, 1.07 mM) in magnesium chloride (5 mM) and pH 8.0 Tris buffer (50 mM) at 30 °C with stirring. Through the incubation, the reaction was monitored by HPLC using a 4 x 250 mm Econosil C18 column (Alltech). The product was detected by absorbance at 254 nm, and column eluted at 1 mL/min with water (A) and acetonitrile (B) using the following gradient. Initially the solution was 30% B, then raised linearly to 45% over 30 min, further raised to 80% linearly over 3 min, and finally decreased linearly to 30% over 3 min. After incubation for 1.5 hr, at which point the reaction had completed, the mixture was directly filtered through a YM-10 membrane filter by centrifugation at 4,000 rpm for 40 min. The clear filtrate was purified by semi-preparative HPLC using a 10 x 250 mm Econosil C18 column (Alltech). The column was eluted at 4 mL/min with water (A) and acetonitrile (B) using the same gradient as the above analytic HPLC. Collected fractions were pooled, extracted with ethylacetate (50 mL x 3 times), dried over an anhydrous sodium sulfate, and concentrated under reduced pressure to afford the target compound (2.0 mg, 62%). All spectral data was identical to the literature reference.

3.2.4. Synthesis of the [C12-²H] SpnL Substrate Analog

A. Enzymatic conversions: The overall scheme for enzymatic conversions is shown in **Scheme 3-2**.



Scheme 3-2. Preparation of [C12-²H] SpnL substrate analog

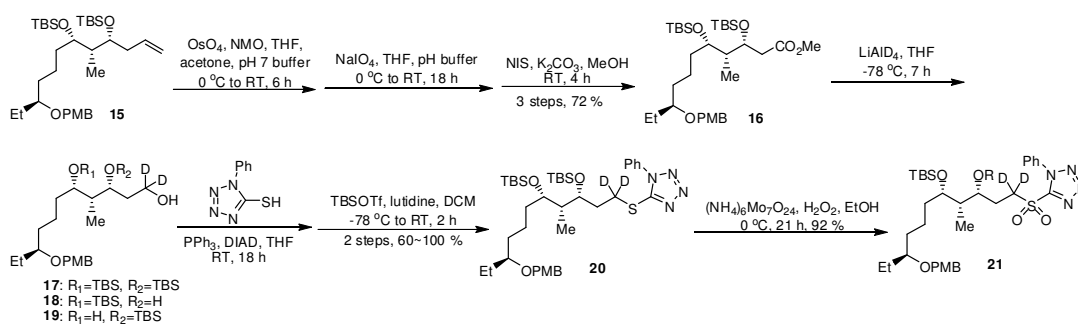
[C12-²H] SpnL substrate analog (4): [C12-²H] SpnG substrate analog (**14**) was prepared following the same procedure as compound (**11**) using [C12-²H] SpnM substrate analog. [C12-²H] SpnG substrate analog was prepared following the same procedure as compound (**2**) using [C12-²H] SpnG substrate analog (**14**) with a yield of 38% for 2 steps.

¹H NMR (DMSO-d₆, 500 MHz) δ (ppm) 6.76 (d, 1H, J = 16.6 Hz, 13-H), 6.47 (dd, 1H, J = 9.5, 15.5 Hz, 3-H), 6.12 (d, 1H, J = 16.6 Hz, 14-H), 5.93 (d, 1H, J = 9.7 Hz, 6-H), 5.74 (d, 1H, J = 15.5 Hz, 2-H), 5.37 (dt, 1H, J = 3.0, 9.7 Hz, 7-H), 4.75-4.70 (m, 1H, 21-H), 4.57 (d, 1H, J = 1.3 Hz, 1'-H), 4.31-4.26 (m, 1H, 9-H), 3.52-3.50 (m, 1H, 20-H), 3.41-3.26 (m, 4H, 4-H, 17-H, 3'-H, 4'-H), 3.18-3.13 (m, 1H, 5'-H), 2.67-2.62 (m, 1H, 16-H), 2.46-2.41 (m, 1H, 11-H), 2.18-2.12 (m, 1H, 7-H), 1.84-1.13 (m, 12H, 8-Hs+10-Hs+18-Hs+19-Hs+20-Hs+22-Hs), 1.11 (d, 3H, J = 6.2 Hz, 6'-Hs), 1.05 (d, 3H, J = 6.8

Hz, 16-CH₃), 0.79 (t, 3H, J = 7.4 Hz, 23-Hs); ¹³C NMR (DMSO-d₆, 125 MHz) δ (ppm) 202.70, 164.77, 148.22, 147.42, 130.71, 129.07, 127.98, 122.00, 98.62, 75.85, 74.52, 72.53, 72.04, 70.79, 70.63, 68.56, 63.06, 49.79, 41.82, 41.77, 37.08, 36.07, 35.41, 31.79, 28.97, 26.64, 21.69, 17.86, 14.53, 9.82; HRMS (ESI, positive) *m/z* for C₃₀H₄₃DO₉ [M+Na]⁺: calcd 572.2940, found: 572.2939.

3.2.5. Synthesis of the [C13-²H] SpnL Substrate Analog

A. Synthesis of Fragment A: The overall synthetic scheme is shown in **Scheme 3-3**.



Scheme 3-3. Preparation of fragment A in the synthesis of [C13-²H] substrate analog

(3R,4R,5S,9S)-methyl 3,5-bis(tert-butyl dimethylsilyloxy)-9-(4-methoxybenzyloxy)-4-methylundecanoate (16): 1) Allyl compound (**15**; 3.9 g, 6.74 mmol) was dissolved in a solution of THF (20 mL), acetone (20 mL), and pH 7 buffer (20 mL), and cooled to 0 °C with stirring for 10 min. Osmium tetroxide (86 mg, 0.34 mmol) and N-methylmorpholine N-oxide (1.18 g, 10.11 mmol) were subsequently added into the reaction mixture, which was allowed to stir at room temperature for 24 hr. The reaction mixture was quenched with the subsequent addition of aqueous 10% sodium thiosulfate solution (20 mL) and pH 7 buffer (10 mL) at room temperature. After stirring at room temperature for 30 min, the aqueous phase was extracted with ethyl acetate (30 mL x 3 times). The combined

organic phases were washed with brine (50 mL), dried over an anhydrous sodium sulfate pad, and concentrated to give a pale yellow residue, which was subjected to the next step without further purification. 2) This residue was dissolved in a solution of THF (150 mL) and pH 7 buffer (60 mL) at room temperature. Sodium (meta)periodate (4.76 g, 22.24 mmol) was added portionwise into the reaction mixture for 1 hr at 0 °C, followed by stirring at room temperature for 24 hr. The suspension was filtered through a filter paper, and the organic phase of the filtrate was then separated by extracting the aqueous phases with ethyl acetate (30 mL x 3 times). The combined organic phases were washed with brine (30 mL), dried over an anhydrous sodium sulfate pad, and concentrated by rotary-evaporation. The resulting residue was used directly for the next step without further purification. 3) N-iodosuccinimide (NIS; 3.79 g, 16.85 mmol) and potassium carbonate (2.33 g, 16.85 mol) were added to a solution of the aldehyde from the previous step in anhydrous methanol (40 mL) at room temperature. The reaction mixture was stirred at room temperature for 38 hr, and quenched with saturated aqueous sodium thiosulfate solution (200 mL). The aqueous phase was extracted with dichloromethane (40 mL x 3 times), and the collected organic phases were dried over an anhydrous sodium sulfate pad, filtered and concentrated under reduced pressure. The resulting residue was subjected to flash column chromatography on silica gel. The target compound was eluted with 3% to 5% EtOAc/Hexane solution (1.94 g, 47%).

¹H NMR (CDCl₃, 400 MHz) δ (ppm) 7.25 (d, 2H, *J* = 7.2 Hz, PhH of PMB), 6.84 (d, 2H, *J* = 7.2 Hz, PhH of PMB), 4.42-4.41 (m, 2H, CH₂ of PMB), 4.15-4.11 (m, 1H, 3-CH), 3.77-3.75 (m, 4H, 5-CH and OCH₃ of PMB), 3.61 (s, 3H, OMe of CO₂Me), 3.30-

3.26 (m, 1H, 9-CH), 2.55-2.45 (m, 2H, 2-CH₂), 1.69-1.23 (m, 8H, 6-CH₂+7-CH₂+8-CH₂+10-CH₂), 0.92-0.81 (m, 24H, CH₃ of ^tBu of TBS, 11-CH₃, 4-CH₃), 0.06-(-0.02) (m, 12H, CH₃ of TBS); ¹³C NMR (CDCl₃, 100 MHz) δ 172.47 (C=O of COOMe), 158.99 (Ph of PMB), 131.25 (Ph of PMB), 129.15 (Ph of PMB), 113.67 (Ph of PMB), 79.80 (C-10), 72.17 (C-6), 70.65 (C-4), 70.44 (CH₂ of PMB), 55.24 (OCH₃ of PMB), 51.37 (OCH₃ of COOMe), 41.93, 40.31, 35.04 (C-5), 33.86 (C-7), 26.22 (C-9), 25.97 (CH₃ of ^tBu of TBS), 25.83 (CH₃ of ^tBu of TBS), 20.88 (C-8), 18.10 (Me₃C-Si), 18.02 (Me₃C-Si), 9.98, 9.49, -3.79 (CH₃ of TBS), -4.37 (CH₃ of TBS), -4.46 (CH₃ of TBS), -4.52 (CH₃ of TBS)(ppm) ; HRMS (ESI, positive) *m/z* for C₃₅H₆₆O₆Si₂ [M+Na]⁺: calcd 633.3977, found 633.3968.

(3R,4R,5S,9S)-3,5-bis(tert-butyldimethylsilyloxy)-9-(4-methoxybenzyloxy)-4-methylundecan-1-ol with di-deuteride at the C-1 position (17): Lithiumaluminum deuteride (180 mg, 4.30 mmol) was added to a solution of compound (**16**; 1.75 g, 2.86 mmol) in anhydrous diethyl ether (50 mL) portionwise over 5 min at 0 °C. The reaction mixture was then stirred at 0 °C for 30 min. After quenching with water (25 mL), the aqueous phase was extracted with diethyl ether (20 mL x 2 times). The combined organic phases were washed with brine (30 mL), dried over an anhydrous sodium sulfate, filtered, and concentrated under reduced pressure. The resulting residue was subjected to flash column chromatography on silica gel. The target compound was eluted with 10 % EtOAc/Hexanes (**17**; 82 mg, 0.14 mmol, 5%). A side product was also isolated (**18** and **19**; combined yield: 852 g, 1.81 mol, 63%) with 50% EtOAc/Hexane solution.

Compound **17**: ¹H NMR (CDCl₃, 400 MHz) δ (ppm) ; 7.24 (d, 2H, *J* = 8.4 Hz,

PhH of PMB), 6.85 (d, 2H, $J = 8.4$ Hz, PhH of PMB), 4.44 (d, 1H, $J = 11.2$ Hz, CH₂ of PMB), 4.37 (d, 1H, $J = 11.2$ Hz, CH₂ of PMB) 3.88-3.83 (m, 1H, 3-CH), 3.77 (s, 3H, OCH₃ of PMB), 3.69-3.65 (m, 1H, 5-CH), 3.28-3.25 (m, 1H, 9-CH), 1.87-1.14 (m, 11H, 2-CH₂+4-CH+6-CH₂+7-CH₂+8-CH₂+10-CH₂), 0.92-0.84 (m, 24H, CH₃ of ^tBu of TBS, 11-CH₃, 4-CH₃), 0.07-(-0.01) (m, 12H, CH₃ of TBS); ¹³C NMR (CDCl₃, 100MHz) δ (ppm) ; HRMS (ESI, positive) m/z for C₃₂H₆₀D₂O₅Si₂ [M+Na]⁺: calcd 607.4154, found 607.4169.

Mono-protected product **18** and **19**: HRMS (ESI, positive) m/z for C₂₆H₄₆D₂O₅Si₂ [M+Na]⁺: calcd 493.3289, found 493.3301.

5-((3R,4R,5S,9S)-3,5-bis(tert-butylidimethylsilyloxy)-9-(4-methoxybenzyloxy)-4-methylundecylthio)-1-phenyl-1H-tetrazole with di-deuteride at C-1 position (20):

Method A: A solution of the alcohol (**17**, 142 mg, 0.24 mmol), 1-phenyl-1*H*-tetrazole-5-thiol (65 mg, 0.36 mmol), triphenylphosphine (96 mg, 0.36 mmol), and diisopropyl azodicarboxylate (DIAD; 74 mg, 0.36 mmol) in anhydrous THF (5 mL) was stirred at room temperature for 15 hr. The resulting yellow suspension was concentrated under reduced pressure and subjected directly to flash column chromatography. An intermediate was eluted with 10% EtOAc/Hexane (**20**, 203 mg, 0.27 mmol, quantitative).

Method B: 1) A solution of the mono-TBS protected products from the previous step (**18** and **19**; 852 mg, 1.81 mmol), 1-phenyl-1*H*-tetrazole-5-thiol (645 mg, 3.62 mmol), triphenylphosphine (475 mg, 1.81 mmol), and diisopropylazodicarboxylate (DIAD; 366 mg, 1.81 mmol) in anhydrous THF (15 mL) was stirred at room temperature for 15 hr. The resulting yellow suspension was concentrated under reduced pressure and subjected

directly to flash column chromatography, and the intermediate was eluted with 20% EtOAc/Hexane (1.03 g, 1.63 mmol). 2) TBSOTf (1.30 g, 4.90 mmol) was added to a solution of the above intermediate (1.03 g, 1.63 mmol) and 2,6-lutidine (0.88 g, 8.10 mmol) in anhydrous dichloromethane (20 mL) at -78 °C over 5 min. The reaction mixture was then slowly warmed to room temperature with stirring for 20 hr. After quenching with water (20 mL), the aqueous phase was extracted with dichloromethane (20 mL x 3 times). The collected organic phases were dried over an anhydrous sodium sulfate pad, filtered, and concentrated under reduced pressure. The resulting residue was subjected to flash column chromatography. The target compound was eluted with 10% EtOAc/Hexane (729 mg, 0.98 mmol, 54% for 2 steps).

¹H NMR (CDCl₃, 400 MHz) δ (ppm) ; 7.56-7.50 (m, 5H, PhH), 7.24-7.22 (m, 2H, PhH of PMB), 6.85-6.81 (m, 2H, PhH of PMB), 4.43-4.39 (dd, 2H, *J* = 16.0, 11.2 Hz, CH₂ of PMB), 3.84-3.74 (m, 5H, OCH₃ of PMB, 3-CH, 5-CH), 3.29-3.26 (9-CH), 2.14 (dd, 1H, *J* = 14.0, 4.8 Hz, 2-CH₂), 1.95 (dd, 1H, *J* = 14.0, 4.8 Hz, 2-CH₂), 1.68-1.24 (m, 8H, 6-CH₂+7-CH₂+8-CH₂+10-CH₂), 0.92-0.79 (m, 24H, CH₃ of ^tBu of TBS, 11-CH₃, 4-CH₃), 0.03-(-0.02) (m, 12H, CH₃ of TBS); ¹³C NMR (CDCl₃, 100 MHz) δ (ppm) 158.92(Ph(C) of PMB), 154.21 (C=N of tetrazole), 133.69 (Ph(C) of PMB), 131.14 (Ph(C) of Ph), 129.94 (Ph(C) of PMB), 129.68 (Ph(C) of Ph), 129.18(Ph(C) of Ph), 123.70 (Ph(C) of Ph), 113.61 (Ph(C) of PMB), 79.65 (C-10), 72.31 (C-4), 71.99 (C-6), 70.39 (CH₂ of PMB), 55.16 (OCH₃ of PMB), 40.61 (C-11), 35.34 (C-5), 33.77 (C-7), 33.59 (C-3), 26.20 (C-9), 25.90 (CH₃ of ^tBu of TBS), 25.87 (CH₃ of ^tBu of TBS), 25.71 (C-2), 21.13 (C-8), 18.04 (Me₃(C)-Si), 9.70 (C-12), 9.46 (5-CH₃), -3.71 (CH₃ of TBS), -

4.15 (CH₃ of TBS), -4.43 (CH₃ of TBS), -4.47 (CH₃ of TBS); HRMS (ESI, positive) *m/z* C₃₉H₆₄D₂N₄O₄SSi₂ for [M+H]⁺: calcd 745.4542, found 745.4553.

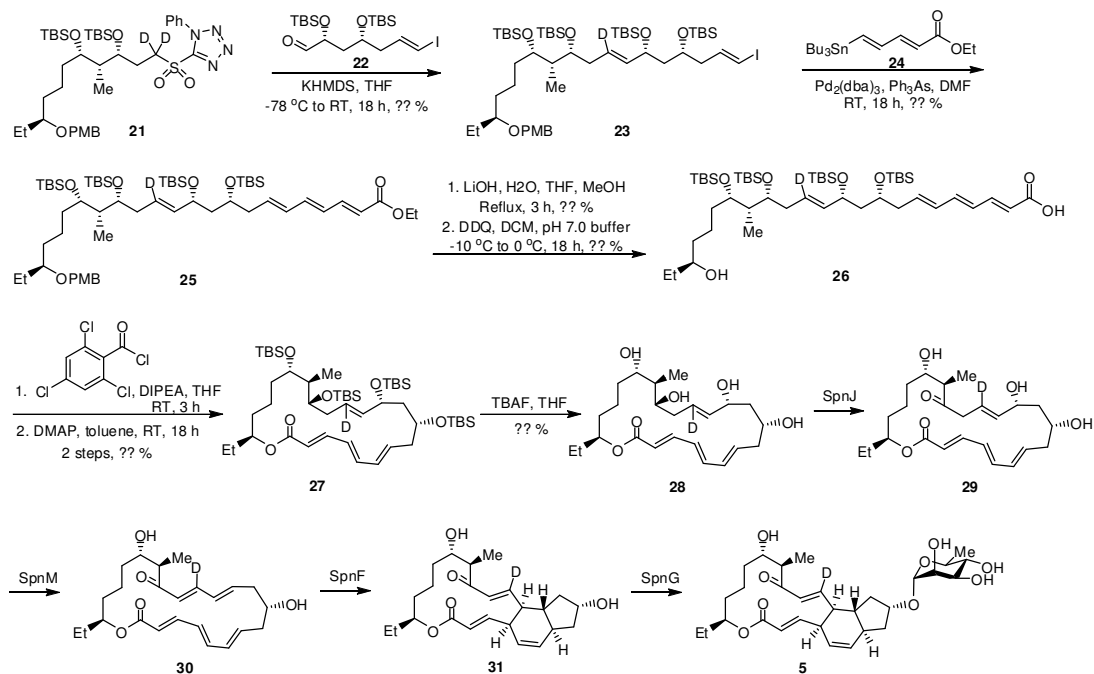
5-((3R,4R,5S,9S)-3,5-bis(tert-butyl dimethylsilyloxy)-9-(4-methoxybenzyloxy)-4-methylundecylsulfonyl)-1-phenyl-1H-tetrazole with di-deuteride at C-1 position (21)

: A solution of ammonium heptamolybdate tetrahydrate (302 mg, 0.24 mmol) in 30% hydrogen peroxide (1.17 mL) was added to a solution of thioether compound (**20**; 720 mg, 0.98 mmol) in ethanol (25 mL) at 0 °C. The reaction mixture was stirred at 0 °C for 21 hr, and the suspension was then filtered through a filter paper. The resulting filtrate was evaporated under reduced pressure, and partitioned between ethyl acetate (20 mL x 2 times) and brine. The combined organic phases were dried over an anhydrous sodium sulfate, filtered, and concentrated under reduced pressure. The resulting residue was purified with flash column chromatography on silica gel. The target compound was eluted with 10% EtOAc/Hexane (697 mg, 0.90 mmol, 92%).

¹H NMR (DMSO-d₆, 400 MHz) δ (ppm) 7.69-7.66 (m, 2H, PhH), 7.60-7.55 (m, 3H, PhH), 7.23 (d, 2H, *J* = 8.0 Hz, PhH of PMB), 6.83 (d, 2H, *J* = 8.4 Hz, PhH of PMB), 4.45-4.36 (m, 2H, CH₂ of PMB), 3.88-3.76 (m, 5H, OCH₃ of PMB, 3-CH, 5-CH), 3.30-3.27 (m, 1H, 9-CH), 2.25 (dd, 1H, *J* = 13.6 Hz, 4 Hz, 2-CH₂), 2.12 (dd, 1H, *J* = 13.6 Hz, 4.4 Hz, 2-CH₂), 1.59-1.24 (m, 9H, 4-CH+6-CH₂+7-CH₂+8-CH₂+10-CH₂), 0.90-0.82 (m, 24H, CH₃ of ^tBu of TBS+12-CH₃+4-CH₃), 0.07-0.00 (m, 12H, CH₃ of TBS); ¹³C NMR (DMSO-d₆, 100MHz) δ (ppm) 158.96 (Ph(C) of PMB), 153.39 (C=N of tetrazole), 133.00 (Ph(C) of PMB), 131.32 (Ph(C) of Ph), 131.08 (Ph(C) of PMB), 129.63 (Ph(C) of Ph), 129.22 (Ph(C) of PMB), 124.91 (Ph(C) of Ph), 113.64 (Ph(C) of PMB), 79.55 (C-

10), 71.58 (C-4), 71.44 (C-6), 70.43 (CH₂ of PMB), 55.16 (OCH₃ of PMB), 40.58 (C-11), 35.37 (C-5), 33.65 (C-7), 26.20 (C-9), 26.03, 25.84 (CH₃ of ^tBu of TBS), 25.83 (CH₃ of ^tBu of TBS), 21.37 (C-8), 18.04 (Me₃(C)-Si), 18.00(Me₃(C)-Si), 9.56 (C-12), 9.45 (5-CH₃), -3.60 (CH₃ of TBS), -4.33 (CH₃ of TBS), -4.54 (CH₃ of TBS), -4.58 (CH₃ of TBS); HRMS (ESI, positive) *m/z* for C₃₉H₆₄D₂N₄O₆SSi₂ [M+H]⁺: calcd 777.4440, found 777.4440.

B. Synthesis of [C13-²H] SpnL Substrate Analog by Coupling reactions and enzymatic conversions: The overall synthetic scheme is pictured in **Scheme 3-4**.



Scheme 3-4. Preparation of [C13-²H] SpnL substrate analog

(1E,4R,6R,7E,10R,11R,12S,16S)-4,6,10,12-Tetrakis(tert-butyldimethylsilyloxy)-11-methyl-16-(4-methoxybenzyloxy)octadeca-1,7-diene with mono-deuteride at C-8 position (23): Potassium hexamethyldisilazide (KHMDs; 0.5 M in toluene, 2.0 mL, 1.00

mmol) was added dropwise to a solution of fragment A (**21**) (706 mg, 0.91 mmol) in THF (20 mL) at -78 °C over 10 min. The reaction mixture was stirred at -78 °C for 30 min, at which time fragment B (**22**) (546 mg, 1.09 mmol) in THF (10 mL) was added to the resulting yellow solution at -78 °C over 30 min. The reaction temperature was slowly raised to room temperature, and the reaction mixture was further stirred at room temperature for 19 hr. The mixture was then poured into a saturated aqueous sodium bicarbonate solution (20 mL). After stirring for 10 min, the aqueous phase was extracted with diethyl ether (30 mL × 2 times). The combined organic phases were then washed with brine, dried over an anhydrous sodium sulfate pad, filtered, and concentrated under reduced pressure. The residue was subjected to flash column chromatography. The target compound was eluted with 2% EtOAc/Hexanes (827 mg, 0.79 mmol, 87%).

¹H NMR (CDCl₃, 400 MHz) δ (ppm) 7.25-7.23 (m, 2H, PhH of PMB), 6.85-6.82 (m, 2H, PhH of PMB), 6.50-6.43 (m, 1H, 2-CH), 6.06-5.96 (ddt, J =26.4, 14.4, 1.2 Hz), 5.37 (d, 1H, 6.4 Hz, 7-CH), 4.41 (s, 2H, CH₂ of PMB), 4.10-4.06 (m, 1H, 6-CH), 3.77 (s, 3H, OCH₃ of PMB), 3.75-3.71 (m, 1H, 10-CH), 3.67-3.66 (m, 1H, 12-CH), 3.28-3.26 (m, 16-CH), 2.24-2.05 (m, 4H, 3-CH₂ and 9-CH₂), 1.81-1.23 (m, 11H, 5-CH₂, 11-CH, 13-CH₂, 14-CH₂, 15-CH₂ and 17-CH₂), 0.91-0.82 (m, 42H, 11-CH₃, 18-CH₃ and CH₃ of ^tBu of TBS), 0.07-(-0.02) (m, 24H, CH₃ of TBS); ¹³C NMR (CDCl₃, 100 MHz) δ 159.01(Ph(C) of PMB), 143.29 (C-2), 135.42 (C-7), 131.29(Ph(C) of PMB), 129.16(Ph(C) of PMB), 113.70(Ph(C) of PMB), 79.77 (C-16), 76.45 (C-1), 72.89 (C-12), 72.23 (C-10), 70.68(C-4), 70.45(CH₂ of PMB), 68.21, 55.25(OCH₃ of PMB), 46.02, 43.56, 43.46, 41.25 (C-11), 40.23 (C-5), 37.75, 35.39 (C-15), 33.90 (C-13), 26.24

(C-17), 25.97(CH₃ of ^tBu of TBS), 25.89(CH₃ of ^tBu of TBS), 25.85(CH₃ of ^tBu of TBS), 25.74(CH₃ of ^tBu of TBS), 21.28 (C-14), 18.13(Me₃(C)-Si), 18.01(Me₃(C)-Si), 9.51 (C-18), -3.74(CH₃ of TBS), -3.91(CH₃ of TBS), -4.26(CH₃ of TBS), -4.35(CH₃ of TBS), -4.43(CH₃ of TBS), -4.49(CH₃ of TBS), -4.61(CH₃ of TBS), -4.72 (CH₃ of TBS)(ppm) ; HRMS (ESI, positive) *m/z* for C₅₁H₉₈DIO₆Si₄ [M+Na]⁺: calcd 1070.5518, found 1070.5522.

(2E,4E,6E,9R,11R,12E,15R,16R,17S,21S)-Ethyl 9,11,15,17-Tetrakis(tert-butyltrimethylsilyloxy)-16-methyl-21-(4-methoxybenzyloxy)tricosanoate with mono-deuteride at 13-position (25):

Tris(dibenzylideneacetone) dipalladium (Pd₂(dba)₃; 36 mg, 0.04 mmol) and triphenylarsine (48 mg, 0.16 mmol) were added to a solution of vinyl iodide (**23**, 827 mg, 0.79 mmol) and fragment C (**24**) (491 mg, 1.18 mmol) in anhydrous *N,N*-dimethylformamide (15 mL) at room temperature. The reaction mixture was stirred for 19 hr at room temperature, at which time water (30 mL) was added. The reaction mixture was extracted with diethyl ether (25 mL × 2 times), and the resulting organic phases were washed with brine (20 mL), dried over an anhydrous sodium sulfate pad, filtered, and concentrated under reduced pressure. The residue was subjected to flash column chromatography. The target compound was eluted with 2% to 5% EtOAc/Hexane (602 mg, 0.58 mmol, 74%).

¹H NMR (CDCl₃, 400 MHz) δ (ppm);) 7.28-7.23 (m, 3H, 3-CH and PhH of PMB), 6.84 (d, 2H, *J* = 8.4 Hz, PhH of PMB), 6.50 (dd, 2H, *J* = 14.8 Hz, 10.4 Hz, 5-CH), 6.22-6.07 (m, 2H, 4-CH and 6-CH), 5.92-5.87 (m, 1H, 7-CH), 5.82 (d, 1H, *J* = 15.2 Hz, 2-CH), 5.37 (d, 1H, *J* = 6.8 Hz, 12-CH), 4.40 (s, 2H, CH₂ of PMB), 4.18 (q,

2H, $J = 7.2$ Hz, $\underline{\text{CH}_2\text{CH}_3}$ of OEt), 4.12-4.08 (m, 1H, 11-CH), 3.84-3.79 (m, 1H, 9-CH), 3.77 (s, 3H, OCH_3 of PMB), 3.74-3.70 (m, 1H, 15-CH), 3.68-3.64 (m, 1H, 17-CH), 3.28-3.24 (m, 1H, 21-CH), 2.37-2.32 (m, 1H, 8- CH_2), 2.23-2.18 (m, 3H, 14- CH_2 and 8- CH_2), 1.73-1.66 (m, 1H, 10- CH_2), 1.61-1.23 (m, 13H, 10- CH_2 , 16-CH, 18- CH_2 , 19- CH_2 , 20- CH_2 , 22- CH_2 and $\underline{\text{CH}_2\text{CH}_3}$ of OEt), 0.91-0.82 (m, 42H, 16- CH_3 , 23- CH_3 and CH_3 of ^tBu of TBS), 0.01--0.02 (m, 24H, CH_3 of TBS); ^{13}C NMR (CDCl_3 , 100 MHz) δ (ppm) 167.19 (1-C=O), 158.99(Ph(C) of PMB), 144.74 (C-3), 140.91 (C-5), 136.55 (C-7), 132.02 (C-6), 131.25(Ph(C) of PMB), 129.19(Ph(C) of PMB), 128.12 (C-4), 120.23 (C-2), 113.68(Ph(C) of PMB), 79.77 (C-21), 72.84 (C-17), 72.21 (C-9), 70.75, 70.45(CH_2 of PMB), 68.92, 60.20 (CH_2 of OEt), 55.25(OCH_3 of PMB), 46.12, 41.20, 40.74, 37.75, 35.38 (C-20), 33.88 (C-18), 26.22 (C-22), 25.96(CH_3 of ^tBu of TBS), 25.89(CH_3 of ^tBu of TBS), 25.85(CH_3 of ^tBu of TBS), 21.27 (C-19), 18.13(Me_3C -Si), 18.03(Me_3C -Si), 14.31 (CH_3 of OEt), 9.49 (C-23), -3.74(CH_3 of TBS), -3.94(CH_3 of TBS), -4.32(CH_3 of TBS), -4.39(CH_3 of TBS), -4.53(CH_3 of TBS), -4.75(CH_3 of TBS); HRMS (ESI, positive) m/z for $\text{C}_{58}\text{H}_{107}\text{DO}_8\text{Si}_4$ [$\text{M}+\text{Na}$] $^+$: calcd 1068.7076, found 1068.7096.

(2E,4E,6E,9R,11R,12E,15R,16R,17S,21S)-9,11,15,17-Tetrakis(tert-butyltrimethylsilyloxy)-21-hydroxy-16-methyltricoso-2,4,6,12-tetraenoic acid with mono-deuteride at 13-position (26): Lithium hydroxide (140 mg, 5.83 mg) was added to a solution of long-chain compound (**25**, 602 mg, 0.58 mmol) in a solution of THF (12 mL), methanol (12 mL), and water (12 mL) at room temperature. The reaction mixture was stirred under reflux for 3 hr, at which time volatile solvents were evaporated under reduced pressure. The pH of the aqueous solution was adjusted to approximately 7 by

addition of 1 N aqueous hydrochloric acid solution, and the mixture was extracted with ethyl acetate (20 mL \times 3 times). The organic extracts were pooled, dried over an anhydrous sodium sulfate, and concentrated under reduced pressure. The residue was subjected to flash column chromatography. The target carboxylic acid compound was eluted with 20% to 35% EtOAc/Hexane (483 mg, 0.47 mmol, 81%).

^1H NMR (CDCl_3 , 400 MHz) δ (ppm) 7.36 (dd, 1H, $J = 14.4$ Hz, 12.0 Hz, 3-CH), 7.25 (d, 2H, $J = 8.0$ Hz, PhH of PMB), 6.85 (d, 2H, $J = 8.4$ Hz, PhH of PMB), 6.55 (dd, $J = 14.0$, 11.2 Hz, 5-CH), 6.25-6.10 (m, 2H, 4-CH and 6-CH), 5.96-5.90 (m, 1H, 7-CH), 5.83 (d, 1H, $J = 15.6$ Hz, 2-CH), 5.39 (d, 1H, $J = 6.8$ Hz, 12-CH), 4.41 (s, 2H, CH_2 of PMB), 4.12-4.11 (m, 1H, 11-CH), 3.84-3.82 (m, 1H, 9-CH), 3.78 (s, 3H, OCH_3 of PMB), 3.76-3.73 (m, 1H, 15-CH), 3.68-3.66 (m, 1H, 17-CH), 3.29-3.28 (m, 1H, 21-CH), 2.39-2.36 (m, 1H, 8- CH_2), 2.25-2.23 (m, 3H, 14- CH_2 and 8- CH_2), 1.73-1.24 (m, 11H, 10- CH_2 , 16-CH, 18- CH_2 , 19- CH_2 , 20- CH_2 , 22- CH_2), 0.91-0.82 (m, 42H, 16- CH_3 , 23- CH_3 and CH_3 of ^tBu of TBS), 0.02-0.00 (m, 24H, CH_3 of TBS); ^{13}C NMR (CDCl_3 , 125 MHz) δ (ppm) 159.02(Ph(C) of PMB), 147.08 (C-3), 142.09(C-5), 137.51 (C-7), 135.49 (C-12), 131.94 (C-6), 131.29(Ph(C) of PMB), 129.19(Ph(C) of PMB), 127.86 (C-2), 118.84 (C-2), 113.71(Ph(C) of PMB), 79.79 (C-21), 72.89 (C-17), 72.26, 70.77, 70.46(CH_2 of PMB), 68.92, 55.25 (OCH_3 of PMB), 46.15, 44.36, 41.27, 40.77, 37.77, 35.41, 33.91, 33.17, 31.42, 29.69, 26.26 (C-22), 25.97(CH_3 of ^tBu of TBS), 25.91(CH_3 of ^tBu of TBS), 25.85(CH_3 of ^tBu of TBS), 21.30 (C-19), 18.17(Me_3C -Si), 18.14(Me_3C -Si), 18.04(Me_3C -Si), 9.50, -3.73(CH_3 of TBS), -3.76(CH_3 of TBS), -3.92(CH_3 of TBS), -4.26(CH_3 of TBS), -4.32(CH_3 of TBS), -4.37(CH_3 of TBS), -

4.51(CH₃ of TBS), -4.72(CH₃ of TBS); HRMS (ESI, positive) *m/z* for C₅₆H₁₀₃DO₉Si₄ [M+Na]⁺: calcd 1040.6763, found 1040.6747.

2) 2,3-Dichloro-5,6-dicyano-*p*-benzoquinone (DDQ; 269 mg, 1.19 mmol) was added to a solution of the carboxylic acid from the previous step (483 mg, 0.47 mmol) in dichloromethane (45 mL) and pH 7 phosphate buffer (5 mL) at 0 °C. The reaction mixture was stirred at 0 °C for 17 hr, at which time saturated aqueous ammonium chloride solution (20 mL) was added. The aqueous phase was extracted with dichloromethane (20 mL × 3 times). The combined organic phases were dried over an anhydrous sodium sulfate, and concentrated under reduced pressure. The residue was subjected to flash column chromatography. The target compound was eluted with 20% to 35% EtOAc/Hexanes (126 mg, 0.14 mmol, 30%).

¹H NMR (CDCl₃, 500 MHz) δ (ppm) 7.37 (dd, 1H, *J* = 15.1, 11.5 Hz, 3-CH), 6.57 (dd, 1H, *J* = 14.6, 11.0 Hz, 5-CH), 6.24 (dd, 1H, *J* = 14.6, 11.4 Hz, 4-CH), 6.16 (dd, 1H, *J* = 15.1, 11.0 Hz, 6-CH), 5.96 (quint, 1H, *J* = 7.5 Hz, 7-CH), 5.85 (d, 1H, *J* = 15.5 Hz, 2-CH), 5.41 (d, 1H, *J* = 6.5 Hz, 12-CH), 4.14 (br q, 1H, *J* = 7.0 Hz, 11-CH), 3.86-3.81 (m, 1H, 9-H), 3.75 (q, 1H, *J* = 5.5 Hz, 15-CH), 3.69 (q, 1H, *J* = 5.5 Hz, 1H, 17-CH), 3.53-3.49 (m, 1H, 21-H), 2.41-2.37 (m, 1H, 8-CH₂), 2.26-2.22 (m, 3H, 8-CH₂, 14-CH₂), 1.75-1.25 (m, 11H, 10-CH₂, 16-CH, 18-CH₂, 19-CH₂, 20-CH₂, 22-CH₂), 0.90-0.88 (m, 42H, 16-CH₃, 23-CH₃ and CH₃ of ^tBu of TBS), 0.06-0.02 (m, 24H, CH₃ of TBS); ¹³C NMR (CDCl₃, 125 MHz) δ (ppm) 171.21 (1-C=O), 147.03 (C-3), 142.04 (C-5), 137.38 (C-7), 132.00 (C-6), 127.91 (C-4), 119.03 (C-2), 73.08 (C-21), 72.63, 72.19, 70.82 (C-9), 68.97, 46.15, 40.82 (C-16), 40.65, 40.11, 37.57, 37.43, 35.71, 35.06, 30.12, 29.70, 27.84

(C-22), 26.84, 25.95(CH₃ of ^tBu of TBS), 25.93(CH₃ of ^tBu of TBS), 25.87(CH₃ of ^tBu of TBS), 21.33 (C-19), 18.19(Me₃(C)-Si), 18.16(Me₃(C)-Si), 18.12(Me₃(C)-Si), 18.05(Me₃(C)-Si), 9.88 (C-23), 9.32 (16-CH₃), -3.77(CH₃ of TBS), -3.82(CH₃ of TBS), -3.98(CH₃ of TBS), -4.29(CH₃ of TBS), -4.38(CH₃ of TBS), -4.59(CH₃ of TBS), -4.71(CH₃ of TBS); HRMS (ESI, positive) *m/z* for C₄₈H₉₅DO₇Si₄ [M+Na]⁺: calcd 920.6188, found 920.6159.

(3E,5E,7E,10R,12R,13E,16R,17R,18S,22S)-10,12,16,18-tetrakis(tert-butyltrimethylsilyloxy)-22-ethyl-17-methyloxacyclodocosa-3,5,7,13-tetraen-2-one with mono-deuteride at 13-position (27): A solution of *N,N*-diisopropylethylamine (0.6 mL, 0.4 M, 0.24 mmol) in THF was mixed with acid compound (**26**; 108 mg, 0.12 mmol) in THF (15 mL). A 2,4,6-Trichlorobenzoyl chloride solution (0.33 mL, 0.4 M, 0.13 mmol) in THF was added to the mixture at room temperature. The reaction mixture was stirred at room temperature for 3 hr, and concentrated under reduced pressure to afford the crude anhydride intermediate. A solution of the obtained anhydride in toluene (6 mL) was added to a solution of *N,N*-dimethylaminopyridine (DMAP; 44 mg, 0.36 mmol) in toluene (17 mL) was added using a syringe pump over 3 hr. At the end of the addition, the syringe was rinsed with additional toluene (2 mL). After stirring for 14 hr, the mixture was quenched with a saturated aqueous sodium bicarbonate solution (10 mL), and the aqueous phase was extracted with ethyl acetate (10 mL x 3 times). The combined organic phases were washed with brine (20 mL), dried over an anhydrous sodium sulfate pad, and concentrated under reduced pressure. The crude residue was purified with flash column chromatography. The target compound was eluted with 4% EtOAc/Hexanes (55

mg, 0.06 mmol, 52%).

^1H NMR (CDCl_3 , 500 MHz) δ (ppm); ^{13}C NMR (CDCl_3 , 125 MHz) δ (ppm) ;
HRMS (ESI, positive) m/z for $\text{C}_{48}\text{H}_{93}\text{DO}_6\text{Si}_4$ $[\text{M}+\text{Na}]^+$: calcd 902.6082 , found 902.6062.

(3E,5E,7E,10R,12R,13E,16R,17R,18S,22S)-22-ethyl-10,12,16,18-tetrahydroxy-17-methyloxacyclodocosa-3,5,7,13-tetraen-2-one with mono-deuteride at 13-position (28): A solution of the macrolactone (mg, mmol) in hydrogen fluoride-pyridine complex (mL) was stirred at 0 °C for 4 days until the starting material was no longer detectable. After quenching with a saturated aqueous sodium bicarbonate solution (mL) at 0 °C, the aqueous phase was extracted with dichloromethane (mL x 3 times). The combined organic phases were dried over an anhydrous sodium sulfate pad, and concentrated under reduced pressure. The resulting residue was purified with flash column chromatography on silica gel. The target compound was elute with 5% MeOH/DCM solution (mg, mmol, %).

^1H NMR (DMSO-d_6 , 500 MHz) δ (ppm) ; ^{13}C NMR (DMSO-d_6 , 125 MHz) δ (ppm) ; HRMS (ESI, positive) m/z for $\text{C}_{24}\text{H}_{37}\text{DO}_6$ $[\text{M}+\text{Na}]^+$: calcd 446.2629, found .

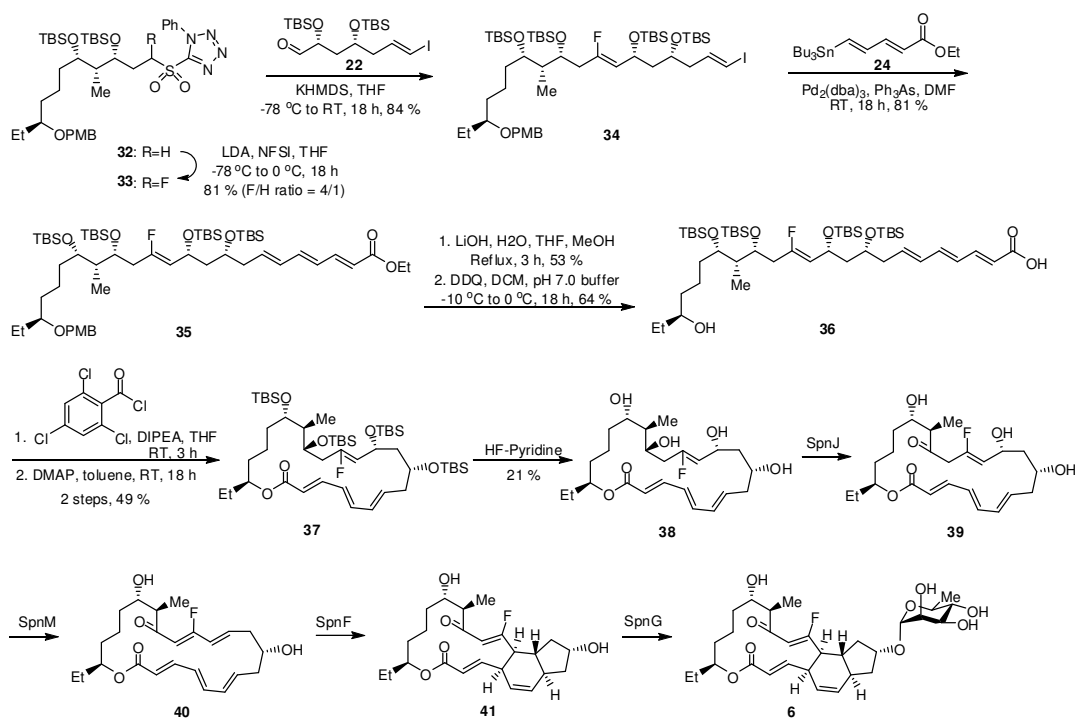
[C13- ^2H] SpnL substrate analog (5): SpnJ (μM), SpnM (μM), SpnF (μM) and SpnG (μM) were added to a solution of macrolactone (**28**; mg, mM in DMSO) and TDP-L-rhamnose (mM) in magnesium chloride (mM) and Tris·HCl buffer (50 mM) at 30 °C with stirring. Through the incubation, the reaction was monitored by HPLC using a 4 x 250 mm Econosil C18 column (Alltech). Compounds were detected by their absorbance at 254 nm, and the column was eluted at a rate of 1 mL/min with water (A) and acetonitrile (B) using the following gradient. Initially the eluting solution was only 30%

B, then increased at a linear rate to 45% in 30 min, then linearly to 80% in 3 min, and finally decreased linearly back to 30% in 3 min. After incubation at 30 °C for 2.5 hr, at which point the reaction was completed, the reaction mixture was directly filtered through a YM-10 membrane filter by centrifugation at 4,000 rpm over 40 min. The clear filtrate was purified by semi-preparative HPLC using a 10 x 250 mm Econosil C18 column (254 nm, Alltech). The column was eluted at 4 mL/min with water (A) versus acetonitrile (B) and the following gradient. Initially the concentration of B in the elution solution was 30%. This was raised linearly to 45% in 30 min, then again to 80% linearly over 3 min, and finally decreased linearly to 30% in 3 min. Collected fractions were pooled, extracted with EtOAc (50 mL x 3 times), dried over an anhydrous sodium sulfate pad, and concentrated under reduce pressure to produce a target compound (mg,%).

^1H NMR (DMSO- d_6 , 500 MHz) δ (ppm) ; ^{13}C NMR (DMSO- d_6 , 125 MHz) δ (ppm) ; HRMS (CI, negative) m/z for $\text{C}_{30}\text{H}_{43}\text{DO}_9$ $[\text{M}+\text{Na}]^+$: calcd 572.2940, found .

3.2.6. Synthesis of the C13-F SpnL Substrate Analogue

A. Synthesis of C13-F SpnL Substrate Analog by Fragment A Modification, Coupling reactions, and enzymatic conversions: The overall synthetic scheme is pictured in **Scheme 3-5**.



Scheme 3-5. Preparation of C13-F SpnL substrate analog

5-((3R,4R,5S,9S)-5-(tert-butyldimethylsilyloxy)-1-fluoro-9-(4-methoxybenzyloxy)-4-methyl-3-(triethylsilyloxy)undecylsulfonyl)-1-phenyl-1H-tetrazole (33): Lithium diisopropylamide solution (1.5 mL, 2.0 M, 3.0 mmol) was added dropwise to a solution of the sulfone (1.7 g, 2.2 mmol) in anhydrous THF (50 mL) over 15 min at $-78\text{ }^{\circ}\text{C}$, and the reaction mixture was stirred at $-78\text{ }^{\circ}\text{C}$ for 1 hr. N-fluorobenzenesulfonylimide solution (NFSI; 830 mg, 2.6 mmol) in THF (10 mL) was then added to the reaction mixture via cannular over 40 min at $-78\text{ }^{\circ}\text{C}$. The reaction mixture was allowed to warm to room temperature with stirring for 18 hr. After quenching by addition of a saturated aqueous ammonium chloride solution (10 mL) at $0\text{ }^{\circ}\text{C}$, the aqueous phase was extracted with ethyl acetate (50 mL x 3 times). The combined organic phases were washed with brine (40 mL), dried over an anhydrous sodium sulfate pad, filtered, and concentrated under

reduced pressure. The resulting residue was subjected to flash column chromatography. The fluoro-compound was eluted with 10% EtOAc/Hexanes (1.4 g, 1.8 mmol). Spectral data was not the collected.

HRMS (ESI, positive) m/z for $C_{39}H_{65}FN_4O_6SSi_2$ $[M+Na]^+$: calcd 815.4045, found 815.4043.

(5R,7R,11R,12R,13S,Z)-7,11-bis(tert-butyldimethylsilyloxy)-9-fluoro-5-((E)-3-iodoallyl)-13-((S)-4-(4-methoxybenzyloxy)hexyl)-2,2,3,3,12,15,15,16,16-nonamethyl-4,14-dioxa-3,15-disilaheptadec-8-ene (34): Compound (34) was prepared following the same procedure as compound (23) using compound (33) and compound (22) with a yield of 84%. No spectral data was the collected.

(2E,4E,6E,9R,11R,12Z,15R,16R,17S)-ethyl 9,11,17-tris(tert-butyldimethylsilyloxy)-13-fluoro-21-(4-methoxybenzyloxy)-16-methyl-15-(triethylsilyloxy)tricoso-2,4,6,12-tetraenoate (35): Compound (35) was prepared following the same procedure as compound (25) with a yield of 81%.

1H NMR ($CDCl_3$, 500 MHz) δ (ppm) 7.27 (dd, 1H, $J = 11.1, 15.2$ Hz, 3-H), 7.24 (d, 2H, $J = 8.5$ Hz, PhH of PMB), 6.84 (d, 2H, $J = 8.5$ Hz, PhH of PMB), 6.49 (dd, 1H, $J = 11.0, 14.8$ Hz, -CH), 6.18 (dd, 1H, $J = 11.3, 14.9$ Hz, 4-H), 6.10 (dd, 1H, $J = 10.7, 15.1$ Hz, 6-H), 5.92-5.86 (m, 1H, 7-H), 5.82 (d, 1H, $J = 15.2$ Hz, 2-H), 4.62-4.52 (m, 2H, 21-H+12-H), 4.41 (s, 2H, CH_2 of OMB), 4.18 (q, 2H, $J = 7.1$ Hz, CH_2CH_3 of OEt), 4.02-3.99 (m, 1H, 11-H), 3.84-3.80 (m, 1H, 9-H), 3.77 (s, 3H, OCH_3 of PMB), 3.68-3.63 (m, 1H, 15-H), 3.28-3.25 (m, 1H, 17-H), 2.42-2.18 (m, 1H, 8-H), 2.41-2.20 (m, 5H, 8-H,+10-Hs+14-Hs), 1.73-1.59 (m, 1H, 10-Hs), 1.54-1.46 (m, 9H, 16-H+18-Hs+19-Hs+20-

Hs+22-Hs), 1.27 (t, 3H, $J = 5.2$ Hz, CH₂CH₃ of OEt), 0.95-0.90 (m, 5H, CH₂CH₃ of TES+23-CH₃), 0.88-0.84 (m, 30H, 3xtBu of TBS+16-CH₃), 0.58 (t, 3H, $J = 7.9$ Hz, CH₂CH₃ of TES), 0.039-0.002 (m, 24H, CH₃ of TBS); ¹³C NMR (CDCl₃, 125 MHz) δ (ppm) 167.18 (1-C=O), 159.01, 158.05, 144.75 (C-3), 136.67 (C-5), 132.04 (C-7), 131.34 (C-6), 129.17, 128.10 (C-4), 120.22 (C-2), 113.71, 79.83 (C-17), 78.46 (C-21), 72.06 (C-9), 70.47 (CH₂ of PMB), 69.11 (C-15), 68.28 (C-11), 60.18 (OCH₂CH₃ of OEt), 55.25 (OCH₃ of PMB), 47.27, 40.88 (C-8), 37.43 (C-10), 34.55 (C-14), 30.90, 30.12, 25.96, 21.03, 18.11 (Me₃C of tBu of TBS), 18.02 (Me₃C of tBu of TBS), 18.01 (Me₃C of tBu of TBS), 14.31 (OCH₂CH₃ of OEt), 9.50 (16-CH₃), 9.32 (C-23) 6.99 (CH₂CH₃ of TES), 5.28 (CH₂CH₃ of TES), 3.90 (CH₃ of TBS), 4.23 (CH₃ of TBS), 4.46 (CH₃ of TBS), 4.57 (CH₃ of TBS), 4.71 (CH₃ of TBS), 5.02 (CH₃ of TBS); ¹⁹F NMR (CDCl₃, 470 MHz) δ (ppm) 105.51 (ddd, $J = 17.3, 23.2, 39.5$ Hz); HRMS (ESI, positive) m/z for C₅₈H₁₀₇FO₈Si₄ [M+Na]⁺: calcd 1085.6925, found 1085.6916.

(2E,4E,6E,9R,11R,12Z,15R,16R,17S,21S)-9,11,17-tris(tert-butyldimethylsilyloxy)-13-fluoro-21-hydroxy-16-methyl-15-(triethylsilyloxy)tricoso-2,4,6,12-tetraenoic acid (36): Compound **(36)** was prepared following the same procedure as compound **(26)** with a yield of 34% for 2 steps.

¹H NMR (CDCl₃, 600 MHz) δ (ppm) 7.35 (dd, 1H, $J = 11.2, 15.0$ Hz, 3-H), 6.55 (dd, 1H, $J = 11.1, 14.9$ Hz, 5-H), 6.22 (dd, 1H, $J = 11.5, 14.8$ Hz, 4-H), 6.15 (dd, 1H, $J = 10.3, 14.8$ Hz, 6-H), 5.99-5.92 (m, 1H, 7-H), 5.83 (d, 1H, $J = 15.2$ Hz, 2-H), 4.63-4.55 (m, 2H, 21-H+12-H), 3.99-3.97 (m, 1H, 11-H), 3.85-3.81 (m, 1H, 9-H), 3.68-3.63 (m, 1H, 15-H), 3.51-3.47 (m, 1H, 17-H), 2.64-2.60 (m, 1H, 8-H), 2.41-2.20 (m, 4H, 8-H+10-

H+14-Hs), 2.15-1.50 (m, 10H, 10-H+16-H+18-Hs+19-Hs+20-Hs+22-Hs), 0.95-0.90 (m, 5H, CH₂CH₃ of TES+23-Hs), 0.88-0.84 (m, 30H, 3 x tBu of TBS+16-CH₃), 0.58 (t, 3H, $J = 7.9$ Hz, CH₂CH₃ of TES), 0.039 (s, 3H, CH₃ of TBS), 0.024 (s, 3H, CH₃ of TBS), 0.021 (s, 3H, CH₃ of TBS), 0.014 (s, 3H, CH₃ of TBS), 0.009 (s, 3H, CH₃ of TBS), 0.003 (s, 3H, CH₃ of TBS); ¹³C NMR (CDCl₃, 150 MHz) δ (ppm) 158.06 (1-C=O), 147.00 (C-3), 142.07 (C-5), 137.54 (C-7), 132.02 (C-6), 127.85 (C-4), 121.37 (C-2), 118.70 (d, $J = 12.2$ Hz, C-12), 77.70 (C-17), 76.32 (C-21), 73.09 (C-9), 69.61 (C-15), 68.91 (C-11), 46.17, 40.98 (C-8), 37.42 (C-10), 34.58 (C-14), 30.91, 30.10, 25.94, 21.00, 18.13 (Me₃C of tBu of TBS), 18.06 (Me₃C of tBu of TBS), 18.04 (Me₃C of tBu of TBS), 9.86 (16-CH₃), 9.38 (C-23) 6.98 (CH₂CH₃ of TES), 5.27 (CH₂CH₃ of TES), 3.94 (CH₃ of TBS), 4.33 (CH₃ of TBS), 4.46 (CH₃ of TBS), 4.57 (CH₃ of TBS), 4.71 (CH₃ of TBS), 5.06 (CH₃ of TBS); ¹⁹F NMR (CDCl₃, 564 MHz) δ (ppm) 105.41 (ddd, $J = 17.2, 23.0, 39.6$ Hz); HRMS (ESI, negative) m/z for C₄₈H₉₄FO₇Si₄ [M-H]⁻: calcd 913.6066, found 913.6079.

(3E,5E,7E,10R,12R,13Z,16R,17R,18S,22S)-10,12,18-tris(tert-butyldimethylsilyloxy)-22-ethyl-14-fluoro-17-methyl-16-(triethylsilyloxy)oxacyclodocosa-3,5,7,13-tetraen-2-one (37): Compound (37) was prepared following the same procedure as compound (27) with a yield of 49% for 2 steps. No spectral data was the collected.

(3E,5E,7E,10R,12R,13Z,16R,17R,18S,22S)-22-ethyl-14-fluoro-10,12,16,18-tetrahydroxy-17-methyloxacyclodocosa-3,5,7,13-tetraen-2-one (38): Hydrogen fluoride-pyridine complex (0.38 mL) was added to a solution of the macrolactone (41 mg, 0.046 mmol) in ethanol (3.8 mL) at 0 °C. The reaction mixture was stirred at 4 °C for

4 days, at which time the reaction mixture was quenched by adding a saturated aqueous sodium bicarbonate solution (5 mL) at 0 °C. The aqueous phase was extracted with dichloromethane (25 mL x 3 times), and the combined organic phases were dried over an anhydrous sodium sulfate pad, and concentrated under reduced pressure. The resulting residue was purified with flash column chromatography on silica gel. The target compound was eluted with 7% MeOH/DCM solution (8.5 mg, 0.056 mmol).

¹H NMR (CDCl₃, 600 MHz) δ (ppm) 7.23 (dd, 1H, *J* = 11.3, 15.6 Hz, 3-H), 6.52 (dd, 1H, *J* = 10.8, 14.8 Hz, 5-H), 6.24 (dd, 1H, *J* = 11.2, 14.9 Hz, 4-H), 6.16 (dd, 1H, *J* = 10.9, 15.3 Hz, 6-H), 5.81 (d, 1H, *J* = 15.3 Hz, 2-H), 5.82-5.76 (m, 1H, 7-H), 4.91-4.87 (m, 1H, 21-H), 4.73 (dd, 1H, *J* = 3.8, 8.7 Hz, 12-H), 4.64 (dt, 1H, *J* = 3.8, 8.7 Hz, 11-H), 4.07-4.05 (m, 1H, 9-H), 3.95-3.91 (m, 1H, 15-H), 3.78-3.75 (m, 1H, 17-H), 2.64-2.60 (m, 1H, 8-H), 2.43-2.36 (m, 1H, 10-H), 2.34-2.15 (m, 3H, 8-H+14-Hs), 1.71-1.38 (m, 10H, 10-H+16-H+18-Hs+19-Hs+20-Hs+22-Hs), 0.89 (t, 3H, *J* = 7.5 Hz, 23-Hs), 0.77 (t, 3H, *J* = 7.1 Hz, 16-CH₃); ¹³C NMR (CDCl₃, 150 MHz) δ (ppm) 166.39 (1-C=O), 144.58 (C-3), 140.73 (C-5), 134.94 (C-7), 133.31 (C-6), 128.36 (C-4), 120.93 (C-2), 111.28 (d, *J* = 12.4 Hz, C-12), 77.74 (C-17), 76.02 (C-21), 73.34 (C-9), 70.70 (C-15), 65.48 (d, *J* = 6.2 Hz, C-11), 43.29, 41.44 (C-8), 40.08, 38.21 (C-10), 35.91 (C-14), 34.77, 32.73, 27.68, 9.74 (C-23), 4.18 (16-CH₃); ¹⁹F NMR (CDCl₃, 564 MHz) δ (ppm) -105.38 (ddd, *J* = 17.3, 23.1, 39.8 Hz); HRMS (ESI, positive) *m/z* for C₂₄H₃₇FO₆ [M+Na]⁺: calcd 463.24664, found 463.24736.

C13-F SpnL substrate analog (6): 1) A 35 mL solution of fluoro-macrolactone (31.0 mg, 70.4 μmol), SpnJ (17.4 μM), SpnM (2.5 μM), and SpnF (19.5 μM) in 50 mM

Tris·HCl (pH 8) was incubated at 30 °C for 4 hr. The reaction was monitored by HPLC for the appearance of product and consumption of substrate, using a 4 x 250 mm Econosil C18 column (Alltech). Compounds were detected using absorbance at 254 nm, and the column was eluted at a rate of 1mL/min with water (A) and acetonitrile (B) using the following gradient. Initially the concentration of B was 30%, it was increased linearly to 40% over 36 min, then to 80% over 3 min, kept constant at 80% concentration for 5 min, and finally decreased linearly to 30% over 3 min. The product was eluted with a retention time of 32.1 min. Based on HPLC analysis, the reaction was almost complete (>95%) after 4 hr of incubation. The product was extracted with ethyl acetate (20 mL x 3 times), dried over an anhydrous sodium sulfate pad, and concentrated under reduced pressure. The residue was purified by flash column chromatography on silica and Prep-HPLC to afford a tricyclic aglycone (15.3 mg, 0.0364 mmol, 52%).

2) A 6.8 mL solution including above compound (11.4 mg, 0.0704 mmol), TDP-L-rhamnose (9.2 mg, 16.8 μmol), MgCl₂ (5 mM), and SpnG (80 μM) in 50 mM Tris·HCl (pH 8) was incubated at 30 °C for 4 hr. The reaction was monitored by HPLC for the appearance of product and consumption of substrate, using a 4 x 250 mm Econosil C18 column (Alltech). The compounds were detected by absorption at 254 nm, and the column was eluted at a rate of 1mL/min with water (A) and acetonitrile (B) using the following gradient. Initially the concentration of B was 30%, this was increased linearly to 40% in 36 min, then to 80% in 3 min, kept constant at 80% for 5 min, and finally decreased linearly to 30% in 3 min. The product eluted had a retention time of 22.1 min. Based on HPLC analysis, the reaction was almost complete (>95%) after 4 hr of incubation. The product was extracted

with ethyl acetate (20 mL x 3 times), dried over an anhydrous sodium sulfate pad, and concentrated under reduced pressure. The resulting residue was directly purified with Prep-HPLC to produce a target compound (9.8 mg, 0.0173 mmol, 64%).

^1H NMR (DMSO- d_6 , 600 MHz) δ (ppm) 6.58 (dd, $J = 15.5, 10.0$ Hz, 1H, 3-H), 5.94 (d, $J = 9.6$ Hz, 1H, 6-H), 5.85 (dd, $J = 15.6, 0.6$ Hz, 1H, 2-H), 5.57 (d, $J = 40.8$ Hz, 1H, 14-H), 5.38 (dt, $J = 10.8, 4.2$ Hz, 1H, 5-H), 4.78-4.74 (m, 1H, 21-H), 4.65-4.63 (m, 1H, 3'-H), 4.58-4.56 (m, 1H, 1'-H), 4.30-4.26 (m, 1H, 17-H), 3.53-3.51 (m, 1H, 2'-H), 3.48-3.45 (m, 1H, 9-H), 3.42-3.35 (m, 2H, 4-H, 5'-H), 3.16 (dt, $J = 13.2, 5.4$ Hz, 1H, 4'-H), 2.97-2.91 (m, 1H, 12-H), 2.57-2.54 (m, 1H, 7-H), 2.41-2.37 (m, 1H, 16-H), 2.01-1.93 (m, 3H, 8-Ha, 10-H), 1.84-1.82 (m, 1H, 8-Hb), 1.52-1.34 (m, 5H, 11-H, 18-H, 22-H), 1.28-1.18 (m, 4H, 19-H, 20-H), 1.12 (d, $J = 15.6$ Hz, 3H, 6'-H), 1.05 (d, $J = 6.6$ Hz, 3H, 24-H), 0.81 (t, $J = 7.8$ Hz, 3H, 23-H); ^{13}C NMR (DMSO- d_6 , 150 MHz) δ (ppm) 201.1 (C-15), 174.2 (C-13), 164.7 (C-1), 145.7 (C-3), 130.7 (C-6), 127.2 (C-5), 122.8 (C-2), 107.7 (C-14), 98.6 (C-1'), 75.7 (C-21), 74.2 (C-17), 72.0 (C-4'), 71.6 (C-9), 70.7 (C-2'), 70.6 (C-3'), 68.6 (C-5'), 53.1 (C-16), 45.5 (C-12), 41.0 (C-7), 40.4 (C-4), 36.9 (C-11), 35.41 (C-10), 35.38 (C-8), 35.1 (C-18), 31.2 (C-20), 27.0 (C-22), 22.0 (C-19), 17.8 (C-6'), 13.9 (C-24), 9.8 (C-23). HRMS (ESI, positive) m/z for $\text{C}_{30}\text{H}_{43}\text{FO}_9$ $[\text{M}+\text{Na}]^+$: calcd 589.2789, found 589.2794.

3.2.7. *In vitro* activity assay of SpnL

In order to verify the activity of SpnL, a solution containing SpnL natural substrate (**2**; 100 μM) in pH 8.0 Tris buffer (50 mM) was incubated with SpnL (10 μM) at 30 $^\circ\text{C}$. Through the incubation, the reaction was monitored by HPLC analysis. HPLC

condition was as follows: C18 analytical column (250 x 4.6 mm, 5 μ m), gradient from 30 to 45% acetonitrile in water for 30 min at a rate of 1 mL/min, detected by UV absorption at 254 nm. Each aliquot was transferred into half its volume of 1:1 DMSO/acetonitrile solution at 0 °C after 1 min, 2 min, 5 min, or 30 min. The quenching mixture was centrifuged to precipitate proteins, and the resulting supernatant was subjected to HPLC analysis to measure the rate of substrate consumption and product formation.

3.2.8. Isotope Trace Experiment for the SpnL Reaction

The pH 8.0 Tris·HCl buffer in a stock solution of SpnL was switched with pD 8.0 Tris·DCl buffer by centrifugal filtration through a YM 10 membrane filter followed by resuspension of the concentrated enzyme in pD 8.0 Tris·DCl buffer. This process was repeated twice. A solution containing SpnL natural substrate (**2**; 500 μ M) and SpnL (10 μ M) in pD 8.0 Tris·DCl buffer (50 mM; total volume of 50 μ L) was incubated at 30 °C for 2 hr. The products were then extracted with ethyl acetate (100 μ L) and directly analyzed by MS. As a control, SpnL natural product (**3**; 500 μ M) in pD 8.0 Tris·DCl was incubated under the same condition, which was extracted with ethyl acetate (100 μ L) and directly analyzed by MS.

3.2.9. Kinetic Isotope Effect Studies of the SpnL Reaction Using SpnL Natural Substrate and Deuterium-Labeled SpnL Substrate Analogs

3.2.9.1. Determination of concentration of SpnL natural substrate and deuterium-labeled SpnL substrate analog

Prior to the determination of SpnL's kinetic parameters, concentrations of SpnL natural substrate and deuterium-labeled SpnL substrate analog were first standardized

based on the area integration of HPLC analysis using *para*-methoxyacetophenone (PMAP) as a reference.

3.2.9.2. Determination of kinetic parameters for SpnL reaction for SpnL natural substrate and deuterium-labeled SpnL substrate analog

In order to determine kinetic parameters for SpnL reaction, SpnL natural substrate (2; 2, 4, 6, 8, 10, 25, 50, 100, 200, and 400 μM ; 10 points) and *para*-methoxyacetophenone (PMAP; 0.25 equivalent to SpnL natural substrate, used as a reference for the reaction progress) was incubated with SpnL (0.5 μM) in pH 8.0 Tris buffer (50 mM) containing DMSO (10% v/v) at 30 °C for 1 min and 2 min, which were selected to measure the rate of substrate consumption and product formation (**Table 2-1**). After quenching with a half volume of 1:1 DMSO/acetonitrile solution and precipitating by centrifugation, the supernatant was subjected to HPLC analysis as described above. The same procedure was conducted with the deuterium-labeled SpnL substrate analogs, C12-D and C13-D analog. All of the experiments were duplicated at the same time period.

Entry No.	[SpnL] (μM)	[substrate] (μM)	[PMAP] (μM)	Total volume (μL)	Quenching volume (μL)	Injecting volume (μL)
1	0.5	2.0	0.5	500.0	250.0	500.0
2	0.5	4.0	1.0	400.0	200.0	400.0
3	0.5	6.0	1.5	300.0	150.0	300.0
4	0.5	8.0	2.0	200.0	100.0	200.0
5	0.5	10.0	2.5	200.0	100.0	200.0
6	0.5	25.0	6.25	100.0	50.0	100.0
7	0.5	50.0	12.5	50.0	25.0	50.0
8	0.5	100.0	25.0	20.0	10.0	20.0
9	0.5	200.0	50.0	10.0	5.0	10.0
10	0.5	400.0	100.0	5.0	2.5	5.0

Table 2-1. *In vitro* activity assay of SpnL for SpnL natural substrate and deuterium-labeled SpnL substrate analog

3.2.10. Biochemical Studies of the SpnL-Catalyzed Cyclization Using C13-F Substrate Analog

3.2.10.1. *In vitro* activity assay of SpnL with C13-F SpnL substrate analog

A solution containing C13-F SpnL substrate analog (=the C13-F analog, **6**; 100 μM), DMSO (5% v/v) in pH 8.0 Tris buffer (50 mM) was pre-incubated at 30 °C for 2 min, and then the reaction initiated by addition of SpnL (5 μM). Several aliquots were quenched with an equal volume of 1:1 DMSO/acetonitrile solution at 0 °C for 30 min and 4 hr, and the protein precipitated by centrifugation. The resulting supernatant was subjected to HPLC analysis as described above. The control reaction was performed with SpnL natural substrate under the same condition.

3.2.10.2. Competition assay of SpnL with SpnL natural substrate and C13-F SpnL substrate analog

A solution containing a mixture of SpnL natural substrate and the C13-F analog (totally 500 μM with a ratio of 1:4 by molar concentration) in pH 8.0 Tris buffer (50 mM containing 5% v/v of DMSO) was incubated at 30 °C. Two aliquots were quenched with an equal volume of 1:1 DMSO/acetonitrile solution at 0 °C, and the protein precipitated by centrifugation. The resulting supernatant was subjected to HPLC analysis.

3.2.10.3. Preincubation *in vitro* activity assay of SpnL with SpnL natural substrate and the C13-F analog

A solution containing SpnL (20 μM) and the C13-F analog (500 μM) in pH 8.0 Tris buffer (50 mM) containing (5% v/v) was incubated at 30 °C for various times (5, 10,

15, and 30 min), at which point SpnL natural substrate (500 μM) was added to each of the reaction mixtures. After continued incubation at 30 $^{\circ}\text{C}$ for 40 min, the reaction mixture was quenched with an equal volume of 1:1 DMSO/acetonitrile solution at 0 $^{\circ}\text{C}$, and the precipitate removed by two rounds of centrifugation and supernatant transfer. The resulting supernatant was subjected to HPLC analysis. As a control reaction, the same experiment was performed for SpnL preincubation without the C13-F analog.

3.2.10.4. *In vitro* activity assay of SpnL with SpnL natural substrate, the C13-F analog, and L-glutathione

A solution containing SpnL (10 μM), L-glutathione (0, 250, or 2,000 μM) and the C13-F analog (250 μM) in pH 8.0 Tris buffer (50 mM) containing DMSO (5% v/v) was preincubated at 30 $^{\circ}\text{C}$ for 5 min, after which SpnL natural substrate (125 μM) was added to each of the reaction mixtures. After additional incubation at 30 $^{\circ}\text{C}$ for 30 min, the reaction mixture was quenched with an equal volume of 1:1 DMSO/acetonitrile solution at 0 $^{\circ}\text{C}$, and the precipitate was removed by two rounds of centrifugation and supernatant transfer. The resulting supernatant was subjected to HPLC analysis. As a control reaction, the same experiment was performed for SpnL preincubation without the C13-F analog.

In order to detect the covalent adduct of the C13-F analog and L-glutathione, a solution containing the C13-F analog (3 mM) in pH 8.0 Tris buffer (50 mM) or pH 12.0 NaOH solution was incubated with L-glutathione (15 mM) at 30 $^{\circ}\text{C}$ in the absence or presence of dithiothreitol (100 mM) for 18 hr. The reaction mixture was directly subjected to MS analysis.

3.2.10.5. Inhibition kinetic study of SpnL with SpnL natural substrate and C13-F SpnL substrate analog

A solution containing the C13-F analog (1.5 μM) and DMSO (6.6%) in pH 8.0 Tris buffer (50 mM) was preincubated at 30 °C for 2 min. SpnL (1.0 μM) was then added into the reaction mixture. After incubation at 30 °C for a specific period of time (10 seconds and 20 seconds), SpnL natural substrate (125 μM) was added and the reaction mixture incubated at 30 °C for additional 30 min. After quenching and two rounds of precipitation, the resulting supernatant was subjected to HPLC analysis. As a control reaction, the same procedure was conducted without the C13-F analog.

3.2.10.6. Detection of covalently-modified SpnL with the C13-F analog

For the inhibition assay, a solution containing SpnL (152 μM) and the C13-F analog (300 μM or 75 μM) in pH 8.0 Tris buffer (50 mM) was incubated at 30 °C for 1 hr, and dialyzed at 4 °C against ammonium bicarbonate buffer (50 mM) thoroughly (4 times) to remove excess amount of the C13-F analogue. Half of the solution (175 μL) was then subjected to ESI-MS analysis. The other half (175 μL) was treated with trypsin (5 μg) at 37 °C for 6 hr, and then subjected to ESI-MS analysis. Two sets of reactions were prepared as control. One containing only SpnL (152 μM) in pH 8.0 Tris buffer (50 mM), and the other containing SpnL (152 μM) and SpnL natural substrate (300 μM) in pH 8.0 Tris buffer. Both were followed by the same incubation and treatment conditions as the inhibition assay.

3.2.10.7. Detection of covalently-modified SpnL mutant (C71A) with the C13-F analog

In order to investigate the effect of cysteine residue 71 in the SpnL reaction with the C13-F analog, a SpnL mutant (C71A) prepared by Dr. Kim, was used under the same experimental conditions described in Section 3.2.9.6. Three trials were performed. SpnL C71A alone, SpnL C71A incubated with SpnL natural substrate, and SpnL C71A incubated with the C13-F analog. Each trial was analyzed by MALDI-ESI-MS.

3.2.10.8. Single turnover experiment

A solution containing the C13-F analog (25 μ M or 50 μ M) in pH 8.0 Tris buffer (50 mM) was preincubated at 30 °C for 2 min. The reaction was initiated by addition of SpnL (22.5 μ M) at 30 °C, and the reaction mixture incubated at 30 °C for either 5 min or 30 min. After quenching and two rounds of precipitation, the resulting supernatant was analyzed by HPLC.

3.2.11. Studies on the SAM-dependence of SpnF and SpnL reactions

3.2.11.1. *In vitro* activity assay of “as isolated” SpnF and SpnL with external SAM

First, the content of SAM in as isolated SpnF and SpnL was determined as follows. A SpnL solution (210 μ M) was denatured with 3 N aqueous hydrochloric acid solution at 0 °C, and the protein removed by YM-10 filtration. The resulting filtrate was subjected to the UV-VIS and HPLC analysis. The HPLC analysis was conducted with Dionex analytical column (CarboPac PA20, 250 x 4.6 mm) eluting with a gradient of 5% to 35% aqueous 1 M ammonium acetate solution for 30 min by flow rate of 1.0 mL/min, and the compounds detected by UV absorbance at 257 nm. The same procedure was used for SpnF.

Second, for the control reaction, a solution containing SpnL natural substrate (250 μM) in pH 8.0 Tris buffer (50 mM) was preincubated without SAM at 30 °C for 2 min, and the reaction was then initiated by addition of SpnL (10 μM) at 30 °C. After incubation at 30 °C for 3 min, the reaction mixture was quenched with an equal volume of 1:1 DMSO/acetonitrile solution at 0 °C, and the protein precipitated by centrifugation. The resulting supernatant was subjected to HPLC analysis as described above.

Third, a solution containing SpnL natural substrate (250 μM) in pH 8.0 Tris buffer (50 mM) was preincubated with SAM (500 μM) at 30 °C for 2 min, and the reaction then initiated with addition of SpnL (10 μM) at 30 °C. The reaction mixture was treated as described above, and submitted to HPLC analysis.

Lastly, SpnL (10 μM) was preincubated with SAM (500 μM) at 0 °C for 2 hr, and then added into a solution containing SpnL natural substrate (250 μM) in pH 8.0 Tris buffer (50 mM) at 30 °C. The reaction mixture was treated as described above, and submitted to HPLC analysis.

The same experiments were performed for SpnF in a similar manner using SpnM natural substrate combined with SpnM.

3.2.11.2. *In vitro* activity assay of apo-SpnF and apo-SpnL with external SAM

First, A solution containing 1 mL of SpnL (125 μM) in Tris buffer (50 mM) was denatured with 2.6 mL of 3 M aqueous KBr solution containing glycerol (20% v/v) at 0 °C for 2 min, and the protein refolded with 6.6 mL of pH 2.5 saturated aqueous ammonium sulfate solution over 5 min. The precipitate was the collected by ultracentrifugation (18,000 xg) and resuspended in 4 mL of pH 8.0 Tris buffer (50 mM).

The solution was treated again with 3 M KBr solution and 6.6 mL of pH 2.5 saturated aqueous ammonium sulfate solution in the same manner described above. The precipitate obtained after ultracentrifugation was dissolved in 10 mL of Tris buffer and dialyzed against pH 8.0 Tris buffer three times. The dialyzed protein was centrifugally concentrated through a YM-10 membrane filter. The supernatant (ca. 1.5 mL) was used to determine the SAM content and *in vitro* activity assay. The same procedure was conducted for SpnF using pH 5.5 saturated aqueous ammonium sulfate solution instead of pH 2.5 solution.

Second, the content of SAM in apo-SpnF and apo-SpnL was determined as described above with the UV-VIS analysis and HPLC analysis.

Third, an *in vitro* activity assay of apo-SpnF and apo-SpnL in the presence of SAM was performed in the same manner as described above.

Lastly, an *in vitro* activity assay of apo-SpnF and apo-SpnL was performed in the presence of S-adenosyl-l-homocysteine (SAH), 5'-deoxyadenosine, and/or methionine in the same manner as described above.

3.2.11.3. *In vitro* activity assay of reconstituted-SpnF and reconstituted-SpnL with external SAM

First, a solution containing apo-SpnL (100 μ M) in pH 8.0 Tris buffer (50 mM) was incubated with SAM (2.5 mM) at 4 °C for 2 hr, at which time excess SAM was removed by dialysis against pH 8.0 Tris buffer (50 mM) four times. The dialyzed enzyme solution was used to determine the SAM content and *in vitro* activity assay. The same procedure was conducted for SpnF.

Second, the content of SAM in reconstituted-SpnF and reconstituted-SpnL was determined as described above with the UV-VIS analysis and HPLC analysis.

Third, an *in vitro* activity assay of reconstituted-SpnF and reconstituted-SpnL in the absence or presence of SAM was performed in the same manner as described above.

3.2.11.4. Circular dichroism (CD) experiment

To compare the overall change of conformation between holo-SpnL (as isolated SpnL) and apo-SpnL, two protein samples of holo-SpnL and apo-SpnL were subjected to CD analysis. In addition, the conformational changes were monitored from apo-SpnL to reconstituted-SpnL during the reconstitution process by adding various equivalencies of SAM into apo-SpnL.

3.2.12. SpnL mutant study using SpnL D57N, E96Q, and E96L

3.2.12.1. *In vitro* activity assay of SpnL mutants

For the saturation *in vitro* activity assay, a solution containing SpnL natural substrate (20 μM) and SpnL mutant (40) in pH 8.0 Tris buffer (50 mM) was incubated at 37 °C for 3 hr and 20 hr. After quenching with an equal volume of ethanol at 0 °C and precipitating proteins by centrifugation, the resulting supernatant was analyzed by HPLC.

For the time-course *in vitro* activity assay, a solution containing SpnL natural substrate (80 μM) and SpnL mutant (10 μM) in pH 8.0 Tris buffer (50 mM) was incubated at 37 °C, and several aliquots were transferred into an equal volume of ethanol solution at 0 °C for either 10, 20, 30, 60, 240, or 1,200 min. After removal of protein by centrifugation, the resulting supernatants were analyzed by HPLC.

3.2.12.2. Detection of covalently-modified SpnL mutants with SpnL natural substrate

To detect the covalent adduct of SpnL mutant with SpnL natural substrate, the same procedure was conducted as described in Section 3.2.9.6. The protein samples were not treated with trypsin due to no evidence for the formation of the covalent adduct of SpnL mutant with SpnL natural substrate.

3.2.13. Chemoenzymatic total synthesis of spinosyn A

3.2.13.1. Enzymatic transformation of SpnJ substrate to 17-pseudoaglycone of spinosyn A

A solution containing SpnJ substrate (5 mM) in pH 8.0 Tris buffer (50 mM) was incubated at 30 °C. SpnJ (5 μM), SpnM (2.5 μM)/SpnF (10 μM), SpnG (20 μM)/MgCl₂ (2 mM)/TDP-l-rhamnose (1.5 mM), SpnL (20 μM), SpnI (20 μM)/SAM (5 mM), SpnK (20 μM)/SAM (5 mM), and SpnH (20 μM)/SAM (5 mM) were added subsequently into the reaction mixture at 30 °C every 2 hr. The reaction was monitored by HPLC for the appearance of product and consumption of substrate, using a 4 x 250 mm Econosil C18 column (Alltech). The compounds were detected by absorption at 254 nm, and the column was eluted at a rate of 1mL/min with water (A) and acetonitrile (B) using the following gradient. Initially the concentration of B was 30%, this was increased linearly to 60% in 60 min, then to 30% in 2 min, kept constant at 30% for 3 min. HPLC analysis was performed after 2 hr of incubation for each enzyme (in other word, just before the addition of each enzyme).

3.2.13.2. Chemical conversion of 17-pseudoaglycone to spinosyn A (1)

BF₃-Et₂O (0.2 mL, 0.21 mmol) was added into a reaction mixture containing D-forosamine (30 mg, 0.18 mmol) and 17-pseudoaglycone of spinosyn A (122 mg, 0.21 mmol) in dichloromethane (1.5 mL) at 0 °C with vigorous stirring. After 6 hr, the reaction mixture was quenched with 2~3 drops of saturated aqueous sodium bicarbonate. The aqueous phase was extracted with dichloromethane (1.0 mL x 3 times). The combined organic phase was dried over an anhydrous sodium sulfate pad, filtered, and concentrated under reduced pressure. The resulting residue was analyzed by HPLC.

HPLC analysis was performed using a 4 x 250 mm Econosil C18 column (Alltech). The compounds were detected by absorbance at 254 nm, and the column was eluted at a rate of 1 mL/min with aqueous 20 mM ammonium acetate solution (A) and 20 mM ammonium acetate in methanol/acetonitrile (1/1) solution (B) using the following gradient. Initially the concentration of B was 80%, this was increased linearly to 90% in 30 min, then back to 80% in 2 min, and kept constant at 80% for 3 min. The 17-pseudoaglycone was eluted at 9 min, and spinosyn A was eluted at 20 min.

3.3. RESULTS AND DISCUSSION

3.3.1. Synthesis of the SpnL Natural Substrate, and Deuterium-Labeled SpnL Substrate Analogs

SpnL-catalyzed cyclization is suggested to proceed through either a Rauht-Currier type mechanism^{29, 30} or a Michael addition mechanism,³¹ depending on how the conjugated system of C-11 to C-15-oxygen is activated, as shown in **Figure 3-2**. During the SpnL reaction, the rate determining step is thought to be either the nucleophilic

addition step for the Rauhut-Currier type mechanism or the deprotonation step for the Michael addition mechanism (**Figure 3-6, Left dotted box**). However, the possibility that the rate determining step may be the last step of deprotonation cannot be ruled out (**Figure 3-6, Right dotted box**). Two steps are found in both mechanisms, namely the C-C bond formation by cyclization and protonation at the C-2 position, so neither step is likely to show any kinetic difference. The expected kinetic isotope effects are summarized in **Figure 3-6 (table)**.

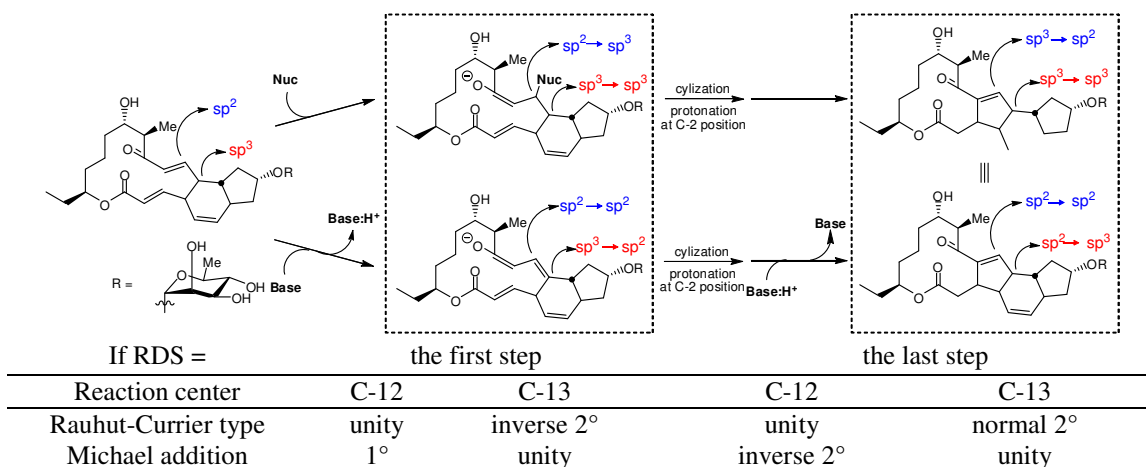


Figure 3-6. Hybrid changes of carbons at C-12 and C-13 positions, and the summary of the expected kinetic isotope effects during the SpnL reaction. 1° = primary kinetic isotope effect, 2° = secondary kinetic isotope effect.

If the kinetic isotope effect is used to distinguish between the SpnL reaction mechanisms, it should be measured for at least two reaction centers to avoid incorrect interpretation. The C14-D analog is excluded because the sp^2 carbon at the C-14 position does not undergo a hybrid change in both mechanisms, leading to a unity kinetic isotope effect for both cases.

The SpnL natural substrate and C12-D SpnL substrate analog were prepared from the corresponding SpnM natural substrate and C12-D SpnM substrate analog, respectively, by enzymatic conversions using SpnM (dehydratase), SpnF ([4+2] cyclase), and SpnG (rhamnosyl transferase at the C-9-OH).²² In order to prepare the C13-D analog, an intermediate (**21**) containing two deuteriums at the position adjacent to the sulfone moiety was used. The methyl ester precursor (**16**) was first prepared by a NIS-mediated esterification developed by McDonald and co-workers.^{152, 153} Deuteriums were then introduced by a lithiumaluminum hydride (LiAlD₄) reaction. The issue of TBS-deprotection during the deuteration reaction was overcome by selective thioetherification on the primary alcohol, followed by TBS reprotection of the exposed secondary alcohol. During the Julia-Kocienski olefination,^{134, 135} one deuterium at the C-13 position was removed (**21** to **23**). The C13-D analog was finally prepared by chemoenzymatic synthesis. **Figure 3-7** shows the enzymatic conversion of SpnM natural substrate (**9**) to SpnG product (**5**, identical to SpnL natural substrate).

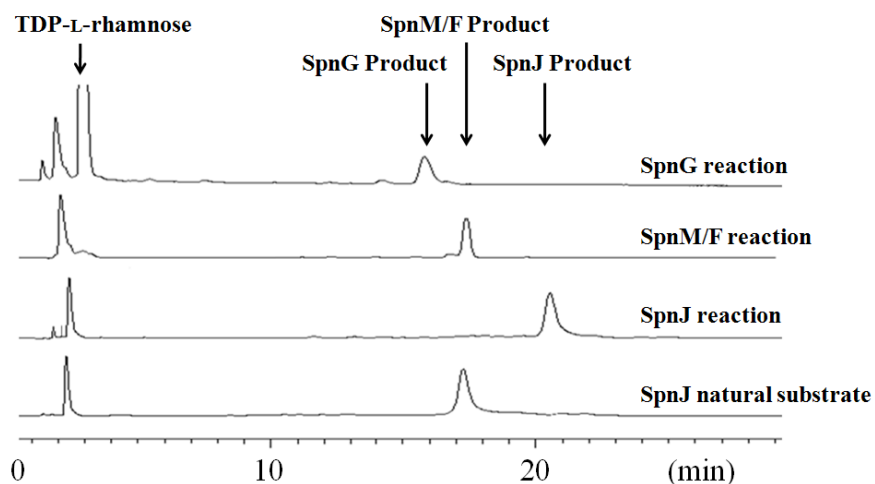


Figure 3-7. HPLC trace of SpnM natural substrate (**9**) into SpnG product (**2**, SpnL natural substrate).

3.3.2. Synthesis of the C13-F SpnL Substrate Analog

Suicide inactivation, or mechanism-based inactivation, is a widely used technique to capture an enzyme active-site nucleophile by a substrate analog which can be converted through the normal enzymatic reaction mechanism to generate a negative species and form a covalent adduct of the enzyme.^{62, 63, 154, 155, 156, 157, 158} Usually, suicide inactivation occurs at the active site of the enzyme of interest, so the analysis of the covalent adduct gives useful information about the reaction mechanism. Because it is a good leaving group, fluorine has been widely used in the design of suicide inactivators.^{84, 85, 159} Attaching a fluorine atom at the C-13 position on the SpnL natural substrate may cause the fluorine to be removed from the reaction intermediate instead of a nucleophile in the Rauhut-Currier type mechanism, resulting in the inactivation of SpnL. Retrosynthetic analysis was performed to facilitate the design of synthetic scheme for the preparation of the C13-F analog. As shown in **Scheme 3-5**, the fluorination on the C-13 position was incorporated into a modification of fragment A through electrophilic fluorination by *N*-fluorobenzenesulfonimide (NFSI) with lithium diisopropylamide (LDA) (**32** to **33**).¹⁶⁰ The best results were obtained using 2.0 equivalents of LDA and 1.5 equivalents of NFSI, which yielded a mixture of mono-fluorinated and non-fluorinated (starting material) product in a ratio of >85:15. At this stage, these two compounds were not separable, so the mixture was directly used for the following coupling reactions. A mixture of the two resulting chemical reaction products (**38**) containing a fluorine or hydrogen at the C-13 position was subjected to enzymatic conversions by SpnJ, SpnM,

SpnF, and SpnG,^{20, 22} where the C13-F analog showed similar reactivity as the natural substrate for all enzymatic reactions. The mixture was then separated by preparative-HPLC as the C13-F SpnL substrate analog or SpnL natural substrate. The HPLC trace of the SpnG reaction is shown in **Figure 3-8**.

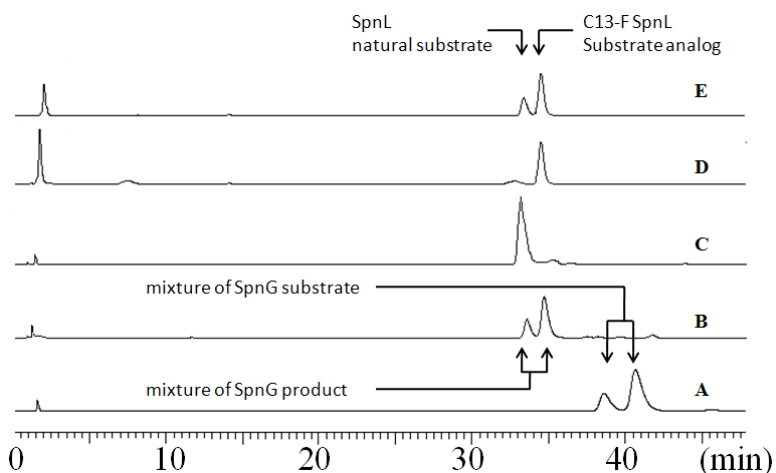


Figure 3-8. HPLC trace of the SpnG reaction for a mixture of C13-F and natural substrate. (A) a mixture of SpnG substrates, (B) a mixture of SpnG products, (C) isolated SpnL natural substrate, (D) isolated C13-F SpnL substrate analog, and (E) coinjection of C and D. HPLC condition: 30% to 45% aqueous acetonitrile with a flow rate of 1 mL/min over 60 min.

3.3.3. *In vitro* activity assay of SpnL

Prior to the kinetic isotope effect study and biochemical study of SpnL, the activity of SpnL was verified with the SpnL natural substrate. A solution containing SpnL natural substrate (100 μ M) with SpnL (10 μ M) in pH 8.0 Tris buffer (50 mM) was incubated at 30 °C for several time periods (1 min, 2 min, 5 min, and 30 min). HPLC analysis showed complete conversion in 30 min (**Figure 3-9**).

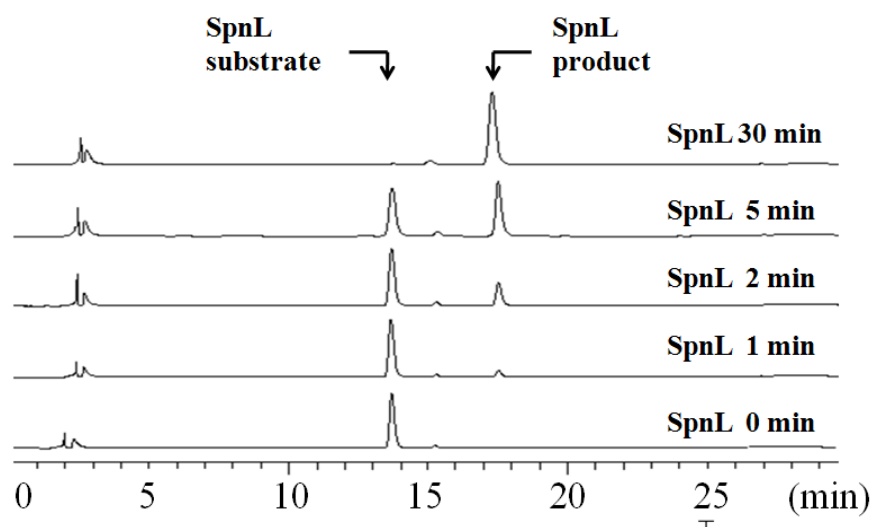


Figure 3-9. HPLC trace of SpnL reaction for the SpnL natural substrate.

3.3.4. Isotope Trace Experiment for the SpnL Reaction

Deuterium isotope trace experiments are one of a biochemical method which is widely used for the mechanistic studies, where an enzymatic reaction involves a protonation and deprotonation step with its substrate and product.^{161, 162, 163, 164} If the reaction is carried out in D₂O, the newly introduced deuterium from D₂O in the product can be traced by NMR or mass spectroscopy.

According to the Rauhut-Currier type mechanism, the reaction involves one protonation step and one deprotonation step, while the Michael addition mechanism includes two protonation steps and two deprotonation steps. If these protonation and deprotonation steps are mediated by an amino acid residue carrying a solvent exchangeable functional group or a microenvironmental water molecule in the active site of SpnL, a solvent hydrogen atom will be incorporated during the protonation steps of the SpnL reaction. Namely, if the hydrogen atoms on the general acid/general base group are

exchanged with deuterium atoms during the SpnL reaction running in D_2O , a deuterium atom will be introduced on the SpnL product instead of hydrogen atom (**Figure 3-10**). Therefore, an isotope trace experiment may provide evidence to distinguish between the two proposed mechanisms for the SpnL reaction, depending on how many deuteriums are introduced into the SpnL product.

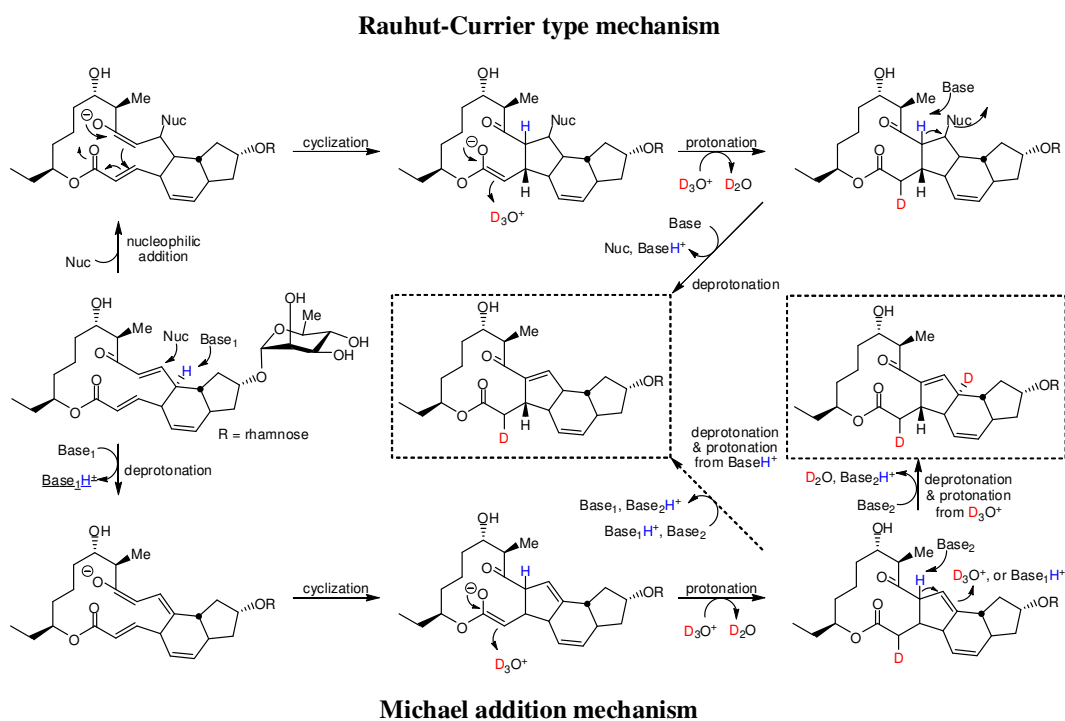


Figure 3-10. Deuterium(s) incorporation during the SpnL reaction, depending on the mechanisms.

To exclude the possibility of the deuterium exchange between D_2O and SpnL product, a control reaction was performed with SpnL product in the deuterated buffer solution. SpnL product ($500 \mu M$) was incubated with SpnL ($10 \mu M$) in pH 8.0 Tris buffer (50 mM) at $30 \text{ }^\circ C$ for 2 hr, extracted with ethyl acetate, and analyzed by MS. This SpnL product showed a peak of 571.3 m/z , corresponding to the sodium salt form and was identical to the peak of SpnL product produced by SpnL in pH 8.0 Tris buffer. This

demonstrated that no proton in SpnL product is easily interchangeable with hydrogens of the water molecules in the buffer solution under the incubation conditions.

Deuterium isotope experiments were performed by incubation of SpnL natural substrate (500 μM) with SpnL (10 μM ; buffer of stock solution was exchanged to the deuterated buffer as described in Section 3.2.7) in pD 8.0 Tris buffer (50 mM) at 30 $^{\circ}\text{C}$ for 2 hr. The product was extracted with ethyl acetate and analyzed by MS. This SpnL product showed a peak of 572 m/z , corresponding to the monodeuterated sodium salt form of the SpnL product. The MS results are shown in **Figure 3-11**.

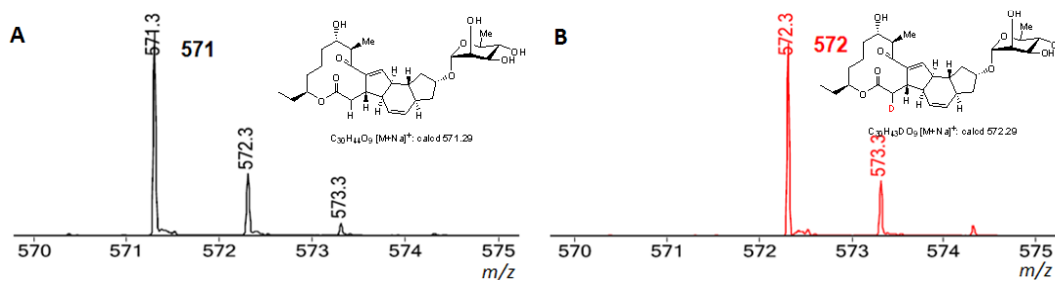


Figure 3-11. MS (ESI, positive) results for the isotope trace experiment. (A) Incubation of SpnL natural substrate in pD 8.0 Tris buffer, and (B) incubation of SpnL product in pD 8.0 Tris buffer.

The observed increase of one mass unit from the SpnL product enzymatically generated in the deuterated buffer solution is consistent with the expected result when the SpnL reaction proceeds through the Rauhut-Currier type mechanism. However, if SpnL has two different specific bases (base₁ and base₂) to remove the protons at the C-12 position and the C-14 position, it is possible to produce the monodeuterated SpnL product when incubated in deuterated buffer. For example, base₁ is located adjacent to the proton at C-12 position, and removes the C-12-H in the first step. This proton may be exchanged with deuterium from the deuterated buffer or not. After base₂ removes the C-14-H in the

last step, the proton or deuterium from base₁ will be transferred to the product. If the proton bound to base₁ is not exchanged, this proton, which originates from C-12-H, is rebound to the C-12 position, yielding the M+1 Da SpnL product (monodeuterated at C-14 in the SpnL product). If the proton bound on base₁ is exchangeable with D₂O, a new deuterium will be introduced at the C-12 position, producing the M+2 Da SpnL product (dideuterated SpnL product).

The results of isotope trace experiments gave information of the middle steps of the cyclization reaction, especially the protonation at the C-2 position. However, the results could not differentiate between the two plausible mechanisms.

3.3.5. Kinetic Isotope Effect Studies of the SpnL Reaction Using SpnL Natural Substrate and Deuterium-Labeled SpnL Substrate Analogs

The SpnL-catalyzed cyclization seems to proceed by four steps no matter which mechanism is applied. In the case of the Rauhut-Currier type mechanism, the nucleophilic addition at the C-13 position activates the conjugated π -system for the C-C bond formation. The Michael addition begins with the deprotonation at the C-12 position, which activates the conjugated system to generate a closed related enolate intermediate as the Rauhut-Currier type mechanism. The cyclization and protonation at the C-2 position are the same in both reaction mechanisms. A deprotonation at the C-14 position concomitant with removal of nucleophile completes the SpnL reaction in the Rauhut-Currier type mechanism, whereas a deprotonation at the C-14 position concomitant with protonation at the C-12 position finishes the SpnL reaction in the Michael addition mechanism. The cyclization and protonation at the C-2 position is known to occur very

quickly, compared to the first nucleophilic addition and the last removal of nucleophile in the Rauhut-Currier type mechanism or the first deprotonation and the last protonation at the C-12 position in the Michael addition mechanism. Thus, the kinetic isotope effect studies are focused on the first step and the last step during the SpnL-catalyzed cyclization reaction. The expected results are already shown in **Figure 3-6**.

The kinetic isotope effect of the SpnL reaction can be measured by two ways.¹⁶⁵ One utilizes the direct comparison activity assay, where the kinetic parameters are measured for SpnL natural substrate and deuterium-labeled SpnL substrate analogs, and the kinetic isotope effects are determined from those kinetic parameters. The other takes advantage of a competitive activity assay, where a mixture of SpnL natural substrate and deuterium-labeled SpnL substrate analog are incubated with SpnL under the same conditions, and the kinetic isotope effect is determined from the change of the enrichment ratio in the remaining SpnL substrate or the resulting SpnL product, which is the same method applied for the kinetic isotope effect studies of the SpnF reaction. In the latter case, it is possible to determine the kinetic isotope effect regardless of the concentration of labeled and unlabeled substrate. However, the former case requires the precise measurement of the concentrations of the labeled and unlabeled substrates because kinetic parameters such as V_{\max} or K_M are determined based on knowing the concentrations of substrate and enzyme. Thus, the concentration of SpnL natural substrate and deuterium-labeled SpnL substrate analog were determined using par-methoxyacetophenone as an internal reference, which was selected due to its high

stability and lack of inhibitory activity towards SpnL and non-interference with both substrate and product in HPLC analysis.

Initially, the kinetic parameters of SpnL natural substrate and C12-D SpnL substrate analog were determined by general kinetic experiments, as described in Section 3.2.8, followed by statistical analysis (**Figure 3-12**).^{166, 167} The kinetic isotope effect was calculated based on these kinetic parameters (**Figure 3-13**). The value of $^{12}\text{C}(V/K)$ corresponds to an inverse secondary kinetic isotope effect. In addition, measurement by the competitive experiment of SpnL reaction with SpnL natural substrate and C12-D substrate analog gave a kinetic isotope effect of 0.965 ± 0.005 , which also corresponds to an inverse kinetic isotope effect (**Figure 3-14**). Thus, the overall result is a slightly inverse kinetic isotope effect at the C-12 position. If the rate determining step is the first step, this result can rule out the Michael addition mechanism. However, the kinetic isotope effect data is more consistent with the Michael addition mechanism if the rate determining step is the last step because the expected kinetic isotope effect is a unity for the Rauhut-Currier type mechanism, and inverse for the Michael addition mechanism, as depicted in **Figure 3-6**. Thus, it is ambiguous to conclude which mechanism is operative in the SpnL reaction.

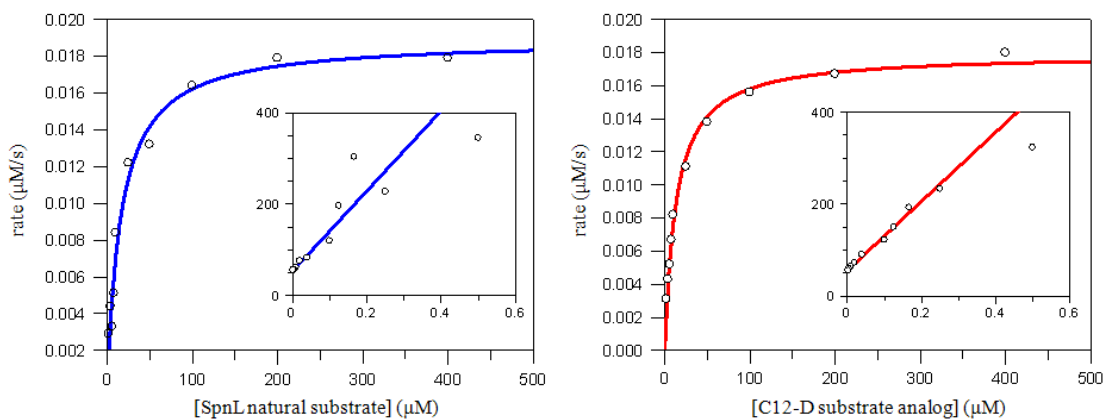


Figure 3-12. Determination of kinetic parameters for the SpnL natural substrate and C12-D substrate analog

	SpnL natural substrate	C12-D SpnL substrate analog
V_{\max}	0.0189 ± 0.0008 ($\mu\text{M/s}$)	0.0179 ± 0.0003 ($\mu\text{M/s}$)
K_M	16.6410 ± 2.4549 (μM)	13.4508 ± 0.9267 (μM)
$^{12}\text{C}/^{13}\text{C} (V/K) = 0.88 \pm 0.12$		

Figure 3-13. Kinetic parameters for the SpnL natural substrate and C12-D substrate analog, and the kinetic isotope effect determined under the direct comparison conditions.

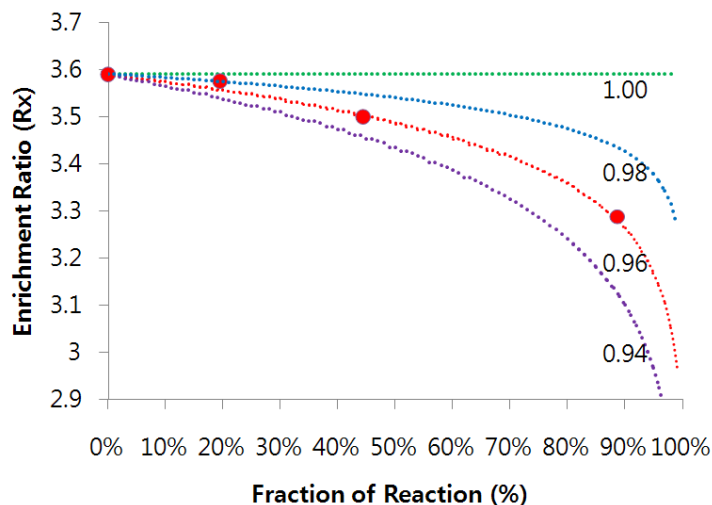


Figure 3-14. Plot of enrichment ratio (R_x) versus reaction progress for C12-D kinetic isotope effect of the SpnL.

Apparently, additional kinetic isotope effect experiments with the C13-D SpnL substrate analog should be performed to differentiate the hypothetical SpnL reaction

mechanisms. As of current, the kinetic isotope effect study with this deuterium-labeled SpnL substrate analog is still in progress. Taken together of the kinetic isotope effect results for both the C-12 and the C-13 position will give sufficient information to determine the mechanism of the SpnL reaction conclusively.

3.3.6. Biochemical Studies of the SpnL-Catalyzed Cyclization using the C13-F SpnL Substrate Analog

3.3.6.1. *In vitro* activity assay of SpnL with C13-F SpnL substrate analog

The SpnL-catalyzed cyclization reaction is considered to be initiated by either nucleophilic addition at the C-13 position in the Rauhut-Currier type mechanism or deprotonation at the C-12 position in the Michael addition mechanism. To distinguish between the two mechanisms, a C13-F SpnL substrate analog was designed for the detection of SpnL-substrate adduct. The C13-F SpnL substrate analog is expected to inactivate the catalytic function of SpnL as a suicide inactivator by covalent modification of the nucleophilic amino acid residue in SpnL, if it proceeds through the Rauhut-Currier type mechanism. In contrast, the C13-F SpnL substrate analog is expected to be a substrate for SpnL, which should be able to transform it to the C13-F-containing tetracyclic product, if it uses the Michael addition mechanism (**Figure 3-5**).

In order to test whether the C13-F analog is a substrate for SpnL, an *in vitro* activity assay of SpnL was performed by incubating the C13-F analog (100 μ M) with SpnL (5 μ M) in pH 8.0 Tris buffer (50 mM) at 30 °C for 30 min or for 4 hr. No turnover was observed for the C13-F analog, while SpnL natural substrate was completely transformed into SpnL product in 30 min (**Figure 3-15**). This result clearly demonstrated

that C13-F analog was not a substrate for SpnL. However, it is not clear whether SpnL-catalyzed cyclization proceeds through the Rauhut-Currier type mechanism. The strong electronegativity of fluoride at C-13 position could affect the reactivity with SpnL. Also, the slightly bulkier fluoride in the C13-F analog could make it difficult to fit in the active site of SpnL. Overall, many factors can have an effect on the activity of SpnL towards C13-F analog leading to no turnover of C13-F analog into C13-F-containing SpnL product. Therefore, another set of *in vitro* activity assays of SpnL was used to verify the possible inhibitory activity of C13-F analog for SpnL-catalyzed cyclization.

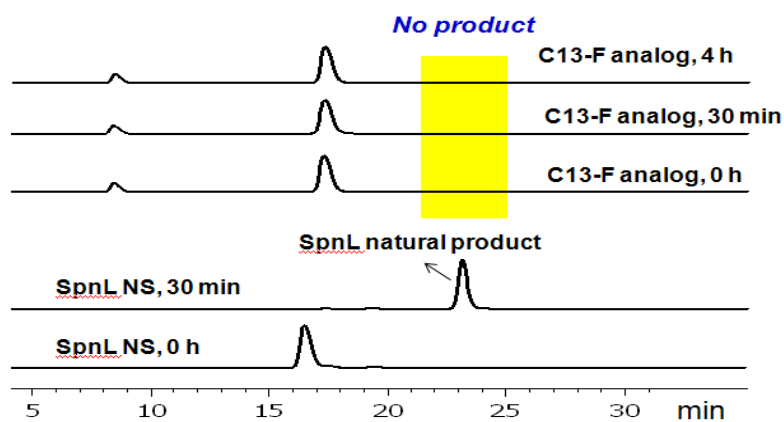


Figure 3-15. HPLC trace of SpnL-catalyzed cyclization using C13-F analog

3.2.6.2. Competition assay of SpnL with SpnL natural substrate and C13-F SpnL natural substrate analog

To test the inhibitory activity of C13-F analog on SpnL-catalyzed cyclization, SpnL (10 μM) was incubated with a 1:4 mixture of SpnL natural substrate and C13-F analog (100 μM and 400 μM) at 30 $^{\circ}\text{C}$ for several hr. The results of the *in vitro* activity assay are shown in **Figure 3-16**, depicting that a small amount of SpnL natural substrate was transformed into SpnL product, and a large amount of SpnL natural substrate still

remained in the mixture. In addition, there was no obvious change of the C13-F analog peak, even after 4 hr of incubation. Although the inhibitory mode of action was elusive, this result demonstrated that C13-F analog seemed to block the SpnL-catalyzed cyclization of SpnL natural substrate into SpnL product. Originally, C13-F analog was designed as a suicide inactivator (namely, mechanism-based inhibitor) to covalently modify the amino acid residue in the active site of SpnL if the SpnL reaction proceeds through the Rauhut-Currier type mechanism. Based on the above preliminary data, further experiments were performed to verify the inhibitory activity of C13-F analog in SpnL-catalyzed cyclization.

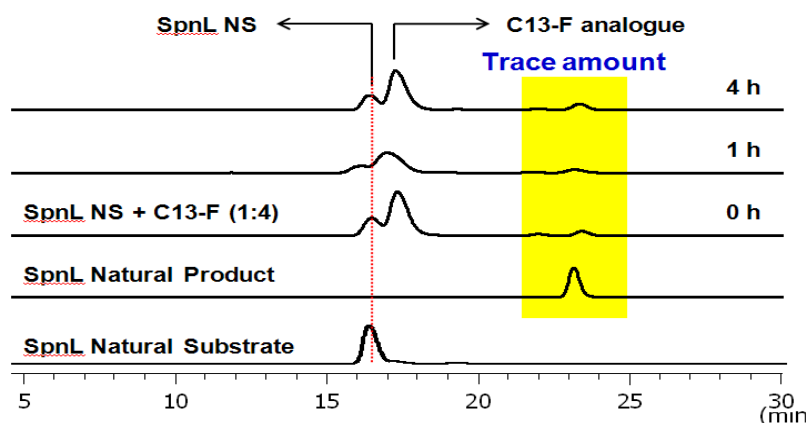


Figure 3-16. HPLC trace of SpnL-catalyzed cyclization using SpnL and C13-F analog

3.3.6.3. Preincubation *in vitro* activity assay of SpnL with SpnL natural substrate and C13-F SpnL substrate analog

A mechanism-based inhibitor is defined as a substrate analog, which can form an irreversible complex with an enzyme through a covalent bond during normal reaction catalysis, resulting in the complete inactivation of the enzyme. Thus, if an enzyme reacts with a mechanism-based inhibitor, its catalytic activity should decrease in proportion to

the exposure time to the inhibitor without recovery. Preincubation *in vitro* activity assays were subsequently carried out to detect the change in activity of SpnL, depending on the preincubation time with the C13-F analog.

A solution containing SpnL (20 μM) and C13-F analog (500 μM) in pH 8 Tris buffer (50 mM) was incubated at 30 $^{\circ}\text{C}$ for varied length of time (5, 10, 15, and 30 min). SpnL natural substrate (500 μM) was then added to each of the reaction mixtures. After additional incubation at 30 $^{\circ}\text{C}$ for 40 min to complete the SpnL-catalyzed reaction for SpnL natural substrate, the reaction mixture was quenched, precipitated, and analyzed by HPLC (**Figure 3-17, Right**). As a control reaction, the same procedure was performed without C13-F analog (**Figure 3-17, Left**). In the case of SpnL preincubation with C13-F analog, no conversion of SpnL natural substrate to SpnL product was observed even after only 5-min preincubation, and C13-F analog remained unchanged for both the given reaction time, and after 24 hr (data not shown). In contrast, SpnL preincubated without C13-F analog was still able to catalyze the SpnL reaction, although its catalytic ability decreased depending on the preincubation time.

These observations suggest two possible explanations for the inhibitory mechanism of C13-F analog for SpnL reaction. First, the C13-F analog may bind tightly to the active site of SpnL, and inactivate the activity of SpnL even though the C13-F analog is still technically a reversible inhibitor. Second, the C13-F analog may be a true suicide inactivator of SpnL. In order for the C13-F analog to be a suicide inactivator, the C13-F analog should play its role to covalently modify an active site residue in SpnL.

Thus, the next experiment was focused on elucidating the target of the C13-F analog inhibition, assuming that C13-F analog is an irreversible inhibitor.

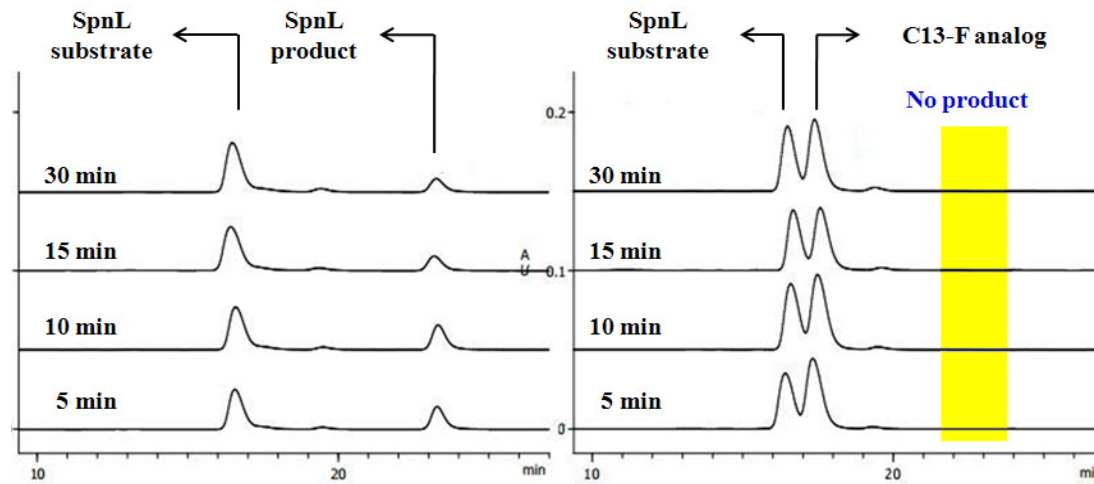


Figure 3-17. HPLC trace of the SpnL reaction for the preincubation experiment. Left: preincubation of SpnL without C13-F analog, Right: preincubation of SpnL with C13-F analog

3.3.6.4. *In vitro* activity assay of SpnL using the SpnL natural substrate and C13-F analog with L-glutathione

In this experiment, the effect of L-glutathione as a mimic of the active site to react with the C13-F analog was studied. According to Hak Joong Kim's thesis, incubation of SpnL natural substrate (2 mM) with L-glutathione (3 mM) in pH 8 Tris buffer (50 mM) at 30 °C overnight resulted in the formation of an adduct between SpnL natural substrate and L-glutathione as determined by MS. Thus, addition of L-glutathione may trigger the SpnL catalysis as glutathione may act as an exogenous nucleophile to initiate the SpnL reaction.

A solution containing SpnL (10 μ M), L-glutathione (0, 250, or 2,000 μ M) and C13-F analog (250 μ M) in pH 8.0 Tris buffer (50 mM) was preincubated at 30 °C for 5

min, after which time SpnL natural substrate (125 μM) was added to each of the reaction mixtures. After additional incubation at 30 $^{\circ}\text{C}$ for 30 min to complete the SpnL reaction, the reaction mixture was quenched, the protein precipitated, and the supernatant analyzed by HPLC. As a control reaction, the same experiment was performed with SpnL preincubation in the presence of L-glutathione, but without C13-F analog. SpnL preincubated with C13-F analog didn't catalyze the reaction in the presence of L-glutathione regardless of its concentration. Even though there has been no obvious evidence for L-glutathione to play a role as a cofactor in SpnL, this result demonstrated that L-glutathione is at least not the nucleophile to initiate the SpnL reaction, and inactivation of SpnL is not related to the depletion of L-glutathione. Thus, the focus was turned to the covalent modification of SpnL by C13-F analog, as originally intended. Before going to the part of covalent modification study, some of kinetic experiments were performed in next section to show the inhibition mode of C13-F analog.

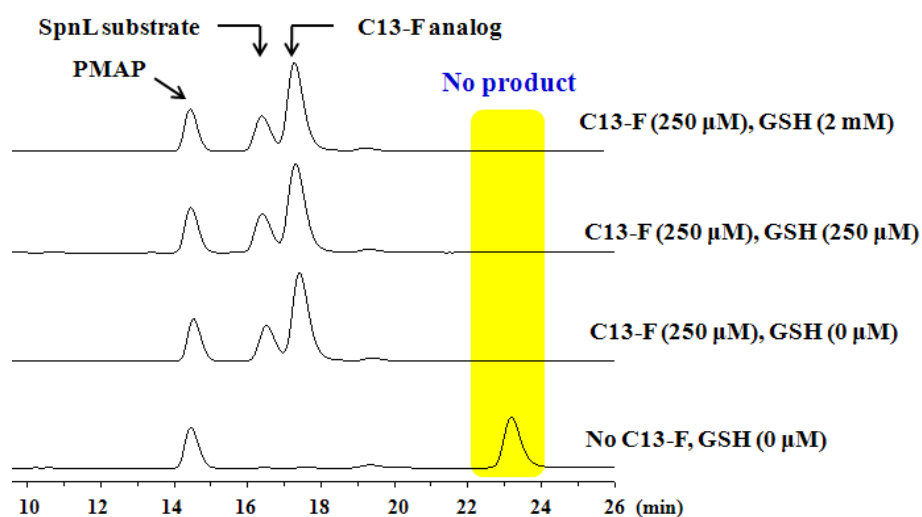
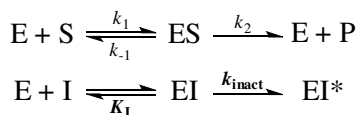


Figure 3-18. HPLC trace of SpnL reaction for the test of l-glutathione depletion by C13-F analog.

3.3.6.5. Inhibition kinetic study of SpnL using SpnL natural substrate and C13-F SpnL substrate analog

A. Theoretical background for irreversible inactivation by mechanism-based inhibitor

The efficiency of mechanism-based inhibitors, such as suicide inhibitors, can be expressed in terms of the kinetic parameters K_I and k_{inact} , and the partition ratio, which are conventionally determined by a dilution assay. In this method, the enzyme is preincubated with the suicide inhibitor followed by adding the substrate and measuring the product formation. Kinetic parameters are then determined from the rate of irreversible loss of enzyme activity at various inhibitor concentrations.¹⁶⁹ Kinetic calculation is shown as follows:



The general expression for the velocity (or rate) of enzymatic reaction can be expressed as:

$$d[P]/dt = k_2[ES] \dots\dots\dots (1)$$

The overall rate of production of [ES] is expressed as below. It is assumed that [ES] remains constant until the substrate for the enzymatic reaction is almost depleted, if the substrate is in excess of the enzyme. The change of [ES] over time should be zero at the steady-state.

$$d[ES]/dt = k_1[E][S] - k_{-1}[ES] - k_2[ES] = 0 \dots\dots\dots (2)$$

which can be rearranged to

$$[ES] = k_1[E][S]/(k_{-1}+k_2) \dots\dots\dots (3)$$

Dividing both sides by k_1 and solving for $[ES]$,

$$[ES] = k_1[E][S]/(k_{-1}+k_2) = [E][S]/K_M \dots\dots\dots (4)$$

where $K_M = (k_{-1}+k_2)/k_1$, which is also known as the Michaelis constant.

In the presence of inhibitor, the total enzyme concentration can therefore be expressed as below:

$$K_I = [E][I]/[EI] \dots\dots\dots (5)$$

$$[E]_T = [E] + [ES] + [EI] + [EI^*] \dots\dots\dots (6)$$

which can be rearranged to

$$[E]_T - [EI^*] = [E] + [EI] + [ES] = [E] + [E][I]/K_I + [E][S]/K_M = [E](1 + [I]/K_I + [S]/K_M) \dots\dots\dots (7)$$

$$[E] = ([E]_T - [EI^*])/(1 + [I]/K_I + [S]/K_M) \dots\dots\dots (8)$$

If it is substituted for the equation (4),

$$[ES] = k_1[E][S]/(k_{-1}+k_2) = [E][S]/K_M = ([S]/K_M) \cdot \{([E]_T - [EI^*])/(1 + [S]/K_M + [I]/K_I)\} \dots\dots\dots (9)$$

$$d[P]/dt = k_2[ES] = (k_2[S]) \cdot \{([E]_T - [EI^*])/(1 + [S]/K_M + [I]/K_I)\}/K_M \dots\dots\dots (10)$$

The same procedure can be used for the second part of inhibition reaction.

$$d[EI^*]/dt = k_{inact}[EI] = k_{inact}[E][I]/K_I = k_{inact}([I]/K_I) \cdot ([E]_T - [EI^*])/(1 + [I]/K_I + [S]/K_M) \dots\dots\dots (11)$$

$$d[EI^*]/([E]_T - [EI^*]) = k_{inact} \cdot ([I]/K_I)/(1 + [I]/K_I + [S]/K_M) \dots\dots\dots (12)$$

If $[EI^*] = 0$ at $t = 0$, it integrates to:

$$-\ln\{([E]_T - [EI^*])/[E]_T\} = k_{inact} \cdot ([I]/K_I)/(1 + [I]/K_I + [S]/K_M) \cdot t \dots\dots\dots (13)$$

Solving for $[EI^*]$ yields

$$[EI^*] = [E]_T \cdot \{1 - e^{-(k_{inact} \cdot ([I]/K_I)) / (1 + [I]/K_I + [S]/K_M)} \cdot t\} \dots\dots\dots (14)$$

$$\begin{aligned} d[P]/dt &= (k_2[S]/K_M) \cdot \{([E]_T - [EI^*]) / (1 + [S]/K_M + [I]/K_I)\} \\ &= (k_2[S]/K_M) \cdot \{([E]_T - [E]_T \cdot \{1 - e^{-(k_{inact} \cdot [I]) / (K_I(1 + [I]/K_I + [S]/K_M))} \cdot t\}) / (1 + [S]/K_M + [I]/K_I)\} \\ &= (k_2[S][E]_T / K_M) \cdot \{e^{-(k_{inact} \cdot [I]) / (K_I(1 + [I]/K_I + [S]/K_M))} \cdot t\} / (1 + [S]/K_M + [I]/K_I) \end{aligned} \dots\dots\dots (15)$$

If $[P] = 0$ at $t = 0$, it integrates to

$$[P] = (k_2[S][E]_T K_I / K_M k_{inact} [I]) \cdot \{1 - e^{-(k_{inact} \cdot [I]) / (K_I(1 + [I]/K_I + [S]/K_M))} \cdot t\} \dots\dots\dots (16)$$

where $K_M = 16.64 \pm 2.46 \text{ M}^{-1}$ and $V_{max} = 0.0189 \pm 0.0008 \text{ s}^{-1}$ for SpnL natural substrate.

It is simplified to

$$[P] = m_1 \cdot (1 - e^{-(m_2 t + m_3)}) \dots\dots\dots (17)$$

The parameters k_{inact} and K_I can be obtained by analyzing the plot between m_2 and $[I]$.

$$m_2 = k_{inact} \cdot ([I]/K_I) / (1 + [I]/K_I + [S]/K_M) \dots\dots\dots (18)$$

$$1/m_2 = (1 + [I]/K_I + [S]/K_M) / (k_{inact} \cdot ([I]/K_I)) = (K_I \cdot (1 + [S]/K_M)) / (k_{inact} \cdot [I]) + 1/k_{inact} \dots (19)$$

A plot of $1/m_2$ versus $1/[I]$ should result in a linear curve and the value of k_{inact} and K_I can be obtained from the intercept and slope of that curve.

If an inhibition assay is set up so that the concentration of inhibitor (C13-F analog) present in the incubation after addition of SpnL natural substrate is relatively small compared to the concentration of SpnL natural substrate and is assumed to have little effect on the SpnL reaction, the rate of SpnL natural substrate turnover is expected to be directly proportional to the remaining active enzyme concentration expressed in %

activity by measuring the ratio of substrate and product. Experimentally, there are three options to measure the progress of the reaction, consumption of substrate, appearance of product, and inactivation of enzyme. In this inhibition assay, the concentration of remaining active enzyme was calculated by measuring the substrate turnover to product after a given preincubation period with inhibitor followed by additional incubation with an excess amount of substrate to complete turnover. For the calculation, integrated areas of substrate and product were normalized by an internal standard, and its turnover rate expressed in % activity of enzyme. The equation (14) doesn't need a term [S], a concentration of substrate because the remaining enzyme doesn't compete with inhibitor and

$$[EI^*]' = [E]_T \cdot \{1 - e^{-(k_{inact} \cdot ([I]/K_I) / (1 + [I]/K_I)) \cdot t}\} = [E]_T \cdot \{1 - e^{-k_{obs} \cdot t}\} \dots\dots\dots (20)$$

$$[E]_T - [EI^*]' = e^{-k_{obs} \cdot t} \dots\dots\dots (21)$$

where $k_{obs} = k_{inact} \cdot ([I]/K_I) / (1 + [I]/K_I)$, and its reciprocal is expressed as

$$1/k_{obs} = K_I/k_{inact} \cdot (1/[I]) + 1/k_{inact} \dots\dots\dots (22)$$

Thus, a plot of $1/k_{obs}$ versus $1/[I]$ is a straight line and the kinetic parameters, k_{inact} and K_I can be determined from the intercept and slope of this line.

B. *In vitro* inhibition assay of SpnL with C13-F analog

In order to determine the kinetic constants, K_I and k_{inact} , for the inhibition caused by the C13-F analog, an *in vitro* inhibition assay of SpnL was performed as follows. A solution containing the C13-F analog (1.5 μ M, 3.0 μ M, or 4.5 μ M) in pH 8.0 Tris buffer was preincubated with SpnL (1.0 μ M) at 30 °C for 10 sec or 20 sec. SpnL natural substrate (125 μ M) was then added into the reaction mixture. After incubation at 30 °C

for 30 min, the reaction mixture was quenched, the protein precipitated, and the supernatant analyzed by HPLC. As a control, the reaction was repeated without C13-F analog. The results are summarized in **Figure 3-19**, **Figure 3-20**, and **Figure 3-21**, showing that the averaged $k_{\text{obs}}[I]$ was $18,518 \text{ M}^{-1}\cdot\text{s}^{-1}$. According to Equation (19), the plot for $1/k_{\text{obs}}$ versus $1/[I]$ gave two kinetic parameters: $K_I = 0.58 \text{ } (\mu\text{M})$, and $k_{\text{inact}} = 0.058 \text{ (s}^{-1}\text{)}$.

Time (sec)	Control (no C13-F)		[C13-F] = 1.5 μM		[C13-F] = 3.0 μM		[C13-F] = 4.5 μM	
	% activity	$[E]_{\text{T}}-[EI^*]$	% activity	$[E]_{\text{T}}-[EI^*]$	% activity	$[E]_{\text{T}}-[EI^*]$	% activity	$[E]_{\text{T}}-[EI^*]$
Zero	100%	1.0 μM	100%	1.00 μM	100%	1.00 μM	100%	1.00 μM
10 sec	-	-	54%	0.54 μM	51%	0.51 μM	46%	0.46 μM
20 sec	-	-	47%	0.47 μM	43%	0.43 μM	41%	0.41 μM
k_{obs}	-		0.042 s^{-1}		0.048 s^{-1}		0.052 s^{-1}	
$k_{\text{obs}}/[I]$	-		$28,000 \text{ M}^{-1}\cdot\text{s}^{-1}$		$16,000 \text{ M}^{-1}\cdot\text{s}^{-1}$		$11,555 \text{ M}^{-1}\cdot\text{s}^{-1}$	
Avg ($k_{\text{obs}}/[I]$)	-		$18,518 \text{ M}^{-1}\cdot\text{s}^{-1}$					

Figure 3-19. Inhibition assay of SpnL with C13-F analog. As a control, SpnL activity was measured as 98.6% at 10 sec, and 94.5% at 20 sec)

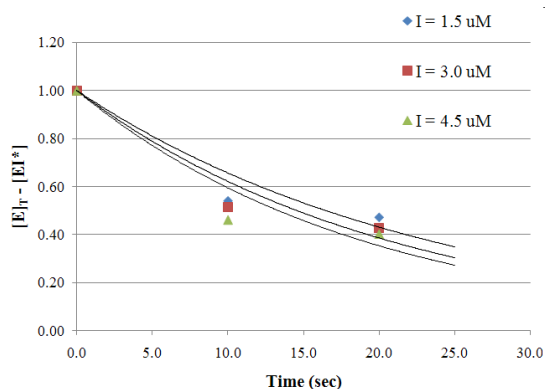


Figure 3-20. Inhibition assay results for various concentrations of the C13-F analog

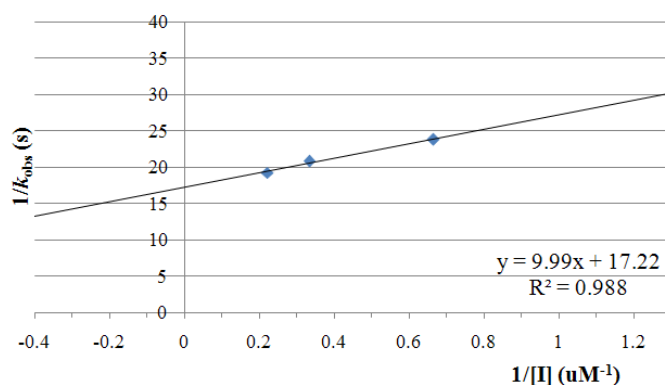


Figure 3-21. Plot for $1/k_{\text{obs}}$ versus $1/[I]$

The inhibition assays allowed the determination of two parameters of C13-F analog for the SpnL reaction: K_I and k_{inact} , showing both tight binding and rapid inactivation. The definition of k_{inact} is the rate when the inhibition occurs at maximal inactivation, and the definition of K_I is the concentration at which the rate is 50% k_{inact} . Thus, a low K_I value means tight binding between the inhibitor and enzyme at the first stage, and a high k_{inact} value means a rapid inactivation of enzyme. From the kinetic perspective, C13-F analog seems to be a good inhibitor of SpnL. These kinetic data justified for the next experimental step, MS experiment to find covalently modified SpnL.

3.3.6.6. MS experiments for the detection of covalently-modified SpnL with C13-F analog

The C13-F analog was designed to demonstrate the inactivation of SpnL by covalent modification based on the Rauhut-Currier type mechanism. A series of *in vitro* activity assays and inhibition assays seem to support the Rauhut-Currier type mechanism because the C13-F analog shows the inhibitory activity for SpnL reaction although the mechanism is still unknown. If SpnL makes a covalent bond with the C13-F analog by

excluding the fluorine atom during normal catalysis, the mass of the modified SpnL should increase by the molecular weight of the C13-F analog without the fluorine atom.

A solution containing SpnL (152 μ M) and C13-F analog (300 μ M) in pH 8.0 Tris buffer (50 mM) was incubated at 30 °C for 1 hr, and dialyzed at 4 °C against ammonium bicarbonate buffer (50 mM) to remove excess C13-F analog. The resulting solution was analyzed by MS. For comparison, a solution containing SpnL (152 μ M) and SpnL natural substrate (300 μ M) in pH 8.0 Tris buffer was also analyzed by MS. MS of SpnL itself was used as a reference.

The MS for the control reaction using SpnL treated with SpnL natural substrate shows two characteristic peaks of SpnL (MW 32,754 Da; calculated isotopically averaged MW 32,782 Da) and the glucuronylated SpnL (MW 32,931 Da = 32,754 + 177 Da), which is a common post-translational modification observed for His₆-tagged proteins produced in *E. coli* (**Figure 3-22**).¹⁶⁹ The MS for the control reaction using SpnL only also gave two peaks, corresponding to the native SpnL and the glucuronylated SpnL. This is identical to the control reaction of SpnL treated with SpnL natural substrate (**Figure 3-23**). This means that SpnL performs its catalytic role without any modification of its active-site residue. However, MS data for SpnL incubated with C13-F analog presents an interesting result showing the two peaks of putative SpnL and its glucuronylated form increased by approximately 545 Da (**Figure 3-24**). The first peak corresponds to the native form of SpnL covalently modified with the C13-F analog (MW 33,300 Da = 32,754 + 547 - 1 Da), and the second peak corresponds to the glucuronylated form of SpnL covalently modified with the C13-F analog (MW 33,477

$\text{Da} = 32,754 + 547 + 177 - 1 \text{ Da}$). A plausible covalent modification of SpnL by the C13-F analog is depicted in **Figure 3-25**.

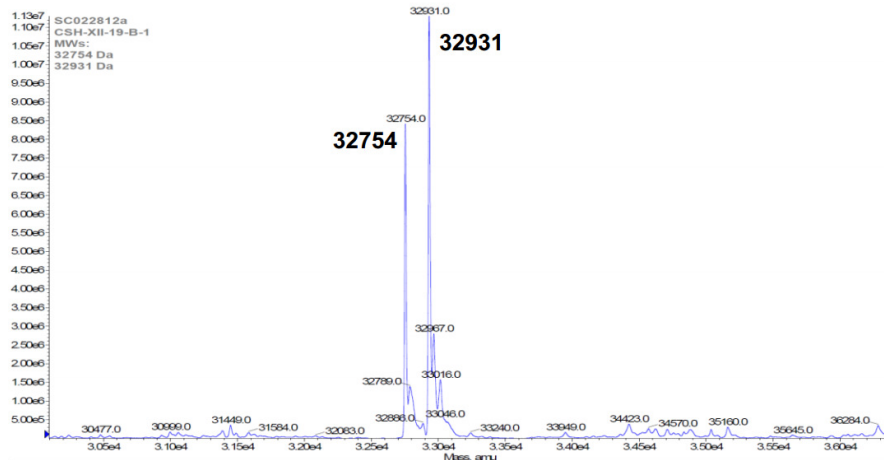


Figure 3-22. ESI-MS data of SpnL incubated with SpnL natural substrate

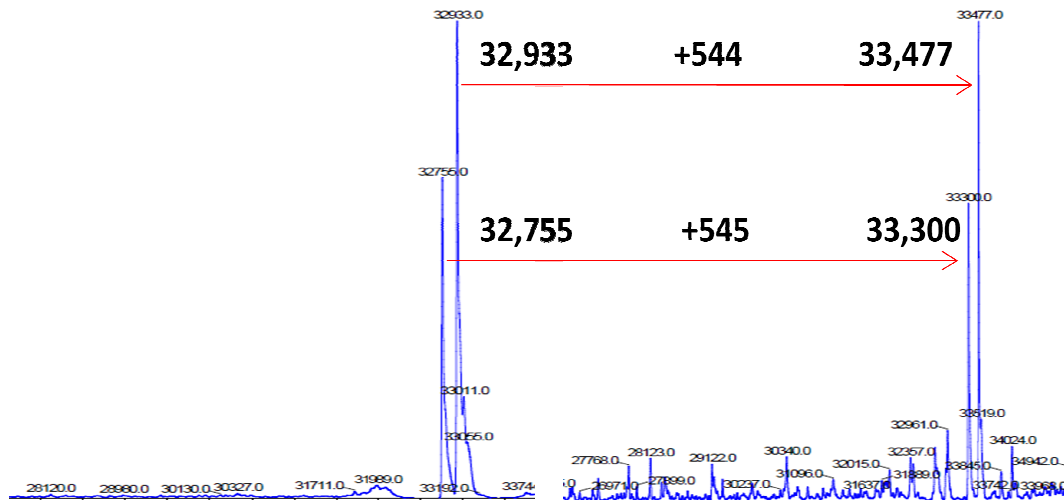


Figure 3-23. ESI-MS spectroscopic data of SpnL

Figure 3-24. ESI-MS data of SpnL incubated with C13-F analog

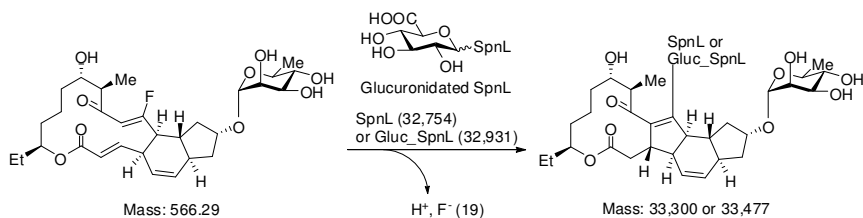


Figure 3-25. Plausible covalent-modification of SpnL (or glucuronylated SpnL) by the C13-F analog

Above MS data strongly suggests that the C13-F analog is first attacked by a nucleophile of SpnL (or its glucuronylated form) and covalently bound to SpnL by expelling a fluoride anion (**Figure 3-25**). Put in another way, a deprotonated nucleophilic residue of SpnL (such as a cysteine) attacks an electrophilic position of C13-F analog (almost certainly the C-13 position, due to the strongly electronegative fluorine-substituent) to make a covalent intermediate. After cyclization and protonation at the C-2 position, deprotonation at the C-14 position coupled with removal of the fluoride anion at the C-13 position instead of the SpnL nucleophile produced a covalently-modified SpnL (or its glucuronylated form). The position of nucleophilic attack from SpnL on the C13-F analog is expected to be the C-13 position, but the identity of the nucleophilic residue of SpnL is not immediately apparent. The following experiments were conducted to detect the nucleophile of SpnL after covalent modification of SpnL with the C13-F analog.

To identify the covalent modification site of SpnL, SpnL was first incubated with the C13-F analog, and then was digested with trypsin, a serine protease, which cleaves peptide chain mainly at the carboxyl side of amino acids lysine and arginine, except when either is followed by a proline. This resulting solution was subjected to ESI-MS analysis, which is expected to show the change in the mass of fragments from SpnL and SpnL covalently-modified with C13-F analog. **Figure 3-26** lists the possible fragments of SpnL

after treatment with trypsin (SpnL used in this experiment was SpnL-Hi6-tag, but its sequence numbering corresponds to natural SpnL. Natural SpnL starts with the residues MESIF, noted as number 1). The recorded MS data is shown **Figure 3-27**. Most peaks in the MS are assigned based on their expected MS values, shown in **Figure 3-26**. By comparing the MS from the control (SpnL only) and C13-F (SpnL incubated with C13-F) reactions, two new peaks are identified (**a**=*ModiFrag5* and **b**=*ModiFrag4* in **Figure 3-27**) which show a mass increase of 547 Da, corresponding to that of the C13-F analog without fluoride. They have been designated “*ModiFrag4*” and “*ModiFrag5*” in **Figure 3-26**. The calculated molecular weight of Fragment 4 is 2248.58 (corresponding to 2249.14 in MS), and that of its modified fragment, *ModiFrag4*, is 2795.25 (calculated as 2248.58 + 546.67; corresponding to 2795.40 in MS). The calculated molecular weight of Fragment 5 is 733.84 (corresponding to 734.36 in MS), and that of its modified fragment, *ModiFrag5*, is 1280.51 (calculated as 733.84 + 546.67; corresponding to 1280.64 in MS). These results indicate that both fragment 4 and fragment 5 may contain the amino acid residue covalently linked to the C13-F analog. Interestingly, both fragments have a cysteine residue, Cys60 and Cys71, respectively. Another cysteine residue-containing fragment 16 is not modified by the C13-F analog (there is no peak near 2060.45, corresponding to the sum of 1513.78 + 546.67).

Fragment	Amino acids sequences and its calculated mass
Fragment 1	MGSSHHHHHHSSGLVPR; 1900.06
Fragment 2	GSH ₁ MESIFDALAHGRPLHHGYWAGGYR; 3023.33
Fragment 3	₂₅ EDAGATPWSDAADQLTDLFIDK; 2379.51
Fragment 4	₄₇ AALRPGAHFLDLGCGNGQPVVR; 2248.58
ModiFrag 4	₄₇ AALRPGAHFLDLGCGNGQPVVR-(C13-F); 2795.25 (= 2248.58 + 546.67)
Fragment 5	₆₉ AACASGVR; 733.84
ModiFrag 5	₆₉ AACASGVR-(C13-F); 1280.51 (= 733.84 + 546.67)
Fragment 6	₇₇ VTGITVNAQHLAAATR; 1622.84
Fragment 7	₉₃ LANETGLAGSLEFDLVDGAQLPYPDGFFQAAWAMQSVVQIVDQAAAIR; 5095.70
Fragment 8	₁₄₁ EVHR; 539.59
Fragment 9	₁₄₅ ILEPGGR; 740.86
Fragment 10	₁₅₂ FVLGDIITR; 1033.23
Fragment 11	₁₆₁ VR; 273.33
Fragment 12	₁₆₃ LPEEYAAVWTGTTAHTLNSFTALVSEAGFEILEVTDLTAQTR; 4555.02
Fragment 13	₂₀₅ CMVSWYVDELLR; 1513.78
Fragment 14	₂₁₇ K; 146.19
Fragment 15	₂₁₈ LDELAGVEPAAVGTYQQR; 2045.27
Fragment 16	₂₃₆ YLGDIAAK; 849.98
Fragment 17	₂₄₄ HGPGPAQLIAVAEYR; 1649.87
Fragment 18	₂₆₀ K; 146.19
Fragment 19	₂₆₁ HPDYAR; 757.80
Fragment 20	₂₆₇ NEESMGFMLLQAR; 1525.75
Fragment 21	₂₈₀ K; 146.19
Fragment 22	₂₈₁ K; 146.19
Fragment 23	₂₈₂ QS; 232.22

Figure 3-26. Expected MS of fragments of SpnL treated with trypsin after incubation with the C13-F analog

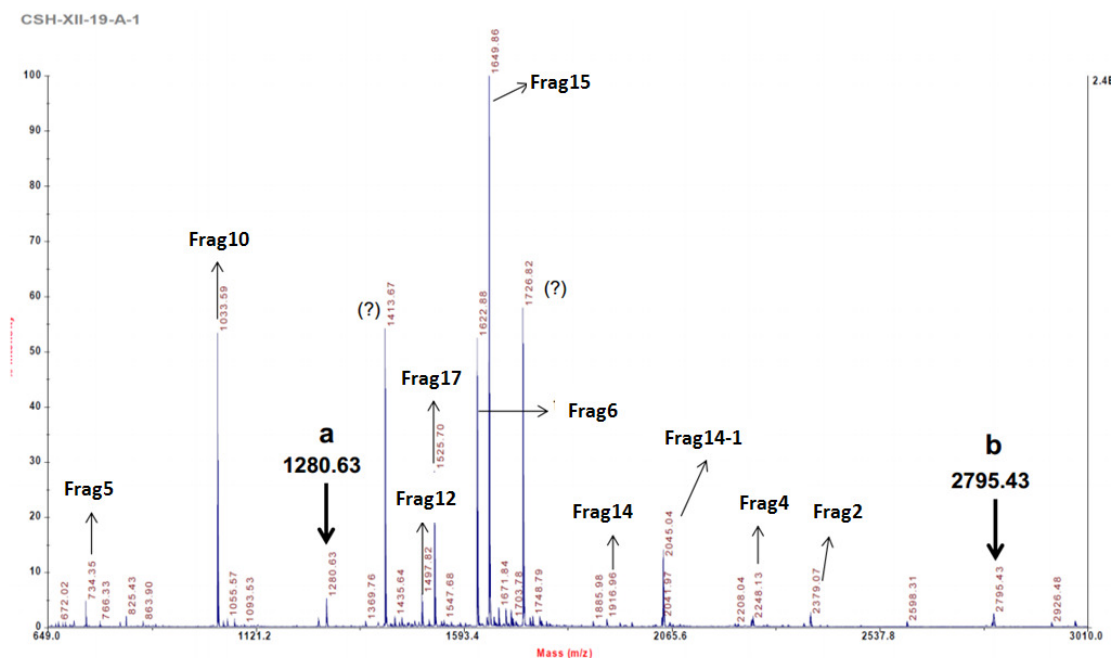


Figure 3-27. MS for SpnL, which was treated with 2 equivalent of C13-F analog and trypsin. Peaks **a** and **b** are new peaks not found in the MS of the trypsin-digested sample that wasn't incubated with C13-F analog.

However, it is unexpected that two different sites on SpnL are modified by the C13-F analog. It is probable that the 2:1 ratio of C13-F analog versus SpnL caused the modification of two sites in one SpnL. In other words, it is possible that either *ModiFrag4* and/or *ModiFrag5* may be an artifact, which is modified by the C13-F analog regardless of the reaction mechanism. While 1 equivalent of SpnL and C13-F analog may make an interaction which results in the inactivation of SpnL (namely, specific covalent modification based on the reaction mechanism), the extra C13-F analog may further modify a different site of the inactivated SpnL (namely, non-specific modification). Thus, the next experiment was designed to show the “real” modification site of SpnL by using a 0.5:1.0 ratio of C13-F analog to SpnL. In theory, a half equivalent of C13-F analog is expected to modify one specific site of SpnL (specific covalent modification) based on

the Rauhut-Currier type mechanism. After incubation of SpnL (152 μM) and the C13-F analog (75 μM) at 30 $^{\circ}\text{C}$ for 1 hr, followed by dialysis and trypsin-digestion at 37 $^{\circ}\text{C}$ for 6 hr, the resulting solution was analyzed by MS. This MS looks very similar to the previous MS result although the peaks corresponding to *ModiFrag4* and *ModiFrag5* became smaller than the unmodified peaks of Fragment 4 and Fragment 5 (**Figure 3-28**). This means that formation of either Fragment 4 and/or Fragment 5 may reflect a non-specific nucleophilic addition of SpnL towards its substrate. In other word, Fragment 4 and/or Fragment 5 are covalently bound to the C13-F analog in a manner that doesn't depend on the reaction mechanism.

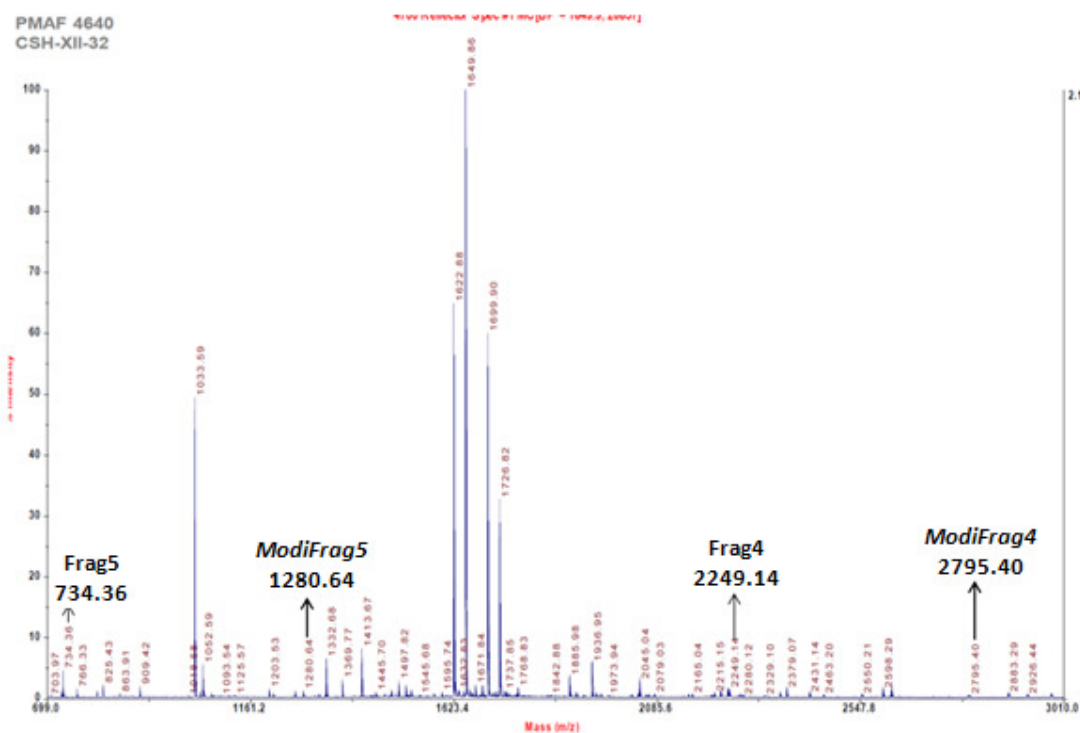


Figure 3-28. MS for SpnL, which was treated with 0.5 equivalent of C13-F analog and trypsin.

The two sites of SpnL, corresponding to Fragment 4 and Fragment 5, seem to be covalently modified with the C13-F analog independently and by different mechanisms.

Notably, the peak corresponding to doubly modified SpnL, with two molecules of C13-F analog, was not observed in any of the MS. The next experiments were focused on finding the amino acid residues of Fragment 4 and Fragment 5, which are involved in the covalent modification of SpnL with the C13-F analog.

3.3.6.7. MS experiments for the detection of covalently-modified SpnL mutant (C71A) with C13-F analog

Based on the Rauhut-Currier type mechanism, any close by nucleophile in the catalytic site of SpnL may make a covalent bond with C13-F analog. Many different residues can play a role as the nucleophile, such as lysine, serine, threonine, cysteine, tyrosine, asparatate, and glutamate. From the amino acid sequence of Fragment 4 and Fragment 5, the cysteine residue in each fragment is the most likely nucleophilic amino acid residue. To verify the modification site of SpnL, three mutants of SpnL (C60A, C71A, and C205A), prepared by Dr. Kim, a former lab member, were used instead of SpnL. Previous *in vitro* activity assays by Dr. Kim showed that C71A and C205 mutations had no effect on the activity of SpnL, while the C60A mutant lost its catalytic activity. This result suggested that the C60 residue in SpnL is important for its activity. Based on the results from the *in vitro* activity assay of SpnL mutants and MS experiments of SpnL modification with the C13-F analog, SpnL C60A and C71A mutants were chosen for the MS experiments to determine the specific residue involved in the covalent bond formation of SpnL with the C13-F analog.

As a control, a solution containing SpnL mutant (152 μ M) and SpnL natural substrate (300 μ M) in pH 8.0 Tris buffer (50 mM) was incubated at 30 °C for 1 hr,

dialyzed at 4 °C against ammonium bicarbonate buffer (50 mM), trypsin-digested at 37 °C for 6 hr, and analyzed by MALDI-ESI-MS. For the preparation of *ModiFrag4* and *ModiFrag5* for MS analysis, the C13-F analog (300 μM) was included instead of SpnL natural substrate for the SpnL modification in a separate solution, followed by the same procedures. The result for the SpnL C71A mutant is shown in **Figure 3-29**, indicating that only Fragment 4 is modified to *ModiFrag4*, corresponding to the molecular weight of 2794.40 in MS. Interestingly, Fragment 5, containing C71A, is not modified with the C13-F analog because there is no peak at $1248.45 = 701.78 + 546.67$; ${}_{69}\text{AAAASGVR} = 701.78$). This result clearly demonstrated that Cys60 is modified and Cys71 may also be a modification site on SpnL of the C13-F analog. Unfortunately, the result for SpnL C60A mutant didn't show the proper MS (data not shown) due to problems of low expression and poor purification. Overall, the SpnL mutant study supported that Cys60 and Cys71 are the modification sites of SpnL by the C13-F analog. To pursue the direct evidence for the covalent bonding of cysteine residue with C13-F analog, ESI MS/MS experiments were performed as follows.

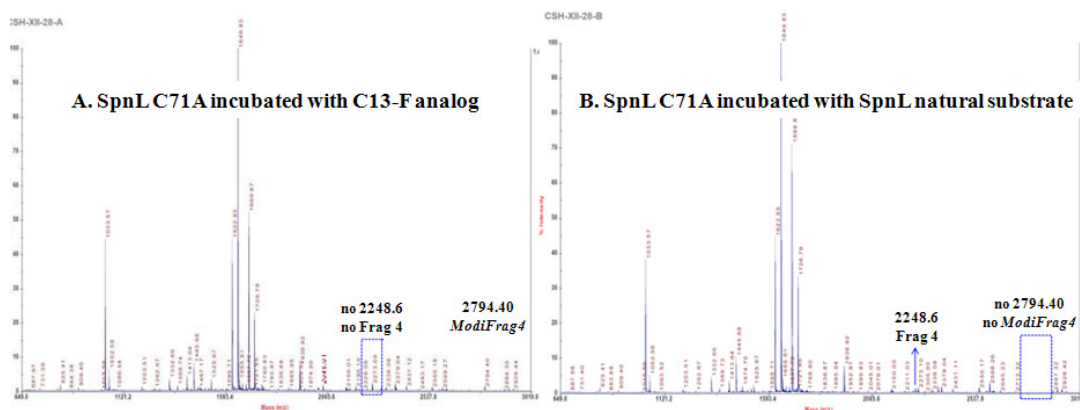


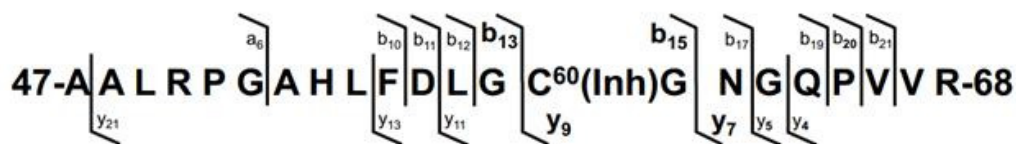
Figure 3-29. MS for SpnL C71A mutant. (A) SpnL C71A incubated with C13-F analog, and (B) SpnL

C71A incubated with SpnL natural substrate.

After SpnL (152 μ M) was incubated with the C13-F analog (300 μ M) at 30 $^{\circ}$ C for 1 hr, dialyzed against ammonium bicarbonate buffer (50 mM), and trypsin-digested at 37 $^{\circ}$ C for 6 hr, the resulting solution was analyzed by ESI MS/MS. Prior to the analysis of the MS results, the ion re-fragmentation of fragment 4 is analyzed based on the protein fragmentation ion calculator, which is provided by the website (<http://db.systemsbiology.net/proteomicsToolkit/FragIonServlet.html>, accessed Nov 1, 2013, **Figure 3-30** and **Figure 3-31**).

Seq	#	A	B	C	X	Y	Z	# (+1)
A	1	44.07669	72.08679	89.11735	-	2249.59871	2232.56815	22
A	2	115.15549	143.16558	160.19615	2204.51413	2178.51991	2161.48935	21
L	3	228.31493	256.32503	273.35559	2133.43533	2107.44111	2090.41055	20
R	4	384.50241	412.51251	429.54307	2020.27589	1994.28167	1977.25111	19
P	5	481.61909	509.62919	526.65975	1864.08841	1838.09419	1821.06363	18
G	6	538.67101	566.68111	583.71167	1766.97173	1740.97751	1723.94695	17
A	7	609.74981	637.75991	654.79047	1709.91981	1683.92559	1666.89503	16
H	8	746.89089	774.90099	791.93155	1638.84101	1612.84679	1595.81623	15
L	9	860.05033	888.06043	905.09099	1501.69993	1475.70571	1458.67515	14
F	10	1007.22689	1035.23699	1052.26755	1388.54049	1362.54627	1345.51571	13
D	11	1122.31549	1150.32559	1167.35615	1241.36393	1215.36971	1198.33915	12
L	12	1235.47493	1263.48503	1280.51559	1126.27533	1100.28111	1083.25055	11
G	13	1292.52685	1320.53695	1337.56751	1013.11588	987.12166	970.09110	10
C	14	1395.66565	1423.67575	1440.70631	956.06396	930.06975	913.03919	9
G	15	1452.71757	1480.72767	1497.75823	852.92517	826.93095	809.90039	8
N	16	1566.82141	1594.83151	1611.86207	795.87324	769.87903	752.84846	7
G	17	1623.87333	1651.88343	1668.91399	681.76940	655.77519	638.74462	6
Q	18	1752.00405	1780.01415	1797.04471	624.71749	598.72327	581.69271	5
P	19	1849.12073	1877.13083	1894.16139	496.58677	470.59254	453.56199	4
V	20	1948.25329	1976.26339	1993.29395	399.47008	373.47586	356.44530	3
V	21	2047.38585	2075.39595	2092.42651	300.33753	274.34331	257.31275	2
R	22	2203.57333	2231.58343	-	201.20496	175.21075	158.18018	1

Figure 3-30. Fragment ion table in average mass for Fragment 4 in SpnL.



N-terminal												
b-NH ₃	---	---	---	395.2	492.3	549.3	620.4	757.4	870.5	1017.6	1132.6	
b-H ₂ O	---	---	---	---	---	---	---	---	---	---	1131.6	
b	---	143.1	256.2	412.3	509.3	566.3	637.4	774.4	887.5	1034.6	1149.6	
b+H ₂ O	---	---	---	---	---	---	---	---	---	---	---	
#	1	2	3	4	5	6	7	8	9	10	11	
47 -	A	A	L	R	P	G	A	H	L	F	D	-
#	22	21	20	19	18	17	16	15	14	13	12	
C-terminal												
y	---	2177.1	2106.1	1993.0	1836.9	1739.9	1682.8	1611.8	1474.7	1361.7	1214.6	
y-NH ₃	---	2160.1	2089.1	1976.0	1819.9	1722.8	1665.8	1594.8	1457.7	1344.6	1197.6	
y-H ₂ O	---	2159.1	2088.1	1975.0	1818.9	1721.9	1664.8	1593.8	1456.7	1343.7	1196.6	
N-terminal												
b-NH ₃	1245.7	1302.7	1405.7	1462.7	1576.8	1633.8	1761.8	1858.9	1958.0	2057.0	---	
b-H ₂ O	1244.7	1301.7	1404.7	1461.7	1575.8	1632.8	1760.9	1857.9	1957.0	2056.1	---	
b	1262.7	1319.7	1422.7	1479.8	1593.8	1650.8	1778.9	1875.9	1975.0	2074.1	---	
b+H ₂ O	---	---	---	---	---	---	---	---	1993.0	2092.1	---	
#	12	13	14	15	16	17	18	19	20	21	22	
-	L	G	C	G	N	G	Q	P	V	V	R	- 68
#	11	10	9	8	7	6	5	4	3	2	1	
C-terminal												
y	1099.6	986.5	929.5	826.5	769.4	655.4	598.4	470.3	373.3	274.2	175.1	
y-NH ₃	1082.5	969.5	912.4	809.4	752.4	638.4	581.3	453.3	356.2	257.2	158.1	
y-H ₂ O	---	---	---	---	---	---	---	---	---	---	---	

Figure 3-31. Re-fragmentation of unmodified fragment 4 from the trypsin-digested SpnL C71A mutant after preincubation with the C13-F analog

The MS results are shown in **Figure 3-32**. The re-fragmented ion corresponding to b_{12} was expected to have a $m/z = 1262.70$ for b_{12}^+ and 631.35 for b_{12}^{2+} , but the latter was shown to have an actual $m/z = 631.85$ in **Figure 3-32 (B)**. Although the re-fragmented ion corresponding to b_{13} was not shown in the MS, modified re-fragmented ion corresponding to b_{15} was shown with a $m/z = 676.02$ for $\text{Modi-}b_{15}^{3+}$ ($m/z = 2026.4$ from summation of b_{15}^+ (1479.75) and C13-F analog (546.67)) for $\text{Modi-}b_{15}^+$ in **Figure 3-32 (B)**. The re-fragmented ion corresponding to unmodified b_{15} was not found in the MS ($m/z = 1479.75$ for b_{15}^+ and $m/z = 739.88$ for b_{15}^{2+}). The re-fragmented ion

corresponding to y_7 was shown at $m/z = 752.41$ for y_7^+ and modified re-fragmented ion corresponding to Modi- y_{11} was also revealed at $m/z = 814.92$ for $(\text{Modi-}y_{11}\text{-NH}_3)^{2+}$ ($m/z = 1628.94$ from summation of $(y_{11}\text{-NH}_3)^+$ (1082.27) and C13-F analog (546.67) for $(\text{Modi-}y_{11}\text{-NH}_3)^+$). Additionally, re-fragmented ions of de-rhamnosylated modified fragment such as b_{15}^{2+} at $m/z = 940.49$ and $(y_{13}\text{-H}_2\text{O})^{2+}$ at $m/z = 872.43$ were observed in **Figure 3-32 (C)**, which indicated the existence of modification of the amino acids between 56F and 61G. Based on these observations, the modification site of SpnL should be within the amino acid sequence 59-GCG-61 of Fragment 4. Considering that glycine residues have no capability to make any covalent bonding, due to their lack of a reactive side chain such as amino alcohol or thiol, it is more likely that Cys60 is the modification site of SpnL through formation of covalent bond with the C13-F analog.

Although the MS of Fragment 5 was not good enough to analyze the re-fragmented ions (data not shown), Cys71 is the most likely nucleophile to make a covalent modification with C13-F analog based on similar reasoning to Fragment 4. The amino acid sequence of Fragment 5 is 69-AACASGVR-76, which contains only one cysteine residue at 71 position. Serine at 73 might be another option, so more careful analysis of Fragment 5 was required in future work. At this stage, these observations suggested that Cys60 and Cys71 (or Ser73) are the covalent modification sites of SpnL, and support the Rauhut-Currier type mechanism for SpnL-catalyzed cyclization.

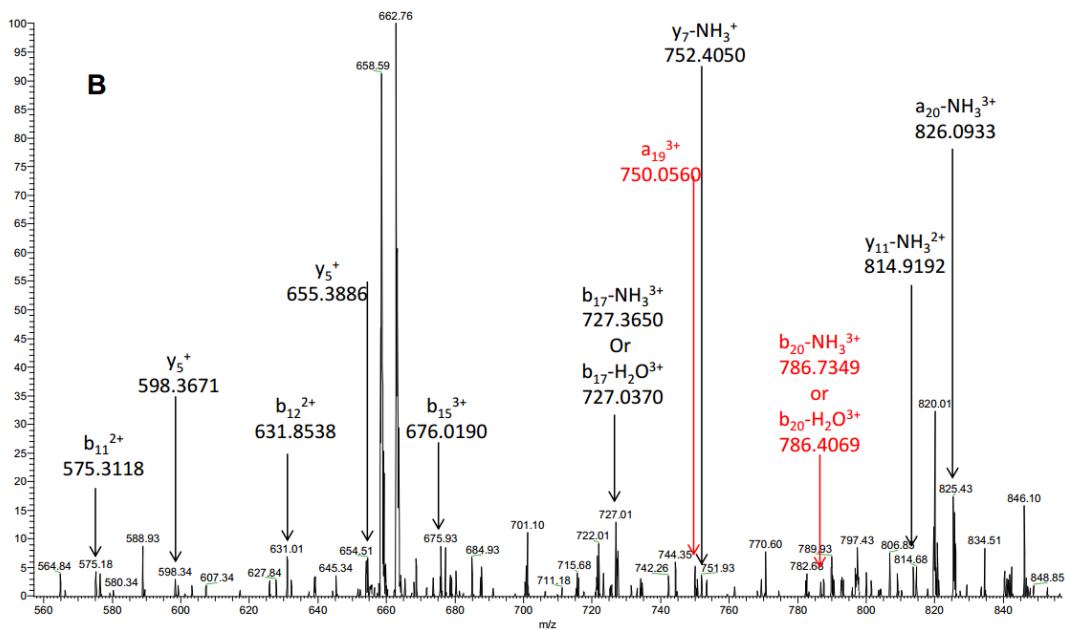
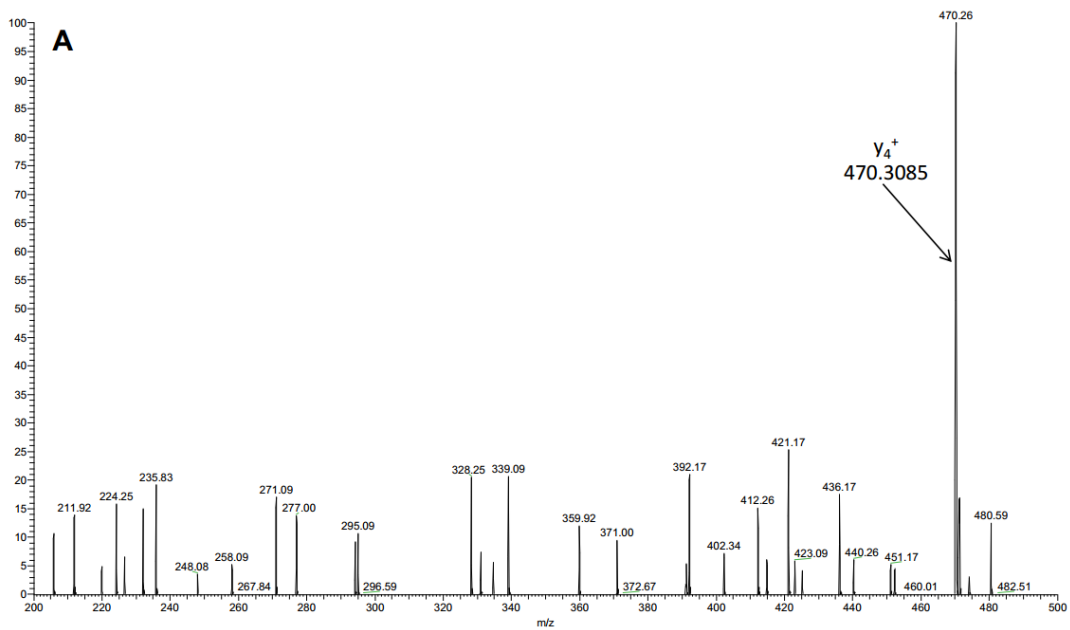


Figure 3-32. ESI MS/MS for SpnL C71A mutant, trypsin-digested after incubation with C13-F analog (continued).

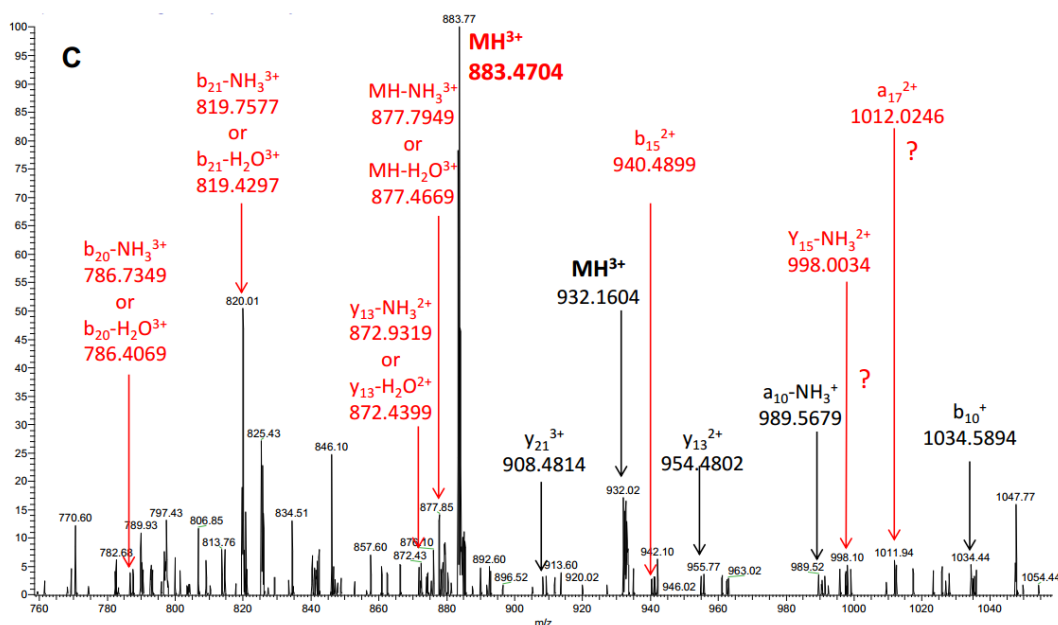


Figure 3-32. ESI MS/MS for SpnL C71A mutant, trypsin-digested after incubation with C13-F analog. Expanded MS of (A) 200-500 m/z region, (B) 550-850 m/z region, (C) 750-1050 m/z region. The black colored arrows indicates the re-fragmented ions originated from the intact inhibitor-bound fragment 4, and the red arrows shows the re-fragmented ions derived from the de-rhamnosylated inhibitor-bound fragment 4.

All of the experimental observations strongly support the hypothesis that Cys60 and/or Cys71 (and/or Ser73) are the modification sites of SpnL with the C13-F analog. However, it is still unusual that two or three nucleophiles in the active site of SpnL, are able to make a covalent bond with the substrate analog. Dr. Choi, a former graduate student, suggested a few possible models to explain these unusual observations. The first two scenarios require the two cysteine residues, Cys60 and Cys71, to be positioned in the same phase. The first scenario is that the C13-F analog is twisted in the SpnL active site, which may be different from the positioning of the natural substrate due to the fluoride atom at C-13 position. It is well known that carbon-fluoride bonding is more hydrophobic than carbon-hydrogen bonding and that fluoride is the most electronegative element.

These properties may cause the C13-F analog to bind in a twisted conformation in the active site of SpnL. Thus, assuming that the spatial distance of Cys60 and Cys71 are in a close proximity, both of the cysteine residues may have access to the electrophilic C-13 position of the C13-F analog, as depicted in **Figure 3-33 (A)**. Second scenario is also based on the structural difference of the C13-F analog from the natural substrate. That is, the C13-F analog may have two different binding modes in the active site of SpnL, compared to the one binding mode of natural substrate. The C-13 center of the natural substrate is positioned toward one of the two cysteines, while the C-13 center of C13-F analog can be reached by both cysteines by flipping itself in the active site, as shown in **Figure 3-33 (B)**. However, the flipping model is less likely since it is not easy to reverse the binding in the active site.

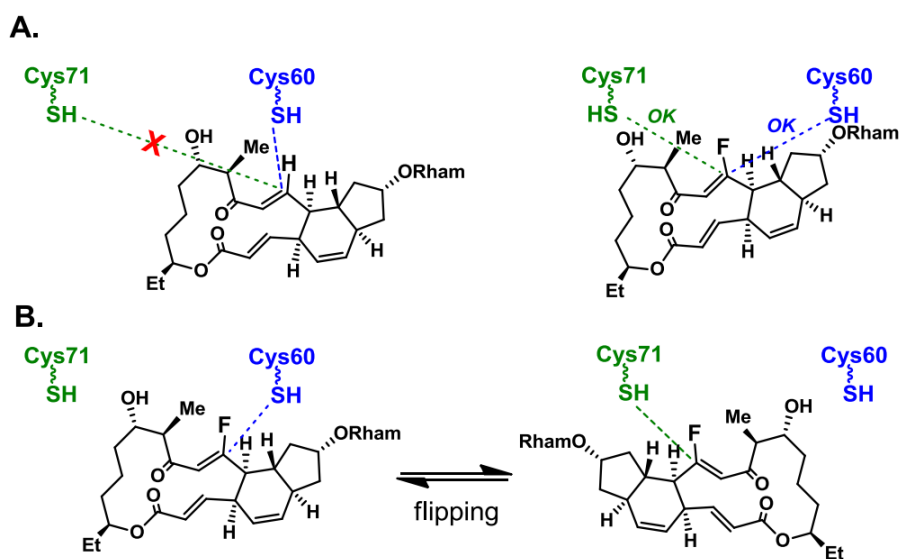


Figure 3-33. Two possible scenarios if Cys60 and Cys71 are located in close proximity. (A) Twisted positioning scenario, and (B) flipping scenario.

Before going to the third scenario, it is worthwhile to mention that Dr. Choi tried to detect the covalent adduct formation of L-glutathione and C13-F analog by incubation

at 30 °C for 24 hr, the same way Dr. Kim did with the natural substrate. However, there was no evidence for the covalent adduct. Recently, a similar experiment was performed for L-glutathione and C13-F analog in pH 12.0 NaOH solution, to enhance the nucleophilicity of L-glutathione. Also, an excess of dithiothreitol (DTT) and/or magnesium (II) chloride was added into the reaction mixture to avoid the oxidation of L-glutathione. However, MS still didn't show any evidence for the covalent adduct (**Figure 3-34**). In addition, Dr. Kim found that SpnL C71A and C205A mutants could catalyze the SpnL natural substrate cyclization with similar activity as the wild-type SpnL, whereas SpnL C60A didn't show any activity. Dr. Choi reconfirmed this result by HPLC analysis (**Figure 3-35**).

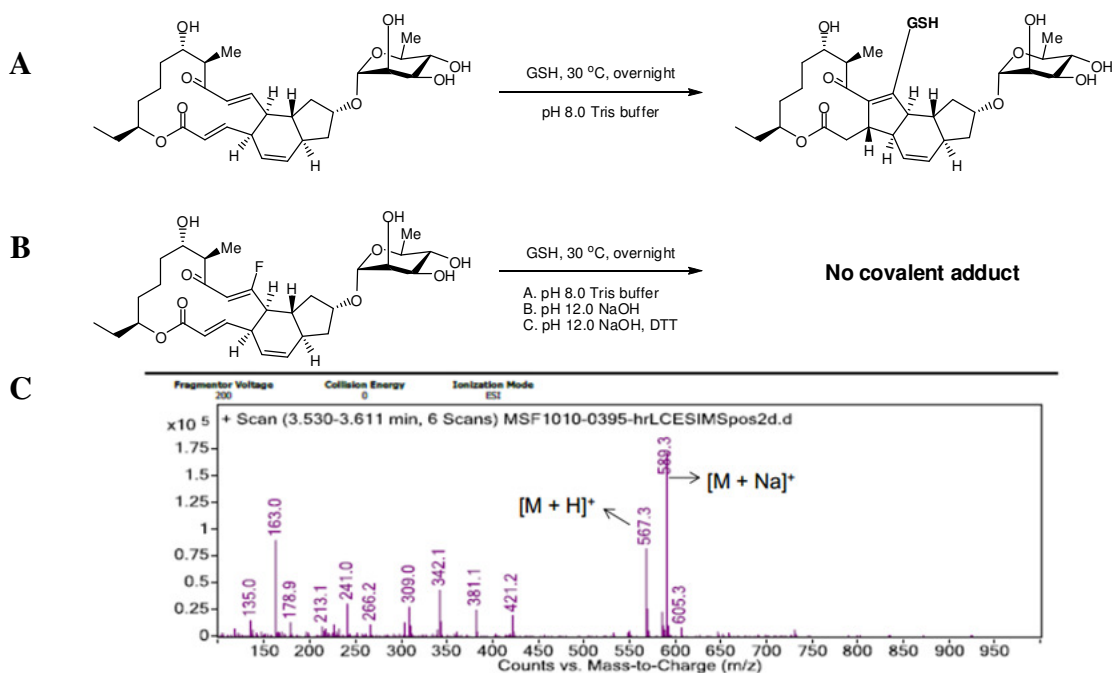


Figure 3-34. Expected non-enzymatic covalent adduct formation of L-glutathione with SpnL natural substrate and C13-F analog. (A) Reaction with SpnL natural substrate, (B) reaction with C13-F analog, and (C) MS (ESI, positive mode) result of reaction (B), showing no adduct formation (GSH = L-glutathione).

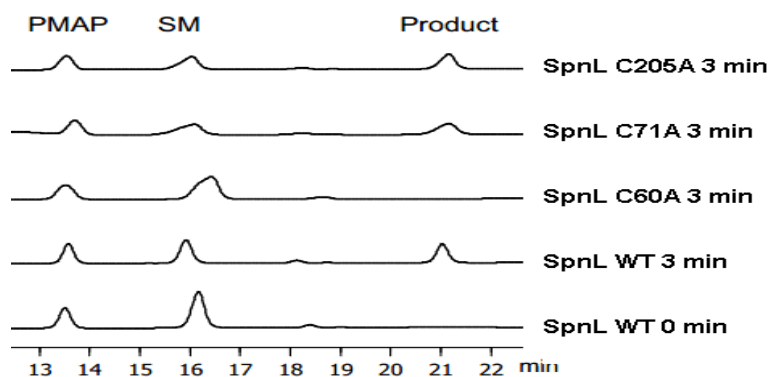


Figure 3-35. *In vitro* activity assay of SpnL and three mutants.

The Aroyan group and Wang group reported an investigation of fluoride-containing α,β -unsaturated ketones, describing its low electrophilicity due to the instability induced by the fluoride atom (**Figure 3-36**).^{30, 170} Generally, the β position in α,β -unsaturated ketones becomes more electrophilic due to the partially positive charge developed on it in a resonance structure (**Figure 3-36 (A)**),³⁰ while the β position in fluoride-containing α,β -unsaturated ketones becomes less electrophilic due to the unstable positive charge developed next to a strongly electron-withdrawing fluoride atom (**Figure 3-36 (B)**).¹⁷⁰ Thus, the relative reactivity of fluoride-containing α,β -unsaturated ketones and α,β -unsaturated esters are similar (**Figure 3-36 (C)**).

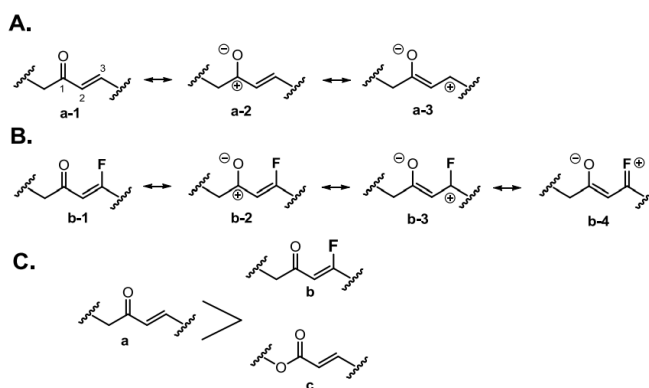


Figure 3-36. Comparison of reactivity of three α,β -unsaturated ketones toward nucleophilic addition in

Rauhut-Currier reaction

The third scenario is based on the assumption that both Cys60 and Cys71 are closely located but in the opposite positions. In this scenario, the C13-F analog is bound to the active site in the same location as the natural substrate, and Cys60, the more likely nucleophile of SpnL, can initiate the SpnL reaction through the covalent bond formation to the C-13 center. However, the low electrophilicity of the C-13 center could cause the alternative nucleophilic attack of Cys71 onto the C-3 center due to its relatively higher susceptibility than the C-13 position to nucleophilic attack (**Figure 3-37 (B)**). It is worth mentioning that Arg68 and/or Asp57 which are close to the cysteine nucleophile in the primary sequence may play a role as the general acid/base required for SpnL reaction (**Figure 3-37 (A)**).

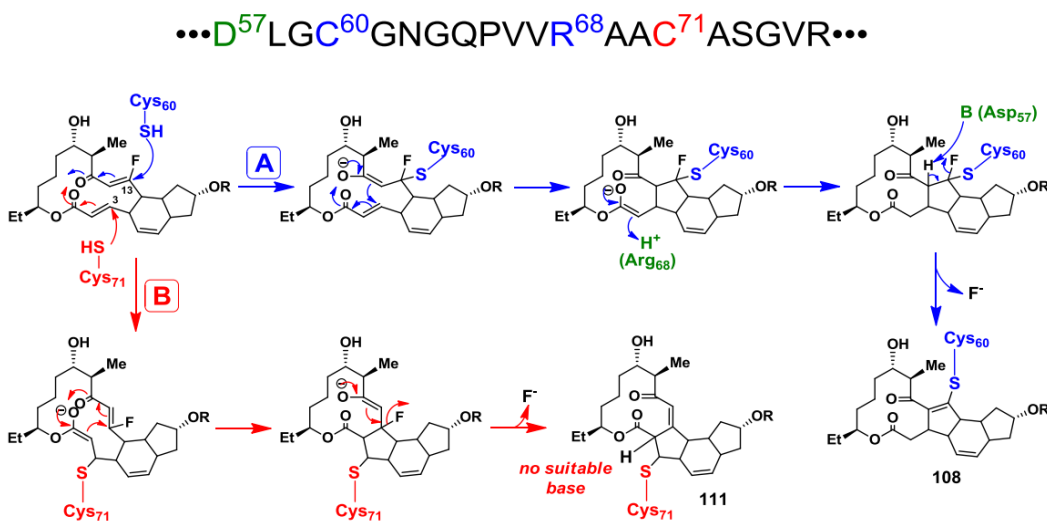


Figure 3-37. The third possible scenario if Cys60 and Cys71 are located opposite to the other and in close proximity. (A) Route A can occur in the reaction with SpnL natural substrate and C13-F analog, and (B) Route B is only possible in the reaction with C13-F analog due to its low electrophilicity at C-13 center.

3.3.6.8. Single turnover experiment

To trap an F-containing product (namely, C13-F SpnL product), a single turnover condition was investigated because the newly produced C13-F containing turnover product may also be an inhibitor for SpnL. A solution containing SpnL (22.5 μM) and the C13-F analog (50 μM or 25 μM) in pH 8.0 Tris buffer (50 mM) was incubated at 30 °C for 5 min or 30 min, precipitated, and subjected to HPLC analysis. The HPLC trace from the single turnover experiment is shown in **Figure 3-38**. During the incubation of SpnL with the C13-F analog, all the SpnL was expected to be completely inactivated, there should be only unreacted C13-F analog and the possible C13-F containing SpnL product on HPLC trace. The peak near 15 min was speculated to be the C13-F containing SpnL product, and the amount was calculated by comparison with the internal standard. A 3% conversion from the C13-F analog as “substrate” was estimated for all of the conditions. There was no difference for two sets of experiments (2.0 : 0.9 or 1:0 : 0.9 ratios of C13-F analogs to SpnL) or incubation time. When compared with SpnL natural substrate and SpnL product, the new peak near 15 min is very likely to be the C13-F containing SpnL product (data not shown).

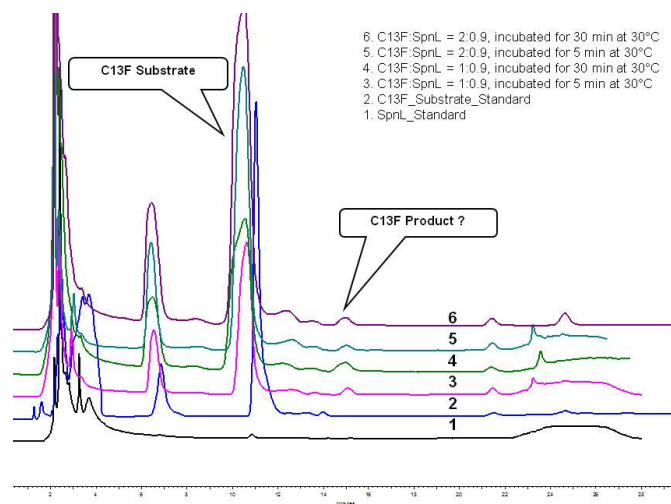


Figure 3-38. HPLC trace for the single turnover experiments. (1) SpnL, (2) C13-F analog, and (3)–(6) single turnover experimental result. Here, a peak at 6.6 min is PMAP as an internal reference.

The mass data of this peak is shown in **Figure 3-39**, showing that $[M+H]^+$ equals to 585.5 (100%), 586.5 (31%), 587.5 (7%), which did not correspond to the expected molecular weight (calculated MW = 566.29, and $[M+H]^+ = 567.30$). If C13-F SpnL product was hydrated with one molecule of water, its calculated molecular weight, $[M+H_2O+H]^+ = 585.31$, matched with the experimental data. Thus, one possible way to explain the data is that this isolated compound is a mono-fluoro mono-hydroxyl product at the C-13 center, which is produced by hydration at the C-13 position during the SpnL reaction (**Figure 3-40**).

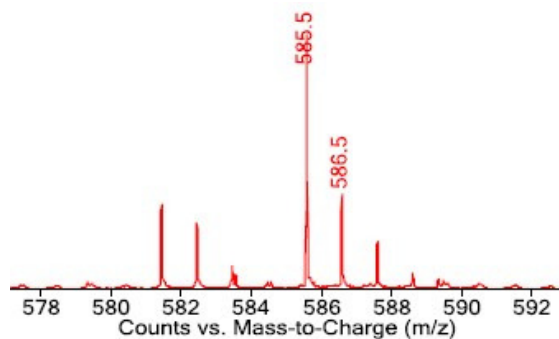


Figure 3-39. MS of isolated compound

It was uncertain when the water molecule was added onto the C-13 position. Considering the previous result that the C-13 position is not susceptible to water or L-glutathione attack under physiological conditions, one molecule of water might be added to the C-13 position after formation of C13-F containing SpnL product (**Figure 3-40, dotted box**). Initially, the single turnover experiment was designed to differentiate the two mechanisms, and the observation of C13-F containing SpnL product is evidence for the Michael addition mechanism. However, it is also possible that the fluoride anion and nucleophile can compete to be removed at the last step of the SpnL reaction (**Figure 3-5**). Although the C13-F containing SpnL product was observed as a hydrated form by MS, it didn't conclusively differentiate between the Rauhut-Currier type mechanism and the Michael addition mechanism.

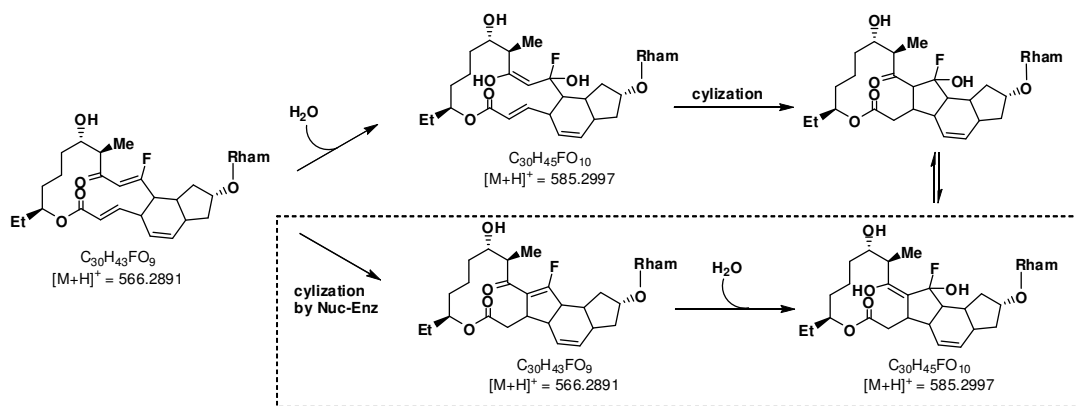


Figure 3-40. Proposed mechanism of H₂O incorporation into C13-F containing SpnL product

3.3.6.9. Future works

Even though C13-F analog inactivated SpnL, it is uncertain whether the nucleophilic addition of cysteine or serine (Cys60 or Cys71 or Ser73) occurs at the C-13 position of C13-F analog because ESI-MS only showed the formation of covalent adduct between SpnL and the C13-F analog, and ESI MS/MS only revealed the modification site of SpnL as being on Fragment 4 and Fragment 5 (as *ModiFrag4* and *ModiFrag5*). That is, it only narrowed down the possible modification sites of SpnL. The ¹³C13-F analog is designed to address the site of covalent bonding on the substrate (**Figure 3-41**). After SpnL is incubated with ¹³C13-F analog and trypsin-digested, the solution will be subjected to ESI-MS and ¹³C-NMR analysis. ESI-MS is expected to show the formation of a covalent adduct the same as the C13-F analog, and ¹³C-NMR is expected to show a peak shift of C-13 from a peak corresponding to sp² (substrate) to a peak corresponding to sp³ (covalent adduct).

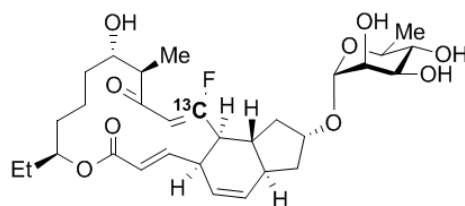


Figure 3-41. Mechanistic probes for SpnL reaction: $^{13}\text{C}^{13}\text{-F}$ analog

3.3.6.10. Conclusion

Experiments in Section 3.3.4 to 3.3.6 are focused on the identification of the inhibition mode for the SpnL-catalyzed cyclization reaction using isotope trace experiments, kinetic isotope effect experiments and biochemical experiments mainly measured by MS. Isotope trace experiments and kinetic isotope effect experiments show that if the rate determining step of SpnL is the first step and all protons in SpnL are exchangeable with water, then the Rauhut-Currier type mechanism is more likely. MS of SpnL incubated with $\text{C}^{13}\text{-F}$ analog shows a characteristic peak corresponding to the covalently-modified SpnL with $\text{C}^{13}\text{-F}$ analog by removal of fluoride atom. MS of fragmented SpnL, which was incubated with $\text{C}^{13}\text{-F}$ analog, shows that the two modifications occur in the amino acid sequences of Fragment 4 and Fragment 5 of SpnL. MS using SpnL C71A mutant indirectly supported the existence of covalent modification on Cys71 and also Cys60. ESI MS/MS of SpnL from the re-fragmentation result of Fragment 4 revealed that Cys60 was the most likely nucleophile to initiate the SpnL reaction, although there is no evidence for Cys71 due to lack of MS for Fragment 5. The conclusion from the overall experimental observations is that SpnL-catalyzed cyclization follows the Rauhut-Currier type mechanism through the covalent bonding of the substrate

with Cys60, Cys71, or Ser73 of SpnL as the first step. If combined with the *in vitro* activity assay of SpnL mutants (C60A, C71A, and C205A), Cys60 may be the most likely residue to initiate the SpnL reaction through the covalent bonding in the first step. However, additional biochemical experiments should follow to elucidate the details of the mechanism in the future.

3.3.7. Studies on the SAM-dependence of SpnF and SpnL reactions

S-Adenosylmethionine (SAM or AdoMet) is a biological sulfonium compound used in many biological reactions, which was discovered by Cantoni group in 1952.¹⁷¹ It is made from adenosine tri-phosphate (ATP) and methionine by methionine adenosyltransferase. SAM is involved in numerous biologically important methylation reactions, ACP transfer reactions, methylene transfer reactions, amino group transfer reactions, ribosyl group transfer reactions, and aminopropyl group transfer reactions.¹⁷² However, the mechanisms of most of these reactions have not been extensively characterized. Furthermore, the structural role of SAM has not yet been reported.

In the biosynthesis of Spinosyn A, SpnF and SpnL have been identified as members of the S-adenosyl-l-methionine (SAM) dependent methyltransferase superfamily, based on sequence homology (**Figure 3-42**).^{15, 19} However, neither of them catalyze the methyl transfer reaction.²² Rather, SpnF catalyzes the [4+2] cycloaddition to form a cyclohexene ring through bond formation between C-4-C-12 and C-7-C-11, and SpnL catalyzes the cyclization which forms a cyclopentene ring through C-3-C-14 bond formation. So, a question arose as to what the role of SAM is for SpnF and SpnL enzymes. To address this question and to characterize the role of SAM in these two

enzymes, various biochemical studies were designed and performed. The same experimental procedures were used to show the role of SAM for SpnF and SpnL.

PCC7420	•••ENIL	DVGC G	I	G	G	S	S	L	D	L	A	Q	R	F	G	A	Q	V	Q	G	I
DSM44928	•••ARVL	DVGC G	I	G	G	P	A	L	Y	L	A	G	A	L	G	C	A	V	V	G	V
ABC84455	•••DRVLL	DVGC G	I	G	K	P	A	M	R	V	A	T	S	T	G	A	D	V	L	G	I
SnogM	•••QRVLL	DVGC G	A	G	R	P	A	A	D	L	S	R	A	T	G	A	S	V	V	G	V
ACY01395	•••QRVLL	DVGC G	V	G	Q	P	A	M	R	I	A	R	R	T	G	A	H	V	T	G	I
MitM	•••SRVLL	DVGC G	V	G	T	P	G	V	R	I	A	R	L	S	G	A	H	V	T	G	I
MA4680	•••RRVLL	DVGC G	S	G	K	P	A	V	R	L	A	L	S	A	P	V	D	V	V	G	V
BAF85841	•••RRVLL	DVGC G	S	G	R	P	A	L	R	L	A	H	S	E	P	V	D	I	V	G	I
ATCC27064	•••RHLL	DVGC G	I	G	V	P	A	L	R	I	A	G	A	H	G	V	R	V	T	G	V
RS-1	•••QTL	DVGC G	V	G	R	P	A	V	R	L	S	Q	Q	T	G	A	A	V	V	G	I
CNB440	•••HRVLL	DVGC G	T	G	G	P	A	R	R	I	A	Q	V	T	G	A	T	V	T	G	V
MonE	•••LRVLL	DVGC G	S	G	A	P	A	C	E	L	A	T	D	H	G	V	E	V	V	G	I
UbiE/COQ5	•••MHILL	DVGC G	V	G	G	S	T	R	R	L	S	H	E	T	G	C	H	V	T	G	I
SpnF	•••VRLL	DVGC G	T	G	Q	P	A	L	R	V	A	R	D	N	A	I	Q	I	T	G	I
SpnL	•••AHLF	DVGC G	N	G	Q	P	V	V	R	A	A	C	A	S	G	V	R	V	T	G	I

Figure 3-42. Sequence comparison of SpnL and SpnF with known SAM-dependent methyltransferases.

3.3.7.1. *In vitro* activity assay of as-isolated SpnF and SpnL in the presence of exogenous SAM

The SAM content of SpnF and SpnL was first measured by UV and HPLC analysis. After denaturation of the as-isolated SpnF and SpnL by treatment with strong acid, the resulting solution was subjected to UV and HPLC analysis. As-isolated SpnF contains 1.0 equivalent of SAM, and the as-isolated SpnL contains 0.60~0.75 equivalent of SAM (**Figure 3-43** and **Figure 3-44**).

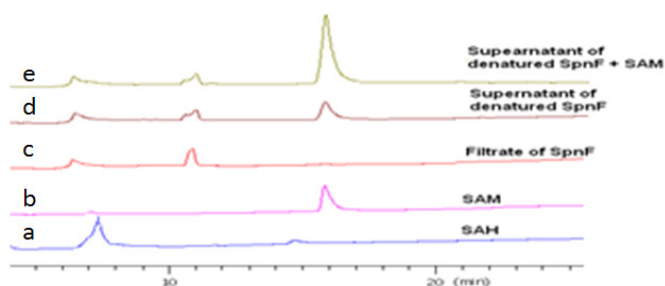


Figure 3-43. HPLC traces of SAM in SpnF. (a) SAH standard, (b) SAM standard, (c) filtrate of SpnF, (d) supernatant of denatured SpnF and (e) coinjection of SAM with supernatant of denatured SpnF.

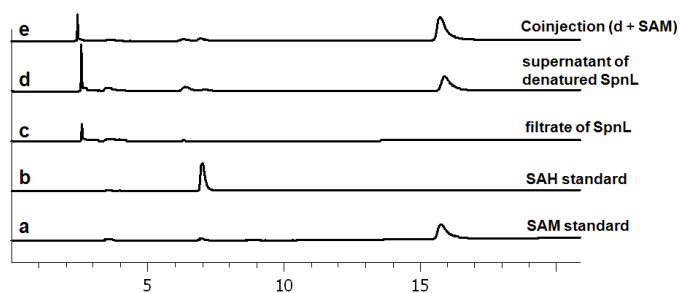


Figure 3-44. HPLC traces of SAM in SpnL. (a) SAM standard, (b) SAH standard, (c) filtrate of SpnL, (d) supernatant of denatured SpnL, (e) coinjection of SAM with supernatant of denatured SpnL.

An *In vitro* activity assay of SpnF and SpnL was then performed to show the change in activity of SpnF and SpnL with external SAM. A solution containing SpnL natural substrate (250 μ M) in pH 8.0 Tris buffer (50 mM) was incubated with SpnL (10 μ M) at 30 °C for 3 min. Another solution contained SpnL natural substrate (250 μ M) and SpnL (10 μ M) preincubated with SAM (500 μ M) for 2 hr. As a control, a solution containing SpnL natural substrate (250 μ M) and SpnL (10 μ M) in pH 8.0 Tris buffer was also incubated under the same conditions. Three solutions were analyzed by HPLC after quenching and precipitation of proteins. The same procedure was also performed for the SpnF. There was no obvious change between the control reaction and SAM-treated reactions (data not shown). In other word, the external SAM didn't affect the activity of

SpnF and SpnL.

3.3.7.2. *In vitro* activity assay of apo-SpnF and apo-SpnL with external SAM

At first, apo-SpnF and SpnL were prepared following the procedure as described in Section 3.2.11.2. SAM content and *in vitro* activity of apo-SpnF and SpnL were determined. As expected, apo-SpnF and apo-SpnL didn't show any trace of SAM, and didn't catalyze their expected reaction, namely [4+2] cycloaddition and cyclization, respectively (**Figure 3-45** and **Figure 3-46**).

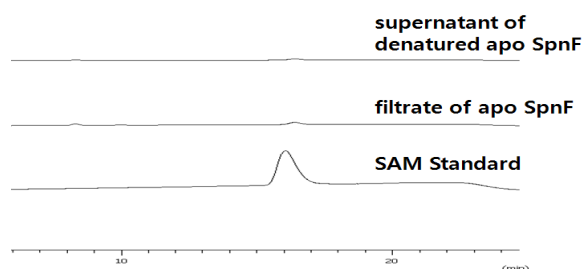


Figure 3-45. HPLC traces of apo-SpnF. (a) SAM standard, (b) filtrate of apo-SpnF, and (c) supernatant of denatured apo-SpnF

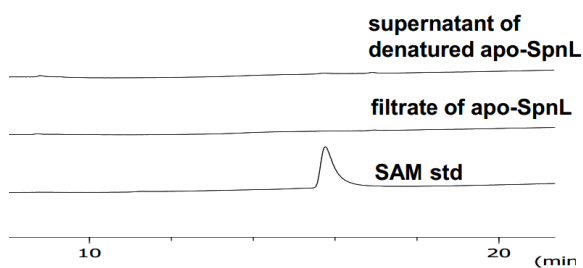


Figure 3-46. HPLC traces of apo-SpnL. (a) SAM standard, (b) filtrate of apo-SpnL, and (c) supernatant of denatured apo-SpnL

Apo-enzymes were then incubated with their substrates in the presence of external SAM. Apo-SpnF didn't show any activity (**Figure 3-47**; SpnF product shown in (b) was non-enzymatic product), while apo-SpnL showed activity in a SAM concentration-

dependent manner (**Figure 3-48 (A)**). Similarly, SAH increased the activity of apo-SpnL (**Figure 3-48 (B)**), whereas SAH didn't affect the activity of apo-SpnF (data not shown). However, apo-SpnF and apo-SpnL showed no change in activity when 5'-deoxyadenosine and/or methionine was added (**Figure 3-48 (C)**).

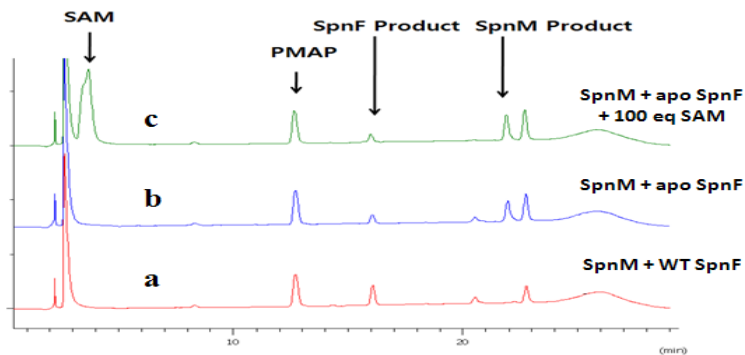


Figure 3-47. HPLC traces for *in vitro* activity assay of apo-SpnF with external SAM.

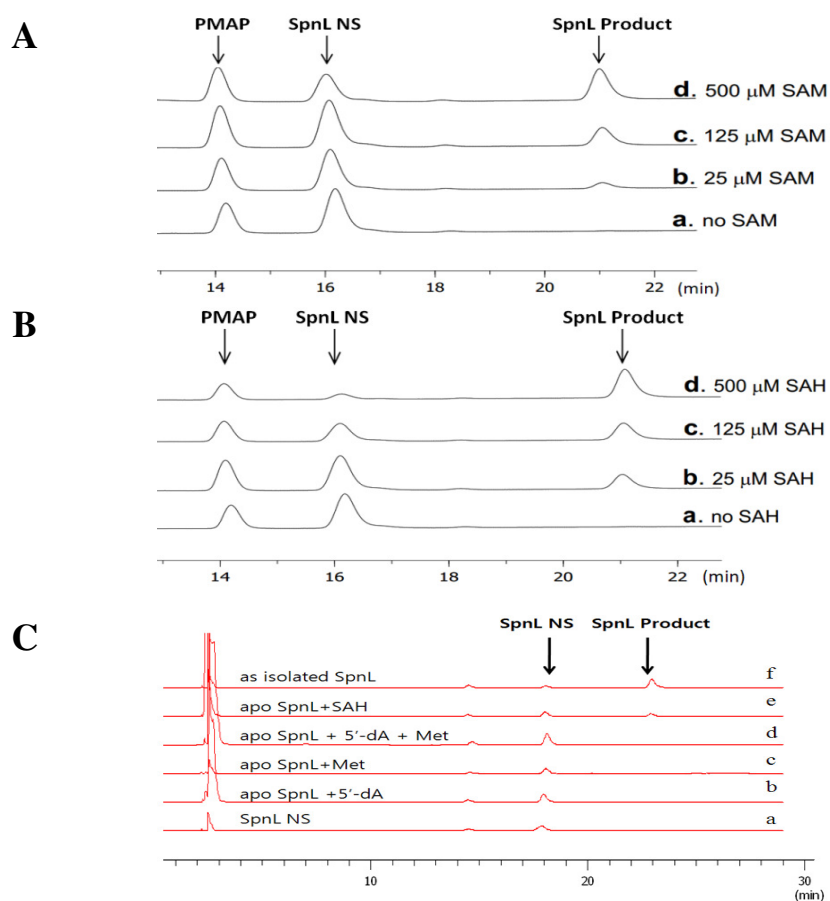


Figure 3-48. HPLC trace of *in vitro* activity assay of apo-SpnL in the presence of (A) SAM, (B) SAH, and (C) 5'-deoxyadenosine and/or methionine.

3.3.7.3. *In vitro* activity assay of reconstituted SpnF and reconstituted SpnL with external SAM

Reconstituted enzymes were prepared by incubation of apo-enzymes (100 μ M) with an excess SAM (2.5 mM) in pH 8.0 Tris buffer at 4 $^{\circ}$ C for 2 hr, followed by repeated dialyses to remove excess SAM in the buffer solution. The SAM content and *in vitro* activity of the reconstituted SpnF and reconstituted SpnL were then determined. UV and HPLC analysis revealed that reconstituted SpnF had no SAM, while reconstituted SpnL contained 0.70 equivalent of SAM, which is similar to the value of 0.60~0.75

equivalent for the as-isolated SpnL (**Figure 3-49**). Furthermore, the reconstituted SpnL didn't show any activity even with external SAM, whereas reconstituted SpnL showed activity without external SAM (**Figure 3-50**).

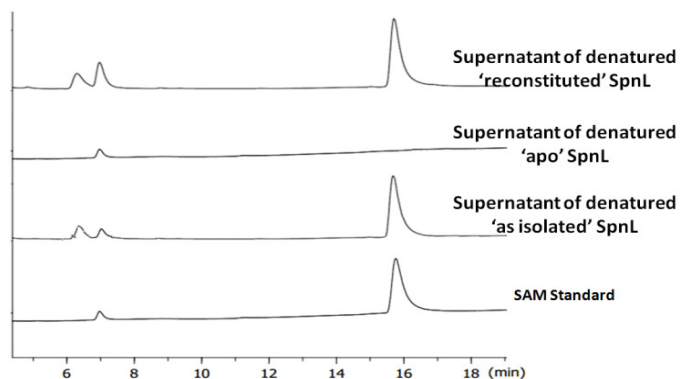


Figure 3-49. HPLC trace of SAM for (a) SAM standard, (b) as-isolated SpnL, (c) apo-SpnL, and (d) reconstituted SpnL

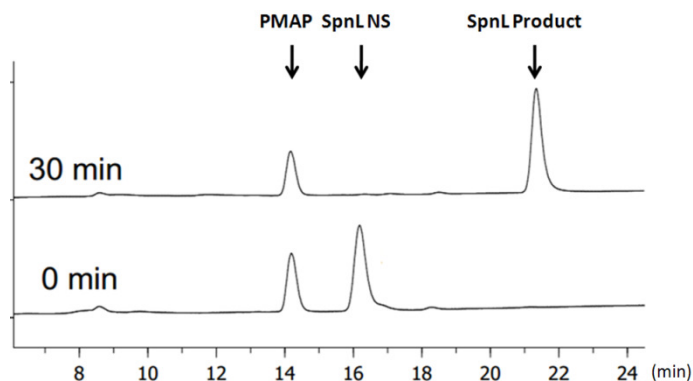


Figure 3-50. HPLC trace of SpnL reaction with the reconstituted SpnL

SAM is a common co-substrate for the methyl transfer reactions in biological systems.^{173, 174, 175, 176, 177} The sulfonium ion's highly reactive methyl group makes it an important biological methylating agent. The function of SpnL is to catalyze the cyclization of tricyclic aglycone into the tetracyclic aglycone by carbon-carbon bond formation between at C-3 and C-14 in the biosynthesis of spinosyn A.²² Thus, SpnL is

not considered a methyltransferase. On the other hand, SAM can also be cleaved reductively to produce 5'-deoxyadenosyl 5'-radical as an intermediate in many iron-sulfur cluster-containing radical SAM enzymes. The hallmark of those radical SAM enzymes is the well-conserved CxxxCxxC motif, which coordinates a [4Fe-4S] cluster in the active site. The amino acid sequence of SpnL revealed three cysteine residues, Cys60, Cys71, and Cys205. However, those three cysteines are located far from each other, indicating that SpnL is not a member of the radical SAM enzyme superfamily. SAM is also used in the biosynthesis of polyamine. After decarboxylation, the remaining S-adenosylmethioninamine donates its n-propylamine group to the biosynthesis of polyamine such as spermidine and spermine. This is also not the case for SpnL. Thus, the role of SAM in SpnL reactions warrants investigation.

Several biochemical experiments to assay the *in vitro* activity of as-isolated SpnF, apo-SpnF, and reconstituted SpnF didn't show any clue for the role of SAM in SpnF. However, a series of *in vitro* activity assays of as-isolated SpnL, apo-SpnL, and reconstituted SpnL showed that SAM is required for the activity of SpnL, although the actual role of SAM is still unknown. Previously, Dr. Choi suggested several possibilities for the role of SAM in SpnL, delineated as following.¹⁵¹ First, SAM is simply involved in the folding of SpnL (**Figure 3-51 (A)**). Second, SAM binding to SpnL helps substrate binding by inducing a conformational change of SpnL into an active form (**Figure 3-51 (B)**). Third, SAM binding fills the active site so that the substrate can bind to the active site more tightly (space filling), rather than inducing a conformational change (**Figure 3-51 (C)**). Lastly, SAM can be involved in other unknown functions during catalysis. Thus,

the next experiment, using circular dichroism spectroscopy, was performed to prove the structural change of SpnL during the reconstitution process.

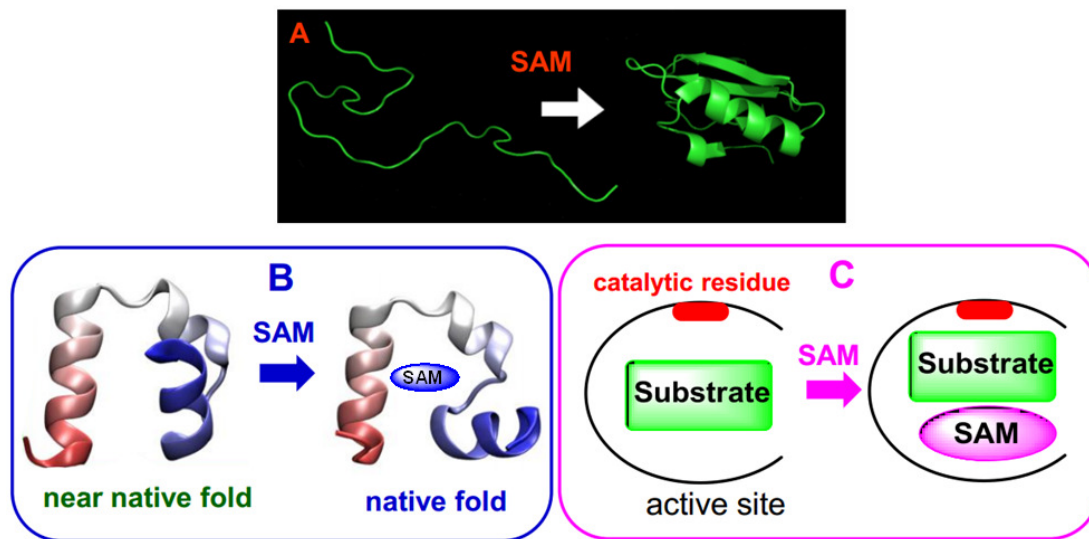


Figure 3-51. Three proposed structural roles of SAM in SpnL reaction. (A) assistance in the folding process, (B) assistance in proper folding (native folding), and (C) assistance by filling the active site to make a substrate near to catalytic residue.

3.3.7.4. Circular dichroism (CD) experiments

The far-UV circular dichroism (CD) spectrum of proteins can show the conformation of their secondary structure as fractions in α -helix and β -sheet.^{178, 179, 180} It is possible that the comparison of the conformations of the as-isolated SpnL, apo-SpnL, and reconstituted SpnL may give different results, depending on whether SAM is present. Due to the difficulties in measuring CD in typical aqueous buffer systems, the CD analysis was optimized to meet the criteria of these experiments. The circular dichroism spectrum of SpnL was then measured for the as-isolated SpnL and apo-SpnL. Finally, the change of CD of apo-SpnL was measured by the addition of SAM during the reconstitution process. The results are shown in **Figure 3-52** and **Figure 3-53**. The

conformational analysis of the fraction of α -helix and β -sheet gave similar results. However, apo-SpnL has similar values of ellipticity at 210 nm and 219 nm, while the as-isolated SpnL has different values of ellipticity at these regions (**Figure 3-52**). In addition, the change in the CD spectra at 210 nm and 219 nm shows concentration dependence of SAM during the reconstitution process, although the difference is not very significant (**Figure 3-53**).

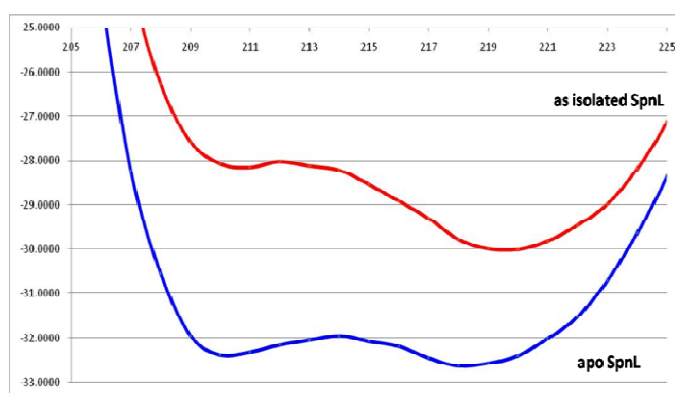


Figure 3-52. CD spectrum of as-isolated SpnL and apo-SpnL (not scaled).

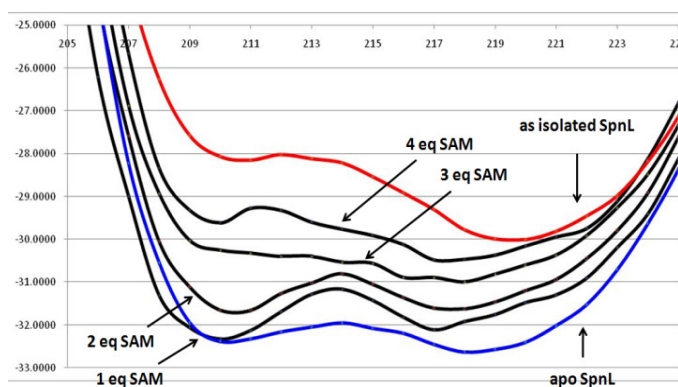


Figure 3-53. CD spectrum change during the reconstitution process (not scaled).

Circular dichroism spectrum of the apo-SpnL indicated that the secondary structure of apo-SpnL is already similar to that of the as-isolated SpnL before reconstitution with external SAM (i.e., apo-SpnL is at the very least not a random coil).

Moreover, the conformation of apo-SpnL changed to that of the as-isolated SpnL depending on the amount of SAM added, as shown in **Figure 3-53**.

In **Section 3.3.7.3.**, several possibilities are proposed for the role of SAM in the SpnL reaction. The first possibility that SAM is simply involved in the proper folding of SpnL, can be ruled out because apo-SpnL already has a folded structure similar to the as-isolated SpnL. The second and third suggestions are very similar in that SAM binds to SpnL to make the substrate bind more tightly to its active site. The second role proposed is a conformational change of the active site, and the third role proposed is the space filling model, allowing the substrate to contact the catalytic residue(s) more tightly in the active site. These possible structural roles conceptually explain how the activity of SpnL might be reliant on the presence of SAM, by making the active site of SpnL more suitable for catalysis. Here, it is worthwhile to note that SAH as well as SAM restored the activity of apo-SpnL, but the two fragments of SAM, 5'-deoxyadenosine and methionine, didn't. The methyl group in SAM is missing in SAH, indicating that methyl group is not required for the activity of SpnL. The remaining two parts corresponding to 5'-deoxyadenosine and methionine are connected through a sulfur linkage in SAH and SAM. If SAM participates in the space filling model, the two fragment molecules, 5'-deoxyadenosine and methionine should be able to activate the apo-SpnL, especially when they are used together. However, there was no restoration of apo-SpnL activity even in the presence of both fragment molecules in high concentrations. Rather, the second model, suggesting conformational changes of the active site, seems to be more likely, if combined with space filling model (third model). That is, assuming that the active site or

any other important site for the activity of apo-SpnL has two separated pockets (namely, a 5'-deoxyadenosine pocket and a methionine pocket; **Figure 3-54, Left: open-shape**), which can bind to an adenine moiety and the amino acid moiety of SAM, only sulfur-linked SAM and SAH can restore the activity of apo-SpnL by contracting these two pockets more tightly (**Figure 3-54, Right: closed-shape**). If there's no linker, the two pockets should be still far away and couldn't affect the activity of apo-SpnL even though the two pockets were filled with 5'-deoxyadenosine and methionine. This concept is depicted in **Figure 3-53**.

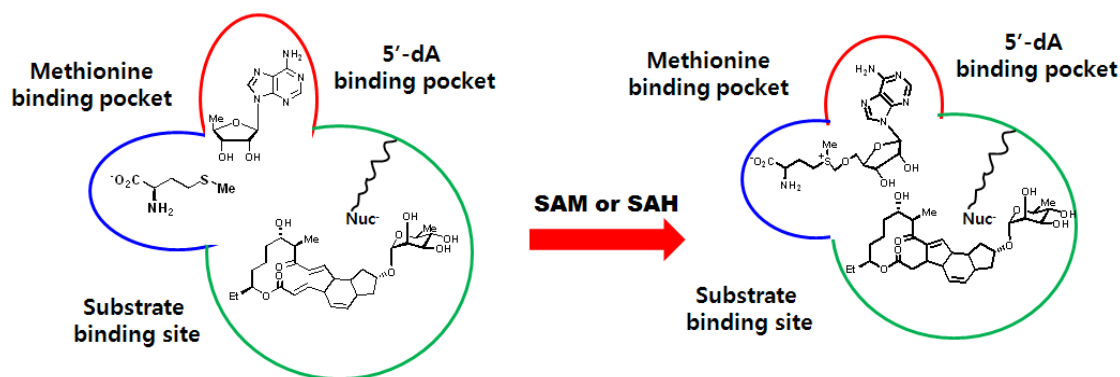


Figure 3-54. New proposed role of SAM in the SpnL reaction. Left: open-shaped, and Right: closed-shaped.

SpnF and SpnL, in the biosynthesis of spinosyn A, have been classified as members of SAM-dependent methyltransferase superfamily due to their characteristic DxGCG motif, based on sequence homology. However, SpnF was proved to be involved in the [4+2] cycloaddition as part of the formation of cyclohexene ring and SpnL was shown to be involved in the ring closure to form the cyclopentene ring during the biosynthesis of spinosyn A aglycone. Initially, four possibilities about the structural role of SAM in SpnF and SpnL were suggested in Section 3.3.7.3. To verify these hypotheses,

several experiments were conducted. The SpnL content of SAM was determined by UV and HPLC analysis to be 0.60~0.75 equivalents. A series of *in vitro* activity assays of as-isolated SpnL, apo-SpnL, and reconstituted SpnL revealed that SAM is apparently required for the SpnL reaction. It was also found that SAH as well as SAM could restore the activity of apo-SpnL, but 5'-deoxyadenosine and methionine couldn't. In addition, the circular dichroism spectroscopy disclosed that the conformation of apo-SpnL becomes more similar to that of as-isolated SpnL in a SAM concentration dependent manner during the reconstitution process. Combined results lead to a slightly modified hypothesis about the role of SAM in SpnL, namely that SAM plays a structural role to connect two pockets in the active site or any important site for the activity of SpnL, to activate the enzyme. At this stage, it is hard to say how SpnL binds to SAM and the substrate, as well as which residues of SpnL interact with SAM and the substrate due to the lack of a crystal structure containing SAM and the substrate. The crystal structure of SpnL will likely reveal the binding site of SAM and the active site, as well as show the structural role of SAM in the SpnL reaction. To our knowledge, the structural role of SAM is necessarily performed first in the SpnL reaction. Further research will give additional clues as other role of SAM in the SpnL reaction, as well as the SpnF reaction.

3.3.8. SpnL mutant study using SpnL D57N, E96Q, and E96L

When a known catalytic base, Glu358, in m⁵U-tRNA methyltransferase was mutated to glutamine, the X-ray crystal structure of the mutant enzyme revealed a covalently modified enzyme-substrate adduct.¹⁸¹ So far, the X-ray crystal structure of SpnL has not been solved yet. However, the non-enzymatic incubation of SpnL with L-

glutathione led to a Michael addition adduct, although the site of covalent modification is not known. Based on the proposed Rauhut-Currier type mechanism, deprotonation after the cyclization reaction will expel SpnL and release the SpnL product. If this deprotonation step is blocked, the covalently-modified enzyme-substrate adduct will be accumulated leading to enzyme inactivation. Recently, it was found that two cysteine residues (Cys60 and Cys71) of SpnL are the possible residues to form covalent bonds with the substrate/inhibitor during the enzymatic cyclization reaction, as demonstrated by the inhibition study using the C13-F analog. Thus, it is proposed that several aspartate or glutamate residues near these two cysteine residues are the catalytic base necessary to complete the deprotonation and removal of the SpnL active site nucleophile from its product. There are total 33 aspartate and glutamate residues in SpnL. Three residues, Asp45, Asp57 and Glu96, were selected as the most likely catalytic base involved in the deprotonation step. The disappearance of SpnL natural substrate and the absence of any product formation upon incubation of SpnL natural substrate with the SpnL mutants is expected due to the accumulation of the covalent adduct if one of these selected residues is involved in the deprotonation reaction. Furthermore, it is expected that MS or X-ray crystallography will show the presence of the SpnL-substrate complex. Three single-point SpnL mutants were made by Dr. Y.-n. Liu, the research associate in the Liu Lab. SpnL D57N, SpnL E96Q, and SpnL E96L were well expressed and purified. However, SpnL D45N was not well expressed due to unknown reasons. So, all of the SpnL mutant studies were performed using three SpnL mutants, SpnL D57N, SpnL E96Q, and SpnL E96L.

The *in vitro* time-course activity assays of the three SpnL mutants were performed using the same procedure for assaying the wild type SpnL. A solution containing SpnL natural substrate (80 μ M) and SpnL mutant proteins (10 μ M) in pH 8.0 Tris buffer (50 mM) was incubated at 37 °C for 20 hr with activity monitored by HPLC analysis. The HPLC analysis showed that the activity of SpnL D57N was very similar to that of SpnL, while the activity of SpnL E96Q and SpnL E96L were less than that of SpnL (**Figure 3-55**). If either Asp57 or Glu96 is the general base responsible for the deprotonation step of the reaction, this last step should be prevented and no SpnL product would be detected. Specifically, if the SpnL reaction follows the Rauhut-Currier type mechanism, SpnL natural substrate should disappear, but SpnL product is expected not to appear because the SpnL mutant should be inactivated by covalent modification. If the SpnL reaction follows the Michael addition mechanism, SpnL natural substrate should disappear, and an isomer of SpnL product should be produced, not the SpnL natural product. However, this result clearly showed that all three SpnL mutants catalyze the cyclization reaction, although to varying in degrees. Next, to detect the covalent adduct of SpnL mutant with SpnL natural substrate, a solution containing SpnL natural substrate and the SpnL mutant was incubated at 30 °C for given time, in which time half of SpnL substrate was converted into SpnL product. It was assumed that there should be a covalent adduct of a SpnL mutant with an intermediate trapped in the middle of the SpnL reaction. The reaction mixture was quenched, dialyzed, and submitted to ESI MS analysis. MS result didn't give any promising peaks, corresponding to the covalent adduct for any of the three SpnL mutants (data not shown).

	0 min	10 min	20 min	30 min	60 min	240 min	1200 min
SpnL WT	0%	53%	97%	100%	100%	100%	100%
SpnL D57N	0%	47%	75%	89%	96%	99%	99%
SpnL E96Q	0%	20%	30%	44%	49%	55%	70%
SpnL E96L	0%	4%	5%	7%	11%	12%	24%

SpnL WT (30 oC) vs SpnL D57N, E96Q, and E96L (37 oC)

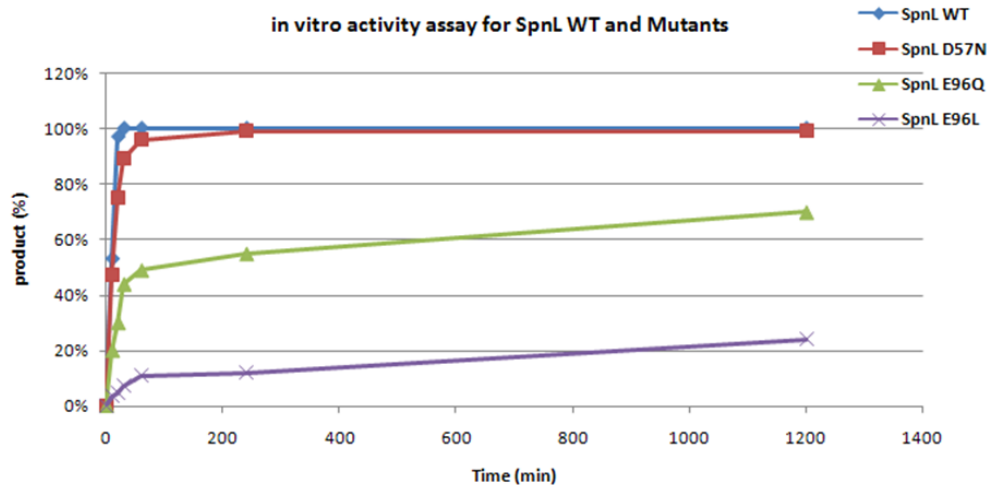


Figure 3-55. HPLC trace of the *in vitro* activity assay for SpnL and SpnL mutants.

These results can be explained in two ways, proper-folded or improper-folded (or misfolded) SpnL mutants. If the SpnL mutants are properly-folded as the wild type SpnL, the slow but complete conversion of SpnL natural substrate into SpnL product means that the selected aspartate or glutamate are not directly involved in the deprotonation step. Instead, it is possible that other amino acid residues or a water molecule is involved in the deprotonation at the C-12 position of SpnL substrate and the enzyme covalent adduct. The slow rate of reaction can be explained by low catalytic diad formation of amide residue in the SpnL mutants (asparagines in SpnL D57N, and glutamine in SpnL E96Q) with the water molecule due to its low hydrogen bonding ability compared to the carboxylate moiety of Asp57 or Glu96. In this case, a weakly deprotonated water molecule is only able to inefficiently carry out deprotonation. Thus, the reaction rate

should be slow. In the case of SpnL E96L, this catalytic diad is less likely to capture a water molecule due to its increased lipophilicity from the lysine residue. Another possibility is that these asparagine or glutamine may be used as a very weak base for the deprotonation. Based on the current evidence, these two amino acid residues (D57 and E96) seem not to be involved in the deprotonation step directly,.

Another possibility is the folding problem. It is conceivable that the SpnL mutants are improperly folded and therefore have lower activity compared to the wild type SpnL. There are two scenarios in this case. One is that the catalytic active site might be distorted resulting in a low binding affinity of SpnL mutants for SpnL substrate. Simultaneously, the distorted active site may partially block the insertion of SpnL substrate and/or release of SpnL product, resulting in the slow cyclization reaction. The other scenario is that the misfolded SpnL mutants may place the catalytic asparagine (D57N) or glutamine (E96Q) in a less ideal position, although those could still act as a general base involved in the deprotonation reaction. During the dynamic protein folding cycle, some of properly-folded SpnL mutants may function well enough to catalyze the cyclization reaction, resulting in complete but slow conversion.

Initially, the purpose of the SpnL mutant study was to identify the covalent adduct of SpnL mutants and SpnL natural substrate to distinguish between the two plausible mechanisms: the Rauhut-Currier type mechanism and Michael addition mechanism. From the *in vitro* activity test of three SpnL mutants, Glu96 appears to play an important role in the SpnL reaction, compared to Asp57. However, the covalent adduct of SpnL mutant and SpnL natural substrate was not detected by ESI MS, so it is still uncertain

which mechanism the SpnL reaction follows. However, the *in vitro* activity difference between SpnL E96Q and E96L indicated that the hydrophilic environment near Glu96 is more favored and consequently a water molecule in this site can be used as a catalytic base as a deprotonated hydroxide ion or partially negative charged water molecule. In this case, turnover of SpnL natural substrate into the product occurs regardless of the reaction mechanism. Although the reaction mechanism is not distinguished by these experiments, Glu96 seems to be an important residue in the SpnL reaction.

3.3.9. Chemoenzymatic total synthesis of spinosyn A

The spinosyns exhibit neuronal activity against insects mainly by interacting with nicotinic acetylcholine receptors. A mixture of spinosyn A and spinosyn D, namely Spinosad[®], has been worldwide used in agriculture as a highly potent and selective insecticide.^{5, 6, 7} Since Spinosad[®] resistance has been recently reported, the importance of developing modified spinosyns to increase their insecticidal activity against Spinosad[®]-resistant insects should not be understated.^{182, 183, 184, 185}

As described earlier, spinosyn A, which contains a tetracyclic aglycone and two appended sugars, is an interesting natural product due to its structural complexity. Many research groups have reported the total synthesis of spinosyn A and spinosyn analogs. The Evans group¹⁸⁶ and Paquette group^{187, 188} reported the synthesis of the tricyclic perhydro-*as*-indacene in spinosyn A. The Roush group^{79, 80} and Tietze group¹⁸⁹ have also reported the total synthesis of spinosyn A.

The Roush group utilized a nucleophile induced Michael cyclization (corresponding to an intramolecular Rauhut-Currier reaction) and transannular [4+2]

cycloaddition from a multi-conjugated macrolactone ring as the key reactions in their total synthesis of spinosyn A (**Figure 3-56**).^{79, 80}

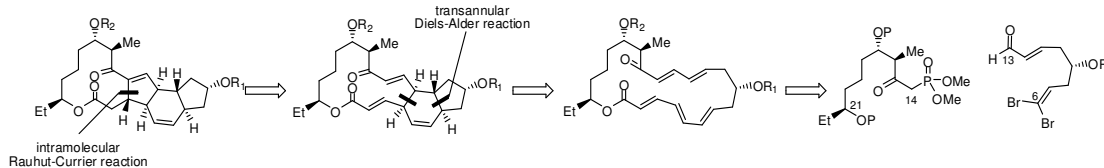


Figure 3-56. Retrosynthetic analysis of spinosyn A by the Roush group. (P: protecting group, R₁: α -trimethylrhannosyl, and R₂: forosamine)

Tietze and co-workers reported a synthesis of a novel spinosyn A analog, which contains a benzene ring instead of cyclopentene moiety in the aglycone, by two fold Pd-mediated Heck reaction in 2008 (**Figure 3-57**).¹⁸⁹

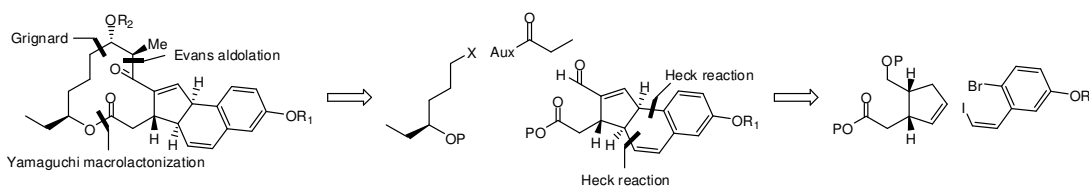


Figure 3-57. Retrosynthetic analysis of spinosyn A analog by the Tietze group. (P: protecting group, Aux: Evans chiral auxiliary, R₁: α -trimethylrhannosyl, and R₂: pivaloyl)

To my knowledge, the chemoenzymatic total synthesis of spinosyn A is another approach to complete the synthesis of the natural product by both organic synthesis and biosynthesis containing multi-enzymes. The precursor for the SpnJ reaction was synthesized based on organic synthesis utilizing Yamaguchi macrolactonization,¹³³ Julia-Kocienski olefination,^{134, 135} and Stille cross-coupling reaction,¹³⁶ as shown in **Figure 2-8**. A series of enzymatic transformations including SpnJ (oxidase), SpnM (dehydratase), SpnF (cyclase), SpnG (glycosyltransferase), SpnL (cyclase), SpnI, SpnK, and SpnH (*O*-methyltransferases) was then performed in one pot to produce a 17-pseudoaglycone of spinosyn A (**Figure 1-4**, and **Figure 3-58**).^{20, 21, 22} Interestingly, it was found that the

three methyltransferases could catalyze a series of methylations on the tricyclic aglycone substrate, which has not been reported before (**Figure 3-59**). The final step is expected to be a SpnP-catalyzed glycosylation with TDP-D-forosamine, but this has not been established yet due to the difficulty to prepare TDP-D-forosamine. Thus, etherification of D-forosamine and the tetracyclic precursor was performed by using $\text{BF}_3\text{-Et}_2\text{O}$ in dichloromethane at 0 °C for 6 hr and the desired product was isolated in 38% yield (**Figure 3-60**).

In conclusion, although the organic synthesis of the macrolactone precursor for the enzymatic reactions takes a great deal of time and labor, the final 8 enzymatic transformations only take several hr with high stereospecificity and yield. If the final step catalyzing the forosamine transfer is established, it will give a more efficient way to synthesize spinosyn A.

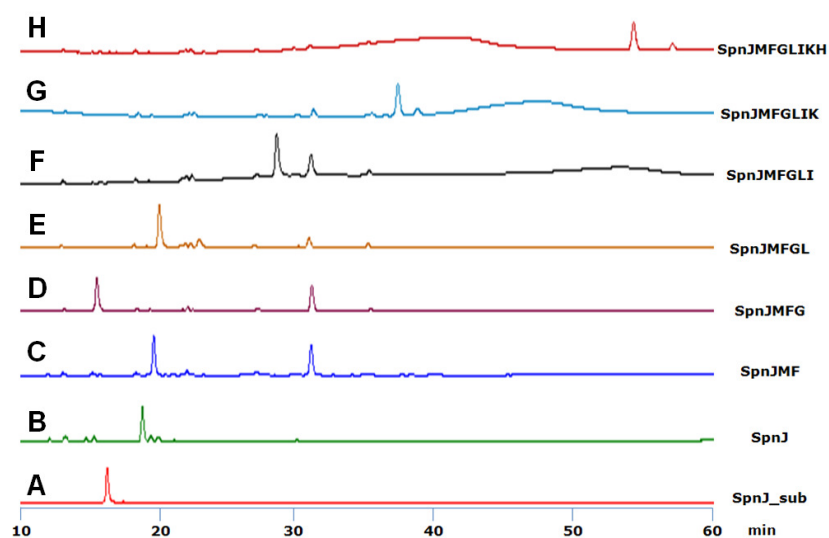


Figure 3-58. HPLC trace of enzymatic transformations using SpnJ, SpnM, SpnF, SpnG, SpnL, SpnI, SpnK, and SpnH to produce 17-pseudoaglycone of spinosyn A. (A) SpnJ substrate, (B) SpnJ product, (C) SpnM/F product, (D) SpnG product, (E) SpnI product, (F) SpnK product, and (G) SpnH product. (a peak near 31 min is a side product of SpnM reaction)

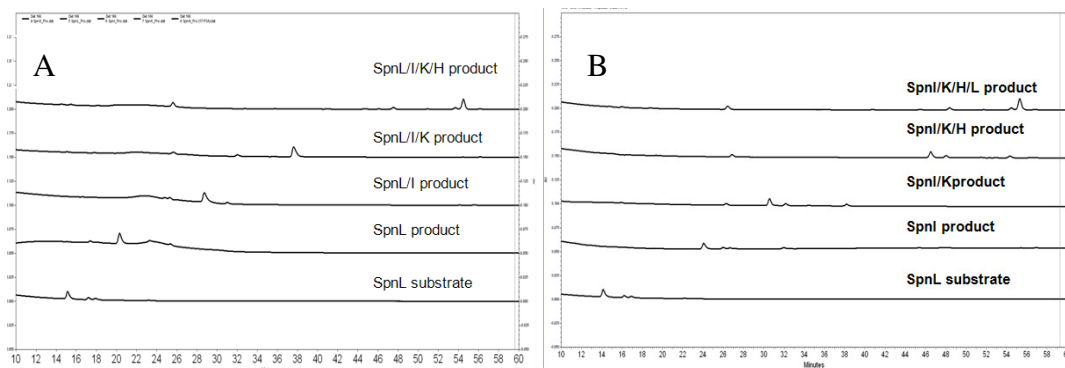


Figure 3-59. HPLC trace of SpnL/I/K/H reaction (left) versus SpnI/K/H/L reaction (right). HPLC conditions: C18 analytic column (250 x 4.6 mm, 5 μ m), aqueous acetonitrile: 30% to 60% over 60 min at a flow rate of 1 mL/min with detection at 267 nm.

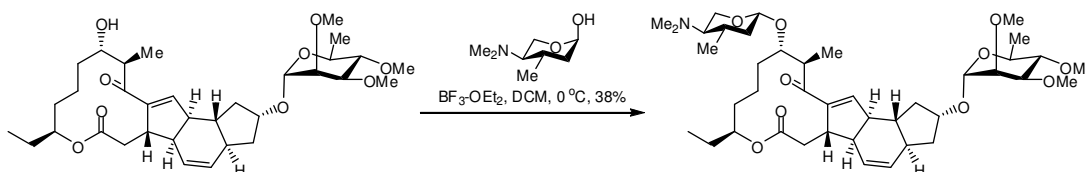


Figure 3-60. Etherification of D-forosamine to 17-pseudoaglycone of spinosyn A.

3.4. CONCLUSION

SpnL-catalyzed cyclization is the second “cross-bridging” process to produce a cyclopentene moiety in a perhydro-*as*-indacene core of spinosyn A. As mechanistic studies of SpnF-catalyzed [4+2] cycloaddition have been focused on verifying whether it is a true “Diels-Alderase”, mechanistic studies of SpnL-catalyzed cyclization have been concentrated on verifying whether it is a “Rauhut-Currierase”, which catalyzes the dimerization of two alkenes activated by nucleophilic addition. Since formation of the cyclopentene moiety can also proceed through the Michael addition mechanism, by which the activation of the conjugated system is initiated by deprotonation at the C-12 position, many biochemical studies were designed and described in Chapter 3 to differentiate the two plausible mechanisms for SpnL reaction.

First, the isotope trace experiment showed that one deuterium is introduced in the SpnL product, which seems to support the Rauhut-Currier type mechanism. However, it is possible that a proton abstracted by the active site base in the first step can return to the C-12 position in the last step through the Michael addition mechanism, resulting in the same monodeuterated SpnL product. A slightly inverse kinetic isotope effect for the C12-D SpnL substrate analog is too ambiguous to draw the conclusion because the result can be differently interpreted depending on the rate determining step. If the first step is the rate determining step, it is obvious that the Michael addition mechanism can be excluded based on the slightly inverse kinetic isotope effect at the C-12. However, we cannot rule out the possibility that the last deprotonation step is the more sensitive step for the SpnL reaction. Additional kinetic isotope effect studies using the C13-D analog is in progress, and expected to give more information about the SpnL mechanism.

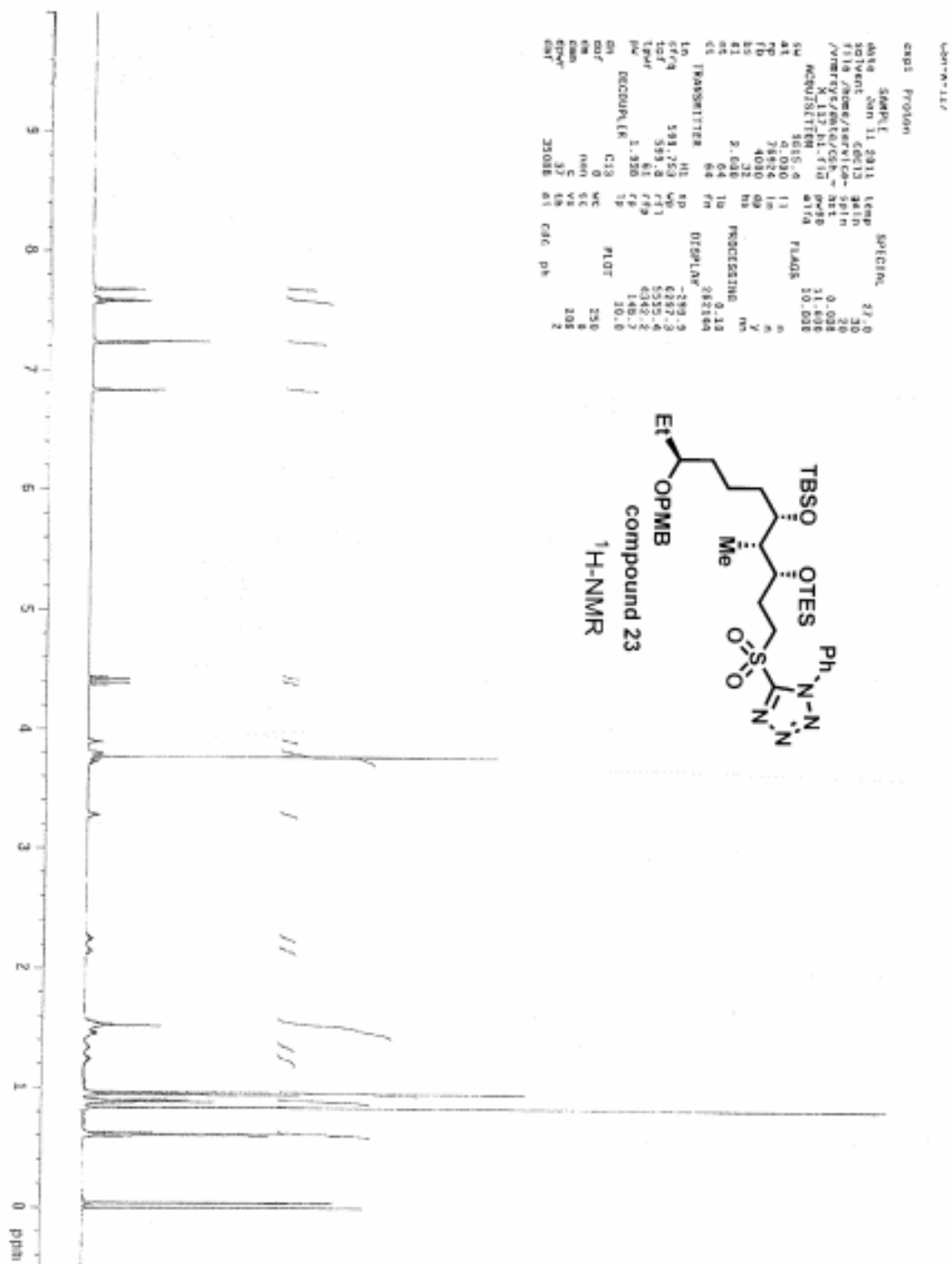
The C13-F SpnL substrate analog was initially designed to inactivate the SpnL reaction by covalent modification of active site residue, if the SpnL utilizes the Rauhut-Currier type mechanism. Biochemical studies show that the C13-F analog is indeed a mechanism-based inhibitor which makes a covalent adduct with SpnL. Furthermore, ESI MS/MS analysis of the covalent adduct reveals that the amino acid residue responsible for the nucleophilic attack is probably Cys60, Cys71, or Ser73, although the exact structure of the covalent adduct is still unknown. The newly designed ¹³C13-F SpnL substrate analog is expected to give more evidence for the Rauhut-Currier type mechanism.

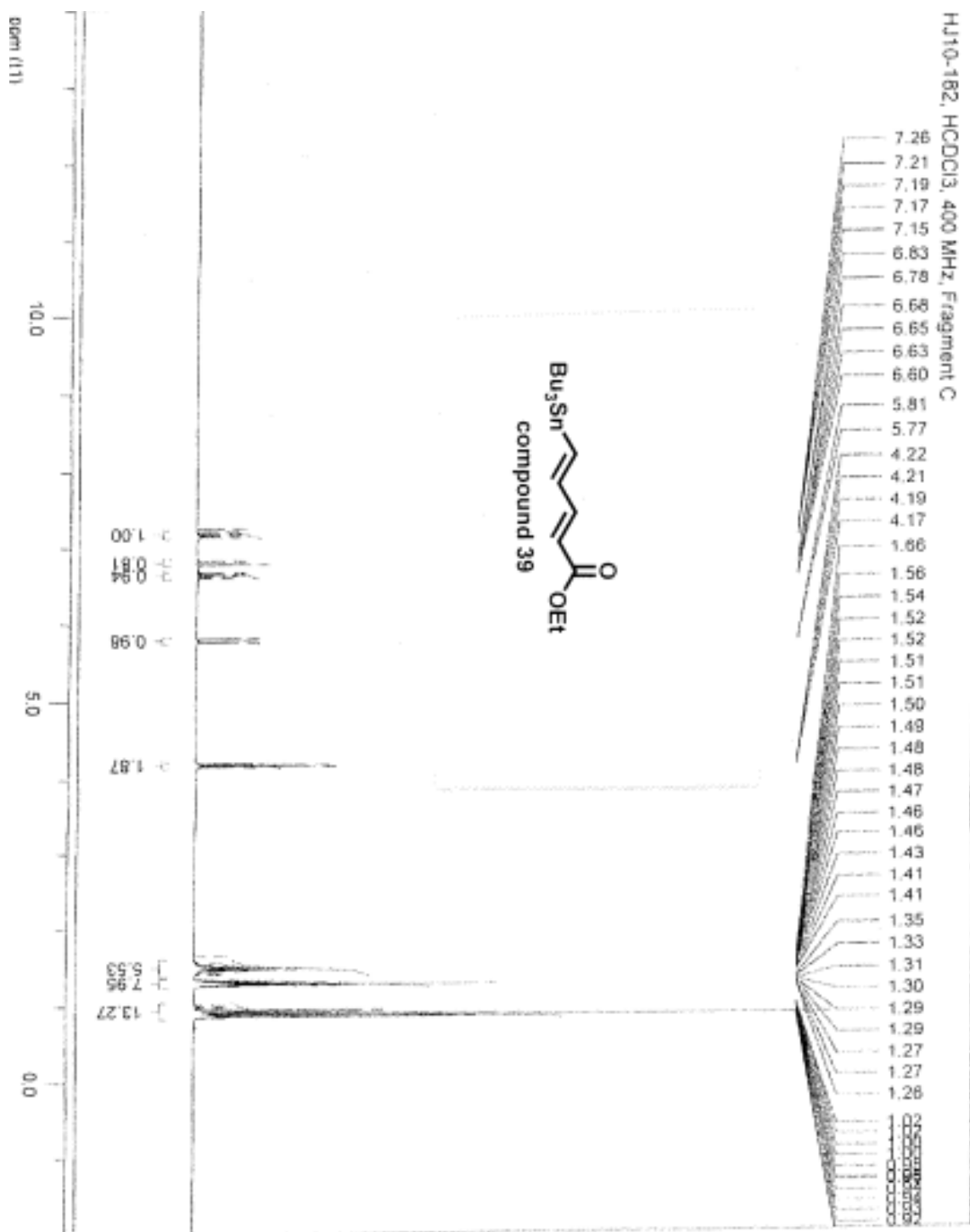
Biochemical studies about the role of SAM in SpnF and SpnL were performed using the denaturation and reconstitution of enzymes, and showed that the existence of SAM is required for the activity of SpnL, although it is uncertain for SpnF. Moreover, CD spectroscopy led to the hypothesis that SAM has a structural function. SAM may make the substrate binding site more active by connecting a methionine binding pocket and a 5'-deoxyacenosine binding pocket, as described in **Section 3.3.6**. In addition, SpnL mutant studies showed that Glu96 may play an important role in the catalysis of SpnL. Finally, the chemoenzymatic total synthesis of spinosyn A was completed by etherification of 17-pseudoaglycone and D-forosamine. In the near future, it is expected that SpnP, the glycosyltransferase, will be established to catalyze the final step of the biosynthesis of spinosyn A.

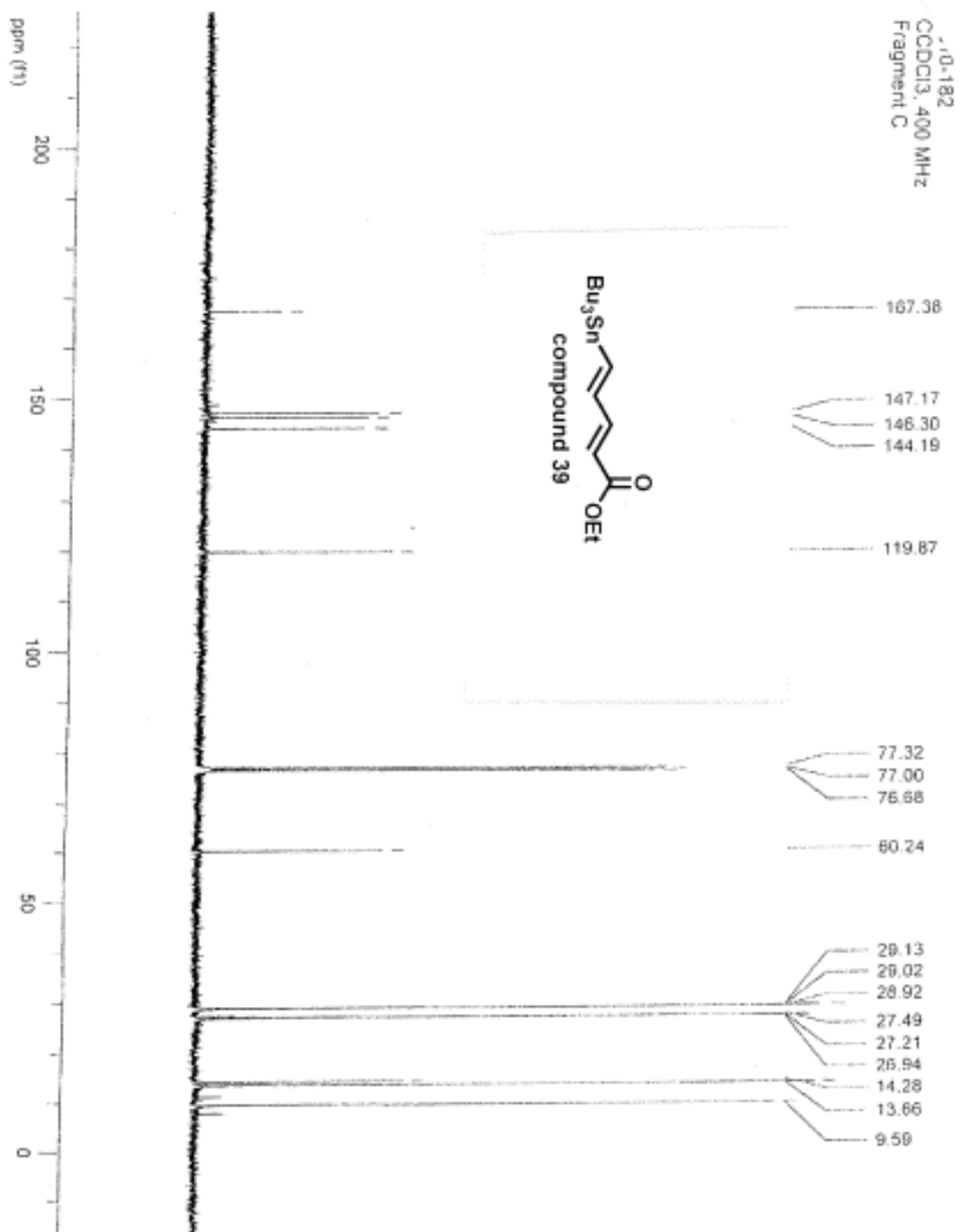
In conclusion, many interesting aspects of SpnL-catalyzed cyclization have been studied in Chapter 3. Mechanistically, SpnL reaction seems to proceed through the Rauhut-Currier type mechanism, based on the biochemical studies using the C13-F analog. Additional experimental data on the SpnL-catalyzed reaction will give more insights of the reaction mechanism. Also, several other interesting questions, such as why SpnF and SpnL are dependent on SAM, and what is the order of enzymatic transformations in the biosynthesis of spinosyn A will be further investigated in the future.

Appendix

A.1. Spectral Data for Chapter 2



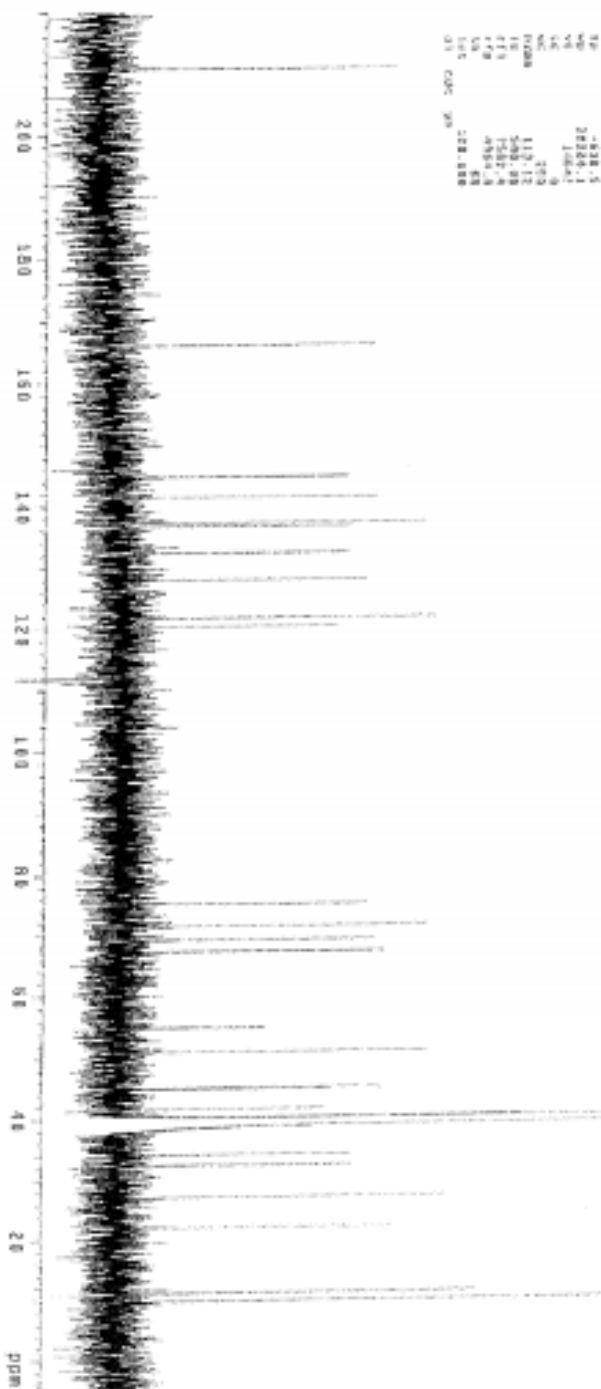
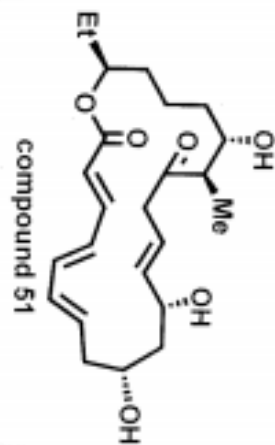




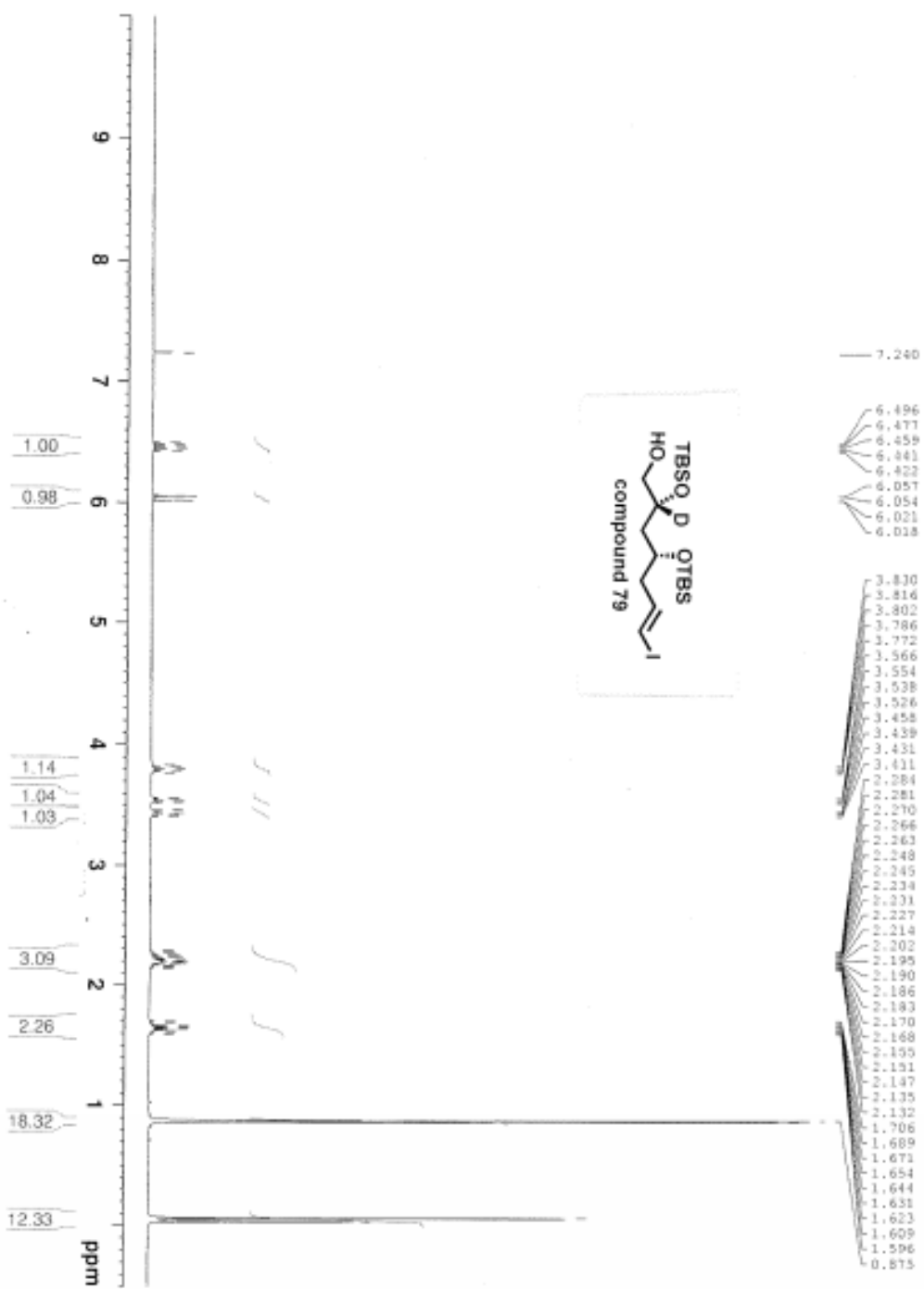

```

NAME: 5p1
NAME2: 51
EXPNO: 1
PROCNO: 1
PROCPS: 1
SOLVENT: DMSO
CONC: 228.888
AQ: 0.156137
RG: 320
RT: 1.00
F2: 100.626177
F3: 100.626177
F4: 100.626177
F5: 100.626177
F6: 100.626177
F7: 100.626177
F8: 100.626177
F9: 100.626177
F10: 100.626177
F11: 100.626177
F12: 100.626177
F13: 100.626177
F14: 100.626177
F15: 100.626177
F16: 100.626177
F17: 100.626177
F18: 100.626177
F19: 100.626177
F20: 100.626177
F21: 100.626177
F22: 100.626177
F23: 100.626177
F24: 100.626177
F25: 100.626177
F26: 100.626177
F27: 100.626177
F28: 100.626177
F29: 100.626177
F30: 100.626177
F31: 100.626177
F32: 100.626177
F33: 100.626177
F34: 100.626177
F35: 100.626177
F36: 100.626177
F37: 100.626177
F38: 100.626177
F39: 100.626177
F40: 100.626177
F41: 100.626177
F42: 100.626177
F43: 100.626177
F44: 100.626177
F45: 100.626177
F46: 100.626177
F47: 100.626177
F48: 100.626177
F49: 100.626177
F50: 100.626177
F51: 100.626177
F52: 100.626177
F53: 100.626177
F54: 100.626177
F55: 100.626177
F56: 100.626177
F57: 100.626177
F58: 100.626177
F59: 100.626177
F60: 100.626177
F61: 100.626177
F62: 100.626177
F63: 100.626177
F64: 100.626177
F65: 100.626177
F66: 100.626177
F67: 100.626177
F68: 100.626177
F69: 100.626177
F70: 100.626177
F71: 100.626177
F72: 100.626177
F73: 100.626177
F74: 100.626177
F75: 100.626177
F76: 100.626177
F77: 100.626177
F78: 100.626177
F79: 100.626177
F80: 100.626177
F81: 100.626177
F82: 100.626177
F83: 100.626177
F84: 100.626177
F85: 100.626177
F86: 100.626177
F87: 100.626177
F88: 100.626177
F89: 100.626177
F90: 100.626177
F91: 100.626177
F92: 100.626177
F93: 100.626177
F94: 100.626177
F95: 100.626177
F96: 100.626177
F97: 100.626177
F98: 100.626177
F99: 100.626177
F100: 100.626177

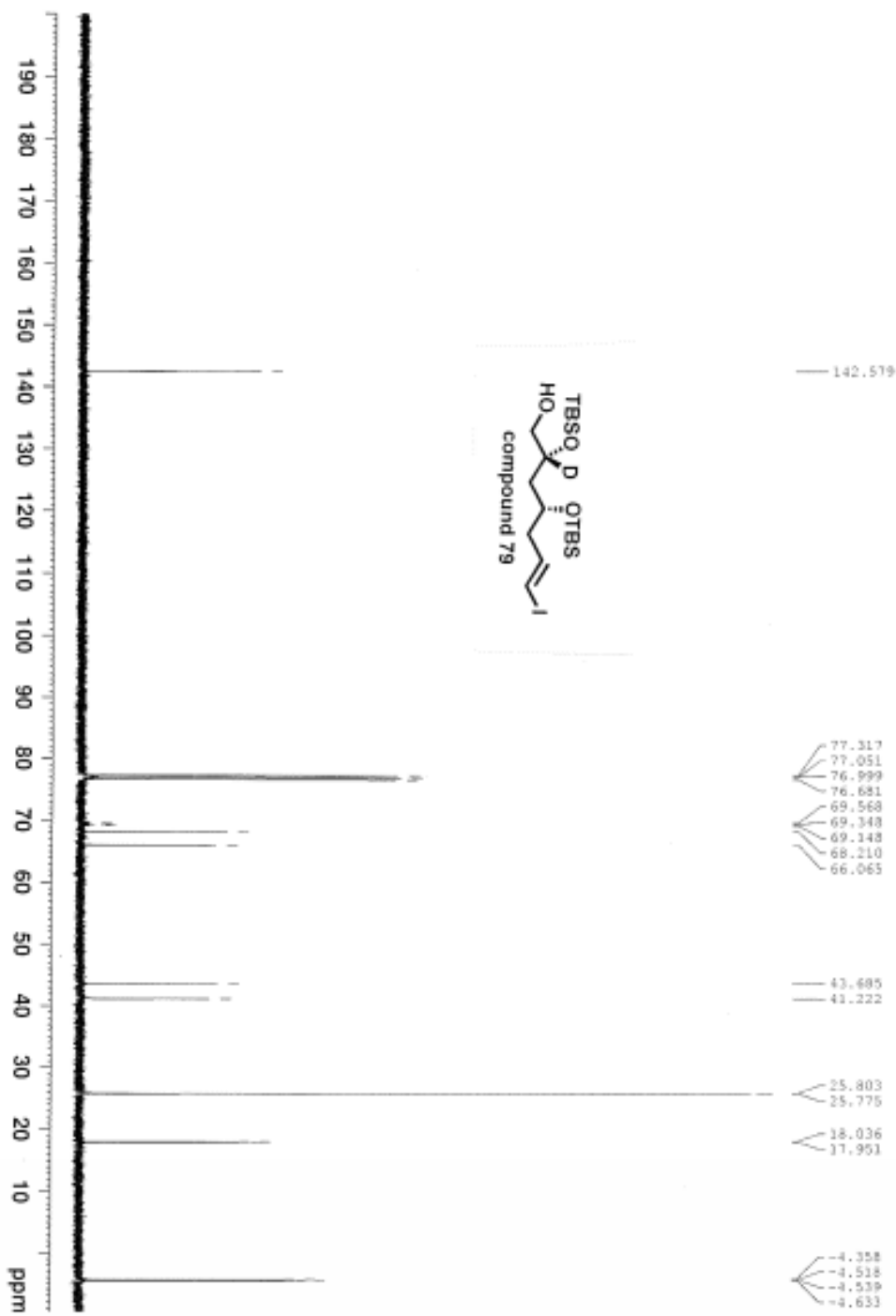
```



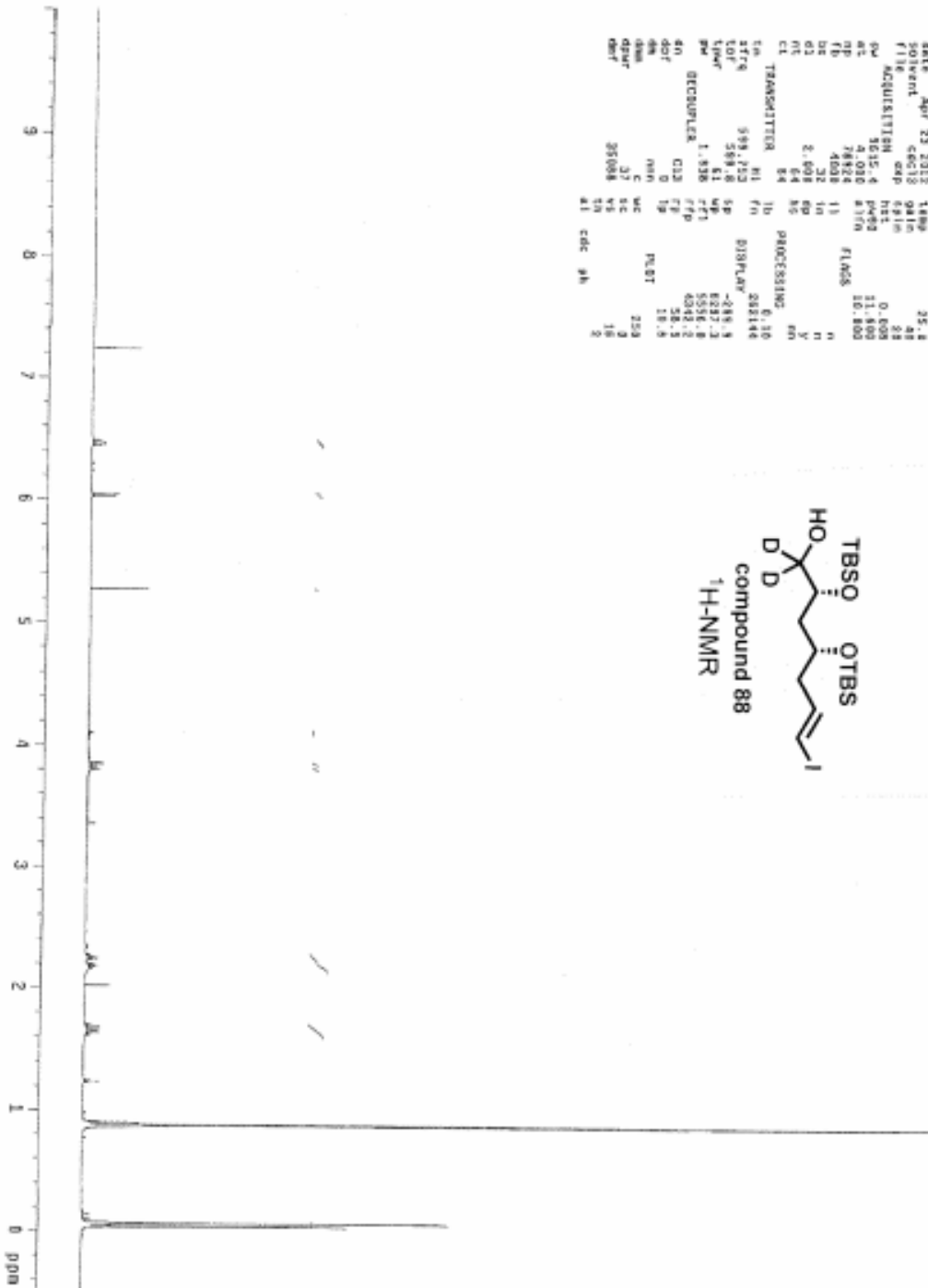
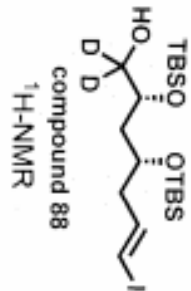
GML2150B 20130613 CDCl3 400MHz



GML21508 20130614 CDCl3 13C 100MHz



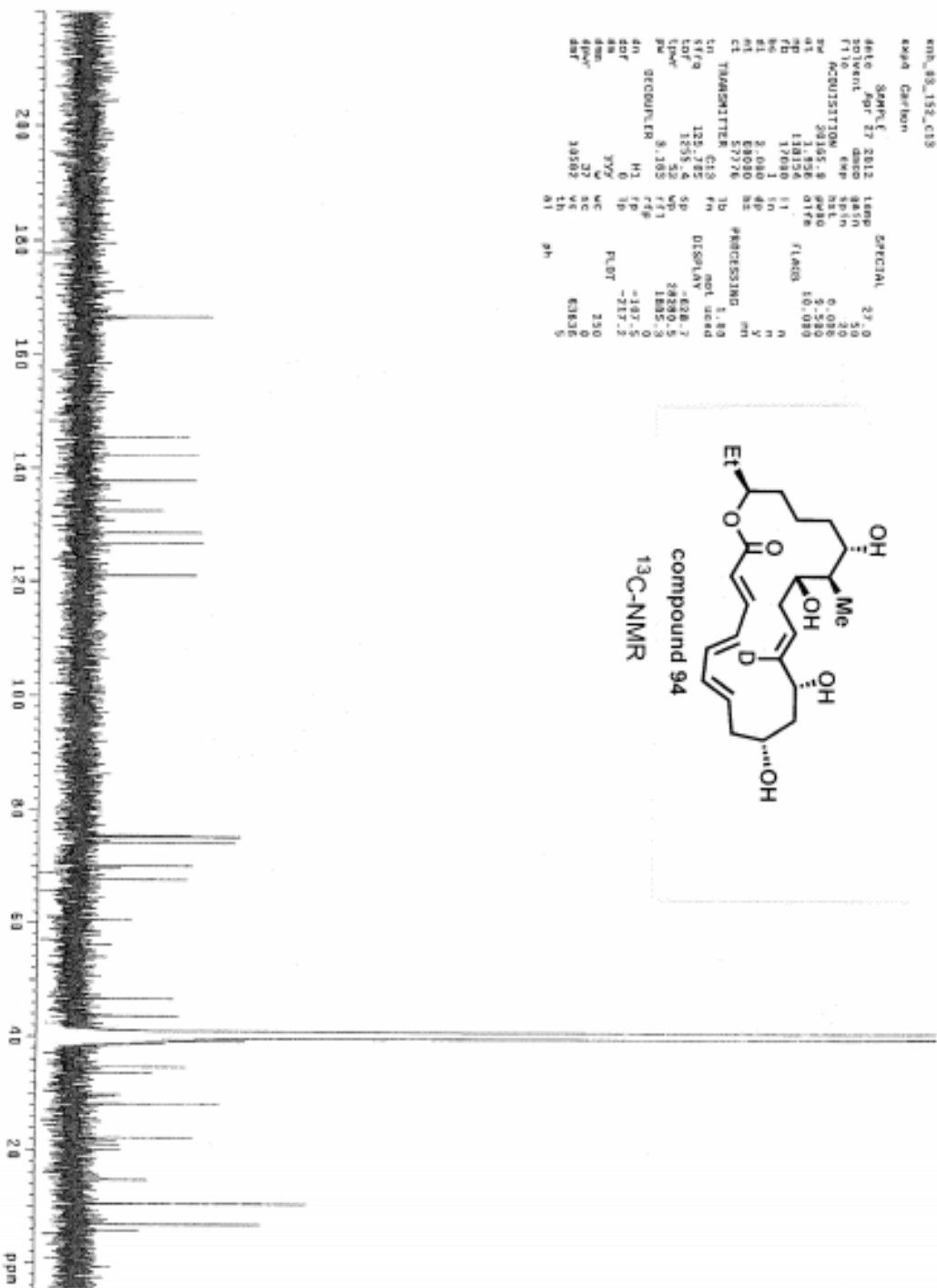
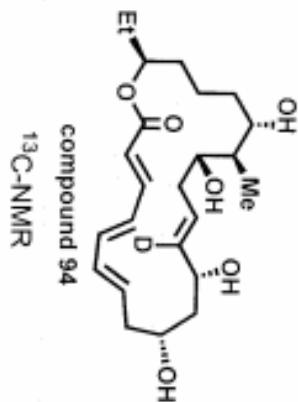
4KX1 F70108
 SAMPLE
 DATE Apr 23 2012 1809 SPECIAL 25.1
 SOLVENT cdc13d gain 48
 FILE ACQUISITION exp 691h 28
 NO 2635.4 p493 0.009
 QZ 78820 817H 21.800
 FB 4008 13 10.800
 DC 32 1h n
 Q3 2.408 6p v
 Q5 64 85 m
 CL TRANSMITTER 84 1b PROCESSING 6.10
 1a 1179 599.253 1h 018FLAF 208144
 LOF 598.2 5p
 TMR 61 4p 6287.2
 PM 1.836 7f1 5556.8
 DECOUPLE C12 7f 4049.2
 AQ 0 1p 28.5
 DRP 0 1p PLST 18.5
 DM n/n
 DM 5 w/c 259
 dpr 3 v/c 13
 dpr 35008 1h 2
 AT cdc gh



expd_88_152_C13

expd Carbon

date	SAMPLE	1800	SPECIAL	27.0
2012	27	1800		27.0
solvent	dmso	gash		30
FTIR	exp	nat		0.080
ACQUISITION	2012.8	9W80	FLA00	5.250
41	13526	0176	FLA00	10.080
70	17080	1		0
80	1	1		0
81	2.080	4P		0
82	80080	82	PROGRESSING	00
83	27276	70		1.80
CT	TAMMCHITTER	C13	PH	not used
STFQ	125.725	5P	DISPLAY	-828.7
LOF	1255.4	5P		28280.5
CPW	52	WP		1885.3
PR	8.185	FFI		-197.0
DECOUPLER	H1	FFP		-217.2
40	0	7P	FLDT	250
80F	0	MC		0
88	YYY	MC		0
89	27	SC		0
90W	38582	VC		0
90F	0	VC		0
91	0	VC		0

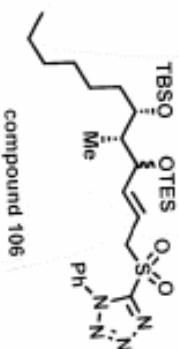


500 MHz nmr

knr_5_163.n1

exp4 Corson

SAMPLE SPECIAL 27.0
date apr 26 2013 1400 0010
solvent ccd13 5.0
file exp 301n
ACQUISITION 8.008
S1 32673.7 8439 11.600
01 1.158 4174 18.000
F2 12808 11
F3 18008 11
F4 18008 11
F5 2.000 10
F6 2.000 10
F7 10000 10
F8 10000 10
F9 18000 10
F10 18000 10
F11 18000 10
F12 18000 10
F13 18000 10
F14 18000 10
F15 18000 10
F16 18000 10
F17 18000 10
F18 18000 10
F19 18000 10
F20 18000 10
F21 18000 10
F22 18000 10
F23 18000 10
F24 18000 10
F25 18000 10
F26 18000 10
F27 18000 10
F28 18000 10
F29 18000 10
F30 18000 10
F31 18000 10
F32 18000 10
F33 18000 10
F34 18000 10
F35 18000 10
F36 18000 10
F37 18000 10
F38 18000 10
F39 18000 10
F40 18000 10
F41 18000 10
F42 18000 10
F43 18000 10
F44 18000 10
F45 18000 10
F46 18000 10
F47 18000 10
F48 18000 10
F49 18000 10
F50 18000 10
F51 18000 10
F52 18000 10
F53 18000 10
F54 18000 10
F55 18000 10
F56 18000 10
F57 18000 10
F58 18000 10
F59 18000 10
F60 18000 10
F61 18000 10
F62 18000 10
F63 18000 10
F64 18000 10
F65 18000 10
F66 18000 10
F67 18000 10
F68 18000 10
F69 18000 10
F70 18000 10
F71 18000 10
F72 18000 10
F73 18000 10
F74 18000 10
F75 18000 10
F76 18000 10
F77 18000 10
F78 18000 10
F79 18000 10
F80 18000 10
F81 18000 10
F82 18000 10
F83 18000 10
F84 18000 10
F85 18000 10
F86 18000 10
F87 18000 10
F88 18000 10
F89 18000 10
F90 18000 10
F91 18000 10
F92 18000 10
F93 18000 10
F94 18000 10
F95 18000 10
F96 18000 10
F97 18000 10
F98 18000 10
F99 18000 10
F100 18000 10

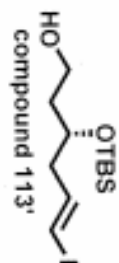


LSM-91-137

exp1 Proton

```

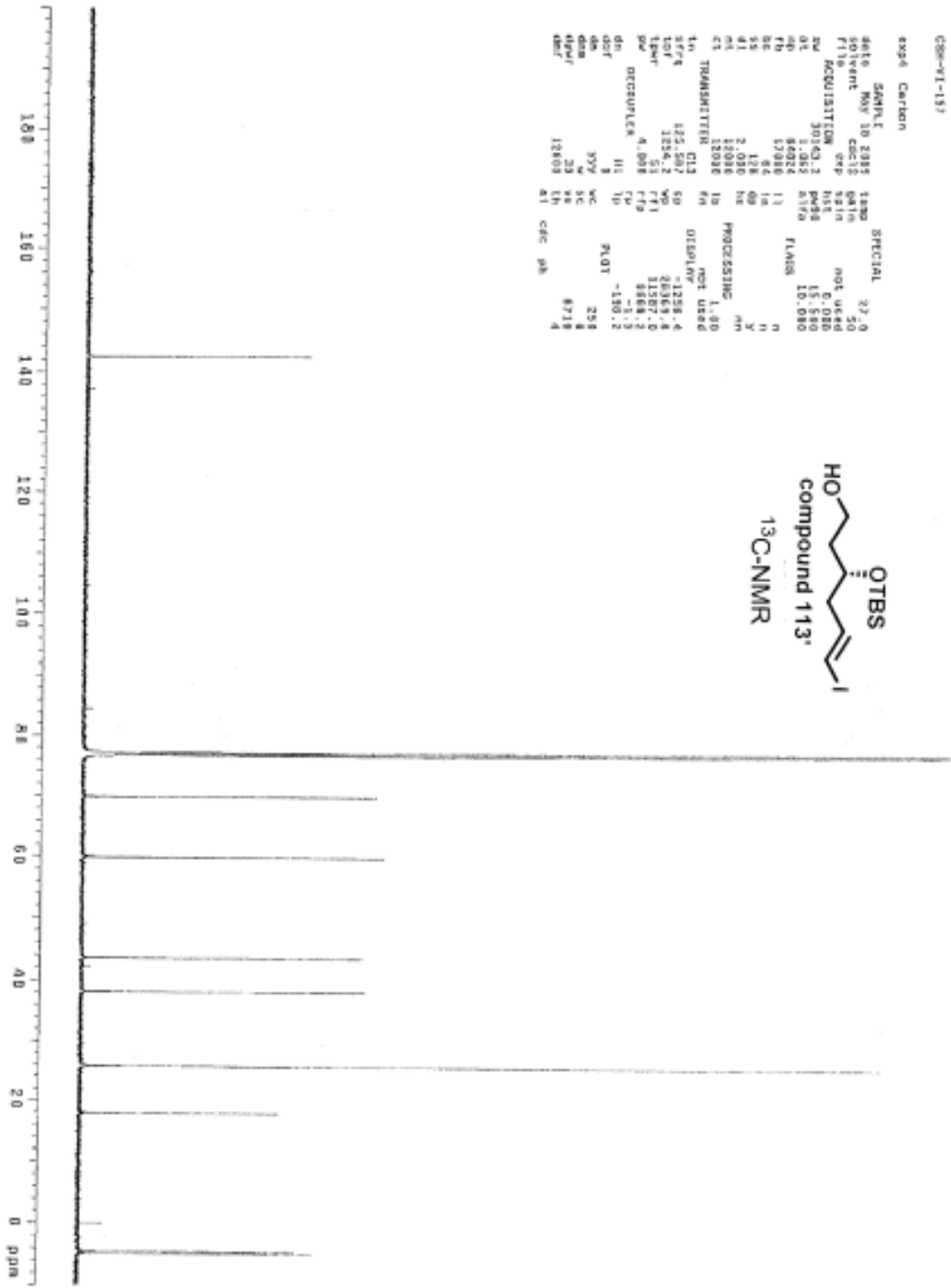
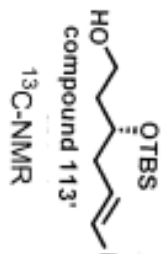
NAME      MAY 28 2085 1000 SPECIAL 27.4
DATE      66613 0010  58
FILE      A00033710M 449 1010  not used
LV        7290.4  P045  15.100
GC        6.095  0174  6.080
NU        64605  11  FLAG5  0
NU        4609  11
NU        22  14
NU        2.322  02  Y
NU        64  04  NO
NU        84  10  PROCESSING 0.18
NU        84  10  DISPLAY 85326
NAME      TRANSMITTER H1
TO        459.402  4P  -249.6
TGT       459.4  4P  3242.5
LSMR      1.529  7FD  4828.2
PW        2.553  7P  3052.4
DECIMATE  C19  1/2  3.7
AQ        0
AM        000  UC  259
SM        32  SC  0
DM        32  SC  159
DBF       32258  14  CQC  0
  
```



08-11-13

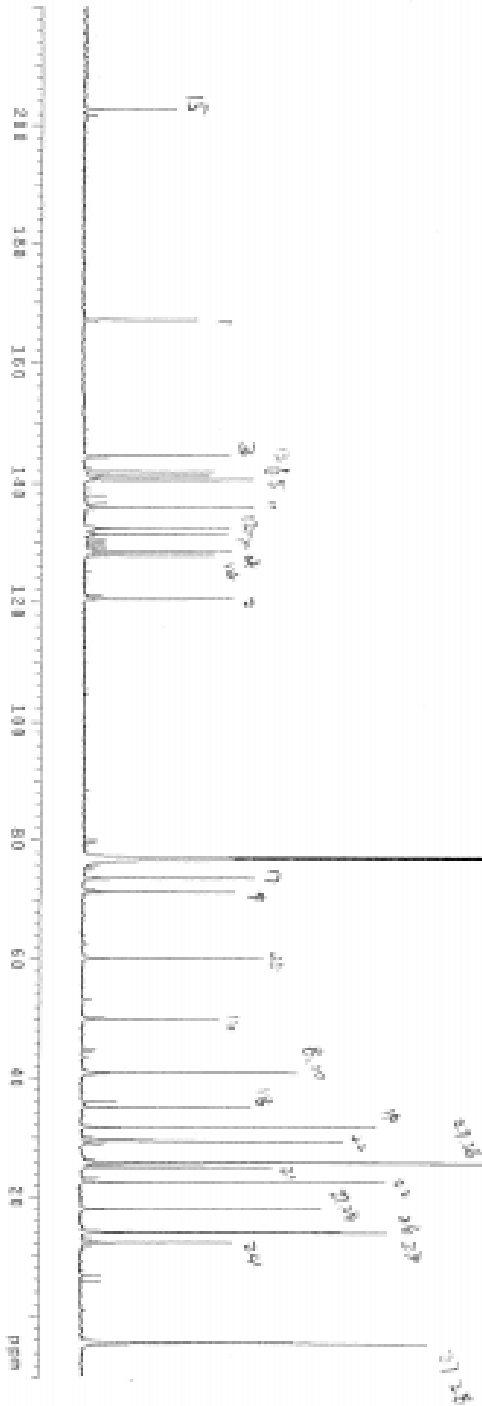
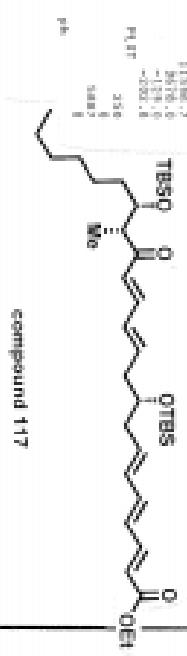
expd Carbon

DATE	SAMPLE	NOV 10 2013	1830	SPECIAL	27.50
FILE	00012	0414	0414	NOT UP	50
ACQUISITION	01	01	01	15.580	15.580
	1.013	ALFA	FLAHS	10.080	10.080
01	8024	11			
02	1798	11			
03	17	08			
04	12	08			
05	2.030	HE	PROCESSING	AM	3
06	12036	10			
07	12036	10			
08	12036	10			
09	12036	10			
10	12036	10			
11	12036	10			
12	12036	10			
13	12036	10			
14	12036	10			
15	12036	10			
16	12036	10			
17	12036	10			
18	12036	10			
19	12036	10			
20	12036	10			
21	12036	10			
22	12036	10			
23	12036	10			
24	12036	10			
25	12036	10			
26	12036	10			
27	12036	10			
28	12036	10			
29	12036	10			
30	12036	10			
31	12036	10			



500 MHz NMR
 exp_05_181_0_018

Signal	Chemical Shift (ppm)	Integration	Assignment
1	7.15	1.00	CH=CH-
2	6.85	1.00	CH=CH-
3	6.55	1.00	CH=CH-
4	6.25	1.00	CH=CH-
5	5.95	1.00	CH=CH-
6	5.65	1.00	CH=CH-
7	5.35	1.00	CH=CH-
8	5.05	1.00	CH=CH-
9	4.75	1.00	CH=CH-
10	4.45	1.00	CH=CH-
11	4.15	1.00	CH=CH-
12	3.85	1.00	CH=CH-
13	3.55	1.00	CH=CH-
14	3.25	1.00	CH=CH-
15	2.95	1.00	CH=CH-
16	2.65	1.00	CH=CH-
17	2.35	1.00	CH=CH-
18	2.05	1.00	CH=CH-
19	1.75	1.00	CH=CH-
20	1.45	1.00	CH=CH-
21	1.15	1.00	CH=CH-
22	0.85	1.00	CH=CH-
23	0.55	1.00	CH=CH-
24	0.25	1.00	CH=CH-
25	0.00	1.00	TMS

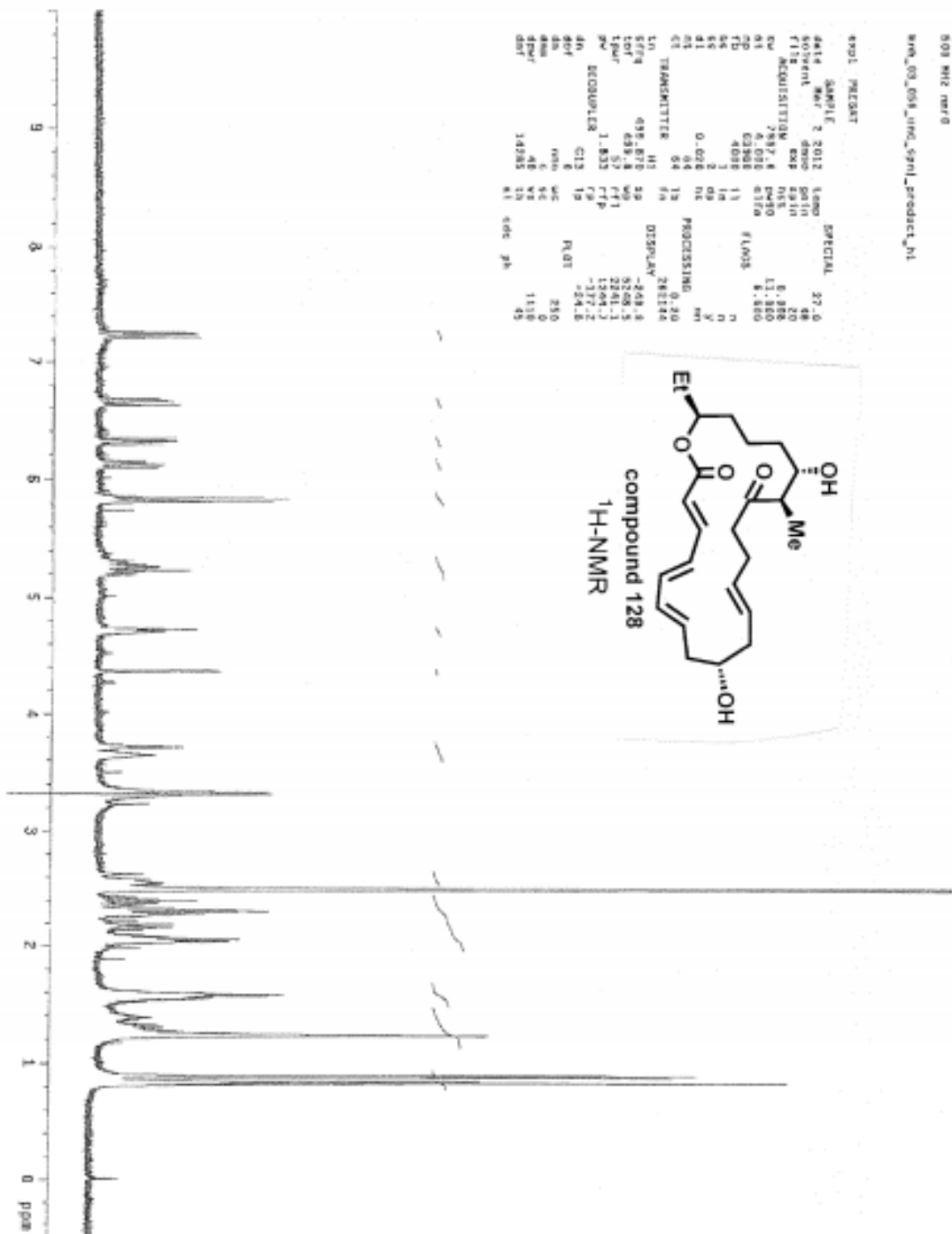
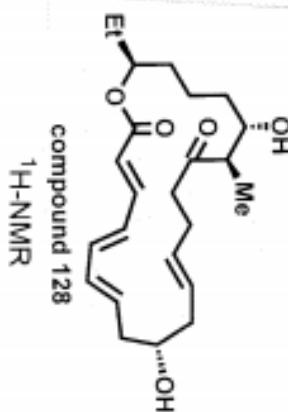


808 MHz NMR

exp_03_054_1mg_Spnl_Product_01

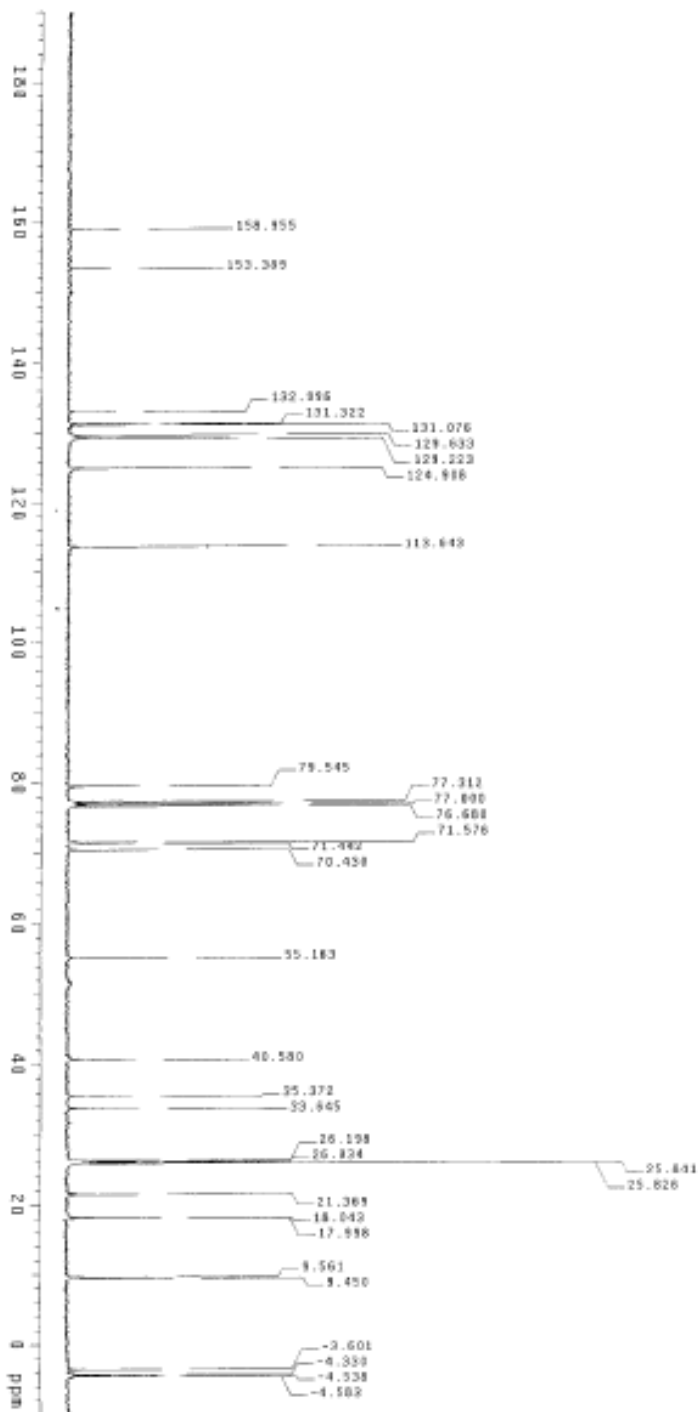
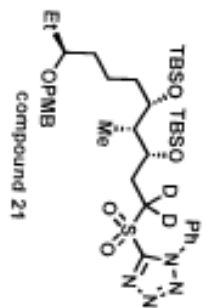
PRESENT

DATA	SAMPLE	NAME	2012	LEMO	SPECIAL	27.0
SOLVENT	DMF	DMF-D ₂				48
FTIR	ACQUISITION	EXP	0410			20
EXP	7587.8	PMW0				5.850
CP	4.078	6170	FLW05			13.850
TD	4038	11				5.850
SC	1	18				7
SE	1	18				7
SI	0.678	18				7
ST	04	18				7
CT	04	18				7
TRANSMITTER	H1	FH				0.20
RECEIVER	H1	SD				28184
CONV	438.878	UC				458.8
TDI	638.8	UC				9208.8
TDPI	57	FT1				2581.2
PC	1.833	FTP				1304.2
DECORREL	C12	TA				-177.2
AN						-24.8
SDI	8	UC				R.03
SDI	8	UC				250
AM	4	UC				0
DMF	48	UC				1310
DMF	18285	TA				45
DMF	41	608	PH			



20130916_040811_23060613
 Acquire directory:
 Sample directory:
 Pulse sequence: zgpg30
 Solvent: CDCl3
 Acquire temperature
 User: jh144
 F2: 101.625 MHz
 F1: 500.136 MHz
 FWHM: 508 Hz
 Aquisition

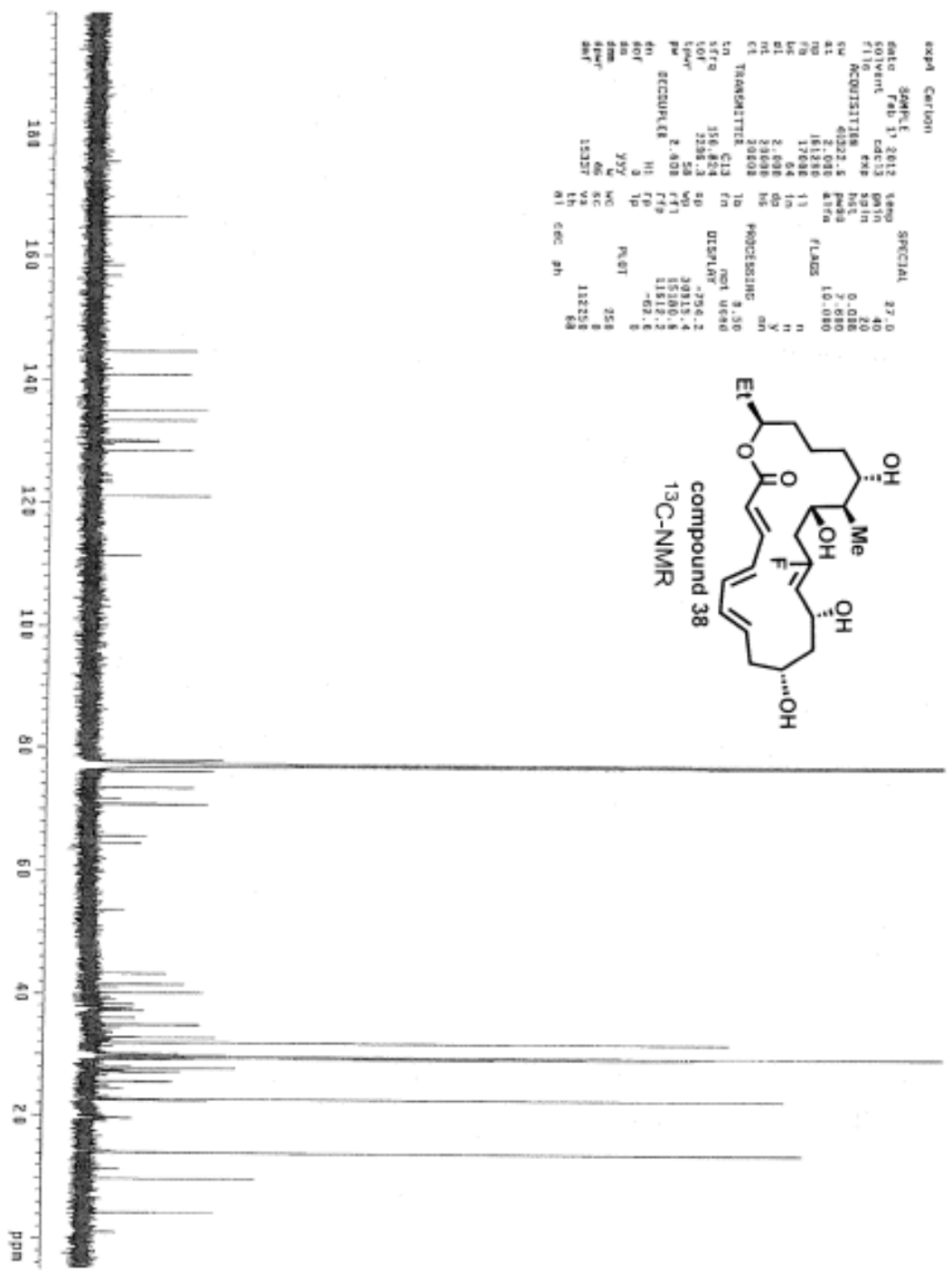
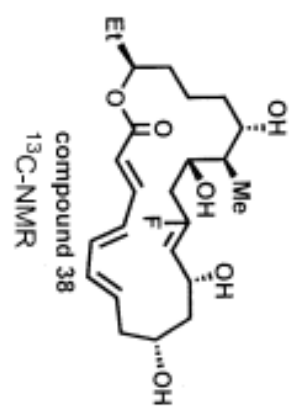
Relax. delay: 2.000 sec
 Pulse: 30.0 degrees
 Acq. time: 1.389 sec
 Width: 24500.0 Hz
 256 FID points
 256 F2 points
 256 F1 points
 256 FWHM
 Power: 44.00
 Continuously on
 MWTZ-16 not loaded
 DATA PROCESSING
 Line broadening: 2.0 Hz
 F1 size: 65536
 Total time: 14 min, 7 sec




```

expd Carbon
=====
date_ 04APR 17 2012 temp SPECIAL 27.0
solvent_ CDCl3 shift 40
F1 F2 ACQUISITION exp 561
NUC1 13C 40027.5 PWR 0.030
NUC2 13C 161280 ALFA 7.080
NUC3 13C 17092 11 FLAOS 10.080
NUC4 13C 17092 11
NUC5 13C 17092 11
NUC6 13C 17092 11
NUC7 13C 17092 11
NUC8 13C 17092 11
NUC9 13C 17092 11
NUC10 13C 17092 11
NUC11 13C 17092 11
NUC12 13C 17092 11
NUC13 13C 17092 11
NUC14 13C 17092 11
NUC15 13C 17092 11
NUC16 13C 17092 11
NUC17 13C 17092 11
NUC18 13C 17092 11
NUC19 13C 17092 11
NUC20 13C 17092 11
NUC21 13C 17092 11
NUC22 13C 17092 11
NUC23 13C 17092 11
NUC24 13C 17092 11
NUC25 13C 17092 11
NUC26 13C 17092 11
NUC27 13C 17092 11
NUC28 13C 17092 11
NUC29 13C 17092 11
NUC30 13C 17092 11
=====

```



Bibliography

1. Hutchinson, C. R. Microbial polyketide synthases: More and more prolific. *Proc. Natl. Acad. Sci. U.S.A.* **1999**, *96* (7), 3336–3338.
2. Staunton, J.; Weissman, K. J. Polyketide biosynthesis: a millennium review. *Nat. Prod. Rep.* **2001**, *18*, 380-416.
3. Zhang, W.; Tang, Y. Combinatorial biosynthesis of natural products. *J. Med. Chem.* **2008**, *51* (9), 2629-2633.
4. Kirst, H. A.; Michel, K. H.; Martin, J. W.; Creemer, L. C.; Chio, E. H.; Yao, R. C.; Nakatsukasa, W. M.; Boeck, L. D.; Oocolowitz, J. L.; Paschal, J. W.; Deeter, J. B.; Jones, N. D.; Thompson, G. D. A83543A-D, unique fermentation-derived tetracyclic macrolides. *Tetrahedron Lett.* **1991**, *32* (37), 4839-4842.
5. Thompson G. D.; Dutton R.; Sparks T. C. Spinosad - a case study: an example from a natural products discovery programme. *Pest. Manag. Sci.* **2000**, *56*, 696–702.
6. Sparks, T. C.; Crouse, G. D.; Durst, G. Natural products as insecticides: the biology, biochemistry and quantitative structure-activity relationships of spinosyns and spinosoids. *Pest. Manag. Sci.* **2001**, *57* (10), 896-905.
7. Kirst, H. A. The spinosyn family of insecticides: realizing the potential of natural products research. *J. Antibiot.* **2010**, *63* (93), 101-111.
8. Salgado, V. L. Studies on the mode of action of spinosad: insect symptoms and physiological correlates. *Pest. Biochem. Physiol.* **1998**, *60* (2), 91-102
9. Salgado, V. L.; Sheets, J. J.; Watson, G. B.; Schmidt, A. L. Studies on the mode of action of spinosad: the internal effective concentration and the concentration dependence of neural excitation. *Pest. Biochem. Physiol.* **1998**, *60* (2), 103-110.

10. Watson, G. B. Action of insecticidal spinosyns on γ -aminobutyric acid responses from small-diameter cockroach neurons. *Pest. Biochem. Physiol.* **2001**, *71* (1), 20-28.
11. Orr, N.; Shaffner, A. J.; Richey, K.; Couse, G. D. Novel mode of action of spinosad: receptor binding studies demonstrating lack of interaction with known insecticidal target sites. *Pest. Biochem. Physiol.* **2009**, *95* (1), 1-5.
12. Millar, N. S.; Denholm, I. Nicotinic acetylcholine receptors: targets for commercially important insecticides. *Invert Neurosci.* **2007**, *7* (1), 53-66.
13. Salgado, V. L.; Saar, R. Desensitizing and non-desensitizing subtypes of alpha-bungarotoxin-sensitive nicotinic acetylcholine receptors in cockroach neurons. *J. Insect Physiol.* **2004**, *50* (10), 869-879.
14. Orr, N.; Hasler, J.; Watson, G.; Mitchell, J.; Gustafson, G.; Gifford, J.; Geng, C.; Chouinard, S.; Cook, K. Spinosad: from nature to green chemistry to novel mode of action. **2006**, In: 11th UPAC International Congress of Pesticide Chemistry Abstracts, Kobe, Japan, p 27
15. Madduri, K.; Waldron, C.; Merlo, D. J. Rhamnose biosynthesis pathway supplies precursors for primary and secondary metabolism in *Saccharopolyspora spinosa*. *J. Bacteriol.* **2001**, *183* (19), 5632-5638.
16. Zhao, Z. B.; Hong, L.; Liu, H.-w. Characterization of protein encoded by SpnR from the spinosyn gene cluster of *Saccharopolyspora spinosa*: Mechanistic implications for forosamine biosynthesis. *J. Am. Chem. Soc.* **2005**, *127* (21), 7692-7693.
17. Hong, L.; Zhao, Z. B.; Liu, H.-w. Characterization of SpnQ from the spinosyn biosynthetic pathway of *Saccharopolyspora spinosa*: Mechanistic and evolutionary implications for C-3 deoxygenation in deoxysugar biosynthesis. *J. Am. Chem. Soc.* **2006**, *128* (44), 14262-14263.

18. Hong, L.; Zhao, Z. B.; Melancon, C. E.; Zhang, H.; Liu, H.-w. In vitro characterization of the enzymes involved in TDP-d-foresamine biosynthesis in the spinosyn pathway of *Saccharopolyspora spinosa*. *J. Am. Chem. Soc.* **2008**, *130* (14), 4954-4967.
19. Waldron, C.; Matsushima, P.; Rosteck, P. R.; Broughton, M. C.; Turner, J.; Madduri, K.; Crawford, K. P.; Merlo, D. J.; Baltz, R. H. Cloning and analysis of the spinosad biosynthetic gene cluster of *Saccharopolyspora spinosa*. *Chem. Biol.* **2001**, *8* (5), 487-499.
20. Kim, H. J.; Pongdee, R.; Wu Q.; Hong, L.; Liu, H.-w. The biosynthesis of spinosyn in *Saccharopolyspora spinosa*: synthesis of the cross-bridging precursor and identification of the function of SpnJ. *J. Am. Chem. Soc.* **2007**, *129* (47), 14582-14584.
21. Kim, H. J.; White-Phillip, J. A.; Ogasawara, Y.; Shin, N.; Isiorho, E. A.; Liu, H.-w. Biosynthesis of Spinosyn in *Saccharopolyspora spinosa*: Synthesis of Permethylated Rhamnose and Characterization of the Functions of SpnH, SpnI, and SpnK. *J. Am. Chem. Soc.* **2010**, *132* (9), 2901-2903.
22. Kim, H. J.; Ruszczychy, M. W.; Choi, S. H.; Liu, Y. N.; Liu, H.-w. Enzyme-catalyzed [4+2] cycloaddition is a key step in the biosynthesis of spinosyn A. *Nature* **2011**, *473* (7345), 109-112.
23. Martin, C. J.; Timoney, M. C.; Sheridan, R. M.; Kendrew, S. G.; Wilkinson, B.; Staunton, J.; Leadlay, P. F. Heterologous expression in *Saccharopolyspora erythraea* of a pentaketide synthase derived from the spinosyn polyketide synthase. *Org. Biomol. Chem.* **2003**, *1* (23), 4144-4147.
24. Oikawa, H. Biosynthesis of structurally unique fungal metabolite GKK1032A (2): Indication of novel carbocyclic formation mechanism in polyketide biosynthesis. *J. Org. Chem.* **2003**, *68* (9), 3552-3557.

25. Diels, O.; Alder, K. Synthesesen in der hydroaromatischen Reihe. *Justus Leibig's Annalen der Chemie* **1928**, *460*, 98-122.
26. Synthesis of the hydro aromatic sequence, *Ann.* **1929**, *470*, 62.
27. Diels, O.; Alder, K. Synthesis in the hydroaromatic series, IV. Announcement: the rearrangement of malein acid anhydride on arylated diene, triene, and fulvene. *Ber.* **1929**, *62*, 2081 & 2087.
28. Huisgen, R. Cycloaddition – definition, classification, and characterization. *Angew. Chem. Int. Ed.* **1968**, *7* (5), 321-406.
29. Rauhut, M. M.; Currier, H. U. Preparation of dialkyl-2-methylene glutamates. **1963**, U. S. Patent 3074999, American Cyanamid Co.
30. Aroyan, C. E.; Dermenci, A.; Miller, S. J. The Rauhut-Currier reaction: a history and its synthetic application. *Tetrahedron* **2009**, *65* (21), 4069-4087.
31. Michael, A. Ueber die addition von natriumacetessigund natriummalonsaureathern zu den aethern ungesattigter sauren. *Journal fur Praktische chemie* **1887**, *35*, 349-356.
32. Little, R. D.; Masjedizadeh, M. R.; Wallquist, O.; McLoughlin, J. I. The intramolecular Michael reaction. *Org. React.* **1995**, *47*, 315-552.
33. Smith, J. G.; The Diels-Alder Reaction. Organic Chemistry, 3rd Ed. New York, NY, McGraw-Hill, **2011**, 588–89.
34. Sauer, J.; Sustmann, R. Mechanistic aspects of Diels-Alder reactions: a critical survey. *Angew. Chem. Int. Ed.* **1980**, *19*, 779-807.
35. Goldstein, E.; Beno, B.; Houk, K. N. Density functional theory prediction of the relative energies and isotope effects for the concerted and stepwise mechanisms

- of the Diels-Alder reaction of butadiene and ethylene. *J. Am. Chem. Soc.* **1996**, *118*, 6036-6043.
36. Nicolaou, K. C.; Snyder, S. A.; Motagnon, T.; Vassilkogiannakis, G. The Diels-Alder reaction in total synthesis. *Angew. Chem. Int. Ed.* **2002**, *41*, 1668-1698.
 37. Stocking, E. M.; Williams, R. M. Chemistry and biology of biosynthetic Diels-Alder reactions. *Angew. Chem. Int. Ed.* **2003**, *42*, 3078-3115.
 38. Oikawa, H. Involvement of the Diels-Alderase in the biosynthesis of natural products. *Bull. Chem. Soc. Jpn.* **2005**, *78*, 537-554.
 39. Kim, H. J.; Ruszczycky, M. W.; Liu, H.-w. Current developments and challenges in the search for a naturally selected Diels-Alderase. *Current Opinion in Chem. Biol.* **2012**, *16*, 1-8.
 40. Kelly, W. L. Intramolecular cyclizations of polyketide biosynthesis: mining for a “Diels-Alderase”? *Org. Biomol. Chem.* **2008**, *6*, 4483-4493.
 41. Oikawa, H.; Katayama, K.; Suzuki, Y.; Ichihara, A. Enzymatic-activity catalyzing exo-selective Diels-Alder reaction in solanapyrone biosynthesis. *J. Chem. Soc. Chem. Comm.* **1995**, (13), 1321-1322.
 42. Katayama, K.; Kobayashi, T.; Oikawa, H.; Honma, M.; Ichihara, A. Enzymatic activity and partial purification of solanapyrone synthase: first enzyme catalyzing Diels-Alder reaction. *Biochimica et Biophysica Acta – Protein Struct. Mol. Enzymol.* **1998**, *1384* (2), 387-395.
 43. Kasahara, K.; Miyamoto, T.; Fujimoto, T.; Oquri, H.; Tokiwano, T.; Oikawa, H.; Ebizuka, Y.; Fujii, I. Solanapyrone synthase, a possible Diels-Alderase and iterative type I polyketide synthase encoded in a biosynthetic gene cluster from *Alternaria solani*. *ChemBioChem* **2010**, *11* (9), 1245-1252.

44. Auclair, K.; Sutherland, A.; Kennedy, J.; Witter, D. J.; Van den Heever, J. P.; Hutchinson, C. R.; Vederas, J. C. Lovastatin nonaketide synthase catalyzes an intramolecular Diels-Alder reaction of a substrate analogue. *J. Am. Chem. Soc.* **2000**, *122* (46), 11519-11520.
45. Ma, S. M.; Tang, Y. Biochemical characterization of the minimal polyketide synthase domains in the lovastatin nonaketide synthase LovB. *FEBS J.* **2007**, *274* (11), 2854-2864.
46. Oikawa, H.; Yagi, K.; Watanabe, K.; Honma, M.; Ichihara, A. Biosynthesis of macrophomic acid: Plausible involvement of intermolecular Diels-Alder reaction. *Chem. Comm.* **1997**, (1), 97-98.
47. Oikawa, H.; Watanabe, K.; Yagi, K.; Ohashi, S.; Mie, T.; Ichihara, A.; Honma, M. Macrophomate synthase: unusual enzyme catalyzing multiple reactions from pyrones to benzoates. *Tetrahedron Lett.* **1999**, *40* (38), 6983-6986.
48. Ose, T.; Watanabe, K.; Mie, T.; Honma, M.; Watanabe, H.; Yao, M.; Oikawa, H.; Tanaka, I. Insight into a natural Diels-Alder reaction from the structure of macrophomate synthase. *Nature* **2003**, *422* (6928), 185-189.
49. Watanabe, K.; Mie, T.; Ichihara, A.; Oikawa, H.; Honma, M. Detailed reaction mechanism of macrophomate synthase: extraordinary enzyme catalyzing five-step transformation from 2-pyrones to benzoates. *J. Biol. Chem.* **2000**, *275*, 38393-38401.
50. Sakurai, I.; Suzuki, H.; Shimizu, S.; Yamamoto, Y. Novel Biotransformation of a 2-Pyrone to a Substituted Benzoic-Acid. *Chem. Pharm. Bull.* **1985**, *33* (11), 5141-5143.
51. Guimaraes, C. R. W.; Udier-Blagovic, M.; Jorgensen, W. L. Macrophomate synthase: QM/MM simulations address the Diels-Alder versus Michael-Aldol reaction mechanism. *J. Am. Chem. Soc.* **2005**, *127* (10), 3577-3588.

52. Serafimov, J. M.; Gillingham, D.; Kuster, S.; Hilvert, D. The putative Diels-Alderase macrophomate synthase is an efficient aldolase. *J. Am. Chem. Soc.* **2008**, *130* (25), 7798-7799.
53. Bouwmeester, H. J.; Gershenzon, J.; Konings, M. C.; Croteau, R. Biosynthesis of the monoterpene limonene and carvone in the fruit of caraway: 1. Demonstration of enzyme activities and their changes with development. *Plant Physiol.* **1998**, *117*, 901-912.
54. Starks, C. M.; Back, K.; Chappell, J.; Noel, J. P. Structural basis for cyclic terpene Biosynthesis by Tobacco 5-epi-Aristolochene Synthase. *Science* **1997**, *277*, 1815-1820.
55. Beckwith, J. L. J. Mechanism and applications of free radical cyclization. *Rev. Chem. Intermed.* **1986**, *7*, 143-154.
56. RajanBabu, T. V. Stereochemistry of intramolecular free-radical cyclization reactions. *Acc. Chem. Res.* **1991**, *24*, 139-145.
57. Curran, D. P.; Sisko, J.; Yeske, P. E.; Liu, H. Recent applications of radical reactions in natural product synthesis. *Pure & Appl. Chem.* **1993**, *65* (6), 1153-1159.
58. Parsons, P. J.; Penkett, C. S.; Shell, A. J. Tandem reactions in organic synthesis: novel strategies for natural product elaboration and the development of new synthetic methodology. *Chem. Rev.* **1996**, *96*, 195-206.
59. Majumdar, K. C.; Karunakar, G. V.; Sinha, B. Formation of five- and six-membered heterocyclic rings under radical cyclization conditions. *Tetrahedron* **2007**, *63* (4) 793-826.

60. Giese, B.; Kopping, B.; Gobel, T.; Dickhaut, J.; Thoma, G.; Kulicke, K. J.; Trach, F. ChemInform Abstract: Radical Cyclization Reactions. *Org. React.* **1996**, *48*, 301-361.
61. Wagner, G. J. *J. Russ. Phys. Chem. Soc.* **1899**, *31*, 690.
62. Meerwein, H. Über den reaktionsmechanismus der umwandlung von borneol in camphen: dritte mitteilung über pinakolinumlagerungen. *Justus Liebig's Annalen der Chemie* **1914**, *405*, 129-175.
63. Ikeda, H.; Nonomiya, T.; usami, M.; Ohta, T.; Omura, S. Organization of the biosynthetic gene cluster for the polyketide anthelmintic macrolide avermectins in *Streptomyces avermitilis*. *Proc. Natl. Acad. Sci. U.S.A.* **1999**, *97* (17), 9509-9514.
64. Hanessian, S.; Ugolini, A.; Hodges, P. J.; Beaulieu, P.; Dube, D.; Andre, C. Progress in natural product chemistry by the Chiron and related approaches - synthesis of avermectins B_{1a}. *Pure & Appl. Chem.* **1987**, *59* (3), 299-316.
65. Fisher, M. H. Recent advances in avermectins research. *Pure & Appl. Chem.* **1990**, *62* (7), 1231-1240.
66. Omura, S.; Shiomi, K. Discovery, chemistry, and chemical biology of microbial products. *Pure & Appl. Chem.* **2007**, *79* (4), 581-591.
67. McGrath, N. A.; Binner, J. R.; Markopoulos, G.; Brichacek, M.; Njardarson, J. An efficient oxidative dearomatization - radical cyclization approach to symmetrically substituted bicyclic guttiferone natural products. *Chem. Commun.* **2011**, *47*, 209-211.
68. Sancar, A. No "end of history" for photolyases. *Science* **1996**, *272*, 48.
69. Thiagarajan, V.; Byrdin, M.; Eker, A. P. M.; Muller, P.; Brettel, K. Kinetics of cyclobutane thymidine dimer splitting by DNA photolyase directly monitored in the UV. *Proc. Natl. Acad. Sci. U.S.A.* **2011**, *108*, 9402-9407.

70. Kim, S. T.; Malhotra, K.; Smith, C. A.; Taylor, J. S.; Sancar, A. Characterization of (6-4) photoproduct DNA photolyase. *J. Biol. Chem.* **1994**, *269*, 8535-8540.
71. Zhao, X.; Liu, J.; Hsu, D. S.; Zhao, S.; Taylor, J. -S.; Sancar, A. Reaction mechanism of (6-4) photolyase. *J. Biol. Chem.* **1997**, *272*, 32580-32590.
72. Baylis, A. B.; Hillman, M. E. D. German Patent 2155113, **1972**.
73. Ciganek, E. Catalyzed α -hydroxyalkylation and α -aminoalkylation of activated olefins (The Morita-Baylis-Hillman Reaction). *Org. React.* **1997**, *51*, 201.
74. Morita, K.; Suzuki, Z.; Hirose, H. A Tertiary. Phosphine-catalyzed Reaction of Acrylic Compounds with Aldehydes. *Bull. Chem. Soc. Jpn.* **1968**, *41*, 2815.
75. Erguden, J. K.; Moore, H. W. A new tandem route to angular tetraquinanes: Synthesis of the waihoensene ring system. *Org. Lett.* **1999**, *1* (5), 375-377.
76. Agapiou, K.; Krische, M. J. Catalytic crossed Michael cycloisomerization of thioenates: total synthesis of (\pm)-ricciocarpin A. *Org. Lett.* **2003**, *5* (10), 1737-1740.
77. Stark, L. M.; Pekari, K.; Sorensen, E. J. A nucleophile-catalyzed cycloisomerization permits a concise synthesis of (+)-harziphiline. *Proc. Natl. Acad. Sci. U.S.A.* **2004**, *101* (33), 12064-12066.
78. Methot, J. L.; Roush, W. R. Synthetic studies toward FR1182877. Remarkable solvent effect in the vinylogous Morita-Baylis-Hillman cyclization. *Org. Lett.* **2003**, *5* (22), 4223-4226.
79. Winbush, S. M.; Mergott, D. J.; Roush, W. R. Total synthesis of (-)-spinosyn A: examination of structural features that govern the stereoselectivity of the key transannular Diels-Alder reaction. *J. Org. Chem.* **2008**, *73* (5), 1818-1829.

80. Mergott, D. J.; Frank, S. A.; Roush, W. R. Total synthesis of (-)-spinosyn A. *Proc. Natl. Acad. Sci. U.S.A.* **2004**, *101* (33), 11955-11959.
81. Mergott, D. J.; Frank, S. A.; Roush, W. R. Application of the intramolecular vinylogous Morita-Baylis-Hillman reaction toward the synthesis of the spinosyn A tricyclic nucleus. *Org. Lett.* **2002**, *4* (18), 3157-3160.
82. Frank, S. A.; Roush, W. R. Studies on the synthesis of (-)-spinosyn A: application of the steric directing group strategy to transannular Diels-Alder reactions. *J. Org. Chem.* **2002**, *67* (12), 4316-4324.
83. Romesberg, F. E.; Spiller, B.; Schultz, P. G.; Stevens, R. C. Immunological origins of binding and catalysis in a Diels-Alderase antibody. *Science* **1998**, *279*, 1929-1933.
84. Carreras, C. W.; Santi, D. V. The catalytic mechanism and structure of thymidylate synthase. *Annu. Rev. Biochem.* **1995**, *64*, 721-762.
85. Gotoh, O.; Shimizu, K.; Kaneda, S.; Nalbantoglu, J.; Takeishi, K.; Seno, T.; Ayusawa, D. Structural and functional analysis of the human thymidylate synthase gene. *J. Biol. Chem.* **1990**, *265* (33), 20277-20284.
86. Wang, Z.; Abeysinghe, T.; Finer-Moore, J. S.; Stroud, R. M.; Kohen, A. A remote mutation affects the hydride transfer by disrupting concerted protein motions in thymidylate synthase. *J. Am. Chem. Soc.* **2012**, *134*, 17722-17730.
87. Halland, N.; Hansen, T.; Jorgensen, K. A. Organocatalytic asymmetric Michael reaction of cyclic 1,3-dicarbonyl compounds and α,β -unsaturated ketones – a highly atom-economic catalytic one-step formation of optically active warfarin anticoagulant. *Angew. Chem.* **2003**, *42*, 4955-4957.

88. Wzorek, J. S.; Knopfel, T. F.; Sapountzis, I.; Evans, D. A. A macrocyclic approach to tetracycline natural products. Investigation of transannular alkylations and Michael additions. *Org. Lett.* **2012**, *14* (23), 5840-5843.
89. Sakaguchi, H.; Tokuyama, H.; Fukuyama, T. Total synthesis of (-)-kainic acid via intramolecular Michael addition: a second-generation route. *Org. Lett.* **2008**, *10* (9), 1711-1714.
90. Morita, Y.; Tokuyama, H.; Fukuyama, T. Stereocontrolled total synthesis of (-)-kainic acid. Regio- and stereoselective lithiation of pyrrolidine ring with the (+)-sparteine surrogate. *Org. Lett.* **2005**, *7* (20), 4337-4340.
91. Takita, S.; Yokoshima, S.; Fukuyama, T. A practical synthesis of (-)-kainic acid. *Org. Lett.* **2011**, *13* (8), 2068-2070.
92. Zdlkow, L.H.; Girota, N.N. Studies in the synthesis of artisine. Terpenes X. *J. Org. Chem.* **1964**, *29*, 1299-1302.
93. Ihara, M.; Fukumoto, K. Syntheses of polycyclic natural products employing the intramolecular double Michael reaction. *Angew. Chem. Int. Ed.* **2003**, *32* (7), 1010-1022.
94. Ihara, M.; Toyota, M.; Fukumoto, K.; Kametani, T. Intramolecular double Michael reaction. Part II. Synthesis of isoatisirene type compound. *Tetrahedron Lett.* **1984**, *25*, 3235-3238.
95. Ihara, M.; Toyota, M.; Fukumoto, K.; Kametani, T. Intramolecular double Michael reaction. Part III. Stereoselective chiral synthesis of atisiran-15-one. *Tetrahedron Lett.* **1985**, *26*, 1537-1540.
96. Ihara, M.; Toyota, M.; Fukumoto, K.; Kametani, T. An enantioselective total synthesis of (+)-atisirene by intramolecular double Michael reaction. *J. Chem. Soc. Perkin Trans. 1*, **1986**, 2151-2161.

97. Vicario, J. L.; Badia, D.; Carrillo, L. Organocatalytic enantioselective Michael and Hetero-Michael reactions. *Synthesis* **2007**, *14*, 2065-2092.
98. Ihara, M. Syntheses of biologically active natural products and leading compounds for new pharmaceuticals employing effective construction of a polycyclic skeleton. *Chem. Pharm. Bull.* **2006**, *54* (6), 765-774.
99. Tokoroyama, T. Discovery of the Michael reaction. *Eur. J. Org. Chem.* **2010**, 2009-2016.
100. Anslyn, E. V.; Dougherty, D. A. Chapter 8. Experiments related to thermodynamics and kinetics. Modern physical organic chemistry. Sausalito, California, University Science Books, 2004, 421-488.
101. Emanuele, J. J.; Heasley, C. J.; Fitzpatrick, P. F. Purification and characterization of the flavoprotein tryptophan 2-monooxygenase expressed at high levels in *Escherichia coli*. *Arch. Biochem. Biophysics* **1995**, *316* (1), 241-248.
102. Ralph, E. C.; Anderson, M. A.; Cleland, W. W.; Fitzpatrick, P. F. Mechanistic studies of the flavoenzyme tryptophan 2-monooxygenase: deuterium and ¹⁵N kinetic isotope effects on alanine oxidation by an L-amino acid oxidase. *Biochemistry* **2006**, *45*, 15844-15852.
103. Emanuele, J. J.; Fitzpatrick, P. F. Mechanistic studies of the flavoprotein tryptophan 2-monooxygenase. 1. Kinetic mechanism. *Biochemistry* **1995**, *34* (11), 3710-3715.
104. Emanuele, J. J.; Fitzpatrick, P. F. Mechanistic studies of the flavoprotein tryptophan 2-monooxygenase. 2. pH and kinetic isotope effects. *Biochemistry* **1995**, *34* (11), 3716-3723.
105. Tishkov, V. I.; Khoronenkova, S. V. D-Amino acid oxidase: structure, catalytic mechanism, and practical application. *Biochemistry* **2005**, *70* (1), 40-54.

106. Pollegioni, L.; Blodig, W.; Chisla, S. On the mechanism of D-amino acid oxidase: structural/linear free energy correlations and deuterium kinetic isotope effects using substituted phenylglycines. *J. Biol. Chem.* **1997**, *272*, 4924-4934.
107. Kurtz, K. A.; Fitzpatrick, P. F. pH and secondary kinetic isotope effects on the reaction of D-amino acid oxidase with nitroalkane anions: evidence for direct attack on the flavin by carbanions. *J. Am. Chem. Soc.* **1997**, *119*, 1155-1156.
108. Walsh, C. T. Suicide substrates, mechanism-based enzyme inactivators: recent developments. *Ann. Rev. Biochem.* **1984**, *53*, 493-535.
109. Pongdee, R. Liu, H.-w. Elucidation of enzyme mechanisms using fluorinated substrate analogues. *Bioorg. Chem.* **2004**, *32* (5), 393-437.
110. O'Hagan D.; Rzepa, H. S. Some influences of fluorine in bioorganic chemistry. *Chem. Commun.* **1997**, 645-652.
111. Santi, D. V.; McHenry, C. S. 5-Fluoro-2'-deoxyuridylate: covalent complex with thymidylate synthetase. *Proc. Natl. Acad. Sci. U.S.A.* **1972**, *69* (7), 1855-1857.
112. Danenberg, P. V.; Danenberg, K. D. Effect of 5,10-methylenetetrahydrofolate on the dissociation of 5-fluoro-2'-deoxyuridylate from thymidylate synthetase: evidence for an ordered mechanism. *Biochemistry* **1978**, *17* (19), 4018-4024.
113. He, X.; Liu, H.-w. Mechanisms of enzymatic C-O bond cleavages in deoxyhexose biosynthesis. *Current. Opinions in Chem. Biol.* **2002**, *6* (5), 590-597.;
114. Chang, C-W. T.; Chen, X. H.; Liu, H.-w. CDP-6-deoxy-6,6-difluoro-D-glucose: a mechanism-based inhibitor for CDP-D-glucose 4,6-dehydratase. *J. Am. Chem. Soc.* **1998**, *120*, 9698-9699.
115. Storer, J.W.; Raimondi, L.; Houk, K.N. Theoretical secondary kinetic isotope effects and the interpretation of transition state geometries. 2. The Diels-Alder transition state geometry. *J. Am. Chem. Soc.* **1994**, *116*, 9675-9683.

116. Henderson, R. W.; Pryor, W.A. Secondary hydrogen isotope effect for the transition from olefin to free radical. *Int. J. Chem. Kinet.* **1972**, *4*, 325-330.
117. Robert F.; Hout, J.; Levi, B. A.; Hehre, W. J. A method for the calculation of normal-mode vibrational frequencies using symmetry coordinates. Application to the calculation of secondary deuterium isotope effects on carbocations. *J. Comp. Chem.* **1983**, *4*, 499-505.
118. Gajewski, J. J.; Peterson, K. B.; Kagel, J. R. Transition-state structure variation in the Diels-Alder reaction from secondary deuterium kinetic isotope effects: The reaction of a nearly symmetrical diene and dienophile is nearly synchronous. *J. Am. Chem. Soc.* **1987**, *109*, 5545-5546.
119. Gajewski, J. J.; Peterson, K. B.; Kagel, J. R.; Huang, Y. C. J. Transition-state structure variation in the Diels-Alder reaction from secondary deuterium kinetic isotope effect: The reaction of nearly symmetrical dienes and dienophiles is nearly synchronous. *J. Am. Chem. Soc.* **1989**, *111*, 9078-9081.
120. Singleton, D. A.; Thomas, A. A. High-precision simultaneous determination of multiple small kinetic isotope effects at natural abundance. *J. Am. Chem. Soc.* **1995**, *117*, 9357-9358.
121. Lowry, T. H.; Richardson, K. S. *Mechanism and Theory in Organic Chemistry*. Harper & Row, Harper-Collins Publishers, Inc., New York, 3rd Edition.
122. Steitwieser Jr, A.; Jagow, R. H.; Rahey, R. C.; Suzuki, S. Kinetic isotope effects in the acetolyses of deuterated cyclopentyl tosylates. *J. Am. Chem. Soc.* **1958**, *80*, 2326-2332.
123. Bahnon, B. J.; Anderson, V. E. Crotonase-catalyzed β -elimination is concerted: A double isotope effect study. *Biochemistry* **1991**, *367*, 28-39.

124. Cassano, A. G.; Wang, B.; Ander, D. R.; Previs, S.; Harris, M. E.; Anderson, V. E. Inaccuracies in selected ion monitoring determination of isotope ratios obviated by profile acquisition nucleotide $^{18}\text{O}/^{16}\text{O}$ measurements. *Anal. Biochem.* **2007**, *367*, 28-39.
125. Page, M. I.; Jencks, W. P. Entropic contributions to rate accelerations in enzymatic and intramolecular reactions and the chelate effect. *Proc. Natl. Acad. Sci. U.S.A.* 1971, *68*, 1678-1683.
126. Jencks, W. P. *Catalysis in Chemistry and Enzymology*. Dover Publications, Inc., New York.
127. Smith, M. B.; March, J. *March's advanced organic chemistry: reactions, mechanisms and structure*. John Wiley & Sons, Inc., New York, 5th Edition.
128. Thomas, K.; Haapalainen, A. M.; Burgos, E. S.; Evans, G. B.; Tyler, P. C.; Gulab, S.; Guan, R.; Schramm, V. L. Femtomolar inhibitors bind to 5'-methylthioadenosine nucleosidases with favorable enthalpy and entropy. *Biochemistry*, **2012**, *51*, 7541-7550.
129. Luo, Q.; Meneely, K. M.; Lamb, A. L. Entropic and enthalpic components of catalysis in the mutase and lyase activities of *Pseudomonas aeruginosa* PchB. *J. Am. Chem. Soc.* **2011**, *133*, 7229-7233.
130. Gloster, T. M.; MacDonald, J. M.; Tarling, C. A.; Stick, R. V.; Withers, S. G.; Davies, G. J. Structural, thermodynamic, and kinetic analyses of tetrahydrooxazine-derived inhibitors bound to β -glucosidases. *J. Biol. Chem.* **2004**, *279* (47), 49236-49242.
131. Richard, J. P. Enzymatic rate enhancements: A review and perspective. *Biochemistry* **2009**, *52*, 2009-2011.

132. Kim, H. J. Investigation of the post-polyketide synthase (PKS) modifications during spinosyn A biosynthesis in *Saccharopolyspora spinosa*. The University of Texas at Austin, Austin, **2010**.
133. Inanaga, J.; Hirata, K.; Saeki, H.; Katsuki, T.; Yamaguchi, M. Rapid esterification by means of mixed anhydride and its application to large-ring lactonization. *Bull. Chem. Soc. Jpn.* **1979**, *52* (7), 1989-1993.
134. Blakemore, P. R.; Cole, W. J.; Kocienski, P. J.; Moreley, A. A stereoselective synthesis of trans-1,2-disubstituted alkenes based on the condensation of aldehydes with metallated 1-phenyl-1H-tetrazol-5-yl sulfones. *Synlett* **1998**, (1), 26-28.
135. Julia, M.; Paris, J.-M. Synthèses à l'aide de sulfones v(+)-méthode de synthèse générale de doubles liaisons. *Tetrahedron Lett.* **1973**, *49*, 4833-4836.
136. Stille, J. K. The palladium-catalyzed cross-coupling reactions of organotin reagents with organic electrophiles. *Angew. Chem. Int. Ed.* **1986**, *25* (6), 508-523.
137. Mukaiyama, T.; Soai, K.; Sato, T.; Shimizu, H.; Suzuki, K. Enantioface-differentiating (asymmetric) addition of allyl lithium and dialkylmagnesium to aldehydes by using (2S, 2'S)-2-hydroxymethyl-1-[(1-alkylpyrrolidin-2-yl)methyl]pyrrolidines as chiral ligands. *J. Am. Chem. Soc.* **1979**, *101* (6), 1455-1460.
138. Evans, D. A.; Takacs, J. M. Enantioselective alkylation of chiral enolates. *Tetrahedron Lett.* **1980**, *21*, 4233-4236.
139. Brown, H. C.; Desai, M. C.; Jadhav, P. K. Hydroboration. 61. Diisopinocampheylborane of high optical purity. Improved preparation and asymmetric hydroboration of representative cis-disubstituted alkenes. *J. Org. Chem.* **1982**, *47* (26), 5065.

140. Brown, H. C.; Singaram, B. Improved procedures for the synthesis of diisopinocampheylborane of high optical purity. *J. Org. Chem.* **1984**, *49* (5), 945-947.
141. Jadhav, P. K.; Bhat, K. S.; Perumal, T.; Brown, H. C. Chiral synthesis via organoboranes. 6. Asymmetric allylboration via chiral allyldialkylboranes. Synthesis of homoallylic alcohols with exceptionally high enantiomeric excess. *J. Org. Chem.* **1986**, *51* (4), 432-439.
142. Seebach, D.; Corey, E. J. Generation and synthetic applications of 2-lithio-1,3-dithianes. *J. Org. Chem.* **1975**, *40* (2), 231-237.
143. Grobel, B.-T.; Seebach, D. Umpolung of the reactivity of carbonyl compounds through sulfur-containing reagents. *Synthesis* **1977**, *6*, 357-402.
144. Pappo, R.; Allen Jr., D. S.; Lemieux, R. U.; Johnson, W. S. Notes – osmium tetroxide-catalyzed periodate oxidation of olefinic bonds. *J. Org. Chem.* **1956**, *21* (4), 478-479.
145. Takai, K.; Nitta, K.; Utimoto, K. Simple and selective method for aldehydes (RCHO) forward (E)-haloalkenes (RCH:CHX) conversion by means of a haloform-chromous chloride system. *J. Am. Chem. Soc.* **1986**, *108* (23), 7408-7410.
146. Horner, L.; Hoffmann, H.; Wippel, H. G. Phosphororganische verbindungen, XII. Phosphinoxyde als olefinierungsreagenzien. *Ber.* **1958**, *91* (1), 61-63.
147. Wadsworth, W. S.; Emmons, W. D. The utility of phosphonate carbanions in olefin synthesis. *J. Am. Chem. Soc.* **1961**, *83* (7), 1733-1738.
148. Wittig, G.; Schollkopf, U. Über triphenylphosphine-methylene als olefinbildende reagenzien I. *Ber.* **1954**, *87* (9), 1318-1330.

149. Wittig, G.; Haag, W. Uber triphenyl-phosphin-methylene als olefinbildende reagenzien II. *Ber.* **1955**, 88 (11), 1654-1666.
150. Brown, H. C. Hydroboration – a powerful synthetic tool. *Tetrahedron Lett.* **1961**, 12, 117-138.
151. Choi, S. H. Synthetic approaches to investigate the chemical mechanism in the biosynthesis of natural products. The University of Texas at Austin, Austin, **2012**.
152. Hurley, P. B.; Dake, G. R.; Synthetic studies toward halichlorine: Complex azaspirocycle formation with use of an NBS-promoted semipinacol reaction. *J. Org. Chem.* **2008**, 73 (11), 4131-4138.
153. McDonald, C.; Holcomb, H.; Kennedy, K.; Kirkpatrick, E.; Leathers, T.; Vanemon, P. N-Iodosuccinimide-mediated conversion of aldehydes to methyl esters. *J. Org. Chem.* **1989**, 54 (5), 1213-1215.
154. Abeles, R. H.; Maycock, A. L. Suicide enzyme inactivators. *Acc. Chem. Res.* **1976**, 9 (9), 313-319.
155. Robertson, J. G. Mechanistic basis of enzyme-targeted drugs. *Biochemistry* **2005**, 44 (15), 5561-5571
156. Kirk, K. L. Fluorination in medicinal chemistry: methods, strategies, and recent developments. *Org. Process Res. Dev.* **2008**, 12 (2), 305-321.
157. Potashman, M. H.; Duggan, M. E. Covalent modifiers: An orthogonal approach to drug design. *J. Med. Chem.* **2009**, 52 (5), 1231-1246.
158. Powers, J. C.; Asgian, J. L.; Ekici, O. D.; James, K. E. Irreversible inhibitors of serine, cysteine, and threonine proteases. *Chem. Rev.* **2002**, 102, 4639-4750.

159. Berkowitz, D. B.; Karukurichi, K. R.; Salud-Bea, R.; Nelson, D. L.; McCune, C. D. Use of fluorinated functionality in enzyme inhibitor development: mechanistic and analytical advantages. *J. Fluor Chem.* **2008**, *129* (9), 731-742.
160. Ghosh, A. K.; Banerjee, S.; Sinha, S.; Kang, S. B.; Zajc, B. α -Fluorovinyl Weinlab amides and α -fluoroenones from a common fluorinated building block. *J. Org. Chem.* **2009**, *74* (10), 3689-3697.
161. Kim, S. C.; Singh, A. N.; Rauchel, F. M. Analysis of the galactosyltransferase reaction by positional isotope exchange and secondary deuterium isotope effects. *Archiv. Biochem. Biophysics.* **1988**, *267* (1), 54-59.
162. Rose, I. A. Mechanisms of enzyme action. *Annu. Rev. Biochem.* **1966**, *35*, 23.
163. Cardinale, G. J.; Abeles, R. H. Purification and mechanism of action of proline racemase. *Biochemistry* **1968**, *7*, 3970.
164. Tanner, M. E.; Gallo, K. A.; Knowles, J. R. Isotope effects and the identification of catalytic residues in the reaction catalyzed by glutamate racemase. *Biochemistry* **1993**, *32*, 3998.
165. Northrop, D. B. Effects on enzyme-catalyzed reactions. *Ann. Rev. Biochem.* **1981**, *50*, 103-131.
166. Northrop, D. B. On the meaning of K_M and V/K in enzyme kinetics. *J. Chem. Ed.* **1998**, *75* (9), 1153-1157.
167. Voet, D.; Voet, J. G. *Biochemistry*, John Wiley & Sons, Inc. 3rd Edition.
168. Krippendorff, B.-F.; Neuhaus, R.; Lienau, P.; Reichel, A.; Huisinga, W. Mechanism-based inhibition: Deriving K_I and K_{inact} directly from time-dependent IC50 values. *J. Biomol. Screening*, **2009**, *14*, 913-923.

169. Geoghegan, K. F.; Dixon, H. B. F.; Rosner, P. J.; Hoth, L. R.; Lanzetti, A. J.; Borzilleri, K. A.; Marr, E. S.; Pezzullo, L. H.; Martin, L. B.; LeMotte, P. K.; McColl, A. S.; Kamath, A. V.; Stroh, J. G. Spontaneous α -N-6-phosphoglucuronylation of a “His-tag” in *Escherichia coli*: The cause of extra mass of 258 or 178 Da in fusion proteins. *Anal. Biochem.* **1999**, *267* (1), 169-184.
170. Wang, L. C.; Luis, A. L.; Agaplou, K.; Jang, H. Y.; Krische, M. J. Organocatalytic Michael cycloisomerization of bis(enones): The intramolecular Rauhut-Currier reaction. *J. Am. Chem. Soc.* **2002**, *124* (11), 2402-2403.
171. Cantoni, G. L. The nature of the active methyl donor formed enzymatically from l-methionine and adenosinetriphosphate. *J. Am. Chem. Soc.* **1952**, *74* (11), 2942-2943.
172. Lu, S. C. S-Adenosylmethionine. *Int. J. Biochem. & Cell Biol.* **2000**, *32* (4), 391-395.
173. Layer, G.; Heinz, D. W.; Jahn, D.; Schbert, W.-D. Structure and function of radial SAM enzymes. *Curr. Opinion Chem. Biol.* **2004**, *8*, 468-476.
174. Ruszczycky, M. K.; Ogasawara, Y. Liu, H.-w. Radical SAM enzymes in the biosynthesis of sugar-containing natural products. *Biochim. Biophys. Acta – Proteins and Proteomics.* **2012**, *1824* (11), 1231-1244.
175. Atta, M.; Arragain, S.; Fontecave, M.; Mulliez, E.; Hunt, J. F.; Luff, J. D.; Forouhar, F. The methylating reaction mediated by the radical SAM enzymes. *Biochim. Biophys. Acta – Proteins and Proteomics.* **2012**, *1824* (11), 1223-1230.
176. Shisler, K.; Broderick, J. B. Emerging themes in radical SAM chemistry. *Curr. Opinion Struc. Biol.* **2012**, *22* (6), 701-710.
177. Fujimori, D. G. Radical SAM-mediated methylation reactions. *Curr. Opinion Chem. Biol.* **2013**, *17* (4), 597-604.

178. Greenfield, N. J. Using circular dichroism spectra to estimate protein secondary structure. *Nat. Protocol.* **2006**, *1*(6), 2876-2890.
179. Greenfield, N. J. Using circular dichroism collected as a function of temperature to determine the thermodynamics of protein unfolding and binding interactions. *Nat. Protocol.* **2006**, *1* (6), 2527-2535.
180. Garbett, N. C.; Ragazzon, P. A.; Chaires, J. B. Circular dichroism to determine binding mode and affinity of ligand-DNA interactions. *Nat. Protoc.* **2007**, *2* (12), 3166-3172.
181. Alian, A.; Lee, T. T.; Griner, S. L.; Stroud, R. M.; Finer-Moore, J. Structure of a TrmA-RNA complex: A consensus RNA fold contributes to substrate selectivity and catalysis in m5U methyltransferases. *Proc. Natl. Acad. Sci. U.S.A.* **2008**, *105* (19), 6876-6881.
182. Bielza, P.; Quinto, V.; Contreras, J.; Torne, M.; Martin, A.; Espinosa, P. J. Resistance to spinosad in the western flower thrips, *Frankliniella occidentalis* (Pergande), in greenhouses of south-eastern Spain. *Pest Manag. Sci.* **2007**, *63* (7), 682-687.
183. Osorio A.; Martinez, A. M.; Schneider, M. I.; Corrales, J. L.; Aviles, M. C.; Smagghe, G.; Pineda, S. Monitoring of beet armyworm resistance to spinosad and methoxyfenozide in Mexico. *Pest Manag. Sci.* **2008**, *64* (10), 1001-1007.
184. Kakani, E. G.; Zygouridis, N. E.; Tsoumani, K. T.; Seraphides, N.; Zalom, F. G.; Mathiopoulos, K. D. Spinosad resistance development in wild olive fruit fly *Bactrocera oleae* (Diptera: Tephritidae) populations in California. *Pest Manag. Sci.* **2010**, *66* (4), 447-453.
185. Lebedev, G.; Abo-Moch, F.; Gafni, G.; Ben-Yakir, D.; Ghanim, M. High-level of resistance to spinosad, emamectin benzoate and carbosulfan in populations of *Thrips tabaci* collected in Israel. *Pest Manag. Sci.* **2013**, *69* (2), 274-277.

186. Evans, D. A.; Black, W. C. Total synthesis of (+)-A83543A [(+)-Lepicidin A] *J. Am. Chem. Soc.* **1993**, *115*, 4497-4513.
187. Paquette, L. A.; Gao, Z.L.; Li, Z.J.; Smith, G. F. Total synthesis of spinosyn A. 1. Enantioselective construction of a key tricyclic intermediate by a multiple configurational inversion scheme. *J. Am. Chem. Soc.* **1998**, *120*, 2543-2552.
188. Paquette, L. A.; Collado, I.; Purdie, M. Total synthesis of spinosyn A. 2. Degradation studies involving the pure factor and its complete reconstitution. *J. Am. Chem. Soc.* **1998**, *120*, 2553-2562.
189. Tietze, L. F.; Kinzel, T. Synthesis of natural products and analogs using multiple Pd-catalyzed transformations. *Pure Appl. Chem.* **2007**, *79* (4), 629-650.

Vita

Nam Ho Kim was born in Seoul, Republic of Korea in 1975. In 1997, he graduated with Bachelor of Science in Chemistry from Korea Advanced Institute of Science and Technology (KAIST). He conducted undergraduate research in the laboratory of Dr. Sung Ho Kang in Chemistry, where he continued pursuing Master degree. After receiving Master of Science degree in 1999, he worked as a research scientist at the Drug Discovery division in SK Chemicals from January 1999 to July 2009. His works were focused on discovering novel anti-cancer, anti-diabetes and anti-obesity drug candidates and on developing new formulations for generic drugs. He also co-authored three research publications and more than fifty Patents. He was admitted to the Medicinal Chemistry Graduate program in the College of Pharmacy at The University of Texas at Austin in 2009. Nam Ho joined the Ben Liu Research Group in September 2009.

Email address: nomis@sk.com; kimnomis@daum.net; kimnomis@gmail.com

This dissertation was typed by Nam Ho Kim.